

1 Atmospheric composition ★ and energy

The earth's atmosphere is vital to terrestrial life. It is believed to have developed in its present form and composition at least some 350 million years ago when extensive vegetation cover originated on land. Its presence provides an indispensable shield from harmful radiation from the sun and its gaseous content sustains the plant and animal biosphere. Within the atmospheric envelope, weather systems form and decay and their development and motion are the basis of most global climates. Yet the atmosphere and its weather phenomena are not fixed and unvarying. The composition of the atmosphere is progressively being modified by man's activities; extreme weather events — gales, tornadoes, hailstorms, floods — can wreak havoc, even when anticipated; weather regimes show significant changes on short and long time scales often with drastic consequences for agriculture and settlement in marginal areas. By seeking to understand the working of the atmosphere and its weather and climate, we can hope to forecast their vagaries and in some instances modify or control them in a beneficial way. This broad endeavour constitutes the field of the atmospheric sciences. *Meteorology* is specifically concerned with the physics of weather phenomena, *climatology* with mean (average) conditions representative of the long term state of the atmosphere and variability. Since weather phenomena range in scale from wind eddies of a metre or so to the global circulation, climate can also refer to conditions within a vegetation canopy (*microclimate*) or to regional and global climate (*macroclimate*).

24 Atmosphere, weather and climate

The structure of the book represents this viewpoint. We will look first at the composition and structure of the atmosphere and its role in the global exchange of energy, the moisture balance and wind systems. The key to atmospheric processes is the radiant energy which the earth and its atmosphere receive from the sun. In order to study the receipt of this energy we need to begin by considering the nature of the atmosphere — its composition and basic properties.

A Composition of the atmosphere

1 Total atmosphere

Air is a mechanical mixture of gases, not a chemical compound. Table 1.1, illustrating the average composition of dry air, shows that four gases — nitrogen, oxygen, argon and carbon dioxide — account for 99.98% of the air by volume. Moreover, rocket observations show that these gases are mixed in remarkably constant proportions up to about 80 km (50 miles).

In addition to these gases, water vapour, which is much more variable in its occurrence in time and space, is a vital atmospheric constituent. This will be discussed more fully below. There are also significant quantities of *aerosols* in the atmosphere. These are suspended particles of sea salt, dust (particularly silicates), organic matter and smoke. They come from both natural and man-made sources.

Having made these generalizations about the atmosphere, we now need to examine the variations which occur in composition with height, latitude and time.

2 Variations with height

The light gases (hydrogen and helium especially) might be expected to become more abundant in the upper atmosphere, but large-scale turbulent mixing of the atmosphere prevents such diffusive separation even at heights of many tens of kilometres above the surface. The height variations which do occur are related to the source-locations of the two major non-permanent gases — water vapour and ozone. Since both absorb some solar and terrestrial radiation the heat budget and vertical temperature structure of the atmosphere are considerably affected by the distribution of these two gases (see ch. 1, D.2 and H).

Water vapour comprises up to 4% of the atmosphere by volume (about 3% by weight) near the surface, but is almost absent above 10 to 12 km. It is supplied to the atmosphere by evaporation from surface water or by transpiration from plants and is transferred upwards by atmospheric tur-

Table 1.1 Average composition of the dry atmosphere below 25 km

Component	Symbol	Volume % (dry air)	Molecular weight
Nitrogen	N ₂	78.08	28.02
Oxygen	O ₂	20.94	32.00
* Argon	Ar	0.93	39.88
Carbon dioxide	CO ₂	0.03 (very variable)	44.00
‡ Neon	Ne	0.0018	20.18
*‡ Helium	He	0.0005	4.00
† Ozone	O ₃	0.00006	48.00
Hydrogen	H	0.00005	2.02
Krypton	Kr	Trace	
‡ Xenon	Xe	Trace	
Methane	Me	Trace	

* Decay products of potassium and uranium.

† Recombination of oxygen.

‡ Inert gases.

bulence. Turbulence is most effective below about 10 km (see ch. 1, H.1) and as the maximum possible water vapour density of cold air is anyway very low (see ch. 1, B.2), there is little water vapour in the upper layers of the atmosphere.

Ozone (O₃) is concentrated mainly between 15 to 35 km. The upper layers of the atmosphere are irradiated by ultraviolet radiation from the sun which causes the break-up of oxygen molecules in the layer between about 80 to 100 km (i.e. O₂ → O + O). These separated atoms (O + O) may then individually combine with other oxygen molecules to create ozone.



where M represents the energy and momentum balance provided by collision with a third atom or molecule. Such three-body collisions are rare at 80 to 100 km because of the very low density of the atmosphere, while below about 35 km most of the incoming ultraviolet radiation has already been absorbed at higher levels. Therefore ozone is mainly formed between 30 and 60 km where collisions between O and O₂ are more likely. Ozone itself is unstable it may be destroyed either by collisions with monatomic oxygen to re-create oxygen (i.e. O₃ + O → O₂ + O₂) or by the action of radiation on it.

26 Atmosphere, weather and climate

The constant metamorphosis of oxygen to ozone and from ozone back to oxygen by photochemical processes maintains an approximate equilibrium above about 40 km, but the ozone mixing ratio is a maximum at about 35 km, whereas maximum ozone density occurs lower down between 20 and 25 km.¹ This is the result of some circulation mechanism transporting ozone downwards to levels where its destruction is less likely, allowing an accumulation of the gas to occur. Even so it is essential to realize that, despite the importance of the ozone layer, if the atmosphere were compressed to sea-level (at normal sea-level temperature and pressure) ozone would contribute only about 3 mm to the total atmospheric thickness of 8 km (fig. 1.1).

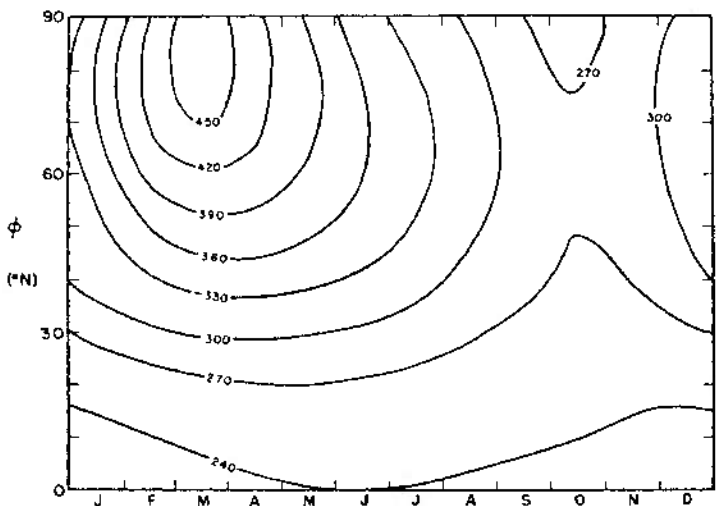


Fig. 1.1. The monthly variation of total atmospheric ozone by latitude (ϕ) in the northern hemisphere. The units are 10^{-3} cm of ozone (at standard atmospheric temperature and pressure) (from Godson 1960).

Aerosols enter the atmosphere by man-made pollution and by agricultural practices as well as through forest fires, sea spray, volcanic activity and wind-raised dust. Large particles rapidly sink back to the surface or are washed out by rain after a few days, but fine particles may reside in the stratosphere above the level of weather processes for 1–3 years.

¹ Mixing ratio = mass of ozone per unit mass of dry air. Density = mass per unit volume.

3 Variations with latitude and season

Variations of atmospheric composition with latitude and season are particularly important in the case of water vapour and ozone.

Ozone content is low over the equator and high over latitudes north of 50°N, especially in spring (fig. 1.1). If the distribution were solely the result of photochemical processes the maximum would occur in June near the equator and the anomalous pattern must be due to a poleward transport of ozone. The movement is apparently from higher levels (30–40 km) in low latitudes towards lower levels (20–25 km) in high latitudes during winter months. Here the ozone is stored during the *polar night* giving rise to an ozone-rich layer in early spring. The type of circulation responsible for this transfer is not yet known with certainty, although it does not seem to be a simple direct one. In the southern hemisphere there is a similar distribution pattern to that of fig. 1.1 except that poleward of 55°S the maximum is later and less pronounced than in the northern hemisphere.

The water-vapour content of the atmosphere is closely related to air temperature (see chs. 1, B.2, 2, A and B) and is therefore greatest in summer and in low latitudes. There are, however, obvious exceptions to this generalization, such as the tropical desert areas of the world.

The carbon dioxide content of the air (averaging about 315 parts per million) has a large seasonal range in higher latitudes in the northern hemisphere. At 50°N the concentration ranges from 310 ppm in late summer to 318 ppm in spring. The low summer values are related to the assimilation of CO₂ by the cold polar seas. Over the year a small net transfer of CO₂ from low to high latitudes takes place to maintain an equilibrium content in the air.

4 Variations with time

The quantities of carbon dioxide, ozone and particles in the atmosphere may be subject to variations over a long time-period and these are of special significance because of their possible effect on the radiation budget.

Carbon dioxide (CO₂) enters the atmosphere mainly by the action of living organisms on land and in the ocean. The decay of organic elements in the soil and the burning of fossil fuels are additional minor sources (fig. 1.2). It is obvious that if this production were not countered in some way the total quantity of carbon would steadily increase. A balance, or dynamic equilibrium, is maintained primarily by photosynthesis which removes approximately 3% of the world's total carbon dioxide annually.

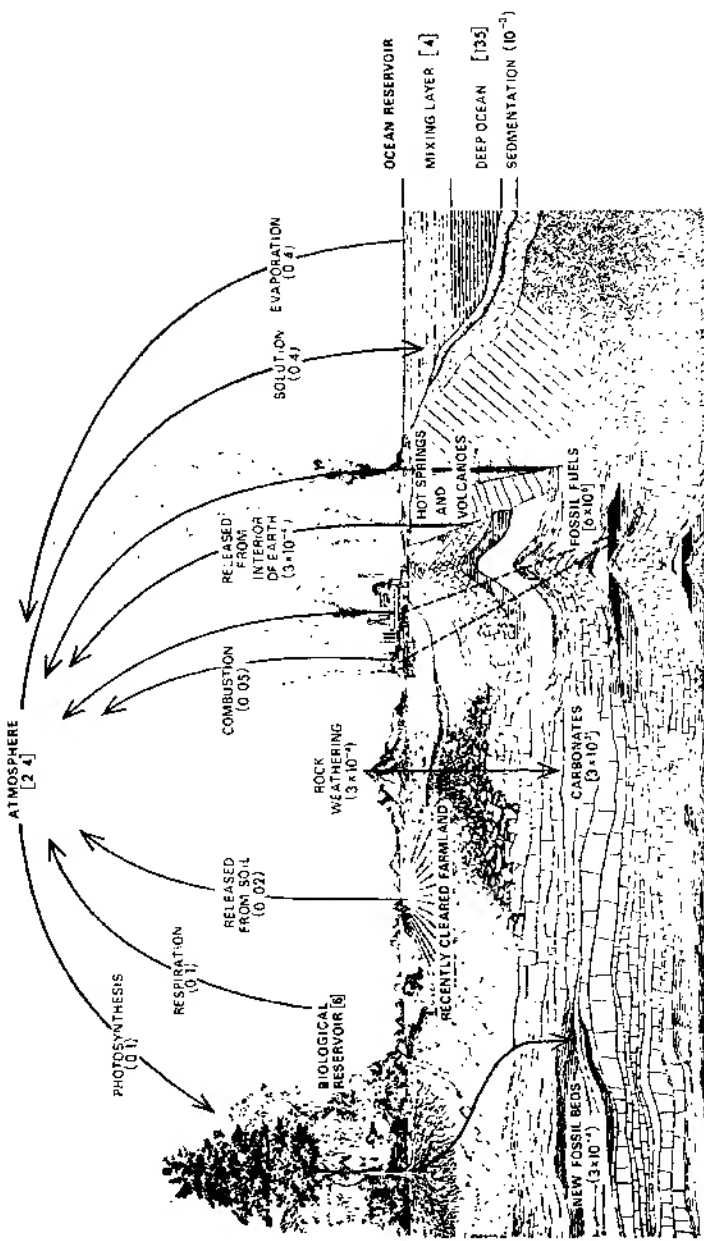


Fig. 1.2. The balance of carbon dioxide in the atmosphere. The numbers in parenthesis indicate CO₂ exchanges (10^{18} g yr $^{-1}$) and those in square brackets storage of CO₂ (10^{18} g) (partly from Plass 1959).

In the oceans the carbon dioxide ultimately goes to produce carbonate of lime, partly in the form of shells and the skeletons of marine creatures. On land the dead matter becomes humus which may subsequently form a fossil fuel. These transfers within the oceans and lithosphere involve very long time scales compared with exchanges involving the atmosphere. As fig. 1.2 showed, the exchanges between the atmosphere and the other reservoirs are more or less balanced.

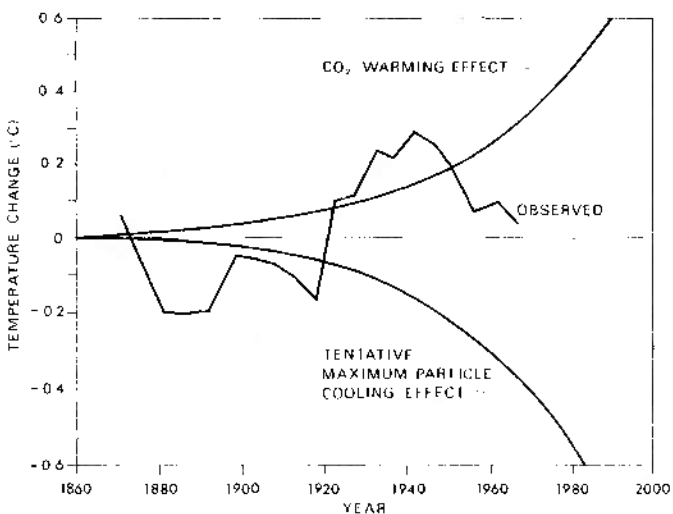


Fig. 1.3. Observed trends in mean temperatures in the northern hemisphere, 1860–1970. The upper smooth curve represents the assumed warming contribution provided by the increase of carbon dioxide, and the lower smooth curve the probable maximum cooling contribution due to increases in the number of atmospheric particles (*after Manabe and Wetherald, and Rasool and Schneider. From Mitchell 1972*).

Yet this balance is not an absolute one, for between 1870 and 1970 the total quantity of atmospheric CO_2 is estimated to have increased by 11% (from 294 to 321 ppm) due to the burning of fossil fuels (fig. 1.3). The actual use of fossil fuels should have produced an increase of about 20% but apparently the excess is taken up by the land biosphere and the oceans.

Carbon dioxide has a significant impact on global temperature by its absorption and re-emission of radiation from the earth and atmosphere

30 Atmosphere, weather and climate

(see fig. 1.6 and ch. 1.E). Calculations suggest that the increase from 320 to 370 ppm expected by AD 2000 could raise the mean air temperature near the surface by 0.5°C (in the absence of other factors).

Changes in particle concentrations with time may be irregular, as with volcanic dust production, or they may be progressive as in the case of man-made particles. At present the man-made contribution (particularly sulphates and soil particles) accounts for about 30% of the total and this figure could double by AD 2000. The overall effect on the lower atmosphere is thought to be one of cooling, such that any warming due to the carbon dioxide increase will tend to be offset until about AD 2000 (fig. 1.3).

Variations in stratospheric ozone may occur as a result of fluctuations in solar ultraviolet radiation. This has been proposed as a mechanism for climatic change (see ch. 8.C), since ozone absorbs solar and terrestrial radiation, but the hypothesis is largely speculative at present.

B Mass of the atmosphere

It is now necessary to examine some of the mechanical laws which the atmospheric gases obey. Two simple laws specify the main factors governing changes in pressure. The first, Boyle's Law, states that, at a constant temperature, the volume (V) of a mass of gas varies inversely as its pressure (P), i.e.

$$P = \frac{k_1}{V}$$

(k_1 is a constant); and the second, Charles's Law, that, at a constant pressure, volume varies directly with absolute temperature (T , measured in °K¹), i.e.

$$V = k_2 T$$

These laws imply that the three qualities of pressure, temperature and volume are completely interdependent, such that any change in one of them will cause a compensating change to occur in one, or both, of the remainder. The gas laws may be combined to give the following relationship:

$$PV = RmT$$

¹ °K = degrees Kelvin (or Absolute). The degree symbol is now customarily omitted.

°C = degrees Celsius

°C = °K - 273

Conversions for °C and °F are given in app. 2.

where m = mass of air

R = a gas constant for dry air.

If m and T are held fixed, we obtain Boyle's law; if m and P are held fixed, we obtain Charles's law. Since it is convenient to use density, ρ (= mass/volume) rather than volume when studying the atmosphere, we can rewrite the equation in the form known as the equation of state

$$P = R\rho T$$

1 Total pressure

Air is highly compressible, such that its lower layers are much more dense than those above. Fifty per cent of the total mass of air is found below 5 km (fig. 1.4) and the average density decreases from about 1.2 kg m^{-3} at the surface to 0.7 kg m^{-3} at 5000 m (approximately 16,000 ft) close to the extreme limit of human habitation.

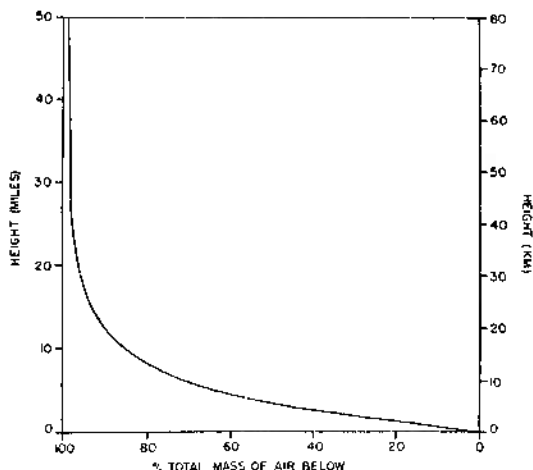


Fig. 1.4. The percentage of the total mass of the atmosphere lying below elevations up to 80 km (50 miles). This illustrates the shallow character of the earth's atmosphere.

Pressure is measured as a force per unit area. The units used by meteorologists are called millibars (mb), 1 mb being equal to a force of 100 newtons acting on 1 m^2 .¹ Pressure readings are made with a mercury

¹ See app. 4.

32 Atmosphere, weather and climate

barometer which in effect measures the weight of the column of mercury that the atmosphere is able to support in a vertical glass tube. The closed, upper end of the tube has a vacuum space and its open, lower end is immersed in a cistern of mercury. By exerting pressure downwards on the surface of mercury in the cistern, the atmosphere is able to support a mercury column in the tube of about 762 mm (30 in or approximately 1016 mb). However, in order to compare the pressure at different geographical locations a further factor must be taken into account. A correction has to be made to mercury barometer readings for variations in pressure attributable to differences in gravity, which at sea-level varies from 9.78 m sec^{-2} at the equator to 9.83 m sec^{-2} at the poles. Pressure readings are referred to the standard value of 9.81 m sec^{-2} for 45° latitude. Mercury barometer readings must also be standardized to allow for the thermal expansion of mercury. The adopted standard temperature is 0°C (32°F).

Atmospheric pressure depending as it does on the weight of the overlying atmosphere, decreases logarithmically with height. Near the surface the rate of decrease of pressure with height is about 1 mb per 10 m. With increasing height, however, the drop in air density causes a decrease in this rate. The temperature of the air can affect this rate of pressure decrease, which is greater for cold dense air (see ch. 3, C.1), although the relationship between pressure and height is so significant that meteorologists often express elevations in millibars, such that 1000 mb represents sea level, 500 mb about 5500 m and 300 mb about 9000 m. A conversion nomogram for an idealized (standard) atmosphere is given in app. 2. Mean sea-level pressure is 1013.25 mb (equivalent to 14.7 lb/in^2). On average, nitrogen contributes about 760 mb, oxygen 240 mb and water vapour 10 mb. In other words, each gas exerts a partial pressure independent of the others.

2 Vapour pressure

At any given temperature there is a limit to the density of water vapour in the air, with a consequent upper limit to the vapour pressure. This is termed the *saturation vapour pressure* (e_s) and fig. 1.5 illustrates how it increases with temperature, reaching a maximum of 1013 mb (1 atmosphere) at boiling point. Attempts to introduce more vapour into the air when the vapour pressure is at saturation produce condensation of an equivalent amount of vapour. Figure 1.5 shows that whereas the saturation vapour pressure has a single value at any temperature above freezing point, below 0°C the saturation vapour pressure above an ice surface is lower than that above a super-cooled water surface. The significance of this will be discussed in ch. 2, G.1.

Vapour pressure (e) varies with latitude and season from about 0.2 mb over northern Siberia in January to over 30 mb in the tropics in July, but this is not reflected in the pattern of surface pressure. Pressure decreases at the surface when some of the overlying air is displaced horizontally,

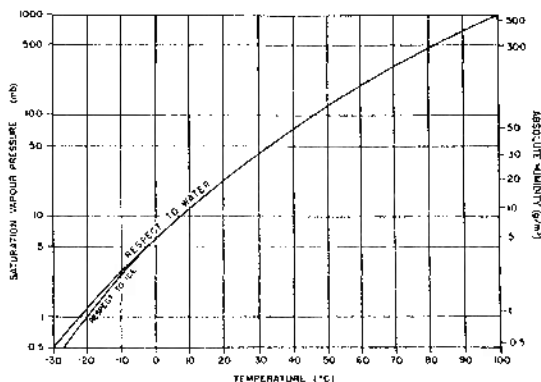


Fig. 1.5. Plot (semi-logarithmic) of the saturation vapour pressure as a function of temperature (i.e. the dew-point curve). Below 0°C the atmospheric saturation vapour pressure is less with respect to an ice surface than with respect to a water drop. Thus, condensation may take place on an ice crystal at lower air humidity than is necessary for the growth of water drops.

and in fact the air in high-pressure areas is generally dry owing to dynamic factors, particularly vertical air motion (see ch. 3, C.5), while air in low-pressure areas is usually moist.

C Solar radiation

The prime source of the energy injected into our atmosphere is the sun, which is continually shedding part of its mass by radiating waves of electromagnetic energy and high-speed particles into space. This constant emission, termed *insolation*, is important because it represents in the long run almost all the energy available to the earth (except for a small amount emanating from the radioactive decay of earth minerals). The amount of insolation received by the earth, assuming for the moment that there is no interference from the atmosphere, is affected by four factors.

34 Atmosphere, weather and climate

1 Solar output

Of the total solar energy sent out into space the earth intercepts only some two thousand millionth, equivalent to a power of 1.8×10^{14} kW. This is because the energy received is inversely proportional to the square of the solar distance (150×10^6 km). The energy received on a surface perpendicular to the solar beam (for mean solar distance) is termed the *solar constant*. This has been variously estimated to be between 1.92–2.02 cal $\text{cm}^{-2} \text{ min}^{-1}$. The most recent measurements indicate a value of 1.95 cal $\text{cm}^{-2} \text{ min}^{-1}$ or 1.36 kW m^{-2} .¹

The small proportion of solar energy available to the earth is reflected in the difference between the surface temperatures of the sun and earth; the temperature at the surface of the former is believed to be about 6000°K, whereas the mean temperature of the earth's atmosphere is only about 250°K (i.e. –23°C) and that of the earth's surface is only 283°K (10°C or 50°F). Figure 1.6 shows the range of wavelengths (mostly short) of the emitted sun's energy, together with the longer-wave re-radiation by the earth and its atmosphere. These curves are constructed on the assumption that the sun and the earth behave as *black bodies*. Such bodies absorb all energy falling on them and, in turn, radiate energy at a rate directly proportional to the fourth power of their absolute temperature (i.e. measured in °K). The radiant energy of a black body is emitted at a rate, F ,

$$F = \sigma T^4$$

where σ = the Stefan–Boltzmann constant; this is known as Stefan's Law. At a given temperature the emission in each wavelength from a black body is the maximum possible. Most solids and liquids behave like black bodies, whereas gases do not. The wavelength of maximum emission (λ_{\max}) varies inversely with the absolute temperature of the radiating body:

$$\lambda_{\max} = \frac{2897}{T} \times 10^{-6} \text{ m} \quad (\text{Wien's Law}).$$

Thus solar radiation is very intense and is mainly short wave between about 0.2 and 4.0 μm, with a peak in the middle part of the spectrum, whereas the much weaker terrestrial radiation has a peak intensity at about 10 μm and a range of about 4 to 100 μm (1 μm = 1 micron = 10^{-6} m).

¹ ‘Calorie’ refers throughout to the ‘small’ or gram-calorie. Another unit in common use is the ‘Langley’ (ly) ($ly \text{ min}^{-1} = 1 \text{ cal cm}^{-2} \text{ min}^{-1}$). A calorie is the heat required to raise the temperature of 1 gram of water from 14.5° to 15.5°C. The units of the international metric system (kW m⁻²) and Joules are given in app. 4. At the present time the data is most references are still in calories.

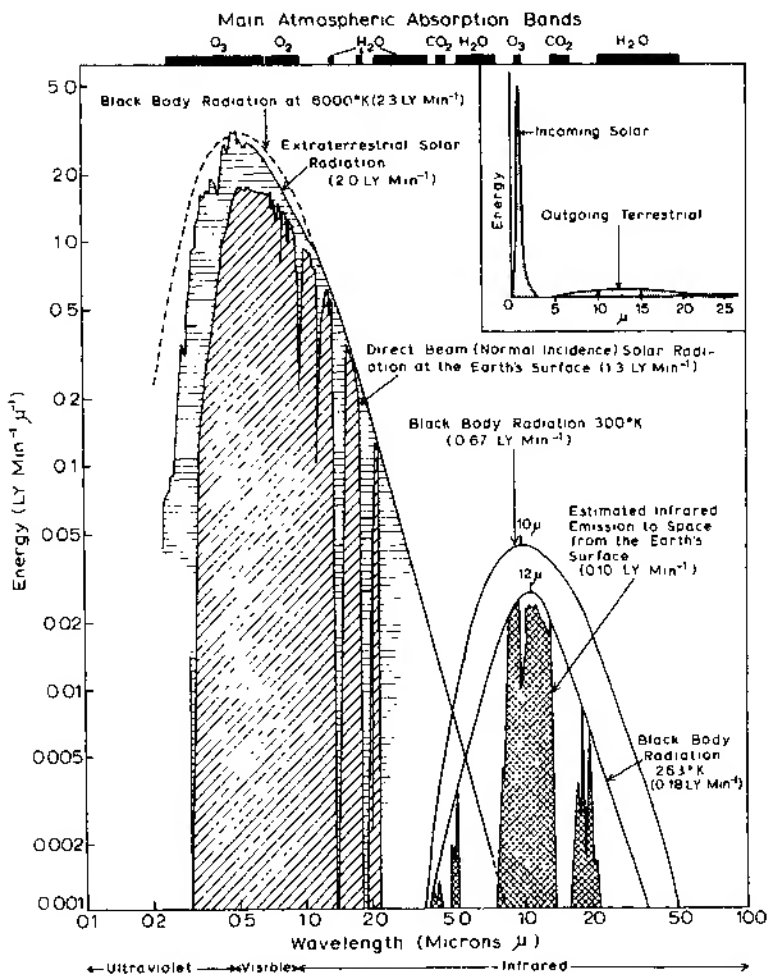


Fig. 1.6. Spectral distribution of solar and terrestrial radiation, plotted logarithmically, together with the main atmosphere absorption bands. The black body radiation at $6000^{\circ}K$ is that proportion of the flux which would be incident on the top of the atmosphere. The inset shows the same curves for incoming and outgoing radiation with the wavelength plotted arithmetically (mostly after Sellers 1963). (μ is now denoted as μm .)

36 Atmosphere, weather and climate

There have been suggestions that the solar constant undergoes small periodic variations of 1 to 2%, perhaps related to the sunspot cycle but, since determinations of the solar constant are subject to errors of similar magnitude, the reality of such fluctuations is still in doubt. Nevertheless, undoubted variations do occur within the ultraviolet band of the spectrum, up to twenty times more ultraviolet radiation may be emitted at certain wavelengths during a sunspot maximum than during a sunspot minimum. However, no clear link between the 11-year sunspot cycle and weather variations has yet been demonstrated, in spite of many attempts to discover such a relationship. In the long term, assuming that the earth behaves as a black body, a long-continued difference of 2% in the solar constant could change the effective mean temperature of the earth's surface by as much as 1.2°C (2.2°F), and a 10% change might alter this temperature by as much as 6°C (10.7°F). The drop in surface temperature often experienced on a sunny day when a cloud temporarily cuts off the direct solar radiation illustrates our reliance upon the sun's radiant energy.

2 Distance from the sun

The ever-changing distance of the earth from the sun produces more frequent variations in our receipt of solar energy. Owing to the eccentricity of the earth's orbit round the sun, the receipt of solar energy on a surface normal to the beam is 7% more on 3 January at the perihelion than on 4 July at the aphelion. In theory (that is, discounting the interposition of the atmosphere and the difference in degree of conductivity between large land and sea masses) this difference should produce an increase in the effective January world surface temperatures of about 4°C (7°F), over those of July. It should also make northern hemisphere winters warmer than those in the southern, and southern hemisphere summers warmer than those in the northern. In practice, atmospheric heat circulation and the effects of continentality substantially mask this global tendency and the actual seasonal contrast between the hemisphere is reversed. Figure 1.7 graphically illustrates the seasonal variations of energy receipt, with latitude. Actual amounts of insolation received on a horizontal surface outside the atmosphere are given in table 1.2. The intensity on a horizontal surface (I_h) is determined from

$$I_h = I_0 \sin d,$$

where I_0 = the solar constant and d = the angle between the surface and the solar beam.

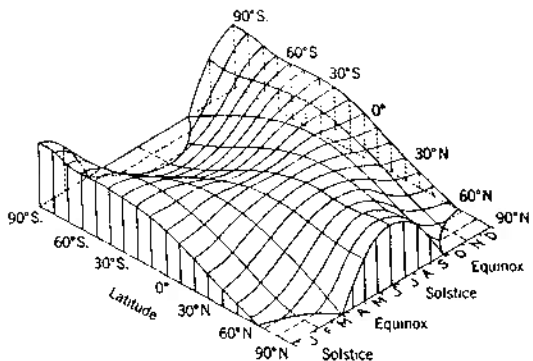


Fig. 1.7. The variations of insolation with latitude and season for the whole globe, assuming no atmosphere. This assumption explains the abnormally high amounts of insolation received at the poles in summer, when daylight lasts for 24 hours each day (after W. M. Davis. From Strahler 1965).

Table 1.2 Insolation on a horizontal surface outside the atmosphere: units, $\text{cal cm}^{-2} \text{ day}^{-1}$ (after K. Ya. Kondratiev)

Date	90°N	70	50	30	0	30	50	70	90°S
Dec 22	0	0	181	480	869	1073	1089	1114	1185
Feb 4	0	25	298	586	905	1003	937	809	834
Mar 21	0	316	593	799	923	799	593	316	0
May 6	796	722	894	958	863	560	285	24	0
June 22	1110	1043	1020	1005	814	450	170	0	0

3 Altitude of the sun

The altitude of the sun (i.e. the angle between its rays and a tangent to the earth's surface at the point of observation) also affects the amount of insolation received at the surface of the earth. The greater the sun's altitude the more concentrated is the radiation intensity per unit area at the earth's surface. There are, in addition, important variations with solar altitude of the proportion of radiation reflected by the surface, particularly in the

38 Atmosphere, weather and climate

case of a water surface (see ch. 1, D.5). The principal factors which determine the sun's altitude are, of course, the latitude of the site, the time of day and the season.

4 Length of day

The length of daylight also affects the amount of insolation which is received. Obviously the longer the time during which the sun shines the greater is the quantity of radiation which a given portion of the earth will be able to receive.

The combination of all these factors produces the pattern of receipt of solar energy at the top of the atmosphere shown by fig. 1.7. The polar regions receive their maximum amounts of insolation during their summer solstices, which is the period of continuous day. The amount of insolation received during the December solstice in the southern hemisphere is greater than that received by the northern hemisphere during the June solstice, due to the previously mentioned elliptical path of the earth round the sun. The equator has two insolation maxima at the equinoxes and two minima at the solstices, due to the apparent passage of the sun during its double annual movement between the northern and southern hemispheres.

D Surface receipt of solar radiation and its effects

1 Energy transfer within the earth-atmosphere system

So far we have described the distribution of insolation as if all of it were available at the earth's surface. This is of course an unreal view because of the effect of the atmosphere on energy transfer. Heat energy can be transferred by the three following mechanisms:

(i) Radiation. Electromagnetic waves can transfer energy (both heat and light) between two bodies without the necessary aid of an intervening material medium. This is so with solar energy through space, whereas the earth's atmosphere only allows the passage of radiation at certain wavelengths and restricts that at others.

(ii) Conduction. Under this mechanism the heat passes through a substance from point to point by means of the transfer of adjacent molecular motions. Since air is a poor conductor this type of heat transfer can be virtually neglected in the atmosphere, but it is important in the ground.

(iii) Convection. This occurs in fluids (including gases) which are able to circulate internally and distribute heated parts of the mass. The low viscosity of air and its consequent ease of motion makes this the chief method of atmospheric heat transfer. It should be noted that *forced con-*

vection (mechanical turbulence) occurs due to the development of eddies as air flows over uneven surfaces, even when there is no surface heating to set up *free* (thermal) convection.

Convection transfers energy in two forms. The first is the *sensible heat* content of the air (called enthalpy by physicists) which is transferred directly by the rising and mixing of warmed air. It is defined as $c_p T$ where T is the temperature and c_p is the specific heat at constant pressure (the heat absorbed by unit mass for unit temperature increase). Sensible heat is also transferred by conduction. The second form of energy transfer by convection is indirect, involving *latent heat*. Whenever water is converted into water vapour by evaporation (or boiling) heat is required. This is referred to as the latent heat of vaporization (L). At 0°C, L is 597 calories per gram of water ($2.50 \times 10^6 \text{ J kg}^{-1}$, where J = Joule; see app. 4). More generally,

$$L (\text{cal g}^{-1}) \approx (597 - 0.56 T)$$

where T is in °C. When water condenses in the atmosphere (see ch. 2C) the same amount of latent heat is given off as is used for evaporation *at the same temperature*. Similarly, for melting ice at 0°C, the latent heat of melting is required which is 80 cal g⁻¹. If ice evaporates, without melting, the latent heat of this sublimation process is 676 cal g⁻¹ at 0°C (i.e., the sum of the latent heats of melting and vaporization). In all of these phase changes of water there is any energy transfer. We shall return to other aspects of these processes in ch. 2.

2 Effect of the atmosphere

Solar radiation is virtually all in the short wave-length range, less than 4 μm (fig. 1.6). About 18% of the incoming energy is absorbed directly by ozone and water vapour. Ozone absorbs all ultraviolet radiation below 0.29 μm (2900 Å) and water vapour absorbs to a lesser extent in several narrow bands between about 0.9 μm to 2.1 μm (see fig. 1.6). About 30% is immediately reflected back into space from the atmosphere, clouds and the earth's surface, leaving approximately 70% to heat the earth and its atmosphere. Of this, the greater part eventually heats the atmosphere, but much of this heat is received secondhand by the atmosphere via the earth's surface. The ultimate retention of this energy by the atmosphere is of prime importance, because if it did not occur the average temperature of the earth's surface would fall by some 40°C (approximately 70°F), making most life obviously impossible. The surface absorbs 45% of the incoming energy available at the top of the atmosphere and re-radiates it

40 Atmosphere, weather and climate

outwards as long (infrared) waves of greater than $3\text{ }\mu\text{m}$ (fig. 1.6). Much of this re-radiated long-wave energy can be absorbed by the water vapour, carbon dioxide and ozone in the atmosphere, the rest escaping through atmospheric windows back into outer space. Figure 1.8 illustrates the relative roles of the atmosphere, clouds and the earth's surface in reflecting and absorbing solar radiation at different latitudes. (A more complete analysis of the total heat budget of the earth-atmosphere system is given in ch. 1, F.)

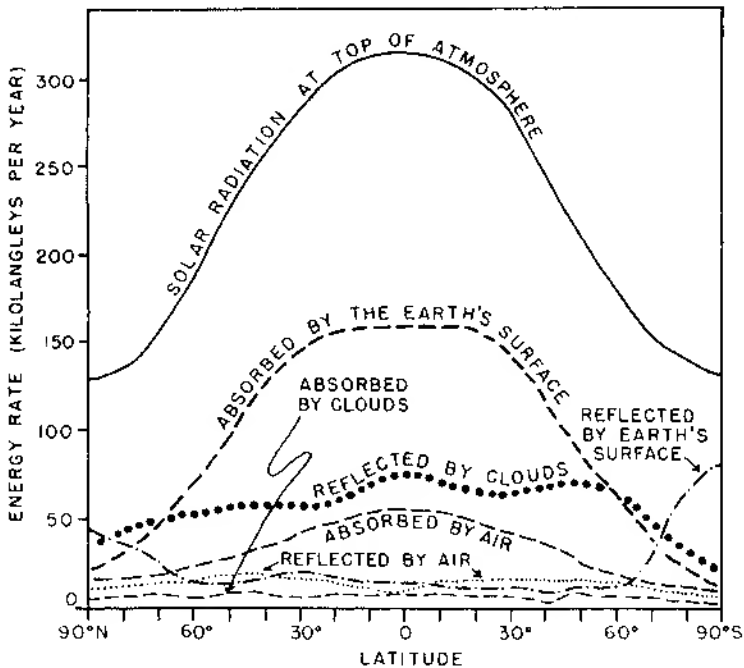


Fig. 1.8. The average annual latitudinal disposition of solar radiation (in kilolangleys; a kilolangley = 1000 cal cm^{-2}). Of 100% radiation entering the top of the atmosphere, 23% is reflected back to space by clouds, 4% by air (plus dust and water vapour), and 4% by the earth's surface. 3% is absorbed by clouds, 21% by the air, and 45% by the earth (from Sellers 1965).

3 Effect of cloud cover

Cloud cover can, if it is thick and complete enough, form a significant barrier to the penetration of insolation. How much insolation is actually reflected depends on the amount of cloud cover and thickness (fig. 1.9).

The proportion of incident radiation that is reflected is termed the albedo or reflection coefficient. Cloud type also affects the albedo. Aircraft measurements show that the albedo of a complete overcast ranges from 44 to 50% for cirrostratus to 55 to 80% for stratocumulus. Average albedos as determined by satellites are summarized in table 1.3.

Table 1.3 Average albedos (from World Meteorological Organization, 1973)

	%
Cumulonimbus: large and thick	92
Cirrostratus: thick and lower clouds and precipitation	74
Stratus: thick (approx. 500 m), over ocean	64
Sand: White Sands, New Mexico	60
Snow: 3-7 days old, covering mountains above timber	59
Stratus: thin, over ocean	42
Cirrus: alone, over land	36
Cumulus: fair-weather, over land (>80% cover)	29
Sand: surface of valleys, plains and slopes	27
Sand and brushwood	17
Coniferous forest	12
Ocean	7-9

The total (or global) solar radiation (direct, Q , and diffuse, q) received at the surface on cloudy days is

$$Q + q = (Q + q)_0 [b + (1 - b)(1 - c)]$$

where $(Q + q)_0$ = global solar radiation for clear skies;

c = cloudiness (fraction of sky covered);

b = a coefficient depending on cloud type and thickness; and the depth of atmosphere through which the radiation must pass. For mean monthly values for the United States $b \approx 0.35$, so that

$$(Q + q) \approx (Q + q)_0 [1 - 0.65c].$$

The effect of a cloud cover also operates in reverse, since it serves to retain much of the heat that would otherwise be lost from the earth by radiation throughout the day and night. This largely negative role of clouds means that their presence appreciably lessens the daily temperature

42 Atmosphere, weather and climate

range by preventing high maxima by day and low minima by night. As well as interfering with the transmission of radiation, clouds act as temporary thermal reservoirs for they absorb a certain proportion of the energy which they intercept. The effect of this absorption of solar radiation is illustrated in figs. 1.8 and 1.9.

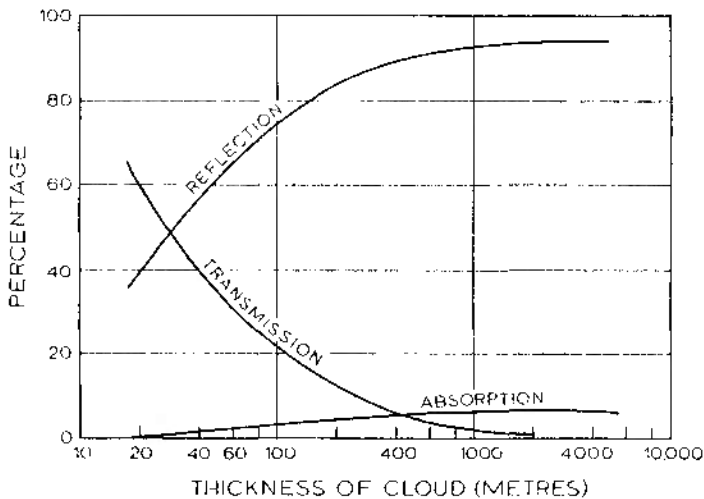


Fig. 1.9. Percentage of reflection, absorption and transmission of solar radiation by cloud layers of different thickness (*from Hewson and Longley 1944*).

4 Effect of latitude

As fig. 1.7 has already shown, different parts of the earth's surface receive different amounts of insolation. The time of the year is one factor controlling this, more insolation being received in summer than in winter because of the higher altitude of the sun and the longer days. Latitude is a very important control over insolation because the geographical situation of a region will determine both the duration of daylight and the distance travelled through the atmosphere by the oblique rays from the sun. However, actual calculations show the effect of the latter to be negligible in the Arctic, apparently due to the low vapour content of the air limiting the tropospheric absorption. Figure 1.10 shows that in the upper atmosphere over the north pole there is a marked maximum of insolation at the June solstice yet only about 30% is absorbed at the surface. This may

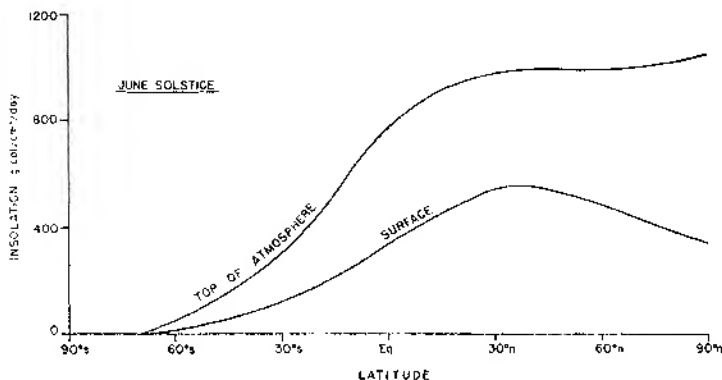


Fig. 1.10. The average receipt of insolation with latitude at the top of the atmosphere and at the earth's surface during the June solstice.

be compared with the global average of 45% of solar radiation being absorbed at the surface. The explanation lies in the high average cloudiness over the Arctic in summer and also in the high reflectivity of the snow and ice surfaces. This example illustrates the complexity of the radiation budget and the need to take into account the interaction of several factors.

A special feature of the latitudinal receipt of insolation is that the maximum temperatures experienced at the earth's surface do not occur at the equator, as one might expect, but at the tropics. A number of factors need to be taken into account. The apparent migration of the vertical sun is relatively rapid during its passage over the equator but its rate slows down as it reaches the tropics. Between 6°N and 6°S the sun's rays remain almost vertically overhead for only 30 days during each of the spring and autumn equinoxes, allowing little time for any large build-up of surface heat and high temperatures. On the other hand, between 17.5° and 23.5° latitude the sun's rays shine down almost vertically for 86 consecutive days during the period of the solstice. This longer sustained period, combined with the fact that the tropics experience longer days than at the equator, makes the maximum zones of heating occur nearer the tropics than the equator. In the northern hemisphere this poleward displacement of the zone of maximum heating is emphasized by the effect of *continentality* (see ch. 1, D.5), while low cloudiness associated with the subtropical high-pressure belts is an additional factor. The clear skies are particularly effective in allowing large annual receipts of solar radiation in these areas (fig. 1.11). The net result of these influences is shown in fig. 1.11 in terms

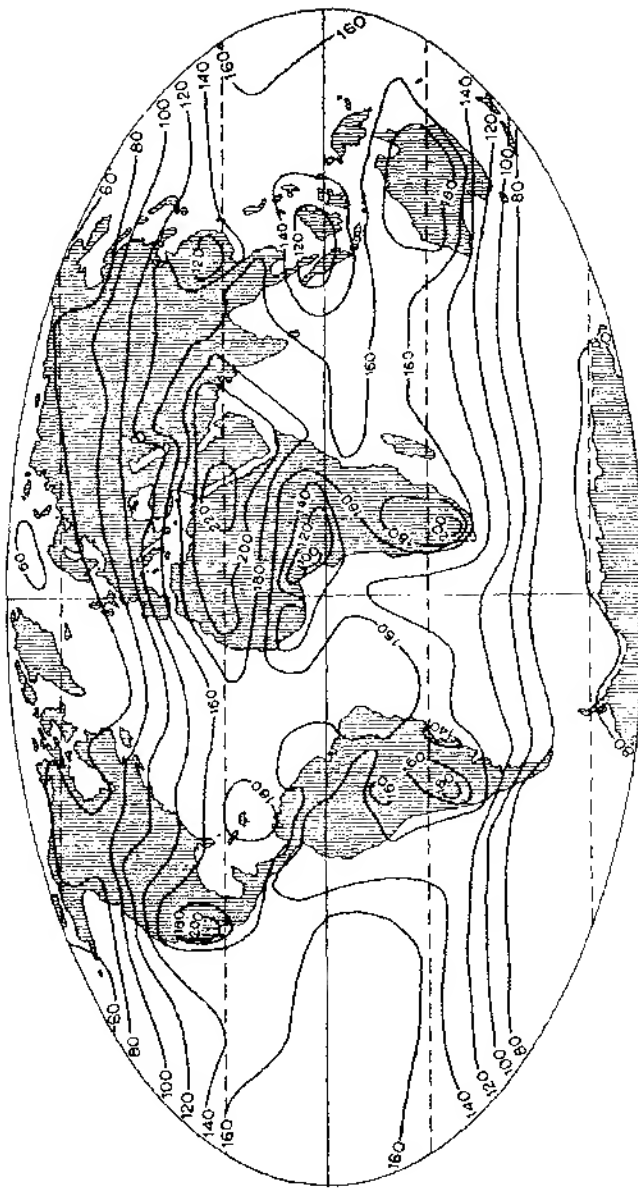


Fig. 1.11. The average annual solar radiation on a horizontal surface at ground level in kilolangleys per year (after Bud'ko. From Selters 1965). Maxima are found in the world's hot deserts, where as much as 80% of the solar radiation annually incident on the top of the unusually clear atmosphere reaches the ground.

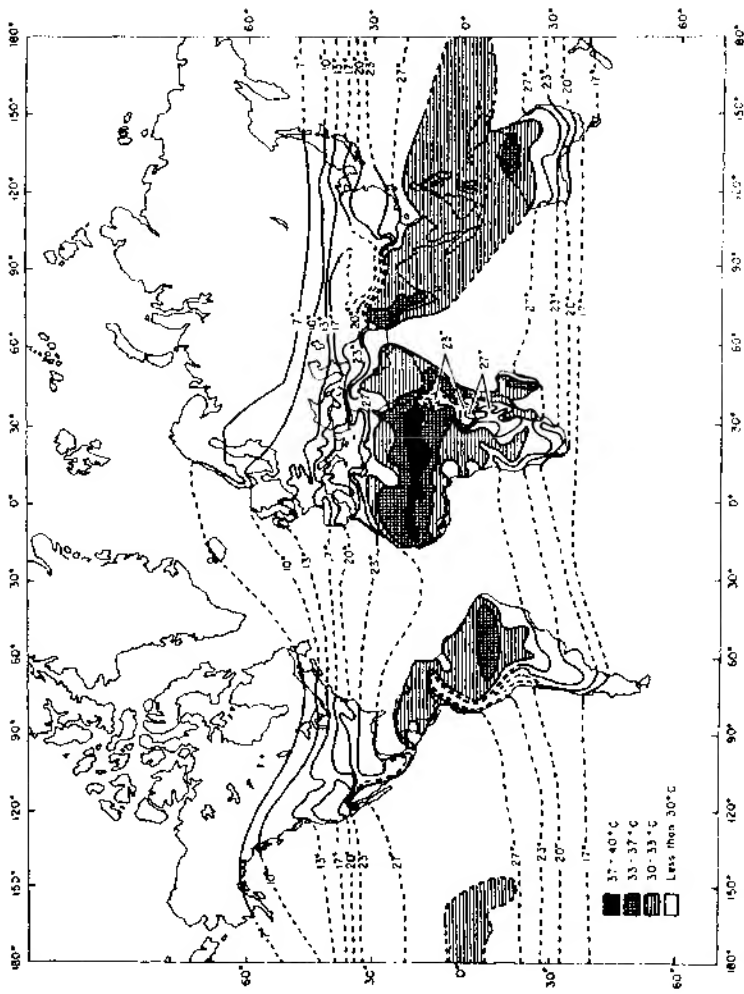
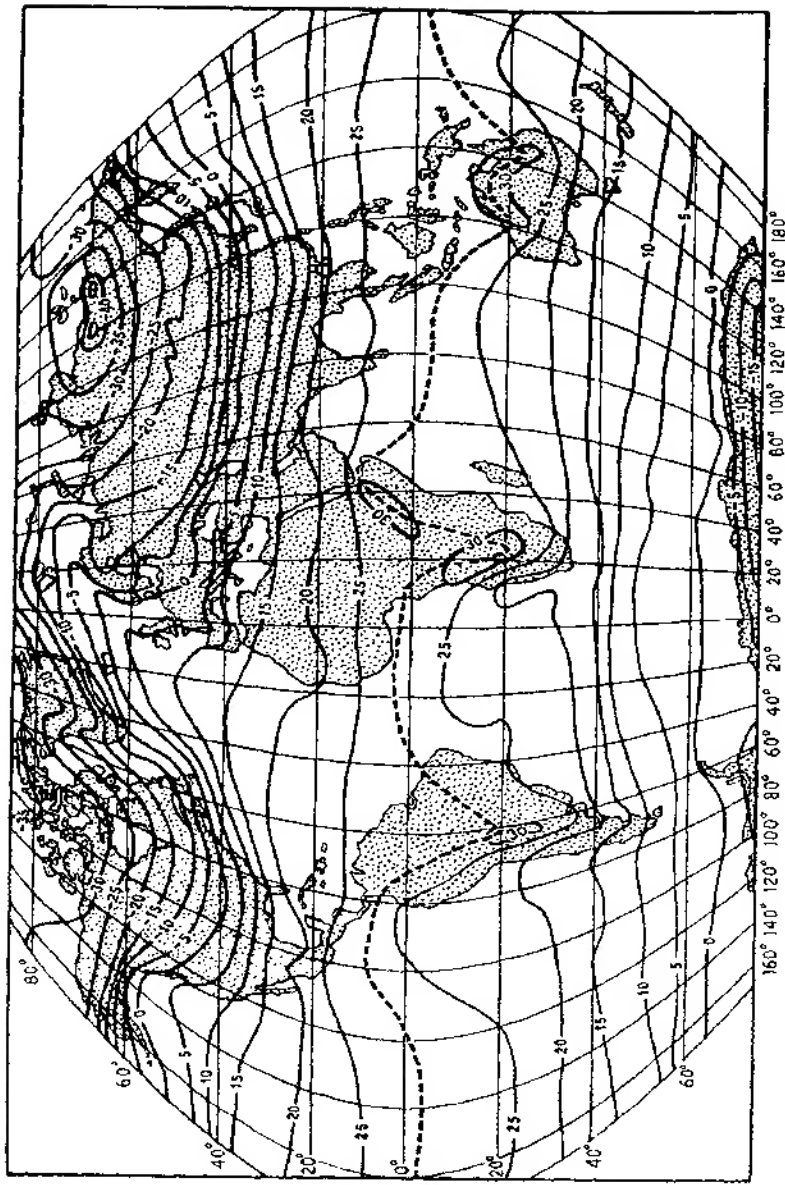


Fig. 1.12. Mean daily maximum shade air temperatures ($^{\circ}\text{C}$) (after Ransom 1963).



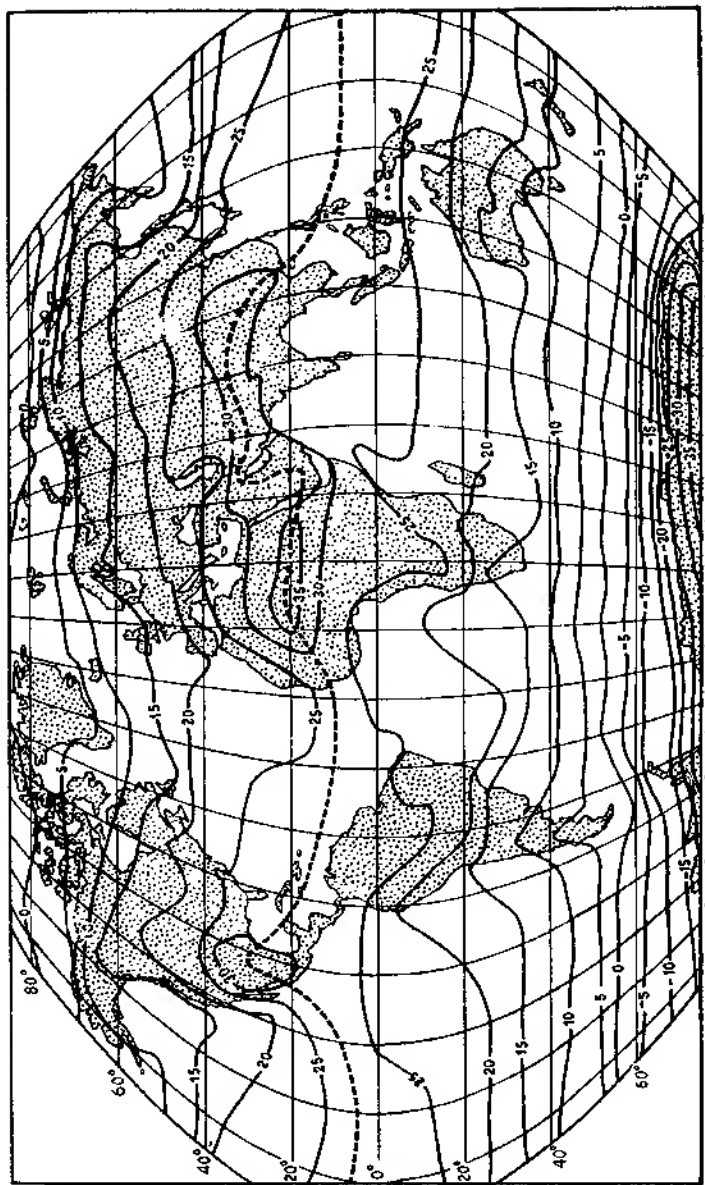


Fig. 1.1.3. Mean sea-level temperatures in January (above) and July (below) ($^{\circ}\text{C}$). The positions of the thermal equator are approximately shown by the dashed line.

of the average annual solar radiation on a horizontal surface at ground level, and by fig. 1.12 in terms of the average daily maximum shade temperatures. Over the continents the highest values occur at about 23°N and $10^{\circ}\text{--}15^{\circ}\text{S}$. In consequence the mean annual *thermal equator* (i.e. the zone of maximum temperature) is located at about 5°N . Nevertheless, the mean air temperatures, reduced to mean sea level, are very broadly related to latitude (fig. 1.13).

5 Effect of land and sea

Another important control on the effect of incoming solar radiation stems from the different ways in which land and sea are able to profit from it. Whereas water has a tendency to store the heat it receives, land, in contrast, quickly returns it to the atmosphere. There are several reasons for this.

A large proportion of insolation is reflected back into the atmosphere without heating the earth's surface at all. The proportion depends upon the type of surface. For land surfaces the albedo is generally between 8 and 40% of the incoming radiation. The figure for forests is about 9 to 18% according to the type of tree and density of foliage (see ch. 7, B), for grass approximately 25%, for cities 14 to 18%, and desert sand 30 to 60%. Fresh, flat snow may reflect as much as 85% of solar radiation,

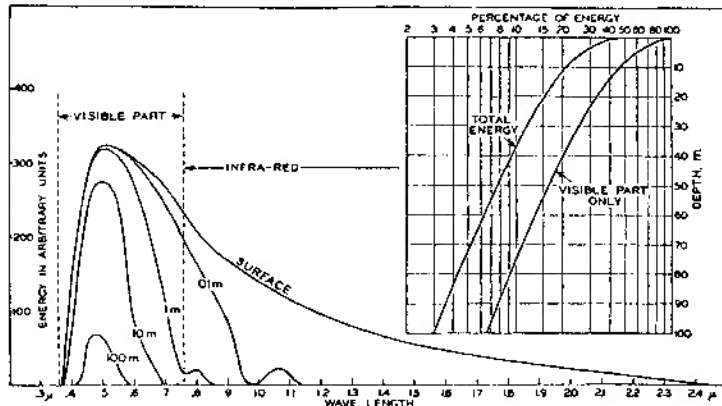


Fig. 1.14. Schematic representation of the energy spectrum of the sun's radiation (in arbitrary units) which penetrates the sea surface to depths of 0, 1, 10 and 100 m. This illustrates the absorption of infra-red radiation by water, and also shows the depths to which visible (light) radiation penetrates (from Sverdrup 1945).

whereas a sea surface reflects very little unless the angle of incidence of the sun's rays is small. The albedo for a calm water surface is only 2 to 3% for a solar elevation angle exceeding 60°, but is more than 50% when the angle is 15°.

The global solar radiation absorbed at the surface is determined from measurements of incident radiation and albedo (a). It may be expressed as

$$(Q + q)(100 - a)$$

where the albedo is a percentage. A snow surface will absorb only about 15% of the incident radiation, whereas for the sea the figure generally exceeds 90%. The ability of the sea to absorb the heat received also depends upon its transparency. As much as 20% of the radiation penetrates as far down as 9 m (30 ft). Figure 1.14 provides some indication of how much

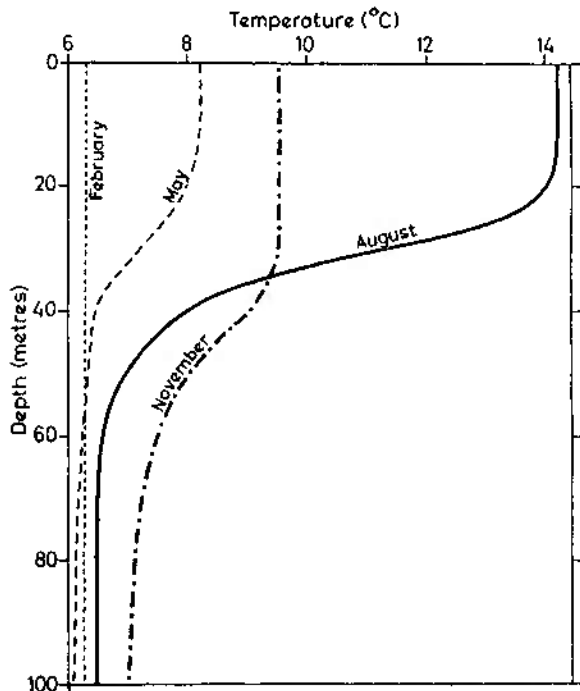


Fig. 1.15. Mean temperatures for the upper 100 m of the North Sea for February, May, August and November (from Lumb 1961) (Crown Copyright Reserved).

50 Atmosphere, weather and climate

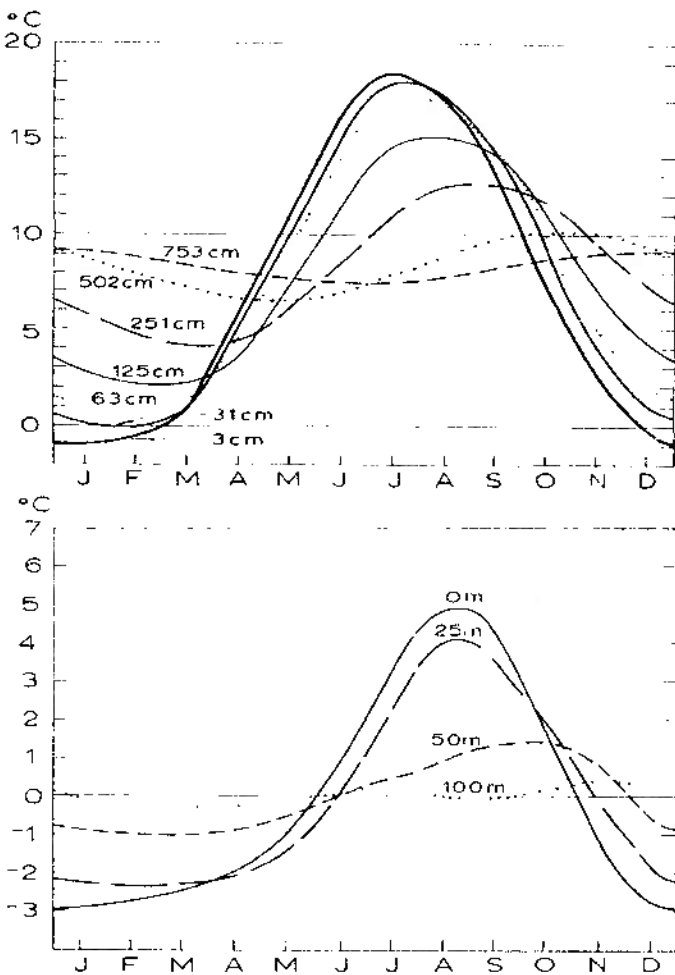


Fig. 1.16. Annual variation of temperature at different depths in soil at Kaliningrad (above) and in the water of the Bay Biscay (at approximately 47°N , 12°W) (below), illustrating the relatively deep penetration of solar energy into the oceans as distinct from that into land surfaces. The bottom figure shows the temperature deviations from the annual mean for each depth (*from Geiger 1965 and Sverdrup 1945*).

energy is absorbed by the sea at different depths. However, the heat absorbed by the sea is carried down to considerable depths by the turbulent mixing of water masses by the action of waves and currents. Figure 1.15, for example, illustrates the warming of the North Sea down to about 40 m in summer. In completely *still* water the annual heat penetration would only be apparent down to about 3–4 m.

A measure of the difference between the subsurfaces of land and sea is given in fig. 1.16, which shows ground temperatures at Kaliningrad (Königsberg) and sea temperature deviations from the annual mean at various depths in the Bay of Biscay. Heat transmission in the soil is carried out almost wholly by conduction and the degree of conductivity varies with the moisture content and porosity of each particular soil.

Air is an extremely poor conductor and for this reason a loose, sandy soil surface heats up rapidly by day, as the heat is not conducted away. Increased soil moisture tends to raise the conductivity by filling the soil pores, but too much moisture increases the soil's heat capacity, thereby reducing the temperature response. The relative depths over which the annual and diurnal temperature variations are effective in wet and dry soils are roughly as follows:

	<i>Diurnal variation</i>	<i>Annual variation</i>
Wet soil	0.5 m	9 m
Dry sand	0.2 m	3 m

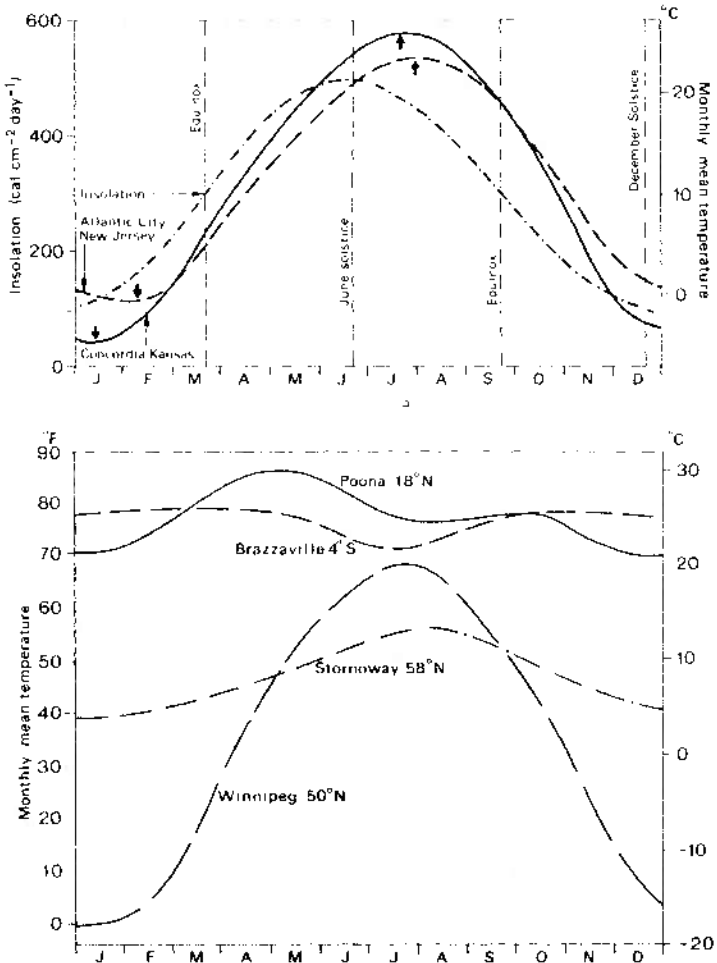
However, the *actual* temperature change is greater in dry soils. For example, the following values of diurnal temperature range have been observed during clear summer days at Sapporo, Japan:

	<i>Sand</i>	<i>Loam</i>	<i>Peat</i>	<i>Clay</i>
Surface	40°C	33°C	23°C	21°C
5 cm	20	19	14	14
15 cm	7	6	2	4

The different heating qualities of land and water are also partly accounted for by their different *specific heats*. The specific heat (*c*) of a sub-

52 Atmosphere, weather and climate

stance can be represented by the number of thermal units (calories) required to raise a unit mass (gram) of it through one degree (Celsius). The specific heat of water is much greater than for most other common substances, and water must absorb five times as much heat energy to raise its temperature by the same amount as a comparable mass of dry soil. Thus for dry sand $c = 0.2 \text{ cal g}^{-1} \text{ deg}^{-1}$ whereas for still water $c = 1.0 \text{ cal g}^{-1} \text{ deg}^{-1}$.



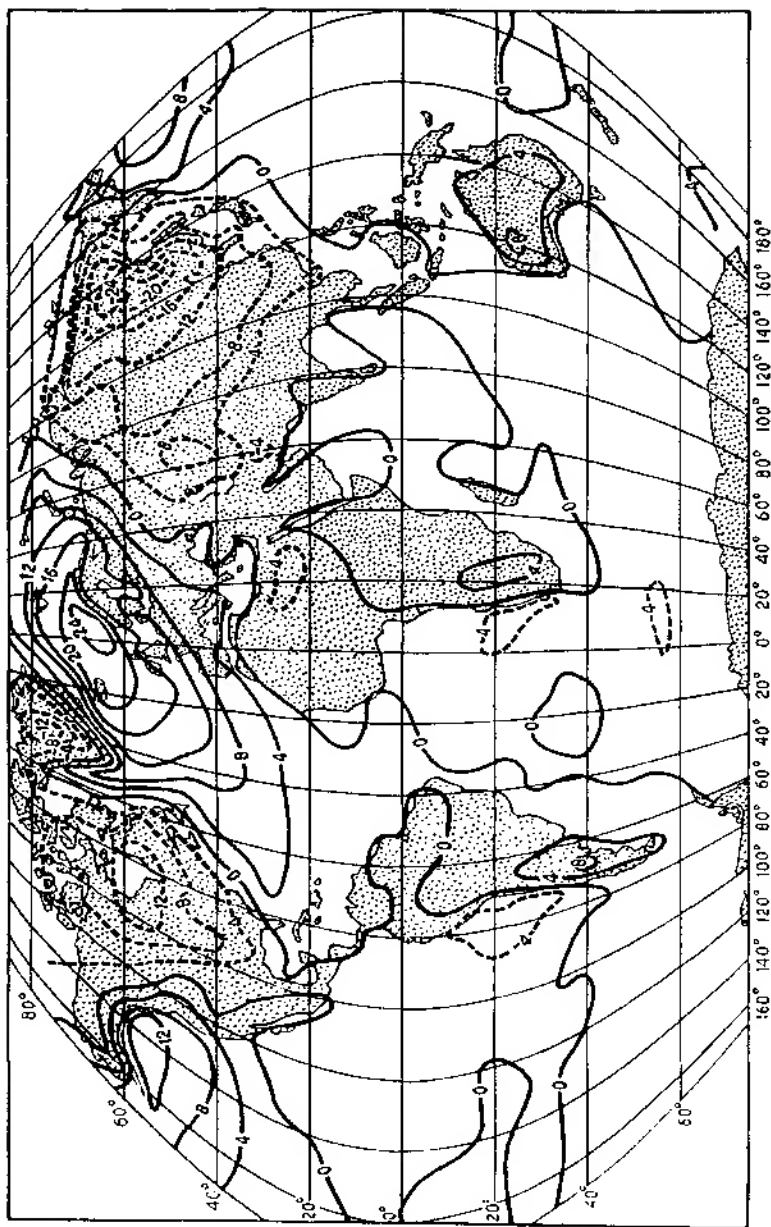
If unit volumes of water and soil are considered the heat capacity, ρc , of the water, where ρ = density, ($\rho c = 1.0 \text{ cal cm}^{-3} \text{ deg}^{-1}$) exceeds that of the sand approximately threefold ($\rho c = 0.3 \text{ cal cm}^{-3} \text{ deg}^{-1}$) if the sand is dry and twofold if it is wet. When this water is cooled the situation is reversed, for then a large quantity of heat is released. A metre-thick layer of sea water being cooled by as little as 0.1°C will release enough heat to raise the temperature of approximately a 30-m thick air layer by 10°C (18°F). In this way the oceans act as a very effective reservoir for much of the world's heat. Similarly evaporation of sea water causes a large heat expenditure because a great amount of energy is needed to evaporate even a small quantity of water (see ch. 2, A).

These differences between land and sea help to produce what is termed *continentality*. Continentality implies, firstly, that a land surface heats and cools much quicker than that of an ocean. Over the land the lag between maximum and minimum periods of insolation and the maximum and minimum surface temperatures is only 1 month, but over the ocean and at coastal stations the lag is as much as 2 months (fig. 1.17). Secondly, the annual and diurnal ranges of temperature are greater in continental than in coastal locations. Figure 1.17 illustrates the annual variation of temperature at Winnipeg and Stornoway, while fig. 1.22c shows the diurnal ranges experienced in continental and maritime areas. This is described more fully below. The third effect of continentality results from the global distribution of the land masses. The small sea area of the northern hemisphere causes the northern hemisphere summer to be warmer but its winters colder on the average than those of the southern hemisphere (summer, 22.4°C (72.3°F) versus 17.1°C (62.7°F); winter, 8.1°C (46.5°F) versus 9.7°C (49.5°F)). Heat storage in the oceans causes them to be warmer in winter and cooler in summer than land in the same latitude, although ocean currents give rise to some local departures from this rule. The distribution of temperature anomalies for the latitude in

Fig. 1.17. Mean annual temperature regimes in various climates and the relationships with solar radiation.

Above. Temperatures at maritime (Atlantic City) and continental (Concordia, Kansas) locations in the middle latitudes. A curve of representative insolation receipts is also given. Maximum and minimum points are indicated on the temperature curves, illustrating the respective time lags behind the insolation curve (*data from Trewartha. After Strahler 1951*).

Below. Mean annual temperature regimes for Poona (Monsoon), Brazzaville (Equatorial), Stornoway (Temperate maritime) and Winnipeg (Temperate continental).



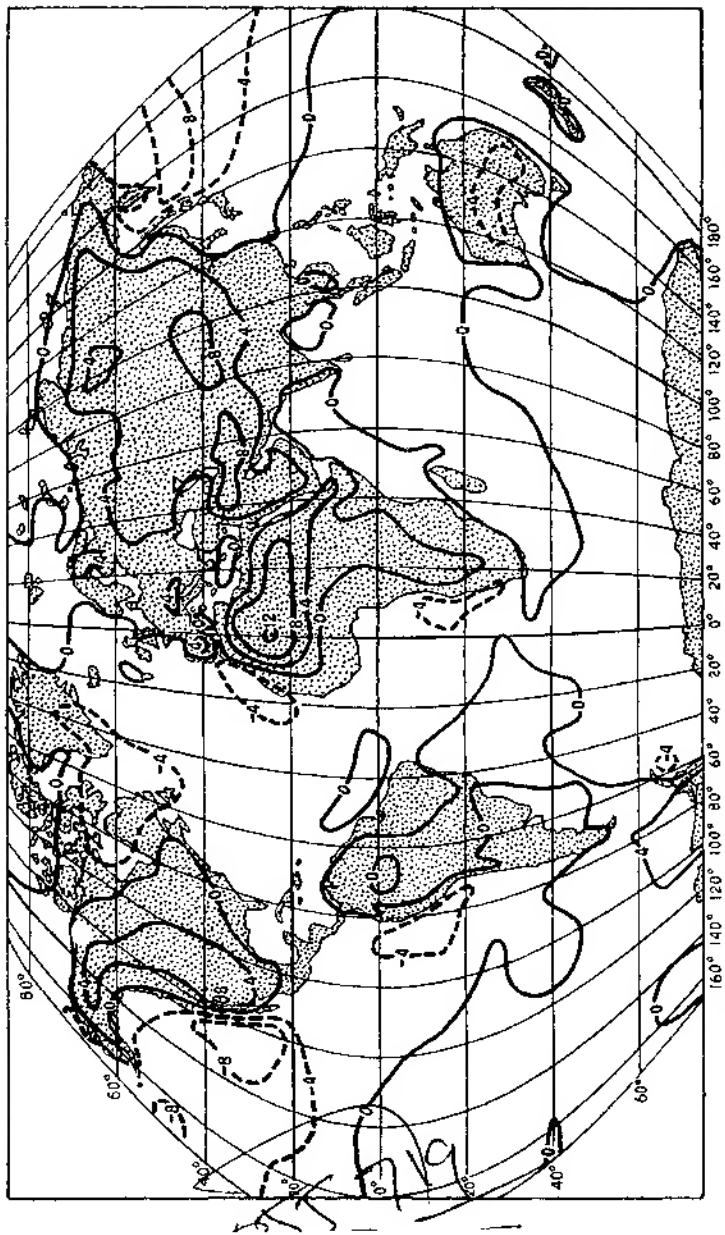


Fig. 1.18. World temperature anomalies (i.e. the difference between recorded temperatures ($^{\circ}\text{C}$) and the mean for that latitude) for January (above) and July (below). Solid lines indicate positive, and dashed lines negative, anomalies.

56 Atmosphere, weather and climate

January and July (fig. 1.18) illustrates the significance of continentality and also the influence of the warm drift currents in the North Atlantic and the North Pacific in winter (compare fig. 3.34).

Sea temperatures can now be estimated by the use of infrared satellite photography (see ch. 1, E). Plate 5 is an infrared photograph taken at night of the south-east coast of the United States in which sea surface temperatures appear in various shades of grey with the darkest areas representing the relatively warm, meandering Gulf Stream. From such photographs, maps of sea temperatures can be constructed, as illustrated in fig. 1.19.

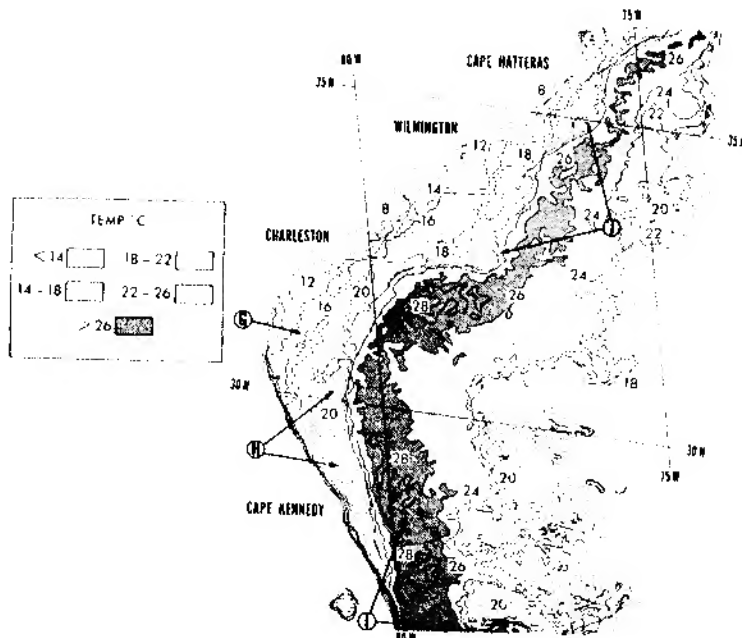


Fig. 1.19. Sea surface temperatures off the east coast of the United States at 0900 GMT on 15 February 1971, estimated from infrared imagery (see pl. 5). Numbers show the point temperatures which were measured by scanning radiometer. The coldest shelf waters (8° - 14°C) are indicated at G; the intermediate slope waters (H) have surface temperatures of 14° - 22°C ; the Gulf Stream surface (I) is at 26 - 28°C and shows steep temperature gradients along certain of its margins (J) (after Rao *et al.* From WMO 1973).

6 Effect of elevation and aspect

When we come down to the local scale, even differences in the elevation of the land and its *aspect* (that is the direction which the surface faces) will strikingly control the amount of insolation received.

Obviously some slopes are more exposed to the sun than others, while really high elevations which have a much smaller mass of air above them (see fig. 1.4) receive considerably more insolation under clear skies than locations near sea-level. On the average in middle latitudes the intensity of incident solar radiation increases by 5–15% for each 1000 m increase in elevation in the lower troposphere. The difference between sites at 200 and 3000 m in the Alps, for instance, can amount to $140 \text{ cal cm}^{-2} \text{ day}^{-1}$ in cloudless summer conditions. However, there is also a correspondingly greater net loss of terrestrial radiation at higher elevations because the low density of the overlying air results in a smaller fraction of the outgoing

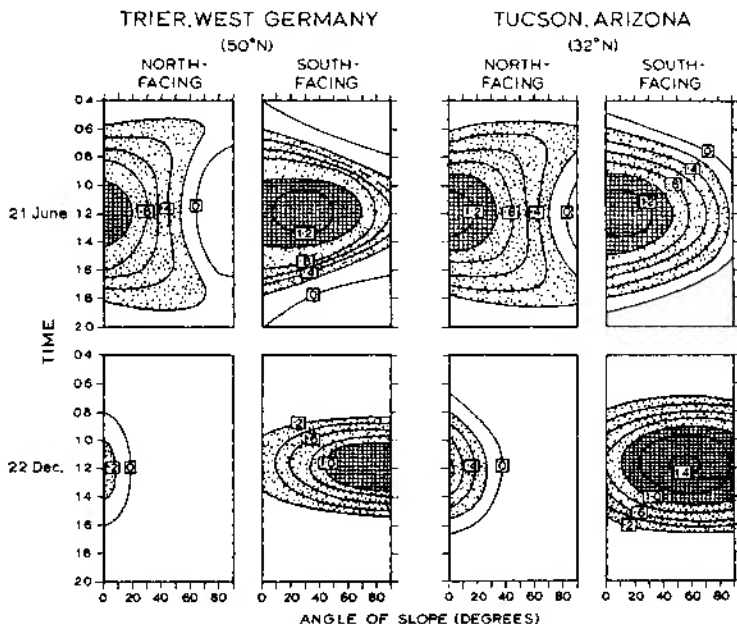


Fig. 1.20. Average direct beam solar radiation ($\text{cal cm}^{-2} \text{ min}^{-1}$) incident at the surface under cloudless skies at Trier, West Germany, and Tucson, Arizona, as a function of slope, aspect, time of day and season of year (after Geiger 1965 and Sellers 1965).

58 Atmosphere, weather and climate

radiation being absorbed. The overall effect is invariably complicated by the greater cloudiness associated with most mountain ranges and it is therefore impossible to generalize from the limited data at present available.

Figure 1.20 illustrates the effect of aspect and slope angle on theoretical maximum insolation receipts at two locations in the northern hemisphere. The general effect of latitude on insolation amounts is clearly shown, but it is also apparent that increasing latitude causes a relatively greater insolation loss for north-facing slopes, as distinct from south-facing ones. The radiation intensity on a sloping surface (I_s) is

$$I_s = I_0 \cos \gamma'$$

where γ' = the angle between the solar beam and a beam normal to the sloping surface. Relief may also affect the quantity of insolation and the duration of direct sunlight when a mountain barrier screens the sun from valley floors and sides at certain times a day. In many alpine valleys settlement and cultivation are noticeably concentrated on southward-facing slopes (the adret or sunny side), whereas northward slopes (ubac or shaded side) remain forested.

E Infrared radiation from the earth

Radiation from the sun is predominantly short wave whereas that leaving the earth is long wave, or infrared, radiation (see fig. 1.6). The infrared emission from the surface is slightly less than that from a black body at the same temperature and, accordingly, Stefan's equation (p. 34) is modified by an emissivity coefficient (ϵ) which is generally between 0.90 and 0.95, i.e. $F = \epsilon \sigma T^4$. Figure 1.6 shows that the atmosphere is highly absorbent to infrared radiation (due to the effects of water vapour, carbon dioxide and ozone), except between about 8.5 and 11.0 μm – the 'atmospheric window'. The opaqueness of the atmosphere to infrared radiation, relative to its transparency to short wave radiation, is commonly referred to as the 'greenhouse effect'. However, in the case of a greenhouse the effect of the glass is probably as significant in reducing cooling by restricting the turbulent heat loss as it is in retaining the infrared radiation.

It is worth emphasizing that long wave radiation is not merely terrestrial in the narrow sense. The atmosphere radiates to space and clouds are particularly effective since they act as black bodies. For this reason cloudiness and cloud top temperature can be mapped from

satellites by day and night using infrared sensors (see pls. 1 and 5). Radiative cooling of cloud layers averages about 1.5°C per day.

F Heat budget of the earth

We can now summarize the net effect of the transfers of energy in the earth atmosphere system averaged over the globe and over an annual period.

The incident solar radiation averaged over the globe is

$$\text{Solar constant} \times \pi R^2 / 4\pi r^2$$

where R = radius of the earth and $4\pi r^2$ is the surface area of a sphere. This figure is approximately $0.5 \text{ cal cm}^{-2} \text{ min}^{-1}$ or $262 \text{ k cal cm}^{-2} \text{ yr}^{-1}$; for convenience we will regard it as 100 units. Referring to fig. 1.21, incoming radiation is absorbed in the stratosphere (4 units) by ozone mainly, and 20 units are absorbed in the troposphere, by carbon dioxide (1), water vapour (13), dust (3) and water droplets in clouds (3). Twenty-three units are reflected back to space from cloud-covered areas, a further 4 units are similarly reflected from the surface and 4 units are returned by atmospheric scattering. The total reflected radiation is the planetary albedo (31% or 0.31). The remaining 45 units reach the earth either directly (24) or as diffuse radiation (21) transmitted via clouds or by downward scattering. The scattering effect of air molecules and dust particles on the visible wavelengths of radiation (blue light = $0.4 \mu\text{m}$, red = $0.7 \mu\text{m}$) is greatest at short wavelengths, and hence the sky light appears blue in colour.

The pattern of outgoing terrestrial radiation is quite different (fig. 1.21). The black-body radiation, assuming a mean surface temperature of 288°K is equivalent to 113 units of infrared (long wave) radiation. However, most of this is absorbed in the atmosphere as described above. Only about 6 units escape through the atmospheric window directly from the surface, but the atmosphere radiates 63 units to space, as well as re-radiating nearly twice as much (97 units) back to the surface (L_d).

These radiation transfers can be expressed symbolically:

$$R_n = (Q + q)(1 - a) + L_n$$

where R_n = net radiation, $(Q + q)$ = global solar radiation, a = albedo and L_n = net longwave radiation. At the surface $R_n = 29$ units. This surplus is conveyed to the atmosphere by the turbulent transfer of sensible heat, or enthalpy (6 units) and latent heat (23 units).

$$R_n = LE + H,$$

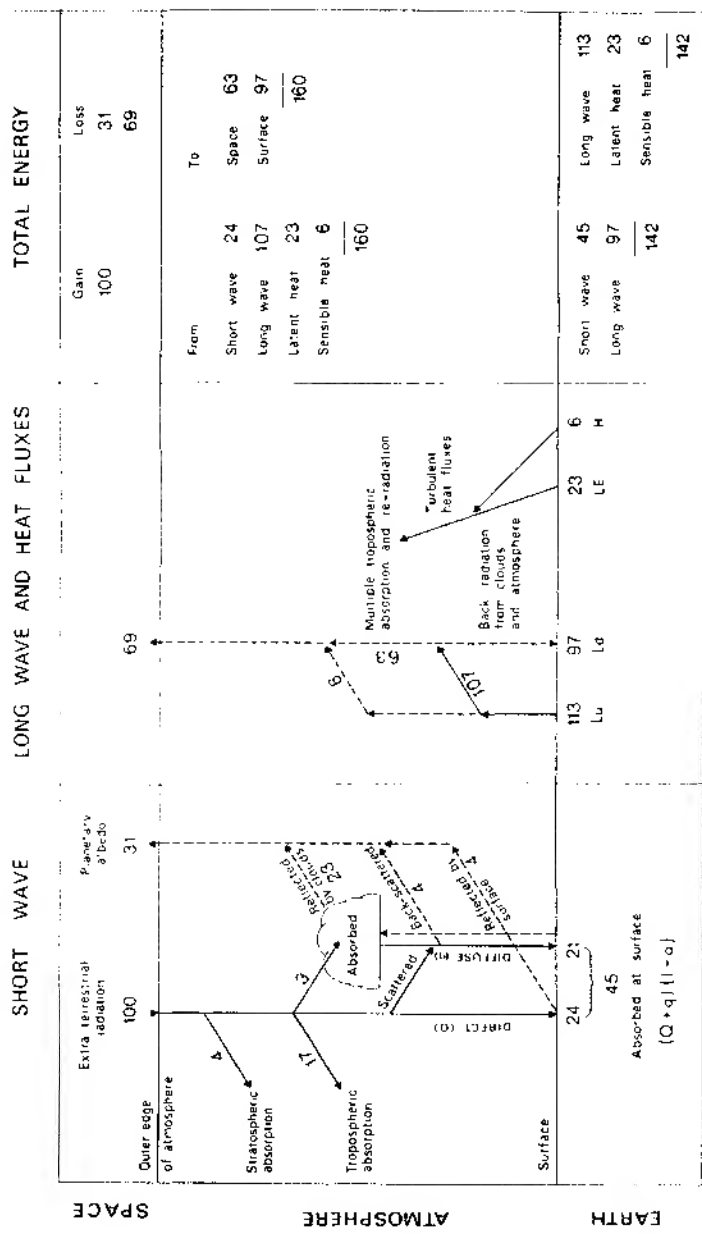


Fig. 1.21. The balance of the atmospheric energy budget (*data after Budko and others*). The transfers are explained in the text. Solid lines indicate energy gains by the atmosphere and surface in the left-hand diagram and the troposphere in the right-hand diagram. The exchanges are referred to 100 units of incoming solar radiation at the top of the atmosphere (equal to $0.5 \text{ cal cm}^{-2} \text{ min}^{-1}$ or $263 \text{ kcal cm}^{-2} \text{ yr}^{-1}$).

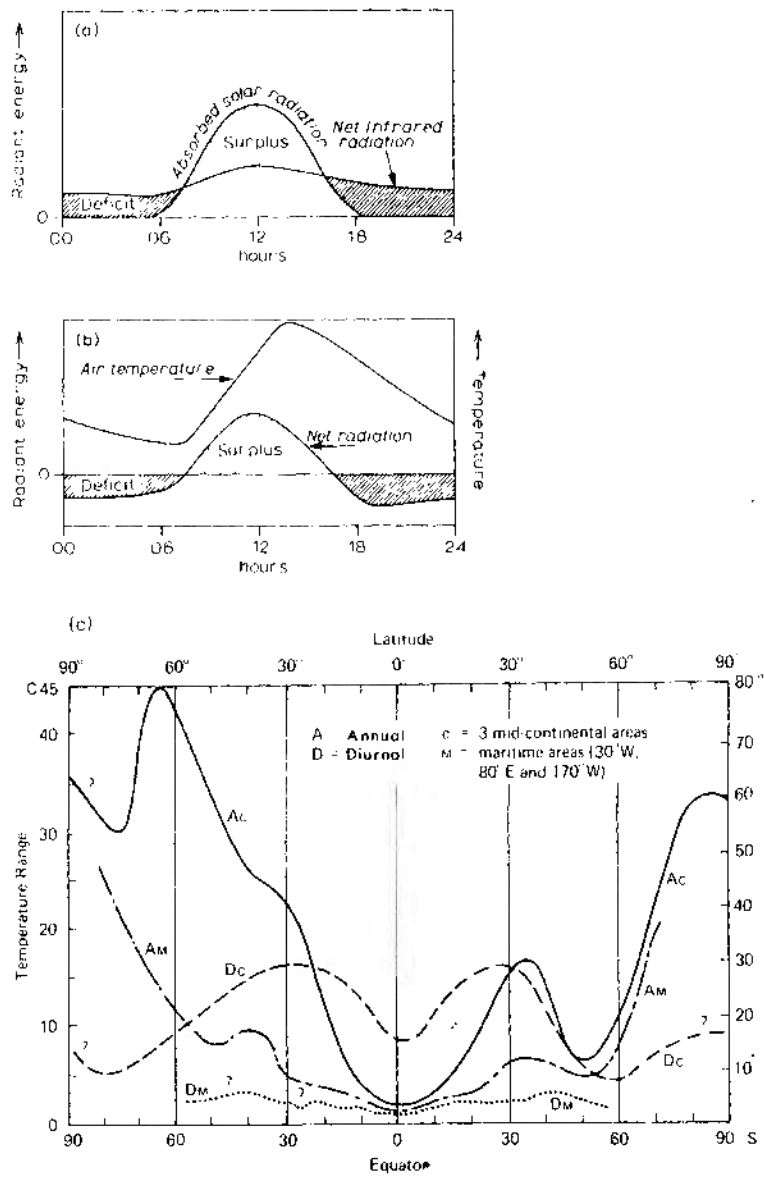
where H = sensible heat transfer and LE = latent heat transfer. There is also a flux of heat into the ground (ch. 1, D.5), but for annual averages this is approximately zero.

Figure 1.21 summarizes the total balances at the surface (± 142 units) and for the atmosphere (± 160 units). The energy balance for the entire earth-atmosphere system is estimated to be $\pm 173 \text{ kcal cm}^{-2} \text{ yr}^{-1}$ (± 66 units). These estimates are still rather crude. Satellites are now providing a 'top-view' of the radiation exchanges (see pls. 1 and 2) and they indicate a planetary albedo of only 0.29, apparently as a result of the measurement of less cloud cover, particularly over the tropical oceans, than had been determined by ground observations. However, various uncertainties are still to be resolved.

The annual and diurnal variations of temperature are directly related to the local radiation budget. Under clear skies, in middle and lower latitudes, the diurnal regime of radiative exchanges generally shows a midday maximum of absorbed solar radiation (fig. 1.22A). A maximum of infrared (longwave) radiation (see fig. 1.6) is also emitted by the heated ground surface at midday when it is warmest. The atmosphere re-radiates infrared radiation downward but there is a net loss at the surface (L_n). The difference between the absorbed solar radiation and L_n is the net radiation, R_n ; this is generally positive between about an hour after sunrise and an hour or so before sunset with a midday maximum. The delay in the occurrence of the maximum air temperature until about 2 p.m. local time (fig. 1.22B) is caused by the gradual heating of the air by convective transfer from the ground. Minimum R_n occurs in the early evening when the ground is still warm; there is a slight increase thereafter. The temperature decrease after midday is slowed by heat supplied from the ground. Minimum air temperature occurs shortly after sunrise due to the lag in the transfer of heat from the surface to the air. The annual pattern of the radiation budget and temperature regime is closely analogous to the diurnal one.

There are marked latitudinal variations in the diurnal and annual ranges of temperature. Broadly, the annual range is a maximum in higher latitudes, with extreme values about 65°N related to the effects of continentality in Asia and North America. The diurnal range reaches a maximum at the tropics over land areas, but it is in the equatorial zone that the diurnal variation of heating and cooling exceeds the annual one (fig. 1.22C). This is of course related to the small seasonal change in solar elevation angle at the equator.

62 Atmosphere, weather and climate



G Atmospheric energy and horizontal heat transport

So far, we have described the gases and other constituents which make up our atmosphere, and have given some account of the earth's heat budget. We have already referred to two forms of energy – internal (or heat) energy due to the motion of individual air molecules and latent energy which is released by condensation of water vapour. Two other forms of energy are important – geopotential energy due to gravity and height above the surface and kinetic energy associated with air motion.

Geopotential and internal energy are interrelated since the addition of heat to an air column not only increases its internal energy, but adds to its geopotential as a result of the vertical expansion of the air column. In a column extending to the top of the atmosphere the geopotential is approximately 40% of the internal energy. These two are therefore usually considered together and termed the total potential energy (*PE*). For the whole atmosphere

$$\text{potential energy} \approx 10^{24} \text{ joules}^1 (23.9 \times 10^{22} \text{ calories})$$

$$\text{kinetic energy} \approx 10^{20} \text{ joules}$$

In a later section (ch. 3, E) we shall see how energy is transferred from one form to another, but here we need only be concerned with heat energy. It is apparent that the receipt of heat energy is very unequal geographically and that this must lead to great lateral transfers of energy across the surface of the earth. Much present-day meteorological research is focused on these transfers, since undoubtedly they give rise, at least indirectly, to the observed patterns of global weather and climate.

The amounts of energy received at different latitudes vary substantially, the equator on the average receiving 2.5 times as much annual solar energy as the poles. Clearly if this process was not modified in some way the variations in receipt would cause a massive accumulation of heat

¹ See app. 4.

Fig. 1.22. Curves showing diurnal and annual variations of radiant energy and temperature.

- Diurnal variations in absorbed solar radiation and infrared radiation in the middle and low latitudes.
- Diurnal variations in net radiation and air temperature in the middle and low latitudes.
- Annual and diurnal temperature ranges as a function of latitude and of continental or maritime location (*from Paffen 1967*).

64 Atmosphere, weather and climate

within the tropics (associated with gradual increases of temperature) and a corresponding deficiency at the poles. Yet this does not seem to happen, and the earth as a whole is roughly in a state of thermal equilibrium in so far as no one region is obviously gaining heat at the expense of another. Some authors believe the Ice Ages to have been an exception to this rule. One explanation of this equilibrium could be that for each region of the world there is an equalization between the amount of incoming and outgoing radiation. Observation shows that this is not so (fig. 1.23), however,

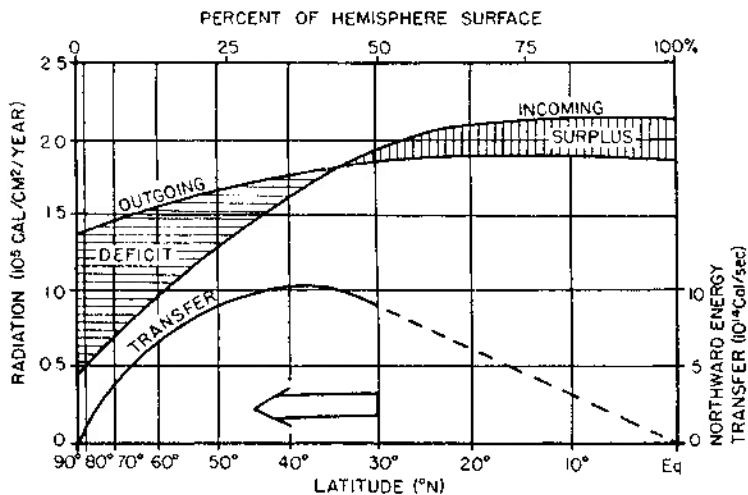


Fig. 1.23. A meridional illustration of the balance between incoming solar radiation and outgoing radiation from the earth and atmosphere (data from Houghton, after Newell 1964), in which the zones of permanent surplus and deficit are maintained in equilibrium by a poleward energy transfer (after Gabites).

for, whereas incoming radiation varies appreciably with changes in latitude, being highest at the equator and declining to a minimum at the poles, outgoing radiation has a more even latitudinal distribution owing to the rather small variations in atmospheric temperature. Some other explanation therefore becomes necessary.

1 The horizontal transport of heat

If the net radiation for the whole earth-atmosphere system is calculated, it

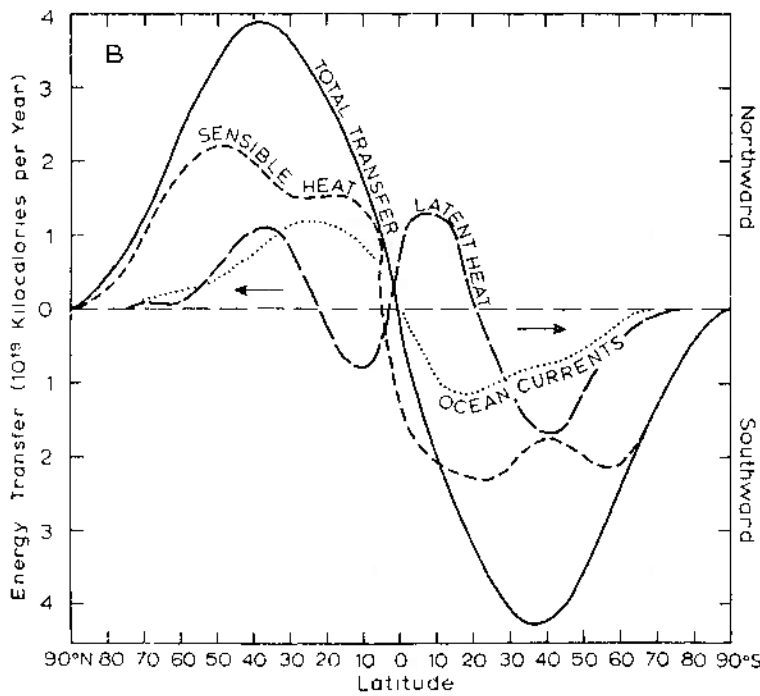
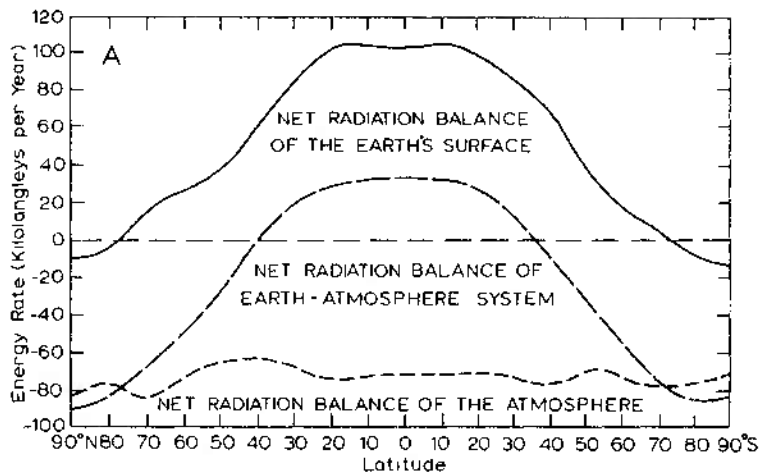
is found that there is a positive budget between 35°S and 40°N as shown in fig. 1.24A. As the tropics do not get progressively hotter or the high latitudes colder, a redistribution of world heat energy must constantly occur, taking the form of a continuous movement of energy from the tropics to the poles. In this way the tropics shed their excess heat and the poles are not allowed to reach extremes of cold. If there were no meridional interchange of heat, a radiation balance at each latitude would only be achieved if the equator were 14°C warmer and the north pole 25°C colder than now. This poleward heat transport takes place within the atmosphere and oceans, and it is estimated that the former accounts for approximately 80% of the required total. The horizontal transport (*advection* of heat) occurs in the form of both latent heat (that is water vapour which subsequently condenses) and sensible heat (that is warm air masses) (fig. 1.24B). It varies in intensity according to the latitude and the season. Figure 1.24B shows the mean annual pattern of energy transfer by the three mechanisms. The latitudinal zone of maximum total transfer rate is found between latitudes 35° and 45° in both hemispheres, although the patterns for the individual components are quite different from one another. The latent heat transport, which occurs almost wholly in the lowest 2 or 3 km, reflects the global wind belts on either side of the subtropical high-pressure zones (see ch. 3, D). The more important meridional transfer of sensible heat has a double maximum not only latitudinally but also in the vertical plane, where there are maxima near the surface and at about 200 mb. The high-level transport is particularly significant over the subtropics, whereas the primary latitudinal maximum about 50° to 60°N is related to the travelling low-pressure systems of the westerlies.

The intensity of the poleward energy flow is closely related to the meridional (that is, north-south) temperature gradient. In winter this temperature gradient is at a maximum and in consequence the hemispheric air circulation is most intense. The nature of the complex transport mechanisms will be discussed in ch. 3, E.

As shown in fig. 1.24B, ocean currents account for a significant proportion of the poleward heat transfer in low latitudes. Indeed, recent satellite estimates of the required total poleward energy transport indicate that the previous figures are too low. The ocean transport may be 47% of the total at 30°–35°N and as much as 74% at 20°N; the Gulf Stream and Kuro Shio currents are particularly important. As a result of this factor, the energy budget equation for an ocean area must be expressed as

$$R_n = LE + H + G + \Delta F,$$

66 Atmosphere, weather and climate



where ΔF = horizontal advection of heat by currents and G = the heat transferred into or out of storage in the water. The latter is more or less zero for annual averages.

2 Spatial pattern of the heat budget components

The mean latitudinal values of the heat budget components discussed above conceal great spatial variations. Figure 1.25 shows the global distribution of the annual net radiation. Broadly, its magnitude decreases poleward from about 25° latitude, although as a result of the considerable absorption of solar radiation by the sea, the net radiation is greater over the oceans – exceeding $120 \text{ kcal cm}^{-2} \text{ yr}^{-1}$ in latitudes $15\text{--}20^\circ$ – than over land areas, where it is about $60\text{--}80 \text{ kcal cm}^{-2} \text{ yr}^{-1}$ in the same latitudes. Net radiation is also rather lower in arid continental areas than in humid ones, because in spite of the increase insolation receipts under clear skies there is at the same time greater net loss of terrestrial radiation.

Figure 1.26 and 1.27 show the vertical transfers of latent and sensible heat to the atmosphere. Both maps show that the fluxes are distributed very differently over land and sea. Heat expenditure for evaporation is at a maximum in tropical and subtropical ocean areas, where it exceeds $120 \text{ kcal cm}^{-2} \text{ yr}^{-1}$. It is less near the equator where wind speeds are somewhat lower and the air has a vapour pressure close to the saturation value (see ch. 2, A). It is clear from fig. 1.26 that the major warm currents considerably augment the evaporation rate. On land the latent heat transfer is greatest in hot, humid regions. It is least in arid areas due to the low precipitation and in high latitudes where there is little available energy.

The largest exchange of sensible heat occurs in the tropical deserts where more than $60 \text{ kcal cm}^{-2} \text{ yr}^{-1}$ is transferred to the atmosphere. In contrast to latent heat, the sensible heat flux is generally small over the oceans, only reaching $20\text{--}30 \text{ kcal cm}^{-2}$ in areas of warm currents. Indeed, negative values occur (transfer to the ocean) where warm continental air masses move offshore over cold currents.

Fig. 1.24. A. Net radiation balance for the earth's surface of +76 kilolangleys/year (incoming solar radiation of 117 kly/yr minus outgoing long-wave energy to the atmosphere of 41 kly/yr); for the atmosphere of -76 kilolangleys/year (incoming solar radiation of 63 kly/yr minus outgoing long-wave energy to space of 139 kly/yr); and for the whole earth-atmosphere system of zero (from Sellers 1965). B. The average annual latitudinal distribution of the components of the poleward energy transfer (in 10^{19} kilocalories) in the earth-atmosphere system (from Sellers 1965).

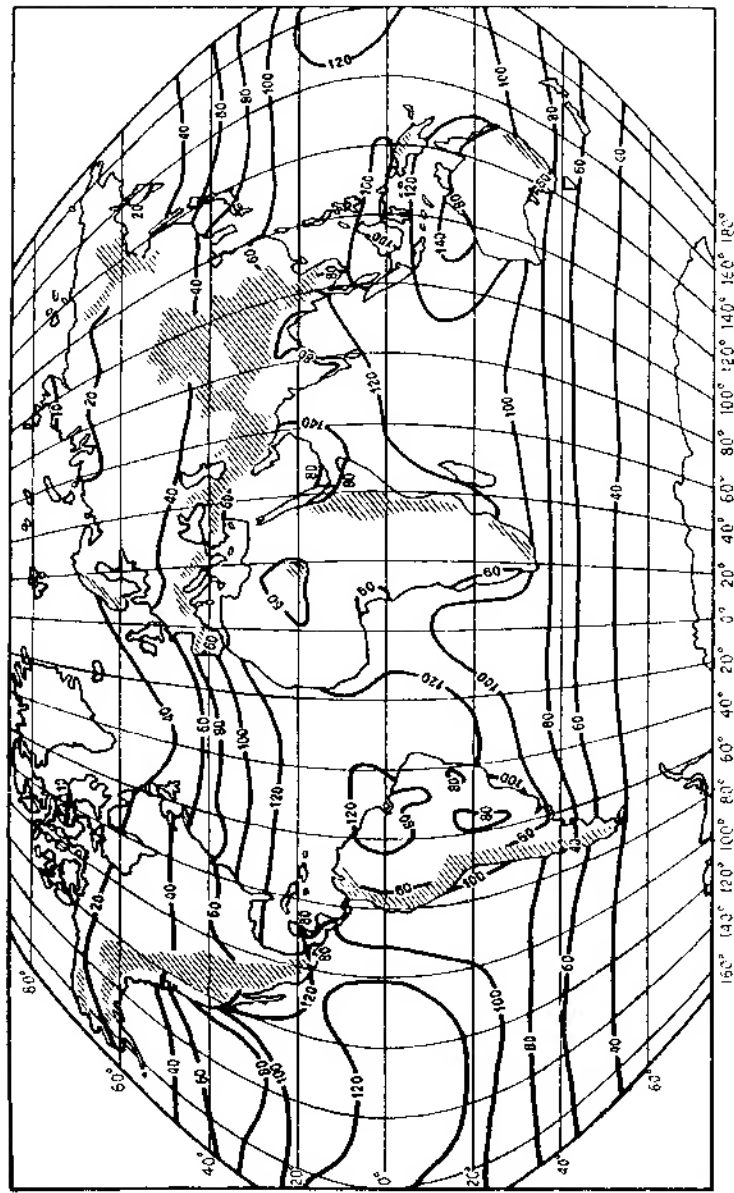


Fig. 1.25. Global distribution of the annual net radiation, in kcal cm^{-2} (after Bud'ko).

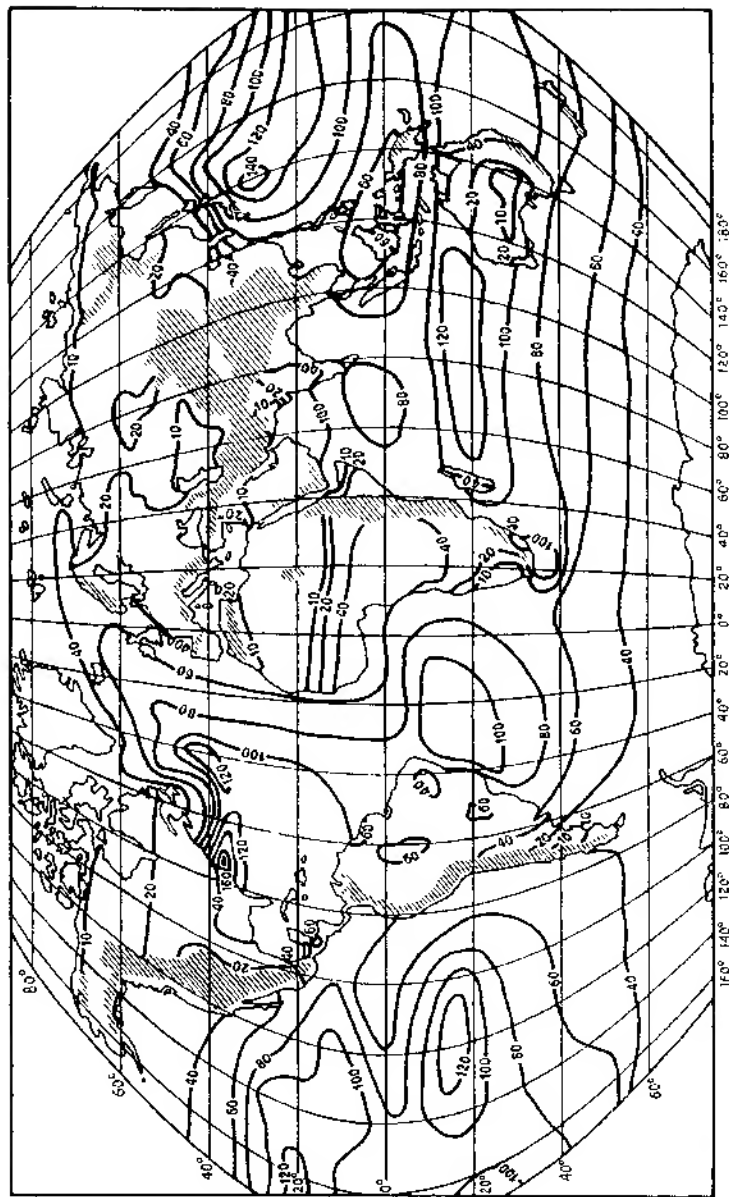


Fig. 1.26. Global distribution of the vertical distribution of latent heat, in kcal cm^{-2} (after Budjko).

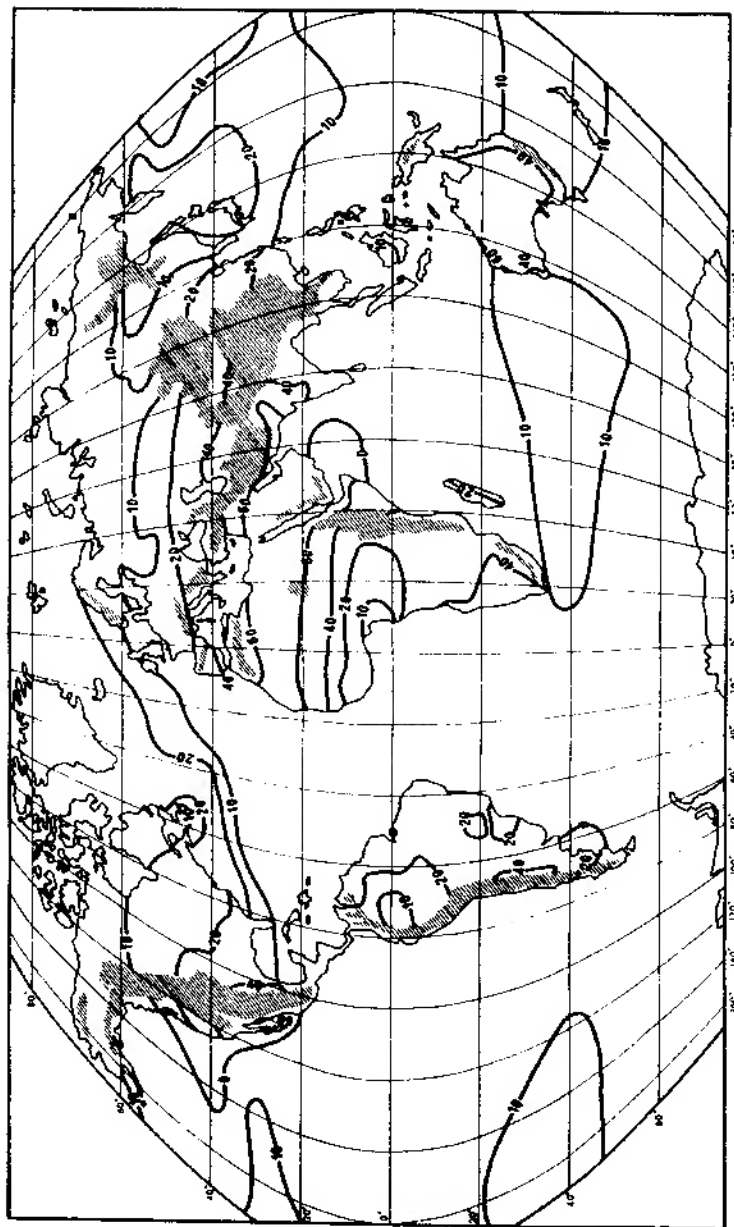


Fig. 1.27. Global distribution of the vertical transfer of sensible heat, in kcal cm^{-2} (after Budýko).

H The layering of the atmosphere

The atmosphere can be divided conveniently into a number of rather well-marked horizontal layers, mainly on the basis of temperature. The evidence for this structure comes from regular RAWINSONDE (radar wind-sounding) balloons, radio-wave investigations, and, more recently, from rocket and satellite flights. Broadly, the pattern (fig. 1.28) consist of three

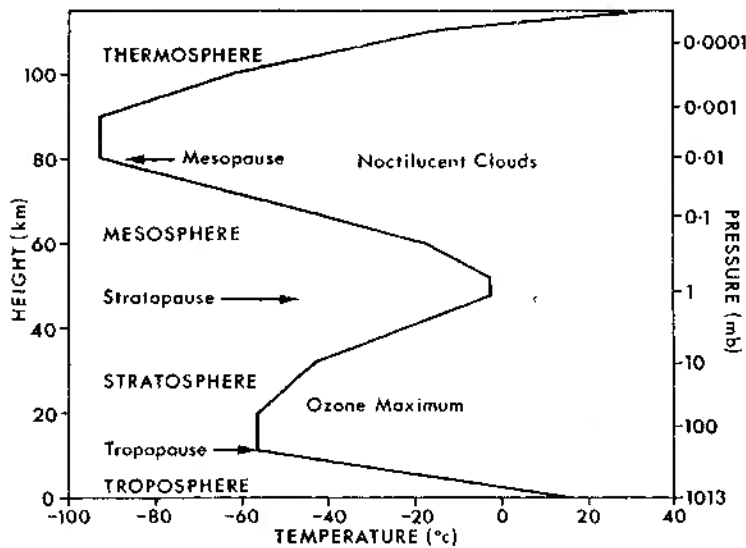


Fig. 1.28. The generalized vertical distribution of temperature and pressure up to about 110 km. Note particularly the tropopause and the zone of maximum ozone concentration with the warm layer above it (*based on data in Valley 1965*).

relatively warm layers (near the surface; between 50 and 60 km; and above about 120 km), separated by two relatively cold layers (between 10 and 30 km; and about 80 km). Mean January and July temperature sections illustrate the considerable latitudinal variations and seasonal trends that complicate the scheme (fig. 1.29).

72 Atmosphere, weather and climate

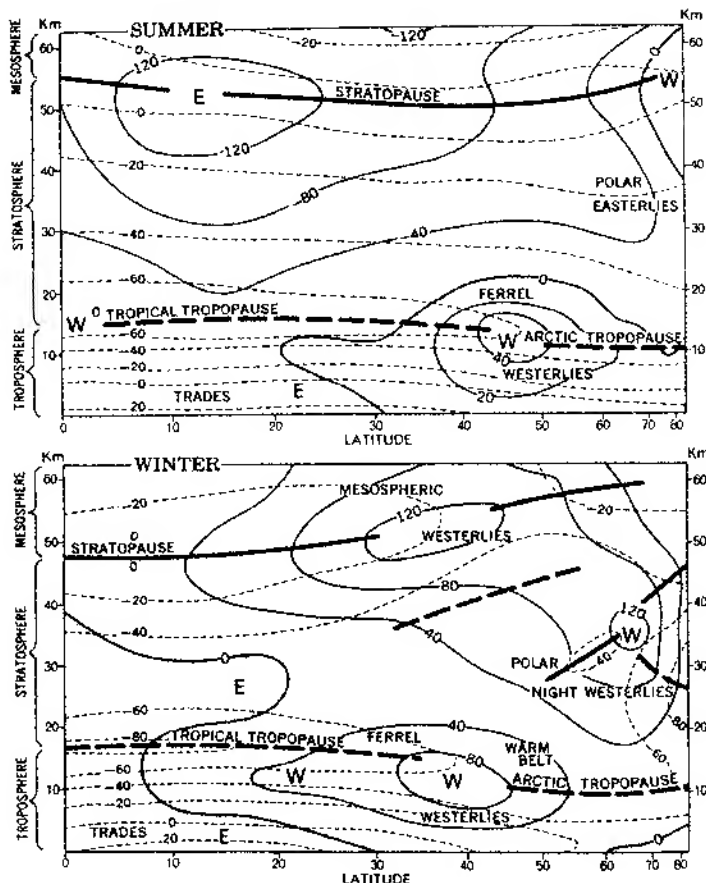


Fig. 1.29. Mean zonal (westerly) winds (solid isolines, in knots. Negative values from the east) and temperatures (in degrees Celsius, dashed isolines), showing the broken tropopause near the mean Ferrel jet stream (after Boville. From Hare 1962). The term 'Ferrel Westerlies' was proposed by F. K. Hare in honour of W. Ferrel (see p. 164). The heavy black lines denote reversals of the vertical temperature gradient of the tropopause and stratopause.

1 Troposphere

The lowest layer of the atmosphere is called the troposphere. It is the zone where weather phenomena and atmospheric turbulence are most marked,

and contains 75% of the total molecular or gaseous mass of the atmosphere and virtually all the water vapour and aerosols. Throughout this layer there is a general decrease of temperature with height at a mean rate of about $6.5^{\circ}\text{C}/\text{km}$ (or $3.6^{\circ}\text{F}/1000 \text{ ft}$), and the whole zone is capped in most places by a temperature inversion level (i.e. a layer of relatively warm air above a colder one) and in others by a zone which is isothermal with height. The troposphere thus remains to a large extent self-contained because the inversion acts as a 'lid' which effectively limits convection (see ch. 2, E). This inversion level or weather ceiling is called the *tropopause*.¹ Its height is not constant, either in space or time. It seems that the height of the tropopause at any point is correlated with sea-level temperature and pressure, which are in turn related to the factors of latitude, season and daily changes in surface pressure. There are marked variations in the altitude of the tropopause as between different latitudes (fig. 1.29), it having an elevation of about 16 km (10 miles) at the equator where there is great heating and vertical convective turbulence and only 8 km (5 miles) at the poles.

The meridional temperature gradients in the troposphere in summer and winter are roughly parallel, as are the tropopauses (fig. 1.29), and the strong lower mid-latitude temperature gradient in the troposphere is reflected in the tropopause breaks (see also fig. 3.19). In these zones important interchanges can occur between the troposphere and stratosphere, or vice versa. Traces of water vapour probably penetrate into the stratosphere by this means, while dry, ozone-rich stratospheric air may be brought down into the mid-latitude troposphere. For example, above-average concentrations of ozone are observed in the rear of mid-latitude low-pressure systems where the tropopause elevation tends to be low. Both facts are probably the result of stratospheric subsidence, which warms the lower stratosphere and causes downward transfer of the ozone.

2 Stratosphere

The second major atmospheric layer is the stratosphere which extends upwards from the tropopause to about 50 km (30 miles). Although the stratosphere contains much of the total atmospheric ozone (it reaches a peak density at approximately 22 km), the maximum temperatures associated with the absorption of the sun's ultraviolet radiation by ozone occur at the *stratopause*, where temperatures may exceed 0°C (fig. 1.29).

¹ The official definition is the lowest level at which the lapse rate decreases to less than, or equal to, $2^{\circ}\text{C}/\text{km}$ (provided that the average lapse rate of the 2-km layer above does not exceed $2^{\circ}\text{C}/\text{km}$).

74 Atmosphere, weather and climate

The air density is much less here so that even limited absorption produces a large temperature increase. Temperatures increase fairly generally with height in summer, with the coldest air at the equatorial tropopause. In winter the structure is more complex with very low temperatures, averaging -80°C , at the equatorial tropopause which is highest at this season. Similar low temperatures are found in the middle stratosphere at high latitudes, whereas over 50° – 60°N there is a marked warm region with nearly isothermal conditions at about -45°C to -50°C . Marked seasonal changes of temperature affect the stratosphere. The cold 'polar night' winter stratosphere undergoes dramatic sudden warmings associated with subsidence due to circulation changes in late winter or early spring when temperatures at about 25 km may jump from -80°C to -40°C over a 2-day period. The autumn cooling is a more gradual process. In the tropical stratosphere recent investigations have identified a quasi-biennial (26 month) wind regime, with easterlies in the layer 18 to 30 km for 12 to 13 months, followed by westerlies for a similar period. The reversal begins first at high levels and takes approximately 12 months to descend from 30 to 18 km (10 to 60 mb).

How far these events in the stratosphere are linked with temperature and circulation changes in the troposphere is a major topic of current meteorological research. Any interactions that do exist, however, are likely to be complex, otherwise they would already have become evident.

3 The upper atmosphere

a Mesosphere. Above the stratopause average temperatures decrease to a minimum of about -90°C (183°K) around 80 km. This layer is commonly termed the mesosphere, although it must be noted that as yet there is no universal acceptance of terminology for the upper atmospheric layers. Indeed, some authors refer to the layer between 20 and 80 km as the mesosphere. Above 80 km temperatures again begin rising with height and this inversion is referred to as the 'mesopause'. It is in this region that 'noctilucent clouds' are observed over high latitudes in summer. Their presence appears to be due to meteoric dust particles which act as nuclei for ice crystals when traces of water vapour are carried upwards by high-level convection caused by the vertical decrease of temperature in the mesosphere.

Pressure is very low in the mesosphere, decreasing from about 1 mb at 50 km to 0.01 mb at 90 km.

b Thermosphere. Above the mesopause atmospheric densities are extremely low, although the tenuous atmosphere still effects drag on space vehicles above 250 km. The lower portion of the thermosphere is com-

posed mainly of nitrogen (N_2) and oxygen in molecular (O_2) and atomic (O) forms, whereas above 200 km atomic oxygen predominates over nitrogen (N_2 and N). Temperatures rise with height, owing to the absorption of ultraviolet radiation by atomic oxygen, probably approaching 1200°K at 350 km, but these temperatures are essentially theoretical. For example, artificial satellites do not acquire such temperatures because of the rarefied air. 'Temperatures' in the upper thermosphere and exosphere undergo wide diurnal variations. They are higher by day and are also higher during a sunspot maximum, although the changes are only represented in varying velocities of the sparse air molecules.

Above 100 km the atmosphere is increasingly affected by solar X-rays and ultraviolet radiation which cause *ionization*, or electrical charging, by separating negatively charged electrons from oxygen atoms and nitrogen molecules, leaving the atom or molecule with a net positive charge (an *ion*). The Aurora Borealis and Aurora Australis are produced by the penetration of ionizing particles through the atmosphere from about 300 to 80 km, particularly in zones about 20°–25° latitude from the earth's magnetic poles. On occasion, however, the aurorae may appear at heights up to 1000 km, demonstrating the immense extension of a rarefied atmosphere. The term *ionosphere* is commonly applied to the layers above 80 km, although sometimes it is used only for the region of high electron density between about 100 and 300 km. In view of these different designations it seems preferable to avoid confusion by using the terminology adopted here.

c *Exosphere and magnetosphere.* The base of the exosphere is between about 500 and 750 km. Here atoms of oxygen, hydrogen and helium (about 1% of which are ionized) form the tenuous atmosphere and the gas laws (see ch. 1, B) cease to be valid. Neutral helium and hydrogen atoms, which have low atomic weights, can escape into space since the chance of molecular collisions deflecting them downwards becomes less with increasing height. Hydrogen is replaced by the breakdown of water vapour and methane (CH_4) near the mesopause, while helium is produced by the action of cosmic radiation on nitrogen and from the slow, but steady, breakdown of radioactive elements in the earth's crust.

Ionized particles increase in frequency through the exosphere and, beyond about 200 km, in the magnetosphere there are only electrons (negative) and protons (positive). These charged particles are concentrated in two bands at about 3000 and 16,000 km above the surface (Van Allen 'radiation' belts), apparently as a result of trapping by the earth's magnetic field. The high energy particles are emitted by the sun in

76 Atmosphere, weather and climate

a stream called the 'solar wind'; some may also derive the cosmic radiation. The magnetosphere has an extended tail on the side of the earth away from the sun, but on the side towards the sun it is compressed by the solar wind to about ten earth radii (57,000 km). Detailed investigation of these regions has been made possible since 1958 by satellites, but study of this outermost fringe lies in the field of *magnetohydrodynamics*. Nevertheless disturbances of these upper regions by solar flares may eventually prove to have meteorological significance at lower levels. At a height of 80,000 km or so the earth's atmosphere probably merges into that of the sun, but even the appropriate definitions of atmosphere, wind and temperature are uncertain in these regions.

I Variation of temperature with height

The last section described the gross characteristics of the vertical temperature profile in the atmosphere, but it is now necessary to examine in more detail some of the features of the temperature gradient at low levels.

Vertical temperature gradients are determined in part by energy transfers and in part by vertical motion of the air. The various factors interact in a highly complex manner. The energy terms are the release of latent heat by condensation (ch. 1, D), radiational cooling of the air and sensible heat transfer from the ground. Horizontal temperature advection may also be important. Vertical motion is dependent on the type of pressure system. High-pressure areas are generally associated with descent and warming of deep layers of air, hence decreasing the temperature gradient and frequently causing temperature inversions in the lower troposphere. In contrast, low-pressure systems are associated with rising air which cools upon expansion and increases the vertical temperature gradient. This is only part of the story since moisture is an additional complicating factor (see ch. 2, E). It remains true, however, that the middle and upper troposphere is relatively cold above a surface low-pressure area, leading to a steeper temperature gradient.

The overall vertical decrease of temperature, or *lapse rate*, in the troposphere is, as has been stated, about $6.5^{\circ}\text{C}/\text{km}$. However, this is by no means constant with height, season, or location. Average global values calculated by C. E. P. Brooks for July show increasing lapse rate with height: $5^{\circ}\text{C}/\text{km}$ in the lowest 2 km, $6^{\circ}\text{C}/\text{km}$ between 4 and 6 km, and $7^{\circ}\text{C}/\text{km}$ between 6 and 8 km. Winter values are generally smaller and in continental areas, such as central Canada or eastern Siberia, may even be negative (i.e. temperatures increase with height in the lower layer) as a

result of excessive radiational cooling over a snow surface. (fig. 1.30.) A similar situation occurs when dense, cold air accumulates in mountain basins on calm, clear nights. On such occasions the mountain tops may be many degrees warmer than the valley floor below (see ch. 3, B.2). For this reason the adjustment of average temperatures of upland stations to mean sea level may produce misleading results. Observations in Colorado at

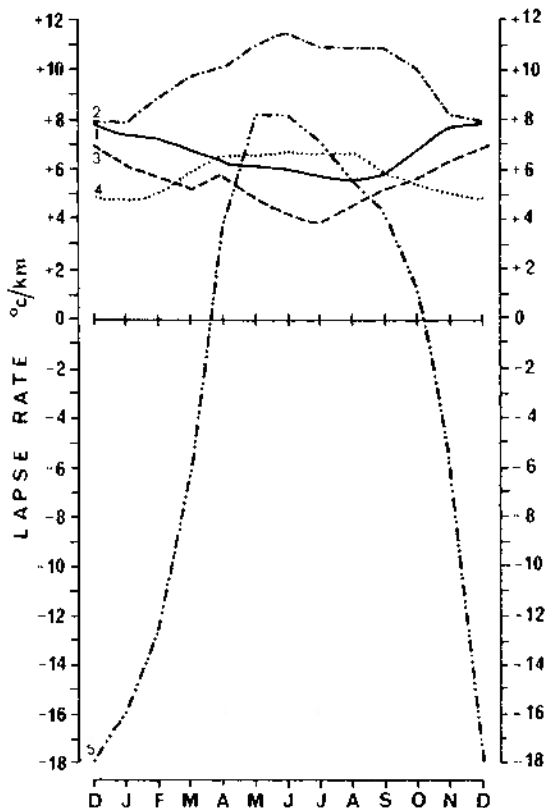


Fig. 1.30. The annual variation of lapse rate in five climatic zones (*from Hastenrath 1968*).

1. Tropical rainy climate (Togo).
2. Tropical desert (Arizona).
3. Mediterranean (Sicily).
4. Mid-latitude, cold winter climate (North Germany).
5. Boreal continental (Eastern Siberia).

78 Atmosphere, weather and climate

Table 1.4 Temperature lapse rates in the lowest 1000–1500 metres (after Lautensach and Bögel)

Climate	Season of maximum	Rate °C/km	Season of minimum	Rate °C/km
Tropical rainy	Dry season	>5	Rainy season	>4.5
Tropical and subtropical deserts	Summer	>8	Winter	>5
Mediterranean	Winter	>5	Summer	<5
Mid-latitudes (cold winter)	Summer	>6	Winter	0–5
Boreal continental	Summer	>5	Winter	<0
Arctic	Summer	≤0	Winter	<0

Pike's Peak (14,111 ft or 4301 m) and Colorado Springs (6098 ft or 1859 m) show the mean lapse rate to be $4.1^{\circ}\text{C}/\text{km}$ ($2.3^{\circ}\text{F}/1000 \text{ ft}$) in winter and $6.2^{\circ}\text{C}/\text{km}$ ($3.4^{\circ}\text{F}/1000 \text{ ft}$) in summer! It should be noted that such topographic lapse rates may bear little relation to free-air lapse rates in nocturnal radiation conditions, and the two must be carefully distinguished.

Table 1.4 summarizes the seasonal characteristics of lapse rates in six major climatic zones and examples of five of these are illustrated in fig. 1.30. The seasonal regime is very pronounced in continental areas with cold winters whereas inversions persist for much of the year in the Arctic. In winter the Arctic inversion is due to intense radiational cooling but in summer it is the result of the surface cooling of advected warmer air. The winter lapse rate is only greater than the summer one in Mediterranean climates. In these regions there is more likelihood of rising air associated with low-pressure areas in winter. In contrast, subsidence is predominant in the desert zones in winter. The tropical and subtropic deserts have very steep lapse rates in summer when there is considerable heat transfer from the surface and generally ascending motion.

2 Atmospheric moisture

Terrestrial moisture is in a constant state of transformation, termed the *hydrologic cycle*, in which the three most important stages are evaporation, condensation and precipitation. Figure 2.1 indicates the

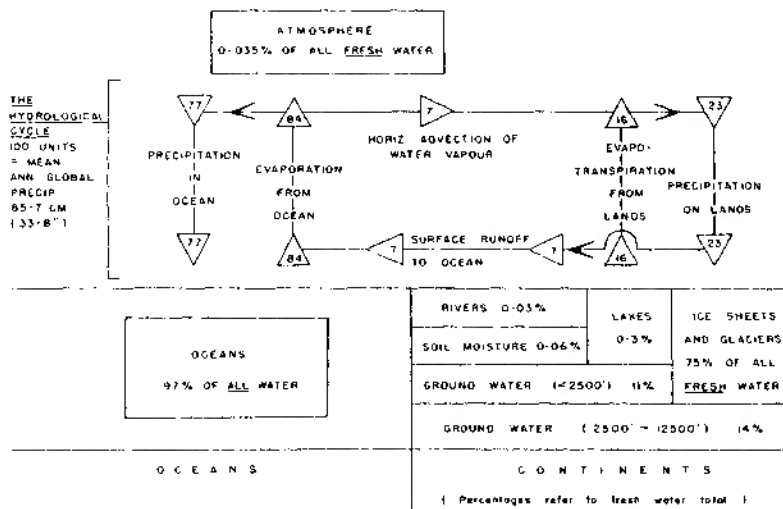


Fig. 2.1. The hydrological cycle and water storage of the globe. The exchanges in the cycle are referred to 100 units which equal the mean annual global precipitation of 85.7 cm (33.8 in). The percentage storage figures for atmospheric and continental water are percentages of all *fresh* water. The saline ocean waters make up 97% of *all* water (*from More 1967*). The horizontal advection of water vapour indicates the *net* transfer.

80 Atmosphere, weather and climate

relative average annual amounts of water involved in each phase of the cycle. It shows that the atmosphere holds only a very small amount of water although the exchanges with the land and oceans are very considerable. This is further emphasized by the following table:

Table 2.1 Mean water content of the atmosphere (in cm of rainfall equivalent) (after Sutcliffe 1956)

	Northern Hemisphere	Southern Hemisphere	World
January	1.9 (0.8 in)	2.5 (1.0 in)	2.2 (0.9 in)
July	3.4 (1.3 in)	2.0 (0.8 in)	2.7 (1.1 in)

The average storage of water in the atmosphere (about 2.5 cm, or 1 in) is only sufficient for some 10 days' supply of rainfall over the earth as a whole. However, intense (horizontal) influx of moisture into the air over a given region makes possible short-term rainfall totals greatly in excess of 1 in. The phenomenal record total of 187 cm (73.6 in) fell on the island of Réunion, off Madagascar, during 24 hours in March 1952, and much greater intensities have been observed over shorter periods (see ch. 2, I.1).

The atmosphere acquires moisture by evaporation from oceans, lakes, rivers and damp soil or from moisture transpired from plants. Taken together, these are often referred to as *evapotranspiration* and the mechanisms involved will now be discussed in detail.

A Evaporation

Evaporation occurs whenever energy is transported to an evaporating surface if the vapour pressure in the air is below the saturated value (e_s). As illustrated in fig. 1.5, the saturation vapour pressure increases with temperature. The change in state from liquid to vapour requires energy to be expended in overcoming the intermolecular attractions of the water particles. This energy is generally provided by the removal of heat from the immediate surroundings causing an apparent heat loss (*latent heat*), as discussed on p. 39, and a consequent drop in temperature. The latent heat of vaporization to evaporate 1 g of water at 0°C is 600 calories. Conversely, condensation releases this heat, and the temperature of an air mass in which condensation is occurring is increased as the water vapour reverts to the liquid state. The diurnal range of temperature is often

moderated by damp air conditions, when evaporation takes place during the day and condensation at night.

Viewed another way, evaporation implies an addition of kinetic energy to individual water molecules and, as their velocity increases, so the chance of individual surface molecules escaping into the atmosphere becomes greater. As the faster molecules will generally be the first to escape, so the average energy (and therefore temperature) of those composing the remaining liquid will decrease and the quantities of energy required for their continued release become correspondingly greater. In this way evaporation decreases the temperature of the remaining liquid by an amount proportional to the latent heat of vaporisation.

The rate of evaporation depends on a number of factors. The two most important are the difference between the saturation vapour pressure at the water surface and the vapour pressure of the air, and the existence of a continual supply of energy to the surface. Wind velocity can also affect the evaporation rate because the wind is generally associated with the importation of fresh, unsaturated air which will absorb the available moisture.

Water loss from plant surfaces, chiefly leaves, is a complex process termed *transpiration*. It occurs when the vapour pressure in the leaf cells is greater than the atmospheric vapour pressure, and is vital as a life function in that it causes a rise of plant nutrients from the soil and cools the leaves. The cells of the plant roots can exert an osmotic tension of up to about 15 atmospheres upon the water films between the adjacent soil particles. As these soil water films shrink, however, the tension within them increases. If the tension of the soil films exceeds the osmotic root tension the continuity of the plant's water supply is broken and wilting occurs. Transpiration is controlled by the atmospheric factors which determine evaporation as well as by plant factors such as the stage of plant growth, leaf area and leaf temperature, and also by the amount of soil moisture (see ch. 7, B.3). It occurs mainly during the day when the *stomata* (i.e. small pores in the leaves) through which transpiration takes place are open. This opening is determined primarily by light intensity. Transpiration naturally varies greatly with season, and during the winter months in mid-latitudes conifers lose only 10–18% of their total annual transpiration losses and deciduous trees less than 4%.

In practice it is difficult to separate water evaporated from the soil, *intercepted moisture* remaining on vegetation surfaces after precipitation and subsequently evaporated, and transpiration. For this reason evaporation is sometimes applied as a general term for all these, or, more correctly, the composite term *evapotranspiration* may be used.

82 Atmosphere, weather and climate

Evapotranspiration losses from natural surfaces cannot be measured directly. There are, however, various indirect methods of assessment, as well as theoretical formulae. One approximate means of indirect measurement is based on the moisture balance equation:

$$\text{Precipitation} = \text{Runoff} + \text{Evapotranspiration} + \text{Soil moisture storage change.}$$

Essentially the method is to measure the percolation through an enclosed block of soil with a vegetation cover (usually grass) and to record the rainfall upon it. The block, termed a *lysimeter*, is weighed regularly so that weight changes unaccounted for by rainfall or runoff can be ascribed to evapotranspiration losses, provided the grass is kept short! The technique allows the determination of daily evapotranspiration amounts.

If the soil block is regularly 'irrigated' so that the vegetation cover is always yielding the maximum possible evapotranspiration the water loss is called the *potential evapotranspiration* (or PE).¹ Assuming a constant soil moisture storage, potential evapotranspiration is calculated as the difference between precipitation and percolation. A simple evapotranspirometer installation is shown in fig. 2.2; the double tank installation ensures that representative readings are obtained. Potential evapotranspiration forms the basis for one system of climate classification developed by C. W. Thornthwaite (see app. I).

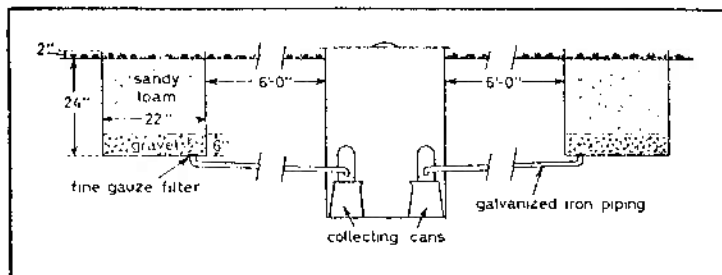


Fig. 2.2. An evapotranspirometer installation for calculating potential evapotranspiration losses. The double installation allows an average of the two results to be determined, giving a more reliable estimate (from Ward 1963).

Theoretical methods for determining evaporation rates have followed two lines of approach. The first relates average monthly evaporation (E) from large water bodies to the mean wind speed (u) and the mean vapour

¹ PE can be defined more generally as the water loss corresponding to the available energy.

pressure difference between the water surface and the air ($e_w - e_d$) in the form:

$$E = Ku(e_w - e_d)$$

where K is an empirical constant. This is termed the aerodynamic approach because it takes account of the factors responsible for removing vapour from the water surface. The second method is based on the energy budget. The *net balance* of solar and terrestrial radiation at the surface (R_n) is used for evaporation (E) and the transfer of heat to the atmosphere (H). A small proportion also heats the soil by day, but since nearly all of this is lost at night it can be disregarded. Thus:

$$R_n = LE + H,$$

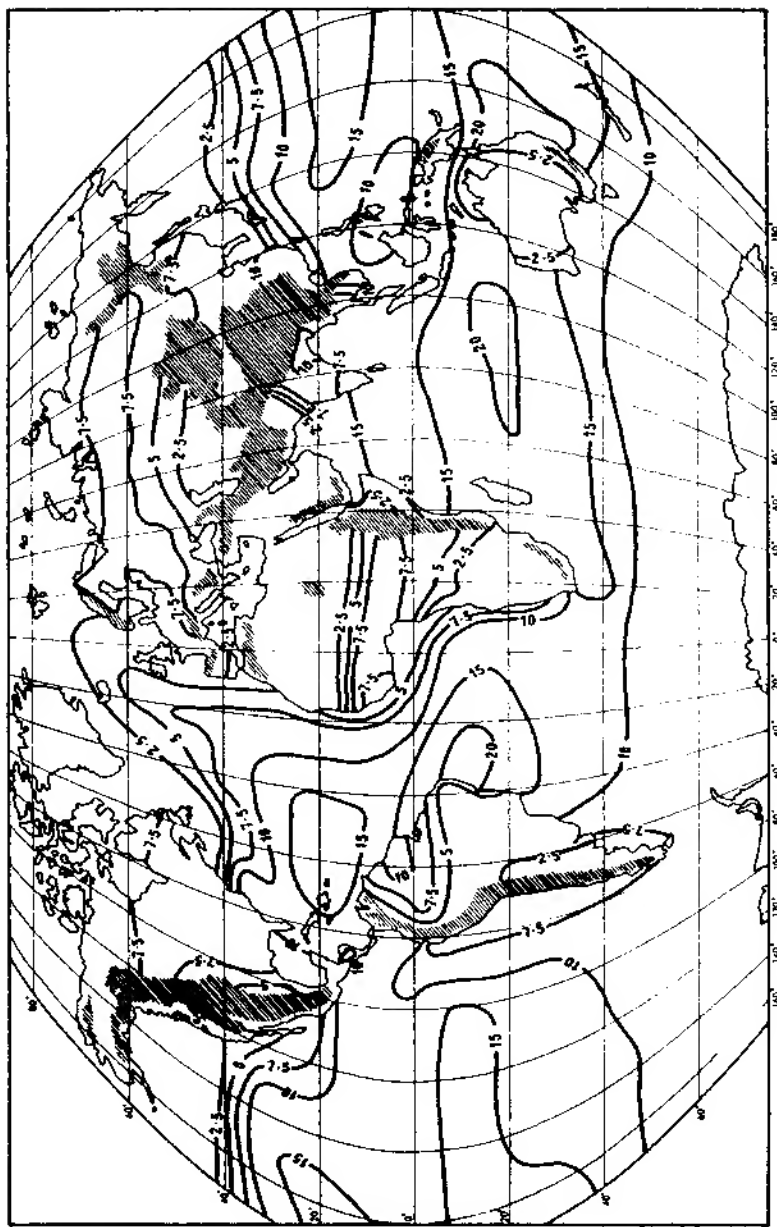
where L is the latent heat of evaporation. R_n can be measured with a net radiometer and the ratio $H/LE = \beta$, referred to as Bowen's ratio, can be estimated from measurements of temperature and vapour content at two levels near the surface. β ranges from < 0.1 for water to ≥ 10 for a desert surface. The use of this ratio assumes that the vertical transfers of heat and water vapour by turbulence takes place with equal efficiency. Evaporation is then determined from an expression of the form:

$$E = \frac{R_n}{L(1 + \beta)}$$

Instruments which will measure the vertical transfers of heat and water vapour have been developed, but at present these are primarily for research purposes.

The most satisfactory climatological method so far devised combines the energy budget and aerodynamic approaches. In this way H. L. Penman eliminated some of the unmeasurable quantities and succeeded in expressing evaporation losses in terms of four meteorological elements which are regularly measured, at least in Europe and North America. These are duration of sunshine (related to radiation amounts), mean air temperature, mean air humidity and mean wind speed (which limit the losses of heat and vapour from the surface).

The relative roles of the factors which have been mentioned are illustrated by the global pattern of evaporation (fig. 2.3). Losses decrease sharply in high latitudes where there is little available energy. In middle and lower latitudes there are appreciable differences between land and sea (fig. 2.4a). Rates are naturally high over the oceans in view of the unlimited availability of water, and on a seasonal basis the maximum rates occur in winter over the western Pacific and Atlantic, where cold con-



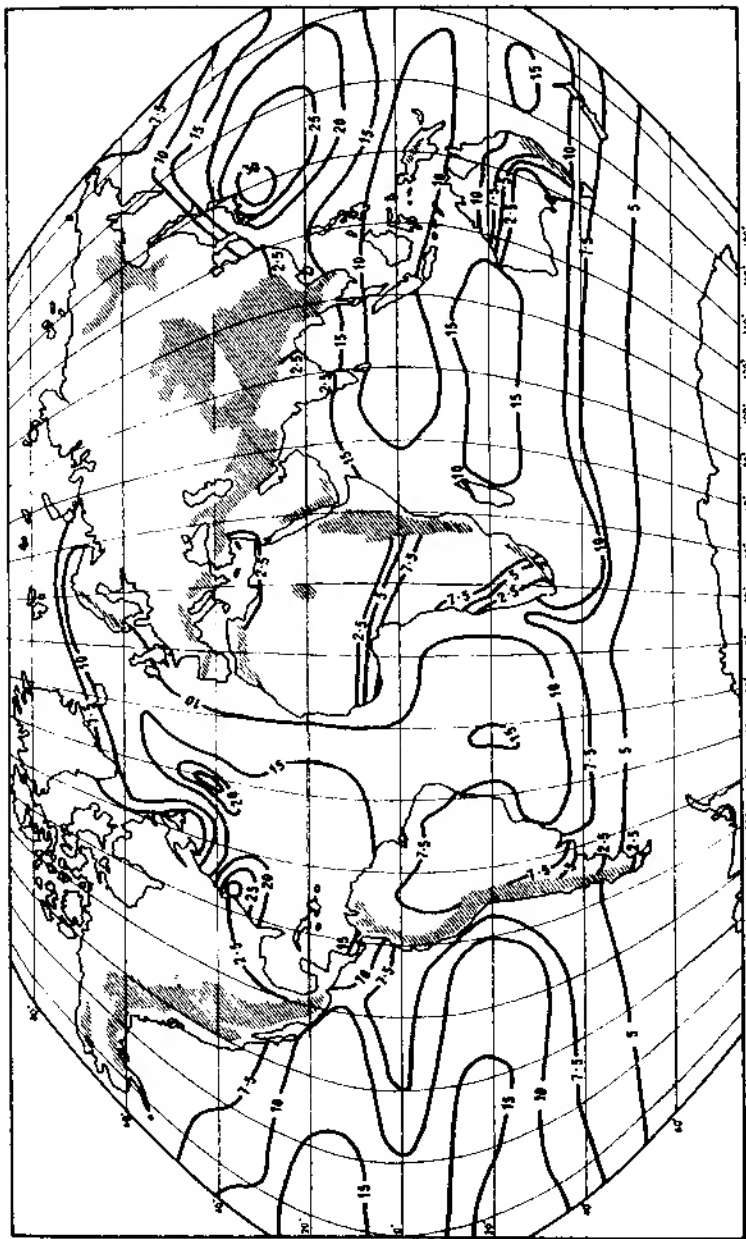


Fig. 2.3. Mean evaporation (cm) for January (above) and July (below).

86 Atmosphere, weather and climate

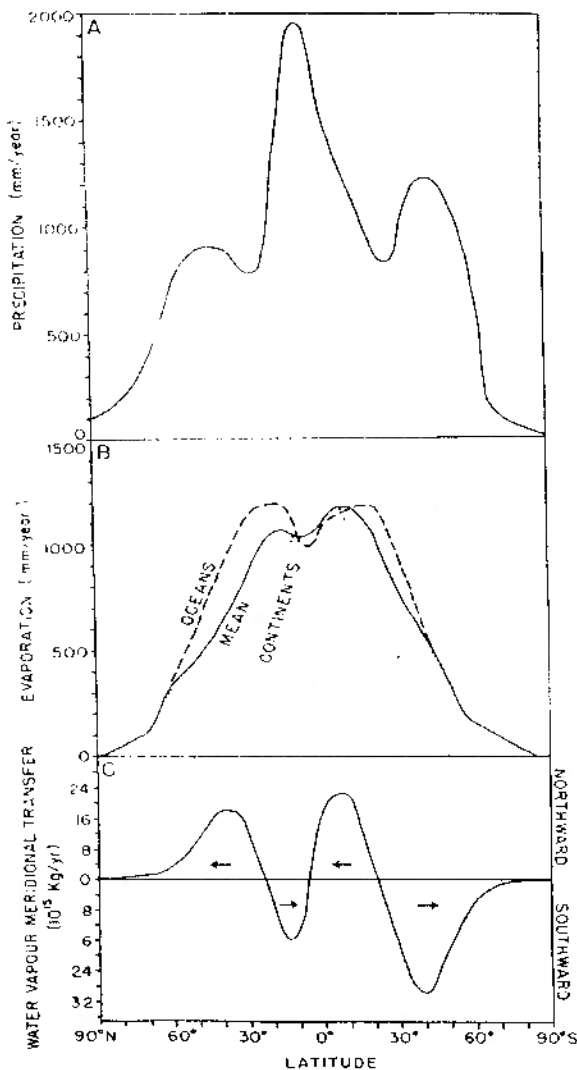


Fig. 2.4. The average annual latitudinal distribution of (A) precipitation (in mm); (B) evaporation (in mm); and (C) meridional transfer of water vapour (in 10^{15} kg) (mostly from Sellers 1965).

tinental air blows across warm ocean currents. On an annual basis maximum oceanic losses occur about 15° – 20° N and 10° – 20° S in the belts of the constant trade winds. The highest annual losses, estimated to be about 200 cm (80 in), are in the western Pacific and central Indian Ocean near 15° S. (cf. fig. 1.26; 100 kcal cm^{-2} is equivalent to an evaporation of 170 cm of water/cm 2). There is a subsidiary equatorial minimum over the oceans mainly as a result of the lower wind speeds in the doldrum belt and the proximity of the vapour pressure in the air to its saturation value, but the land maximum occurs more or less at the equator because of the relatively high solar radiation receipts and the large transpiration losses from the luxuriant vegetation of this region. The secondary maximum over land in mid-latitudes is related to the strong prevailing westerly winds. The other parts of fig. 2.4, incorporated here for convenient comparison, are discussed in later sections.

The annual evaporation over Britain, calculated by Penman's formula, ranges from about 38 cm (15 in) in Scotland to about 50 cm (20 in) in parts of south and south-east England. The annual potential evapotranspiration determined by Thornthwaite's method (based on mean temperature) is over 64 cm (25 in) in most of south-eastern England. Since this loss is concentrated in the period May–September there may be seasonal water deficits of 12–15 cm (5–6 in) in these parts of the country (as shown in fig. 2.5 for Southend), necessitating considerable use of

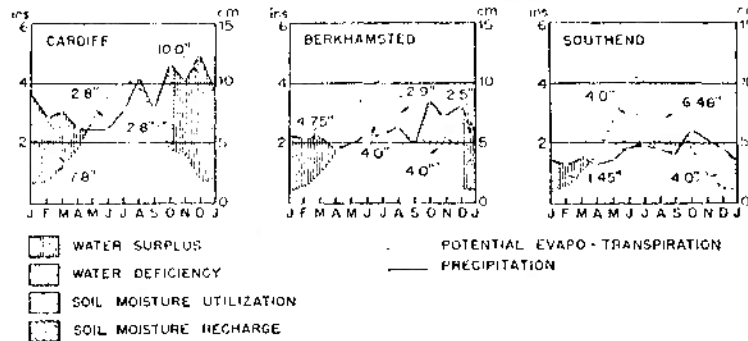


Fig. 2.5. The average annual moisture budget for stations in western, central and eastern Britain determined by Thornthwaite's method (from Howe, 1956).

irrigation water by farmers. Figure 2.6 indicates that in southern and south-eastern England it is necessary to irrigate in about nine years out of ten during the summer six months (April–September), assuming that the crop can extract 6.4 cm (2½ in) of moisture from the soil.



Fig. 2.6. The average number of years in ten when irrigation is theoretically necessary for crops in England and Wales, based on Penman's formula (from Pearl *et al.* 1954) (Crown Copyright Reserved).

B Humidity

I Moisture content

The moisture content of the atmosphere can be measured in a number of ways, apart from the vapour pressure, depending on which aspect the user wishes to emphasize. The total mass of water in a given volume of air, i.e. the density of the water vapour, is one such measure. This is termed the *absolute humidity* (ρ_w) and is measured in grams per cubic metre (g m^{-3}). Volumetric measurements are not greatly used in meteorology and more convenient is the *mass mixing ratio* (x). This is the mass of water vapour in grams per kilogram of dry air. For most practical purposes the *specific humidity* (q) is identical, being the mass of vapour per kilogram of air including its moisture.

The bulk of the atmosphere's moisture content is contained below 500 mb (5574 m), as fig. 2.7 clearly shows. It is also apparent that the

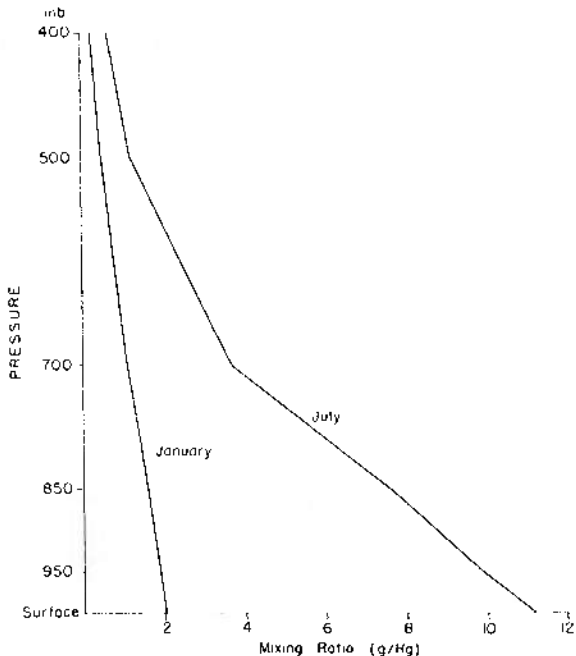
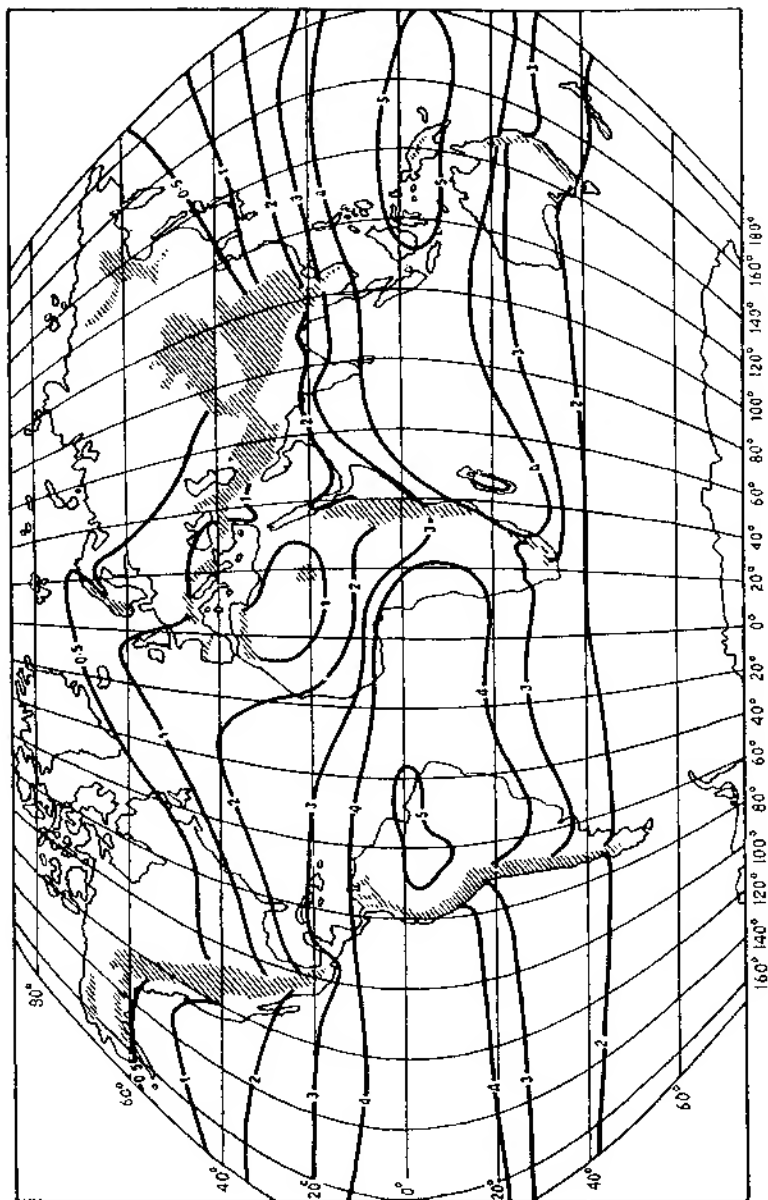


Fig. 2.7. The average vertical variation of atmospheric vapour content at Portland, Maine, between 1946 and 1955 (data from Reitan 1960).



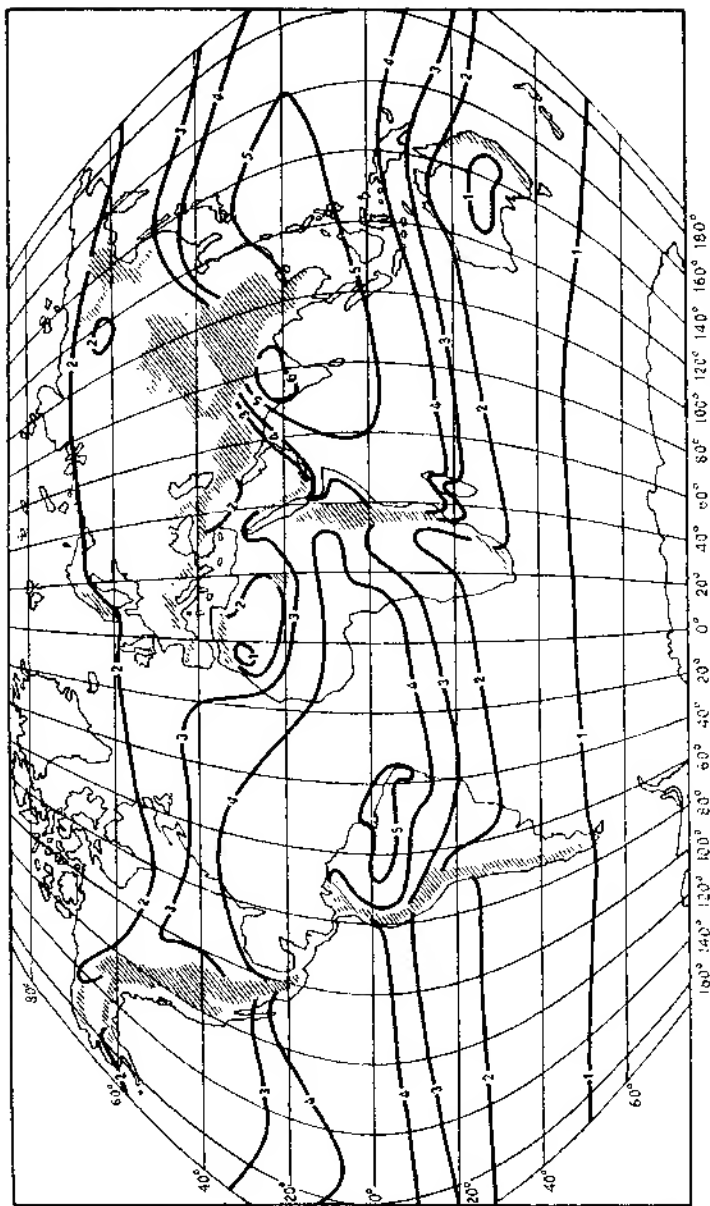


Fig. 2.8. Mean atmospheric water vapour content in January (above) and July (below), 1951–55, in cm of precipitable water (after Bannon and Steele 1960) (Crown Copyright Reserved).

92 Atmosphere, weather and climate

seasonal effect is most marked in the lowest 3000 m (10,000 ft) or so, that is below about 700 mb. The global distribution of atmospheric vapour content in January and July is illustrated in fig. 2.8. Over southern Asia during the summer monsoon an air column holds 5–6 cm of precipitable water, compared with less than 1 cm in tropical desert areas. Minimum values of 0.1–0.2 cm occur over high latitudes and continental interiors of the northern hemisphere in winter.

Another important measure is *relative humidity* (r), which expresses the actual moisture content of a sample of air as a percentage of that contained in the same volume of saturated air at the same temperature. The relative humidity is defined with reference to the mixing ratio, but it can be determined approximately in several ways:

$$r = \frac{x}{x_s} \times 100 \approx \frac{q}{q_s} \times 100 \approx \frac{e}{e_s} \times 100$$

where the subscript s refers to the respective saturation values at the same temperature; e denotes vapour pressure.

A further index of humidity is the dew-point temperature. This is the temperature at which saturation occurs if air is cooled at constant pressure without addition or removal of vapour. When the air temperature and dew point are equal the relative humidity is 100% and it is evident that relative humidity can also be determined from

$$\frac{e_s \text{ at dew point}}{e_s \text{ at air temperature}} \times 100$$

The relative humidity of a parcel of air will obviously change if either its temperature or its mixing ratio is changed. In general the relative humidity varies inversely with temperature during the day, tending to be lower in the early afternoon and higher at night.

2 Moisture transport

It is sometimes overlooked that the atmosphere transports moisture horizontally as well as vertically. Figure 2.4c illustrates the quantities which must be transported meridionally in order to maintain the required moisture balance at a given latitude (i.e. Precipitation – Evaporation = Net horizontal transport of moisture into the air column). A prominent feature is the equatorward transport into low latitudes and the poleward transport in middle latitudes. The reader should inspect this diagram again in the light of the discussion of winds belts in ch 3, E.

At this point it is necessary to stress emphatically the fact that local

evaporation is, in general, not the major source of local precipitation. For example, only 6% the annual precipitation of Arizona and 10% of that over the Mississippi River basin is of local origin, the remainder being transported into these areas (i.e. moisture advection). Even when moisture is available in the atmosphere over a specific region only a small portion of it is usually precipitated. This depends on the efficiency of the condensation and precipitation mechanisms, both microphysical and large-scale, which we shall now consider.

C Condensation

Condensation, the direct cause of all the various forms of precipitation, occurs under varying conditions which in one way or another are associated with change in one of the linked parameters of air volume, temperature, pressure or humidity. Thus, condensation takes place (i) when the temperature of the air is reduced but its volume remains constant and the air is cooled to dew point; (ii) if the volume of the air is increased without addition of heat; this cooling takes place because adiabatic expansion causes energy to be consumed through work (see ch. 2, D); or (iii) when a joint change of temperature and volume reduces the moisture-holding capacity of the air below its existing moisture content. The key to the understanding of condensation clearly lies in the fine balance that exists between these variables. Whenever the balance between one or more of them is disturbed beyond a certain limit condensation may result.

The most common circumstances favourable to the production of condensation are those producing a drop in air temperature; namely contact cooling, mixing of air masses of different temperatures and dynamic cooling of the atmosphere. Contact cooling is produced, for example, within warm, moist air passing over a cold land surface. On a clear winter's night strong radiation will cool the surface very quickly and this surface cooling will gradually extend to the moist lower air, reducing the temperature to a point where condensation occurs in the form of dew, fog or frost, depending on the amount of moisture involved, the thickness of the cooling air layer and the dew-point value. When the latter is below 0°C it is referred to as the hoar frost-point if the air is saturated with respect to ice.

The mixing of the differing layers within a single air mass or of two differing air masses can also produce condensation. Figure 2.9 indicates how the horizontal mixing of two air masses (A and B), of given temperature and moisture characteristics, may produce an air mass (C) which is over-saturated at the intermediate temperature and consequently forms cloud. Vertical mixing of an air layer, which is discussed below (fig.

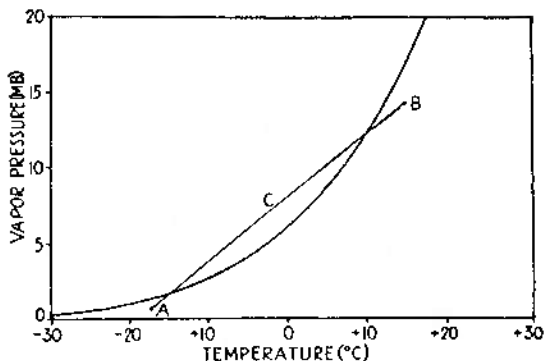


Fig. 2.9. The effect of air-mass mixing (from Petterssen 1941). The horizontal mixing of two unsaturated air masses A and B will produce one supersaturated air mass C. The saturation vapour pressure curve is shown (cf. fig. 1.5 which is a semi-logarithmic plot).

2.15) can have the same effect. Fog, or low stratus, with drizzle – known as ‘crachin’ – which is common along the coasts of South China and the Gulf of Tonkin in February–April, can develop as a result of either air mass mixing or warm advection over a colder surface.

Undoubtedly the most effective cause of condensation, however, is the dynamic process of adiabatic cooling. This is considered in some detail in the next section.

D Adiabatic temperature changes

The displacement of an air parcel to an environment of lower pressure (without heat exchange with surrounding air) causes an increase in its volume and a consequent lowering of its temperature. A volume increase involves work and the consumption of energy, thus reducing the heat available per unit volume and hence the temperature. Such a temperature change, involving no subtraction or addition of heat, is termed *adiabatic*. Vertical displacements of air are obviously a major cause of adiabatic temperature changes.

Near the earth’s surface most processes of change are non-adiabatic (sometimes termed *diabatic*) because of the tendency of air to mix and modify its characteristics by lateral movement, turbulence and related

physical processes. When a parcel of air moves vertically the changes that take place often follow an adiabatic pattern because air is fundamentally a poor thermal conductor, and the air parcel as a whole tends to retain its own thermal identity which distinguishes it from the surrounding air masses. In some circumstances, on the other hand, mixing of air with its surroundings must be taken into account.

We may now consider the changes which occur when an air parcel rises and a decrease of pressure is accompanied by volume increase and temperature decrease (see ch. 1, B). The rate at which temperature decreases in a rising, expanding air parcel is called the *adiabatic lapse rate*. If the upward movement of air does not produce condensation then the energy expended by expansion will cause the temperature of the mass to fall at what is called the *dry adiabatic lapse rate* ($9.8^{\circ}\text{C}/\text{km}$ or $5.4^{\circ}\text{F}/1000 \text{ ft}$). However, prolonged reduction of the temperature invariably produces condensation, and when this happens latent heat is liberated, counteracting the dry adiabatic temperature decrease to a certain extent. It is therefore a distinguishing feature of rising and saturated (or precipitating) air that it cools at a slower rate (i.e. the *saturated adiabatic lapse rate*) than air which is unsaturated. Another difference between the dry and saturated adiabatic rates is that whereas the former remains constant the latter varies with temperature. This is because air masses at higher temperatures are able to hold more moisture and on condensation therefore to release a greater quantity of latent heat. For high temperatures the saturated adiabatic lapse rate may be as low as $4^{\circ}\text{C}/\text{km}$ (or $2.2^{\circ}\text{F}/1000 \text{ ft}$), but this rate increases with decreasing temperatures, approaching $9^{\circ}\text{C}/\text{km}$ ($5^{\circ}\text{F}/1000 \text{ ft}$) at -40°C (-40°F).

In all, three different lapse rates can be differentiated, two dynamic and one static. There is the environmental (or static) rate, which is the actual temperature decrease with height on any occasion, such as an observer ascending with a balloon would record. This is not an adiabatic rate therefore and may assume any form depending on local air temperature conditions. There are also the dynamic adiabatic dry and saturated lapse rates (or cooling rates) which apply to rising parcels of air moving through their environment. Close to the surface the vertical temperature gradient sometimes greatly exceeds the dry adiabatic lapse rate, that is, it is superadiabatic. This is particularly common in arid areas in summer (see table 1.4). Over most ordinary dry surfaces the lapse rate approaches the dry adiabatic value at an elevation of 100 m or so.

The changing properties of moving air parcels can be conveniently expressed by plotting them as path curves on suitably constructed graphs. One such diagram in common use is the tephigram (fig. 2.10). This dis-

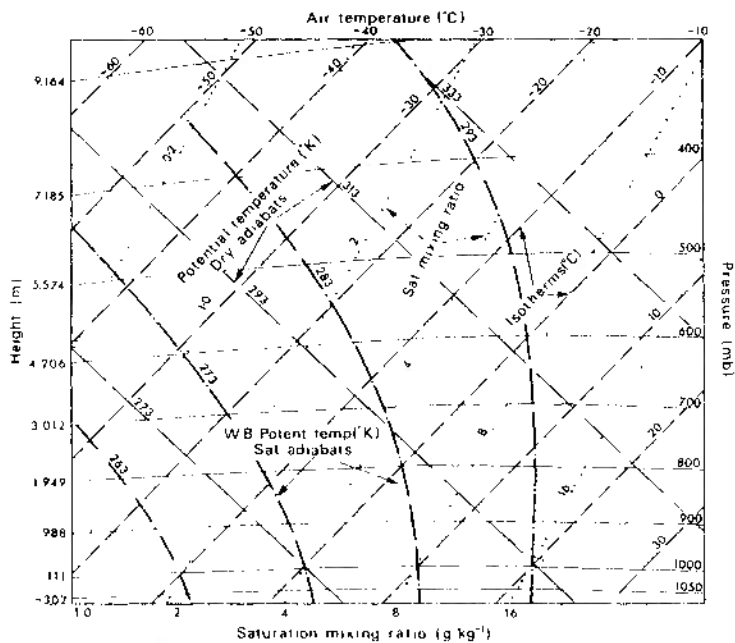


Fig. 2.10. The tephigram, allowing the following properties of the atmosphere to be displayed: isotherms, dry adiabats, isobars, saturated adiabats and the saturation mixing ratio.

plays five properties of the atmosphere:

1. *Isotherms* — i.e. lines of constant temperature (parallel lines from bottom left to top right).
2. Dry adiabats (parallel lines from bottom right to top left).
3. *Isobars* — i.e. lines of constant pressure (slightly curved nearly horizontal lines).
4. Saturated adiabats (curved lines sloping up from right to left).
5. Saturation mixing ratio lines (those at a slight angle to the isotherms).

The dry adiabats are also lines of constant potential temperature, θ , (or isentropes). Potential temperature is the temperature of an air parcel brought dry adiabatically to a pressure of 1000 mb. Mathematically,

$$\theta = T \left(\frac{1000}{p} \right)^{0.286} \quad \text{where } \theta \text{ and } T \text{ are in } {}^\circ\text{K}; p = \text{pressure (mb)}.$$

Figure 2.11 shows schematically the relationship between T and θ ; also between T and θ_w , the wet bulb potential temperature (where the air parcel is brought to a pressure of 1000 mb by a saturated adiabatic

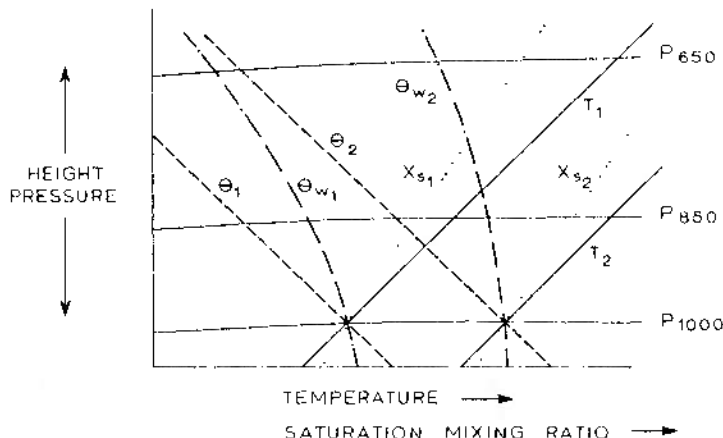


Fig. 2.11. Graph showing the relationships between temperature (T), potential temperature θ , wet bulb potential temperature (θ_w) and saturation mixing ratio (X_s).

process). Figure 2.10 shows, for example, that a saturated air parcel at 1000 mb pressure, with a temperature of 20°C, has a saturation mixing ratio of 16 g/kg. Figure 2.12 illustrates how the tephigram is used to determine the condensation level — the level at which an air parcel becomes saturated if forced to rise. The point at which a line along a dry adiabat through the surface air temperature (T_A) intersects a line of the saturation mixing ratio through the dew-point temperature (T_d) is the *lifting condensation level*. For an air temperature of 20°C and a dew point of 9°C at 1000 mb surface pressure, the lifting condensation level is at 895 mb with a temperature of 8°C. This point on the diagram is termed the 'characteristic point'. It can be estimated by

$$h \text{ (m)} = 120 (T - T_d)$$

where T = air temperature and T_d = dew point temperature at the surface in °C.

For some purposes it is preferable to define a *convective condensation level*. This is the intersection of the environment temperature curve with a saturation mixing ratio line corresponding to the average mixing rating in

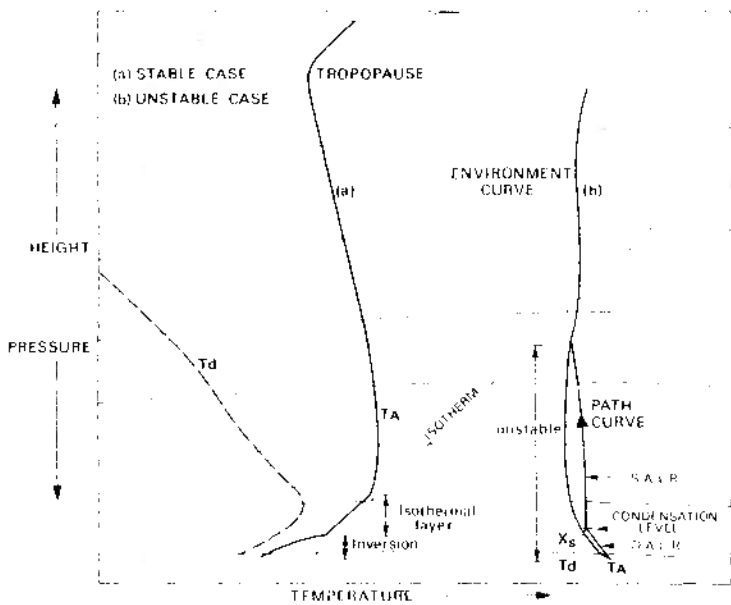


Fig. 2.12. Tephigram used to determine the condensation level and the layering and stability of the atmosphere. Path curve of a rising air parcel is arrowed.

the surface layer (1000–1500 m). Expressed in another way, the surface air temperature is the minimum which will cause cloud to form as a result of free convection.

Experimentation with a tephigram shows that both the convective and lifting condensation levels rise as the surface temperature increases. This is commonly observed in the early afternoon when the base of cumulus clouds tends to be at higher levels.

Potential temperature provides an important yardstick for air mass characteristics, since if the air is only affected by dry adiabatic processes the potential temperature remains constant. This helps to identify different air masses and indicates when latent heat has been released through saturation of the air mass or when non-adiabatic temperature changes have occurred.

E Air stability and instability

The important characteristic of stable air is that if it is forced up or down

it has a tendency to return to its former position once the motivating force ceases. Figure 2.12 shows the reason for this, in that the environmental temperature curve (*a*) lies to the right of any path curve representing the lapse rate of an unsaturated air parcel cooling dry adiabatically when forced to rise. At any level the rising parcel is cooler and more dense than its surroundings and therefore tends to revert to its former level. Similarly, if the air is forced downwards it will gain in temperature at the dry adiabatic rate, always be warmer and less dense than the surrounding air, and tend to return to its former position (unless prevented from doing so). However, if local surface heating causes the environmental lapse rate near the surface to exceed the dry adiabatic lapse rate (*b*), then the adiabatic cooling of a convective air parcel allows it to remain warmer and less dense than the surrounding air so that it continues to rise through buoyancy. Similarly, if an air parcel is impelled downwards under these same conditions from a higher level it will become colder than its surroundings and there will be no check on its downward progress until it reaches the surface. The characteristic of unstable air is a tendency to continue moving away from its original level when set in motion.

Environment curve (*b*) in fig. 2.12 intersects the path curve at a higher level. Above the level of this intersection the atmosphere is stable, but the buoyant energy gained by the rising parcel enables it to move some distance into this region. The theoretical upper limit of cloud development can be estimated from the tephigram by determining an area above the intersection of the environment and path curves equal to that between the two curves from the level of free convection to the intersection (fig. 2.13); the tephigram is so constructed that equal areas represent equal energy. However, this assumes that the air parcel undergoes no mixing (see below).

A further possibility is illustrated in fig 2.13. The air is stable in the lower layers, but if the air is forced to rise, for example by passage over a mountain range, or by local surface heating, the path curve is now to the right of the environment curve and the air, being warmer than its surroundings, is free to rise up. This is termed *conditional instability*, as the development of instability is dependent on the relative humidity of the air. Since the environmental lapse rate is frequently between the dry and saturated adiabatic rates the state of conditional instability is a common one.

These examples assume that a small air parcel is being displaced without any compensating air motion or mixing of the parcel with its surroundings.

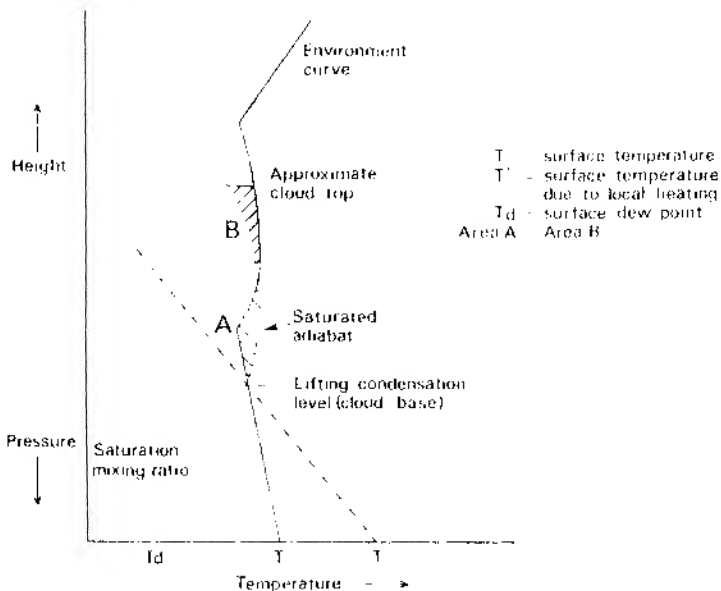


Fig. 2.13. Graph illustrating the conditions associated with the conditional instability of an air mass which is forced to rise.

These assumptions are rather unrealistic since dilution of an ascending air parcel by mixing of the surrounding air with it through *entrainment* will reduce its buoyant energy. However, the method is generally satisfactory for routine forecasting, especially perhaps since the assumptions approximate conditions in the updraught of cumulonimbus clouds.

A further consideration is that a deep layer of air may be displaced by vertical motion over an extensive topographic barrier. Figure 2.14 shows a case where the air in the upper levels is less moist than that at lower levels. If the whole layer is forced bodily upwards the drier air at B follows the dry adiabatic rate, and so, for a while, will the air about A, but there eventually comes a time when the condensation level is reached, after which the lower layers of the rising air mass cool at the saturated adiabatic rate. This has the final effect of increasing the actual lapse rate of the total thickness of the raised layer, and, if this new rate is greater than that of the saturated adiabatic, the air layer becomes unstable, and may overturn. This is termed *convective* (or *potential*) *instability*.

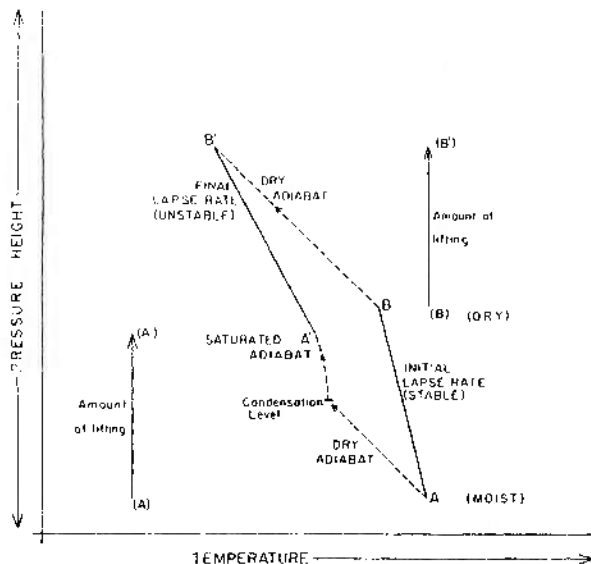


Fig. 2.14. Convective instability. AB represents the initial state of an air column; moist at A, dry at B. After uplift of the whole air column the temperature gradient A'B' exceeds the saturated adiabatic rate so that the air column is unstable.

Vertical mixing of air was referred to earlier as a possible cause of condensation. This is best illustrated by use of a tephigram. Figure 2.15 shows an initial distribution of temperature and dew point. Vertical mixing has the effect of averaging these conditions through the layer affected. Thus, the *mixing condensation level* is determined from the intersection of the

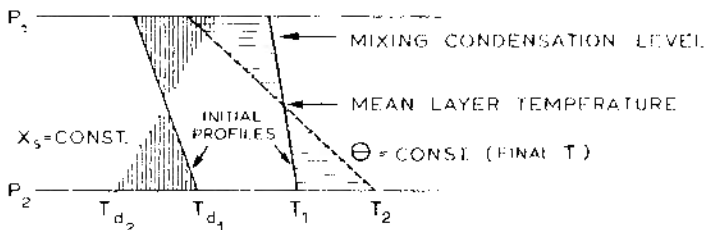


Fig. 2.15. Graph illustrating the effects of vertical mixing in an air mass.

average values of saturation humidity mixing ratio and potential temperature. The areas above and below the points where these average value lines cross the initial environment curves are equal.

Subsidence usually results from either radiational cooling or an excess of horizontal convergence of air in the upper troposphere. Subsiding air generally moves with a vertical velocity of only 1–10 cm/sec (about 100–1000 ft/hr), although convectional conditions provide an exception (see ch. 2, H). Subsidence can produce substantial changes in the atmosphere, and, for instance, if an air mass subsides about 300 m (1000 ft) all average-size cloud droplets will usually be evaporated.

F Cloud formation

The formation of clouds is dependent on atmospheric instability and vertical motion but it is also controlled by microscale processes. These are now discussed before we examine larger scale aspects of cloud development and type.

1 Condensation nuclei

It is very important to note that condensation occurs with the utmost difficulty in *clean* air; moisture must generally find a suitable surface upon which it can condense. If pure air is reduced in temperature below its dew point it becomes *supersaturated* (i.e. relative humidity exceeding 100%). To maintain a pure water drop of radius 10^{-7} cm (0.001 μm) requires a relative humidity of 320%, and for one of 10^{-5} cm (0.1 μm) radius 101%.

Usually condensation occurs on a foreign surface which can be a land or plant surface, as is the case for dew or frost, while in the free air condensation begins around so-called *hygroscopic nuclei*. These particles can be dust, smoke, sulphur dioxide, salts (NaCl) or similar microscopic substances, the surfaces of which (like the weather enthusiast's seaweed!) have the property of *wettability*. Moreover, hygroscopic aerosols are soluble. This is very important since the saturation vapour pressure is less over a solution droplet (for example, sodium chloride or sulphuric acid) than over a pure water drop of the same size and temperature (fig. 2.16). Indeed, condensation begins on hygroscopic particles before the air is saturated; in the case of sodium chloride nuclei at 78% relative humidity. The nuclei range in size from those with a radius of 0.001 μm , which are ineffective because of the high supersaturations required for condensation, to *giants* of over 10 μm which do not remain airborne for very long. Sea salts, which are particularly hygroscopic, enter the atmosphere

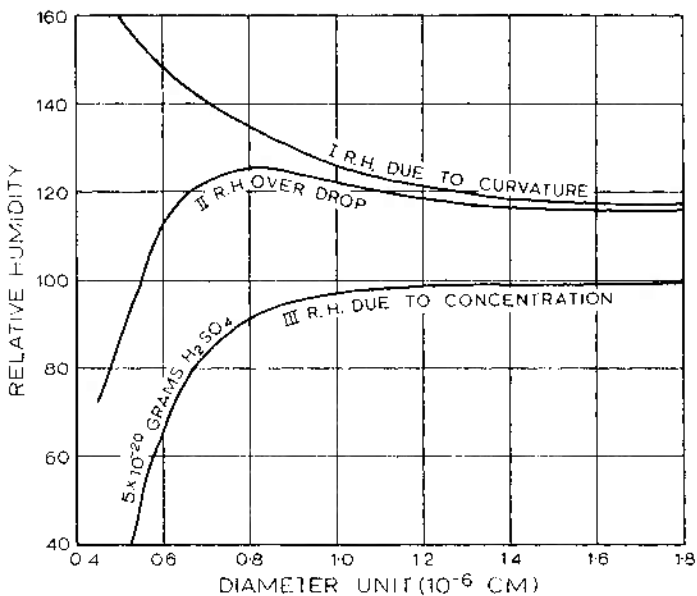


Fig. 2.16. The variation of relative humidity with droplet diameter. Curve I shows the effect due to curvature of the droplet and Curve III that due to a solution of 5×10^{-20} g of sulphuric acid. Curve II is the net result of curvature and solution concentration (from Simpson 1941).

principally by the bursting of air bubbles in foam, but fine soil particles and chemical combustion products raised by the wind are equally important sources of nuclei. On average, oceanic air contains one million condensation nuclei per litre (thousand cm^3) and land air holds some 5 or 6 million.

Once they are initially formed, the process of growth of water droplets is far from simple and much remains to be explained. In the early stages small drops grow more quickly than large ones, but, as the size of a droplet increases its growth rate by condensation decreases, as shown in fig. 2.17. The radial growth rate obviously slows down as the drop size increases because there is an increasingly greater surface area to add to with every increment of radius. However, the condensation rate is limited by the speed with which the released latent heat can be lost from the drop by conduction to the air and this heat reduces the vapour gradient.

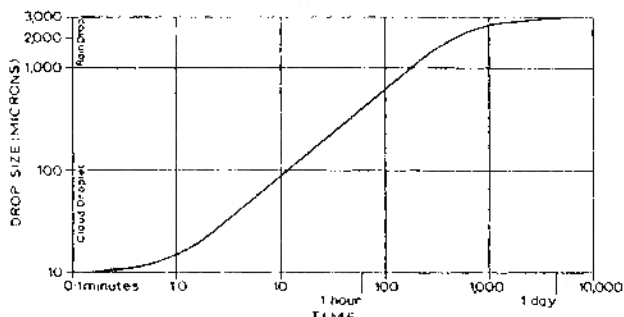


Fig. 2.17. Droplet growth by condensation (note the logarithmic scale).

Moreover competition between droplets for the available moisture increasingly tends to reduce the degree of supersaturation.

Supersaturation in clouds very rarely exceeds 1% and, because the saturation vapour pressure is greater over a curved droplet surface than over a plane water surface, very small droplets ($< 0.1 \mu\text{m}$ radius) are readily evaporated (fig. 2.16). In the early stages the nucleus size is important; for supersaturation of 0.05% a droplet of $1 \mu\text{m}$ radius with a salt nucleus of mass 10^{-13} g reaches $10 \mu\text{m}$ in 30 min, whereas one with a salt nucleus of 10^{-14} g would take 45 min. Later, when the dissolved salt has ceased to have significant effect, the radial growth rate becomes slow as a result of decreasing supersaturation (fig. 2.16).

Figure 2.17 illustrates not only the slow growth of droplets but also the immense size difference between cloud droplets (< 1 to $50 \mu\text{m}$ radius) and raindrops (exceeding 1 mm diameter). These facts strongly suggest that the gradual process of condensation is inadequate to explain the rates of formation of raindrops which are often observed. For example, in most clouds precipitation develops within an hour. It must be remembered too that falling raindrops undergo evaporation in the unsaturated air below the cloud base. A droplet of 0.1 mm radius evaporates after falling only 150 m at a temperature of 5°C and 90% relative humidity, but a drop of 1 mm radius would fall 42 km before evaporating. It seems likely then that cloud droplets are not necessarily the immediate source of raindrops. This point is taken up again in section G.

2 Cloud types

The great variety of cloud forms necessitates a classification for purposes of weather reporting. The internationally adopted system is based upon

(a) the general shape, structure and vertical extent of the clouds, and (b) its altitude.

These primary characteristics are used to define the ten basic groups (or genera) as shown in fig. 2.18. High cirriform cloud is composed of ice crystals giving a generally fibrous appearance. Stratiform clouds are

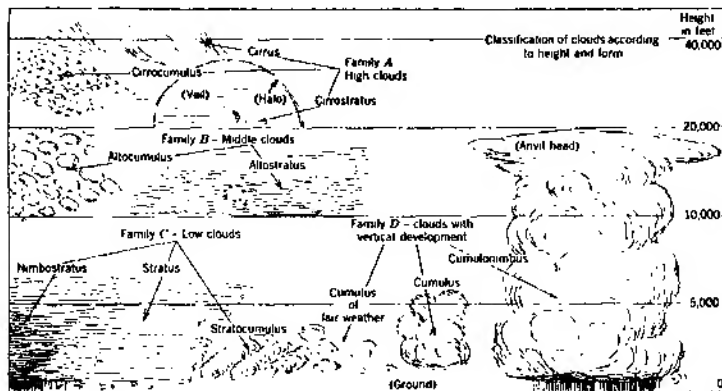


Fig. 2.18. The ten basic cloud groups classified according to height and form (from Strahler 1965).

layer-shaped, while cumuliform ones have a heaped appearance and usually show progressive vertical development. Other prefixes are *alto-* for middle level (medium) clouds and *nimbo-* for low cloud of considerable thickness, which appear dark grey and from which continuous rain is falling.

The height of the cloud base may show a considerable range for any of these types and varies with latitude. The approximate limits in thousands of metres for different latitudes are:

	Tropics	Middle latitudes	High latitudes
High cloud	Above 6	Above 5	Above 3
Medium cloud	2-7	5	2-4
Low cloud	Below 2	Below 2	Below 2

Following taxonomic practice, the classification subdivides the major groups into species and varieties with Latin names according to details of

their appearance. The World Meteorological Organization has produced an *International Cloud Atlas* illustrating all of these types.

Other possible classifications of clouds take into account their mode of origin. For instance, a broad genetic grouping can be made according to the mechanism of vertical motion which produces condensation. Four categories are:

- (a) gradual uplift of air over a wide area in association with a low-pressure system;
- (b) thermal convection (on the local cumulus-scale);
- (c) uplift by mechanical turbulence (*forced convection*);
- (d) ascent over an orographic barrier.

Group (a) includes a wide range of cloud types and will be discussed more fully in ch. 4, D.2. In connection with thermal convection, which forms cumuliform clouds, it is worth noting that upward convection currents (thermals) form plumes of warm air which, as they rise, expand and are carried downwind. Towers (*Castellanus*) in cumulus and other clouds are caused not by thermals of surface origin, but by ones set-up *within* the cloud as a result of the release of latent heat by condensation. Thermals gradually lose their impetus as mixing of cooler, drier air from the surroundings dilutes the more buoyant warm air. Group (c) includes fog, stratus or stratocumulus and is important whenever air near the surface is cooled to dew point by conduction or night-time radiation and the air is stirred by irregularities of the ground. The final group (d) could include stratiform or cumulus clouds produced by forced uplift of air over mountains (see pl. 3). Hill fog is simply stratiform cloud enveloping high ground. A special and important category is the wave (*lenticular*) cloud which develops when air flows over hills setting up a wave motion in the air current downwind of the ridge (see ch. 3, B.2). Clouds form in the crest of these waves if the air reaches its condensation level (see pls. 4, 6 and 7).

A great deal of information on cloud amounts, especially in remote areas, and on cloud patterns in relation to weather systems is now being provided by satellites of the American TIROS, ESSA and NIMBUS series (see eg., pls. 12 and 29). These investigations are supplying data that cannot be obtained by ground observations. Special classifications of cloud elements and patterns have been devised in order to analyse satellite imagery. The most common patterns seen on satellite photographs are cellular, with a typical diameter of 30 km. These develop from the movement of cold air over a warmer sea surface leading to mesoscale convec-

tive mixing. An open cellular pattern forms when there is a large air-sea temperature difference (2°C) (see pl. 16), whereas closed polygonal cells occur if this difference is small ($<0.5^{\circ}\text{C}$) and the vertical motion is limited by a subsidence inversion. Occasionally, subsidence over the tropical oceans leads to a modification of the cellular pattern referred to as actiniform (or radiating) illustrated in pl. 8. Cloud patterns related to frontal cyclonic systems are discussed in ch. 4 D (p. 197).

G Formation of precipitation

The puzzle of raindrop formation has already been briefly mentioned. The simple growth of cloud droplets is apparently an inadequate mechanism by itself, but if this is the case then more complex processes have to be envisaged.

Numerous early theories of raindrop growth have met with objections. For example, it was proposed that differently charged droplets could coalesce by electrical attraction, but it later appeared that distances between drops are too great and the difference between the electrical charges too small for it to happen. It was also suggested that large drops might grow at the expense of small ones, but observations showed that the distribution of droplet size in a cloud tends to maintain a regular pattern, with the average radius between about 10 to $15\ \mu\text{m}$ and a few larger than $40\ \mu\text{m}$. Another proposal was based on the variation of saturation vapour pressure with temperature, such that if atmospheric turbulence brought warm and cold cloud droplets into close conjunction the supersaturation of the air with reference to the cold drop surfaces and the undersaturation with reference to the warm drop surfaces would cause the warm drops to evaporate and the cold ones to develop at their expense. However, except perhaps in some tropical clouds, the temperature of cloud droplets is too low for this differential mechanism to operate. Figure 2.9 shows that below about 10°C the slope angle of the saturation vapour pressure curve is low. Another theory was that raindrops grow around exceptionally large condensation nuclei (such as have been observed in some tropical storms). Large nuclei, it is known, do experience a more rapid rate of initial condensation, but after this stage they are subject to the same limiting rates of growth that apply to all other atmospheric water drops.

The two main groups of current theories which attempt to explain the rapid growth of raindrops involve the growth of ice crystals at the expense of water drops, and the coalescence of small water droplets by the sweeping action of falling drops.

1 Bergeron-Findeisen theory

This theory forms an important part of the presently accepted mechanism of raindrop growth, and is based on the fact that the relative humidity of air is greater with respect to an ice surface than with respect to a water surface. As the air temperature falls below 0°C the atmospheric vapour pressure decreases more rapidly over an ice surface than over water (see fig. 1.5). This results in the saturation vapour pressure over water becoming greater than that over ice, especially between temperatures of -5°C and -25°C where the difference exceeds 0.2 mb, and if ice crystals and supercooled water droplets exist together in a cloud the latter tend to evaporate and direct deposition takes place from the vapour on to the ice crystals (this is often described by meteorologists as *sublimation*, which properly refers to direct evaporation from ice). Just as the presence of condensation nuclei is necessary for the formation of water droplets, so *freezing nuclei* are necessary before ice particles can form – usually at very low temperatures (about -15° to -25°C). Small water droplets can, in fact, be super-cooled in pure air to -40°C before spontaneous freezing occurs, but ice crystals generally predominate in clouds where temperatures are below about -22°C. Freezing nuclei are far less numerous than condensation nuclei; for example there may be as few as 10 per litre at -30°C and probably rarely more than 1000. However, some become active at higher temperatures. Kaolinite, a common clay mineral, becomes initially active at -9°C and on subsequent occasions at -4°C. The origin of freezing nuclei has been the subject of much debate but it is generally considered that very fine soil particles are a major source. Another possibility is that meteoric dust provides the nuclei, although there seems to be no firm evidence of a relationship between meteorite showers and rainfall. Volcanic dust ejected into the upper stratosphere and troposphere during eruptions might be an additional terrestrial source.

Once minute ice crystals have formed they grow readily by deposition from vapour, with different hexagonal forms of crystal developing at different temperature ranges. The number of ice crystals also tends to increase progressively because small splinters become detached during growth by air currents and act as fresh nuclei. The freezing of supercooled water drops may also produce ice splinters (see ch. 2, H). Ice crystals readily aggregate upon collision, due to their frequently branched (dendritic) shape, and tens of crystals may form a single snowflake. Temperatures between about 0°C and -5°C are particularly favourable to aggregation, because fine films of water on the crystals' surfaces freeze

when two crystals touch, binding them together. When the fall-speed of the growing ice mass exceeds the existing velocities of the air upcurrents the snowflake falls, melting into a raindrop if it passes through a sufficient depth of air warmer than 0°C.

This theory seems to fit most of the observed facts, yet it is not completely satisfactory. Cumulus clouds over tropical oceans can give rain when they are only some 2000 m (6500 ft) deep and the cloud-top temperature is 5°C or more. Even in middle latitudes in summer precipitation may fall from cumuli which have no subfreezing layer (*warm clouds*). A suggested mechanism in such cases is that of 'droplet coalescence', which is discussed below.

Practical rainmaking has been based on the Bergeron theory with some success, which at least supports its principal points. The basis of such experiments is the freezing nucleus. Super-cooled (water) clouds between -5°C and -15°C are *seeded* with especially effective nuclei, such as silver iodide or 'dry ice' (CO₂) from aircraft or ground-based generators in the case of silver iodide, promoting the growth of ice crystals and encouraging precipitation. Premature release of precipitation may destroy the updraughts and cause dissipation of the cloud, however. This explains why some seeding experiments have actually *decreased* the rainfall! In other instances cloud growth and precipitation have been achieved, with some individually spectacular results having been obtained by such methods in Australia and the United States. Programs aimed at increasing winter snowfall on the western slopes of the Sierra Nevada and Rocky Mountains by seeding cyclonic storms have been initiated, but it is still too early to regard such rain- (or snow-) making as a routine operation. Its success depends in any case on the presence of suitable super-cooled clouds. When several cloud layers are present in the atmosphere, natural seeding may be important. For example, if ice crystals fall from high-level cirrostratus or altostratus (a 'releaser' cloud) into nimbostratus (a 'spender' cloud) composed of supercooled water droplets, the latter can grow rapidly by the Bergeron process and such situations may lead to extensive and prolonged precipitation. This is a frequent occurrence in cyclonic systems in winter.

2 Collision theories

Alternative raindrop theories use collision, coalescence and 'sweeping' as the drop growth generator. It was originally thought that atmospheric turbulence by making cloud particles collide would cause a significant proportion to coalesce. Unfortunately, it was found that particles might

just as easily break up if subjected to collisions and it was also observed that there is often no precipitation from highly turbulent clouds. Langmuir offered a variation of this simple collision theory by pointing out that falling drops have terminal velocities directly related to their diameters such that the larger drops might overtake and absorb small droplets and that the latter might also be swept into the wake of the former and be absorbed by them. Figure 2.19 gives experimental results

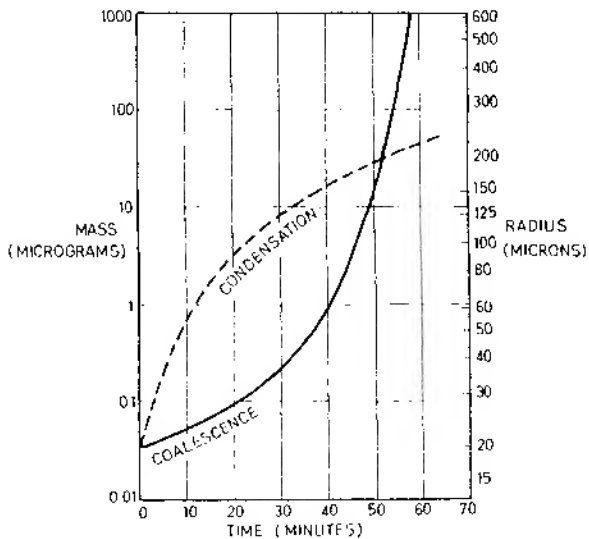


Fig. 2.19. Droplet growth by condensation and coalescence (from East and Marshall 1954).

of the rate of growth of water drops by coalescence and also of ice particles by vapour deposition from an initial radius of $20\text{ }\mu\text{m}$. Although coalescence is initially rather slow, the drop can reach $200\text{ }\mu\text{m}$ radius in just over 50 min. Calculations show that drops must exceed $19\text{ }\mu\text{m}$ in radius before they can coalesce with other droplets — smaller droplets being swept aside without colliding. The initial presence of a few larger drops calls for giant nuclei if the cloud top does not reach above the freezing level. However, if a few ice crystals are present at higher levels in the cloud (or if seeding occurs with ice crystals coming from higher cloud layers) they may eventually fall through the cloud as drops and the coalescence mechanism comes into action. Turbulence, especially in

cumuliform clouds, may serve to encourage collisions in the early stages and cloud electrification also increases the efficiency of coalescence. Thus, the coalescence process allows a more rapid growth than simple condensation can provide and is, in fact, fairly common in clouds in tropical maritime air masses, even in temperate latitudes.

3 Other types of precipitation

Rain has been discussed at length because it is the most common form of precipitation. Snow occurs when the freezing level is so near the surface that aggregations of ice crystals do not have time to melt before reaching the ground. Generally this means that the freezing level must be below 300 m. (1000 ft). Mixed snow and rain ('sleet' in British usage) is especially likely when the air temperature at the surface is about 1.5°C (34° to 35°F). Snow rarely occurs with an air temperature exceeding 4°C (39°F).

Soft hail pellets (roughly spherical, opaque grains of ice with much enclosed air) occur when the Bergeron process operates in a cloud with a small liquid water content and ice particles grow mainly by deposition of water vapour. Limited accretion of small super-cooled droplets forms an aggregate of soft, opaque ice particles 1 mm or so in radius. Showers of such pellets are quite common in winter and spring from cumulonimbus clouds.

Ice pellets may develop if the soft hail falls through a region of large liquid water content above the freezing level. Accretion forms a casing of clear ice around the pellet. Alternatively, an ice pellet consisting entirely of transparent ice may result from the freezing of a raindrop or the re-freezing of a melted snowflake.

True hailstones are roughly concentric accretions of clear and opaque ice. The embryo is a raindrop carried aloft in an updraught and frozen. Successive accretions of opaque ice (rime) occur due to impact of super-cooled droplets which freeze instantaneously, whereas the clear ice (glaze) represents a wet surface layer, developed as a result of very rapid collection of super-cooled drops in parts of the cloud with large liquid water content, which has subsequently frozen. A major difficulty in early theories was the necessity to postulate violently fluctuating upcurrents to give the observed banded hailstone structure, but a new thunderstorm model successfully accounts for this by demonstrating that the growing hailstones are re-cycled by the moving storm (see ch. 4, H). On occasions hailstones may reach giant size, weighing up to 0.76 kg each (recorded in September 1970 at Coffeyville, Kansas). In view of their rapid fallspeeds hailstones may fall considerable distances with little melting.

H Thunderstorms

In temperate latitudes probably the most spectacular example of moisture changes and associated energy releases in the atmosphere is the thunder-storm. Unusually great upward and downward movements of air are both the principal ingredients and motivating machinery of such storms. They occur: (a) as rising cells of excessively heated moist air; (b) along a *squall-line* in association with an air-mass discontinuity (see ch. 4, p. 216); or (c) in association with the triggering-off of conditional instability by uplift over mountains or by excessive local convergence (see ch. 3, B.1).

The life cycle of a storm lasts only 1 to 2 hours, and begins when a parcel of air is either warmer than the air surrounding it or is actively undercut by colder encroaching air. In both instances the air begins to rise and the embryo thunder cell forms as an unstable updraught of warm air (fig. 2.20). As condensation begins to form cloud droplets, latent heat is released and the initial upward impetus of the air parcel is augmented by an expansion and a decrease in density until the whole mass becomes completely out of thermal equilibrium with the surrounding air. At this stage updraughts commonly reach 10 m/sec, and may exceed 30 m/sec. The constant release of latent heat continuously injects fresh supplies of heat energy which accelerate the updraught and do not permit it to slacken. The rise of the air mass will continue as long as its temperature remains greater (or, in other words, its density less) than that of the surrounding air.

Raindrops probably begin to develop rapidly when the ice stage (or *freezing stage*) is reached by the vertical build-up of the cell, but they do not immediately fall to the ground because the updraughts are able to support them. An early and now unacceptable theory of thunderstorm electricity postulated that when raindrops rupture (after reaching a size of about 5 mm diameter) the larger droplets retain a positive charge and the spray from the surface film of water consists of negative ions (*Lenard effect*). This spray was assumed to be carried upwards giving the cloud tops a negative charge while the drops fell and charged the lower parts positively. However, observations demonstrated the opposite distribution of charges in most thunderclouds. One possible explanation is that, since the earth is charged negatively and the ionosphere positively, charged droplets in the atmosphere have an induced positive charge on their lower side and negative charge on their upper side. As the droplets fall they brush aside ions which have the same sign as their lower surface and collect negative ions (ions, it will be recalled, are charged particles formed

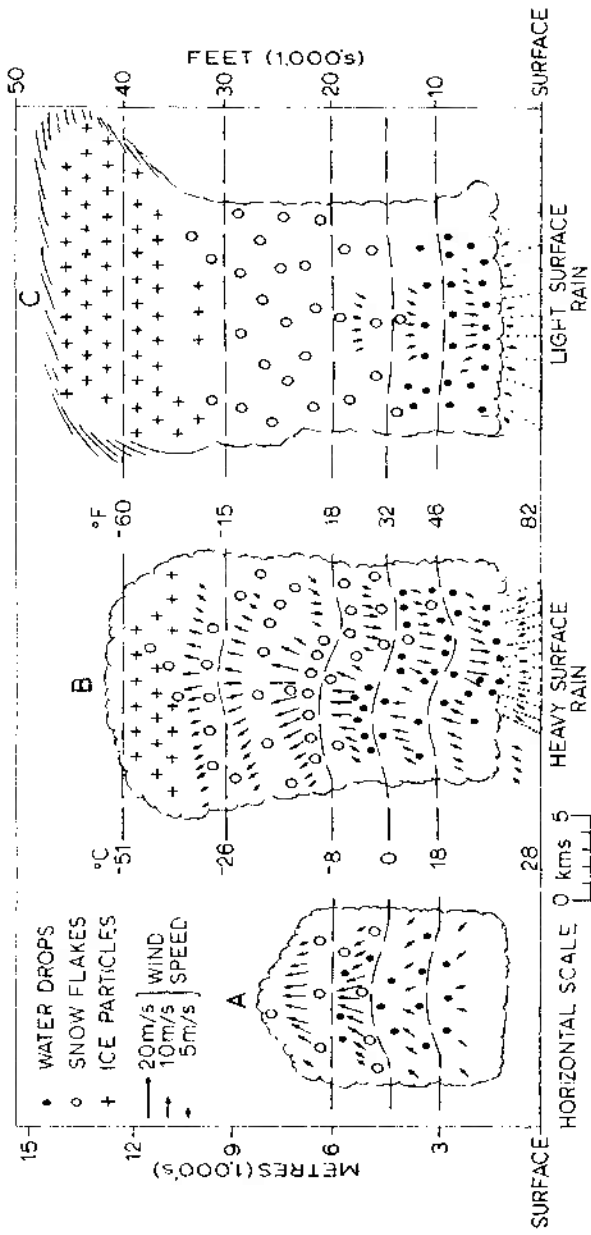


Fig. 2.20. The cycle of thunderstorm development. The arrows indicate the direction and speed of air currents.
 Left. The developing stage of the initial updraught.
 Centre. The mature stage with updraughts and downdraughts.
 Right. The dissipating stage dominated by cool downdraughts.
 (After Byers and Braham. Adapted from Petersen 1938.)

by radioactive gases from the earth or by the action of cosmic and ultraviolet rays). In this way the droplet becomes negatively charged and these falling droplets are naturally concentrated in the lower part of the cloud. This may explain part of the observed distribution of charges shown in fig. 2.21.

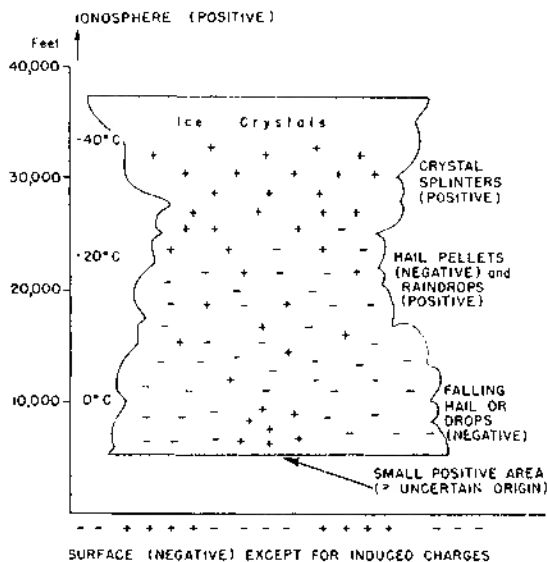


Fig. 2.21. The distribution of electrostatic charges in a thunder-cloud (*after Mason 1962*).

Many current theories of the generation of electrical charges are based on the effects of freezing. A major contribution has been made along these lines by Latham and Mason, involving two related ideas. A super-cooled droplet freezes inwards from its surface and this leads to a negatively-charged warmer core (OH^- ions) and a positively-charged colder surface due to the migration of H^+ ions outwards down the temperature gradient. When this soft hailstone ruptures during freezing small ice splinters carrying a positive charge are ejected by the ice shell and these are preferentially lifted to the top of the convection cell in updraughts. This theory helps to complete our understanding of the charge distribution in fig. 2.21, which shows that the upper part of the cloud (above about the -20°C isotherm) is positively charged. Equally,

the negatively charged hail pellets fall toward the cloud base; this factor is probably more important than the collection of negative ions by drops mentioned previously. Another process by which the thundercloud charges may be created involves the collision between cold ice crystals and warmer pellets of soft hail. Previous accretion of super-cooled droplets on the hail pellets produces an irregular surface which is warmed as the droplets release latent heat on freezing. The impacts of cold ice crystals on this irregular surface then generate negative charge while the colder crystals acquire positive charge. Again the effects of gravitational separation would lead to the observed distribution of charges. The origin of small positive areas near the cloud base (fig. 2.21) is still under discussion. They could arise through the action of convective updraughts carrying positive charge. It is likely that the very varied electrical properties of thunder clouds (from cloud to cloud and within individual clouds as they develop) cannot be explained by any single theory of charge generation.

Lightning commonly begins more or less simultaneously with precipitation downpours. It may occur between the lower part of the cloud and the ground (which locally has an induced positive charge). The first (leader) stage of the flash bringing down negative charge from the cloud is met near the ground by a return stroke which rapidly takes positive charge upward along the already-formed channel of ionized air. Just as the leader is neutralized by the return stroke, so the latter is neutralized in turn within the clouds. Subsequent leaders and return strokes drain higher regions of the cloud until its supply of negative charge is temporarily exhausted. Other more frequent flashes occur within a cloud or between clouds. The extreme heating and explosive expansion of air immediately round the path of the lightning sets up intense sound waves causing thunder to be heard.

Lightning is only one aspect of the atmospheric electricity cycle. During fine weather the earth's surface is negatively charged, the ionosphere positively charged. Atmospheric ions can conduct electricity down to the earth and hence a return supply must be forthcoming to maintain the observed electrical field. One source is the slow *point discharge*, from objects such as buildings and trees, of ions carrying positive charge induced by the negative thundercloud base. Similar upward currents occur above thunderstorm clouds. The other source (estimated to be smaller in its effect over the earth as a whole) is the upward transfer of positive charge by the much more rapid lightning strokes, leaving the earth negatively charged. The joint operation of these supply currents, in approximately 1800 thunderstorms over the globe at any instant, is thought to be suf-

ficient to balance the air-earth leakage, and this number seems to agree reasonably well with observational data.

The middle or mature stage of a storm (fig. 2.20B) is reached when the action of the falling precipitation causes frictional downdraughts of cold air. As these gather momentum cold air may eventually spread out below the thunder cell in a wedge. Gradually, as the moisture of the cell is expended, the supply of released latent heat energy diminishes, the downdraughts progressively gain in power over the warm updraughts, and the cell dissipates.

To simplify the explanation, a thunderstorm with only one cell was illustrated. Usually storms are far more complex in structure and consist of several cells arranged in clusters of 2–8 km across, 100 km or so in length and extending up to 10 km or more (see pl. 13). Such systems are known as squall lines (ch. 4, H).

I Precipitation characteristics and types

Strictly, *precipitation* refers to all liquid and frozen forms of water (p. 111) – rain, snow, hail, dew, hoar-frost, fog-drip and rime (ice accretion on objects through the freezing on impact of super-cooled fog droplets) – but, in general, only rain and snow make significant contributions to precipitation totals. In many parts of the world the term *rainfall* can be used interchangeably with precipitation. The data in the following section refer to rainfall, since snowfall is less easily measured with the same degree of accuracy.

It must be emphasized that precipitation records are only *estimates*. Factors of site location, gauge height, large- and small-scale turbulence in the air flow, splash-in, and evaporation all introduce errors in the catch. Falling snow is particularly subject to wind effects which can result in under-representation of the true amount by 50% or more.

1 *Precipitation characteristics*

There are many measures by which the various attributes of precipitation can be described, both in the long term and from the point of view of individual storms. Traditionally such long-term measures as mean annual precipitation, annual variability and year-to-year trends have been of great interest to the geographer, and these statistical measures are treated in the concluding chapter (see ch. 8, A). However, particularly in terms of hydrological considerations, the characteristics and relationships of individual rainstorms are being studied increasingly, and it is possible here

to point to some of their commonly observed features. Weather observations usually indicate the amount, duration and frequency of precipitation and these enable other derived characteristics to be determined. Three of these are discussed below.

a Rainfall intensity. The intensity (= amount/duration) of rainfall during an individual storm, or a still shorter period, is of vital interest to hydrologists and water engineers concerned with flood forecasting and prevention, as well as to conservationists dealing with soil erosion. Chart records of the rate of rainfall (*hyetograms*) are necessary to assess intensity, which varies markedly with the time interval selected. Average intensities for short periods (thunderstorm-type downpours) are much greater than those for longer time intervals as fig. 2.22 illustrates for Washington,

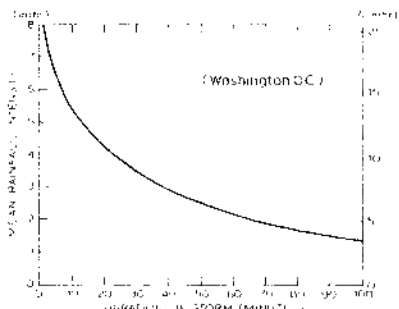


Fig. 2.22. Generalized relationship between precipitation intensity and duration for Washington, D.C. (after Yarnell 1935).

D.C. In the case of extreme rates at different points over the earth (fig. 2.23) the record intensity over 10 min is approximately three times that for 100 mins, and the latter exceeds by as much again the record intensity over 1000 mins (i.e. 16½ hours). High-intensity rain is associated with increased drop size rather than an increased number of drops. For example, with precipitation intensities of 0.1, 1.3 and 10.2 cm/hr (i.e. 0.05, 0.5 and 4.0 in/hr), the most frequent raindrop diameters are 0.1, 0.2 and 0.3 cm, respectively. The occurrence of daily amounts exceeding 1.3 cm (0.5 in) is considered to be important for gully erosion in North America. Such falls account for 90% of the annual rainfall on the Gulf Coast compared with only 20% in the Great Basin.

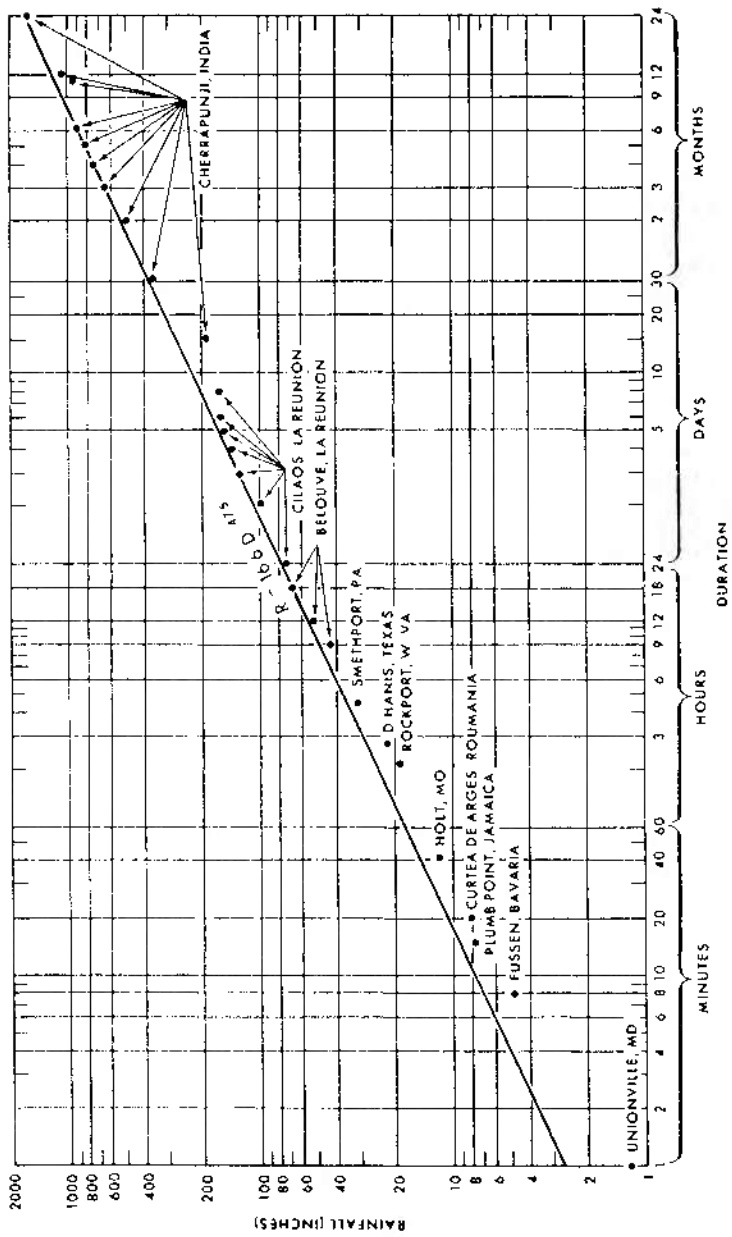


Fig. 2.23. World record rainfalls and the 'envelope' of expected extremes at any place. The equation of the envelope line is given, together with the state or country where each record was established (from Paraphus 1965).

b Areal extent of a rainstorm. The rainfall totals received in a given time interval vary according to the size of the area which is considered, showing a relationship analogous to that of rainfall duration and intensity. The maximum 24-hour rainfalls over areas of different extent in the United States (up to 1960) were as follows:

Sq. miles	Cm	In
10 (25 9 km ²)	98.3	38.7
10 ²	89.4	35.2
10 ³	76.7	30.2
10 ⁴	30.7	12.1
10 ⁵	10.9	4.3

(After Gilman 1964)

Fig. 2.24, based on data of this type, illustrates the maximum rainfall to be expected for a given storm area and given duration in the United States.

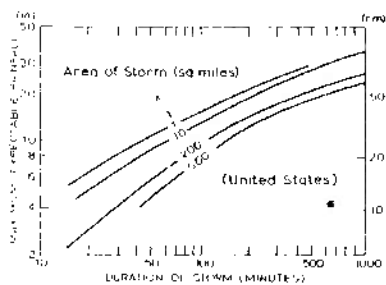


Fig. 2.24. Enveloping depth/duration curves for maximum rainfall for areas of under 500 square miles in the United States (after Berry, Bollay and Beers 1945).

c Frequency of rainstorms. Another useful item is the average time-period within which a rainfall of specified amount or intensity can be expected to occur once. This is known as the *recurrence interval* or *return period*. Figure 2.25 gives this type of information on rainfall amount and duration for Cleveland, Ohio. From this it would appear that a 10-min fall of 2.5 cm (1 in) is likely about once every 20 years, a 24-hour fall of 10 cm (4 in) about once every 30 years. However, this *average return*

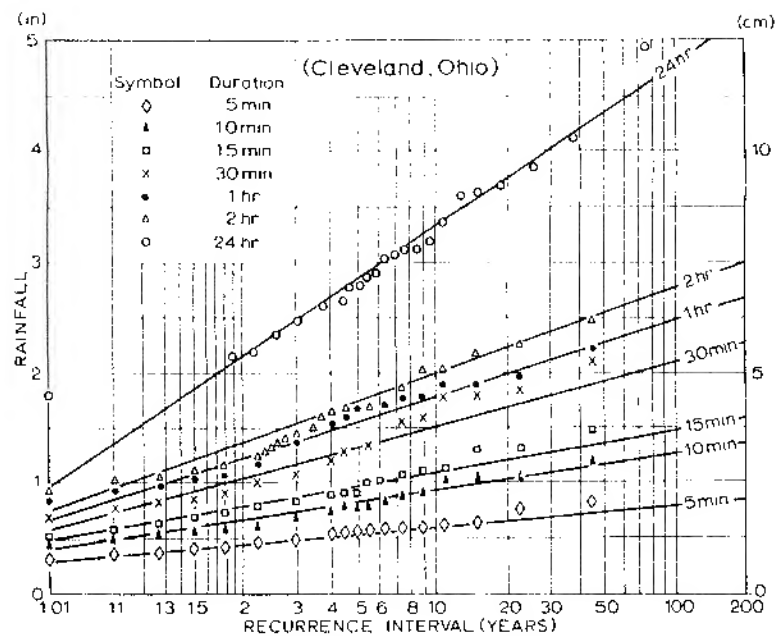


Fig. 2.25. Rainfall/duration/frequency curves for Cleveland, Ohio (1902–1947) (after Linsley and Franzini 1955).

period does not mean that such falls necessarily occur in the twentieth and thirtieth years, respectively, of a selected period. Indeed, they might occur in the first! These estimates require long periods of observational data, but the approximately linear relationships shown by such graphs are of great practical significance for the design of flood-control systems.

2 Precipitation types

The above material can now be related to that of the previous sections in a discussion of precipitation types. A convenient starting point is the usual division into three main types – convective, cyclonic and orographic precipitation – according to the assumed mode of uplift of the air. Essential to this analysis is some knowledge of storm systems. These are treated in later chapters and the newcomer to the subject may prefer to read the following in conjunction with them.

a 'Convective type' precipitation. This is associated with towering

cumulus (*cumulus congestus*) and cumulonimbus clouds. Three sub-categories can be distinguished according to their degree of spatial organization.

(i) Scattered convective cells develop through strong heating of the land surface in summer, especially when lower upper tropospheric temperatures facilitate the release of conditional or convective instability (see ch. 2, E). Precipitation, often including hail, is of the thunderstorm type, although thunder and lightning do not necessarily occur. Limited areas, of the order of 20 to 50 km², are affected by the individual heavy downpours, which generally last for about $\frac{1}{2}$ to 1 hour.

(ii) Showers of rain, snow or soft hail pellets may form in cold, moist unstable air passing over a warmer surface. Convective cells moving with the wind can produce a streaky distribution of precipitation parallel to the wind direction, although over a period of several days the variable paths and intensities of the showers tend to obscure this pattern.

Two locations in which these occur are parallel to a surface cold front in the warm sector of a depression (sometimes as a squall line) or parallel to and ahead of the warm front. Hence the precipitation is widespread, though of brief duration at any locality.

(iii) In tropical cyclones cumulonimbus cells become organized about the vortex in spiralling bands (see ch. 6, C.2). Particularly in the decaying stages of such cyclones, typically over land, the rainfall can be very heavy and prolonged, affecting areas of thousands of square kilometres.

b 'Cyclonic type' precipitation. Precipitation characteristics vary according to the type of low-pressure system and its stage of development, but the essential mechanism is ascent of air through horizontal convergence of airstreams in an area of low pressure (see ch. 3, B.1). In extra-tropical depressions this is reinforced by uplift of warm, less-dense air along an air-mass boundary (see ch. 4, D.2). Such depressions give moderate and generally continuous precipitation over very extensive areas as they move usually eastward in the westerly wind belts between about 40° and 65° latitude. The precipitation belt in the forward sector of the storm can affect a locality in its path for 6 to 12 hours, whereas the belt in the rear gives a shorter period of thunderstorm-type precipitation. These sectors are, therefore, sometimes distinguished in precipitation classifications, and a more detailed breakdown is illustrated in table 5.4. Polar lows (see ch. 4, G.3) combine the effects of airstream convergence and convective activity of category *a(ii)*, above, whereas troughs in the equatorial low-pressure area give convective precipitation as a result of airstream convergence in the easterlies (see ch. 6, C.1).

c *Orographic precipitation.* Orographic precipitation is commonly regarded as a distinct type, but this requires careful qualification. Mountains are not especially efficient in causing moisture to be removed from airstreams crossing them, yet because precipitation falls repeatedly in more or less the same locations the cumulative totals are large. Orography, dependent on the alignment and size of the barrier, may (i) trigger conditional or convective instability by giving an initial upward motion or by differential heating of the mountain slopes, (ii) increase cyclonic precipitation by retarding the rate of movement of the depression system, (iii) cause convergence and uplift through the funnelling effects of valleys on airstreams. In mid-latitude areas where precipitation is predominantly of cyclonic origin, orographic effects tend to increase both frequency and intensity of winter precipitation, whereas during summer and in continental climates with a higher condensation level the main effect of relief is the occasional triggering of intense thunderstorm-type precipitation. The orographic influence occurs only in the proximity of high ground in the case of a stable atmosphere. Recent radar studies show that the main effect in this case is one of redistribution, whereas in the case of an unstable atmosphere precipitation appears to be increased, or at least redistributed on a larger scale, since the orographic effects may extend well downwind due to the activation of the mesoscale rain bands (see fig. 4.10).

Two special cases of orographic effects may be mentioned. One is the general influence of surface friction which by turbulent uplift may assist the formation of stratus or stratocumulus layers when other conditions are suitable (see ch. 2, C.2). Only light precipitation (drizzle, light rain or snow grains) is to be expected under these circumstances. The other case arises through frictional slowing down of an airstream moving inland over the coast. A particular instance of the convergence and uplift which this may initiate has been reported by Bergeron. During a 24-hour period in October 1945, a west-south-westerly airstream over Holland produced a belt of precipitation (3 cm or more) — a result of frictional convergence and uplift — in crossing the narrow zone of coastal sand dunes only a few metres high. Over the remainder of that virtually flat country a series of lee waves developed in the tropospheric airflow downwind from the coast (see fig. 3.9, for example), and these gave a series of transverse (north-south) bands of precipitation up to 2 cm in amount. On the following day the surface flow had changed little, but a temperature decrease from -20°C to -28°C at the 500-mb level altered the vertical stability so that the lee waves broke down and the precipitation distribution showed

convective streaks, up to 4 cm per day, parallel to the surface wind direction.

3 Regional variations in the altitudinal maximum of precipitation

The increase of precipitation with height is a world-wide characteristic with only a few exceptions. In middle and higher latitudes this is particularly pronounced on west-coast mountain ranges, but is less apparent inland. In North America the Sierras and Coast Ranges, on the one hand, compared with the Rockies on the other, clearly demonstrate this effect (see ch. 5, B.2). In Western Britain with mountains of about 1000 m, the maximum falls are recorded to leeward of the summits. This probably reflects the general tendency of air to go on rising for a while after it has crossed the crestline and the time-lag involved in the precipitation process after condensation. Over narrow uplands the horizontal distance may allow insufficient time for maximum cloud build-up and the occurrence of precipitation. However, a further factor may be the effect of eddies, set up in the airflow by the mountains, on the catch of rain gauges. Studies in Bavaria at the Hohenpeissenberg observatory show that standard rain gauges may overestimate amounts by about 10% on the lee slopes and underestimate them by 14% on windward slopes.

In the tropics and subtropics the maximum precipitation occurs below the higher mountain summits, from which level it decreases upwards towards the crests. Observations are generally sparse in the tropics, but numerous records from Java show that the average elevation of greatest precipitation is approximately 1200 m (4000 ft). Above about 2000 m the decrease in amounts becomes quite marked. Similar features are reported from Hawaii and, at a rather higher elevation, on mountains in East Africa (see ch. 6, E.3). Figure 2.26A shows that, despite the wide range of records for individual stations, this effect is clearly apparent along the Pacific flank of the Guatemalan Highlands. Further north along the coast, the occurrence of a precipitation maximum below the mountain crest is observed in the Sierra Nevadas, despite some complication introduced by the shielding effect of the Coast Ranges (fig. 2.26B), but in the Olympic Mountains of Washington precipitation increases right up to the summits (fig. 2.26C). As has been previously mentioned, precipitation catches on mountain crests may underestimate the actual precipitation due to the effect of eddies, and this is particularly true where much of the precipitation falls in the form of snow which is very susceptible to blowing by the wind.

One explanation of this orographic difference between tropical and

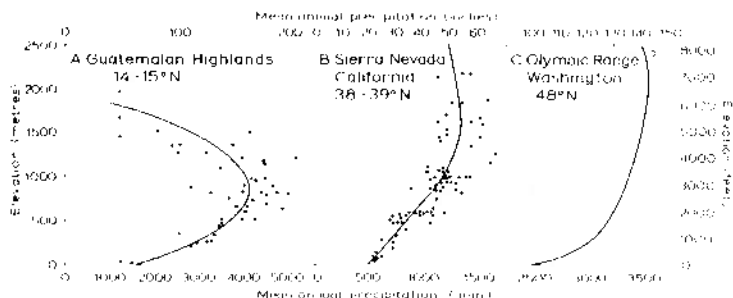


Fig. 2.26. Generalized curves showing the relationship between elevation and mean annual precipitation for west-facing mountain slopes in Central and North America. The dots give some indication of the wide scatter of individual precipitation readings (*adapted from Hastenrath 1967 and Armstrong and Stidd 1967*).

temperate rainfall is based on the concentration of moisture in a fairly shallow layer of air near the surface in the tropics (see ch. 6, A). Much of the orographic precipitation seems to derive from warm clouds (particularly cumulus congestus), composed of water droplets, which commonly have an upper limit at about 3000 m. It is probable that the height of the maximum precipitation zone is close to the mean cloud base since the maximum size and number of falling drops will occur at that level. Thus, stations located above the level of mean cloud base will receive only a proportion of the orographic increment. In temperate latitudes much of the precipitation, especially in winter, falls from stratiform cloud which commonly extends through a considerable depth of the troposphere. In this case there tends to be a smaller fraction of the total cloud depth below the station level. These differences according to cloud type and depth are apparent even on a day-to-day basis in middle latitudes, as has been shown by detailed studies in the Bavarian Alps. Seasonal variations in the altitude of the mean condensation level and zone of maximum precipitation are similarly observed. In the mountains of central Asia (the Pamirs and Tien Shan), for instance, the maximum is reported to occur at about 1500 m (5000 ft) in winter and at 3000 m (9900 ft) in summer.

4 The world pattern of precipitation

A glance at the maps of precipitation amount for December–February and June–August (fig. 2.27) indicates that the distributions are considerably more complex than those, for example, of mean temperature

(see fig. 1.13). Comparison of fig. 2.27 with the meridional profile or average precipitation for each latitude (see fig. 2.4A) brings out the marked longitudinal variations that are superimposed on the zonal pattern. The latter has three main features: an equatorial maximum which, like the thermal equator, is slightly displaced into the northern hemisphere; very low totals in high latitudes; and secondary minima in subtropical latitudes. Fig. 2.27 demonstrates why the subtropics do not appear as particularly dry on the meridional profile in spite of the known aridity of the subtropical high pressure areas (see ch. 3, C.3 and 5, D.2). In these latitudes the eastern sides of the continents receive considerable rainfall in summer.

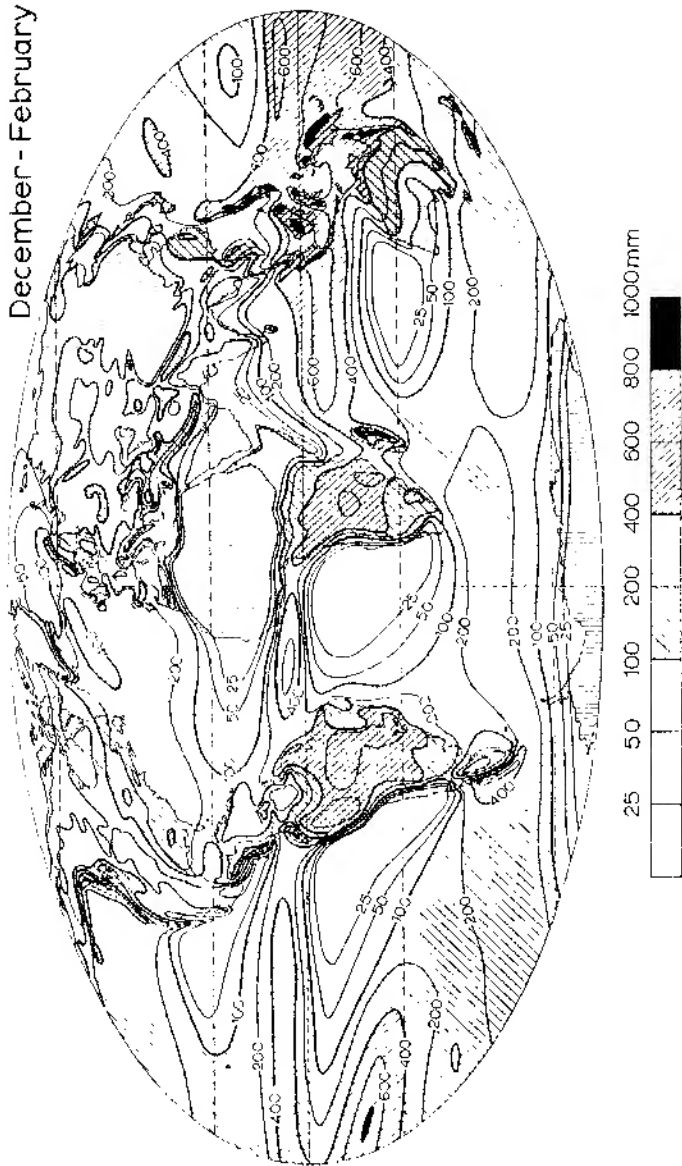
In view of the complex controls involved, no brief explanation of these precipitation distributions can be very satisfactory. Various aspects of selected precipitation regimes are examined in chs. 5 and 6, after consideration of the fundamental ideas about atmospheric motion, air masses and frontal zones. A classification of wind belts and precipitation characteristics is outlined in app. 1.C. It must suffice at this stage simply to note the factors which have to be taken into account in studying fig. 2.27.

- (i) The limit imposed on the maximum moisture content of the atmosphere by air temperature. This is important in high latitudes and in winter in continental interiors.
- (ii) The major latitudinal zones of moisture influx due to atmospheric advection. This in itself is a reflection of the global wind systems and their disturbances (i.e. the converging trade wind systems and the cyclonic westerlies, in particular).
- (iii) The distribution of the land masses. It is noteworthy that the southern hemisphere lacks the vast, arid, mid-latitude continental interiors of the northern. The oceanic expanses of the southern hemisphere allow the mid-latitude storms to increase the zonal precipitation average for 45°S by about one third compared with that of the northern hemisphere for 50°N (see fig. 2.4A). Another major non-zonal feature is the occurrence of the monsoon regimes, especially in Asia.
- (iv) The distribution of mountain areas with respect to the locally prevailing winds.

5 *Drought*

The term drought implies an absence of significant precipitation for a period which is long enough to cause moisture deficits in the soil due to evapotranspiration and decreases in stream flow, thereby disrupting the

December - February



June - August



Fig. 2.27. Mean global precipitation (in mm) for the periods December–February and June–August (from Möller 1991).

normal biological and human activities. Thus a drought condition may obtain after only three weeks without rain in parts of Britain, whereas some areas of the tropics regularly experience many successive dry months. All regions suffer the temporary but irregularly-recurring condition of drought, but particularly those with marginal climates alternately influenced by differing climatic mechanisms. Drought is therefore especially associated with:

- (i) Increases in area and persistence of the subtropical high pressure cells. Drought in southern Israel has been shown to be significantly related to this mechanism.
- (ii) Changes in the summer monsoonal circulation, causing a postponement or failure of incursions of maritime tropical air, such as may occur in northern Nigeria or the Punjab.

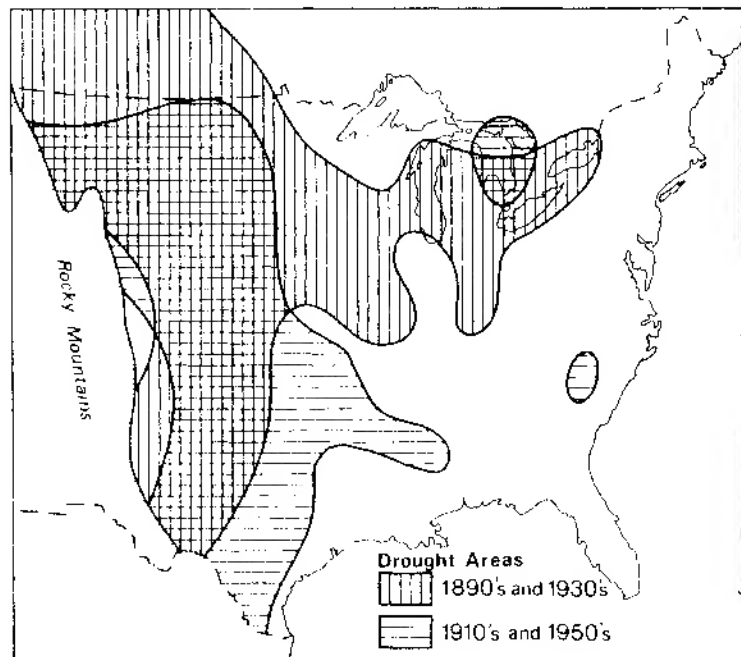


Fig. 2.28. Drought areas for the central USA based on areas receiving less than 80% of the normal July–August precipitation (after Borchert 1971).

- (iii) Lower ocean surface temperatures produced by changes in currents or increased upwelling of cold waters. Rainfall in California and Chile may be affected by such mechanisms (see p. 180).
- (iv) Southward displacement of the mid-latitude storm tracks associated with an expansion of the circumpolar vortex, the development of large-amplitude quasi-stationary long waves in the westerlies and the contraction equatorwards of the meridional circulation in the tropics (see p. 363). It has been suggested that droughts on the Great Plains east of the Rockies in the 1890s and 1930s were due to such changes in the general circulation. However, the droughts of the 1910s and 1950s in this area were caused by persistent high pressure in the southeast and the northward displacement of storm tracks (see fig. 2.28).

Clearly, the most severe and prolonged droughts involve combinations of the above mechanisms, and it is possible that the present drought in the Sudano-Sahelian zone is due to an eastwards strengthening of the Azores high pressure cell, lower surface temperatures in the eastern North Atlantic and an expansion of the circumpolar vortex.

3 Atmospheric motion

The atmosphere acts somewhat in the same manner as a gigantic heat engine in which the constantly maintained difference in temperature existing between the poles and the equator provides the energy supply necessary to drive the planetary atmospheric circulation. The conversion of the heat energy into kinetic energy to produce motion must involve rising and descending air, but vertical movements are generally much less in evidence than horizontal ones, which may cover vast areas and persist for periods of a few days to several months.

Before considering these global aspects, however, it is important to look at the immediate controls on air motion. The downward-acting gravitational field of the earth sets up the observed decrease of pressure away from the earth's surface that is represented in the vertical distribution of atmospheric mass (fig. 1.4). This mutual balance between the force of gravity and the vertical pressure gradient is referred to as *hydrostatic equilibrium*. This state of balance, together with the general stability of the atmosphere and its shallow depth, greatly limits vertical air motion. Average horizontal wind speeds are of the order of one hundred times greater than average vertical movements, though individual exceptions occur – particularly in convective storms.

A Laws of horizontal motion

There are four controls on the horizontal movement of air near the earth's surface: pressure gradient force, Coriolis force, centripetal acceleration

and frictional forces. The primary cause of air movement is the development of a horizontal pressure gradient and the fact that such a gradient can persist (rather than being destroyed by air motion towards the low pressure) results from the effect of the earth's rotation in giving rise to the Coriolis force.

1 The pressure gradient force

The pressure gradient force has vertical and horizontal components but, as already noted, the vertical component is more or less in balance with the force of gravity. Horizontal differences in pressure can be due to thermal or mechanical causes (often not easily distinguishable), and these differences control the horizontal movement of an air mass. In effect the pressure gradient serves as the motivating force which causes the movement of air away from areas of high pressure and towards areas where it is lower, although other forces prevent air from moving directly across the isobars (lines of equal pressure). The pressure gradient force per unit mass is expressed mathematically as

$$-\frac{1}{\rho} \frac{dp}{dn}$$

where ρ = air density and dp/dn = the horizontal gradient of pressure. Hence the closer the isobar spacing the more intense is the pressure gradient and the greater the wind speed. The pressure gradient force is also inversely proportional to air density and this relationship is of particular importance in understanding the behaviour of upper winds.

2 The earth's rotational deflective (Coriolis) force

The Coriolis force arises from the fact that the movement of masses over the earth's surface is usually referred to a moving co-ordinate system (i.e. the latitude and longitude grid which 'rotates' with the earth). The simplest way to begin to visualize the manner in which this deflecting force operates to picture a rotating disc on which moving objects are deflected. Figure 3.1 shows the effect of such a deflective force operating on a mass moving outward from the centre of a spinning disc. The body follows a straight path in relation to a fixed frame of reference (for instance, a box which contains a spinning disc), but viewed relative to co-ordinates rotating with the disc the body swings to the right of its initial line of motion. This effect is readily demonstrated if a pencil line is drawn across a white disc on a rotating turntable. Figure 3.2 illustrates a case where the movement is not from the centre of the turntable and the object possesses an initial momentum in relation to its distance from the axis of

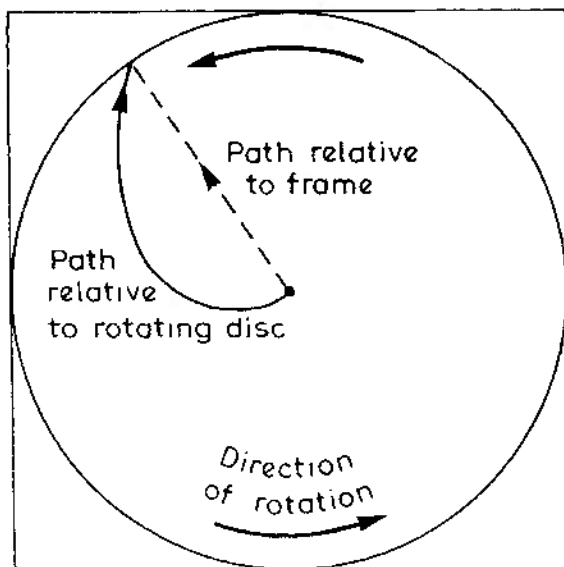


Fig. 3.1. The Coriolis deflecting force operating on a body moving outward from the centre of a rotating turntable.

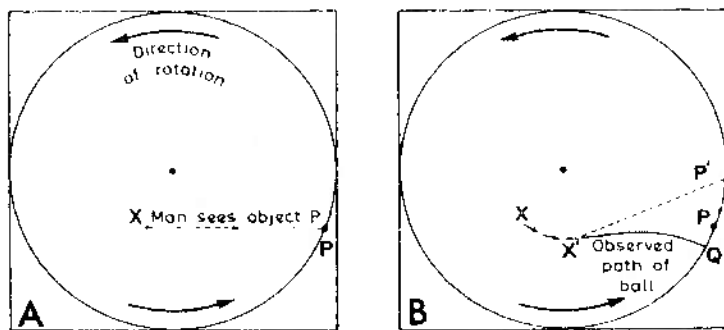


Fig. 3.2. The Coriolis deflecting force on a rotating turntable.

- A. A man at X sees the object P and attempts to throw a ball towards it. Both locations are rotating anticlockwise.
- B. The man's position is now X' and the object is at P'. To the man, the ball appears to follow a curved path and lands at Q. The man overlooked the fact that P was moving to his left and that the path of the ball would be affected by the initial impetus due to the man's own rotation.

rotation. In the analogous case of the rotating earth (with rotating reference co-ordinates of latitude and longitude), there is apparent deflection of moving objects to the right of their line of motion in the northern hemisphere and to the left in the southern hemisphere, as viewed by observers on the earth. The deflective force (per unit mass) is expressed by:

$$-2\omega V \sin \phi$$

where ω = the angular velocity of spin ($15^\circ/\text{hr}$ or $2\pi/24$ radians/hr for the earth = 7.29×10^{-5} radians/sec); ϕ = the latitude and V = the velocity of the mass. $2\omega \sin \phi$ is referred to as the Coriolis parameter (f).

The magnitude of the deflection is directly proportional to: (a) the horizontal velocity of the air (i.e. air moving at 11 m/sec (25 mph) having half the deflective force operating on it as that moving at 22 m/sec (50 mph)); and (b) the sine of the latitude ($\sin 0^\circ = 0$; $\sin 90^\circ = 1$). The effect is thus a maximum at the poles (i.e. where the plane of the deflecting force is parallel with the earth's surface) and decreases with the sine of the latitude, becoming zero at the equator (i.e. where there is no component of the deflection in a plane parallel to the surface). Values of f vary with latitude as follows:

Latitude	0°	10°	20°	43°	90°
$f(10^{-4}/\text{sec})$	0	0.25	0.50	1.00	1.458

The Coriolis force always acts at right angles to the direction of the air motion to the right in the northern hemisphere and to the left in the southern hemisphere.

The earth's rotation also produces a vertical component of rotation about a horizontal axis. This is a maximum at the equator (zero at the poles), but it is much less important to atmospheric motions due to the existence of hydrostatic equilibrium.

3 The geostrophic wind

Observations in the *free atmosphere* (above the level affected by surface friction at about 500 to 1000 m) show that the wind blows more or less at right angles to the pressure gradient (i.e. parallel to the isobars) with, for the northern hemisphere, the high-pressure core on the right and the low-pressure on the left when viewed downwind. This implies that for steady motion the pressure gradient force is exactly balanced by the Coriolis deflection acting in the diametrically opposite direction (fig. 3.3). The

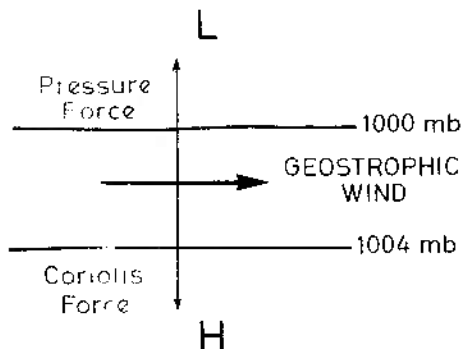


Fig. 3.3. The geostrophic wind case of balanced motion (northern hemisphere).

wind in this idealized case is called a *geostrophic wind*, the velocity (V_g) of which is given by the following formula:

$$V_g = \frac{1}{2\omega \sin \phi \rho} \cdot \frac{dp}{dn}$$

where dp/dn = the pressure gradient. The velocity is thus inversely dependent on latitude, such that the same pressure gradient which will be associated with geostrophic wind speeds of 15 m/sec (34 mph) at latitude 43° will produce a velocity of only 10 m/sec (23 mph) at latitude 90° . Except in low latitudes, where the Coriolis deflection approaches zero, the geostrophic wind is a close approximation to the observed air motion in the free atmosphere. Since pressure systems are rarely stationary this fact implies that air motion must continually change towards a new balance. In other words mutual adjustments of the wind and pressure fields are constantly taking place. The common 'cause-and-effect' argument that a pressure gradient is formed and air begins to move towards low pressure before coming into geostrophic balance is an unfortunate oversimplification of reality.

4 The centripetal acceleration

For a body to follow a curved path there must be an inward acceleration towards the centre of rotation. This acceleration (c) is expressed by:

$$c = -\frac{mV^2}{r}$$

where m = the moving mass, V = its velocity and r = the radius of curvature. This factor is sometimes regarded for convenience as a centrifugal force operating radially outward¹. In the case of the earth itself this is valid. The centrifugal effect due to rotation has in fact resulted in a slight bulging of the earth's mass in low latitudes and a flattening near the poles. The decrease in apparent gravity towards the equator reflects the effect of the centrifugal force working against the gravitational attraction directed towards the earth's centre. It is only necessary therefore to consider the forces involved in the rotation of the air about a local axis of high or low pressure. Here the curved path of the air (parallel to the isobars) is maintained by an inward-acting, or centripetal, acceleration.

Figure 3.4 shows (for the northern hemisphere) that in a low-pressure system balanced flow is maintained in a curved path (referred to as the *gradient wind*) by the Coriolis force being weaker than the pressure force.

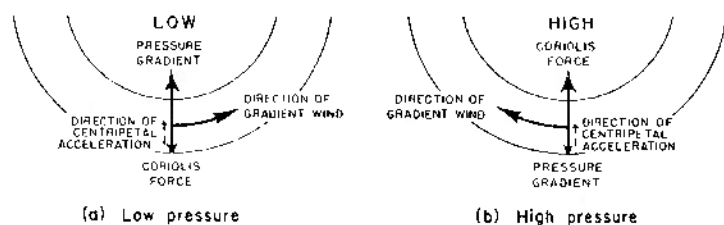


Fig. 3.4. The gradient wind case of balanced motion around a low pressure (a) and a high pressure (b) in the northern hemisphere.

The difference between the two gives the net centripetal acceleration inward. In the high-pressure case the inward acceleration is provided by the Coriolis force exceeding the pressure force. Since the pressure gradients are assumed to be equal, the different contributions of the Coriolis force in each case imply that the wind speed around the low-pressure must be less than the geostrophic value (*subgeostrophic*) whereas in the high-pressure case it is *supergeostrophic*. In reality this effect is obscured by the fact that the pressure gradient in a high is usually much weaker than in a low. Moreover, the fact that the earth's rotation is cyclonic imposes a limit on the speed of anticyclonic flow. The maximum occurs when the angular velocity is $f/2 (= \omega \sin \phi)$, at which value the absolute rotation of the air (viewed from space) is just cyclonic. Beyond this point anticyclonic flow breaks down ('dynamic instability'). There is no maximum speed in the case of cyclonic rotation.

¹ The centrifugal force is equal in magnitude and opposite in sign to the centripetal acceleration.

The magnitude of the centripetal acceleration is generally small, and it only becomes really important where high-velocity winds are moving in very curved paths (i.e. about an intense low-pressure system). Two cases are of meteorological significance: firstly, in intense cyclones near the equator where the Coriolis force is negligible; and, secondly, in a narrow vortex such as a tornado. Under these conditions, when the large pressure gradient force provides the necessary centripetal acceleration for balanced flow parallel to the isobars, the motion is called *cyclostrophic*.

The above arguments all assume steady conditions of balanced flow. This simplification is useful, but it must be noticed that two factors prevent a continuous state of balance. Latitudinal motion changes the Coriolis parameter and the movement or changing intensity of a pressure system leads to acceleration or deceleration of the air, causing some degree of cross-isobaric flow. Pressure change itself depends on air displacement through the breakdown of the balanced state. If air movement were purely geostrophic there would be no growth or decay of pressure systems. The acceleration of air in moving at upper levels from a region of cyclonic isobaric curvature (subgeostrophic wind) to one of anticyclonic curvature (supergeostrophic wind) causes a fall of pressure at lower levels in the atmosphere through the removal of air aloft. The significance of this fact will be discussed in ch. 4, F. The interaction of horizontal and vertical air motions is outlined in ch. 3, B.2.

5 Frictional forces

The last force which has an important effect on air movement is that due to friction with the earth's surface. If we follow our study of geostrophic wind a little further we find that towards the surface (i.e. below about 500 m for flat terrain) friction begins to decrease the wind velocity below its geostrophic value. This has an effect on the deflective force (which is dependent on velocity) causing it also to decrease. As these two tendencies continue the wind consequently blows more and more obliquely across the isobars in the direction of the pressure gradient. The angle of obliqueness increases with the growing effect of frictional drag due to the earth's surface and it averages about 10° – 20° at the surface over the sea and 25° – 35° over land. The result is to produce a wind spiral with height (fig. 3.5), analogous to the turning of ocean currents as the effect of wind stress diminishes with increasing depth. Both are referred to as 'Ekman spirals', after Ekman who investigated the variation of ocean currents with depth (see ch. 3, F.3).

In summary, the surface wind (neglecting any curvature effects)

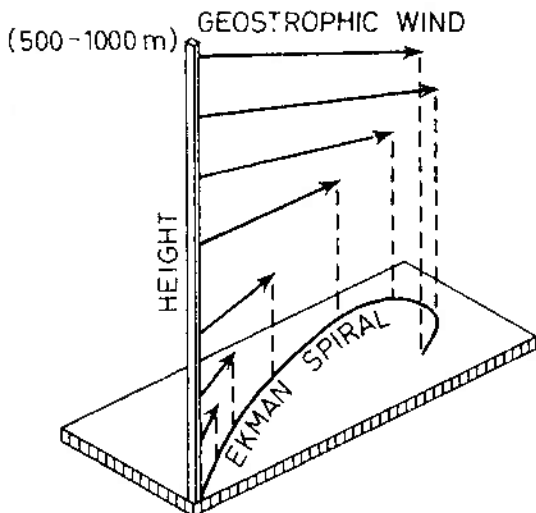


Fig. 3.5. The Ekman spiral of wind with height, in the northern hemisphere. The wind attains the geostrophic velocity at between 500 and 1000 m in the middle and higher latitudes as frictional drag effects become negligible. This is a theoretical profile of wind velocity under conditions of mechanical turbulence.

represents a balance between the pressure gradient force and friction parallel to the air motion and between the pressure gradient force and the Coriolis force perpendicular to the air motion.

B Divergence, vertical motion and vorticity

These three terms essentially hold the key to a proper understanding of modern meteorological studies of wind and pressure systems on a synoptic and global scale. Mass uplift or descent of air occurs primarily in response to dynamic factors related to horizontal airflow and is only secondarily affected by air-mass-stability. Hence the significance of these factors for weather processes.

1 Divergence

Different types of horizontal flow are shown in fig. 3.6A. When streamlines (lines of instantaneous air motion) converge (or diverge) this is

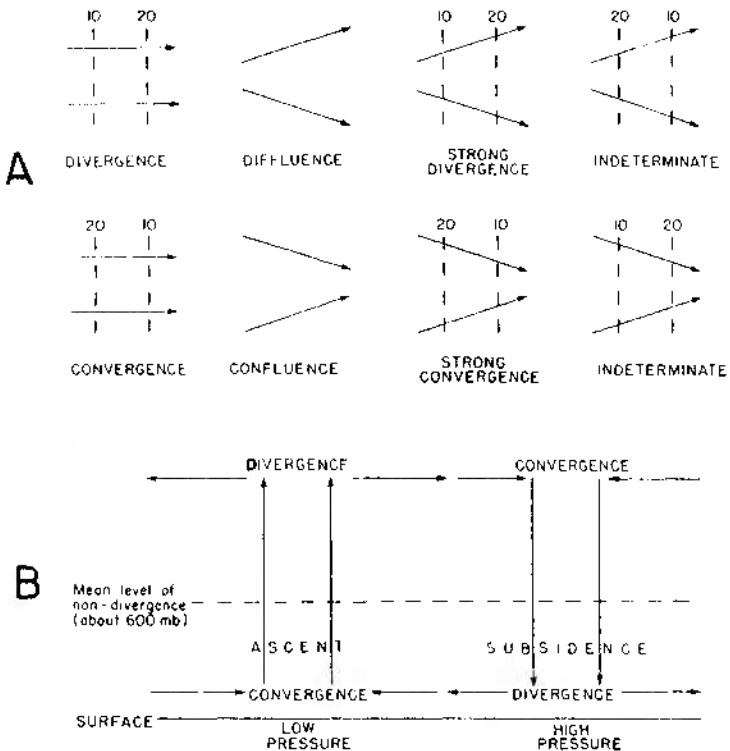


Fig. 3.6. Convergence and divergence.

A. Horizontal flow patterns producing divergence and convergence. The dashed lines are schematic isolaths of wind speed (isotachs).

B. The patterns of vertical motion associated with (mass) divergence and convergence in the troposphere.

termed confluence (or diffluence). Confluence causes an increase in the velocity of the air particles, but no mass accumulation. Convergence occurs when there is a net accumulation of air in a limited sector and divergence when there is net outflow. Confluence may reinforce mass convergence, but sometimes the isotach (line of equal wind speed) pattern cancels out the effect of streamline confluence. It is important to note that if all winds were geostrophic, there could be no convergence or divergence and hence no weather!

Other ways in which convergence or divergence can occur are the result of surface friction effects. Onshore winds undergo convergence at low levels when the air slows down on crossing the coastline owing to the greater friction overland, whereas offshore winds accelerate and become divergent. Frictional differences can also set up coastal convergence (or divergence) if the geostrophic wind is parallel to the coastline with, for the northern hemisphere, land to the right (or left) of the air current, viewed downwind.

2 Vertical motion

Horizontal inflow or outflow near the surface has to be compensated by vertical motion, as illustrated in fig. 3.6a. Air rises above a low-pressure cell and subsides over a high-pressure, with compensating divergence and convergence, respectively, in the upper troposphere. In the middle troposphere there must clearly be some level at which horizontal divergence or convergence is effectively zero; the mean 'level of non-divergence' is generally at about 600 mb. Large-scale vertical motion is extremely slow compared with convective and downdraught currents in cumulus, for example. Typical rates in large depressions and anticyclones are of the order of 5–10 cm sec⁻¹, whereas updraughts in cumulus may exceed 10 m sec⁻¹.

3 Vorticity

Vorticity implies the rotation or angular velocity of minute (imaginary) particles in any fluid system. The air within a depression can be regarded as comprising an infinite number of small air parcels, each rotating cyclonically about an axis vertical to the earth's surface. Vorticity has three elements – magnitude (defined as twice the angular velocity, ω)¹, direction (the horizontal or vertical axis about which the rotation occurs) and the sense of rotation. Rotation in the same sense as the earth's rotation – cyclonic in the northern hemisphere – is defined as positive. Cyclonic vorticity may result from cyclonic curvature of the streamlines, from cyclonic shear (stronger winds on the right side of the current, viewed downwind in the northern hemisphere), or a combination of the two. Anticyclonic vorticity occurs with the corresponding anticyclonic situation (fig. 3.7). The component of vorticity about a vertical axis is referred to as the vertical vorticity. This is generally the most important,

¹ The vorticity, or circulation, about a rotating circular fluid disc is given by the product of the rotation on its boundary (ωR) and the circumference ($2\pi R$) where R = radius of the disc. The vorticity is then $2\omega\pi R^2$, or 2ω per unit area.

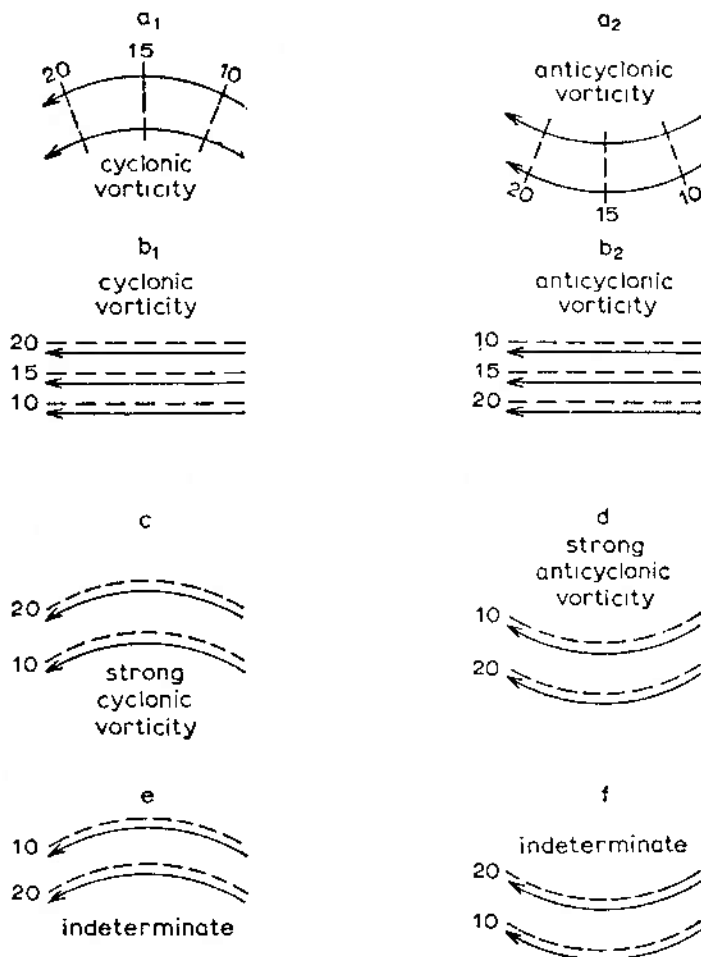


Fig. 3.7. Models illustrating the flow patterns with cyclonic and anticyclonic vorticity in the northern hemisphere (*after Riehl 1954*). In c and d the effects of curvature (a_1 and a_2) and lateral shear (b_1 and b_2) are additive, whereas in e and f they more or less cancel out.

but near the ground surface frictional shear causes vorticity about an axis parallel to the surface and normal to the wind direction.

Vorticity is related not only to air motion about a cyclone or anti-cyclone (*relative vorticity*), but also to the location of that system on the rotating earth. The vertical component of *absolute vorticity* consists of the relative vorticity (ζ) and the latitudinal value of the Coriolis parameter, $f = 2\omega \sin \phi$ (see ch. 3, A.3). At the equator the local vertical is at right angles to the earth's axis so that $f = 0$, but at the north pole cyclonic relative vorticity and the earth's rotation act in the same sense.

C Local winds

To the practising meteorologist the special controls over air movement produced by local conditions often provide more problems than the effects of the major planetary forces just discussed. Diurnal tendencies are superimposed upon both the large- and small-scale patterns of wind velocity. These are particularly noticeable in the case of local winds and therefore are examined before we consider the major types of local wind regime.

In normal conditions there is a general tendency for wind velocities to be least about dawn, at which time there is little vertical thermal mixing and the lower air does not therefore partake of the velocity of the more freely moving upper air (see ch. 3, C). Conversely, velocities of some local winds are greatest between 1300 and 1400 hours, for this is the time when the air suffers its greatest tendency to move vertically due to terrestrial heating, allowing it, subject to surface frictional effects, to join in the freer upper-air movement. Upper air always moves more freely than air at surface levels because it is not subject to the retarding effects of friction and obstruction.

1 Mountain and valley winds

Terrain irregularities produce special meteorological conditions of their own. During warm afternoons the laterally constricted but vertically expanding air tends to blow up the valley axis. Such winds, termed valley winds, are generally very light and require a weak regional pressure gradient in order to develop. This flow along the main valley develops more or less simultaneously with *anabatic* (upslope) winds which result from greater heating of the valley sides compared with the valley floor. These slope winds rise above the ridge line and feed an upper return current along the line of the valley to compensate for the valley wind. This feature may be obscured, however, by the regional airflow. Speeds reach a maximum around 1400 hours. At night there is a reverse process as the cold denser air at higher elevations drains into depressions and valleys; this is known as a *katabatic* wind (fig. 3.8).

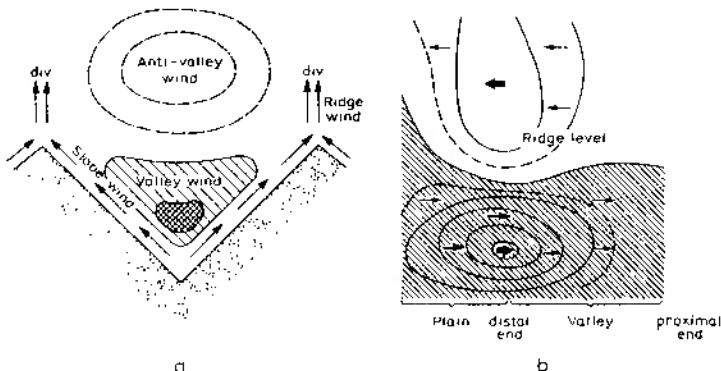


Fig. 3.8. Valley winds in an ideal V-shaped valley. a. Section across the valley. The valley-wind and anti-valley wind are directed at right angles to the plane of the paper. The arrows show the slope and ridge wind in the plane of the paper, the latter diverging (div.) into the anti-valley wind system. b. Section running along the centre of the valley and out on to the adjacent plain, illustrating the valley wind (below) and the anti-valley wind (above) (after Buettner and Thyer 1965).

If the air drains downslope into an open valley, a 'mountain wind' develops more or less simultaneously along the axis of the valley. This flows towards the plain where it replaces warmer, less dense air. The maximum velocity occurs just before sunrise at the time of maximum diurnal cooling. Like the valley wind, the mountain wind is also overlain by an upper return current, in this case upvalley.

Katabatic drainage is usually cited as the cause of frost pockets in hilly and mountainous areas. It is argued that greater radiational cooling on the slopes, especially if they are snow-covered, leads to a gravity flow of cold, dense air into the valley bottoms. Recent observations in California, however, suggest that the valley air remains colder than the slope air from the onset of nocturnal cooling, so that the air moving downslope slides over the denser air in the valley bottom. Moderate drainage winds will also act to raise the valley temperatures through turbulent mixing. Clearly, this problem requires further study. Plate 4 illustrates the effect of large-scale cold air drainage around the Norwegian coast.

2 Winds due to topographic barriers

Mountain ranges have important effects on the airflow across them. The displacement of air upwards over the obstacle may trigger instability if the

air is conditionally unstable (see ch. 2, E), whereas stable air returns to its original level in the lee of the barrier and this descent often forms the first of a series of *lee waves* (or *standing waves*) downwind as shown in fig. 3.9. The wave form remains more or less stationary relative to the barrier

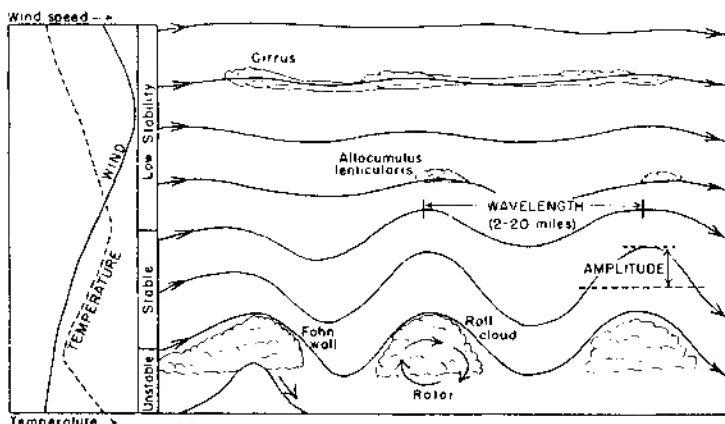


Fig. 3.9. Lee waves and rotors are produced by air flow across a long mountain range. The first wave crest usually forms less than one wavelength downwind of the ridge. There is a strong surface wind down the lee slope. Wave characteristics are determined by the wind speed and temperature relationships, shown schematically on the left of the diagram. The existence of an upper stable layer is particularly important (after Wallington 1960).

with the air moving quite rapidly through it. Below the crest of the waves there may be circular air motion in a vertical plane which is termed a *rotor*. The formation of such features is naturally of vital interest to airmen. The development of lee waves is commonly disclosed by the presence of lenticular clouds (pl. 6), and on occasion a rotor causes reversal of the surface wind direction in the lee of high mountains (see pl. 7).

A related and locally very important type of wind is the *föhn* or *chinook*. It is a strong, gusty, dry and warm wind which develops on the lee side of a mountain range when stable air is forced to flow over the barrier by the regional pressure gradient. Sometimes, there is a loss of moisture by precipitation on the mountains (fig. 3.10) and the air, having cooled at the saturated adiabatic lapse rate above the condensation level, subsequently warms at the greater dry adiabatic lapse rate as it descends on the lee side with a consequent lowering of both the relative and ab-

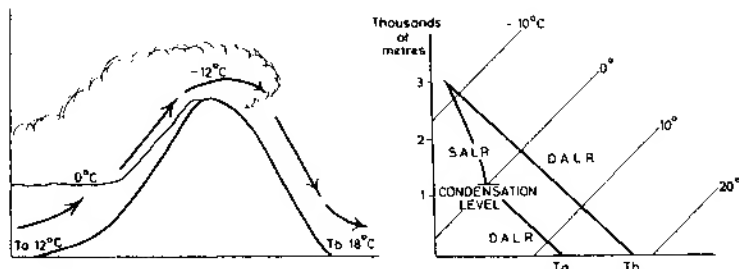


Fig. 3.10. The fohn effect when an air parcel is forced to cross a mountain range. T_a refers to the temperature at the windward foot of the range and T_b to that at the leeward foot.

solute humidity. Recent investigations show, however, that in many instances there is no loss of moisture over the mountains and in such cases the fohn effect is the result of wave motions forcing air from higher levels to descend. Föhn winds are common along the northern flanks of the Alps and the mountains of the Caucasus and central Asia in winter and spring, when the accompanying rapid temperature rise may help to trigger-off avalanches on the snow-covered slopes. At Tashkent in central Asia, where the mean temperature in winter is about freezing point, temperatures may rise to more than 21°C during a fohn. In the same way the chinook is a significant feature at the eastern foot of the New Zealand Alps and of the Rocky Mountains. At Pincher Creek, Alberta, a temperature rise of 21°C (38°F) occurred in 4 mins with the onset of a chinook on 6 January 1966. Less spectacular effects are also noticeable in the lee of the Welsh mountains, the Pennines and the Grampians, where the importance of fohn winds lies mainly in the dispersal of cloud by the subsiding dry air (see also ch. 5, p. 243 and p. 258).

In some parts of the world, winds descending on the lee slope of a mountain range are cold. The type example of such 'fall-winds' is the *bora* of the northern Adriatic, although similar winds occur on the northern Black Sea coast, in northern Scandinavia, Novaya Zemlya and in Japan. These winds occur when cold continental air masses are forced across a mountain range by the pressure gradient and, despite adiabatic warming, displace warmer air. They are therefore primarily a winter phenomenon.

On the eastern slope of the Rocky Mountains in Colorado, (and probably also in other similar continental locations) winds of either *bora* or chinook type can occur. Locally, at the foot of the mountains, such winds may attain hurricane force with gusts exceeding 45 m sec^{-1} (100

mph). A few downslope storms of this type have caused millions of dollars of property damage in Boulder, Colorado and the immediate vicinity. These windstorms develop when a stable layer close to the mountain-crest level prevents airflow to windward from crossing over the mountains. Extreme amplification of a lee wave (fig. 3.9) drags air from above the summit level (about 4000 m) down to the plains (1700 m) in a very short distance, so that the high velocities occur. However, the flow is not simply 'downslope'; the storm may affect the mountain slopes but not the foot of the slope, or vice versa, depending on the location of the lee wavetrough.

3 Land and sea breezes

Another familiar type of air movement is the land and sea breeze (fig. 3.11). The vertical expansion of the air column which occurs daily during the hours of heating over the more rapidly heated land (see ch. 1, D.5), tilts

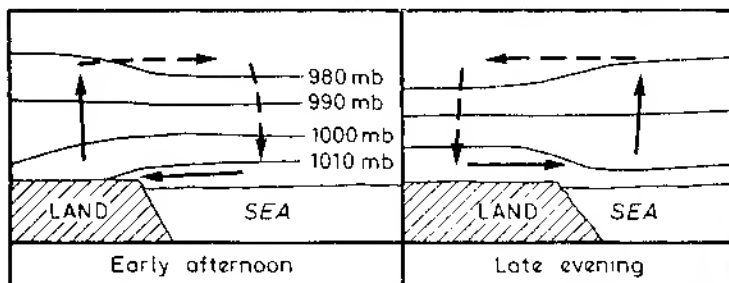


Fig. 3.11. The daytime sea breeze and the nocturnal land breeze.

the isobaric surfaces downwards at the coast, causing onshore winds at the surface and a compensating offshore movement aloft. At night the air over the sea is warmer and the situation is reversed, although much of this reversal is often the effect of downslope winds blowing off the land. Figure 3.12 shows that these local winds can have a decisive effect on coastal temperature and humidity. The advancing cool sea air may form a distinct line (or *front*, see ch. 4, C) marked by cumulus cloud development, behind which there is a distinct wind velocity maximum. This often develops in summer, for example, along the Gulf Coast of Texas. On a smaller scale such features can also be observed in Britain, particularly along the south and east coasts. The sea breeze has a depth of about 1 km (3300 ft), although it thins towards the advancing edge, and may

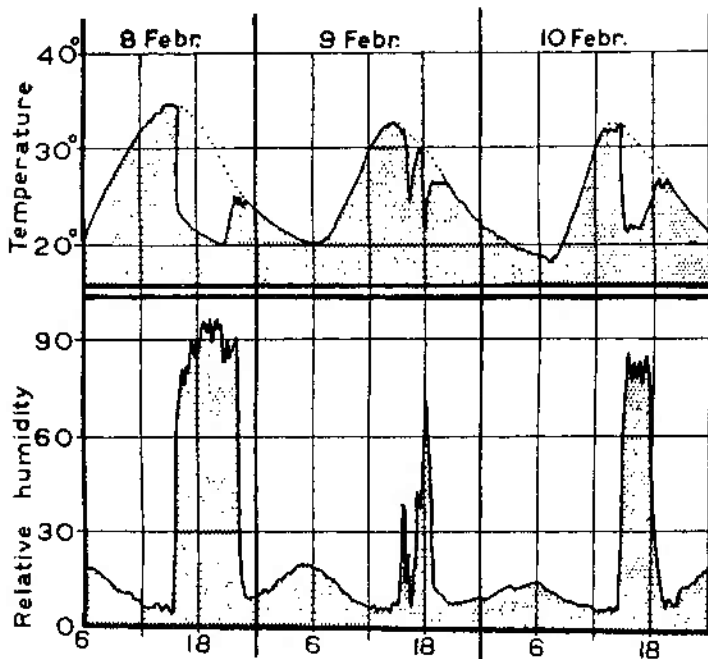


Fig. 3.12. The effect of the afternoon sea breeze on the temperature ($^{\circ}\text{C}$) and relative humidity (%) at Joal on the Senegal coast, 8–10 February 1893 (after Angot and De Martonne. From Kuenen 1955).

penetrate 50 km (30 miles) inland by 2100 hours. Typical wind speeds in such sea breezes are $4\text{--}7 \text{ m sec}^{-1}$ (about 10–15 mph), although these may be greatly increased where a well-marked low-level temperature inversion produces a 'Venturi effect' in constricting and accelerating the flow. The much shallower land breezes are usually only about 2 m sec^{-1} (about 5 mph). The counter currents aloft are generally less evident and may be obscured by the regional airflow, but recent work along the Oregon coast has suggested that under certain conditions this upper return flow may be very closely related to the lower sea breeze conditions, even to the extent of mirroring the surges in the latter. It is worth noting that in middle latitudes the Coriolis deflection causes turning of a well-developed onshore sea breeze (clockwise in the northern hemisphere) so that eventu-

ally it may blow more or less parallel to the shore. Analogous 'lake breeze' systems develop adjacent to large inland water bodies such as the Great Lakes.

D Variation of pressure and wind velocity with height

As might be expected, changes of height reveal variations both of pressure and of wind characteristics. Study of these variations discloses some interesting facts, although explanations of these facts are as yet by no means complete. It is only possible, therefore, to outline some of the existing hypotheses which have been put forward to account for the observed characteristics.

Above the level of surface frictional effects (about 500–1000 m) the wind increases in speed and becomes more or less geostrophic. With further height increase the reduction of air density leads to a general increase in wind speed (see ch. 3, A.1). At 45°N a geostrophic wind of 14 m sec⁻¹ at 3 km is equivalent to one of 10 m sec⁻¹ at the surface for the same pressure gradient. There is also a seasonal variation in wind speeds aloft, these being much greater during winter months when the meridional temperature gradients are at a maximum. In addition, the persistence of these gradients tends to cause the upper winds to be more constant in direction.

1 The vertical variation of pressure systems

The general relationships between surface and tropospheric pressure conditions are illustrated by the models of fig. 3.13. A low-pressure cell at sea-level with a cold core will intensify with elevation, whereas one with a warm core tends to weaken and may be replaced by high pressure. A warm air column of relatively low density causes the pressure surfaces to bulge upwards and conversely a cold, more dense air column leads to downward contraction of the pressure surfaces. Thus, a surface high-pressure cell with a cold core (*a cold anticyclone*), such as the Siberian winter anticyclone, weakens with increasing elevation and is replaced by low-pressure aloft. Cold anticyclones are shallow and rarely extend their influence above about 2500 m (8000 ft). By contrast a surface high with a warm core (*a warm anticyclone*) intensifies with height. This is characteristic of the large subtropical cells which maintain their warmth through dynamic subsidence. The high surface pressure in a warm anticyclone is linked hydrostatically with cold, relatively dense air in the lower stratosphere. Conversely a cold depression (fig. 3.13A) is associated with a warm lower stratosphere.

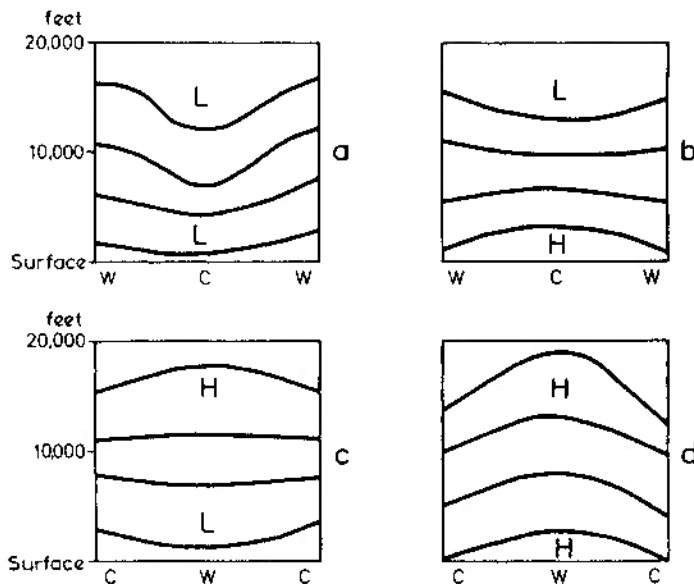


Fig. 3.13. Models of the vertical pressure distribution in cold and warm air columns. a. A surface low pressure intensifies aloft in a cold air column. b. A surface high pressure weakens aloft and may become a low pressure in a cold air column. c. A surface low pressure weakens aloft and may become a high pressure in a warm air column. d. A surface high pressure intensifies aloft in a warm air column.

Mid-latitude low-pressure cells have cold air in the rear and in consequence the axis of low pressure slopes with height towards the colder air to the west. High-pressure cells slope towards the warmest air (fig. 3.14) and in this manner the northern hemisphere subtropical high-pressure cells are displaced 10° – 15° south in latitude at the 3000-m level, as well as towards the west (fig. 3.15). Even so, this slope of the high-pressure axes is not constant through time and stations located between the cells may experience widely fluctuating upper winds associated with variations in the inclination of the axes.

2 Mean upper-air patterns

It is helpful to begin by considering the patterns of pressure and wind in the middle troposphere. These are less complicated in appearance than

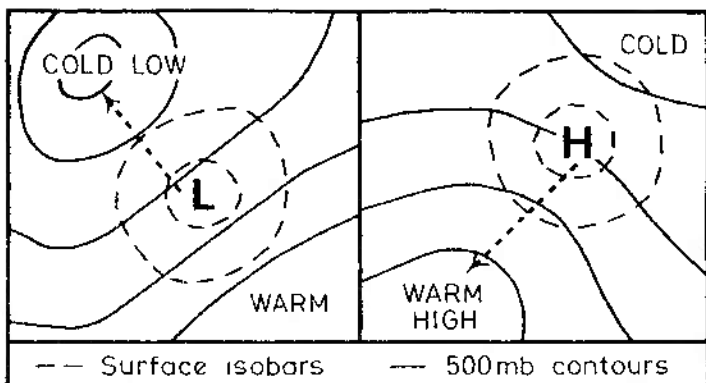


Fig. 3.14. The characteristic slope of the axes of low- and high-pressure cells with height in the northern hemisphere.

surface maps as a result of the diminished effects of the land masses. Rather than using pressure maps at a particular height it is convenient to depict the height of a selected pressure surface; this is termed a *contour chart* by analogy with topographic relief maps.¹ Figure 3.16 shows that in the middle troposphere of the southern hemisphere there is a vast circum-polar cyclonic vortex poleward of latitude 30°S in summer and winter. The vortex is more or less symmetrical about the pole although the low centre is towards the Ross Sea sector. Corresponding charts for the northern hemisphere (fig. 3.17) also show an extensive cyclonic vortex, but one which is markedly more asymmetric with a primary centre over the eastern Canadian Arctic and a secondary one over eastern Siberia. The major troughs and ridges form what are referred to as *long waves* (or *Rosshy waves*) in the upper flow (see ch. 4, F). The two major troughs at about 70°W and 150°E are thought to be induced by the combined influence on upper-air pressure and winds of large orographic barriers, like the Rockies, and heat sources such as warm ocean currents (in winter) or land masses (in summer). The subtropical high-pressure belt has only one clearly distinct cell in January over the eastern Caribbean, whereas in July cells are well developed over the Atlantic and the Pacific. In addition, the July map shows greater prominence of the subtropical high over the Sahara and southern North America.

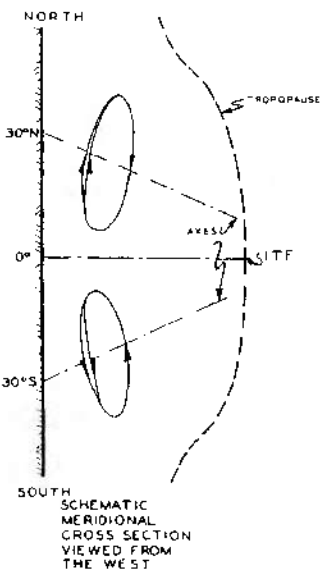
¹ The geostrophic wind concept is equally applicable to contour charts. Heights on these charts are given in geopotential metres (g.p.m.).

In the southern hemisphere, the predominance of ocean surface (which comprises 81% of the hemisphere) considerably reduces the development of long waves in the upper westerlies. Nevertheless, asymmetries are initiated by the effects on the atmosphere of such geographical features as the Andes, the elevated and extensive dome of eastern Antarctica, and ocean currents, particularly the Humboldt and Benguela Currents (see fig. 3.34) and the associated cold coastal upwellings. Both hemispheres show a summer to winter intensification of the mean circulation which is explained below.

3 Upper winds

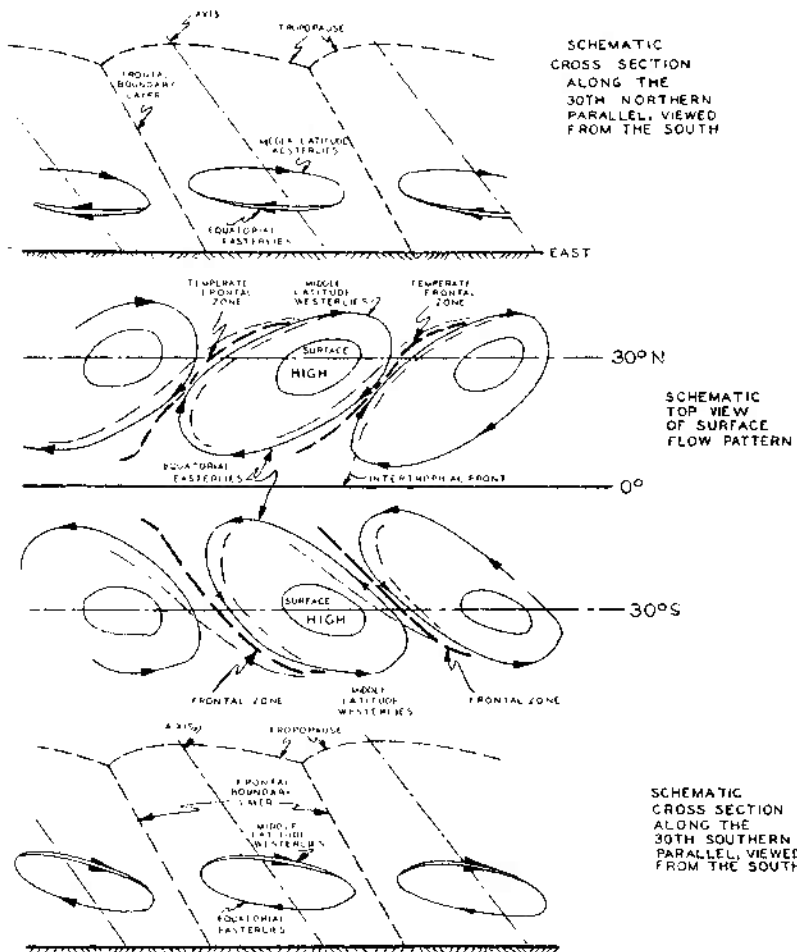
It is a common observation that clouds at different levels move in different directions. The wind speeds at these levels may also be markedly different, although this is not so evident to the casual observer. The

Fig. 3.15. Schematic horizontal and vertical structure of the subtropical high-pressure cells. Note particularly the convergence along the belts between the cells, the slope of the axes with height westward and equatorward, and the inclined spiral of air motion in the middle troposphere - up on the west sides (dynamically unstable air) and down on the east sides (dynamically stable air) (from Garbell 1947).



gradient of wind velocity with height is referred to as the (vertical) *wind shear*, and in the free air, above the friction level, the amount of shear depends upon the temperature structure of the air. This important relationship is illustrated in fig. 3.18. The diagram shows hypothetical

contours of the 1000 and 500 mb pressure surfaces. The thickness of the 1000–500 mb layer is proportional to its mean temperature – low thickness values correspond to cold air, high thickness values to warm air. This relationship is apparent in the vertical sections of fig. 3.13. The theoretical wind vector (V_t) blowing parallel to the thickness lines, with a velocity proportional to their gradient, is termed the *thermal wind*. The



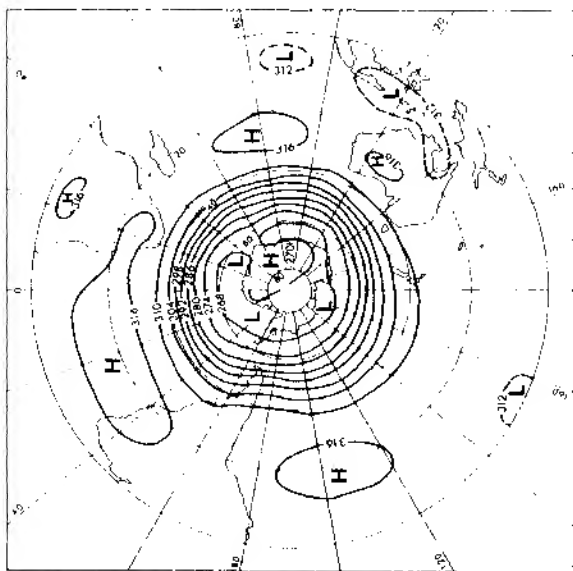
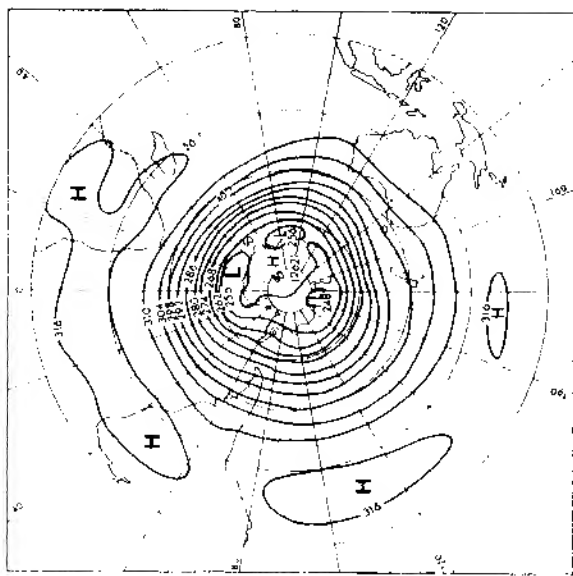


Fig. 3.16. The mean contours (g.p.d.km.) of the 700 mb pressure surface in January (left) and July (right) for the southern hemisphere, 1949-6 (after Taljaard *et al.* 1969).

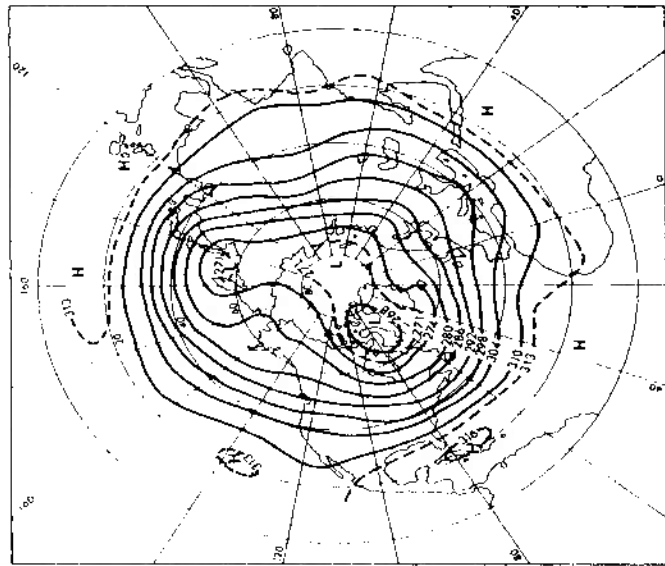
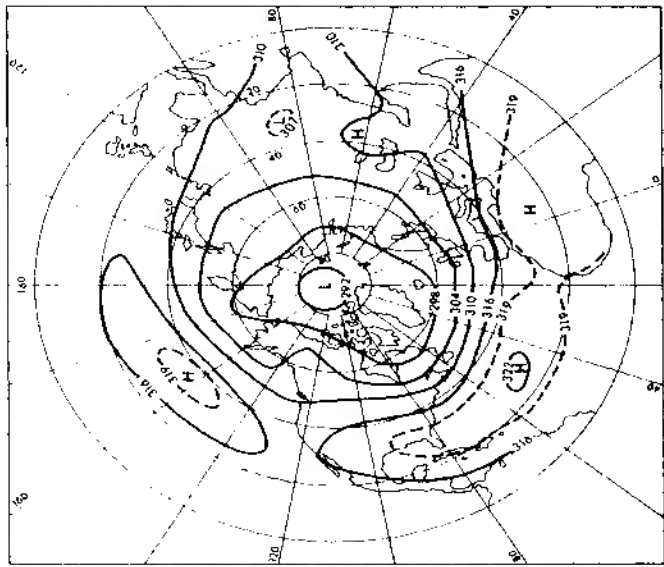


Fig. 31.7. The mean contours (g.p.dkm.) of the 700 mb pressure surface in January (left) and July (right) for the northern hemisphere, 1950-59 (adapted from O'Connor 1961).

geostrophic wind velocity at 500 mb (G_{500}) is the vector sum of the 1000 mb geostrophic wind (G_{1000}) and the thermal wind (V_T), as shown in fig. 3.18.

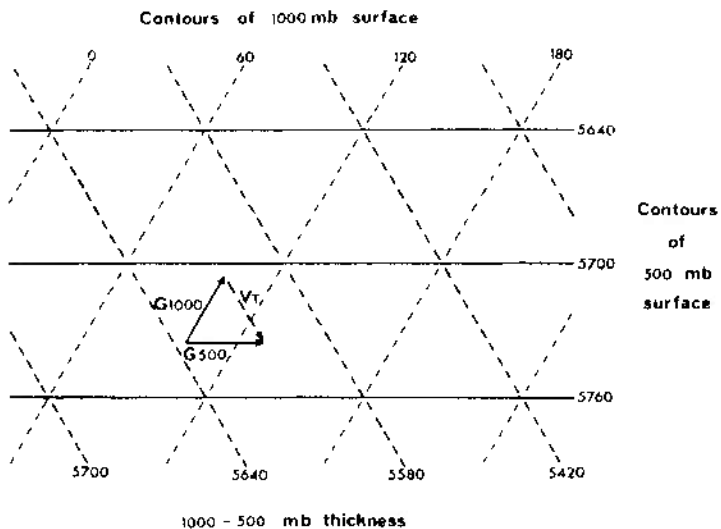


Fig. 3.18. The thermal wind and the thickness of the 1000–500-mb layer (in metres). G_{1000} is the geostrophic velocity at 1000 mb, G_{500} that at 500 mb, and V_T is the resultant 'thermal wind' blowing parallel to the thickness lines.

Since the thermal wind blows with cold air (low thickness) to the left in the northern hemisphere, when viewed downwind, it is readily apparent that in the troposphere the poleward decrease of temperature should cause a large westerly component in the upper winds. Furthermore, since the meridional temperature gradient is steepest in winter the zonal westerlies are most intense at this time.

The total result of the above influences is that in the northern hemisphere most upper geostrophic winds are dominantly westerly between the subtropical high-pressure cells (centred aloft about 15°N) and the polar low-pressure centre aloft. Between the subtropical high-pressure cells and the equator they are easterly. This dominant, westerly circulation reaches maximum speeds of 100–150 mph (45–67 m sec⁻¹), which even increase to 300 mph (135 m sec⁻¹) in winter. These maximum speeds are concentrated in a narrow band often situated at about 30°

latitude, between 9000 and 15,000 m, called the *jet stream*.¹ Plate 10 shows bands of cirrus cloud which may have been related to jet-stream systems.

This stream, which is essentially a fast-moving mass of laterally concentrated air, is in some way connected with the zone of maximum slope, folding, or fragmentation of the tropopause, which in turn coincides with the latitude of maximum poleward temperature gradient and energy transfer. The thermal wind, as described above, is a major component of the jet stream, but the basic reason for the concentration of the meridional temperature gradient in a narrow zone (or zones) is still uncertain. One theory is that the temperature gradient becomes accentuated when the upper wind pattern is confluent (see ch. 3, B.1). Fig. 3.19, giving a

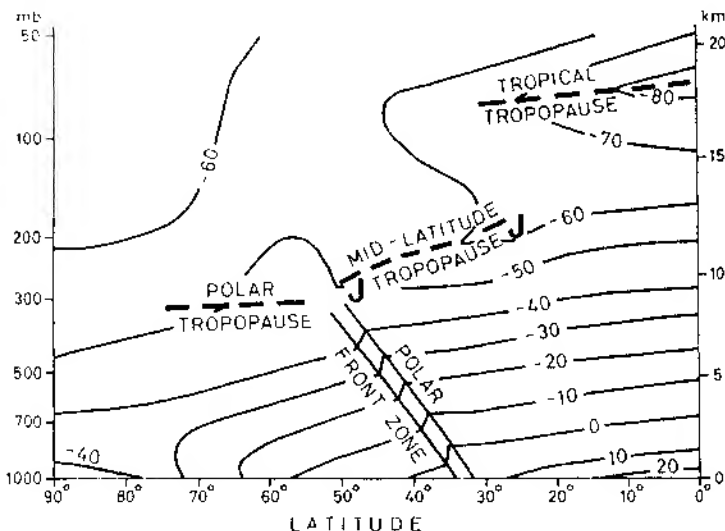


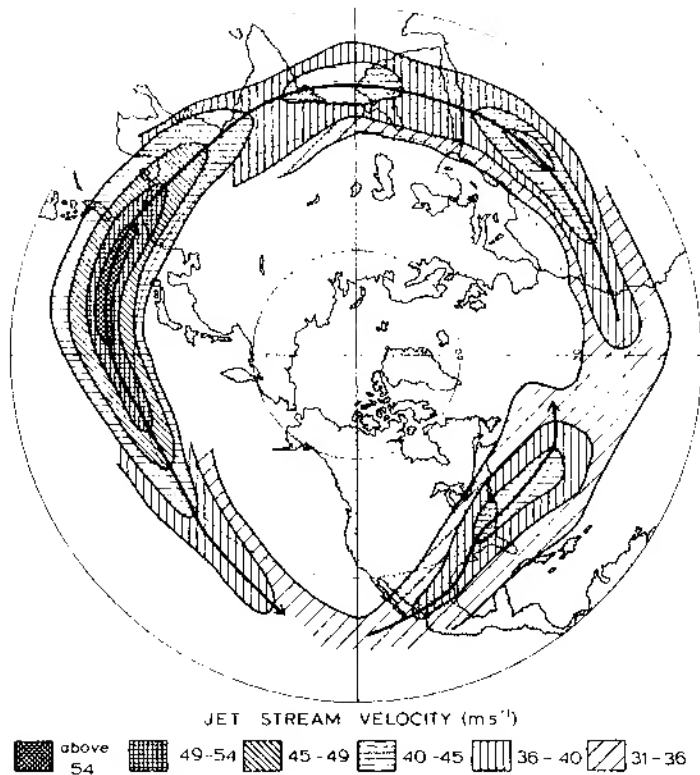
Fig. 3.19. The typical distribution of temperature and the location of the westerly jet streams (J) in the northern hemisphere in winter (after Defant and Taba, and Newton and Persson).

generalized view of the wind and temperature distribution in the troposphere in winter, shows that there are two westerly jet streams. (see fig. 1.29) The more northerly one, termed the *Polar Front Jet Stream* (see ch. 4, E), is associated with the steep temperature gradient where polar

¹The World Meteorological Organization recommends an arbitrary lower limit of 30 m sec⁻¹.

156 Atmosphere, weather and climate

and tropical air interact, but the *Subtropical Jet Stream* is related to a temperature gradient confined to the upper troposphere. The Polar Front Jet Stream is very irregular in its longitudinal location and is commonly discontinuous, whereas the Subtropical Jet Stream is much more per-



sistent. For these reasons the location of the mean jet stream (fig. 3.20) primarily reflects the position of the Subtropical Jet Stream. The synoptic pattern of jet stream occurrence may be further complicated in some sectors by the presence of additional frontal zones (see ch. 4, E), each associated with a jet stream. This situation is common in winter over North America.

Comparison of figs. 3.17 and 3.20 indicates that the main jet stream cores are associated with the principal troughs of the Rossby long waves. The relationships between these upper tropospheric wind systems and surface weather and climate will be considered in chs. 4, 5, and 6.

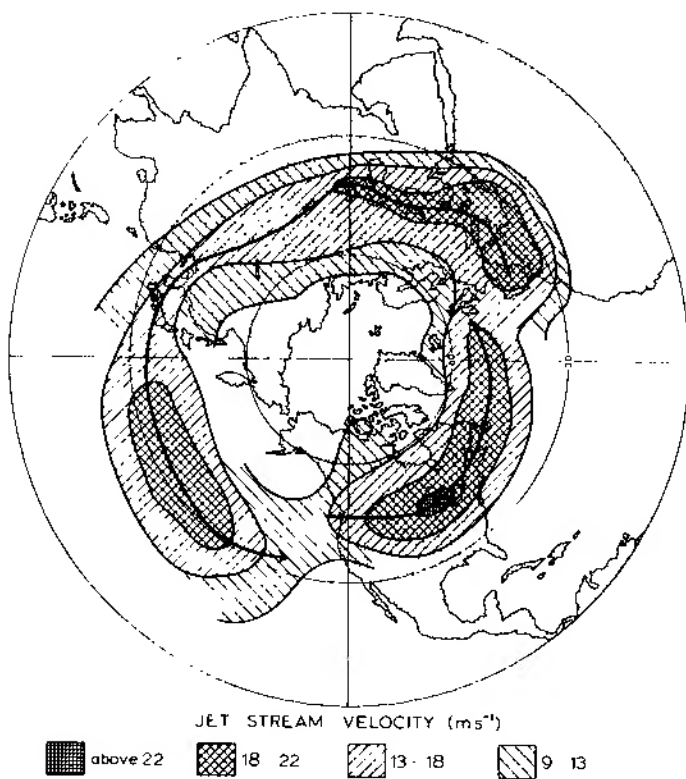
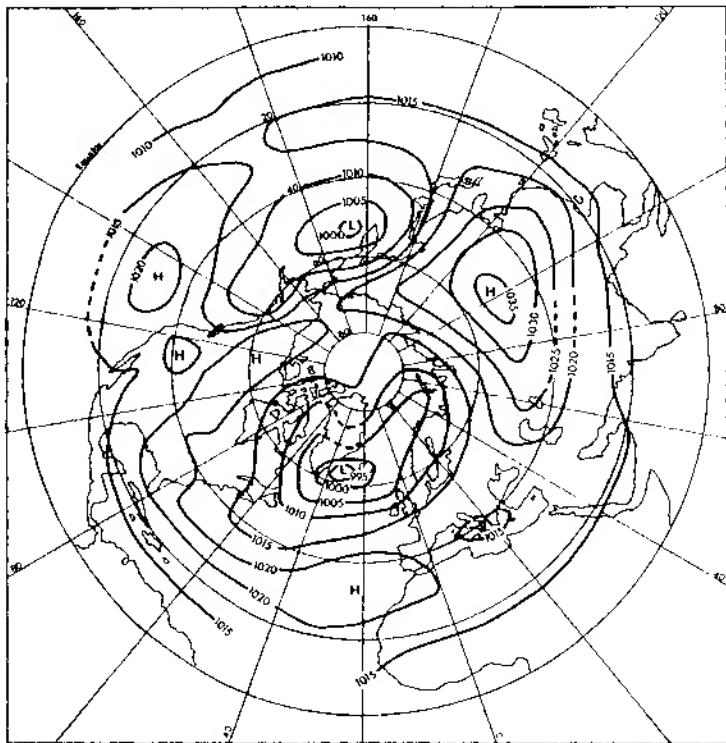


Fig. 3.20. The mean location and velocities ($m s^{-1}$) of the westerly jet stream in the northern hemisphere in January (opposite) and July (above) (after Namias and Clapp. Adapted from Petterssen 1958).

4 Surface pressure conditions

The most permanent features of the mean surface pressure maps are the oceanic subtropical high pressure cells (figs. 3.21 and 3.22). These anticyclones are located at about 30° latitude, suggestively situated below

the mean Subtropical Jet Stream. They move a few degrees equatorward in winter and poleward in summer in response to the seasonal expansion and contraction of the two circumpolar vortices. In the northern hemisphere the subtropical ridges of high pressure are weakened over the heated continents in summer but are thermally intensified over them in



winter. The principal subtropical high-pressure cells are located: (a) over the Bermuda-Azores ocean region (aloft the centre of this cell lies over the east Caribbean); (b) over the south and south-west United States (the Great Basin or Sonoran cell) - this continental cell is naturally prone to seasonal decline, being replaced by a thermal surface low in summer; (c) over the east and north Pacific - a large and powerful cell (sometimes dividing into two, especially during the summer); and (d) over the Sahara - this, like other continental source areas is, seasonally variable both in

intensity and extent, being most prominent in winter. In the southern hemisphere the subtropical anticyclones are oceanic, except over southern Australia in winter.

Equatorward of the subtropical anticyclones there is an equatorial trough of low pressure, associated broadly with the zone of maximum insolation and tending to migrate with it, especially towards the heated con-

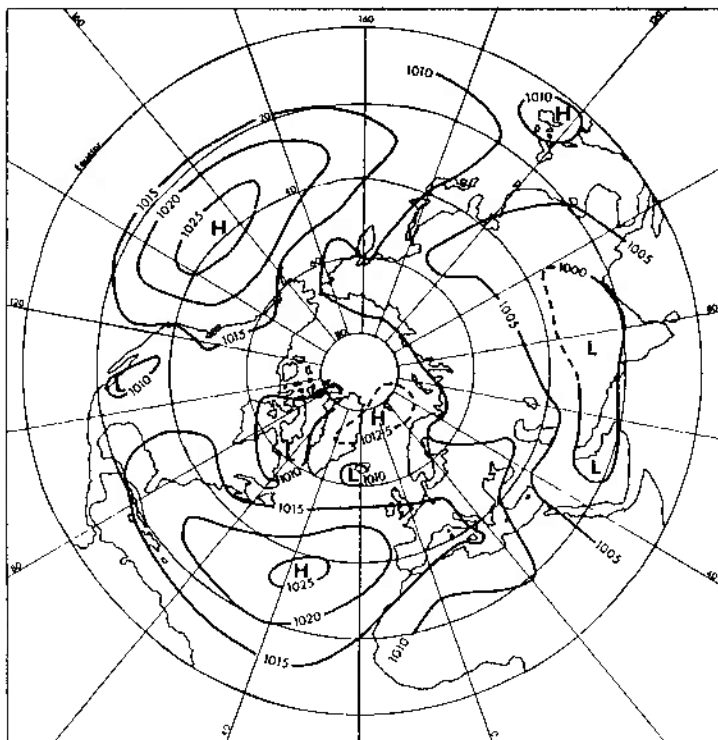
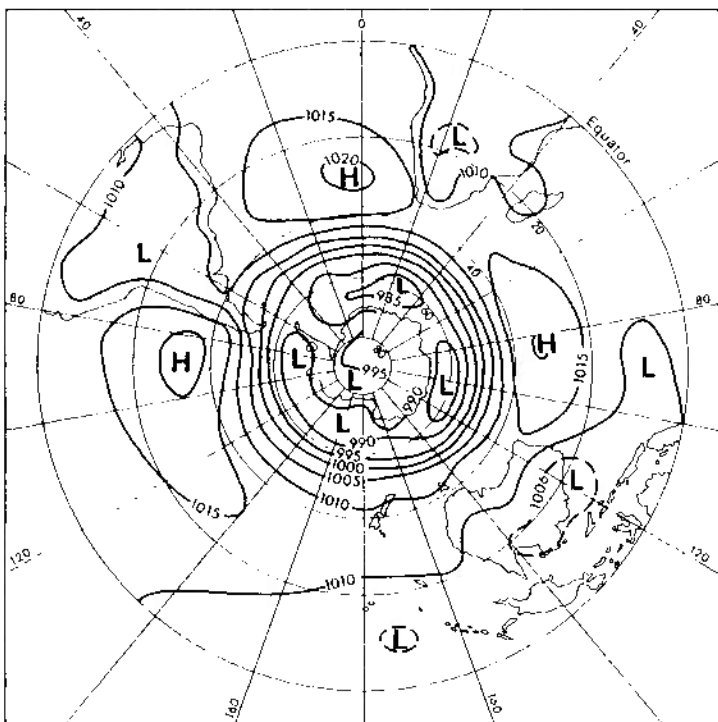


Fig. 3.21. The mean surface pressure distribution (mb) in January (opposite) and July (above) for the northern hemisphere, 1950–59 (*after O'Connor 1961*).

tinental interiors of the summer hemisphere. Poleward of the subtropical anticyclones lies a general zone of subpolar low pressure. In the southern hemisphere this is virtually circumpolar (fig. 3.22) whereas in the northern hemisphere the major centres are near Iceland and the Aleutians in winter and primarily over continental areas in summer. It is commonly stated

that in high latitudes there is a surface anticyclone due to the cold polar air, but in the Arctic this is true only in spring over the Canadian Arctic Archipelago. In winter the Polar Basin is affected by high and low pressure cells with the major semi-permanent cold air anticyclones over Siberia and, to a lesser extent, northwestern Canada. The shallow Siberian



high is in part a result of the exclusion of tropical air masses from the interior by the Tibetan and massif and the Himalayas. Over Antarctica it is meaningless to speak of sea-level pressure but, on average, there is high pressure over the high eastern Antarctic plateau between 800 and 500 mb.

It is important at this point to differentiate between mean pressure patterns and the highs and lows shown on synoptic weather maps. The synoptic map is one which shows the principal pressure systems over a very large area at a given time; local wind features, for example, are

ignored. The lows over Iceland and the Aleutians (fig. 3.21) shown on mean pressure maps represent the frequent passage of deep depressions across these areas. The mean high-pressure areas, however, relate to more or less permanent highs. The intermediate areas, such as the zone about 50° - 55° N, affected by travelling depressions and ridges of high pressure,

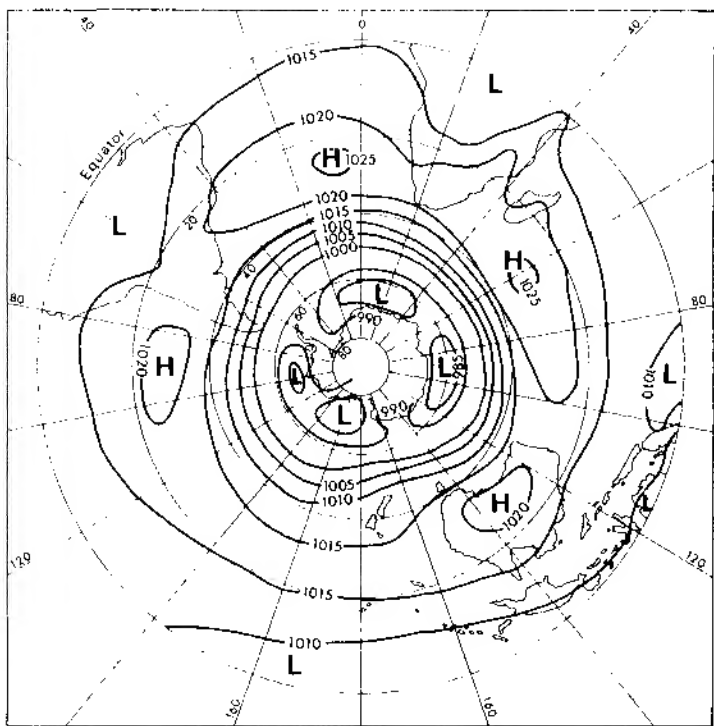


Fig. 3.22. The mean surface pressure distribution (mb) in January (opposite) and July (above) for the southern hemisphere (from Taljaard et al. 1969).

appear on the mean maps as being of neither markedly high nor markedly low pressure. The movement of depressions is considered in ch. 4, F.

On comparing the surface and tropospheric pressure distributions for January (figs. 3.17 and 3.21) it will be noticed that only the subtropical high-pressure cells extend to high levels. The reasons for this are evident from fig. 3.13B and D. In summer the equatorial low-pressure belt is also

162 Atmosphere, weather and climate

evident aloft over southern Asia. The subtropical cells are still discernible at 300 mb, showing them to be a fundamental feature of the global circulation and not merely a response to surface conditions.

E The global wind belts

One fact which emerged from the preceding discussion was the importance of the subtropical high-pressure cells. Dynamic, rather than immediately thermal, in origin, and situated between 20° and 30° latitude, they seem to provide the key to the world's surface wind circulation. In the northern hemisphere the pressure gradients surrounding these cells are strongest between October and April. In terms of actual pressure, however, oceanic cells experience their highest pressure in summer, the belt being counterbalanced at low levels by thermal low-pressure conditions over the continents. Their strength and persistence clearly mark them as the dominating factor which controls the position and activities of both the trades and westerlies.

1 The trade winds

The trades (or tropical easterlies) are important because of the great extent of their activity; they blow over nearly half the globe. They originate at low latitudes on the margins of the sub-tropical high-pressure cells, and their constancy of direction and speed is remarkable (fig. 3.23). Trade winds, like the westerlies, are strongest during the winter half-year, which suggests they are both controlled by the same fundamental mechanism.

The two trade-wind systems tend to converge in the *Equatorial Trough* (of low pressure). Over the oceans, particularly the central Pacific, the convergence of these air streams is pronounced and in this sector the term *Inter-Tropical Convergence Zone* (ITCZ) is applicable. Elsewhere the convergence is by no means continuous in space or time (pl. 12). Equatorward of the main *root zones* of the trades over the eastern Pacific and eastern Atlantic are regions of light, variable winds, known traditionally as the *doldrums* and much feared in past centuries by the crews of sailing ships. Their seasonal extent varies considerably; from July to September they spread westward into the central Pacific while in the Atlantic they extend to the coast of Brazil. A third major doldrum zone is located in the Indian Ocean and western Pacific. In March–April it stretches 16,000 km from east Africa to 180° longitude and it is again very extensive during October–December.

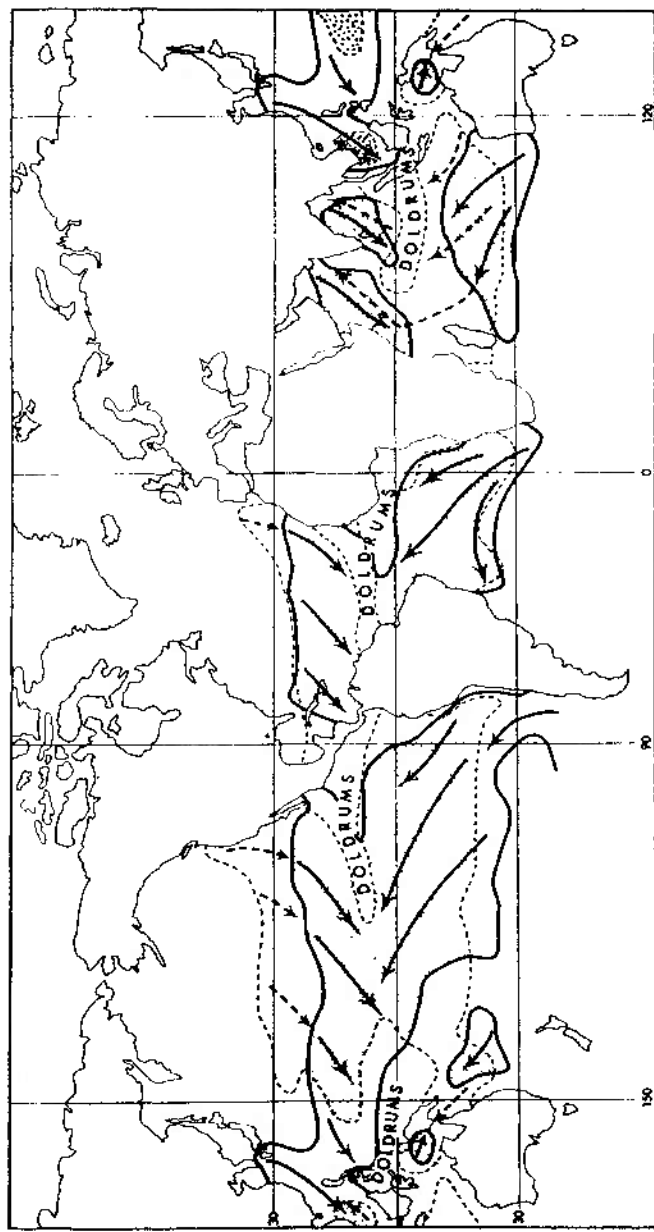


Fig. 3.23. Map of the trade wind belts and the doldrums. The limits of the trades - enclosing the area within which 50% of all winds are from the predominant quadrant - are shown by the solid (January) and the dashed (July) lines. The stippled area is affected by trade-wind currents in both months. Schematic streamlines are indicated by the arrows - dashed (July) and solid (January, or both months) (based on Crowe 1949 and 1950).

2 *The equatorial westerlies*

In the summer hemisphere, and over continental areas especially, there is a zone of generally westerly winds intervening between the two trade-wind belts (fig. 3.24). This westerly system is well marked over Africa and southern Asia in the northern hemisphere summer, when thermal heating over the continents assists the northward displacement of the Equatorial Trough (fig. 3.23). Over Africa the westerlies reach to 2–3 km and over the Indian Ocean to 5–6 km. In the northern section these winds are known as the 'Indian Monsoon' but this is now recognized to be a complex phenomenon the cause of which is partly global and partly regional in origin (see ch. 6, D). The equatorial westerlies are not simply trades of the opposite hemisphere which recurve (due to the changed direction of the Coriolis deflection) on crossing the equator, since there is *on average* a westerly component in the Indian Ocean at 2°–3°S in June and July and at 2°–3°N in December and January. Over the Pacific and Atlantic Oceans the ITCZ does not shift sufficiently far from the equator to permit the development of this westerly wind belt.

3 *The mid-latitude (Ferrel) westerlies*

These are the winds of the mid-latitudes emanating from the poleward sides of the subtropical high-pressure cells. They are far more variable than the trades both in direction and intensity, for in these regions the path of air movement is frequently affected by cells of low and high pressure which travel generally eastwards within the basic flow (pl. 13). Also in the northern hemisphere the preponderance of land areas with their irregular relief and changing seasonal pressure patterns tend to obscure the generally westerly air flow. The Scilly Islands, lying in the south-westerlies, record 46% of winds from between south-west and north-west, but fully 29% from the opposite sector between north-east and south-east.

The westerlies of the southern hemisphere are stronger and more constant in direction than those of the northern hemisphere because the broad expanses of ocean rule out the development of stationary pressure systems (fig. 3.25). Kerguelen Island (49°S, 70°E) has an annual frequency of 81% of winds from between south-west and north-west and the comparable figure of 75% for Macquarie Island (54°S, 159°E) shows that this predominance is widespread over the southern oceans. However, the apparent zonality of the southern circumpolar vortex (fig. 3.22) conceals considerable synoptic variability in winter and summer.

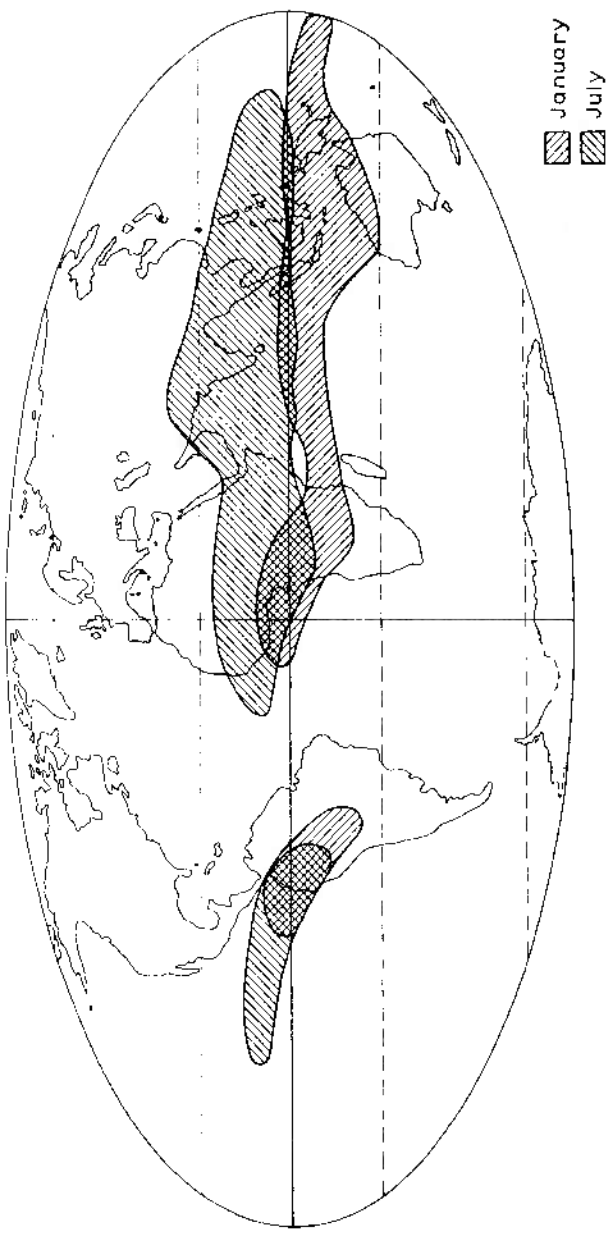


Fig. 3.24. Distribution of the equatorial westerlies in any layer below 3 km (about 10,000 ft) for January and July (after Flöhn 1960, in Indian Meteorological Department 1960).

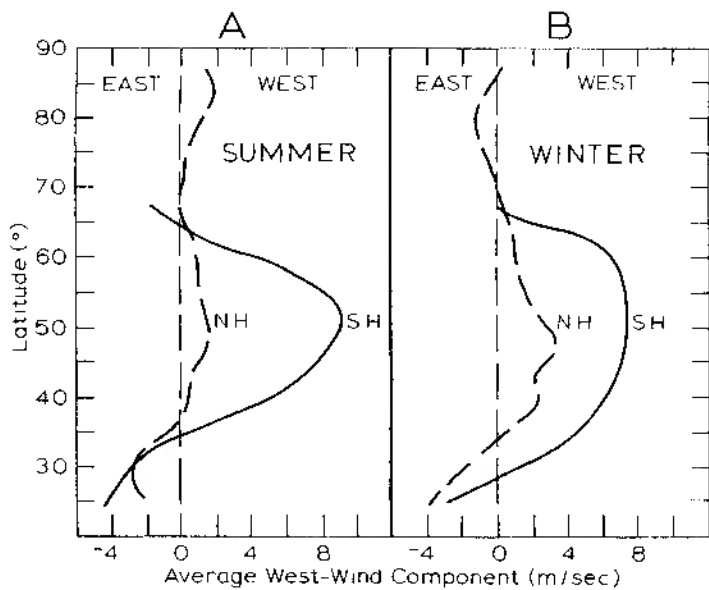


Fig. 3.25. Profiles of the average west-wind component m sec^{-1} at sea-level in the northern and southern hemispheres during their respective summer (A) and winter (B) seasons (after Van Loon 1964).

4 The polar easterlies

This term is applied to winds which are supposed to occur between a polar high pressure and the belt of low pressure of the higher mid-latitudes. The polar high, as has already been pointed out, is by no means a quasi-permanent feature of the arctic circulation. Easterly winds occur mainly on the poleward sides of depressions over the North Atlantic and North Pacific and if average wind directions are calculated for entire latitude belts in high latitudes there is found to be little sign of a coherent system of polar easterlies. The situation in high latitudes of the southern hemisphere is complicated by the presence of Antarctica, but anticyclones appear to be frequent over the high plateau of eastern Antarctica and easterly winds prevail over the Indian Ocean sector of the Antarctic coastline. For example, in 1902–3 the expedition ship *Gauss* at 66°S , 90°E observed winds between north-east and south-east for 70% of the time, and at many coastal stations the constancy of easterlies may be compared with that of the trades. However, westerly components predominate over the sea areas off west Antarctica.

F The general circulation

The observed patterns of wind and pressure prompt consideration of the mechanisms maintaining the *general circulation* of the atmosphere – the large-scale patterns of wind and pressure which persist throughout the year or recur seasonally. Reference has already been made to one of the primary driving forces, the imbalance of radiation between lower and higher latitudes (see ch. 1, G.1), but it is important also to appreciate the significance of energy transfers in the atmosphere. Energy is continually undergoing changes of form as shown schematically in fig. 3.26. Unequal

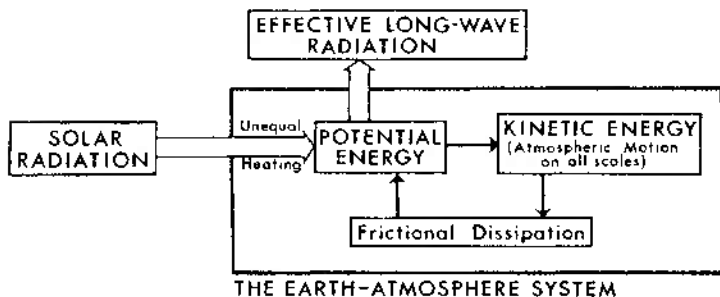


Fig. 3.26. Schematic changes of energy involving the earth-atmosphere system.

heating of the earth and its atmosphere by solar radiation generates potential energy, some of which is converted into kinetic energy by the rising of warm air and the sinking of cold air. Ultimately, the kinetic energy of atmospheric motion on all scales is dissipated by friction and small scale turbulent eddies (i.e. internal viscosity). In order to maintain the general circulation, the rate of generation of kinetic energy must obviously balance its rate of dissipation. These rates are estimated to be about 2 W m^{-2} , which amounts only to some 1% of the average global solar radiation absorbed at the surface and in the atmosphere. In other words the atmosphere is a highly inefficient heat engine (see ch. 1, G).

A second controlling factor is the angular momentum of the earth and its atmosphere. This is the tendency for the earth's atmosphere to move, with the earth, around the axis of rotation. Angular momentum is proportional to the rate of spin (that is the angular velocity) and the square of the distance of the air parcel from the axis of rotation. With a uniformly rotating earth and atmosphere, the total angular momentum must remain constant (in other words, there is a *conservation of angular momentum*).

If, therefore, a large mass of air changes its position on the earth's surface such that its distance from the axis of rotation also changes, then its angular velocity must change in a manner so as to allow the angular momentum to remain constant. Naturally angular momentum is high at the equator¹ and decreases with latitude to become zero at the pole (that is, the axis of rotation), so air moving poleward tends to acquire progressively higher eastward velocities. For example, air travelling from 42° to 46° latitude and conserving its angular momentum, would increase its speed relative to the earth's surface by 29 m sec⁻¹. This is the same principle which causes an ice skater to spin more violently when her arms are progressively drawn into the body. In practice this increase of air-mass velocity is countered or masked by the other forces affecting air movement (particularly friction), but there is no doubt that many of the important features of the general atmospheric circulation result from this poleward transfer of angular momentum.

The necessity for a poleward momentum transport is readily appreciated in terms of the maintenance of the mid-latitude westerlies. These winds continually impart westerly (relative) momentum to the earth by friction and it has been estimated that they would cease altogether due to this frictional dissipation of energy in little over a week if their momentum were not continually replenished from elsewhere. In low latitudes the extensive tropical easterlies are gaining westerly (relative) momentum by friction, as a result of the earth rotating in a direction opposite to their flow, and this excess is transferred polewards with the maximum poleward transport occurring, significantly, in the vicinity of the sub-tropical jet stream at about 250 mb at 30°N and 30°S.

1 Circulations in the vertical and horizontal planes

There are two possible ways in which the atmosphere can transport heat and momentum. One is by circulation in the vertical plane as indicated in fig. 3.27 which shows three meridional cells. The low-latitude (or Hadley) cell and its counterpart in the southern hemisphere were considered to be analogous to the convective circulations set-up when a pan of water is heated over a flame and are referred to as *thermally direct* cells. Warm air near the equator was thought to rise and generate a low-level flow towards the equator, the earth's rotation deflecting these currents which thus form the north-east and south-east trades. This explanation was put forward by G. Hadley in 1735, although in 1856 W. Ferrel pointed out that the conservation of angular momentum would be a more effective

¹ Equatorial speed of rotation is 465 m sec⁻¹.

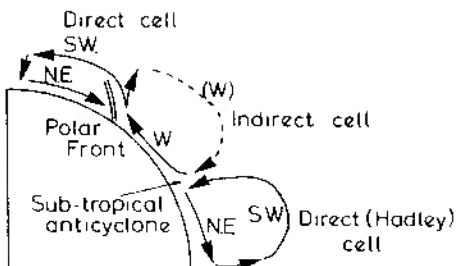


Fig. 3.27. Three-cell model of the northern hemisphere meridional circulation (*after Rossby 1941. From Barry 1967*).

factor in causing easterlies because the Coriolis force is small in low latitudes. The low-latitude cell, according to the above scheme, would be completed by poleward counter-currents aloft with the air sinking at about 30° latitude as it is cooled by radiation. However, this scheme is not entirely correct since the atmosphere does not have a simple heat source at the equator, the trades are not continuous around the globe (fig. 3.23) and poleward upper flow is restricted mainly to the western ends of the subtropical high-pressure cells aloft (see fig. 3.17).

Figure 3.27 shows another thermally direct cell in high latitudes with cold dense air flowing out from a polar high pressure. The reality of this is doubtful, but it is in any case of limited importance to the general circulation in view of the small mass involved. It is worth noting at this point that a single direct cell in each hemisphere is not possible, because the easterly winds near the surface would slow down the earth's rotation. On average the atmosphere must rotate with the earth, requiring a balance between easterly and westerly winds over the globe.

The mid-latitude cell in fig. 3.27 is thermally indirect and it would need to be driven by the other two. Momentum considerations indicate the necessity for upper easterlies in such a scheme, yet observations with upper-air balloons during the 1930s and 1940s demonstrated the existence of strong westerlies in the upper troposphere (see ch. 3, D.3). Rossby modified the three-cell model to incorporate this fact, proposing that westerly momentum was transferred to middle latitudes from the upper branches of the cells in high and low latitudes. Such horizontal mixing could, for example, be accomplished by troughs and ridges in the upper flow.

These views underwent radical amendment from about 1948 onwards.

The alternative means of transporting heat and momentum – by horizontal circulations – had been suggested in the 1920's by A. Defant and H. Jeffreys but could not be tested until adequate upper-air data became available. Calculations for the northern hemisphere by V. P. Starr and R. M. White at Massachusetts Institute of Technology showed that in middle latitudes horizontal cells transport most of the required heat and momentum polewards. This operates through the mechanism of the quasi-stationary highs and the travelling highs and lows near the surface acting in conjunction with their related wave patterns aloft. The importance of such horizontal eddies for energy transport is shown in fig. 3.28 (see also

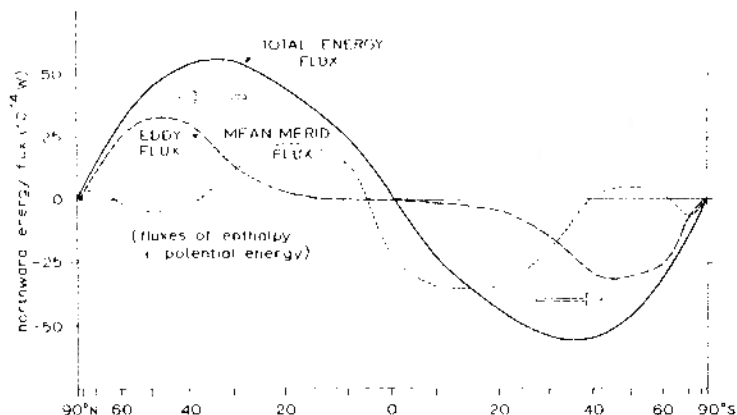


Fig. 3.28. The poleward transport of energy, showing the importance of horizontal eddies.

fig. 1.24B). The modern concept of the general circulation therefore views the energy of the zonal winds as being derived from travelling waves, not from meridional circulations. In lower latitudes, however, this mechanism may be insufficient by itself to account for the total energy transport estimated to be necessary for energy balance. For such reasons the mean Hadley cell still features in current representations of the general circulation, as fig. 3.29 shows, but the low-latitude circulation is recognized as being complex. In particular, the vertical heat transport in the Hadley cell is effected by giant cumulonimbus clouds in disturbance systems associated with the Equatorial Trough (of low pressure), which is located on average at 5°S in January and at 10°N in July (see ch. 6, B). The Hadley cell of the winter hemisphere is by far the most important and it

gives rise to low-level transequatorial flow into the summer hemisphere. The traditional model with twin cells, symmetrical about the equator, is found only in spring/autumn. Longitudinally, the Hadley cells are linked with the monsoon regimes of the summer hemisphere. Rising air over southern Asia (and also South America and Indonesia) is associated with east-west (zonal) outflow and these are systems known as 'Walker circulations'. The poleward return transport of the meridional Hadley cells takes place in troughs which extend into low latitudes from the mid-latitude westerlies. This tends to occur at the western ends of the upper tropospheric subtropical high pressure cells (see fig. 3.15). Horizontal

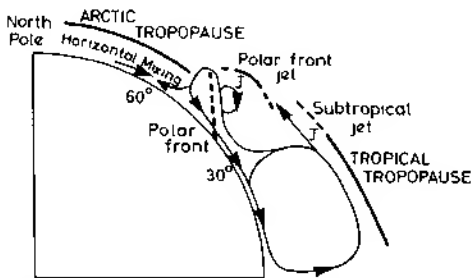


Fig. 3.29. General meridional circulation model for the northern hemisphere in winter (*after Palmén 1951. From Barry 1967*).

mixing predominates in middle and high latitudes although it is also thought that there is a weak indirect mid-latitude cell in much reduced form (fig. 3.29). The relationship of the jet streams to regions of steep meridional temperature gradient has already been noted (see fig. 3.19). A complete explanation of the two wind maxima and their role in the general circulation is still lacking, but they undoubtedly form an essential part of the story.

In the light of these theories the origin of the subtropical anticyclones which play such an important role in the world's climates may be re-examined. Their existence has been variously ascribed to the piling-up of poleward-moving air as it is increasingly deflected eastwards through the earth's rotation and the conservation of angular momentum; to the sinking of poleward currents aloft by radiational cooling; to the general necessity for high pressure near 30° latitude separating approximately equal zones of east and west winds; or to combinations of such

mechanisms. An adequate theory must account not only for their permanence but also for their cellular nature and the vertical inclination of the axes. The preceding discussion shows that ideas of a simplified Hadley cell and momentum conservation are only partially correct. Moreover, recent studies rather surprisingly show no relationship, on a seasonal basis, between the intensity of the Hadley cell and that of the subtropical highs.

It is probable that the high-level anticyclonic cells which are evident on *synoptic* charts (these tend to merge on mean maps) are related to anticyclonic eddies on the equatorward side of jetstreams. Theoretical and observational studies show that, as a result of the latitudinal variation of the Coriolis parameter, cyclones in the westerlies tend to move poleward and anticyclonic cells equatorward. Hence the subtropical anticyclones are constantly regenerated. The cellular pattern at the surface clearly reflects the influence of heat sources. The cells are stationary and elongated north-south over the northern hemisphere oceans in summer

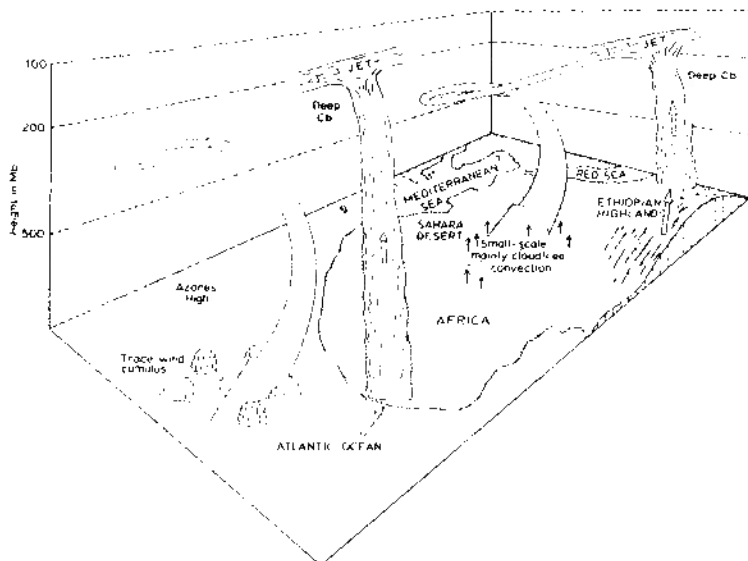


Fig. 3.30. Tentative flow model relating summer convection, the easterly jet stream and high-pressure subsidence over northern Africa and the eastern North Atlantic (adapted from Walker 1972) (Crown Copyright Reserved).

when continental heating creates low pressure and also the meridional temperature gradient is weak. In winter, on the other hand, the zonal flow is stronger in response to a greater meridional temperature gradient and continental cooling produces east-west elongation of the cells. Undoubtedly surface and high-level factors reinforce one another in some sectors and tend to cancel out in others. Indeed, it has been suggested that the Azores high pressure cell, in particular, owes part of its summer intensification and its tendency to extend eastward to air masses which rise locally in areas of high monsoonal rainfall over Africa, enter the tropical easterly jet stream circulation (see ch. 6, p. 308) and then subside over the western Sahara and the eastern North Atlantic (fig. 3.30).

2 Variations in the circulation of the northern hemisphere

The pressure and contour patterns during certain periods of the year may be radically different from those indicated by the mean maps (see figs. 3.17, 3.32 and 3.33). These variations, of three to 8 weeks' duration, occur irregularly but are rather more noticeable in the winter months when the general circulation is strongest. The nature of the changes is illustrated schematically in fig. 3.31. The zonal westerlies over middle latitudes develop waves and the troughs and ridges become accentuated, ultimately splitting up into a cellular pattern with pronounced meridional flow at certain longitudes. The strength of the westerlies between 35° and 55°N is termed the *zonal index*; strong zonal westerlies are representative of high index and marked cellular patterns occur with low index. A relatively low index may also occur if the westerlies are well south of their usual latitudes and, paradoxically, such expansion of the zonal circulation pattern is associated with strong westerlies in lower latitudes than usual. Figures 3.32 and 3.33 illustrate the mean 700 mb contour patterns and zonal wind speed profiles for two contrasting months. In December 1957 the westerlies were stronger than normal north of 40°N and the troughs and ridges were weakly developed, whereas in February 1958 there was low zonal index and an expanded circumpolar vortex, giving rise to strong low-latitude westerlies. The 700 mb pattern shows very weak subtropical highs, deep meridional troughs and blocking anticyclone off Alaska (see fig. 3.31D). The cause of these variations is still uncertain although it would appear that fast zonal flow is unstable and tends to break down. This tendency is certainly increased in the northern hemisphere by the arrangement of the continents and oceans.

Detailed studies are now beginning to show that the irregular index fluctuations, together with secondary circulation features, such as cells of

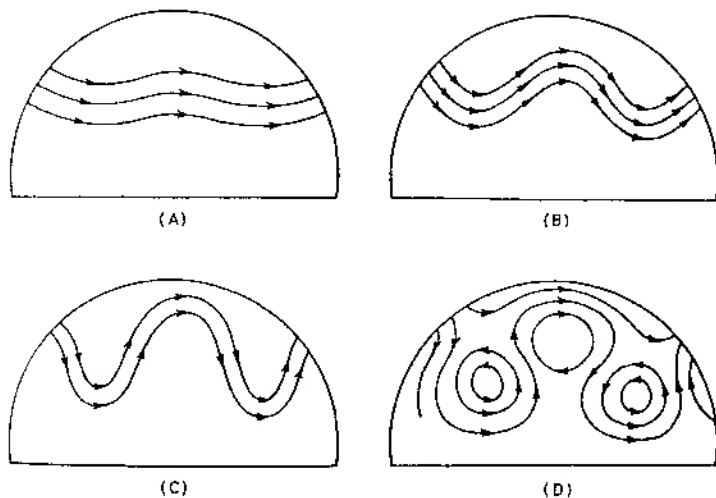


Fig. 3.31. The index cycle. A schematic illustration of the development of cellular patterns in the upper westerlies, usually occupying 3–8 weeks and being especially active in February and March in the northern hemisphere. Statistical studies indicate no regular periodicity in this sequence.

A. High zonal index. The jet stream and the westerlies lie north of their mean position. The westerlies are strong, pressure systems have a dominantly east–west orientation, and there is little north–south air-mass exchange.

B and C. The jet expands and increases in velocity, undulating with increasingly larger oscillations.

D. Low zonal index. Complete break-up and cellular fragmentation of the zonal westerlies. Formation of stationary deep occluding cold depressions in lower mid-latitudes and deep warm blocking anticyclones at higher latitudes. This fragmentation commonly begins in the east and extends westward at a rate of about 60° of longitude per week (*after Namlas. From Haltiner and Martin 1957*).

low and high pressure at the surface or long waves aloft, play a major role in redistributing momentum and energy. Laboratory experiments with rotating ‘dishpans’ of water to simulate the atmosphere, and computer studies using numerical models of the atmosphere’s behaviour demonstrate that a Hadley circulation cannot provide an adequate mechanism for transporting heat poleward. In consequence, the meridional temperature gradient increases and eventually the flow becomes unstable in the Hadley mode, breaking down into a number of cyclonic and anticyclonic eddies. This phenomenon is referred to as

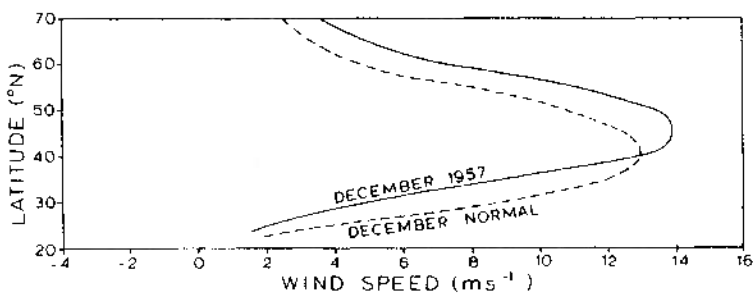
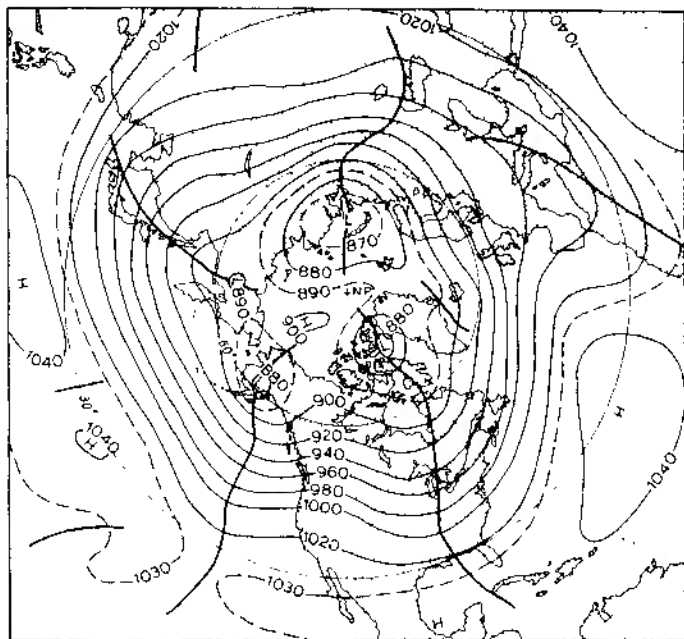


Fig. 3.32. *Above.* Mean 700-mb contours (in tens of feet) for December 1957, showing a fast, westerly, small-amplitude flow typical of a high zonal index. *Below.* Mean 700-mb zonal wind speed profiles ($m s^{-1}$) in the Western Hemisphere for December 1957, compared with those of a normal December. The westerly winds were stronger than normal and displaced to the north (after *Monthly Weather Review* 85, 1957, 410–11).

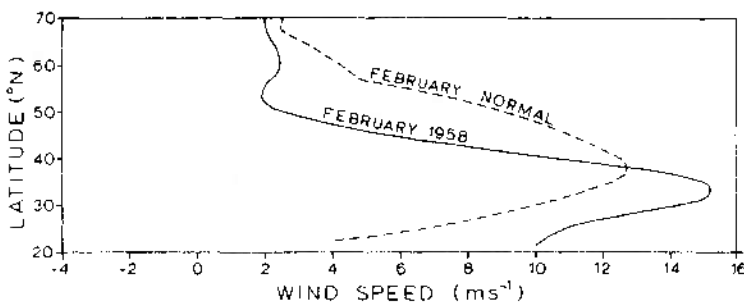
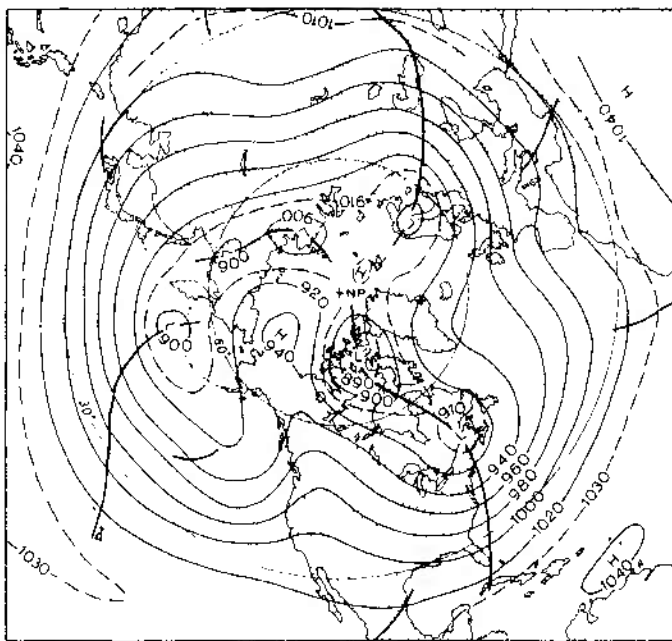


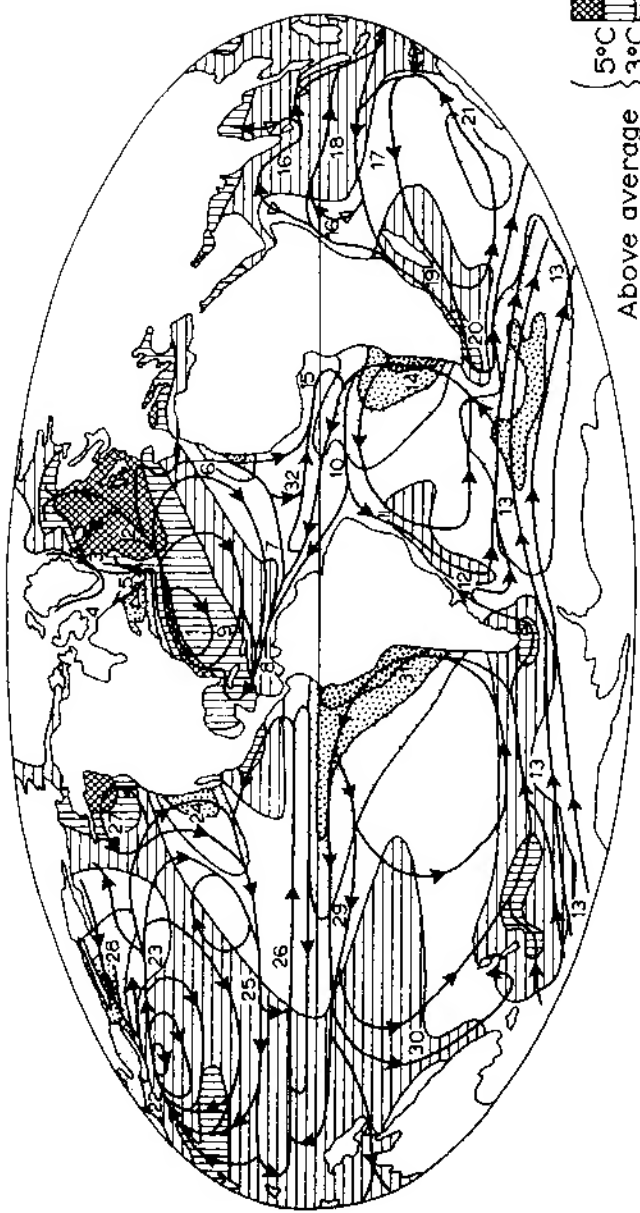
Fig. 3.33. Above. Mean 700-mb contours (in tens of feet) for February 1958. Below. Mean 700-mb zonal wind speed profiles ($m s^{-1}$) in the Western Hemisphere for February 1958, compared with those of a normal February. The westerly winds were stronger than normal at low latitudes, with a peak at about $33^{\circ}N$ (after *Monthly Weather Review* 86, 1958, 62-3).

baroclinic instability. In energy terms, the potential energy in the zonal flow is converted into potential and kinetic energy of the eddies. It is also now known that the kinetic energy of the zonal flow is derived from the eddies, the reverse of the classical picture which viewed the disturbances within the global wind belts as super-imposed detail. The significance of atmospheric disturbances and the variations of the circulation are becoming increasingly evident. The mechanisms of the circulation are, however, greatly complicated by numerous interactions and *feedback* processes, one of the most important of which involves the oceanic circulation as outlined below. The significance of interactions between the oceanic and atmospheric heat and moisture budgets has already been discussed in ch. 1, G, and ch. 2, A.

3 The circulation of the ocean surface

The most obvious feature of the surface oceanic circulation is the control exercised over it by the low-level planetary wind circulation, especially by the subtropical oceanic high pressure circulations and the westerlies. The oceanic circulation even partakes of the seasonal reversals of flow in the monsoonal regions of the northern Indian Ocean, off East Africa and off northern Australia (fig. 3.34). The Ekman effect (see ch. 3, A.5) causes the flow to be increasingly deflected to the right (in the northern hemisphere) and to decrease in velocity as the influence of the wind stress diminishes with depth. However, the rate of change of flow direction with depth increases with latitude, such that near the equator there are no flow reversals at depth which are characteristic of higher latitudes. The depth at which this reversal occurs decreases poleward, but averages about 50 m over large areas of the ocean. In addition, as water moves meridionally the conservation of angular momentum implies changes in relative vorticity (see p. 139 and p. 167), with poleward-moving currents acquiring anticyclonic vorticity and equatorward-moving currents acquiring cyclonic vorticity.

Equatorward of the subtropical high pressure cells the persistent trade winds generate the broad North and South Equatorial Currents (fig. 3.34). On the western sides of the oceans most of this water swings poleward with the airflow and thereafter increasingly comes under the influence of the Ekman deflection and of the anticyclonic vorticity effect. However, some water tends to pile up near the equator on the western sides of oceans, partly because here the Ekman effect is virtually absent with little poleward deflection and no reverse current at depth. To this is added some of the water which is displaced northward into the equatorial



zone by the especially active subtropical high-pressure circulations of the southern hemisphere. This accumulated water flows back eastward down the hydraulic gradient as compensating narrow surface Equatorial Counter Currents, unimpeded by the weak surface winds. As the circulations swing poleward round the western margins of the oceanic subtropical high-pressure cells there is the tendency for water to pile up against the continents giving, for example, an appreciably higher sea level in the Gulf of Mexico than that along the Atlantic coast of the United States. This accumulated water cannot escape by sinking because of its relatively high temperature and resulting vertical stability, and it consequently continues poleward in the dominant direction of surface airflow. As a result of this movement the current gains anticyclonic vorticity which reinforces the similar tendency imparted by the winds, leading to relatively narrow currents of high velocity (for example, the Kuro Shio, Brazil, Mozambique-Agulhas and, to a less-marked extent, the East Australian Current). In the North Atlantic the configuration of the Caribbean Sea and Gulf of Mexico especially favours this pile-up of water, which is released poleward through the Florida Straits as the particularly narrow and fast Gulf Stream.

These poleward currents are opposed both by their friction with the nearby continental margins and by energy losses due to turbulent diffusion, such as those accompanying the formation and cutting off of meanders in the Gulf Stream. On the poleward sides of the subtropical high-pressure cells westerly currents dominate, and where they are un-

Fig. 3.34. The general ocean current circulation of the globe, showing the mean temperature anomalies of surface ocean temperatures.

1. Gulf Stream
2. North Atlantic Drift
3. East Greenland Current
4. West Greenland Current
5. Labrador Current
6. Canary Current
7. North Equatorial Current
8. Caribbean Current
9. Antilles Current
10. South Equatorial Current
11. Brazil Current
12. Falkland Current
13. West Wind Drift
14. Benguela Current
15. Guinea Current
16. Southwest and Northeast Monsoon Drift
17. South Equatorial Current
18. Equatorial Counter Current
19. Mozambique Current
20. Agulhas Current
21. West Australian Current
22. Kuro Shio Current
23. North Pacific Drift
24. California Current
25. North Equatorial Current
26. Equatorial Counter Current
27. Alaska Current
28. Kamchatka Current
29. South Equatorial Current
30. East Australian Current
31. Peru or Humboldt Current
32. Equatorial Counter Current

impeded by landmasses in the southern hemisphere they form the broad and swift West Wind Drift. In the northern hemisphere a great deal of the eastward-moving current in the Atlantic swings northward, leading to very anomalously high sea temperatures, and is compensated for by a southward flow of cold Arctic water at depth. However, more than half of the water mass comprising the North Atlantic Drift, and almost all that of the North Pacific Drift, swings south round the east sides of the sub-tropical high-pressure cells, forming the Canary and California Currents. Their Southern-hemisphere equivalents are the Benguela, Humboldt or Peru, and West Australian Currents. In contrast with the currents on the west sides of the oceans, these currents acquire cyclonic vorticity which is in opposition to the anticyclonic wind tendency, leading to relatively broad flows of low velocity. In addition the deflection due to the Ekman effect causes the surface water to move westward away from the coasts, leading to upwelling of cold water from depths of 100–300 m. Although the band of upwelling may be quite narrow (about 200 km wide for the Benguela Current) the Ekman effect spreads this cold water westward. On the poleward margins of these cold-water coasts the meridional swing of the wind belts imparts a strong seasonality to the upwelling, the California Current upwelling, for example, being particularly well marked during the period, March–July.

4 Air masses, fronts and depressions

An air mass may be defined as a large body of air whose physical properties, especially temperature, moisture content and lapse rate, are more or less uniform horizontally for hundreds of kilometres. The theoretical ideal is an atmosphere where surfaces of constant pressure are not intersected by isosteric (constant-density) surfaces, so that in any vertical cross-section, as shown in fig. 4.1, isobars and isotherms are parallel. Such an atmosphere is referred to as *barotropic*.

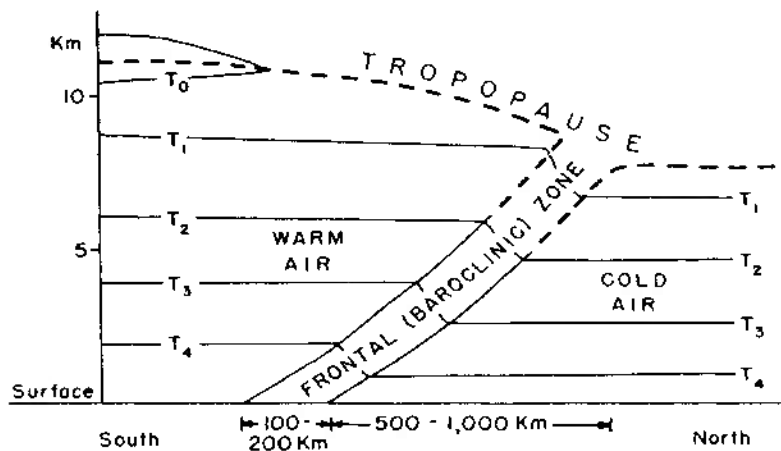
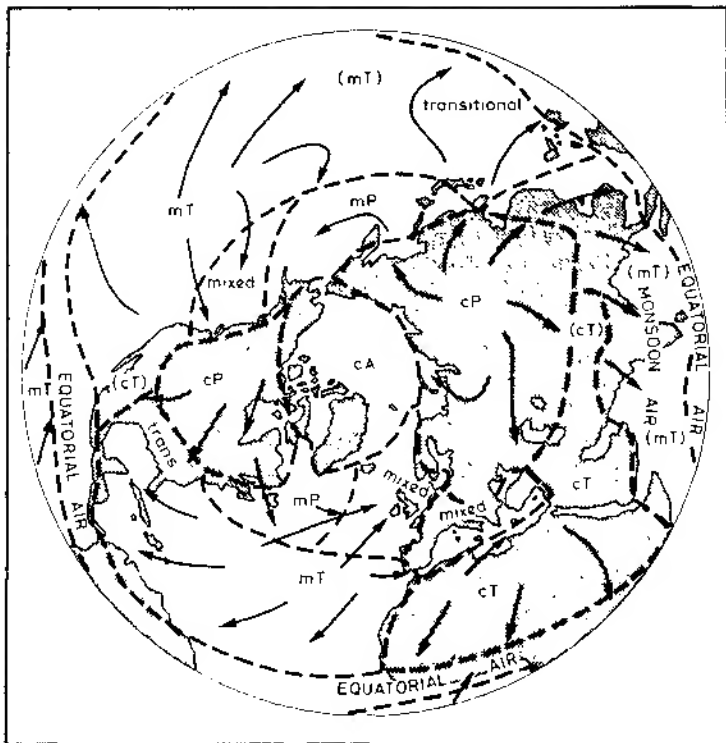


Fig. 4.1. A schematic temperature section showing barotropic air masses and a baroclinic frontal zone (assuming that density decreases with height only).



Three main factors tend to determine the nature and degree of uniformity of air-mass characteristics. They are: (a) the nature of the source area (from which the air mass obtains its original qualities), and the direction of movement (the physical properties of all air masses are classified according to the way in which they compare with the corresponding properties of the underlying surface region or with those of adjacent air masses); (b) changes that occur in the constitution of an air mass as it moves over long distances; and (c) the age of the air mass.

Study of the contrasting properties of different air masses leads naturally on to a consideration of air-mass boundaries or *fronts*. Their relationship to low-pressure centres and to the patterns of airflow aloft are also discussed in this chapter, and this is followed by a brief examination of the various approaches adopted in weather forecasting.

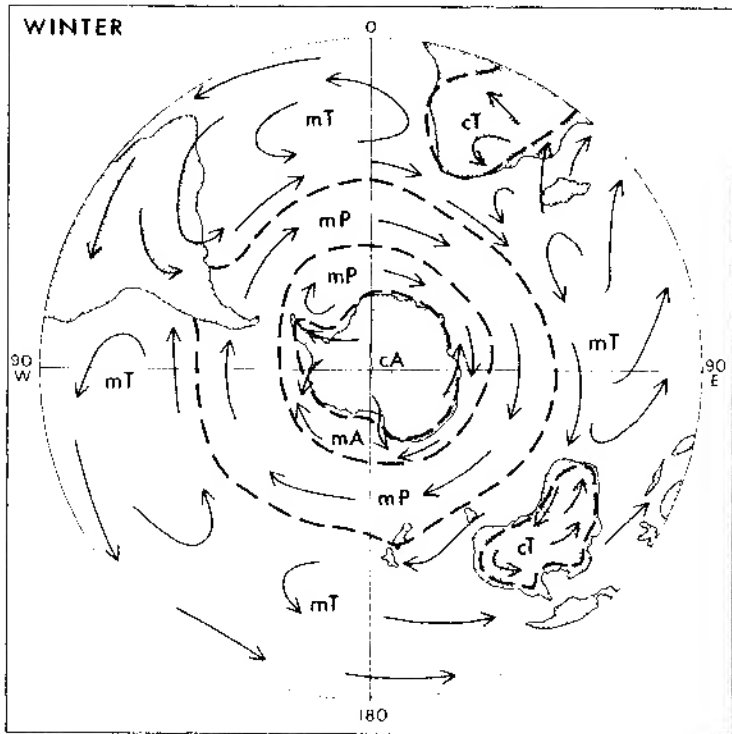


Fig. 4.2. Air masses in winter.

Left. Northern hemisphere (after Pettersen 1958 and Crowe 1965).

Above. Southern hemisphere (after Taljaard 1972).

A Nature of the source area

We have already observed how most of the physical processes of our atmosphere result from self-regulating attempts to equalize the major differences that arise from inequalities in the world distribution of heat, moisture and pressure. On the world scale the heat and momentum balances refer only to long-term average conditions. However, on a smaller scale, radiation and vertical mixing can produce some measure of equilibrium between the surface conditions and the properties of the overlying air mass if air remains over a given geographical region for a period of about 3 to 5 days. Naturally the chief source regions of air

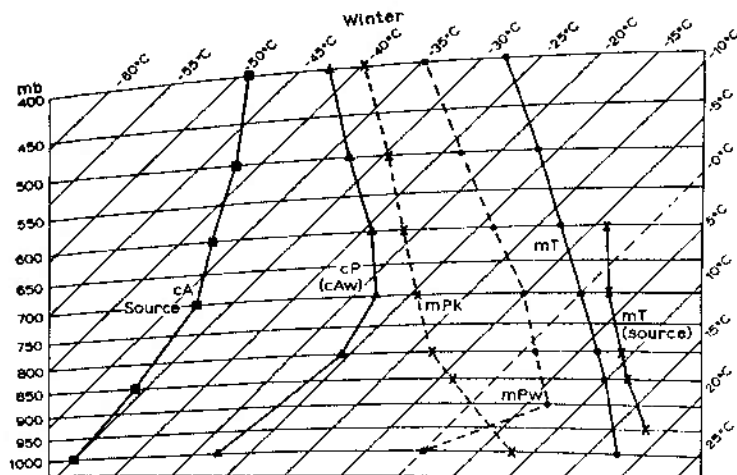


Fig. 4.3. The average vertical temperature structure for selected air masses affecting North America at about 45°–50°N, recorded over their source areas or over North America in winter (after Godson, Showalter and Willett).

Table 4.1 Air-mass characteristics in winter

- (1) Typical values in North America, 45–50°N (after Godson 1950)
 - (2) Monthly means over the British Isles, using surface data at Kew in place of the 1000 mb values (after Belasco 1952)
 - (3) Typical values in the Mediterranean (after 'Weather in the Mediterranean', M.O. 391, 1962)
 - (4) Typical values in Australia, 33°S
 - (5) Typical values in Antarctica, 75°S
 - (6) Typical values in the Southern Oceans, 50°S
- } (after Taljaard 1969)

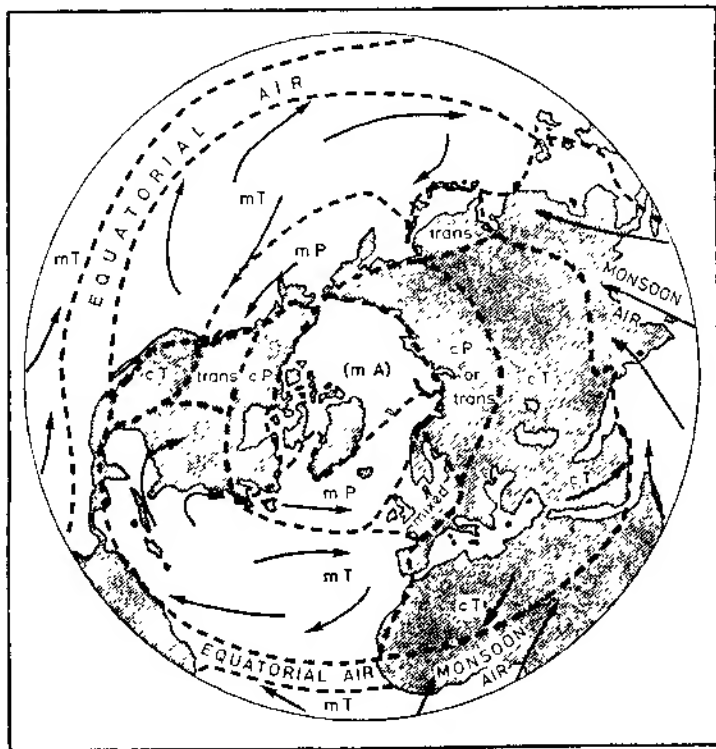
T = air temperature (°C) x = humidity mixing ratio (g/kg)

Air Mass	Level (mb)			
	1000	850	700	500
cA (1) T	—	-31	-33	-42
(3) T	1	-8	-21	-36
(3) x	2.4	1.7	0.4	0.2
(5) T	(0.33)††	-28	-30	-42
(5) x	(0.2)††	0.3	0.2	0.1

Air Mass	Level (mb)	1000	850	700	500
mA (1) T	—	—10	21	—38	
† (2) T	1	—9	—20	—40	
(2) x	3 1	1 7	0 7	0 6	
(3) T	4	—6	—14	—33	
(3) x	4 6	2 2	1 3	0 3	
(6) T	0	—10	—20	—35	
(6) x	3 0	1 6	0 8	0 2	
cP (1) T	—	—18	—20	—33	
* (2) T	—2	—12	—22	—41	
(2) x	2 6	1 5	0 6	0 1	
(3) T	7	—2	—13	—24	
(3) x	4 5	2 6	1 3	0 4	
mPw (1) T	—	5	—4	—23	
** (2) T	8	1	—9	—27	
(2) x	5 8	4 0	2 1	0 6	
(3) T	12	2	—7	—23	
(3) x	7 8	4 0	1 6	0 4	
(4) T	10	2	—7	—25	
(4) x	5 5	3 4	1 8	0 4	
mT (1) T	—	10	0	—17	
† (2) T	11	6	—2	—17	
(2) x	6 8	5 6	3 5	1 2	
(3) T	—	10	2	—14	
(3) x	—	6 0	2 5	1 0	
(4) T	14	6	—2	—18	
(4) x	7 8	5 3	2 5	0 9	
cT (3) T	—	19	5	—17	
(3) x	—	1 8	1 3	0 6	
Med (3) T	14	3	—3	—19	
(3) x	7 0	3 7	2 5	0 9	

Belasco's classification: † P₁, * A₁, ** P₂, † T₁, ‡ 950 mb level.

masses are areas of extensive, uniform surface type which are normally overlain by quasi-stationary pressure systems. These requirements are fulfilled where there is slow divergent flow from the major thermal and dynamic high-pressure cells, whereas low-pressure regions are zones of convergence into which air masses move (see ch. 4, E).



Air masses are classified on the basis of two primary factors. The first is the temperature, giving arctic, polar and tropical air, and the second is the type of surface in their region of origin, giving maritime and continental categories. The major cold and warm air masses will now be discussed.

1 Cold air masses

The principal sources of cold air in the northern hemisphere are: (a) the continental anticyclones of Siberia and northern Canada, which originate continental polar (cP) air masses, and (b) the Arctic Basin, when it is dominated by high pressure (fig. 4.2). Some classifications designate air

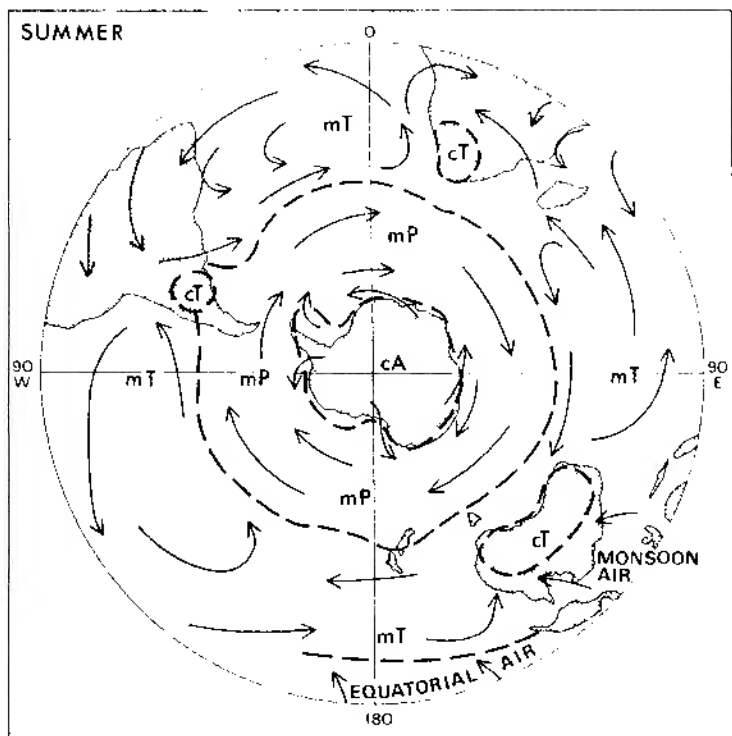


Fig. 4.4. Air masses in summer.

Left. Northern hemisphere (after Petterssen 1958 and Crowe 1965).
Above. Southern hemisphere (after Taljaard 1972).

of the latter category as continental arctic (cA), but the differences between cP and cA air masses are limited mainly to the middle and upper troposphere, where temperatures are lower in the cA air (table 4.1).

The snow-covered source regions of these two air masses lead to

marked cooling of the lower layers (see fig. 4.3) and, since the vapour content of cold air is very limited, the air masses generally have a mixing ratio of only 0.1–0.5 g/kg near the surface. The stability produced by the effect of surface cooling prevents vertical mixing so that further cooling occurs more slowly by radiation losses only. The effect of this radiative cooling and the tendency for air-mass subsidence in high-pressure regions combine to produce a prominent temperature inversion from the surface up to about 850 mb in typical cA and cP air. In view of their extreme dryness these air masses are characterized by small cloud amounts and only occasional light snowfalls. In summer continental heating over northern Canada and Siberia causes the virtual disappearance of their sources of cold air. The Arctic Basin source remains (see fig. 4.4A), but the cold air here is very limited in depth at this time of year. In the southern hemisphere, the Antarctic continent and the ice shelves are a source of cA air in all seasons (figs. 4.2B and 4.4B). There are no sources of cP air, however, due to the dominance of ocean areas in middle latitudes. At all seasons cA or cP air is greatly modified by a passage over the ocean. Secondary types of air mass are produced by such means and these will be considered in ch. 4, B.

2 Warm air masses

These have their origins in the subtropical high-pressure cells and, during the summer season, in the great accumulations of warm surface air which characterize the heart of large land areas.

The tropical (T) sources are either maritime (mT), originating in the oceanic subtropical high-pressure cells, or continental (cT), originating either from the continental parts of these subtropical cells (e.g. as does the North African *Harmattan*) or simply associated with regions of generally light variable winds, assisted by upper tropospheric subsidence, over the major continents in summer (e.g. Central Asia). In the southern hemisphere, the source area of mT air covers about half of the hemisphere. There is no zone of significant temperature gradient between the Equator and the oceanic Subtropical Convergence about 40°S.

The maritime type is characterized by high temperatures (accentuated by the warming action to which the descending air is subjected), high humidity of the lower layers over the oceans, and stable stratification. Since the air is warm and moist near the surface, stratiform cloud commonly develops as the air moves polewards from its source. The continental type in winter is restricted mainly to North Africa (fig. 4.2, table 4.1), where it is a warm, dry and stable air mass. In summer, warming of the

lower layers by the heated land generates a steep lapse rate, but despite its instability the low relative and specific humidity prevent the development of cloud and precipitation. In the southern hemisphere, cT air is rather more prevalent in winter over the subtropical continents except South America. In summer, much of southern Africa and northern Australia is affected by mT air, while there is a small source of cT air over Argentina (fig. 4.4B).

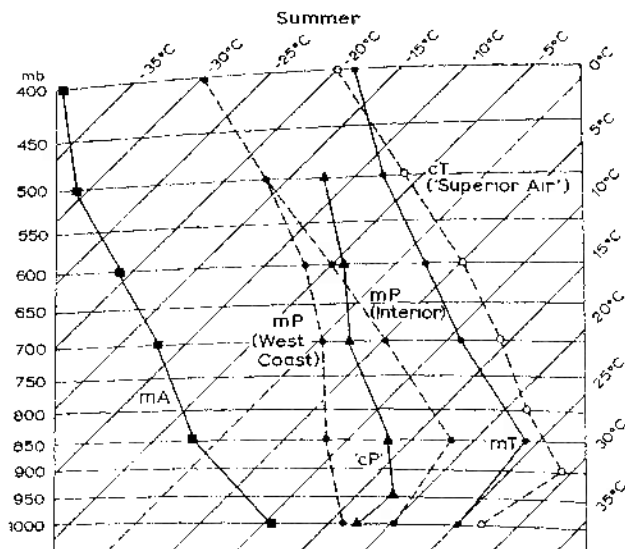


Fig. 4.5. The average vertical temperature structure for selected air masses affecting North America in summer (after Godson, Showalter and Willett).

The characteristics of the primary air masses are illustrated in figs. 4.3 and 4.5 and tables 4.1 and 4.2. In some cases their properties have been considerably affected by movement away from the source region, and it is this question which will now be considered.

B Air-mass modification

As air masses move away from their source region they are affected by different heat and moisture exchanges with the ground surface and by

190 Atmosphere, weather and climate

Table 4.2 Air-mass characteristics in summer (Key as for Table 4.1)

Air Mass	Level (mb)			
	1000	850	700	500
cA (5) T	(-9) ‡	-13	-20	-33
(5) x	(1.8) ‡	1.1	0.7	0.2
mA (1) T	—	-4	-14	-33
(2) T	14	2	-7	-25
(2) x	6.3	4.3	2.5	0.1
mP (1) T	—	11	0	-19
* (2) T	16	4	-6	-24
(2) x	8.4	3.9	2.2	0.4
(3) T	—	18	-2	-19
(3) x	—	6.0	2.5	0.8
(4) T	17	8	0	-14
(4) x	8.0	6.0	3.1	1.0
cP (3) T	26	13	4	-14
(3) x	16.1	6.7	3.4	0.9
mT (1) T	—	18	8	-8
(2) T	19	12	4	-11
(2) x	10.8	8.1	4.5	2.4
(4) T	22	16	5	-11
(4) x	13.4	8.0	4.8	1.7
cT (1) T	—	22	10	-11
(2) T	21	16	6	-11
(2) x	12.1	3.9	3.4	1.1
† (3) T	—	26	13	-10
(3) x	—	4.5	2.5	0.5
(4) T	27	20	7	-12
(4) x	8.0	4.7	3.6	1.2
Med (3) T	29	19	12	-6
(3) x	14.1	7.4	3.0	0.9

Belasco's classification: * P_j. † cT originating over Africa, ‡ 950 mb.

dynamic processes in the atmosphere. Thus an initially barotropic air mass is gradually changed into a moderately *baroclinic* airstream in which isosteric and isobaric surfaces intersect one another. The presence of horizontal temperature gradients means that air cannot travel as a solid block maintaining an unchanging internal structure. The trajectory (i.e. actual path) followed by an air parcel in the middle or upper troposphere will normally be quite different from that of a parcel nearer the surface, due to the increase of westerly wind velocity with height in the troposphere. The actual structure of an airstream at a given instant is determined to a large extent by the past history of air-mass modification processes. In spite of these qualifications the air-mass concept nevertheless remains of considerable practical value.

1 Mechanisms of modification

The mechanisms by which air masses are modified are, for convenience, treated separately, although this rigid distinction is often not justified in practice.

a Thermodynamic changes. An air mass may be heated from below either by passing from a cold to a warm surface or by solar heating of the ground over which the air is located. Similarly, but in reverse, it can be cooled from below. Heating from below acts to increase air-mass instability so that the effect may be spread rapidly through a considerable thickness of air, whereas surface cooling produces a temperature inversion which greatly limits the vertical extent of the cooling. For this reason cooling mainly occurs through radiative heat loss by the air, a process which takes place only very gradually.

Changes can also occur through increased evaporation, the moisture being supplied either from the underlying surface or by precipitation from an overlying air mass layer. In reverse, the abstraction of moisture by condensation or precipitation can also cause changes. A parallel, and most important, change is the respective addition or loss of latent heat accompanying this condensation or evaporation. The distribution of latent and sensible heat transfers to the atmosphere are illustrated in figs. 1.26 and 1.27, although it must be noticed that these refer to annual values.

b Dynamic changes. Dynamic (or mechanical) changes are, superficially at any rate, different from thermodynamic changes because they involve mixing or pressure changes associated with the actual movement of the air mass. The distribution of the physical properties of air masses has been shown to be considerably modified, for example, by a prolonged

192 Atmosphere, weather and climate

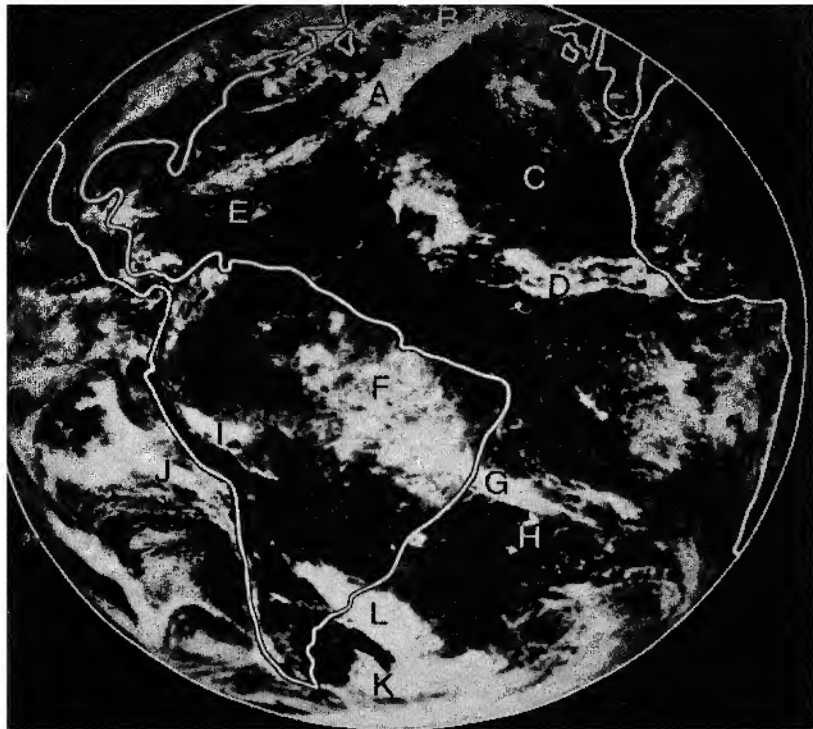
period of turbulent mixing (see fig. 2.15). This process is particularly important at low levels where surface friction intensifies the natural turbulence of airflow, providing a ready mechanism for the upward transfer of the effects of thermodynamic processes.

The radiative and advective exchanges discussed previously are non-adiabatic, but the ascent or descent of air causes adiabatic changes of temperature. Large-scale lifting may result from forced ascent by a mountain barrier or from airstream convergence. Conversely, sinking may occur when high-level convergence sets up subsidence or when stable air, having been forced up over high ground by the pressure gradient, descends in its lee. Dynamic processes in the middle and upper troposphere are in fact a major cause of air-mass modification. The decrease in stability aloft, as air moves away from the areas of subsidence, is a common example of this type of mechanism.

2 The results of modification: secondary air masses

The study of the ways in which air masses change in character tells us a great deal about our weather, for many common meteorological phenomena are the product of such modification.

a Cold air. Continental polar air frequently streams out from Canada over the western Atlantic in winter, where it undergoes rapid transformation. Heating over the Gulf Stream Drift rapidly makes the lower layers unstable and evaporation into the air leads to sharp increases of moisture content (see fig. 1.26). The turbulence associated with the convective instability is marked by gusty conditions. By the time the air has reached the central Atlantic it has become a cool, moist, maritime polar (mP) air mass. Analogous processes occur with outflow from Asia over the north Pacific (see fig. 4.2). Over middle latitudes of the southern hemisphere the circumpolar ocean gives rise to a continuous zone of mP air which, in summer, extends to the margin of Antarctica. In this season, however, there is a considerable gradient of ocean temperatures associated with the Antarctic Convergence that makes the zone far from uniform in its physical properties. The weather in cP airstreams is typically that of bright periods and squally showers, with a variable cloud cover of cumulus and cumulonimbus. As the air moves eastward towards Europe the cooler sea surface may produce a neutral or even stable stratification near the surface, especially in summer, but subsequent heating over land will again regenerate unstable conditions. Similar conditions, but with lower temperatures (table 4.1), result if cA air crosses sea areas in high latitudes producing maritime arctic (mA) air.



A photograph of almost the entire disc of the earth (more than $\frac{1}{2}$ of the total earth's surface) taken from about 36,000 km (about 22,000 miles) above the equator on 10 November 1967 by the US Applications Technology Satellite (ATS-3). This shows depressions over the North (B) and South (K) Atlantic, from which cold fronts (A and L) extend equatorward. The Azores high-pressure area (C) is mostly cloud free, but convective cloud obscures some of the West Indian islands (E), and there are isolated thunderstorms in the South Atlantic (H). The cloud-covered equatorial trough (D) is clearly visible, the lower Amazon Basin (F) is completely obscured by precipitation, and jet-stream clouds extend south-east from Brazil (G). The windward side of the central Andes is bathed in cloud (I), and there is much low cloud off the west coast of South America associated with the cold ocean current (J) (*NASA photograph*).

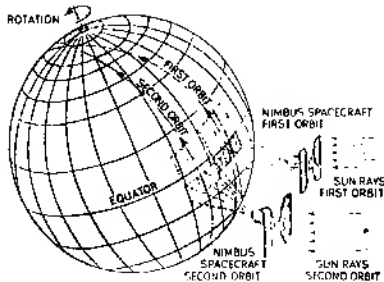
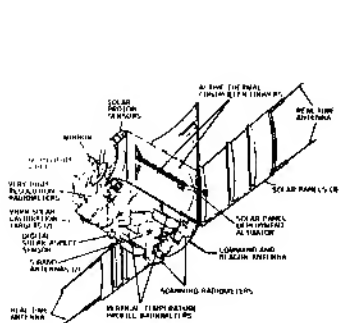


Plate 1. Features of the NOAA 2 spacecraft, which include the capability for obtaining vertical temperature and humidity data twice daily on a global basis (from 'World Weather Program Plan for fiscal year 1974', Dept. of Commerce, Supt. of Documents, Washington, D.C.)

Plate 2. Nimbus II TV camera coverage of approximately 3516×740 km (2185×460 miles). Successive frames at 91-second intervals with about 20% overlap give 32 pictures for each orbit. Orbits are inclined at about 80° to the equator and each successive orbit is displaced about 27° in longitude (*Nimbus II Users' Guide*).

Plate 3. Cumulus orographic clouds developed over the dip-slope of the South Downs in Sussex, England. To the west, southern Hampshire is covered by stratiform clouds. This infrared photograph was taken from an elevation of about 12,000 m (40,000 ft) (B = Burgess Hill; Br = Brighton; H = Haywards Heath; S = Shoreham; W = Worthing) (P.A.—Reuter Ltd).





Plate 4. The snow-covered mountains of southern Norway photographed by *Tiros IX* on 1 April 1965 from a height of 797 km (495 miles). To the west fog and low stratus clouds cover the sea, but near the Norwegian coast cold air draining off the mountains is sweeping the coastal waters giving clear conditions. To the east of the Scandinavian Mountains lee waves have formed in the middle troposphere with wavelengths of approximately 14 km (8.7 miles) (*Environmental Science Services Administration*).



Plate 5. Night-time (0900 GMT) infrared photograph showing sea surface temperatures off the south-east coast of the United States on 15 February 1971 (see fig. 1.19). G-coldest shelf water; H-shelf water of intermediate temperature; I-warm Gulf Stream, clearly showing meanders associated with cold water intrusions (J) (*World Meteorological Organization 1973*).

Plate 6. View north along the eastern front of the Colorado Rockies, showing lee-wave clouds (*NCAR photograph by Robert Bumpas*).





Plate 7. View looking south-south-east from about 9000 m (30,000 ft) along the Owen's Valley, California, showing a roll cloud developing in the lee of the Sierra Nevada mountains. The lee-wave crest is marked by the cloud layer and the vertical turbulence is causing dust to rise high into the air (W = Mount Whitney, 4418 m (14,495 ft); I = Independence) (photograph by Robert F. Simons. Courtesy of R. S. Scorer).

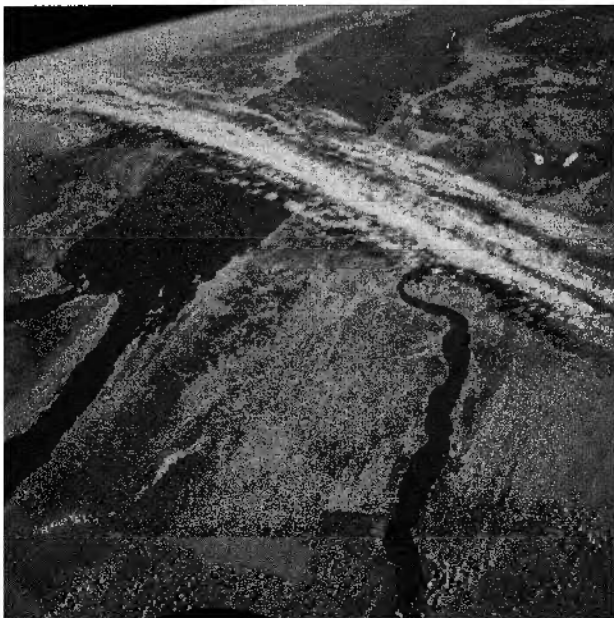


Plate 8. Radiating or dendritic cellular (actiniform) cloud pattern. These complex convective systems, some 150–250 km (90–150 miles) in diameter, were only discovered as a result of satellite photography. They usually occur in groups over areas of subsidence inversions intensified by cold ocean currents (e.g. in the low latitudes of the eastern Pacific) (Environmental Science Service Administration).



Plate 9. Photograph of Decca 45, Mk 1, 3-cm weather radar display of south-eastern England on 8 November 1955 in late afternoon. A warm occlusion had passed north-eastwards over the Straits of Dover at noon on the previous day and was followed by a mild southerly airstream in association with two centres of low pressure lying to the west of the British Isles. The unstable airstream gave temperatures well above the average, light to fresh winds, $\frac{1}{2}$ – $\frac{7}{8}$ cloud cover and showers with scattered thunderstorms over the south-east coast. Coastlines and synoptic data have been superimposed on the radar display. (Temperatures in °F) (courtesy Decca Radar Ltd. The basic display previously appeared in 'Introduction to Hydro-meteorology' by J. P. Bruce and R. H. Clark, Pergamon Press, London, 1966).

Plate 10. Photograph by an astronaut from Gemini XII manned spacecraft from an elevation of some 180 km (112 miles) looking south-east over Egypt and the Red Sea. The band of cirrus clouds is associated with strong upper winds, possibly concentrated as a jet stream (NASA photograph).



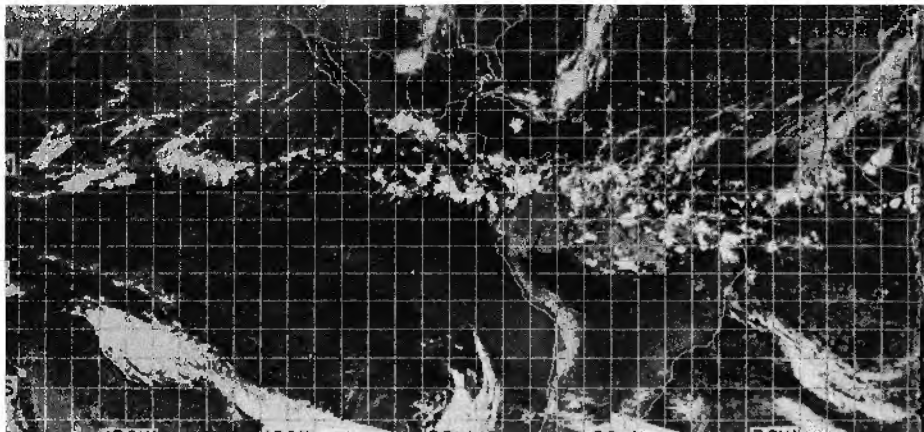


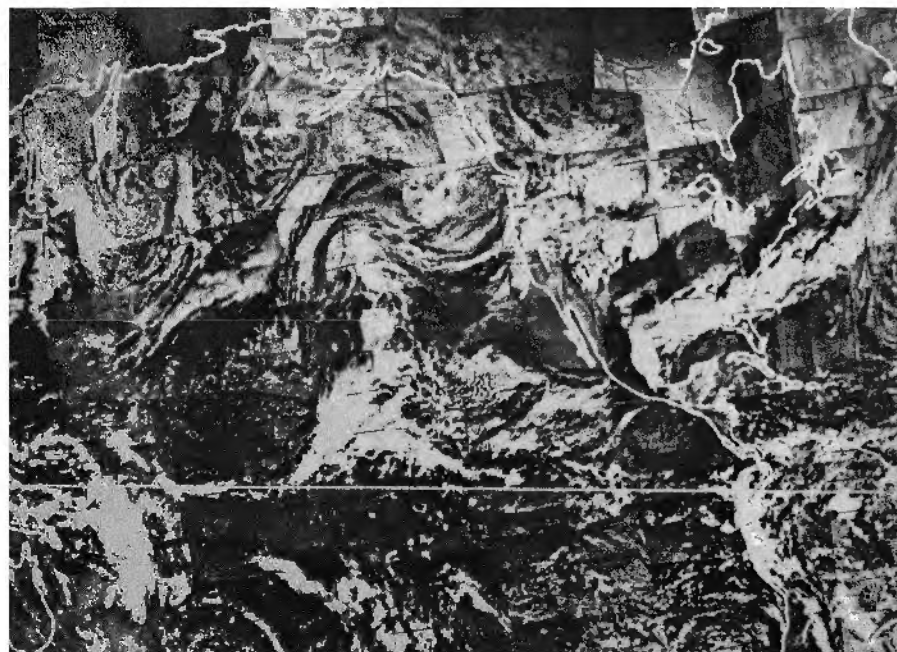
Plate 11. Infrared photograph showing the inter-tropical convergence zone (ITCZ) on 1 June 1971, along which active thunderstorms appear as bright spots (NOAA-1 photograph, World Meteorological Organization 1973).

Plate 12. Mosaic of pictures from Tiros IX covering nearly the whole world taken on 13–14 February 1965. Fronts and depressions in the westerlies are especially apparent in the North Atlantic and the southern hemisphere, whereas anticyclonic clear areas are also evident (e.g. over western Spain and west of California). South of Kamchatka and north-west of the British Isles the characteristic cellular cloud patterns are associated with cold air moving south over warmer ocean surfaces behind cold fronts. The Inter-



Plate 13. Photograph taken at 1446 GMT on 3 April 1968 by the Applications Technology Satellite (ATS-3) from an altitude of about 36,000 km (22,300 miles) above the equator at 84° W. A number of depressions are shown over the United States (A), the North Atlantic (B), the South Atlantic (C) and the South Pacific (D), together with much cloud on the windward (i.e. eastern) side of the Central Andes (E). The depression over the United States was centred on Nebraska (A) and a cold front (F) trailing southward to the Texas coast is clearly visible. This front contained lines of thunderstorms with tops reaching to 12,000–14,000 m (39,000–40,000 ft) and on that day 3 tornadoes and 10 funnel clouds were reported from Iowa, Oklahoma and Nebraska (from *Monthly Weather Review* 96, 1968, 397–8).

Tropical Convergence Zone cloud-belts appear just north of the equator in the Atlantic and eastern Pacific, and south of the equator in the Indian Ocean. Hurricane 'Sarah' is located over the South China Sea and another hurricane over the southern Indian Ocean. North-east to south-west over northern Africa is a possible jet-stream cloud belt (U.S. Weather Bureau and Environmental Science Services Administration).



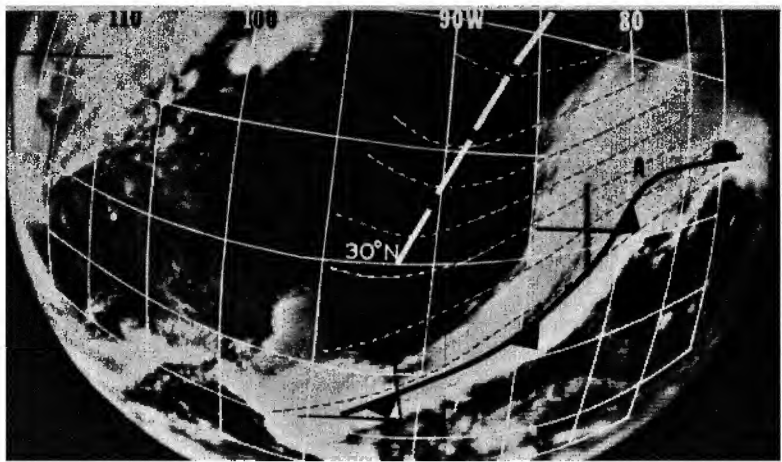


Plate 14. The initiation of a depression, centred (A) south-east of Cape Hatteras, along a frontal belt stretching north-east from the Gulf of Mexico, observed by Tiros IX on 14 February 1965. The 500-mb contour pattern is indicated by the fine dashed lines and a trough at this level (heavy dashed line) is approaching from the west (*APT Users' Guide, Environmental Science Services Administration*).

Plate 15. View looking westward towards an approaching warm front, with lines of jet-stream clouds extending from the north-west, from which trails of ice crystals are falling. In the middle levels are dark wave clouds formed in the lee of small hills by the south-westerly airflow, whereas the wind direction at the surface is more





Plate 16. Cold front lying to the north-west of the British Isles, taken by the ESSA 6 satellite at 1130 GMT on 28 March 1968. Convective cloud is visible in the unstable airflow behind the front, and the glitter on the North Sea is indicative of a fairly smooth sea surface and, consequently, of light surface winds. Scandinavia is in the upper right, and snow-covered Iceland is left of centre with the southern margin of sea ice lying just north-west of it (picture courtesy of Dr. P. A. Sheppard, Department of Meteorology, Imperial College, London).

southerly – as indicated by the smoke from the chimney (photograph copyright by F. H. Ludlam. Diagram by R. S. Scorer. Both published in 'Weather' XVIII (8), 1963, 266–7).

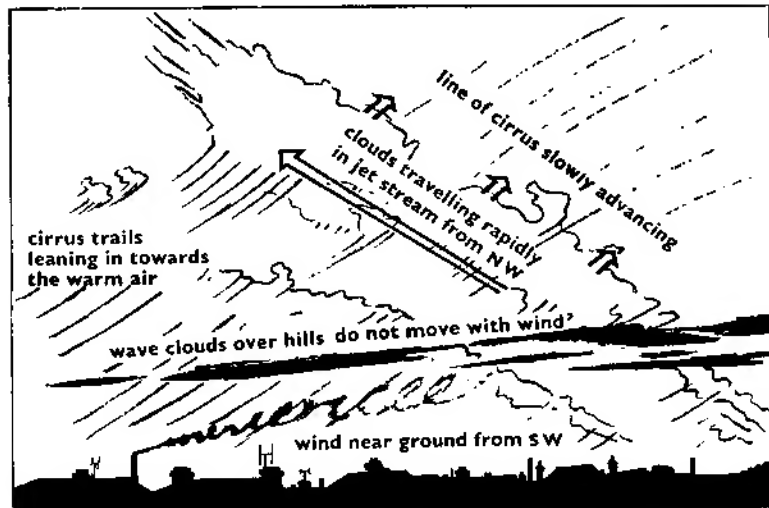




Plate 17. Thunderstorm approaching Östersund, Sweden, during late afternoon on 23 June 1955. Ahead of the region of intense precipitation there are rings of cloud formed over the squall-front (copyright F. H. Ludlam. Originally published in 'Weather' XV (2), 1960, 63).

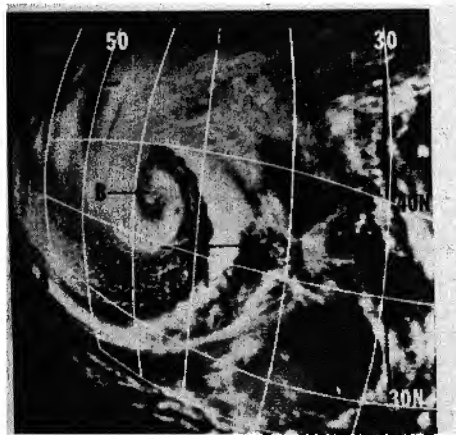


Plate 19. The same depression as shown in pl. 14 two days later, now situated over the central North Atlantic (B), and fully occluded. The continuous cloud spiral (A-B) corresponds to the cold and occluded portions of the frontal system. In the rear of the cold front are cellular cumulus clouds (C) which are very characteristic of cold air moving over a warmer ocean surface (APT Users' Guide, Environmental Science Services Administration).

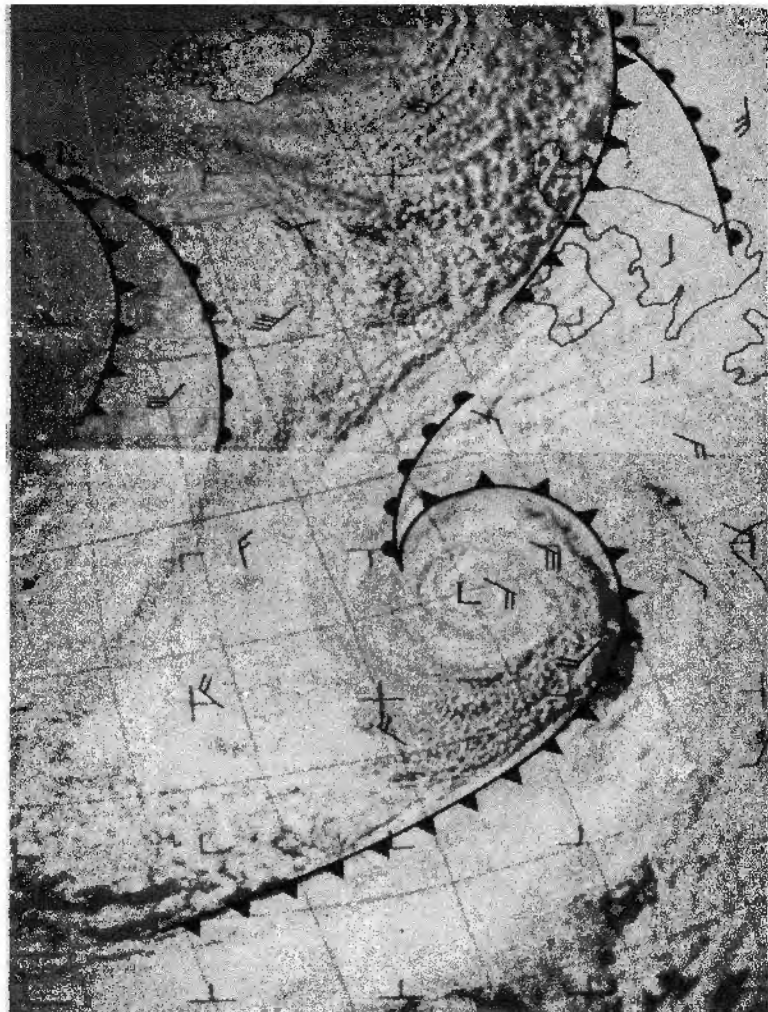
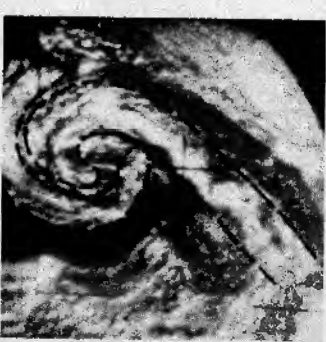
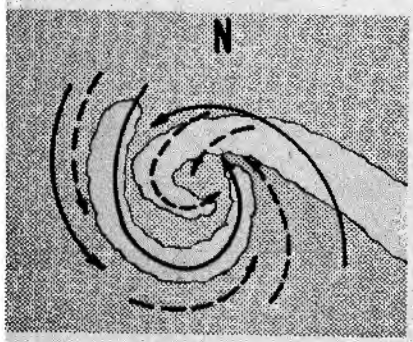
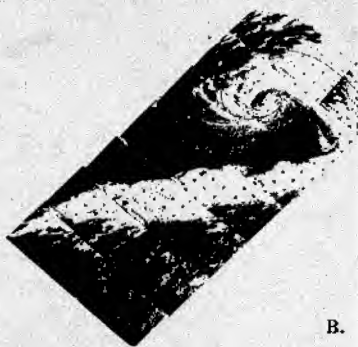
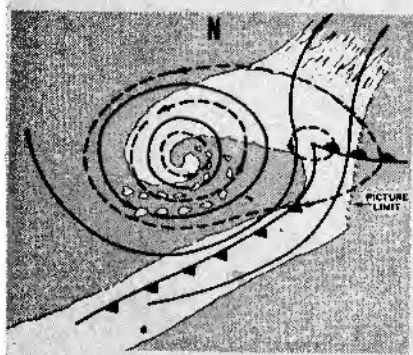
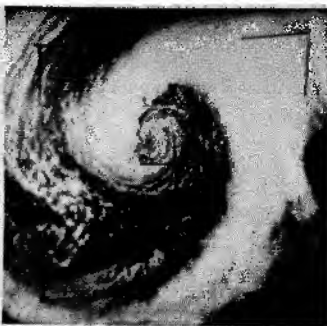
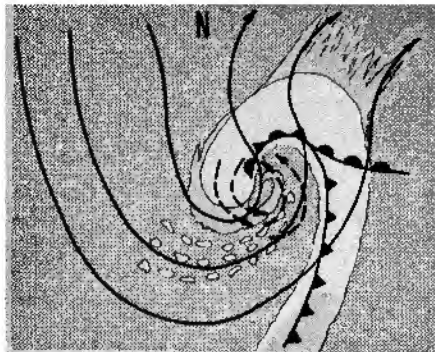


Plate 18. Photograph of a depression to the south-west of the British Isles taken by the ESSA 2 satellite at 1018 GMT on 12 November 1966. The depression began as hurricane 'Lois' in the eastern Caribbean and moved north-eastwards until its winds fell below gale force on 10 November. Thereafter it began to deepen again and the pressure at the centre had dropped to 962 mb when this photograph was taken. The frontal zones are well developed, although the 1000–500-mb wind shear was unusually weak for such a well defined system (courtesy 'Weather' XXIV (6), 1969, 222) (Crown Copyright)



— COVERED

— MOSTLY COVERED

— MOSTLY OPEN

DASHED LINES — LOWER TROPOSPHERE FLOW

SOLID LINE — MIDDLE TROPOSPHERE FLOW



Plate 21. Oblique air photograph of a tornado taken on 15 July 1961, at 1815 hrs local time, from an aircraft about 10 km (6 miles) north-north-east of Otis, Kansas, looking south-west (horizon tilted) from an elevation of about 600 m (2000 ft) above the surface. This tornado occurred near the trailing edge (i.e. to the west) of a squall-line thunderstorm, which is visible with its precipitation on the far left. The top of the tornado parent cloud merged with the thunder cloud, which extended up to some 17,000 m (55,000 ft). No lightning or rain were associated with the tornado cloud base. Little turbulence was encountered by the aircraft, but the high winds in the immediate vicinity of the base of the funnel, some 11 km (7 miles) distant, can be seen to be whipping up a dust-whirl and, in fact, drove a plank of 5 × 15 cm (2 × 6 in) cross-section 45 cm (18 in) into the ground on a farm some 3 km (2 miles) west of Otis (courtesy of F. C. Bates, the National Science Foundation and the University of Kansas).

Plate 20 (left). The decay of a depression (*Nimbus II Users' Guide*, NASA photograph).

- A. Well-developed depression beginning to occlude at the surface and to develop a cyclonic circulation at the 500-mb level. The low clouds are mainly cumuliform.
- B. Fully-occluded depression. The expanded closed circulation at the surface has reached maximum intensity, as has that at the 500-mb level now centred directly above the surface vortex. The heavy overcast in the north-east quadrant is characteristic, as is the spiral pattern of low and middle-level clouds in the west and near the circulation centre.
- C. Decaying depression in which the surface and 500-mb circulations are weakening and the whole organization is breaking up and exhibiting a dominantly annular, as distinct from radial, structure.



Plate 22. View from 5 km (3 miles) distance of a tornado north-east of Tracy, Minnesota, on 13 June 1968 (photograph courtesy of Eric Lantz and Associated Press). A convectively-unstable tongue of warm air extended north from Texas and by mid-afternoon its temperature had risen to 32° C (90° F), and severe thunderstorms had set in ahead of a cold front lying to its west. Surface pressure continued to drop in this belt, which was supported by a trough at 500 mb and surmounted by a jet of over 45 m/sec (100 mph) at the tropopause extending from Oregon to eastern Canada. Thunderstorm activity reached a maximum at about 1800 hrs as the unstable belt moved into Minnesota, and individual cells were shown by radar to have built up to over 15,240 m (50,000 ft). This combination of conditions was ideal for tornado inception and on that afternoon 34 funnels were sighted within 480 km (300 miles) of Minneapolis. The Tracy tornado appeared 13 km (8 miles) south-west of the town at 1900 hrs and moved north-east at 13 m sec⁻¹ (35 mph) for 21 km (13 miles), cutting a 90 to 150 m (300 to 500 ft) wide belt of total destruction through Tracy, killing 9 people, injuring 125 and causing \$3 million worth of damage. Unlike most tornados, it did not lift off the ground on encountering the rough urban surface but 'dug in' for its whole course until it suddenly dissolved a few seconds after the photograph was taken (description courtesy of the Director, National Severe Storms Forecast Center, Kansas City).

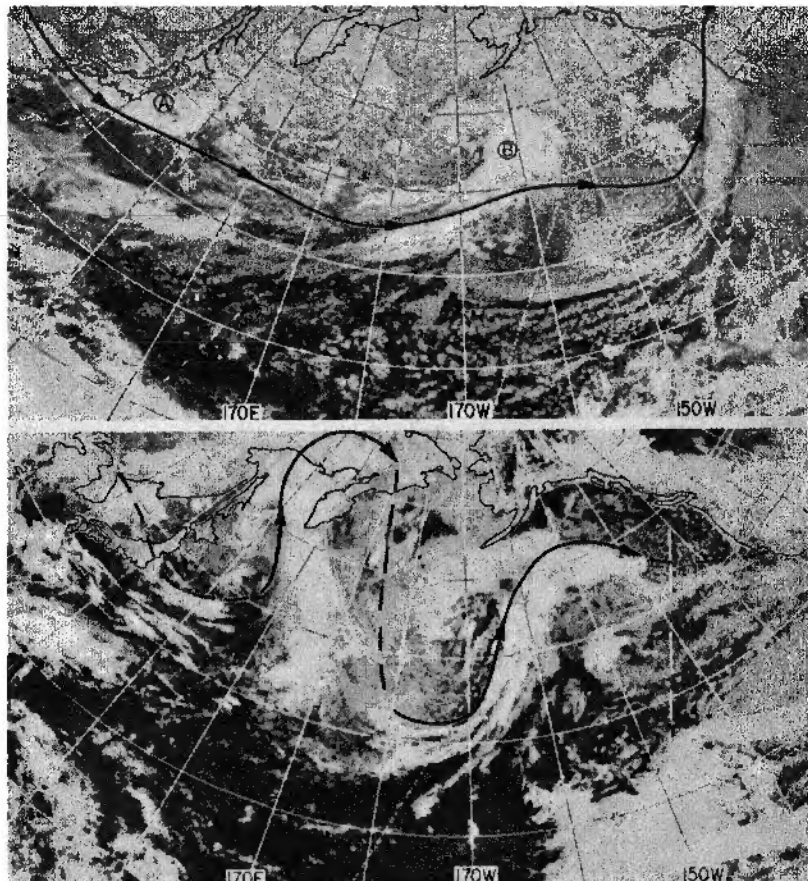


Plate 23. Infrared photographs of the North Pacific, with the 200 mb jet stream inserted.

Above. General zonal flow associated with a high zonal index, 12 March 1971. Three major cloud systems (A, B, C) occur along the belt of zonal flow, and the large east-west belt of cloud (D) to the south of Japan is also characteristic of accentuated zonal flow.

Below. Large amplitude flow regime associated with a lower zonal index, 23 April 1971 (*World Meteorological Organization 1973*).



Plate 24. Tiros IV photograph of part of north-west Europe on 14 April 1962. A large frontal system is located in the Atlantic, minor troughs occur over Biscay and northern France, and cumulus clouds cover much of England (*Environmental Science Services Administration photograph described by E. C. Barrett in 'Geography', 1964, p. 385*).

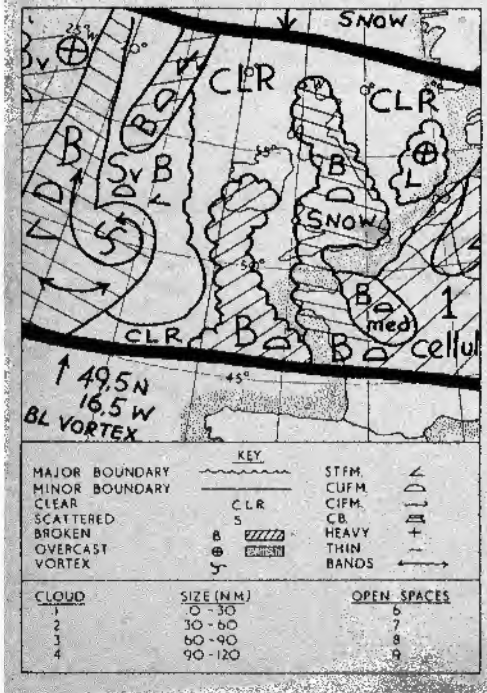


Plate 25. U.S. Weather Bureau nephanalysis for part of north-west Europe on 14 April 1962 (see pl. 24), the two heavy lines indicating the boundary of the area photographed on one orbit. This type of schematic chart is intermediate between satellite photographs and conventional weather maps (*described by E. C. Barrett in 'Geography', 1964, p. 385*).

When cP air moves southward over land in winter, in central North America for example, it acquires higher temperatures and a greater tendency towards instability, but there is little gain in moisture content. The cloud type is scattered shallow cumulus which only rarely gives showers even in the afternoon when convective instability is at a maximum. Exceptions occur in early winter around the eastern and southern shores of Hudson Bay and the Great Lakes. Until these water bodies freeze over, cold airstreams which cross them are rapidly warmed and supplied with moisture leading to locally heavy snowfalls.

Over Eurasia and North America cP air may move southwards and later recurve northwards. Some schemes of air-mass classification cater for such possibilities by specifying whether the air is colder (k), or warmer (w), than the surface over which it is passing. For example, cPk refers to cold, dry continental polar air which is moving over a warmer surface and is thereby likely to become unstable. Likewise, mPw indicates moist, maritime polar air which is being progressively cooled near the surface and, hence, becoming more stable.

In general, a 'k' air mass has gusty, turbulent winds which make for good visibility as smoke and haze are dispersed. The instability leads to cumuliform clouds. A 'w' air mass typically has stable or inversion conditions with stratiform cloud. Limited vertical mixing allows the concentration of smoke, haze and fog at low levels. Clearly, these and similar symbols provide a convenient shorthand description of the important parameters which characterize different air masses.

Many parts of the globe must be regarded as transitional regions where the surface and air circulation produce air masses with intermediate characteristics. Northern Asia and northern Canada fall into this category in summer. In a general sense the air has affinities with continental polar air masses but these land areas, particularly the Canadian shield, have extensive bog and water surfaces so that the air is moist and cloud amounts are quite high. In a similar manner, melt-water pools and leads in the arctic pack-ice make it more appropriate to regard the area as a source of maritime arctic (mA) air in summer (fig. 4.4A). This designation is also applied to air over the Antarctic pack-ice in winter that is much less cold in its lower levels than the air over the continent itself.

b Warm air. The modification of warm air masses is usually a gradual process. Air moving poleward over progressively cooler surface becomes increasingly stable in the lower layers. In the case of mT air with high moisture content, surface cooling may produce advection fog and this is particularly common, for example, in the south-western approaches to the

English Channel during spring and early summer when the sea is still cool. Similar development of advection fog in mT air occurs along the South China coast in February–April, and also off Newfoundland and over the coast of northern California in spring and summer. If the wind velocity is sufficient for vertical mixing low stratus cloud forms in the place of fog, and drizzle may result. In addition, forced ascent of the air by high ground, or by overriding of an adjacent air mass, can produce heavy rainfall.

The cT which originates in those parts of the subtropical anticyclones situated over the arid subtropics in summer is extremely hot and dry (table 4.2). It is typically unstable at low levels and dust-storms may occur, but the dryness and the subsidence of the upper air limit cloud development. In the case of North Africa this cT air may move out over the Mediterranean rapidly acquiring moisture, with the consequent release of potential instability triggering off showers and thunderstorm activity.

The air masses in low latitudes present considerable problems of interpretation. The temperature contrasts found in middle and high latitudes are virtually absent and what differences do exist are due principally to moisture content and, more particularly, to the presence or absence of subsidence. *Equatorial air* is usually cooler than that subsiding in the subtropical anticyclones, for example. *Tropical air* masses can only be differentiated meaningfully in terms of moisture content and the effects of subsidence on the lapse rate. On the equatorial sides of the subtropical anticyclones in summer the air is moving westward from areas with cool sea surfaces (e.g. off north-west Africa and California) towards those of higher sea-surface temperatures. Moreover the south-western parts of the high-pressure cells are affected only by weak subsidence due to the vertical structure of the cells (see fig. 3.15). As a result of these circumstances the mT air moving westwards around the equatorward sides of the subtropical highs becomes much less stable than that on the north-eastern margin of the cells. Eventually such air forms the very warm, moist, unstable 'equatorial air' of the Inter-Tropical Convergence Zone (see figs. 4.2 and 4.4). *Monsoon air* is indicated separately in these figures, although there is no basic difference between it and mT air. The special difficulties of treating tropical climatology in terms of air masses are discussed in ch. 6.

3 The age of the air mass

Eventually the mixing and modification necessarily accompanying the movement of an air mass away from its source will cause the rate of energy exchange with the surroundings to diminish, and the various

weather phenomena associated with these changes will dissipate. This process will be associated with the loss of its original identity, until finally its features merge with those of surrounding airstreams and the air may again become subject to the influence of a new source region.

North-west Europe is shown as an area of 'mixed' air masses in figs. 4.2 and 4.4. This is intended to refer to the variety of sources and directions from which air may invade the region, since weather processes associated with air-mass modification and with the frontal zones separating air masses are very much in evidence. The same is also true of the Mediterranean in winter, although the area does impart its own particular characteristics to polar and other air masses which stagnate over it. Such air is termed *Mediterranean*; typical temperature and humidity values are listed in tables 4.1 and 4.2. In winter it is convectively unstable (see fig. 2.14) as a result of the moisture picked up over the Mediterranean Sea.

The length of time during which an air mass retains its original characteristics depends very much on the extent of the source area and the type of pressure pattern affecting the area. In general the lower air is changed much more rapidly than that at higher levels, although dynamic modifications aloft, which are sometimes overlooked by climatologists, are no less significant in terms of weather processes. Modern air-mass concepts must, therefore, be flexible from the point of view of both synoptic and climatological studies.

C Frontogenesis

The first real advance in our detailed understanding of mid-latitude weather variations was made with the discovery that many of the day-to-day changes are associated with the formation and movement of boundaries, or *fronts*, between different air masses. Observations of the temperature, wind directions, humidity and other physical phenomena during unsettled periods showed that discontinuities often persist between impinging air masses of differing characteristics. The term 'front', for these surfaces of air-mass conflict, was a logical one to be proposed during the First World War by a group of meteorologists (including V. and J. Bjerknes, H. Solberg and T. Bergeron) working in Norway, and their ideas are still an integral part of most weather analysis and forecasting particularly in middle and high latitudes.

1 Frontal waves

It was observed that the typical geometry of the air-mass interface, or

front, resembles a wave form (see fig. 4.6). Similar wave patterns are, in fact, found to occur on the interfaces between many different media, for example, waves on the sea surface, ripples on beach sand, aeolian sand dunes, etc. Unlike these wave forms, however, the frontal waves in the atmosphere are commonly unstable; that is, they suddenly originate, increase in size, and then gradually dissipate. Numerical model calculations

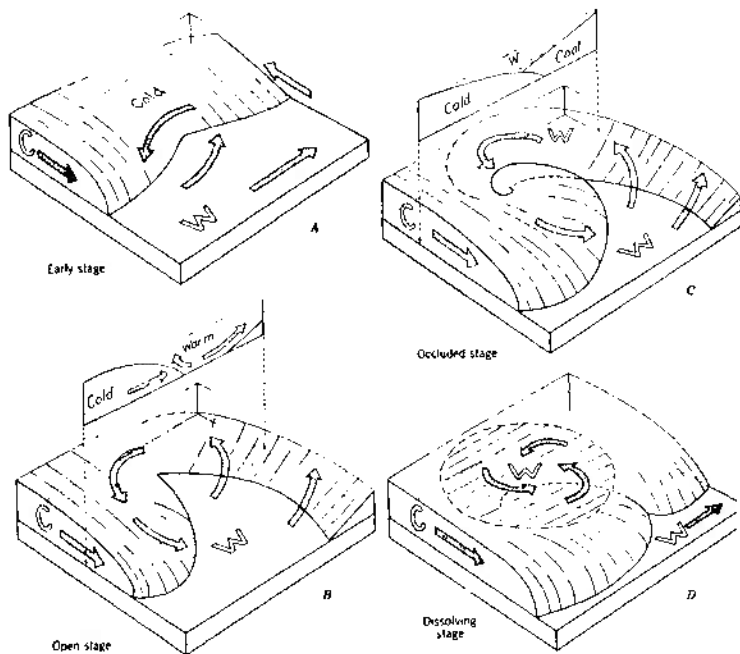


Fig. 4.6. Four stages in the typical development of a mid-latitude depression (*from Strahler 1951*). 'Satellite views' of the cloud systems corresponding to these stages are shown in fig. 4.7.

show that in middle latitudes waves in a baroclinic atmosphere are unstable if their wavelength exceeds a few thousand kilometres. The initially attractive analogy between atmospheric wave systems and waves formed on the interface of other media is, therefore, an insufficient basis on which to develop explanations of frontal waves. In particular, the circulation of the upper troposphere plays a key role in providing appropriate conditions for their development and growth, as will be shown below.

2 The frontal wave depression

A depression (also termed a low or cyclone¹) is an area of relatively low pressure, with a more or less circular isobaric pattern. It covers an area 1500–2000 km in diameter and usually has a life-span of 4–7 days. Systems with these characteristics, which are prominent on daily weather maps, are referred to as *synoptic scale* features. The depression, in mid-latitudes at least, is usually associated with a convergence of contrasting air masses. The interface between these air masses develops into a wave form with its apex located at the centre of the low-pressure area. The wave encloses a mass of warm air between modified cold air in front and fresh cold air in the rear. The formation of the wave also creates a distinction between the two sections of the original air-mass discontinuity for, although each section still marks the boundary between cold and warm air, the weather characteristics found in the neighbourhood of each section are very different. The two sections of the frontal surface are distinguished by the names *warm front* for the leading edge of the wave and *cold front* for that of the cold air to the rear (fig. 4.6 and Plate 14).

The boundary between two adjacent air masses is marked by a strongly baroclinic zone of large temperature gradient 100–200 km wide (see ch. 4, B and fig. 4.1). Sharp discontinuities of temperature, moisture and wind properties at fronts, especially the warm front, are rather uncommon. Such discontinuities are usually the result of a pronounced surge of fresh, cold air in the rear sector of a depression, but in the middle and upper troposphere they are often caused by subsidence and may not coincide with the location of the baroclinic zone.

On satellite imagery, active cold fronts in a strong baroclinic zone commonly show marked spiral cloud bands formed as a result of the thermal advection (see fig. 4.7 B, C and pl. 19). Warm fronts, however, are typically covered by a cirrus shield. As fig. 3.19 shows, an upper tropospheric jet stream is closely associated with the baroclinic zone, blowing roughly parallel to the line of the upper front (see pl. 15). This relationship is examined further in ch. 4, F.

Air behind the cold front, away from the low centre, commonly has an anticyclonic trajectory and hence moves at a greater than geostrophic speed (see ch. 3, A.4) impelling the cold front to acquire a super-geostrophic speed also. The wedge of warm air is pinched out at the surface and lifted bodily off the ground. This stage of *occlusion* eliminates the wave form at the surface (fig. 4.6 and pl. 19). The occlusion gradually

¹ This latter term is tending to be restricted to the tropical (hurricane) variety.

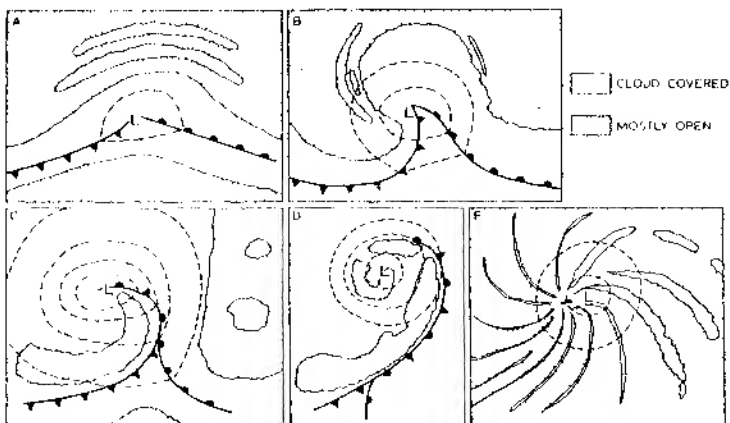


Fig. 4.7. Schematic patterns of cloud cover (white) observed from satellites, in relation to surface fronts and generalized isobars (see pl. 20) (after Bouche and Newcomb 1962). A, B, C and D correspond to the four stages in fig. 4.6.

works outward from the centre of the depression along the warm front. Sometimes, the cold air wedge advances so rapidly that, in the friction layer close to the surface, cold air overruns the warm air and generates a *squall line* (see below, ch. 4, H, p. 216).

The depression usually achieves its maximum intensity 12–24 hours after the beginning of occlusion. This stage is illustrated in pl. 20b.

By no means all frontal lows follow the idealized life cycle illustrated in fig. 4.6 and discussed above. It is generally characteristic of oceanic cyclogenesis, but over North America many lows forming east of the Rocky Mountains in the lee pressure trough develop occluded fronts almost immediately. In winter months, the absence of moisture sources in this region greatly reduces the intensity of frontogenesis until the system moves eastward and draws in warm moist air from the south.

D Frontal characteristics

The activity of a front in terms of weather depends upon the vertical motion in the air masses. If the air in the warm sector is rising relative to the frontal zone the fronts are usually very active and are termed *ana-fronts*, whereas sinking of the warm air relative to the cold air masses gives rise to less intense *kata-fronts* (see figs. 4.8 and 4.9).

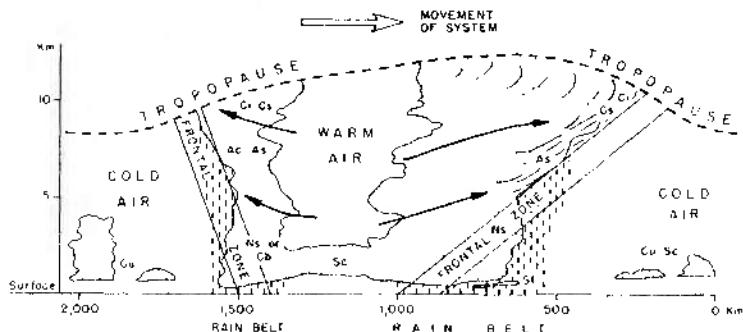


Fig. 4.8. Model of a depression with ana-fronts where the air is rising relative to each frontal surface. Note that an ana-warm front may occur with a kata-cold front (see fig. 4.9) and vice versa (after Pedgley 1962) (Crown Copyright Reserved).

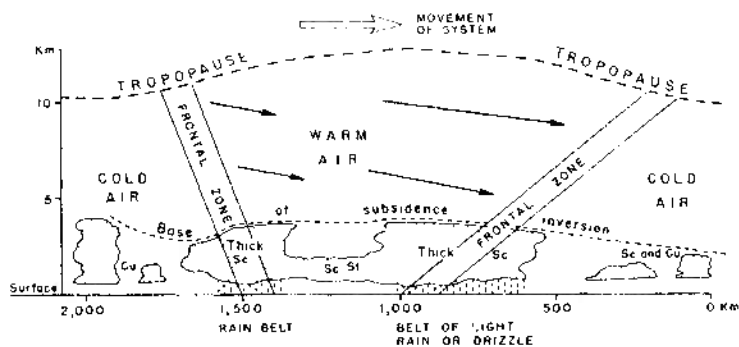


Fig. 4.9. Model of a depression with kata-fronts where the air is sinking relative to each frontal surface (after Pedgley 1962) (Crown Copyright Reserved).

I The warm front

The warm front represents the leading edge of the warm sector in the wave. The frontal zone here has a very gentle slope, of the order $\frac{1}{2}$ – 1° , so that the cloud systems associated with the upper portion of the front herald its approach some 12 hours or more before the arrival of the surface front. The ana-warm front, with rising warm air, has multi-layered cloud which steadily thickens and lowers towards the surface position of the front. The first clouds are thin, wispy cirrus, followed by sheets of cirrus and altostratus, and altostratus (see fig. 4.8). The sun is obscured

200 Atmosphere, weather and climate

as the altostratus layer thickens and drizzle or rain begins to fall. The cloud often extends through most of the troposphere and with continuous precipitation occurring is generally designated as nimbostratus. Patches

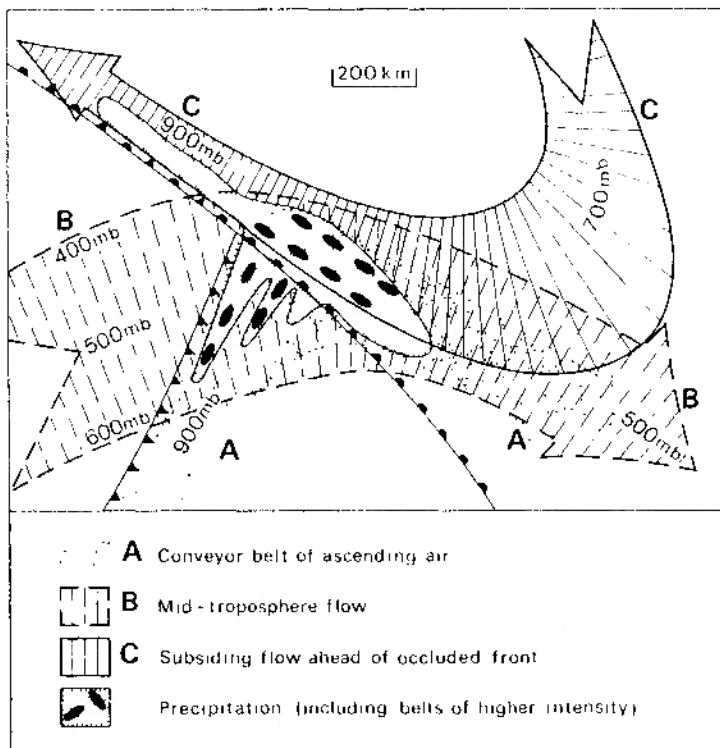


Fig. 4.10. Model of the large-scale flow and mesoscale precipitation structure of a partially-occluded depression typical of those affecting the British Isles. It shows the 'conveyor belt' (A) rising from 900 mb ahead of the cold front over the warm front. This is overlaid by a mid-tropospheric flow (B) of potentially colder air from behind the cold front. Most of the precipitation occurs in the well-defined region shown, within which it exhibits a cellular and banded structure (after Harrold 1973).

of stratus may also form in the cold air as rain falling through this air undergoes evaporation and quickly saturates it.

The descending warm air of the kata-warm front greatly restricts the

development of medium- and high-level clouds. The frontal cloud is mainly stratocumulus, with a limited depth as a result of the subsidence inversions in both air masses (see fig. 4.9). Precipitation is usually light rain or drizzle formed by coalescence since the freezing level tends to be above the inversion level, particularly in summer.

At the passage of the warm front the wind veers, the temperature rises and the fall of pressure is checked. The rain becomes intermittent or ceases in the warm air and the thin stratocumulus cloud sheet may break up.

Forecasting the extent of rain-belts associated with the warm front is complicated by the fact that most fronts are not ana- or kata-fronts throughout their length or even at all levels in the troposphere. For this reason, radar is being used increasingly to determine by direct means the precise extent of rain-belts and to detect differences in rainfall intensity.

Such studies over the British Isles have shown that most of the production and distribution of precipitation is controlled by a broad airflow a few hundred kilometres across and several kilometres deep, which flows parallel to and just ahead of the surface cold front. This air rises over the warm front and turns southward ahead of it (fig. 4.10). The flow has been termed a 'conveyor belt'. Broad-scale convective (potential) instability is generated by the over-running of this low-level flow by potentially colder, drier air in the middle troposphere. Instability is released mainly in small cells which are organized into clusters and the clusters are further arranged in bands within the warm sector and ahead of the warm front (fig. 4.10). Some of the cells and clusters are undoubtedly set up through orographic effects and these influences may extend well downwind when the atmosphere is unstable.

2 *The cold front*

The weather conditions observed at cold fronts are equally variable, depending upon the stability of the warm sector air and the vertical motion relative to the frontal zone. The classical cold-front model is of the ana-type, and the cloud is usually cumulo-nimbus (pl. 16). Over the British Isles air in the warm sector is rarely unstable, so that nimbostratus occurs more frequently at the cold front (fig. 4.8). With the kata-cold front the cloud is generally stratocumulus (fig. 4.9) and precipitation is light. With ana-cold fronts there are usually brief, heavy downpours sometimes accompanied by thunder. The steep slope of the cold front, roughly 2° , means that the bad weather is of shorter duration than at the warm front. With the passage of the cold front the wind veers sharply, pressure begins to rise and temperature falls. The sky may clear very

abruptly, even before the passage of the surface cold front in some cases, although with kata-cold fronts the changes are altogether more gradual.

3 The occlusion

Occlusions are classified as either *cold* or *warm*, the difference depending on the relative states of the cold air masses lying in front and to the rear of the warm sector (fig. 4.11). If the air is colder than the air following it then the occlusion is *warm*, but if the reverse is so (which is more likely over the British Isles) it is termed a *cold* occlusion. The air in advance of the depression is most likely to be coldest when depressions occlude over Europe in winter and very cold cP air is affecting the continent.

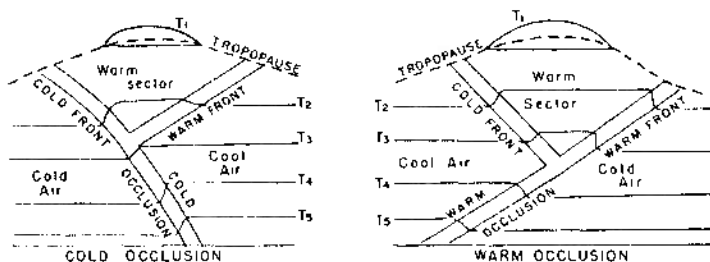


Fig. 4.11. Schematic cross-sections of a cold and a warm occlusion (after Pedgley 1962) (Crown Copyright Reserved).

The line of the warm air wedge aloft is associated with a zone of layered cloud (similar to that found with a warm front) and often of precipitation (see pls. 19 and 20). Hence its position is indicated separately on some weather maps and it is referred to by Canadian meteorologists as a *trowal* (trough of warm air aloft). The passage of an occluded front and trowal brings a change back to polar air-mass weather.

The occurrence of *frontolysis* (frontal decay) is not necessarily linked with occlusion, although it represents the final phase of a front's existence. Decay occurs when differences no longer exist between adjacent air masses. This may arise in four ways: through their mutual stagnation over a similar surface, as a result of both air masses moving on parallel tracks at the same speed, as a result of their movement in succession along the same track at the same speed, or by the system incorporating into itself air of the same temperature.

4 Frontal wave families

Observation has shown that frontal waves, or depressions, do not generally occur as separate units but in *families* of three or four (fig. 4.12) with the depressions which succeed the original one forming as *secondaries* along the trailing edge of an extended cold front. Each new member follows a course which is south of its progenitor as the polar air pushes farther south to the rear of each depression in the series. Eventually the front trails far to the south and the cold polar air forms an extensive meridional wedge of high pressure terminating the sequence.

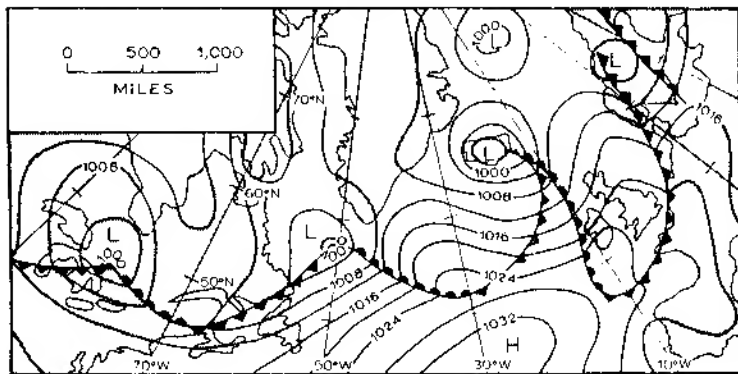


Fig. 4.12. A depression family in the North Atlantic, 22 June 1954 (after Taylor and Yates 1958 (Crown Copyright Reserved).

Another pattern of development may take place on the warm front, particularly at the point of occlusion, as a separate wave forms running ahead of the parent depression. This type of secondary is more likely with very cold (cA, mA or cP) air ahead of the warm front, and its formation is encouraged when the eastward movement of the occlusion is barred by mountains. This situation often occurs when a primary depression is situated in the Davis Strait and a break-away wave forms south of Cape Farewell (the southern tip of Greenland), moving away eastwards. Analogous developments take place in the Skagerrak-Kattegat area when the occlusion is held up by the Scandinavian mountains.

E Zones of wave development and frontogenesis

Fronts and associated depressions do not form everywhere and their development is restricted to well-defined areas. Frontal formation in the

temperate latitudes has been studied intensively for some years and knowledge of the general weather conditions to be expected is reasonably accurate. Not nearly so much is known about the nature of tropical fronts but the conditions of their formation and development are unlike those normally associated with higher-latitude fronts. Increasing world air travel and the need of accurate forecasts for tropical routes is fast filling this gap. At the moment it seems that Arctic and Polar Fronts are caused primarily by gross differences in air-mass characteristics, whereas tropical discontinuities within and between somewhat similar air masses are produced mainly by the nature of the large-scale air motion and especially by confluence within an airstream or between two air currents of different humidity.

The major zones of frontal wave development are naturally those areas which are most frequently baroclinic. This is the case, for instance, off eastern Asia and eastern North America, especially in winter when there is a sharp temperature gradient between the snow-covered land and warm offshore currents. These zones are referred to respectively as the Pacific Polar and Atlantic Polar Fronts (fig. 4.13). Their position is quite variable, but they show a general equatorward shift in winter, when the Atlantic Frontal Zone may extend into the Gulf of Mexico. In this area there is convergence of air masses of different stability between adjacent subtropical high-pressure cells (this frontal zone is sometimes misleadingly termed Temperate). Depressions developing here commonly move north-eastwards, sometimes following or amalgamating with others of the northern part of the Polar Front proper or of the Canadian Arctic Front. Frontal frequency remains high across the North Atlantic, but it decreases eastward in the North Pacific, perhaps owing to a less pronounced gradient of sea-surface temperature. Frontal activity is most common in the central North Pacific when the subtropical high is split into two cells with converging air currents between them.

Another section of the Polar Front, often referred to as the *Mediterranean Front*, is located over the Mediterranean-Caspian Sea areas in winter. At intervals, fresh Atlantic mP air, or cool cP air from south-east Europe, converges with warmer air masses often of North African origin, over the Mediterranean Basin and initiates frontogenesis. In summer the area lies under the influence of the Azores subtropical high-pressure cell and the frontal zone is absent.

The summer locations of the Polar Front over the western Atlantic and Pacific are some 10° further north than in winter (fig. 4.13) although the frontal zone is rather weak at this time of year. There is now a frontal zone over Eurasia and a corresponding one over middle North America.

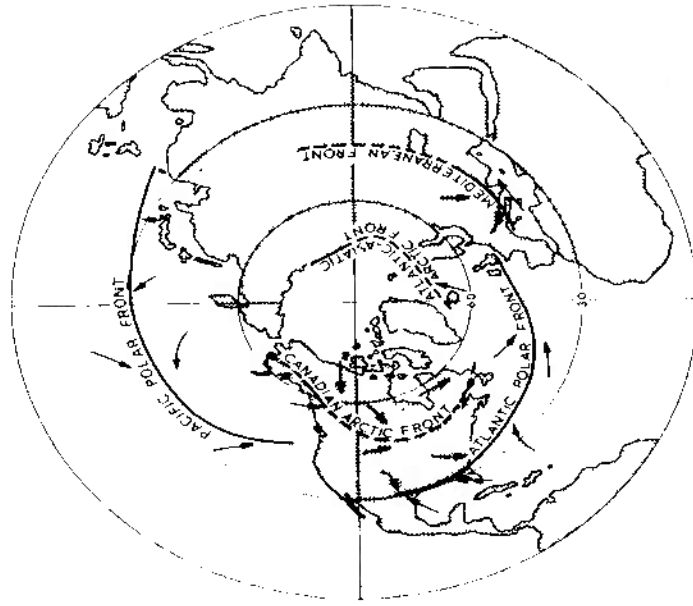
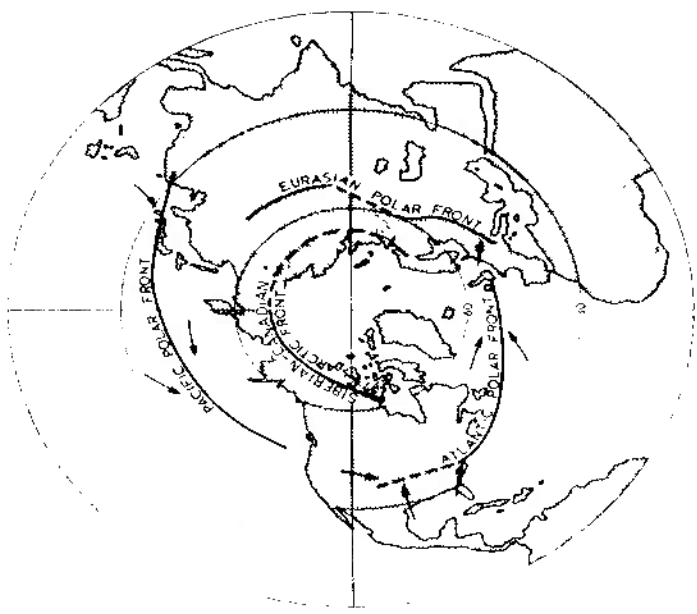


Fig. 4.13. The major northern hemisphere frontal zones in winter (left) and summer (right).

206 Atmosphere, weather and climate

These reflect the general meridional temperature gradient and probably also the large-scale influence of orography on the general circulation (see ch. 4, F).

In the southern hemisphere the Polar Front is on average about 45° S in January (summer) with branches spiralling poleward towards it from

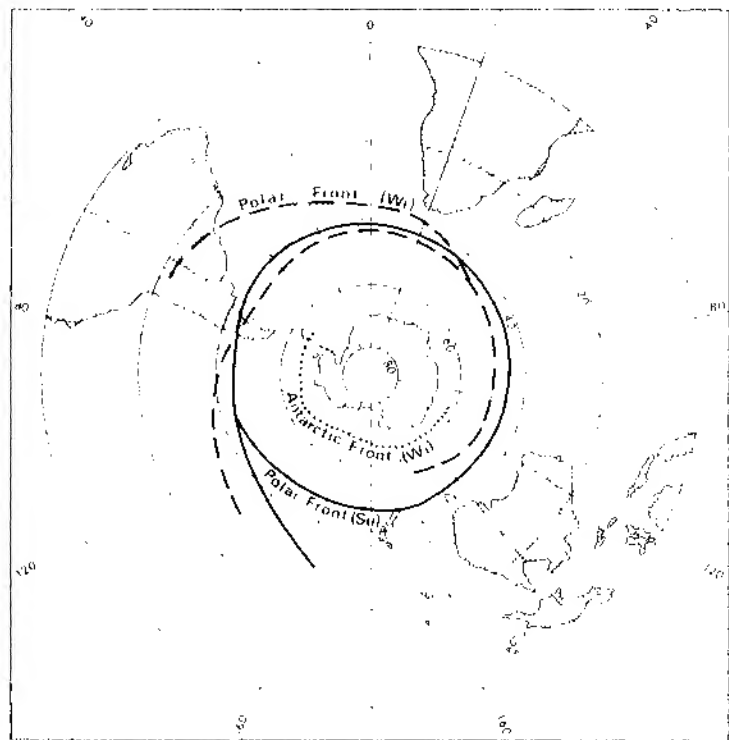


Fig. 4.14. The major southern hemisphere frontal zones in winter (Wi) and summer (Su).

about 32° S off eastern South America and from 30° S, 150° W in the South Pacific (fig. 4.14). In July (winter) there are two Polar Frontal Zones spiralling towards Antarctica from about 20° S; one starts over South America and the other at 170° W. They terminate some $4\text{--}5^{\circ}$ latitude further poleward than in summer.

The second major frontal zone is the Arctic Front, associated with the snow and ice margins of high latitudes (fig. 4.13). In summer this zone is developed along the Arctic coasts of Siberia and North America. In winter over North America it is formed between cA (or cP) air and Pacific maritime air modified by crossing the Coast Ranges and Rockies. There is also a less pronounced Arctic frontal zone in the North Atlantic-Norwegian Sea area, extending along the Siberian coast. A similar weak

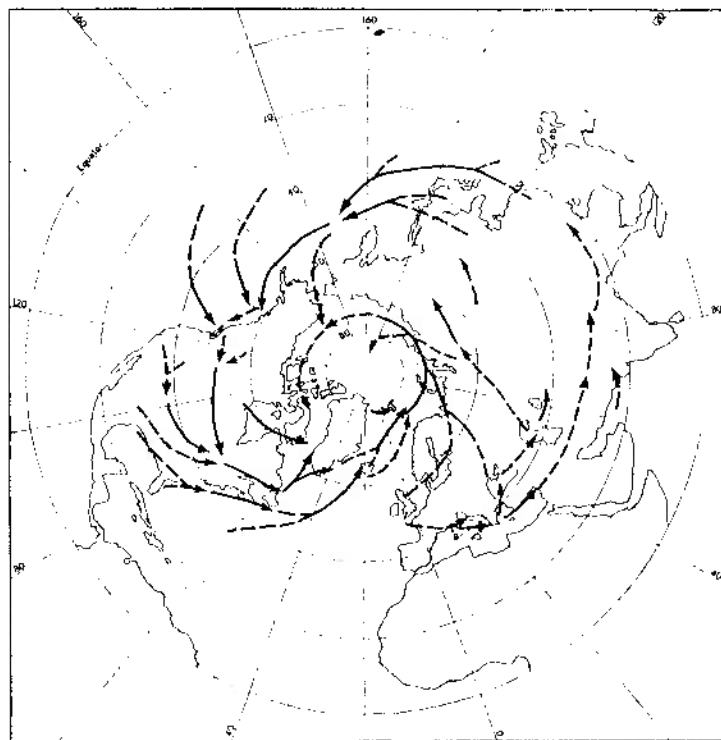


Fig. 4.15. The principal northern hemisphere depression tracks in January. The full lines show major tracks, the dashed lines secondary ones which are less frequent and less well defined. The frequency of lows is a local maximum where arrow-heads end. An area of frequent cyclogenesis is indicated where a secondary track changes to a primary one or where two secondary tracks merge to form a primary (after Klein 1957).

frontal zone is found in winter in the southern hemisphere. It is located at 65–70°S near the edge of the Antarctic pack-ice in the Pacific sector (fig. 4.14) although rather few cyclones form there.

The principal tracks of depressions in the northern hemisphere in January are shown in fig. 4.15. The major ones reflect the primary frontal zones already discussed. In summer the Mediterranean route is absent and lows move across Siberia, but the other tracks are similar although generally more zonal at this season and located in higher latitudes (around 60°N).

Between the two hemispherical belts of subtropical high pressure there is a further major world convergence zone, the Inter-Tropical Convergence Zone (or ITCZ). Formerly this was referred to as the Inter-Tropical Front (ITF), but air-mass contrasts only occur in limited sectors. This zone moves seasonally north and south away from the equator, as the subtropical high-pressure cell activity alternates in opposite hemispheres. The contrast between the converging air masses obviously increases with the distance of the ITCZ from the equator, and the degree of difference in their characteristics is naturally associated with considerable variation in activity along the convergence zone. Activity is most intense in June–July over southern Asia and west Africa, when the contrast between the maritime and continental air masses which are involved is at a maximum. In these sectors the zone merits the term Inter-Tropical Front, although this does not imply that it behaves like a mid-latitude frontal zone. The nature of the ITCZ and its role in tropical weather are discussed in ch. 6.

F Surface/upper-air relationships and the formation of depressions

It has already been pointed out that a wave depression is associated with air-mass convergence, yet the barometric pressure at the centre of the low may decrease by 10–20 mb in 12–24 hours as the system intensifies. The explanation of this apparent discrepancy is that upper air divergence removes rising air more quickly than convergence at lower levels replaces it. The superimposition of a region of upper divergence over a frontal zone is the prime motivating force of *cyclogenesis* (i.e. depression formation). Plate 14 illustrates this relationship between an incipient frontal wave and an advancing upper trough.

The long (or Rossby) waves in the middle and upper troposphere, which were mentioned in ch. 3, D.2, are particularly important in this respect, and it is worth considering first the reason why the hemispheric westerlies

show this large-scale wave motion. The key to this problem lies in the rotation of the earth and the latitudinal variation of the Coriolis parameter (ch. 3, A.2). It has been shown that for large-scale motion the (vertical) absolute vorticity ($f + \zeta$) tends to be conserved, i.e.

$$\frac{d(f + \zeta)}{dt} = 0$$

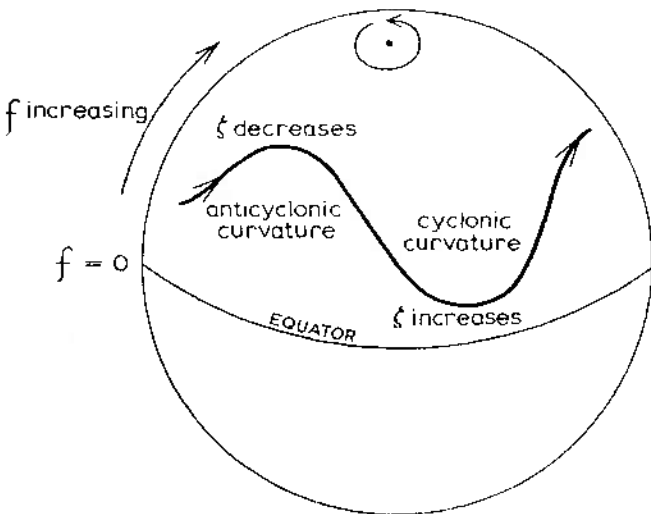


Fig. 4.16. A schematic illustration of the mechanism of long-wave development in the tropospheric westerlies.

The symbol d/dt denotes a rate of change following the motion (a total differential). Consequently, if air moves poleward so that f increases, the cyclonic vorticity tends to decrease. The curvature thus becomes anticyclonic and the current returns towards lower latitudes. If the air moves equatorward of its original latitude f tends to decrease (fig. 4.16), requiring ζ to increase, and the resulting cyclonic curvature again deflects the current polewards. In this manner large-scale flow tends to oscillate in a wave pattern.

210 Atmosphere, weather and climate

Rossby related the motion of these waves to their wavelength (L) and the speed of the zonal current (u). The speed of the wave (or phase speed, c) is:

$$c = u - \beta \left(\frac{L}{2\pi} \right)^2$$

where $\beta = \partial f / \partial t$, i.e. the variation of the Coriolis parameter with latitude (a local, partial differential). For stationary waves, where $c = 0$, $L = 2\pi\sqrt{u/\beta}$. At 45° latitude this stationary wavelength is 3120 km for a zonal velocity of 4 m sec^{-1} , increasing to 5400 km at 12 m sec^{-1} . The wavelengths, at 60°C latitude for zonal currents of 4 and 12 m sec^{-1} are, respectively, 3170 and 6430 km. Long waves tend to remain stationary, or even to move westward against the current, so that $c \leq 0$. Shorter waves travel eastward with a speed close to that of the zonal current and tend to be steered by the quasi-stationary long waves.

The latitudinal circumference limits the circumpolar westerly flow to between three and six major Rossby waves, and these affect the formation and movement of surface depressions. It has been pointed out that the main stationary waves tend to be located about 70°W and 150°E in response to the influence on the atmospheric circulation of orographic barriers, such as the Rocky Mountains and the Tibetan plateau, and of heat sources. On the eastern limb of troughs in the upper westerlies of the northern hemisphere the flow is normally divergent, since the gradient wind is subgeostrophic in the trough but supergeostrophic in the ridge (see ch. 3, A.4). Thus the sector ahead of an upper trough is a very favourable location for a surface depression to form or deepen (see pl. 14), and it will be noted that the mean upper troughs are significantly positioned just west of the Atlantic and Pacific Polar Front Zones in winter.

With these ideas in mind we may now consider further the three-dimensional nature of depression development and the important links existing between upper and lower tropospheric flow. The basic theory relates to the vorticity equation which states that, for frictionless horizontal motion, the rate of change of the vertical component of absolute vorticity (dQ/dt or $d(f + Q)/dt$) is proportional to air-mass convergence ($-D$, i.e. negative divergence):

$$\frac{dQ}{dt} = -DQ \quad \text{or} \quad D = -\frac{1}{Q} \frac{dQ}{dt}$$

The conservation of vorticity equation, which we have already discussed, is in fact a special case of this relationship.

In the sector ahead of an upper trough the decreasing cyclonic vorticity causes divergence (i.e. D positive), since the change in ζ outweighs that in f , thereby favouring surface convergence and low-level cyclonic vorticity. Once the surface cyclonic circulation has become established vorticity production is increased through the effects of thermal advection. Poleward transport of warm air in the warm sector and the eastward advance of the cold upper trough act to sharpen the baroclinic zone, strengthening the upper jet stream through the thermal wind mechanism (see fig. 3.18). The vertical relationship between jet stream and front has already been shown (see fig. 3.19) and the association as seen in plan is illustrated by the model depression sequence in figs. 4.17 and 4.18. The actual relationship between the two may often depart from this idealized case, but the thread of maximum velocity (or core) of the jet is often located to the rear of the cold front.

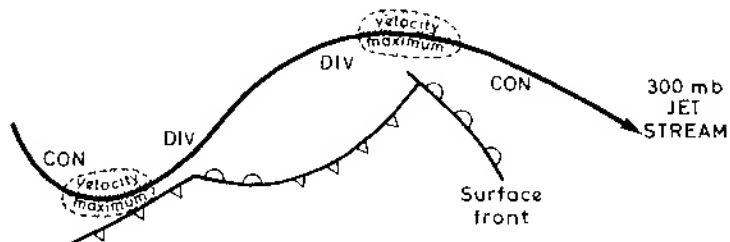


Fig. 4.17. Model of the jet stream and surface fronts, showing zones of upper tropospheric divergence and convergence and the jet stream cores.

The distribution of vertical motion upstream and downstream of this core is known to be quite different. In the area of the jet entrance (i.e. upstream of the core) divergence causes lower-level air to rise on the equatorward (i.e. right) side of the jet, whereas in the exit zone ascent is on the poleward side. It is evident that this pattern confirms the previous interpretation, with the second depression moving eastwards towards the area of maximum cyclogenetic tendency (fig. 4.17). This pattern is of basic importance in the initial deepening stage of the depression. If the upper-air pattern is unfavourable (e.g. beneath left entrance and right exit zones, where there is convergence) the depression will fill. Note that to the rear of the second depression upper convergence will encourage a polar outbreak through subsidence. Figure 4.19 shows how precipitation is often more related to the position of the jet stream than to that of surface fronts. Figure 4.20 illustrates a typical depression family and the associated upper tropospheric jet stream.

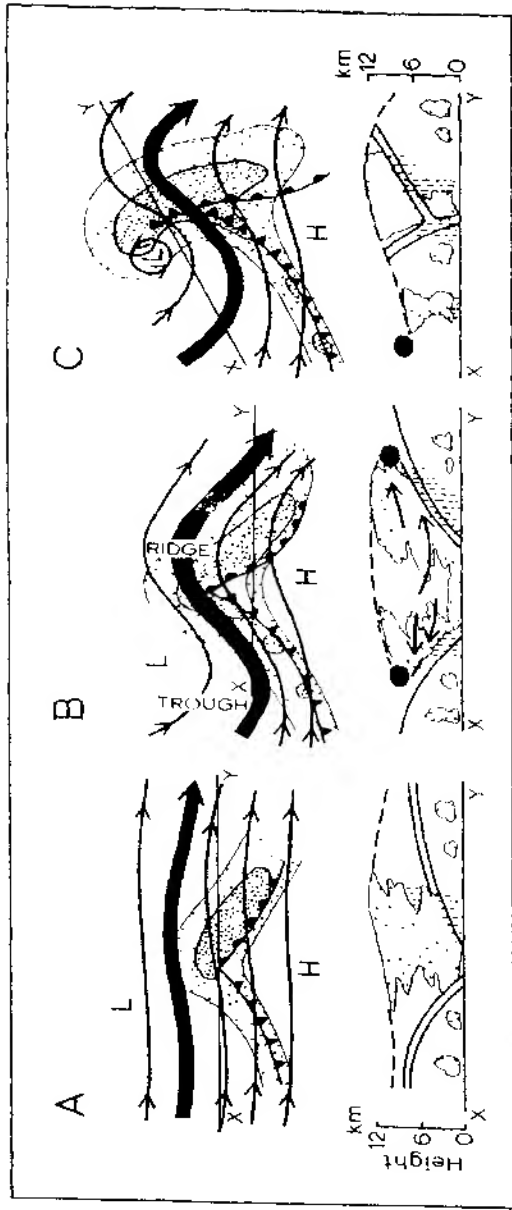


Fig. 4.18. Stages in the development of an occluding depression. Above Upper winds and Polar Jet Stream in relation to surface fronts (see pl. 15), precipitation areas (dark stipple) and cloud (lighter stipple). Below Cross-sections along the lines marked X-Y (after Fjölnir 1969).

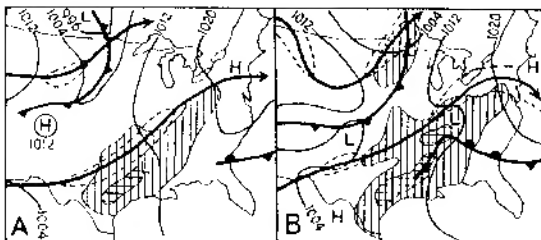


Fig. 4.19. The relations between surface fronts and isobars, surface precipitation (0–1 in vertical hatching; > 1 in cross-hatching), and jet streams (wind speeds in excess of about 100 mph (45 m sec⁻¹) occur within the dashed lines) over the United States on (A) 20 September 1958 and (B) 21 September 1958. This illustrates how the surface precipitation area is related more to the position of the jets than to that of the surface fronts. The air over the south-central United States was close to saturation, whereas that associated with the northern jet and the maritime front was much less moist (*after Richter and Dahl 1958*).

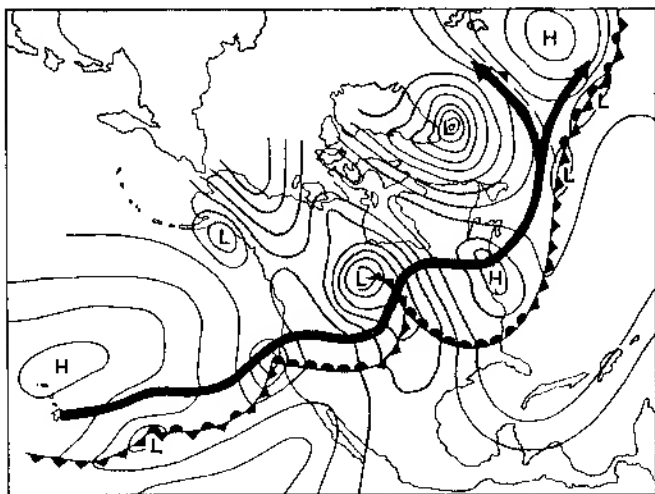


Fig. 4.20. A typical depression family and its relationship with the jet stream. The thin lines are sea-level isobars (*after Vederman 1954*).

The development of a depression can also be considered in terms of energy transfers. A cyclone requires the conversion of potential into kinetic energy and this is achieved by the upward (and poleward) motion of *warm* air. The rising warm air is driven by the vertical wind shear and by the superimposition of upper tropospheric divergence over a baroclinic zone. Intensification of this zone further strengthens the upper winds. The upper divergence allows surface convergence and pressure fall to occur simultaneously. Modern theory relegates the fronts to a quite subordinate role. They develop within depressions as narrow zones of intensified ascent, probably through the effects of cloud formation.

The movement of depressions is determined essentially by the upper westerlies and, as a rule of thumb, a depression centre travels at about 70% of the surface geostrophic wind speed in the warm sector. Records for the United States indicate that the average speed of depressions is 32 kmph (20 mph) in summer and 48 kmph (30 mph) in winter. The higher speed in winter reflects the stronger westerly flow in response to a greater meridional temperature gradient. Shallow depressions are mainly steered by the direction of the thermal wind in the warm sector and hence their path closely follows that of the upper jet stream (see ch. 3, D.3). Deep depressions may greatly distort the thermal pattern, however, as a result of northward transport of warm air and the southward transport of cold air. In such cases the depression usually becomes slow-moving. The movement of a depression may be additionally guided by energy sources such as a warm sea surface, which generates cyclonic vorticity, or by mountain barriers. The depression may cross obstacles, such as the Rocky Mountains or the Greenland Ice Sheet, as an upper low or trough and subsequently redevelop, aided by the lee-effects of the barrier or by fresh injections of contrasting air masses.

G Non-frontal depressions

Not all depressions originate as frontal waves. Tropical depressions are indeed mainly non-frontal and these are considered in ch. 6. In middle and high latitudes four types which develop in distinctly different situations are of particular importance and interest: the lee depression, the thermal low, the polar air depression and the cold low.

1 *The lee depression*

Westerly airflow which is forced over a north-south mountain barrier undergoes vertical contraction over the ridge and expansion on the lee side.

This vertical movement creates compensating lateral expansion and contraction, respectively. Hence there is a tendency for divergence and anticyclonic curvature over the crest, convergence and cyclonic curvature in the lee of the barrier. Wave troughs may be set up in this way on the lee side of low hills (see fig. 3.9) as well as major mountain chains. The airflow characteristics and the size of the barrier determine whether or not a closed low-pressure system actually develops. Such depressions, which at least initially tend to remain 'anchored' by the barrier, are frequent in winter to the south of the Alps and the Atlas Mountains when these regions are under the influence of cold north-westerly airstreams. Fronts may occur in these depressions but it is important to recognize that the low does not form as a wave along a frontal zone.

2 The thermal low

These lows occur almost exclusively in summer, resulting from intense daytime heating of continental areas. The most impressive examples are the summer low-pressure cells over the northern part of the Indian sub-continent and over Arizona. The Iberian peninsula is another region commonly affected by such lows. The weather accompanying them is usually hot and dry, but if sufficient moisture is present the instability caused by heating may lead to showers and thunderstorms. Thermal lows normally disappear at night when the heat source is cut off, but in fact those of India and Arizona persist.

3 Polar air depressions

Polar air depressions develop mainly in winter when very unstable mP or mA air currents stream southwards along the eastern side of an extensive meridional ridge of high pressure, commonly in the rear of an occluding primary depression. The polar low is in the small-synoptic scale (a few hundred km across) with a lifetime of 1–2 days. It is a low level disturbance which may have a closed cyclonic circulation to about 800 mb or it may consist simply of one or more troughs embedded in the polar airflow.

Polar lows affecting northwest Europe usually form in a baroclinic zone in high latitudes over the North Atlantic. A frontal structure is sometimes developed but a key feature is the presence of an ascending, moist, southwesterly flow *relative* to the low centre. This organization accentuates the general instability of the cold air stream to give considerable precipitation often as snow. Heat input to the cold air from the sea continues by night and day so that in exposed coastal districts showers may occur at any time.

4 The cold low

The cold low (or *cold pool*) is usually most evident in the circulation and temperature fields of the middle troposphere. Characteristically it displays symmetrical isotherms about the low centre. Surface charts may show little or no sign of these persistent systems which are frequent over north-eastern North America and north-eastern Siberia. They probably form as the result of strong vertical motion and adiabatic cooling in occluding baroclinic lows along the Arctic coastal margins. Such lows are especially important during the Arctic winter in that they bring large amounts of medium and high cloud which offset radiational cooling of the surface. Otherwise they usually cause no 'weather' in the arctic during this season. It is important to emphasize that tropospheric cold lows may be linked with either low- or high-pressure cells at the surface.

In middle latitudes cold lows may also form during periods of low-index circulation pattern (see fig. 3.33) by the cutting-off of polar air from the main body of cold air to the north (these are sometimes referred to as *cut-off lows*). This gives rise to weather of polar air-mass type, although rather weak fronts may also be present. Such lows are commonly slow-moving and give persistent unsettled weather with thunder in summer. Heavy, early snowfalls over Colorado in October 1969 were associated with upper cold lows.

H Mesoscale phenomena

Mesoscale systems are intermediate in size and life span between synoptic disturbances and individual cumulonimbus cells. They include topographically related wind systems in the boundary layer (ch. 3, B) and organized convective systems such as the *squall line*. The latter consists of a narrow line of thunderstorm cells which may extend for hundreds of kilometres. It is marked by a sharp veer of wind direction and very gusty conditions. The squall line often occurs ahead of a kata-cold front maintained either as a self-propagating disturbance or by thunderstorm downdraughts. It may form a pseudo-cold front between rain-cooled air and a rainless zone within the same air mass. In frontal cyclones, cold air in the rear of the depression may overrun air in the warm sector. The intrusion of this nose of cold air sets up great instability and the subsiding cold wedge tends to act as a scoop forcing up the slower-moving warm air (pl. 17).

Figure 4.21 shows that the *relative motion* of the warm air is towards the squall line. Such conditions generate severe frontal thunderstorms like

that which struck Wokingham, England, in September 1959. This moved from the south-west at about 20 m sec^{-1} , steered by strong south-westerly flow aloft. The cold air subsided from high levels as a violent squall and the updraught ahead of this produced an intense hailstorm. The hailstones grow by accretion in the upper part of the updraught, are blown ahead of the storm by strong upper winds, and begin to fall. This causes surface melting but the stone is caught up again by the advancing squall-line and re-ascends. The melted surface freezes, giving glazed ice as the stone is carried above the freezing level and further growth occurs by the collection of super-cooled droplets (see also ch. 2, p. 108 and p. 111).

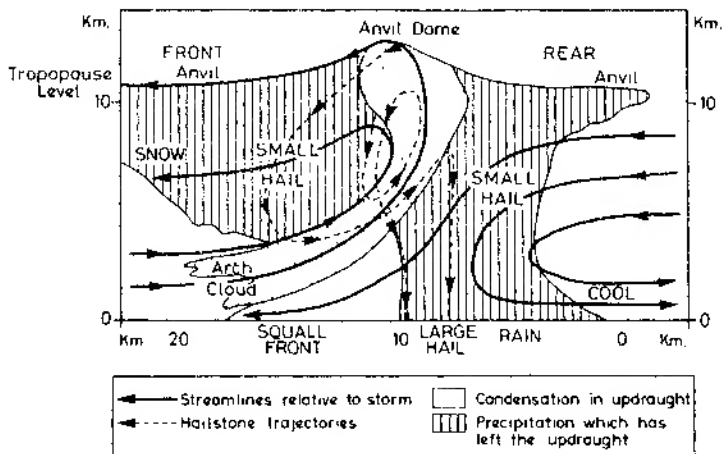


Fig. 4.21. Model of a thunderstorm which gave large hailstones. The air-flow trajectories show movement relative to the storm, which advanced from right to left (*from Ludlam 1961*).

The mesoscale thunderstorm system may also develop from initially isolated cumulonimbus cells. The sequence, which is illustrated in fig. 4.22, appears to be as follows. Evaporational cooling of the air beneath the cloud due to falling rain causes cold downdraughts (see fig. 2.20), and when these become sufficiently extensive they create a local high pressure of a few millibars intensity. As the individual cells become organized in a cluster along the front edge of the high pressure, new cells tend to form on the right flank through the interaction of cold downdraughts which trigger the ascent of displaced warm air. Through this process and the decay of

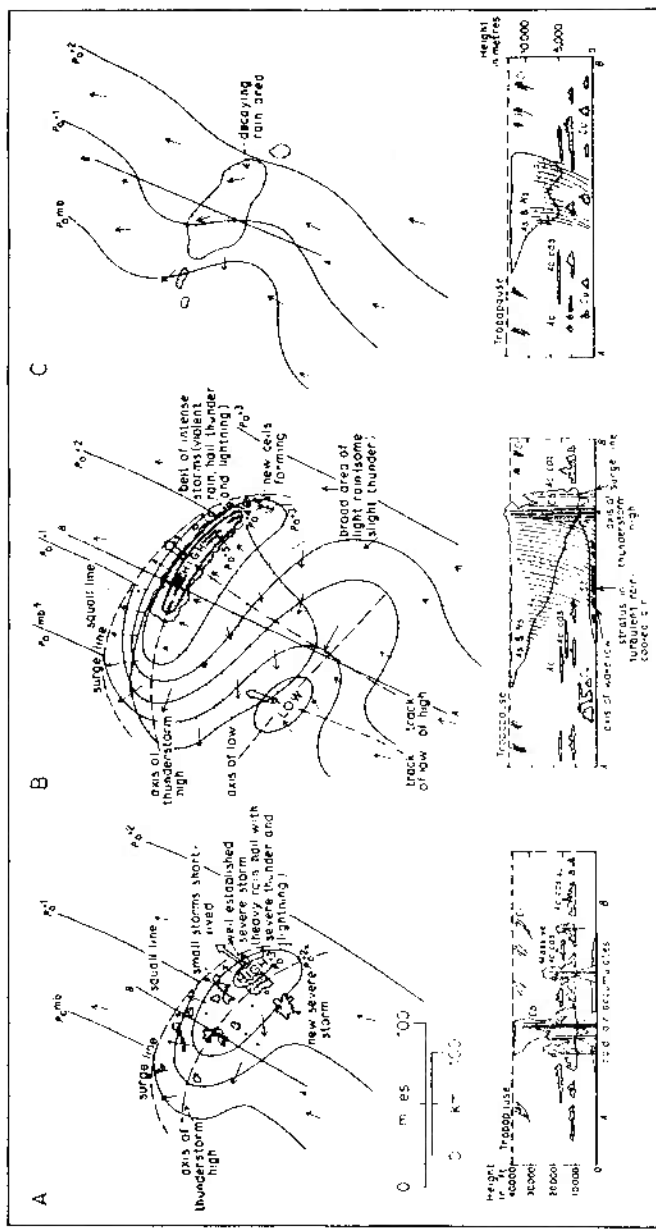


Fig. 4.22. Stages in the development of a meso-scale thunderstorm system: (A) Growth, (B) Maturity, and (C) Decay. The large arrows show the directions of movement of parts of the system, and the small arrows the surface winds. Areas of heavy and light precipitation are delimited (after Pedgley 1962) (Crown Copyright Reserved).

older cells on the left flank, the storm system tends to move 10° – 20° to the right of the mid-tropospheric wind direction. As the thunderstorm high intensifies a 'wake low', associated with clearing weather, develops to the rear of it. The squall-line is now producing violent winds, intense downpours of rain and hail accompanied by thunder. During the triggering of new cells tornadoes may form, as discussed below. The squall-line usually decays when synoptic scale features inhibit its self-propagation. The production is cold air is shut off when new convection ceases, so that the meso-high and low are steadily weakened and the rainfall becomes light and sporadic, eventually stopping altogether.

Tornadoes which may develop from such squall-line thunderstorms, are common over the Great Plains of the United States, especially in spring and early summer (pls. 13, 21 and 22). During this period cold, dry air from the high plateaux may override maritime tropical air.¹ Subsidence beneath the upper troposphere westerly jet (fig. 4.23) caps the low-level

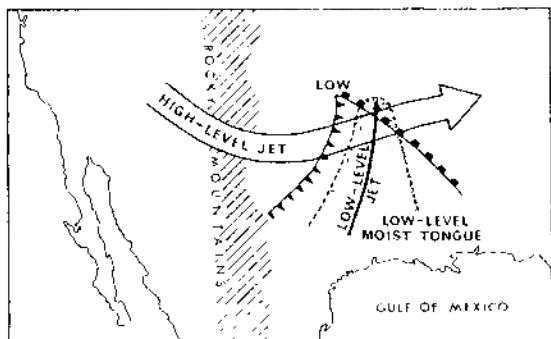


Fig. 4.23. The synoptic conditions favouring severe storms and tornadoes over the Great Plains.

moist air forming an inversion at about 1500–2000 m. The moist air is extended northward by a low-level southerly jet and through continuing advection the air beneath the inversion becomes progressively more warm and moist. Eventually the general convergence and ascent in the depression trigger the potential instability of the air generating large cumulus clouds which penetrate the inversion. The convective trigger is sometimes provided by the approach of the cold front towards the western edge of

¹ It is significant that some storms also occur downwind of other arid plateau regions in Mexico, the Iberian peninsula and West Africa (see ch. 6, C.4).

the moist tongue although tornadoes also occur in association with some tropical cyclones and in other synoptic situations (including high pressure areas!) if the necessary vertical contrast is present in the temperature, moisture and wind fields. The exact tornado mechanism is still not fully understood, because of the observational problems involved. Tornadoes generally form within a rotating thunderstorm system which is identifiable, when seen in plan view on a radar display, by a 'hook echo' pattern representing spiral cloud bands about a small central eye. The pressures in the mesoscale thunderstorm low are only 2–5 mb less than in the surrounding environment. The tornado funnel has been observed to originate in the cloud base and extend towards the surface and one idea is that convergence beneath the base of cumulonimbus clouds, aided by the interaction between cold precipitation downdraughts and neighbouring updraughts, may initiate rotation. Other observations suggest that the funnel forms simultaneously throughout a considerable depth of cloud, usually a towering cumulus. It appears that the upper portion of the tornado spire in this cloud may become linked to the main updraught of a neighbouring cumulonimbus, thereby causing rapid removal of air from the spire and allowing a violent pressure decrease at the surface. The pressure drop is estimated to exceed 200–250 mb in some cases and it is this which makes the funnel visible by causing air entering the vortex to reach saturation. The vortex is usually only a few hundred metres in diameter (pl. 22) and in an even more restricted band around the core the winds can attain speeds of 50–100 m sec⁻¹. Destruction results not only from the high winds, for buildings near the path of the vortex may explode outwards owing to the pressure reduction outside. Tornadoes commonly occur in families and move in rather straight paths (typically for 10 km or so) at velocities dictated by the low-level jet.

I Forecasting

Modern forecasting did not become possible until weather information could be rapidly collected, assembled and processed. The main development came in the middle of the last century with the invention of telegraphy, which for the first time permitted immediate analysis of weather data by the drawing of synoptic charts. These were first displayed in Britain at the Great Exhibition of 1851. Sequences of weather change were correlated with barometric pressure patterns both in space and time by such workers as Fitzroy and Abercromby, but it was not until some time later that the most helpful theoretical models of weather sequences were devised – culminating in the Bjerknes' depression model described earlier.

Forecasts are usually referred to as short-range (1–2 days), medium (or extended) range (up to 5–7 days) and long-range (monthly or seasonal). The first two can for present purposes be considered together.

1 Short-range forecasting

Forecasting procedures developed up to the 1950s were based on synoptic principles but, in the last 10–20 years, practices have been revolutionized by numerical forecasting methods.

a Synoptic methods. Synoptic forecasts use weather maps (see app. 3) of surface and upper air conditions and adiabatic charts, such as the tephigram, of air mass structure. In addition to station weather data, the weather maps show pressure gradients and frontal zones. Formerly, short-range forecasts were based on empirical rules for the movement of surface weather systems and simple frontal concepts were used to predict depression development, but since about 1940 these methods have been greatly improved by study of the relationships between the upper-air circulation and surface systems. Particular attention has been given to long wave structure in relation to the development of surface lows and highs and to divergence-vorticity relationships, based on the work of G.-C. Rossby and R. C. Sutcliffe, respectively.

The initial stage is to predict the future patterns of upper-air contours, surface isobars and the 1000–500 mb thickness, and then to assess what weather conditions are likely to result from the forecast situation. Inaccuracies may arise at both stages. Firstly, the network spacing and arrangement of observing stations determines much of the accuracy of the initial analysis, and since the coverage for ocean areas and for upper-air soundings is sparse only large-scale weather systems can be detected. This situation is now increasingly being remedied by the use of satellite photography of cloud systems including the use of infrared photographs to reveal cloud cover at night (see pls. 11 and 23) and satellite techniques to profile atmospheric temperature and humidity. Secondly, the individual depression may differ considerably from the standard models relating weather systems and weather (such as the Bjerknes' depression model). Thirdly, the small-scale nature of the turbulent motion of the atmosphere means that some weather phenomena are basically unpredictable, for example, the specific locations of shower cells in an unstable air mass. Greater precision than the 'showers and bright periods' or 'scattered showers' of the forecast language is impossible with present techniques, although short-term warnings of rain areas and thunderstorms can be

provided by radar. The procedure for preparing a forecast is becoming much less subjective, although in complex weather situations the skill of the experienced forecaster still makes the technique almost as much an art as a science. Detailed regional or local predictions can only be made within the framework of the general forecast situation for the country and demand thorough knowledge of possible topographic or other local effects by the forecaster.

b Numerical forecasting. This is a much more sophisticated method which attempts to predict the physical processes in the atmosphere by determinations of the conservation of mass, energy and momentum. The basic principle is that the rise or fall of surface pressure is related to mass convergence or divergence, respectively, in the overlying air column. This prediction method was proposed by L. F. Richardson who, in 1922, made a laborious test calculation which gave very unsatisfactory results. The major reason for this lack of success is the fact that the *net* convergence or divergence in an air column is a small residual term compared with the large values of convergence and divergence at different levels in the atmosphere (see fig. 3.6). Small errors arising from observational limitations may, therefore, have a considerable effect on the correctness of the analysis.

Numerical methods developed in the 1950s use a less direct approach. The first developments assumed a one-level barotropic atmosphere with geostrophic winds and hence no convergence or divergence. The movement of systems can be predicted, but not changes in intensity. Despite the great simplifications involved in the barotropic model, it has been used for forecasting 500-mb contour patterns. The latest techniques employ multi-level baroclinic models and include frictional and other effects; hence the basic mechanisms of cyclogenesis are provided for. It is noteworthy that *fields* of continuous variables, such as pressure, wind and temperature, are handled and that fronts are regarded as secondary, derived features. The vast increase in the number of calculations which these models necessitate has required a new generation of larger, faster electronic computers to allow the preparation of a forecast map to keep sufficiently ahead of the weather changes!

The British Meteorological Office uses data from about 1200 land stations, 300 ships and 600 rawinsondes over almost the entire northern hemisphere and up to a height of 12 km as computer input. Values of pressure and temperature are interpolated for 2000 grid points at the surface, 500 and 200 mb levels and computations are then made of the ex-

pected hourly change of these parameters at each grid point. From repeated calculations in one-hour time steps, forecasts of pressure (or height) distribution at the three levels, 1000–500 mb thickness, and large-scale vertical motion are produced for up to 36 hours ahead. The expected 'weather' must be inferred from these maps and in this connection the vertical motion pattern is crucial, since it indicates areas of cloudiness and rain and of dry, clear conditions. Similar techniques are used in the United States and several other countries.

Numerical methods were first used for routine forecasts in the United States in 1955 and in the United Kingdom in 1965. Specific procedures are continually being improved for both meso-scale and continental scale forecasts. Refinements include better spatial and temporal resolution and improved representations of physical processes.

2 Long-range forecasting

The methods discussed above are unsuitable for predicting the probable trend of the weather for periods of a month or more, because they are

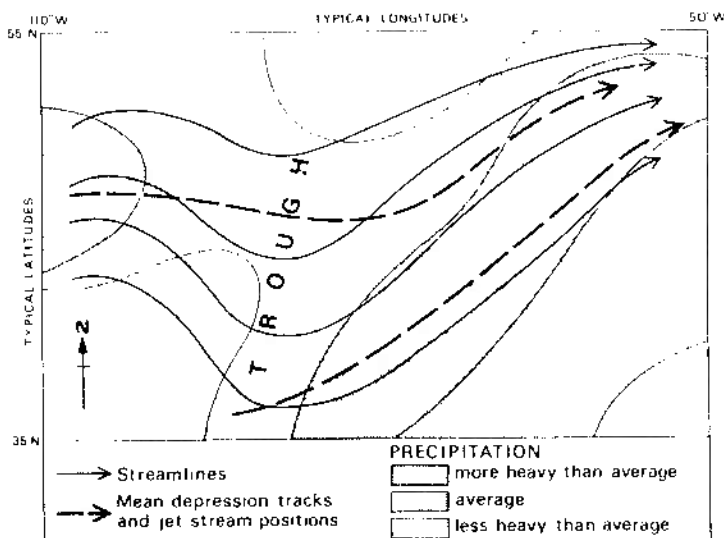
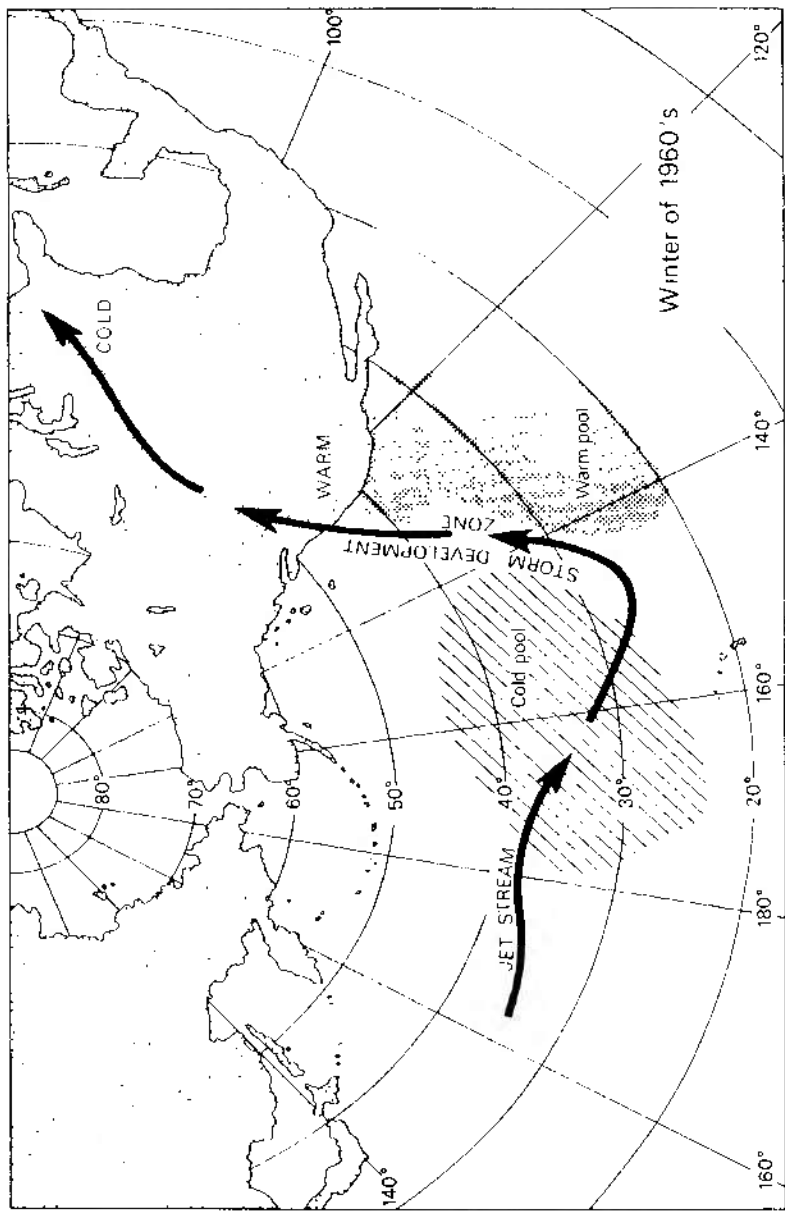


Fig. 4.24. Generalized mean relationships between the westerly air flow pattern, depression tracks, jet stream positions and precipitation zones in mid-latitudes in the northern hemisphere (after W. Klein. From Harman 1971).



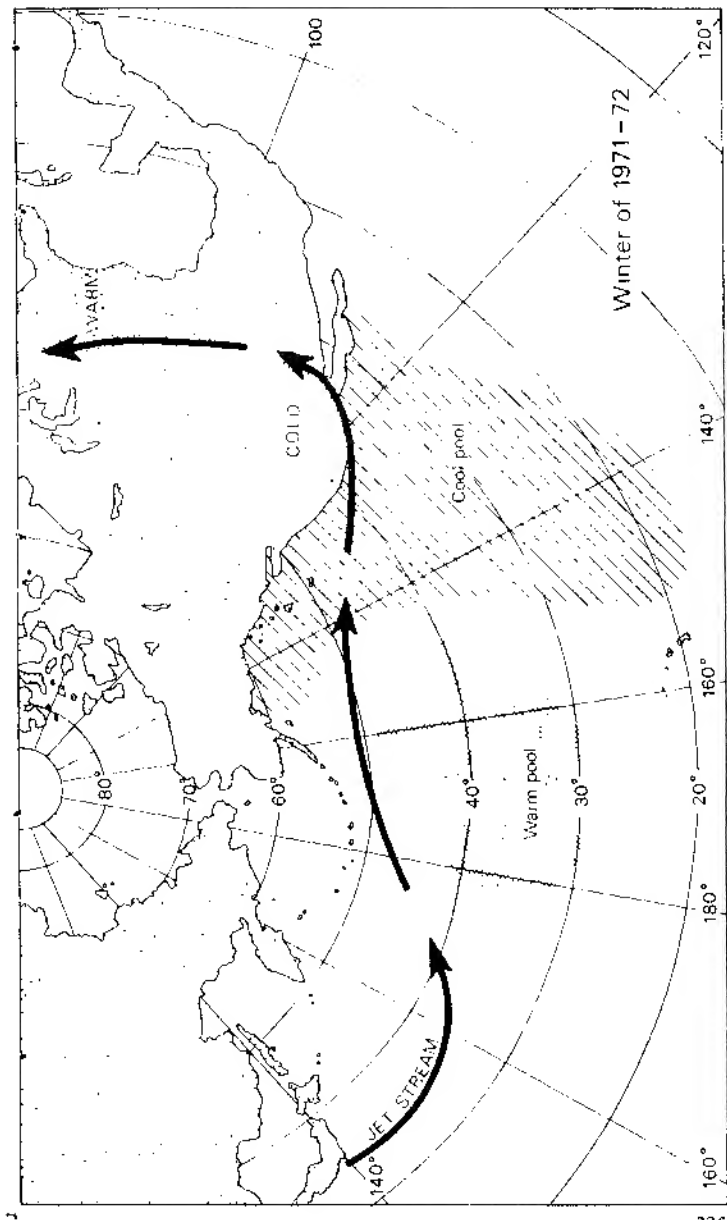


Fig. 4.25. Generalized relationships between ocean surface temperatures, jet stream tracks, storm development zones and land temperatures over the North Pacific and North America during (above) average winter conditions in the 1960s, and (below) the winter of 1971-72 as determined by J. Namias (*after Wick 1973*).

concerned with individual synoptic disturbances with a life cycle of about 3 to 7 days. Theoretical considerations indicate that the limit of synoptic predictability using numerical techniques is less than 15 days. Two rather different techniques will now be described, although these are by no means the only ones.

a Statistical methods. The United States Weather Bureau has issued 30-day forecasts twice monthly since 1948, using a method which has two principal steps. First, a mean 700-mb contour map is predicted for the coming month by a combination of several principles — extrapolation of current tendencies (such as blocking patterns) or the recognition of probable changes of regime in the large-scale atmospheric circulation, study of the possible effects of features such as snow cover and sea-surface temperature anomalies, and the examination of statistical records of the typical locations of troughs and ridges at that season. Second, the most probable anomalies of mean temperature and precipitation amount corresponding to the predicted contour map are derived from known relationships existing between them. For example, Fig. 4.24 shows that more than average precipitation is probable ahead of the trough where there is maximum vorticity advection, especially in association with an active jet stream, whereas less than average precipitation is usual to the rear of the trough axis. With a low zonal index in the westerlies, long waves may persist in more or less stationary positions for periods of several weeks at a time, or even longer, and their mean positions are, therefore, reflected in surface patterns of temperature and precipitation (see also ch. 5, B.1).

The location and intensity of the long waves appears to be critically influenced by ocean surface temperatures. Investigations for the North Pacific and the North Atlantic demonstrate interactions with the atmospheric circulation on a near-hemispheric scale. Figure 4.25A suggests, for example, that an extensive relatively warm surface in the north-central Pacific in the winter of 1971–72 caused a northward displacement of the westerly jet stream together with a compensating southward displacement over the western United States, bringing in cold air there. This pattern contrasts with that observed during the 1960s (fig. 4.25A) when a persistent cold anomaly in the central Pacific, with warmer water to the east, led to frequent storm development in the intervening zone of strong temperature gradient. The associated upper air flow produced a ridge over western North America with warm winters in California and Oregon. Models of the global atmospheric circulation support the view that persis-

tent anomalies of sea surface temperature exert an important control on local and large-scale weather conditions.

b Analogue methods. Another approach to long-term forecasting developed in Britain is based on the principle that sequences of weather events may tend to follow a similar course if the initial conditions are almost identical. The problem is then to find a period with weather conditions as closely analogous as possible to the present one and to use the past sequence of events as a guide to the future. The analogues are matched from a record of patterns of monthly temperature and pressure anomalies, and of sequences of *weather types*. The latter are actually types of pressure pattern or airflow over the country (see ch. 5, A.3). Each category tends to be associated with a particular type of weather. The difficulty in analogue prediction arises from the fact that no two patterns or sequences of weather are ever identical. There may, for example, be five reasonable analogues for a particular month, but examination of the succeeding weather sequences might show mild, rainy weather in two cases and cold spells in the other three. In the preparation of the forecast, therefore, many factors which can affect the weather trends, such as sea temperatures and the extent of snow cover, have to be taken into account. The problems facing the long-range forecasters need to be recognized before criticisms are levelled at them. The complexity of the atmosphere's behaviour makes tentative wording of their predictions necessary and occasional failures inevitable at present.

5 Weather and climate in temperate latitudes

In the two preceding chapters the general structure of the circulation and air-mass characteristics in middle latitudes have been outlined and the behaviour and origin of extra-tropical depressions examined. The direct contribution of pressure systems to the daily and seasonal variability of weather in the westerly wind belt is quite apparent to inhabitants of the temperate lands. Nevertheless there are equally prominent contrasts of regional climate in mid-latitudes which reflect the interaction of geographical and meteorological factors. This chapter gives a selective synthesis of weather and climate in Europe and North America, drawing mainly on the principles already presented. The climatic conditions of the polar and subtropical margins of the Westerly wind belt are examined in the final sections of the chapter. As far as possible different themes are used to illustrate some of the more significant aspects of the climate in each area.

A Europe

1 Pressure and wind conditions

The principal features of the mean North Atlantic pressure pattern are the Icelandic Low and the Azores High. These are present at all seasons (see fig. 3.21), although their location and relative intensity change considerably. The upper flow in this sector undergoes little seasonal change in pattern but the westerlies decrease in strength by over half from winter to summer. The other major pressure system influencing European climates is the Siberian winter anticyclone, the occurrence of which is intensified by the extensive winter snow cover and the marked continentality of

Eurasia. Atlantic depressions frequently move towards the Norwegian or Mediterranean Seas in winter, but if they travel due east they occlude and fill long before they can penetrate into the heart of Siberia. Thus the Siberian high pressure is quasi-permanent at this season and when it extends westward severe conditions affect much of Europe. In summer, pressure is low over all of Asia and depressions from the Atlantic tend to follow a more zonal path. Although the depression tracks over Europe do not shift poleward in summer (as a result of the local *southward* displacement of the Atlantic Arctic Front), the depressions at this season are rather less intense and the diminished airmass contrasts produce weaker fronts.

2 *Oceanicity and continentality*

Winter temperatures in north-west Europe are some 11°C (20°F) or more above the latitudinal average (see fig. 1.19), a fact usually attributed solely to the presence of the North Atlantic Drift. There is, however, a complex interaction between the ocean and atmosphere. The Drift, which originates from the Gulf Stream off Florida strengthened by the Antilles Current, is primarily a wind-driven current initiated by the prevailing south-westerlies. It flows at a velocity of 16 to 32 km (10–20 miles) per day and thus, from Florida, the water takes about eight or nine months to reach Ireland and about a year to Norway (see ch. 3, F.3). The south-westerly winds transport both sensible and latent heat acquired over the western Atlantic toward Europe, and although they continue to gain heat supplies over the north-eastern Atlantic this local warming arises in the first place through the drag effect of the winds on the warm surface waters. Warming of air masses over the north-eastern Atlantic is mainly of significance when polar or arctic air flows south-eastwards from Iceland. For example, the temperature in such airstreams in winter may rise by 9°C (17°F) between Iceland and northern Scotland. By contrast, maritime tropical air cools on average about 4°C (8°F) between the Azores and south-west England in winter and summer. One very evident effect of the North Atlantic Drift is the absence of ice around the Norwegian coastline. However, as far as the climate of north-western Europe is concerned the primary factor is the occurrence of prevailing *onshore* winds transferring heat into the area.

The influence of maritime air masses can extend deep into Europe because there are few major topographic barriers to airflow and because of the presence of the Mediterranean Sea. Hence the change to a more continental climatic regime is relatively gradual except in Scandinavia where the mountain spine produces a sharp contrast between western

Norway and Sweden. There are numerous indices expressing this continentality, but most are based on the annual range of temperature. Gorczynski's continentality index (K) is:

$$K = 17 \frac{A}{\sin \theta} - 20.4$$

where A is the annual temperature range ($^{\circ}\text{C}$) and θ is the latitude angle. K ranges between -12 at extreme oceanic stations and 100 at extreme continental stations. Some values in Europe are London 10, Berlin 21, Moscow 39. Figure 5.1 shows the variation of this index over Europe.

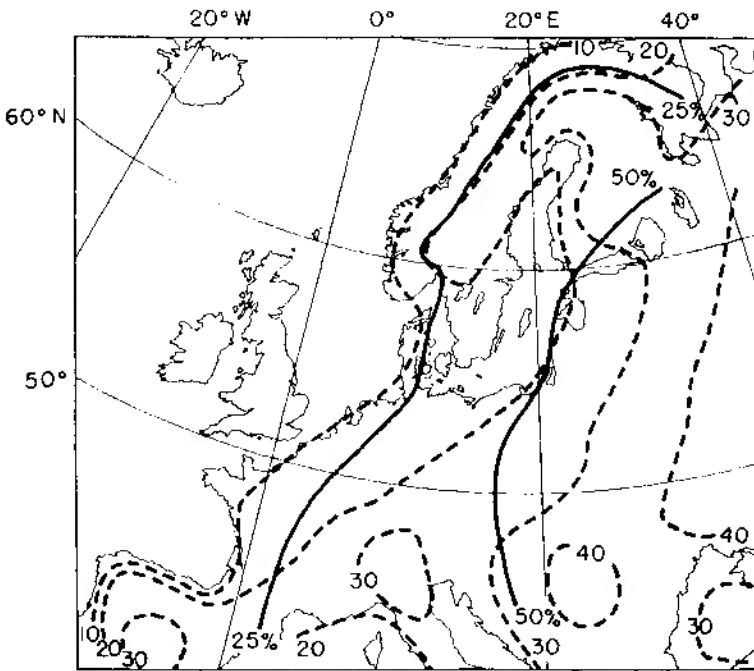


Fig. 5.1. Continentality in Europe. The indices of Gorczynski (dashed) and Berg (solid) are explained in the text (partly after Blüthgen 1966).

A very different approach by Berg relates the frequency of continental air masses (C) to that of all air masses (N) as an index of continentality, i.e. $K = C/N (\%)$. Figure 5.1 shows that non-continental air occurs at least

half the time over Europe west of 15°E as well as over Sweden and most of Finland.

A further illustration of maritime and continental regimes is provided by fig. 5.2. *Hythergraphs* for Valentia (Eire), Bergen and Berlin demonstrate the seasonal changes of mean temperature and precipitation

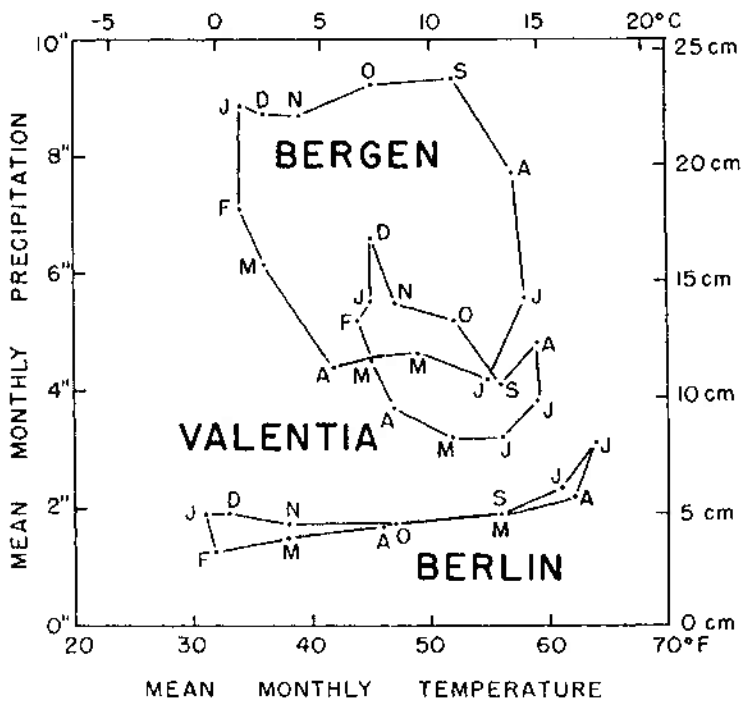


Fig. 5.2. Hythergraphs for Valentia (Eire), Bergen and Berlin. Mean temperature and precipitation values for each month are plotted.

in different locations. Valentia has a winter rainfall maximum and equable temperatures as a result of oceanic situation, whereas Berlin has a considerable temperature range and a summer maximum of rainfall. Bergen receives larger rainfall totals due to orographic intensification and a maximum in autumn and winter, its temperature range being intermediate to the other two. Such averages convey only a very general impression of climatic characteristics and therefore British weather patterns will now be examined in more detail.

3 British airflow patterns and their climatic characteristics

The daily weather maps for the British Isles sector (50° – 60° N, 5° E– 10° W) from 1873 to the present day have been classified by H. H. Lamb according to the movement of pressure systems within the general tropospheric airflow. He identifies seven major categories: Westerly (W), Northwesterly (NW), Northerly (N), Easterly (E) and Southerly (S) types – referring to the compass directions from which the systems are moving – and Cyclonic (C) or Anticyclonic (A) types when depressions or a high-pressure cell respectively dominate the weather map.

In theory, each category should produce a characteristic type of weather, depending on the season, and many writers use the term *weather type* to convey this idea. Nevertheless, few studies have been made of the actual weather conditions occurring in different localities with specific

Table 5.1 General weather characteristics of Lamb's 'Airflow Types'

Type	
Westerly	Unsettled weather with variable wind directions as depressions cross the country. Mild and stormy in winter, generally cool and cloudy in summer.
North-westerly	Cool, changeable conditions. Strong winds and showers affect windward coasts especially, but the southern part of Britain may have dry, bright weather.
Northerly	Cold weather at all seasons, often associated with polar lows or troughs. Snow and sleet showers in winter, especially in the north and east.
Easterly	Cold in the winter half-year, sometimes very severe weather in the south and east with snow or sleet. Warm in summer with dry weather in the west. Occasionally thundery.
Southerly	Generally warm and thundery in summer. In winter it may be associated with a depression in the Atlantic giving mild, damp weather especially in the south-west or with a high over central Europe, in which case it is cold and dry.
Cyclonic	Rainy, unsettled conditions often accompanied by gales and thunderstorms. This type may refer either to the rapid passage of depressions across the country or to the persistence of a deep depression.
Anticyclonic	Warm and dry in summer apart from occasional thunderstorms. Cold in winter with night frosts and fog especially in autumn.

patterns of airflow — a field of study known as *synoptic climatology* — hence the term *airflow type* is used here for Lamb's categories. The general weather conditions which are likely to be associated with a particular airflow type over the British Isles are summarized in table 5.1.

Each airflow pattern may of course result in several air masses affecting an area as it is crossed by depressions travelling within the general airflow. Generalized air-mass relationships for each British airflow type are listed in table 5.2. Such climatological characteristics of

Table 5.2 Airflow types and corresponding air masses

Westerly	mP, mPw, mT
North-westerly	mP, mA
Northerly	mA
Easterly	cA, cP
Southerly	mT or cT (summer); mT or cP (winter)
Cyclonic	mP, mPw, mT

dominant airflows have been quite thoroughly investigated in many countries and the following account of British synoptic climatology can be taken as a typical example of this approach to the study of climatology.

The general properties of air masses have been examined in ch. 4, but certain aspects are of particular interest in respect of the British climate. The frequency of air masses in January, based on a study by Belasco for 1938–49, is illustrated for Kew in fig. 5.3. There is a clear predominance of polar maritime (mP and mPw) air which has a frequency of 30% or more in all months except March. The maximum frequency of mP air at Kew is 33% (with a further 10% mPw) in July. The proportion is even greater in western coastal districts with mP and mPw occurring in the Hebrides, for example, on at least 38% of days throughout the year.

North-westerly mP airstreams produce cool, showery weather at all seasons, especially on windward coasts. The air is unstable with cumuliform cloud, although inland in winter and at night the clouds disperse, giving low night temperatures. Over the sea, however, heating of the lower air continues by day and night in winter months so that showers and squalls can occur at any time, and these may affect windward coastal areas. The average daily mean temperature at Kew with mP air and the difference between this and the average for all air masses (termed the *departure*) during the period 1931–45 are shown in table 5.3. More extreme conditions occur with mA air, the temperature departures at Kew

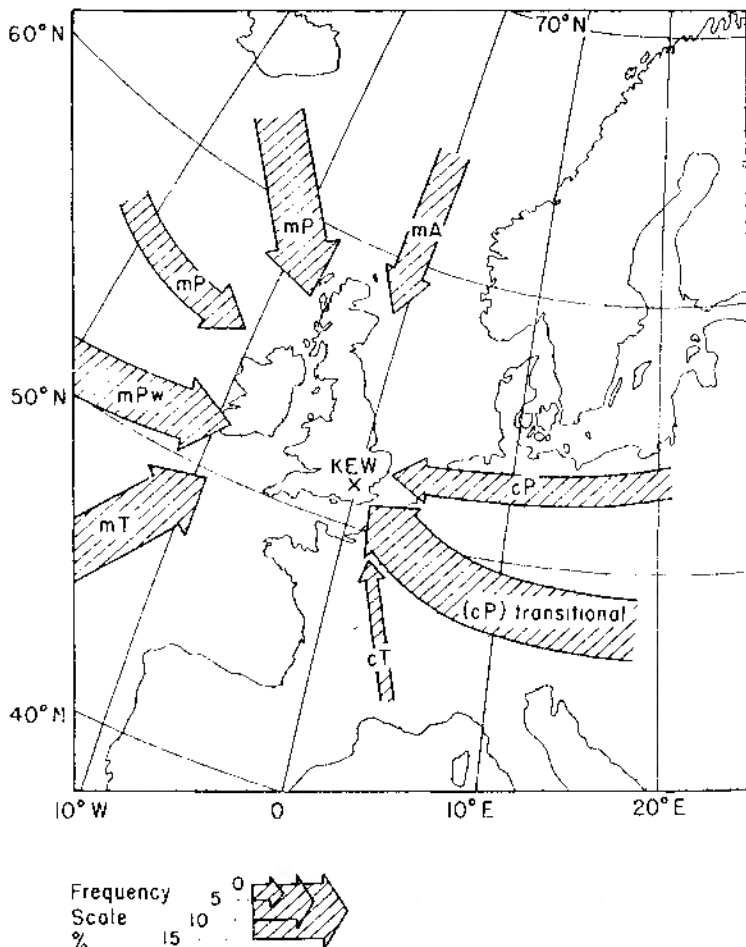


Fig. 5.3. Average air-mass frequencies for Kew (London) in January. Anticyclonic types are included according to their direction of origin (based on Belasco 1952).

being approximately -4°C in summer and winter. The visibility in mA air is usually very good. The contribution of mP and mA air masses to the mean annual rainfall over a 5-year period at three stations in northern England is given in table 5.4, although it should be noted that both air

Table 5.3 Screen-level temperatures occurring with different air masses at Kew ($^{\circ}\text{C}$)
(After Belasco 1952)

	<i>mP</i> (from Iceland)	<i>mP</i> (from mid- Atlantic)	<i>mPw</i>	<i>mA</i>	<i>cP</i>	<i>mT</i>	<i>cT</i>
<i>Winter</i>	<i>T</i>	4	6	8	0	-1	10
	<i>D</i>	-0.8	+1.3	+3.9	-4.4	-5.8	+5.8
<i>Summer</i>	<i>T</i>	16	18	18	14	—	19
	<i>D</i>	-2.8	+0.6	+1.0	-3.3	—	+2.2
							+4.4

T = Average mean daily temperature (to nearest whole degree Celsius).

D = Departure from the average for all air masses (1931-45).

Table 5.4 Percentage of the annual rainfall (1956-60) occurring with different synoptic situations

(After Shaw 1962 and R. P. Mathews unpublished)

Station	Synoptic Categories								
	<i>Warm</i> <i>Front</i>	<i>Warm</i> <i>Sector</i>	<i>Cold</i> <i>Front</i>	<i>Occlu-</i> <i>sion</i>	<i>Polar</i> <i>Low</i>	<i>mP</i>	<i>cP</i>	<i>Arctic</i>	<i>Thunder-</i> <i>storm</i>
Cwm Dyli (99 m or 324 ft)*	18	30	13	10	5	22	0.1	0.8	0.8
Squires Gate (10 m or 33 ft)†	23	16	14	15	7	22	0.2	0.7	3
Rotherham (21 m or 70 ft)‡	26	9	11	20	14	15	1.5	1.1	3

* Snowdonia.

† On the Lancashire coast (Blackpool).

‡ In the Don valley, Yorkshire.

masses may also be involved in non-frontal polar lows. Over much of southern England, and in areas to the lee of high ground, northerly and north-westerly airstreams usually give clear sunny weather with few showers. There is some indication of this in table 5.4, for at Rotherham, in

236 Atmosphere, weather and climate

the lee of the Pennines, the percentage of the rainfall occurring with mP air is much lower than over Lancashire.

Maritime polar air which has followed a more southerly, cyclonic track over the Atlantic, approaching Britain from the south-west, or air which is moving northward ahead of a depression, is shown in mPw in fig. 5.3 and table 5.3. This air has surface properties intermediate with mT air and need not be discussed separately.

Maritime tropical air commonly forms the warm sector of depressions moving from between west and south towards Britain, but fig. 5.3 excludes cases of fronts and depressions (which have a frequency of about 10–12% throughout the year). Hence the characteristic weather conditions of mT air occur rather more often than the percentage frequency might suggest (in January 11% mT air and 4% Anticyclonic air originating from south-west of Britain). The weather is unseasonably mild and damp with mT air in winter. There is generally a complete cover of stratus or stratocumulus cloud and drizzle or light rain (formed by coalescence) may occur, especially over high ground where low cloud produces hill fog. The clearance of cloud on nights with light winds readily cools the moist air to its dew point, forming mist and fog. Table 5.4 shows that a large proportion of the annual rainfall is associated with warm-front and warm-sector situations and therefore is largely attributable to convergence and frontal uplift within mT air. In summer the cloud cover with this air mass keeps temperatures closer to average than in winter (table 5.3); night temperatures tend to be high, but daytime maxima remain rather low.

True continental polar air only affects the British Isles between December and February and even then it is relatively infrequent. Mean daily temperatures are well below average and maxima rise to only a degree or so above freezing point. The air mass is basically very dry and stable but a track over the central part of the North Sea supplies sufficient heat and moisture to cause showers, often in the form of snow, over eastern England and Scotland. *In toto* this provides only a very small contribution to the annual precipitation, as table 5.4 shows, and on the west coast the weather is generally clear. A transitional cP–cT type of air mass reaches Britain from south-east Europe in all seasons, though less frequently in summer. Such airstreams are dry and stable.

Continental tropical air occurs on average about one day per month in summer, which accounts for the rarity of summer heat-waves since these south or south-east winds bring hot, settled weather. The lower layers are stable and the air is commonly hazy, but the upper layers tend to be unstable and occasionally intense surface heating may trigger-off a thunder-

storm. In winter such modified cT air sometimes reaches Britain from the Mediterranean bringing fine, hazy, mild weather.

4 Singularities and natural seasons

Most popular weather lore expresses the belief that each season has its own weather (for example, in England, 'February fill-dyke', 'April showers'), while ancient adages suggest that even the sequence of weather may be determined by the conditions established on a given date (e.g. 40 days of wet or fine weather following St Swithin's day, 15 July). Some of these ideas are quite fallacious, but others contain more than a grain of truth if properly interpreted.

The tendency for a certain type of weather to recur with reasonable regularity around the same date is termed a *singularity*. Many calendars of singularities have been compiled, particularly in Europe, but the early ones (which concentrated upon anomalies of temperature or rainfall) did not prove very reliable. More recently greater success has been achieved by studying singularities of circulation pattern and catalogues have been prepared for the British Isles by Lamb and for central Europe by Flohn and Hess. Lamb's results are based on calculations of the daily frequency of the airflow categories between 1898 and 1947, some examples of which are shown in fig. 5.4. A noticeable feature is the infrequency of the Westerly type in spring, the driest season of the year in the British Isles and also in northern France, northern Germany and in the countries bordering the North Sea. The catalogue of Flohn and Hess is based on a classification of large-scale patterns of airflow in the lower troposphere (*Grosswetterlage*) over central Europe originally proposed by F. Baur.

Some of the European singularities which occur most regularly are as follows:

- (1) A sharp increase in the frequency of Westerly and North-westerly type over Britain takes place about the middle of June. These invasions of maritime air also affect central Europe and this period is sometimes referred to as the beginning of the European 'summer monsoon'.
- (2) About the second week in September Europe and Britain are affected by a spell of Anticyclonic weather. This may be interrupted by Atlantic depressions giving stormy weather over Britain in late September, though anticyclonic conditions again affect central Europe at the end of the month and Britain during early October.
- (3) A marked period of wet weather often affects western Europe and

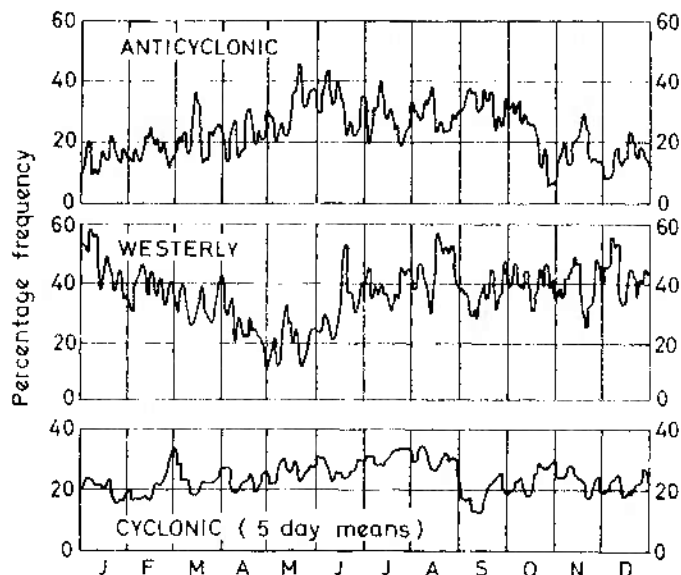


Fig. 5.4. The percentage frequency of anticyclonic, westerly and cyclonic conditions over Britain, 1898–1947 (after Lamb 1950).

also the western half of the Mediterranean at the end of October, whereas the weather in eastern Europe generally remains fine.

- (4) Anticyclonic conditions return to Britain and affect much of Europe about mid-November, giving rise to fog and frost.
- (5) In early December Atlantic depressions push eastwards to give mild, wet weather over most of Europe.

In addition to these singularities, major seasonal trends are recognizable and for the British Isles Lamb identified five *natural seasons* on the basis of spells of a particular type lasting for 25 days or more during the period 1898–1947 (fig. 5.5). In as far as is possible to think in terms of a 'normal year', the seasons are:

- (i) *Spring–early summer* (the beginning of April to mid-June). This is a period of variable weather conditions during which long spells are least likely. Northerly spells in the first half of May are the most significant feature, although there is a marked tendency for anticyclones to occur in late May–early June.

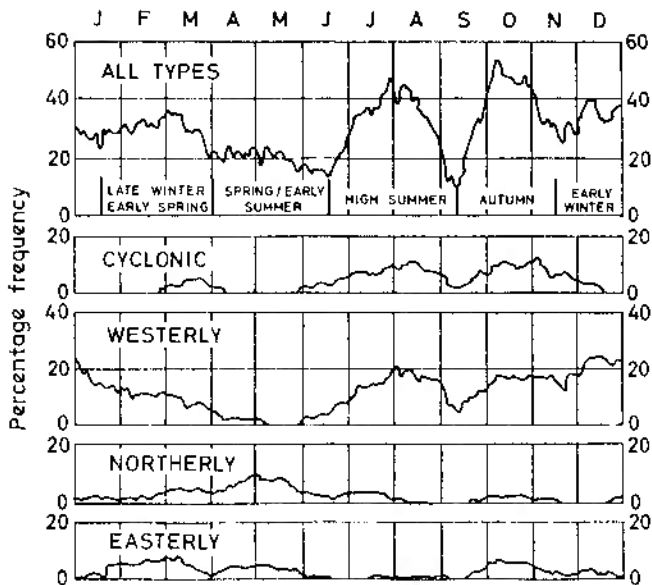


Fig. 5.5. The frequency of long spells (25 days or more) of a given air-flow type over Britain, 1898–1947. The diagram showing all long spells also indicates a division of the year into 'natural seasons' (after Lamb 1950).

- (ii) *High summer* (mid-June to early September). Long spells of various types may occur in different years. Westerly and North-westerly types are the most common and they may be combined with either Cyclonic or Anticyclonic types. Persistent sequences of Cyclonic type occur more frequently than Anticyclonic ones.
- (iii) *Autumn* (the second week in September to mid-November). Long spells are again present in most years, Anticyclonic ones mainly in the first half, Cyclonic and other stormy ones generally in October–November.
- (iv) *Early winter* (from about the third week in November to mid-January). Long spells are less frequent than in summer and autumn. They are usually of Westerly type giving mild, stormy weather.
- (v) *Late winter and early spring* (from about the third week in January to the end of March). The long spells at this time of year

240 Atmosphere, weather and climate

can be of very different types, so that in some years it is mid-winter weather while in other years there is an early spring from about late February.

5 Synoptic anomalies

The mean climatic features of pressure and wind and the typical seasonal airflow regime provide only an incomplete picture of climatic conditions. Some pattern of circulation occur irregularly and yet, because of their tendency to persist for weeks or even months, form an essential element of the climate.

A major example is the occurrence of *blocking* patterns. It was noted in ch. 3, F.2 that the zonal circulation in middle latitudes sometimes breaks down into a cellular pattern. This is commonly associated with a split of the jet stream into two branches over higher and lower middle latitudes and the formation of a cut-off low (see ch. 4, G.4) south of a high-pressure cell. The latter is referred to as a *blocking anticyclone* since it prevents the normal eastward motion of depressions in the zonal flow. A major area of blocking is Scandinavia, particularly in spring. Depressions are forced to move north-eastwards towards the Norwegian Sea or south-eastwards into southern Europe. This pattern, with easterly flow around the southern margins of the anticyclone, produces severe winter weather over much of northern Europe. In January–February 1947, for example, easterly flow across Britain as a result of blocking over Scandinavia led to extreme cold and frequent snowfall. Winds were almost continuously from the east between 22 January and 22 February and even daytime temperatures rose little above freezing point. Snow fell in some part of Britain every day from 22 January to 17 March 1947, and major snowstorms occurred as occluded Atlantic depressions moved slowly across the country. Other notably severe winter months – January 1881, February 1895 and January 1940 – were the result of similar pressure anomalies with pressure much above average to the north of the British Isles and below average to the south.

The average effects of a number of winter blocking situations over north-west Europe are shown in figs 5.6 and 5.7. Precipitation amounts are above normal mainly over Iceland and the western Mediterranean as depressions are steered around the blocking high following the path of the upper jet streams. Over most of Europe precipitation remains below average and this pattern is repeated with summer blocking. Winter temperatures are above average over the north-eastern Atlantic and adjoining land areas, but below average over central and eastern Europe and the Mediterranean due to the northerly outbreaks of cP air (fig. 5.7). The

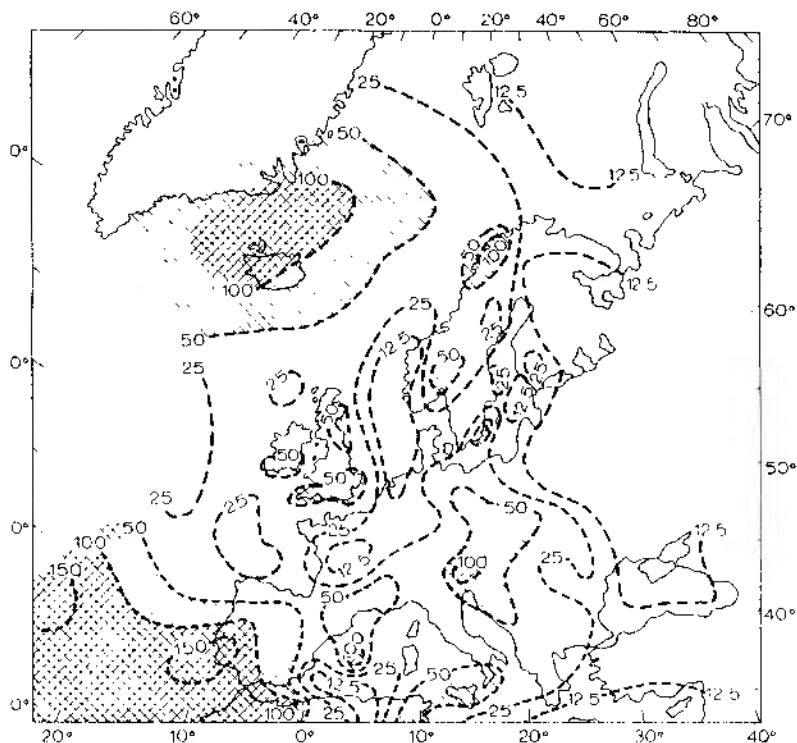


Fig. 5.6. The mean precipitation anomaly, as a per cent of the average during anticyclonic blocking in winter over Scandinavia. Areas above normal are cross-hatched, areas recording precipitation between 50 and 100% of normal have oblique hatching (after Rex 1950).

negative temperature anomalies associated with cool northerly airflow in summer cover most of Europe, and only northern Scandinavia and the north-eastern Atlantic have above-average values.

Despite these generalizations the location of the block is of the utmost importance. For instance, in the summer of 1954 a blocking anticyclone across eastern Europe and Scandinavia allowed depressions to stagnate over the British Isles giving a dull, wet August, whereas in 1955 the blocking was located over the North Sea and a fine, warm summer resulted. Another less common location of blocking is Iceland. A notable example was the 1962–3 winter when persistent high pressure south-east of

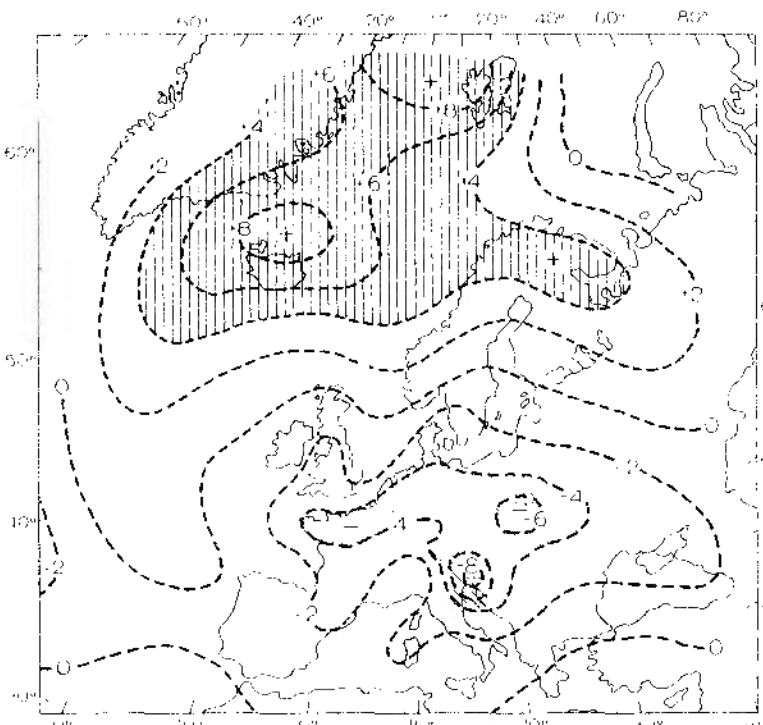


Fig. 5.7. The mean surface temperature anomaly ($^{\circ}\text{C}$) during anticyclonic blocking in winter over Scandinavia. Areas more than 4°C above normal vertical hatching, those more than 4°C below normal have oblique hatching (after Rex 1950).

Iceland led to northerly and north-easterly airflow over Britain. Temperatures in central England at that time were the lowest since 1740, with a mean of 0°C for December 1962 to February 1963. Central Europe was affected by easterly airstreams and mean January temperatures there were 6°C below average.

6 Topographic effects

In various parts of Europe topography has a marked effect on the climate not only of the uplands themselves but also on that of adjacent areas. Apart from the more obvious effects upon temperatures, precipitation amounts and winds, the major mountain masses affect the movement of

frontal systems too. Surface friction over mountain barriers tends to steepen the slope of cold fronts and decrease the slope of warm fronts so that the latter are slowed down and the former accelerated. The cyclogenetic effect of mountain barriers in producing lee depressions has already been discussed (see ch. 4, G.1).

The Scandinavian mountains are one of the most significant climatic barriers in Europe as a result of their orientation with regard to westerly airflow. Maritime air masses are forced to rise over the highland zone giving annual precipitation totals of over 250 cm (100 in) on the mountains of western Norway, whereas descent in their lee produces a sharp decrease in the amounts. The upper Gudbrandsdalen and Osterdalen in the lee of the Jotunheim and Dovre Mountains receive on average less than 50 cm (20 in), and similar low values are recorded in the Jämtland province of central Sweden around Östersund.

The mountains can equally function in the opposite sense. For example, Arctic air from the Barents Sea may move southwards in winter over the Gulf of Bothnia, usually when there is a depression over northern Russia, giving very low temperatures in Sweden and Finland. Western Norway is rarely affected, since the cold wave is contained to the east of the mountains. In consequence there is a sharp climatic gradient across the Scandinavian Highlands in the winter months.

The Alps provide a quite different illustration of topographic effects. Together with the Pyrenees and the mountains of the Balkans, the Alps effectively separate the Mediterranean climatic region from that of Europe. The penetration of warm air masses north of these barriers is comparatively rare and short-lived. However, with certain pressure patterns, air from the Mediterranean and north Italy is forced to cross the Alps, losing its moisture through precipitation on the southern slopes. Dry adiabatic warming on the northern side of the mountains can readily raise temperatures by 5–6°C in the upper valleys of the Aar, Rhine and Inn. At Innsbruck there are approximately 50 days per year with föhn winds, with a maximum in spring, and these occurrences are often responsible for rapid melting of the snow, creating a risk of avalanches. When the airflow across the Alps has a northerly component föhns may occur in northern Italy, but their effects are generally less pronounced.

A more detailed examination of upland climates, with particular reference to Britain, will serve to illustrate some of the diverse effects of altitude. The mean annual rainfall on the west coasts near sea level is about 114 cm (45 in) but on the western mountains of Scotland, the Lake District and Wales averages exceed 380 cm (150 in) per year. The annual record is 653 cm (257 in) in 1954 at Sprinkling Tarn, Cumberland, and

145 cm (57 in) fell in a single month (October 1909) just east of the summit of Snowdon. The annual number of rain-days (days with at least 0.25 mm (0.01 in) of precipitation) increases from about 165 days in south-eastern England and the south coast to over 230 days in north-west Britain. There is little additional increase in the frequency of rainfall with height on the mountains of the north-west, so that the mean rainfall per rain-day rises sharply from 0.5 cm (0.2 in) near sea-level in the west and north-west to over 1.3 cm (0.5 in) in the Western Highlands, the Lake District and Snowdonia. This demonstrates that 'orographic rainfall' here is primarily due to an intensification of the normal precipitation processes and is not a special type. It is more appropriate, therefore, to recognize an orographic component which increases the amounts of rain associated with frontal depressions and unstable airstreams (see ch. 2, 1.2). Even quite low hills such as the Chilterns and South Downs cause a rise in rainfall, receiving about 12–13 cm (5 in) per year more than the surrounding lowlands. Indeed, detailed studies in Sweden show that wooded hills rising only 30–50 m (100–150 ft) above the surrounding plains may cause precipitation amounts during cyclonic spells to be increased by 50–80% compared with the average falls over the lowland. However, in most countries, the rain-gauge networks are too coarse to detect such small-scale variations.

The sheltering effects of the uplands produce low annual totals on the lee side (with respect to the prevailing winds). Thus, the lower Dee valley in the lee of the mountains of north Wales receives less than 75 cm (30 in) per year compared with over 250 cm (100 in) on Snowdonia.

The complexity of the various factors affecting rainfall in Britain is shown by the fact that a close correlation exists between annual totals in north-west Scotland, the Lake District and western Norway, which are directly affected by Atlantic depressions. At the same time there is an inverse relationship between annual amounts in the Western Highlands and lowland Aberdeenshire less than 240 km (150 miles) away. Annual precipitation in the latter area is more closely correlated with that in lowland eastern England. Essentially, the British Isles comprise two major climatic units for rainfall – firstly, an 'Atlantic' one with a winter season maximum, and, secondly, those central and eastern districts with 'continental' affinities in the form of a weak summer maximum in most years. Other areas (eastern Ireland, eastern Scotland, north-east England and most of midland England and the Welsh border counties) generally have a wet second half of the year.

The occurrence of snow is another measure of altitude effects. Near sealevel there are on average approximately 5 days per year with snow

falling in south-west England, 15 days in the south-east and 35 days in northern Scotland. Between 60 and 300 m the frequency increases by about 1 day per 15 m of elevation and even more rapidly on higher ground. Approximate figures for northern Britain are 60 days at 600 m and 90 days at 900 m. The number of mornings with snow lying on the ground (more than half the ground covered) is closely related to mean temperature and hence altitude. Average figures range from about 5 days per year or less in much of southern England and Ireland, to between 30 and 50 days on the Pennines and over 10 days on Grampian Mountains in the last area (on the Cairngorms) and on Ben Nevis there are several semi-permanent snowbeds at about 1160 m and it is estimated that the theoretical climatic snowline – above which there is *net* accumulation of snow – is at 1620 m (5300 ft) over Scotland.

The seasonal variability of lapse rates in mountain areas was mentioned in ch. 1, I. There also exist marked geographical variations even within the British Isles. One measure of these variations is the length of the 'growing season'. Meteorological data can be used to determine an index of growth opportunity by counting the number of days on which the mean daily temperature exceeds an arbitrary threshold value – commonly 6°C (43°F). Along the south-west coasts of England the 'growing season', as calculated on this basis, is nearly 365 days per year and in this area it decreases by about 9 days per 30 m of elevation, but in northern England and Scotland the decrease is only about 5 days per 30 m from between 250–270 days near sea-level. In continental climates the altitudinal decrease may be even more gradual; in central Europe and New England, for example, it is about 2 days per 30 m.

B North America

The North American continent spans nearly 60° of latitude and, not surprisingly, exhibits a wide range of climatic conditions. Unlike Europe, the west coast is backed by the Pacific coast ranges rising to over 2750 m, which lie across the path of depressions in the mid-latitude westerlies and prevent the extension of maritime influences inland. In the interior of the continent there are no significant obstructions to air movement, and the absence of any east–west barrier allows air masses from the Arctic or the Gulf of Mexico to sweep across the interior lowlands, causing wide extremes of weather and climate. Maritime influences in eastern North America are greatly limited by the fact that the prevailing winds are westerly, so that the temperature regime is continental. Nevertheless, the Gulf of Mexico is a major source of moisture supply for precipitation

over the eastern half of the United States and, as a result, the precipitation regimes are different from those found in eastern Asia.

We will look first at the broad characteristics of the atmospheric circulation over the continent.

1 Pressure systems

The mean pressure pattern for the middle troposphere displays a prominent trough over eastern North America in both summer and winter (see fig. 3.17). One theory is that this is a lee trough caused by the effect of the western mountain ranges on the upper westerlies, but at least in winter the strong baroclinic zone along the east coast of the continent is undoubtedly a major contributory factor. The implications of this mean wave pattern are that cyclones tend to move south-eastward over the Midwest carrying continental polar air southward, while the cyclone paths are north-eastward along the Atlantic coast.

In individual months there may of course be considerable deviations from this average pattern, with important consequences for the weather in different parts of the continent, and, in fact, this relationship provides the basis for the monthly forecasts of the United States Weather Bureau. For example, if the trough is more pronounced than usual temperature may be much below average in the central, southern and eastern United States, whereas if the trough is weak the westerly flow is stronger with correspondingly less opportunity for cold outbreaks of polar air masses. Sometimes the trough is displaced to the western half of the continent causing a reversal of the usual weather pattern, since upper north-westerly airflow can bring cold, dry weather to the west while in the east there are very mild conditions associated with upper south-westerly flow. Precipitation amounts also depend on the depression tracks; if the upper trough is far to the west, depressions form ahead of it (see ch. 4, E) over the south central United States and move northeastwards towards the lower St Lawrence, giving more precipitation than usual in these areas and less along the Atlantic coast.

The major features of the surface pressure map in January (see fig. 3.21) are the extension of the subtropical high over the south-western United States (called the Great Basin high) and the separate polar anticyclone of the Mackenzie district of Canada. Mean pressure is low off both the east and west coasts of higher middle latitudes, where oceanic heat sources indirectly give rise to the (mean) Icelandic and Aleutian lows. It is interesting to note that, on average, in December, of any region in the northern hemisphere for any month of the year, the Great Basin region has the most frequent occurrence of highs, whereas the Gulf of Alaska

has the maximum frequency of lows. The Pacific coast as a whole has its most frequent cyclonic activity in winter as does the Great Lakes area, whereas over the Great Plains the maximum is in spring and early summer. Remarkably, the Great Basin in June has the most frequent cyclogenesis of any part of the northern hemisphere in any month of the year. Heating over this area in summer helps to maintain a shallow, quasi-permanent low-pressure cell, in marked contrast with the almost continuous subtropical high-pressure belt in the middle troposphere (fig. 3.17). Continental heating also indirectly assists in the splitting of the Icelandic low to create a secondary centre over north-eastern Canada. The west-coast summer circulation is dominated by the Pacific anticyclone while the south-eastern United States is affected by the Atlantic subtropical anticyclone cell.

Broadly, there are three prominent depression tracks across the continent in winter (see fig. 4.15). One group moves from the west along a more or less zonal path about 45–50°N, whereas a second loops southward over the central United States and then turns north-eastward towards New England and the Gulf of St Lawrence. Some of these depressions originate over the Pacific, cross the western ranges as an upper trough and redevelop in the lee of the mountains. Alberta is a noted area for this process and also for primary cyclogenesis since the arctic frontal zone is over north-west Canada in winter. This frontal zone involves much-modified mA air from the Gulf of Alaska and cold dry cA (or cP) air. Depressions of the third group form along the main polar frontal zone, which in winter is off the east coast of the United States, and move north-eastward towards Newfoundland. Sometimes this frontal zone is present over the continent about 35°N with mT air from the Gulf and cP air from the north or modified mP air from the Pacific. Polar front depressions forming over Colorado move north-eastward towards the Great Lakes and others developing over Texas follow a more or less parallel path, further to the south and east, towards New England.

Between the Arctic and Polar Fronts a third frontal zone is distinguished by Canadian meteorologists. This *maritime* (arctic) frontal zone is present when mA and mP (or mPc and mPw) air masses interact along their common boundary. The three-front (i.e. four air-mass) model allows a detailed analysis to be made of the baroclinic structure of depressions over the North American continent using synoptic weather maps and cross-sections of the atmosphere. Figure 5.8 illustrates the three frontal zones and associated depressions on 29 May 1963. Along 95°W, from 60°N to 40°N, the following dew-point temperatures were reported

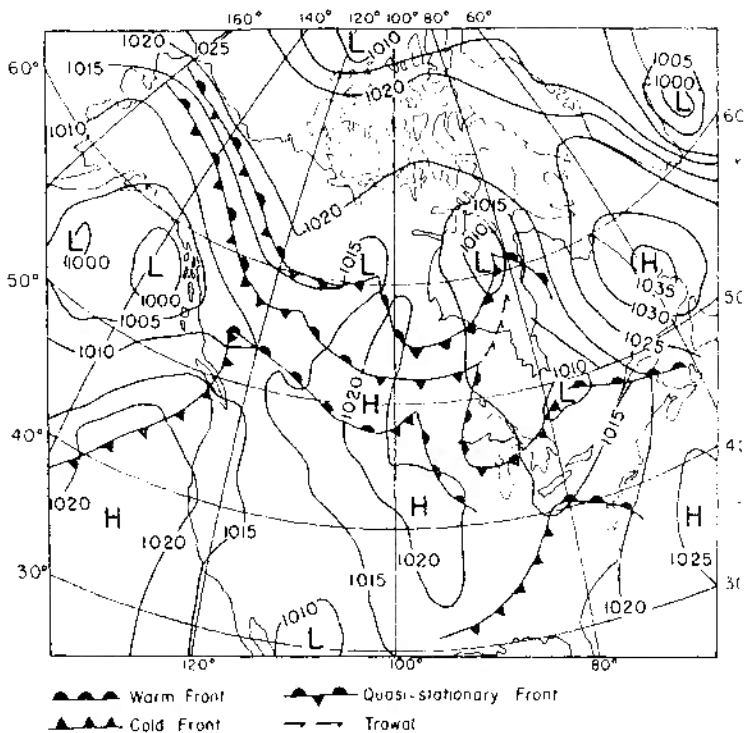


Fig. 5.8. A synoptic example of depressions associated with three-frontal zones on 29 May 1963 over North America (based on charts of the Edmonton Analysis Office and the Daily Weather Report).

in the four air masses: 17°F (-8°C), 33°F (1°C), 40°F (4°C) and 55°F (13°C).

In summer, the east-coast depressions are less frequent and the tracks across the continent are displaced northwards with the main ones moving over Hudson Bay and Labrador-Ungava, or along the line of the St Lawrence. These are associated mainly with a rather poorly-defined Maritime frontal zone. The Arctic Front is usually located along the north coast of Alaska, where there is a strong temperature gradient between the bare land and the cold Polar Sea and pack-ice. East from here the front is very variable in location from day to day and year to year. Broadly, it occurs most often in the vicinity of northern Keewatin and Hudson Strait,

although one study of air-mass temperatures and air-stream confluence regions suggests that an Arctic frontal zone occurs further south over Keewatin in July and that its mean position (fig. 5.9) is closely related to the boreal forest-tundra boundary. This relationship undoubtedly reflects the importance of Arctic air-mass dominance for summer temperatures and consequently for tree-growth possibilities, but the precise nature of the interrelationships between atmospheric systems and vegetation boundaries requires more extensive investigation.

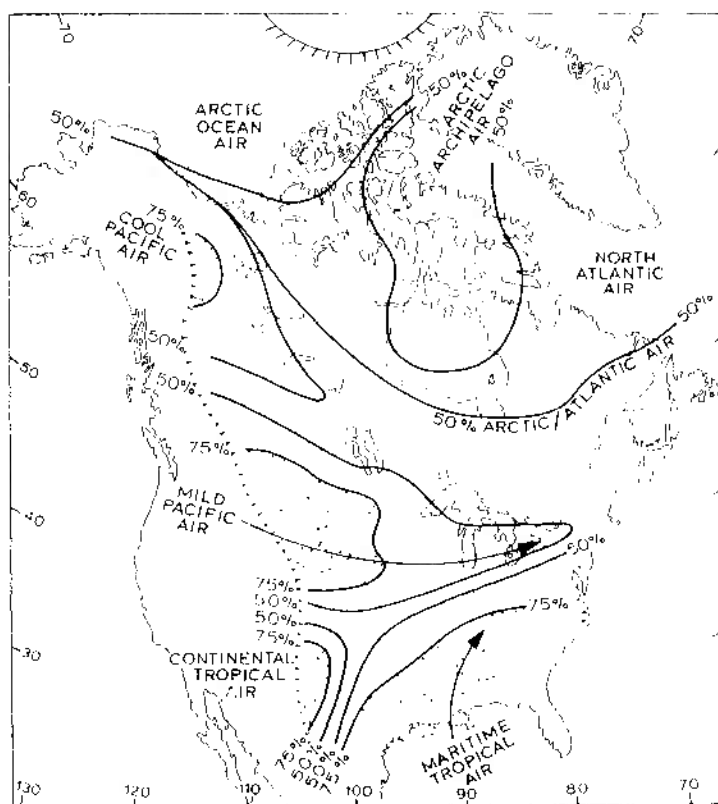


Fig. 5.9. Regions in North America east of the Rocky Mountains dominated by the various air mass types in July for more than 50% and 75% of the time (after Bryson 1966).

250 Atmosphere, weather and climate

A number of circulation singularities have been recognized in North America, as in Europe (ch. 5, A.4). Three which have received considerable attention in view of their prominence are: (i) the advent of spring in late March; (ii) the midsummer high-pressure jump at the end of June; (iii) the Indian summer in late September (and late October).

The arrival of spring is marked by different climatic responses in different parts of the continent. For example, there is a sharp decrease in March to April precipitation in California, due to the extension of the Pacific high, whereas precipitation intensity increases in the Midwest (fig. 5.10A) as a result of more frequent cyclogenesis in Alberta and Colorado

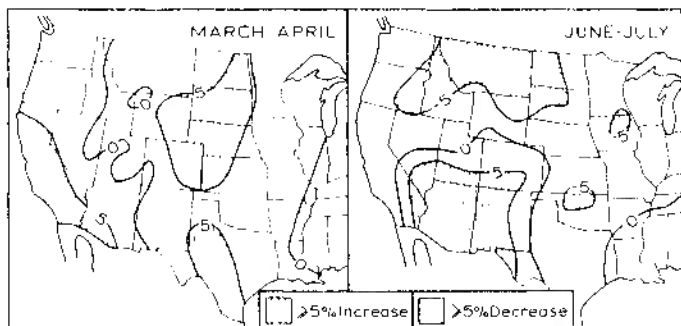


Fig. 5.10. The precipitation changes between March–April (left) and June–July (right), as a percentage of the mean annual total, for the central and western United States (after Bryson and Lahey 1958).

and a northward extension of maritime tropical air over the Midwest from the Gulf of Mexico. These changes are part of a hemispheric readjustment of the circulation since at the beginning of April the Aleutian low-pressure cell, which from September to March is located about 55°N, 165°W, splits into two with one centre in the Gulf of Alaska and the other over northern Manchuria. This represents a decrease in the zonal index (ch. 3, F.2).

In late June there is a rapid northward displacement of the subtropical high-pressure cells in the northern hemisphere. In North America this pushes the depression tracks northward also with the result that precipitation decreases from June to July over the northern Great Plains, parts of Idaho and eastern Oregon (fig. 5.10B). Conversely, the south-westerly anticyclonic flow which affects Arizona in June is replaced by air from the Gulf of California and this causes the onset of the summer rains (fig. 5.10)

(see ch. 5, D.2). It has been suggested by Bryson and Lahey that these circulation changes at the end of June may be connected with the disappearance of snow cover from the Arctic tundra. This leads to a sudden decrease of surface albedo from about 75 to 15% with consequent changes in the heat budget components and hence in the atmospheric circulation.

Frontal wave activity makes the first half of September a rainy period in the northern midwest states of Iowa, Minnesota and Wisconsin, but after about the 20th of the month anticyclonic conditions return with warm air-flow from the dry south-west giving fine weather – the so-called Indian summer. Significantly, the hemispheric zonal index value rises in late September. This anticyclonic weather type has a second phase in the latter half of October, but at this time there are polar outbreaks. The weather is generally cold and dry, although if precipitation does occur there is a high probability of it being in the form of snow.

2 The temperate west coast and cordillera

The oceanic circulation of the North Pacific closely resembles that of the North Atlantic. The drift from the Kuro Shio current off Japan is propelled by the westerlies towards the western coast of North America and acts as a warm current between 40° and 60°N. Sea-surface temperatures are several degrees lower than in comparable latitudes off western Europe, however, due to the smaller volume of warm water involved. Also, in contrast to the Norwegian Sea, the shape of the Alaskan coastline prevents the extension of the drift to high latitudes (see fig. 3.34).

The Pacific coast ranges greatly restrict the inland extent of oceanic influences, and hence there is no extensive maritime temperate climate such as we have described for western Europe. The major climatic features duplicate those of the coastal mountains of Norway and those of New Zealand and southern Chile in the belt of Southern Westerlies. Topographic factors make the weather and climate of such areas very variable over short distances both vertically and horizontally, and, therefore, only a few salient characteristics are selected for consideration.

There is a regular pattern of rainy windward and drier lee slopes across the successive north-west to south-east ranges with a more general decrease towards the interior. The Coast Range in British Columbia has mean annual totals of precipitation exceeding 250 cm (100 in) with 500 cm (200 in) in the wettest places compared with 125 cm (50 in) or less on the summits of the Rockies, yet even on the leeward side of Vancouver Island the average figure at Victoria is only 70 cm (27 in). Analogous to

the 'Westerlies-oceanic' regime of north-west Europe, there is a winter precipitation maximum along the littoral which also extends beyond the Cascades (in Washington) and the Coast Range (in British Columbia), but summers are drier due to the strong North Pacific anticyclone. The regime in the interior of British Columbia is transitional between that of the coastal region and the distinct summer maximum of central North America (fig. 5.11), although at Kamloops in the Thompson valley (annual average 25 cm or 10 in) there is a slight summer maximum associated with thunderstorm type of rainfall. In general, the sheltered interior valleys receive less than 50 cm (20 in) per year and in the driest years certain localities have recorded only 15 cm (6 in). Above 1000 m much of the precipitation falls as snow (fig. 5.11) and some of the

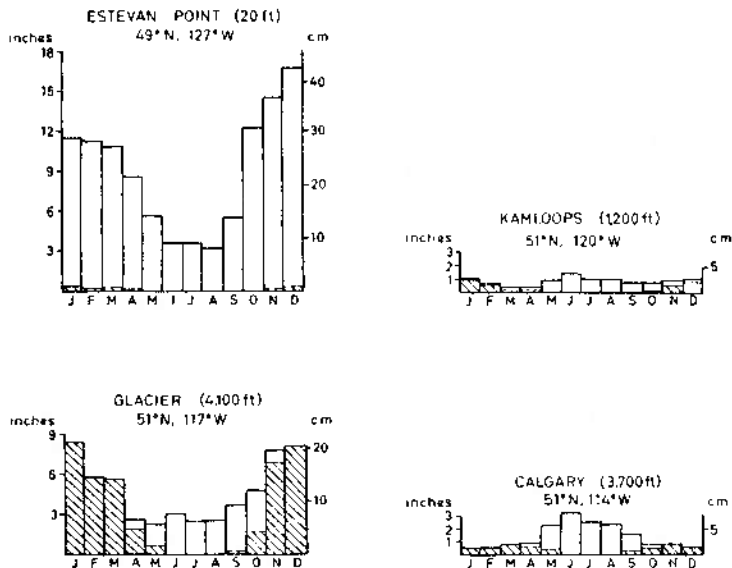


Fig. 5.11. Precipitation graphs for stations in western Canada. The shaded portions represent snowfall, expressed as water equivalent.

greatest snow-depths in the world are reported from British Columbia, Washington and Oregon. For example, between 1000 and 1500 cm (400 and 600 in) falls on the Cascade Range at heights of about 1500 m (5000 ft) and even as far inland as the Selkirk Mountains the totals are con-

siderable. The mean snowfall is 990 cm (390 in) at Glacier, British Columbia (elevation 1200 m) and this accounts for almost 70% of the annual precipitation. In Canada snow-depth is generally measured in inches and ten inches of snow is taken to be equivalent to one inch of water. It is estimated that the climatic snowline rises from about 1600 m (5250 ft) on the west side of Vancouver Island to 2900 m (9500 ft) in the eastern Coast Range. Inland its elevation increases from 2300 m (7550 ft) on the west slopes of the Columbia Mountains to 3100 m (10,170 ft) on the east side of the Rockies. This trend reflects the precipitation pattern referred to above.

Finally, mention must be made of the large diurnal variations which affect the cordilleran valleys. Strong diurnal rhythms of temperature (especially in summer) and wind direction are a feature of mountain climates and their effect is superimposed upon the general climatic characteristics of the area. Cold air drainage produces many remarkably low minima in the mountain valleys and basins. At Princeton, British Columbia (elevation 695 m), where the mean daily minimum in January is -14°C (7°F), there is on record an absolute low of -45°C (-49°F), for example. This leads in some cases to reversal of the normal lapse rate. Golden in the Rocky Mountain Trench has a January mean of -12°C (11°F) whereas 460 m (1500 ft) higher at Glacier (1248 m) it is -10°C (14°F).

3 Interior and eastern North America

Central North America has the typical climate of a continental interior in middle latitudes with hot summers and cold winters (see fig. 5.13), yet the weather in winter is subject to marked variability. This is determined by the steep temperature gradient between the Gulf of Mexico and the snow-covered northern plains; also by shifts of the upper wave patterns and jet stream. Cyclonic activity in winter is much more pronounced over central and eastern North America than in Asia, which is dominated by the Siberian anticyclone (see fig. 4.15), and consequently there is no climatic type with a winter minimum of precipitation in eastern North America.

The general temperature conditions in winter and summer are illustrated in fig. 5.12, showing the frequency with which hourly temperature readings exceed or fall below certain limits. The two chief features of all four maps are: (a) the dominance of the meridional temperature gradient, away from coasts, and (b) the continentality of the interior and east compared with the 'maritimeness' of the west coast. On the July maps additional influences are evident and these are referred to below.

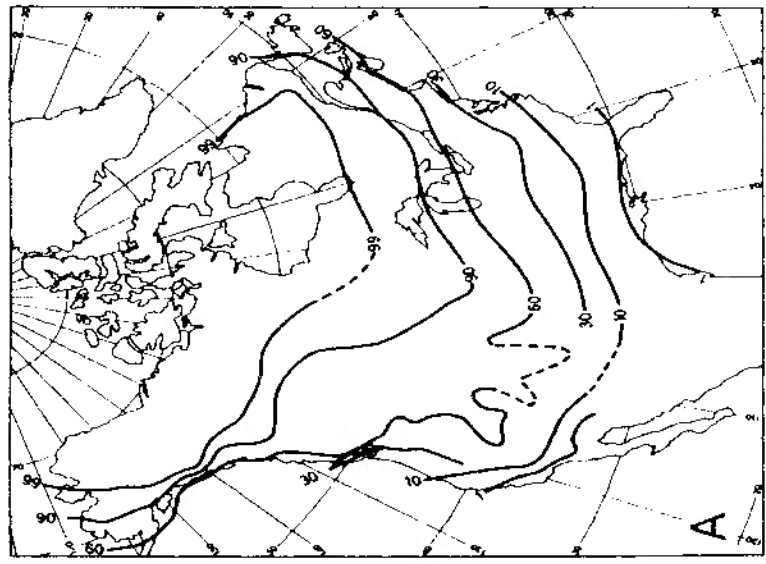
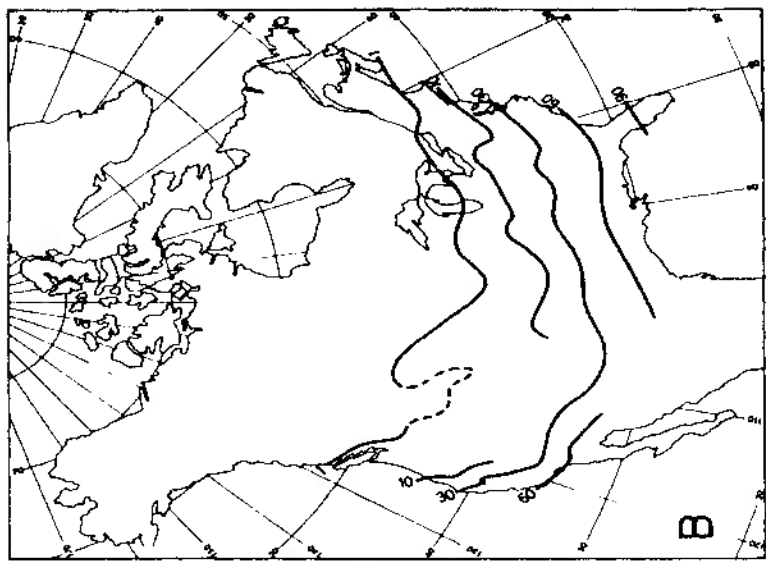
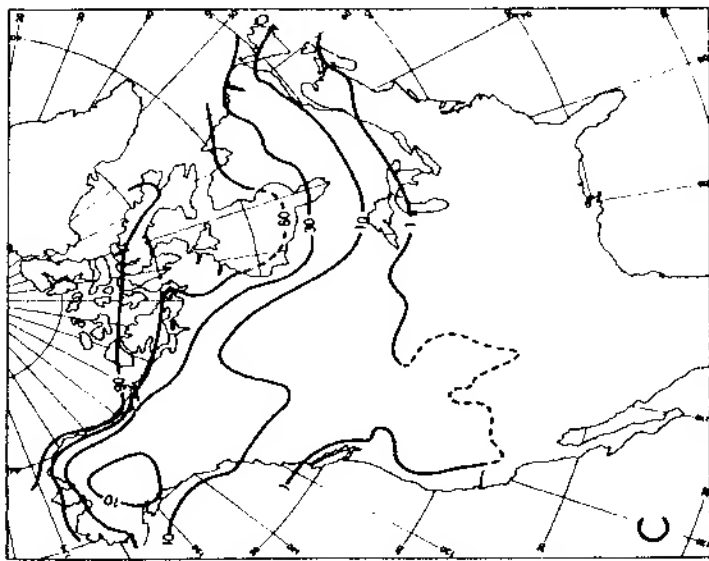
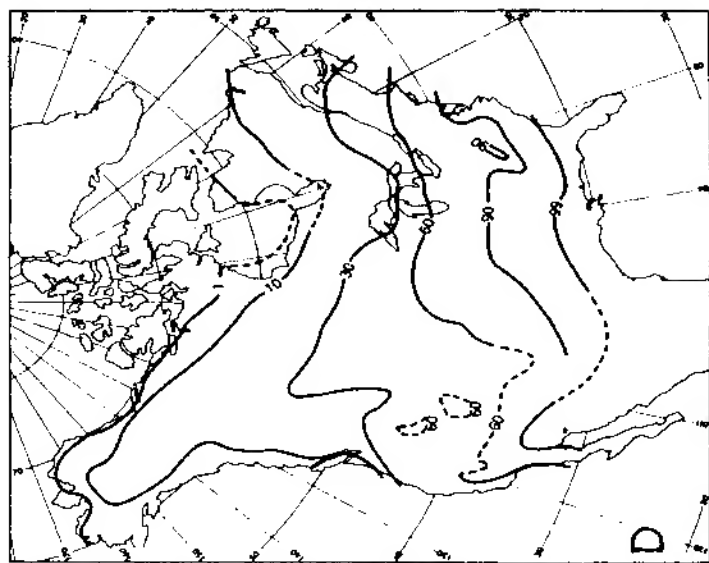


Fig. 5.12. The percentage frequency of hourly temperatures above or below certain limits for North America (after Rayner 1961).
A. January temperatures $< 0^{\circ}\text{C}$. B. January temperatures $> 10^{\circ}\text{C}$. C. July temperatures $< 10^{\circ}\text{C}$. D. July temperatures $> 21^{\circ}\text{C}$.



a Continental and oceanic influences. The Labrador coast is fringed by the waters of a cold current, analogous to the Oya Shio off eastern Asia, but in both cases the prevailing westerlies greatly limit their climatic significance. The Labrador Current maintains drift ice off Labrador and Newfoundland until June and gives very low summer temperatures along the Labrador coast (fig. 5.12 c). The lower incidence of freezing temperatures in this area in January is related to the movement of some depressions into the Davis Strait, carrying Atlantic air northwards. A major role of the Labrador current is in the formation of fog. Advection fogs are very frequent between May and August off Newfoundland, where the Gulf Stream and Labrador Current meet. Warm, moist southerly airstreams are cooled rapidly over the cold waters of the Labrador Current and with steady, light winds such fogs may persist for several days, creating hazardous conditions for shipping. Southward-facing coasts are particularly affected and at Cape Race (Newfoundland), for example, there are on average 158 days per year with fog (visibility less than 1 km) at some time of day. The summer concentration is shown by the figures for Cape Race during individual months: May – 18 (days), June – 18, July – 24, August – 21 and September – 15.

Oceanic influence along the Atlantic coasts of the United States is very limited, and although there is some moderating effect on minimum temperatures at coastal stations this is scarcely evident on generalized maps such as fig. 5.12. More significant climatic effects are in fact found in the neighbourhood of Hudson Bay and the Great Lakes. Hudson Bay remains very cool in summer with water temperatures of about 7–9°C and this depresses temperatures along its shore, especially in the east (fig. 5.12c and d). Mean July temperatures are 12°C (54°F) at Churchill (59°N) and 8°C (47°F) at Port Harrison (58°N), on the west and east shores respectively, compared for instance with 13°C (56°F) at Aklavik (68°N) on the Mackenzie delta. The influence of Hudson Bay is even more striking in early winter when the land is snow-covered. Westerly air-streams crossing the open water are warmed on average by 11°C (20°F) in November, and moisture added to the air leads to considerable snowfall in western Ungava (see the graph for Port Harrison (fig. 5.16)). By the beginning of January the Bay is frozen over almost entirely and no effects are evident. The Great Lakes influence their surroundings in much the same way. Heavy winter snowfalls are a notable feature of the southern and eastern shores of the Great Lakes. In addition to contributing moisture to north-westerly streams of cold cA and cP air, the heat source of the open water in early winter produces a low-pressure trough which increases the snowfall as a result of convergence. Yet a further factor is

frictional convergence and orographic uplift at the shoreline. Mean annual snowfall exceeds 250 cm (100 in) along much of the eastern shore of Lake Huron and Georgian Bay, the south-eastern shore of Lake Ontario, the north-eastern shore of Lake Superior and its southern shore east of about $90^{\circ} 30' W$. Extremes include 114 cm (45 in) in 1 day at Watertown, New York, and 894 cm (352 in) during the 1946–7 winter season at nearby Bennetts Bridge, both of which are close to the eastern end of Lake Ontario. Transport in cities in these snow belts is quite frequently disrupted during winter snowstorms. The Great Lakes also provide an important tempering influence during winter months by raising average daily minimum temperatures at lakeshore stations by some $2-4^{\circ}C$ above those at inland locations.

An indication of the seasonal range of temperature is provided by fig. 5.13, showing continentality (k) based on Conrad's formula:

$$k = \frac{1.7A}{\sin(\phi + 10)} - 14$$

where A is the average annual temperature range in $^{\circ}C$ and ϕ is the latitude angle. The results in middle and high latitudes are similar to those obtained by Gorczynski's method (see ch. 5, A.2); with either of these empirical expressions it is only the relative magnitude of k that is of interest. The highest values form a tongue along the $100^{\circ}W$ meridian with subsidiary areas on the 'Lake Plateau' of central Labrador-Ungava and on the high plateaux of Colorado and Utah. The 'maritimeness' of the Pacific coast, though of very limited inland extent, is pronounced, whereas on the east coast there is relatively high continentality. The map also illustrates the ameliorating effect of the Great Lakes.

b Warm and cold spells. Two types of synoptic condition are of particular significance for temperatures in the interior of North America. One is the 'cold wave' caused by a northerly outbreak of cP air, which in winter regularly penetrates deep into the central and eastern United States and occasionally affects even the Gulf coast (fig. 5.11A), injuring frost-sensitive crops. Cold waves arbitrarily defined as a temperature drop of at least $11^{\circ}C$ ($20^{\circ}F$) in 24 hours over most of the United States, and at least $9^{\circ}C$ ($16^{\circ}F$) in California, Florida and the Gulf Coast, to below a specified minimum depending on location and season. The winter criterion decreases from $0^{\circ}C$ in California, Florida and the Gulf Coast to $\sim 18^{\circ}C$ ($0^{\circ}F$) over the northern Great Plains and the north-eastern States. The cold spells commonly occur with the build-up of a north-south anticyclone in the rear of a cold front. The polar air gives clear, dry weather

with strong, cold winds, although if the winds follow snowfall, fine, powdery snow may be whipped up by the wind, creating blizzard conditions. These are quite common over the northern plains.

Another type of temperature fluctuation is associated with the *Chinook* winds in the lee of the Rockies (see ch. 3, C.2). The Chinook is particularly warm and dry as air of Pacific origin, after losing its moisture over the mountains, descends the eastern slopes and warms at the dry



Fig. 5.13. Continentality in North America according to Conrad's index (*modified after Trewartha 1961*).

adiabatic lapse rate. The onset of the Chinook produces temperatures well above the seasonal normals so that snow is often thawed rapidly, and in fact the Indian word Chinook means snow-eater. Temperature rises of as much as 22°C (40°F) have been observed in 5 min and the occurrence of such warm spells is reflected by the high extreme maxima in winter months at Medicine Hat (fig. 5.14). In Canada the Chinook effect may be observed a considerable distance from the Rockies into south-west Saskatchewan, but in Colorado its influence is rarely felt more than about

50 km from the foothills. No adequate definition of a Chinook has yet been established, but using an arbitrary criterion of winter days with a maximum temperature of at least 4.4°C (40°F), R. W. Longley has shown that in the Lethbridge area Chinooks occur on 40% of days during December–February. However, since the phenomenon is the result of a particular type of airflow, it is evident that some wind characteristic should be included in future definitions.

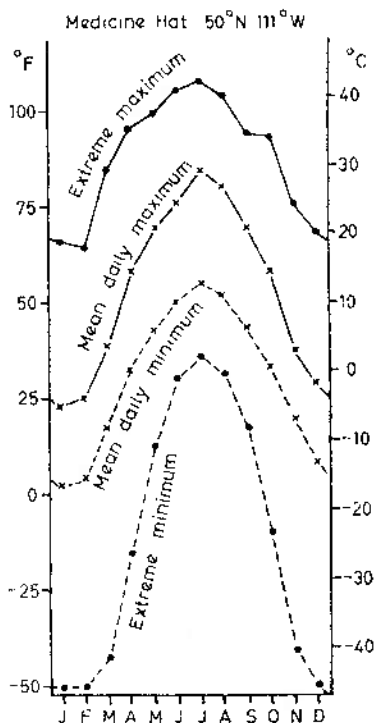


Fig. 5.14. Mean and extreme temperatures at Medicine Hat, Alberta.

Chinook conditions commonly develop in a Pacific airstream which is replacing a winter high-pressure cell over the high western plains. Sometimes the cold, stagnant cP air of the anticyclone is not dislodged by the descending Chinook and a marked inversion is formed, but on other

occasions the boundary between the two air masses may reach ground level locally and, for example, the western suburbs of Calgary may record temperatures above 0°C while those to the east of the city remain below -15°C.

c Precipitation and the moisture balance. Longitudinal influences are apparent in the distribution of annual precipitation, although this is in large measure a reflection of the topography. The 20-in (51-cm) annual isohyet in the United States approximately follows the 100°W meridian (fig. 5.15), and westwards to the Rockies is an extensive dry belt in the rain shadow of the western mountain ranges. In the south-east totals exceed 50 in (127 cm), and 40 in or more is received along the Atlantic coast as far as New Brunswick and Newfoundland.

The major source of moisture for precipitation over North America are the Pacific Ocean and the Gulf of Mexico. The former need not concern us here since comparatively little of the precipitation falling over the interior appears to be derived from that source. The Gulf source is extremely important in providing moisture for precipitation over central and eastern North America, but the predominance of south-westerly airflow means that little precipitation falls over the western Great Plains (fig. 5.16). Over the south-eastern United States there is considerable evapotranspiration and this helps to maintain moderate annual totals northwards and eastwards from the Gulf by providing additional water vapour for the atmosphere. Along the east coast the Atlantic Ocean is an additional significant source of moisture for winter precipitation.

There are at least eight major types of seasonal precipitation regime in North America (fig. 5.16); the winter maximum of the west coast and the transition type of the intermontane region in middle latitudes have already been mentioned and the subtropical types are discussed in the next section. Four primarily mid-latitude regimes are distinguished east of the Rocky Mountains:

- (i) A warm season maximum is found over much of the continental interior (e.g. Rapid City). In an extensive belt from New Mexico to the Prairie Provinces more than 40% of the annual precipitation falls in summer. In New Mexico the rain occurs mainly with late summer thunderstorms, but May-June is the wettest time over the central and northern Great Plains due to more frequent cyclonic activity. Winters are quite dry over the Plains, but the mechanism of the occasional heavy snowfalls is of interest. They occur over the north-western Plains during easterly upslope flow, usually in a

ridge of high pressure. Further north in Canada the maximum is commonly in late summer or autumn when depression tracks are in higher middle latitudes. There is a local maximum in autumn on

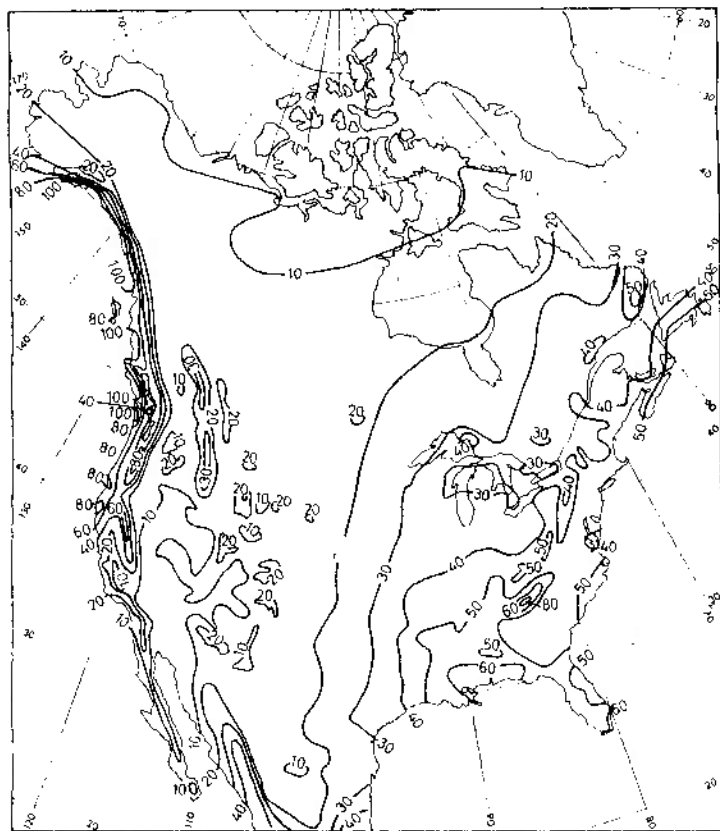


Fig. 5.15. Average annual precipitation (in inches) over North America (after Brooks and Connor, Kendrew and Thomas).

the eastern shores of Hudson Bay (e.g. Port Harrison) due to the effect of open water.

- (ii) Eastward and southward of the first zone there is a double maximum in May and September. In the upper Mississippi region (e.g. Columbia) there is a secondary minimum, paradoxically in

July–August when the air is especially warm and moist, and a similar profile occurs in northern Texas (e.g. Abilene). An upper-level ridge of high pressure over the Mississippi valley seems to be responsible for reduced thunderstorm rainfall in midsummer, and a tongue of subsiding dry air extends southwards from this ridge towards Texas. In September, renewed cyclonic activity associated with the seasonal southward shift of the polar front, at a time

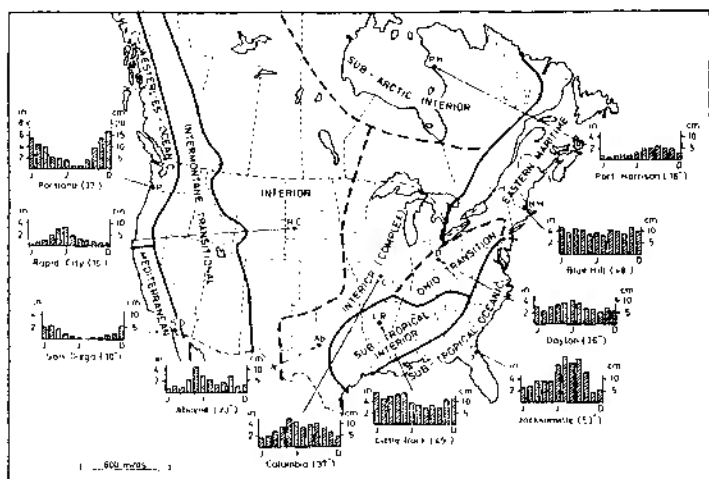


Fig. 5.16. Rainfall regimes in North America. The insert histograms show the mean monthly precipitation; January, June and December are indicated (partly after Trewartha 1961).

when mT air from the Gulf is still warm and moist, causes a resumption of rainfall. Subsequently, however, drier westerly air-streams affect the continental interior as the general airflow becomes more zonal.

The diurnal occurrence of precipitation in the central United States is rather unusual for a continental interior. Sixty per cent or more of the summer precipitation in Kansas, Nebraska and Iowa occurs in the form of thundery downpours between 1800 and 0600 hours. It has been suggested that the nocturnal thunderstorms and rainfall are caused by a slow, large-scale circulation over the plains east of the Rocky Mountains, with a tendency for

low-level divergence and subsidence by day and for convergence and rising air by night. A related concept has been proposed following the discovery of nocturnal southerly 'jets' at only 500–1000 m along 100°W. These winds probably supply the necessary low-level moisture and convergence. Their occurrence is apparently related to a large-scale nocturnal inversion layer over the mountains.

- (iii) East of the upper Mississippi, in the Ohio valley and south of the lower Lakes, there is a transitional regime between that of the interior and the east coast type. Precipitation is reasonably abundant in all seasons but the summer maximum is still in evidence (e.g. Dayton).
- (iv) In eastern North America (New England, the Maritimes, Quebec and south-east Ontario) precipitation is fairly evenly distributed throughout the year (e.g. Blue Hill). In Nova Scotia and locally around Georgian Bay there is a winter maximum, due in the latter case to the influence of open water. In the Maritimes it is related to winter (and also autumn) storm tracks.

It is worth comparing the eastern regime with the summer maximum which is found over eastern Asia. There the Siberian anticyclone excludes cyclonic precipitation in winter and monsoonal influences are felt in the summer months.

The seasonal distribution of precipitation is of vital interest for agricultural purposes. Rain falling in summer, for instance, when evaporation losses are high is less effective than an equal amount in the cool season. Figure 5.17 illustrates the effect of different regimes in terms of the moisture balance, calculated according to Thornthwaite's method. At Halifax (Nova Scotia) there is sufficient moisture stored in the soil to maintain evaporation at its maximum rate (i.e. actual evaporation = potential evaporation), whereas at Berkeley (California) there is a computed moisture deficit of nearly 5 cm in August. This is a guide to the amount of irrigation water which may be required by crops, although in dry regimes the Thornthwaite method generally underestimates the real moisture deficit.

The mean monthly potential evaporation (PE) is calculated in the method developed by C. W. Thornthwaite from tables based on a complex equation relating PE to air temperature. This only gives a general guide to the true PE in view of the different factors which affect evaporation (see ch. 2, A), but the results are reasonably satisfactory in temperate latitudes. By determining the annual moisture surplus and the annual

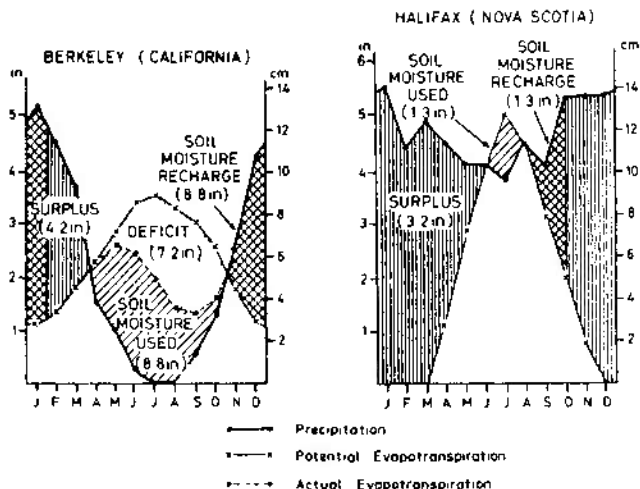


Fig. 5.17. The moisture balances at Berkeley, California and Halifax, Nova Scotia (after Thornthwaite and Mather 1955, and Putnam *et al* 1957).

moisture deficit from graphs such as those in fig. 5.17, or from a monthly 'balance sheet', Thornthwaite obtained an index of aridity and humidity. The humidity index is $100 \times \text{water surplus}/PE$ and the aridity index is $100 \times \text{water deficit}/PE$; there is generally a surplus in one season and a deficit in another. These may then be combined into a single moisture index (Im):

$$Im = \frac{100 \times \text{water surplus} - 60 \times \text{water deficit}}{PE}$$

Here the deficit is given less weight as the surplus is held in the soil, whereas any deficit means that the actual evaporation rate falls below the potential value. The moisture index is used to define the following climatic types (see also app. 1.B):

Im	Climate	Symbol
> 100	Perhumid	A
20 to 100	Humid	B (with 4 subdivisions)
0 to 20	Moist subhumid	C ₂
-20 to 0	Dry subhumid	C ₁
-40 to -20	Semi-arid	D
< -40	Arid	E

Figure 5.18 illustrates the distribution of these moisture regions over the United States. The zero line separating the moist climates of the east from the dry climates of the west (apart from the west coast) follows the 96th meridian almost exactly. The major humid areas are along the Appalachians, in the north-east and along the Pacific coast, while the most extensive arid area is the south-west. Some aspects of the precipitation climatology of this arid area are examined in ch. 5, D.2.

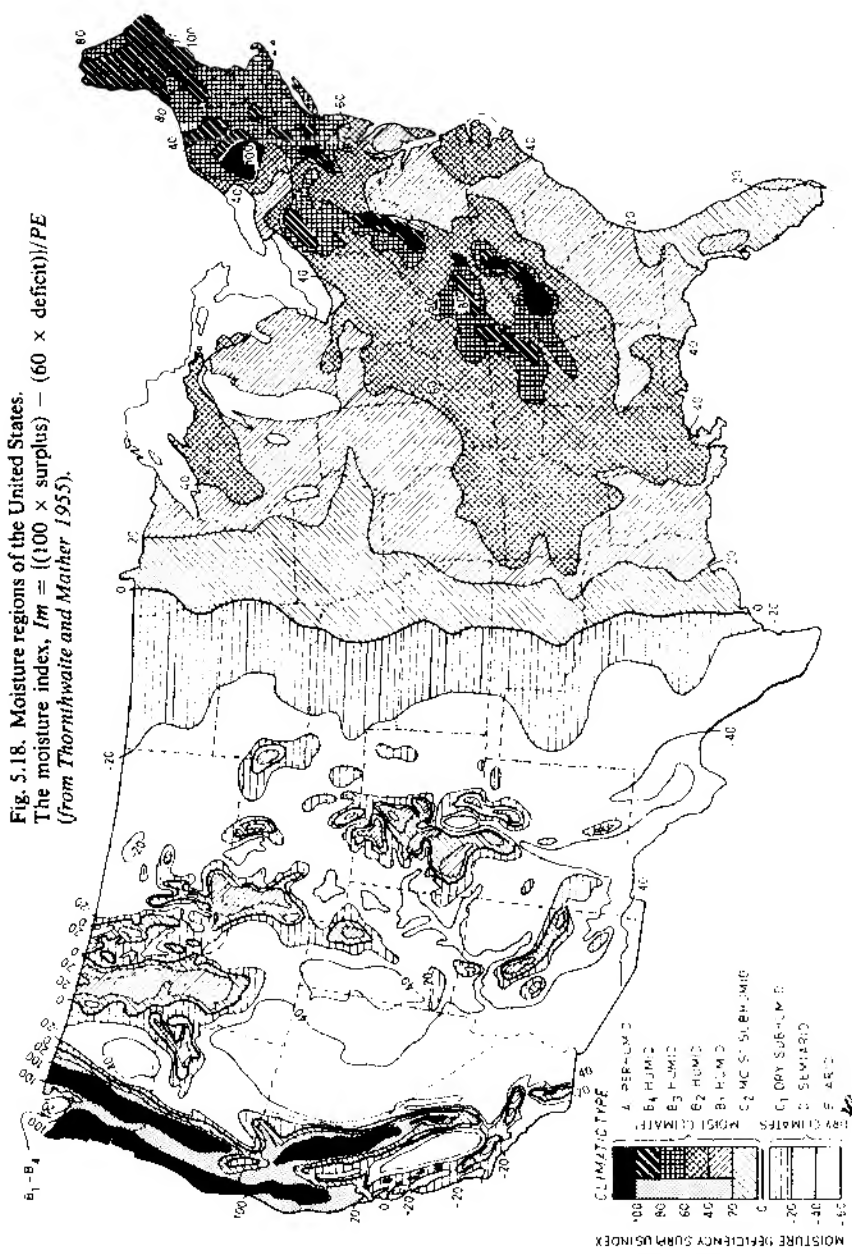
C The polar margins

The longitudinal differences in mid-latitude climates persist into the polar margins, giving rise to maritime and continental sub-types, modified by the extreme radiation conditions in winter and summer. For example, insolation receipts in summer along the arctic coast of Siberia compare favourably, by virtue of the long daylight, with those in lower middle latitudes. The maritime type is found in coastal Alaska, Iceland, northern Norway and adjoining parts of the USSR. Winters are cold and stormy, with very short days. Summers are cloudy but mild with mean temperatures about 10°C. For example, Vardø in north Norway (70°N, 31°E) has monthly mean temperatures of -6°C (21°F) in January and 9°C (48°F) in July, while Anchorage, Alaska (61°N, 150°W) records -11°C (12°F) and 14°C (57°F), respectively. Annual precipitation is generally between 60 and 125 cm (25 and 50 in), with a cool season maximum and about six months of snow cover.

The weather is mainly controlled by depressions which are weakly developed in summer. In winter the Alaskan area is north of the main depression tracks and occluded fronts and upper troughs (trowals) are prominent, whereas northern Norway is affected by frontal depressions moving in to the Barents Sea. Iceland is similar to Alaska, though depressions often move slowly over the area and occlude, whereas others moving north-eastwards along the Denmark Strait bring mild, rainy weather.

The interior, cold-continental climates have much more severe winters although precipitation amounts are less. At Yellowknife (62°N, 114°W), for instance, the mean January temperature is only -28°C (-18°F). In these regions *permafrost* (permanently frozen ground) is widespread and often of great depth. In summer only the top few feet of ground thaw and as the water cannot readily drain away this 'active layer' often remains waterlogged. Although frost may occur in any month, the long summer days usually give three months with mean temperatures above 10°C, and

Fig. 5.18. Moisture regions of the United States.
 The moisture index, $Im = [(100 \times \text{surplus}) - (60 \times \text{deficit})]/PE$
 (from Thornthwaite and Mather 1955).



at many stations extreme maxima are 32°C (90°F) or more (fig. 5.12D). The Barren Grounds of Keewatin, however, are much cooler in summer due to the extensive areas of lake and muskeg, and only July has a mean daily temperature of 10°C. Labrador-Ungava to the east is rather similar, with very high cloud amounts and maximum precipitation in June-September (fig. 5.19). In winter conditions fluctuate between periods of very cold, dry, high-pressure weather and spells of dull, bleak, snowy weather as depressions move eastwards or occasionally northwards over the area. In spite of the very low mean temperatures in winter, there have been occasions when maxima have exceeded 4°C (40°F) during incursions of maritime Atlantic air. Such variability is not found in eastern Siberia which is intensely continental, apart from the

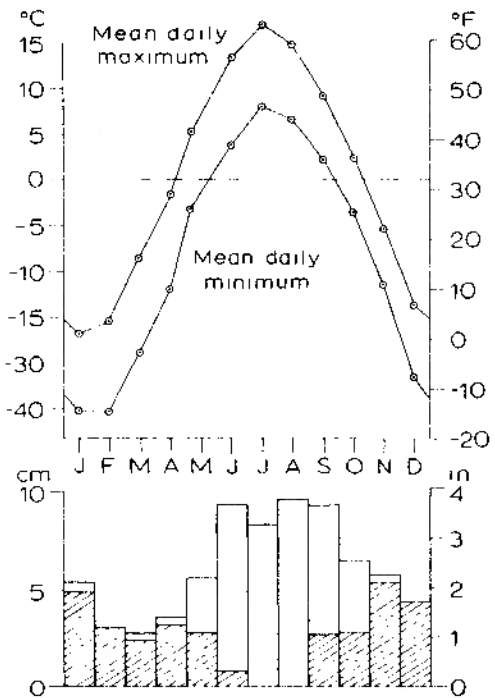


Fig. 5.19. Selected climatological data for McGill Sub-Arctic Research Laboratory, Knob Lake, 1955-62 (data from J. B. Shaw and D. G. Tout). The shaded portions of the precipitation represent snowfall, expressed as water equivalent.

Kamchatka peninsula, with the northern hemisphere's *cold pole* located in the remote north-east (see fig. 1.13). Verkhoyansk and Oimyakon have a January mean of -50°C and both have recorded an absolute minimum of -67.7°C .

D The subtropical margins

1 The Mediterranean

The characteristic west coast climate of the subtropics is the Mediterranean type with hot, dry summers and mild, relatively wet winters. It is interposed between the temperate maritime type and the arid subtropical desert climate, but the Mediterranean regime is transitional in a special way for it is controlled by the westerlies in winter and by the subtropical anticyclone in summer. The seasonal change in position of the subtropical high and the associated subtropical westerly jet stream in the upper troposphere is evident in fig. 5.20. The type region is peculiarly distinctive, extending more than 3000 km into the Eurasian continent. Additionally, the configuration of seas and peninsulas produces great regional variety of weather and climate. The Californian region with similar conditions (fig. 5.16) is of very limited extent, and attention is therefore concentrated on the Mediterranean basin itself.

The winter season sets in quite suddenly in the Mediterranean as the summer eastward extension of the Azores high-pressure cell collapses. This phenomenon can be observed on barographs throughout the region, but particularly in the western Mediterranean where a sudden drop in pressure occurs about 20 October and is accompanied by a marked increase in the probability of precipitation. The probability of receiving rain in any 5-day period increases dramatically from 50–70% in early October to 90% in late October. This change is associated with the first invasions by cold fronts, although thunder-shower rain has been common since August. The pronounced winter precipitation over the Mediterranean largely results from the relatively high sea-surface temperatures at that season; in January the sea temperature being about 2°C higher than the mean air temperature. Incursions of colder air into the region lead to convective instability along the cold front producing frontal and orographic rain. Incursions of arctic air are relatively infrequent (there being, on average 6–9 invasions by cA and mA air each year), but the penetration by unstable mP air is much more common. It typically gives rise to cumulus development to well over 6000 m (20,000 ft) and is critical in the formation of Mediterranean depressions. The initiation and movement of these depressions (see fig. 5.21) is associated with a branch of the Polar Front Jet Stream located about 35°N . This jet develops during low index

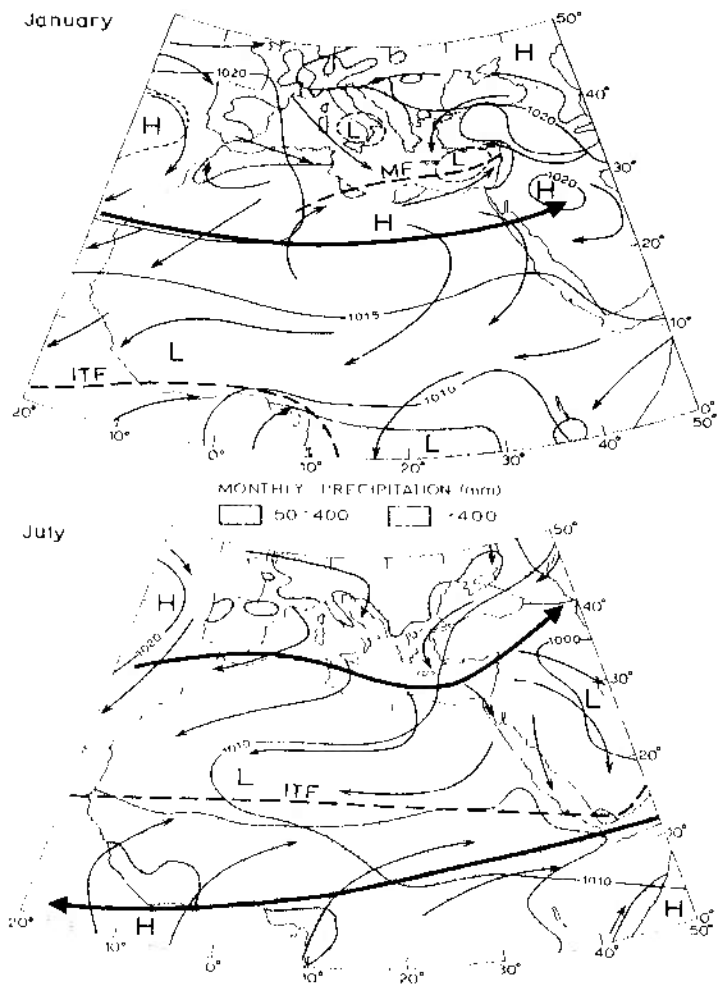


Fig. 5.20. The distribution of surface pressure, winds and precipitation for the Mediterranean and Northern Africa during January and July. The average positions of the Subtropical and Easterly Jet Streams, together with the Inter-tropical (ITF) and Mediterranean (MF) Fronts, are also shown (*partly after 'Weather in the Mediterranean' H.M.S.O. 1962*) (Crown Copyright Reserved).

phases when the westerlies over the eastern Atlantic are distorted by a blocking anticyclone at about 20°W, leading to a deep stream of arctic air flowing southward over the British Isles and France. Although some Atlantic depressions enter the western Mediterranean as surface lows, they make up only 9% of those affecting the region (fig. 5.21), whereas 17% form in the lee of the Atlas Mountains (the so-called *Saharan depressions*, which are most important sources of rainfall in late winter and spring) and fully 74% develop in the western Mediterranean to the lee of the Alps and Pyrenees (see ch. 4, G.1). The combination of the lee effect and that of unstable surface air over the western Mediterranean explains the frequent formation of these *Genoa type depressions* when conditionally unstable mP air invades the region. These depressions are exceptional in that the instability of the local air in the warm sector gives unusually intense precipitation along the warm front, and the unstable mP air produces heavy showers and thunderstorm rainfall to the rear of the cold front, especially between 5° and 25°E. This warming of mP (or mA) air is so characteristic as to produce air designated as *Mediterranean* (see table 4.1). The mean boundary between this Mediterranean air mass and cT air flowing north-eastward from the Sahara is referred to as the Mediterranean front (fig. 5.20). There may be a temperature discontinuity as great as 12–16°C (30–40°F) across it in late winter. Sahara depressions and those from the western Mediterranean move eastward forming a belt of low pressure associated with this frontal zone and frequently draw cT northward ahead of the cold front as the warm, dust-laden *scirocco* (especially in spring and autumn when Saharan air may spread into Europe). The movement of Mediterranean depressions is greatly complicated both by relief effects and by their regeneration in the eastern Mediterranean by fresh cP air from Russia or south-east Europe. Although many depressions travel eastward over Asia, there is a strong tendency for low-pressure centres to move north-eastward over the Black Sea and Balkans, especially as spring advances. Winter weather in the Mediterranean presents considerable variation, however, particularly as the Subtropical Westerly Jet Stream is highly mobile and may occasionally even coalesce with the southerly-displaced Polar Front Jet Stream.

With high index zonal circulation over the Atlantic and Europe, depressions may pass far enough to the north so that their cold-sector air does not reach the Mediterranean, and then the weather there is generally settled and fine. Between October and April, anticyclones are the dominant circulation type for at least 25% of the time over the whole Mediterranean area and in the western basin for 48% of the time. This is

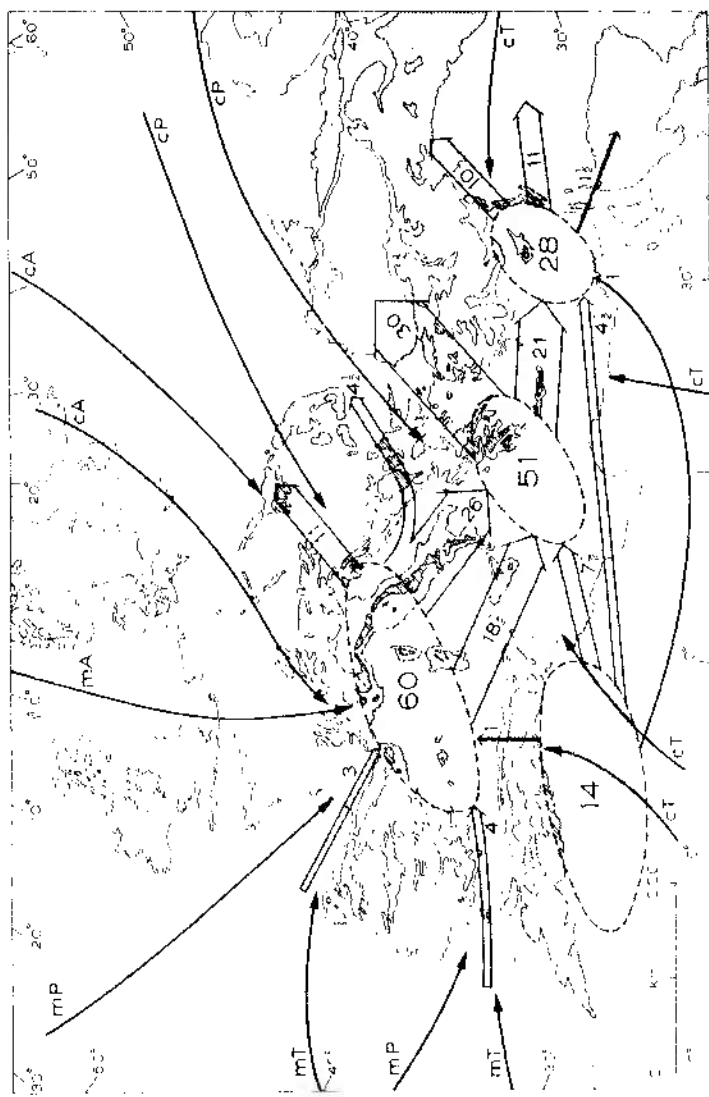


Fig. 5.21. Tracks of Mediterranean depressions, showing average annual frequencies, together with air-mass sources (after 'Weather in the Mediterranean' H.M.S.O. 1962) (Crown Copyright Reserved).

reflected in the high mean pressure over the latter area in January (see fig. 5.20). Consequently, although the winter half-year is the rainy period, there are rather few rain-days. On average, rain falls on only 6 days per month during winter in northern Libya and south-east Spain, yet there are 12 rain-days per month in western Italy, the western Balkan peninsula and the Cyprus area. The higher frequencies (and totals) are related to the areas of cyclogenesis and to the windward side of peninsulas.

Regional winds are also related to the meteorological and topographic factors. The familiar cold, northerly winds of the Gulf of Lions (the *mistral*), which are associated with northerly mP airflows, are best developed when a depression is forming in the Gulf of Genoa east of a high-pressure ridge from the Azores anticyclone. Katabatic and funnelling effects strengthen the flow in the Rhone valley and similar localities so that violent winds are sometimes recorded. The mistral may last for several days until the outbreak of polar or continental air ceases. The frequency of these winds depends on their definition. The average frequency of strong mistral in the south of France is shown in table 5.5 (based on occurrence at one or more stations from Perpignan to the Rhone in 1924-7). Similar winds may occur in the northern Adriatic (the *bora*) and the northern Aegean Seas when polar air flows southward in the rear of an eastward-moving depression and is forced over the mountains (cf. ch. 3, C.2).

**Table 5.5 Number of days with strong mistral in the south of France
(After 'Weather in the Mediterranean', H.M.S.O. 1962)**

Speed	J	F	M	A	M	J	J	A	S	O	N	D	Year
≥11 m/sec (21 kt)	10	9	13	11	8	9	9	7	5	5	7	10	103
≥17 m/sec (33 kt)	4	4	6	5	3	2	0	6	1	0	6	0	30

The generally wet, windy and mild winter season in the Mediterranean is succeeded by a long indecisive spring lasting from March to May, with many false starts of summer weather.

The spring period, like that of early autumn, is especially unpredictable. In March 1966 a trough moving across the eastern Mediterranean, preceded by a warm southerly *khamsin* and followed by a northerly air-stream, brought up to 70 mm (2.8 in) of rain in only 4 hours to a 60 × 120 km (35 × 70 miles) area of the southern Negev desert. Although

April is normally a dry month in the eastern Mediterranean, Cyprus having an average of only 3 days with 1 mm of rainfall or more, high rainfalls can occur as in April 1971 when four depressions affected the region. Two of these were Saharan depressions moving eastward beneath the zone of diffusione on the cold side of a westerly jet and the other two were intensified in the lee of Cyprus. However, the rather rapid collapse of the Eurasian high-pressure cell in April, together with the discontinuous northward and eastward extension of the Azores anticyclone, encourages the northward displacement of depressions, and, even if higher latitude air does penetrate south to the Mediterranean, the sea surface temperature there is relatively cooler and more stable than during the winter. By mid-June the Mediterranean basin is dominated by the expanded Azores anticyclone to the west, while to the south the mean pressure field shows a low-pressure trough extending across the Sahara from southern Asia (fig. 5.20). The winds are predominantly from a northerly direction (e.g. the *etesians* of the Aegean) and represent an eastward continuation of the north-easterly trades. Locally, sea breezes reinforce these winds, but on the Levant coast they cause surface south westerlies. Depressions are by no means absent in the summer months, but they are usually weak since the anticyclonic character of the large-scale circulation encourages subsidence, and air-mass contrasts are much reduced compared with winter (see table 4.2). Thermal lows form from time to time over Iberia and Anatolia, though thundery outbreaks are infrequent due to the low relative humidity.

The most important regional winds in summer are of continental tropical origin. There is a variety of local names for these hot, dry and dusty airstreams — *scirocco* (Algeria and the Levant), *leveche* (south-east Spain) and *khamsin* (Egypt) — which move northwards ahead of eastward-moving depressions. Local winds are often dominant in summer and, for example, the day-to-day weather of many parts of the North African coast is largely conditioned by land and sea breezes, involving air up to 1500 m (5000 ft) deep.

Many stations in the Mediterranean receive only a few mm of rainfall in at least one summer month, yet it is important to realize that the seasonal distribution does not conform to the pattern of simple winter maximum over the whole of the Mediterranean basin. Figure 5.22 shows that this is found in the eastern and central Mediterranean, whereas Spain, southern France, northern Italy and the northern Balkans have more complicated profiles with a maximum in autumn or peaks in both spring and autumn. This double maximum can be interpreted generally as a tran-

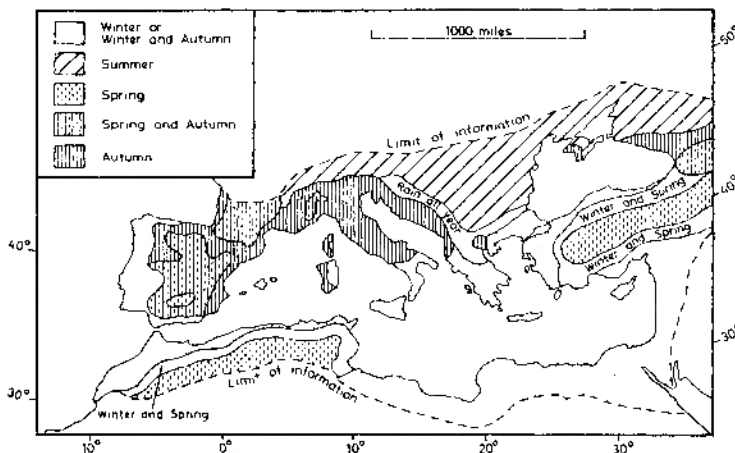


Fig. 5.22. Rainfall regimes in the Mediterranean area (after Huttary 1950).

sition between the continental interior type with summer maximum and the Mediterranean type with winter maximum. A similar transition region occurs in the south-western United States (see fig. 5.16), but local topography in this intermontane zone introduces further irregularities into the regimes.

2 The semi-arid south-western United States

Both the mechanisms and patterns of the climates of areas dominated by the subtropical high-pressure cells are rather obscure at present. On the one hand the inhospitable nature of these arid regions inhibits data collection, and on the other the proper interpretation of the irregular meteorological events requires a close network of stations maintaining continuous records over long periods. This difficulty is especially apparent in the interpretation of desert precipitation data, in that much of the rain falls in very local storms irregularly scattered both in space and time. It is convenient to treat aspects of this climatic type here, in that most of the reliable data relate to the less arid regions marginal to the subtropical cell centres, and in particular to the south-western United States.

A series of observations at Tucson, Arizona, 730 m (2400 ft) between 1895 and 1957 showed a mean annual precipitation of 27.7 cm (10.91 in) falling on an average of about 45 days per year, with extreme mean annual figures of 61.4 cm (24.17 in) and 14.5 cm (5.72 in). Two moister

periods of late November to March (receiving 30% of the mean annual precipitation) and late June to September (50%) are separated by more arid seasons from April to June (8%) and October to November (12%). The winter rains are generally prolonged and of low intensity (more than half the falls have an intensity of less than 0.5 cm (0.2 in) per hour, falling from altostratus clouds at about 2500 m (8000 ft) associated with the cold fronts of depressions which are forced to take southerly routes by strong blocking to the north. These southerly tracks occur during phases of equatorial displacement of the Pacific subtropical high-pressure cell. The re-establishment of the cell in spring before the main period of intense surface heating and convectional showers is associated with the most persistent drought periods, particularly during April to June. Dry westerly to south-westerly flow from the eastern edge of the Pacific subtropical anticyclone is responsible for the low rainfall at this season. During one 29-year period in Tucson there were 8 spells of more than 100 consecutive days of complete drought and 24 periods of more than 70 days.

The period of summer precipitation is quite sharply defined, beginning in the last week in June and lasting until the middle of September. At this time precipitation mainly occurs from convective cells initiated by surface heating, convergence, or, less commonly, orographic lifting. These summer convective storms form in clusters many tens of miles across, the individual storm cells covering together less than 3% of the surface area at any one time, and persisting for less than an hour on average. The storm clusters move across the country in the direction of the upper-air motion, and often seem to be controlled in movement by the existence of low-level jet streams at elevations of about 2500 m. The airflow associated with these storms is generally southerly along the southern and western margins of the Atlantic (or Bermudan) subtropical high, so that in contrast to the winter months the moisture is derived mainly from the Gulf of California. This circulation often sets in abruptly around 1 July and it is therefore recognized as a singularity (see ch. 5, A.4, and fig. 5.10B).

Precipitation from these cells is extremely local, and commonly concentrated in the mid-afternoon and evening. Intensities are much higher than in winter, half the summer rain falling at more than 0.4 in per hour. During the 29-year period about one quarter of the mean annual precipitation fell in storms giving 2.5 cm (1 in) or more per day, and 1.9 cm (0.75 in) in 15 min were recorded. These intensities are much less than those associated with rainstorms in the humid tropics, but the sparsity of vegetation in the drier regions allows the rain to produce considerable sur-

276 Atmosphere, weather and climate

face erosion. Thus the highest measurements of surface erosion in the United States are from areas having 30–40 cm (12–15 in) of rain per year.

3 The interior and east coast of the United States

The climate of the subtropical south-eastern part of the United States has no exact counterpart in Asia, which is affected by the summer and winter monsoon systems. These are discussed in the next chapter and only the distinctive features of the North American subtropics are examined here. Seasonal wind changes are experienced in Florida, which is within the westerlies in winter and lies on the northern margin of the tropical easterlies in summer, but this is not comparable with the regime in southern and south-eastern Asia. Nevertheless, the summer season rainfall maximum (fig. 5.16 for Jacksonville) is a result of this change-over. In June the upper flow over the Florida peninsula changes from north-westerly to southerly as a trough moves westward and becomes established in the Gulf of Mexico. This deep, moist southerly airflow provides appropriate conditions for convection, and indeed Florida probably ranks as the area with the highest annual number of days with thunderstorms – 90 or more, on average, in the vicinity of Tampa. These often occur in late afternoon although two factors apart from diurnal heating are thought to be important. One is the effect of sea-breezes converging from both sides of the peninsula, and the other is the northward penetration of disturbances in the easterlies (see ch. 6). The latter may of course affect the area at any time of day. The westerlies resume control in September–October, although Florida remains under the easterlies during September when Caribbean hurricanes are most frequent and consequently the rainy season is prolonged.

The region of the Mississippi lowlands and the southern Appalachians to the west and north is not simply transitional to the 'Interior type' in terms at least of rainfall regime (fig. 5.16). The profile shows a winter–spring maximum and a secondary summer maximum. The cool season peak is related to westerly depressions moving north-eastward from the Gulf coast area, and it is significant that the wettest month is commonly March when the mean jet stream is farthest south. The summer rains are associated with convection in humid air from the Gulf, though this convection becomes less effective inland as a result of the subsidence created by the anticyclonic circulation in the middle troposphere referred to previously (see ch. 5, B.3.c).

6 Tropical weather and climate

Fifty per cent of the surface of the globe lies between latitudes 30°N and 30°S and over a third of the world's population inhabits tropical lands. Tropical climates are, therefore, of especial geographical interest.

The latitudinal limits of tropical climates vary greatly with longitude and season, and tropical weather conditions may reach well beyond the Tropics of Cancer and Capricorn. For example, the summer monsoon extends to 30°N in southern Asia, but only 20°N in West Africa, while in late summer and autumn tropical hurricanes may affect 'extra-tropical' areas of eastern Asia and eastern North America. Not only do the tropical margins extend seasonally polewards, but in the zone between the major subtropical high-pressure cells there is frequent interaction between temperature and tropical disturbances. Hence the tropical atmosphere is far from being a discrete entity and any meteorological or climatological boundaries must be arbitrary. There are, nevertheless, a number of distinctive features of tropical weather and these are discussed below.

A The assumed simplicity of tropical weather

The study of tropical weather has passed broadly through three stages. Firstly, for a long period which only ended some years before the Second World War, tropical weather conditions, patterns and mechanisms were assumed to be much more simple and obvious than those in higher latitudes. This belief was partly due to the paucity of pre-war meteorological records, particularly over the vast tropical oceans, and

278 Atmosphere, weather and climate

partly due to certain theoretical and practical considerations. One reason was that temperature and hence air-mass contrasts seemed small compared with middle latitudes. Air masses were nevertheless identified on the basis of their moisture content, temperature and stability, although frontal activity was believed to be weak and weather systems correspondingly less evident. Obvious exceptions were tropical cyclones which were thought to result from special conditions of thermal convection. Another reason was the large extent of ocean surface which, it was assumed, would simplify the patterns of weather and climate.

Thus the following simple picture of *trade wind weather* evolved. Maritime tropical air masses, originating by subsidence in the sub-tropical high-pressure cells over the eastern halves of the oceans (see fig. 3.15), move steadily westwards and equatorwards with quite constant speed and direction. Beneath the temperature inversion, formed between about 600 and 800 m by subsidence, the air is moist with a layer of broken cumulus cloud. Conditions are invariably warm and dry, although in certain coastal regions (e.g. south-east Madagascar) the onshore winds can produce periods of thick drizzle. Over the equatorial oceans the surface wind is light and variable (the doldrums) and the air is universally hot, humid and sultry (see ch. 3, E.1).

A further element of simplicity was thought to be provided by the insolation regime. The persistently high altitude of the sun in low latitudes and the equality of length between the days and nights means that seasonal variations of insolation are minimized. Hence the annual rhythm was thought to produce simple rainfall regimes with a single maximum following the summer solstice at the tropics, and a double peak at the equator in response to the passage of the overhead sun at the equinoxes. Diurnal patterns of land and sea breezes giving an afternoon build-up of convective activity and thundery showers were regarded as characteristic features of nearly all tropical climates (see pls 26 and 27).

Following the evolution of this simple picture of tropical weather processes, attempts were made between 1920 and 1940 to introduce mid-latitude frontal concepts. Little real progress was made, however, as a result of the apparent general absence of significant air-mass contrasts. Furthermore, the small surface pressure gradients of most tropical disturbances (other than the hurricane variety) tend to go unnoticed due to the large semi-diurnal pressure oscillation in the tropics. Pressure varies by about 2–3 mb with maxima around 1000 and 2200 hours and minima at 0400 and 1600 hours. It must also be recalled that the wind direction provides no guide to the pressure pattern in low latitudes. The small

Coriolis force prevents the wind from attaining geostrophic balance and consequently the techniques used for analysing mid-latitude weather maps have to be abandoned.

During and after the Second World War more numerous weather observations revealed the inadequacy of the earlier views. It became evident that weather changes are frequent and complex with quite distinct types of weather systems in different tropical lands and with considerable climatic differences even over the ocean areas. It also became apparent that much smaller trigger mechanisms were necessary to produce disturbances in the flow of high-energy, tropical air masses than those associated with mid-latitude depressions, and yet, paradoxically, tropical cyclones are infrequent. The systems responsible for these contrasts are examined in the following sections.

B The intertropical confluence

The tendency for the trade wind systems of the two hemispheres to converge in the Equatorial (low pressure) Trough has already been noted (see ch. 3, E.1, p. 162). Views on the exact nature of this feature have been subject to continual revision. During the 1920s–1940s the frontal concepts developed in mid-latitudes were applied in the tropics and the trade wind confluence was identified as the Intertropical Front (ITF). Over continental areas such as West Africa and southern Asia, where in summer hot, dry continental tropical air meets cooler, humid equatorial air, this term has some limited applicability (fig. 6.1). Sharp temperature and moisture gradients can occur, but the front is seldom a weather-producing mechanism of the mid-latitude type (see fig. 6.21). Elsewhere in low latitudes true fronts (with a marked density contrast) are rare.

Recognition in the 1940s–1950s of the significance of wind field convergence in tropical weather-production led to the designation of the trade wind confluence as the Intertropical Convergence Zone (ITCZ). This confluence is apparent on a *mean* streamline map, but areas of convergence grow and decay, either *in situ* or within disturbances moving westward (pls. 12 and 31), over periods of a few days. Moreover, convergence is infrequent even as a climatic feature in the doldrum zones (see fig. 3.23). Satellite photography has shown that over the oceans the position and intensity of the ITCZ varies greatly, even from day to day. It is possible, however, to show that the convection generated by frictionally-induced convergence in the Trade Wind boundary layer produces individual cumulus clouds 1–10 km in diameter, which group into mesoscale convective

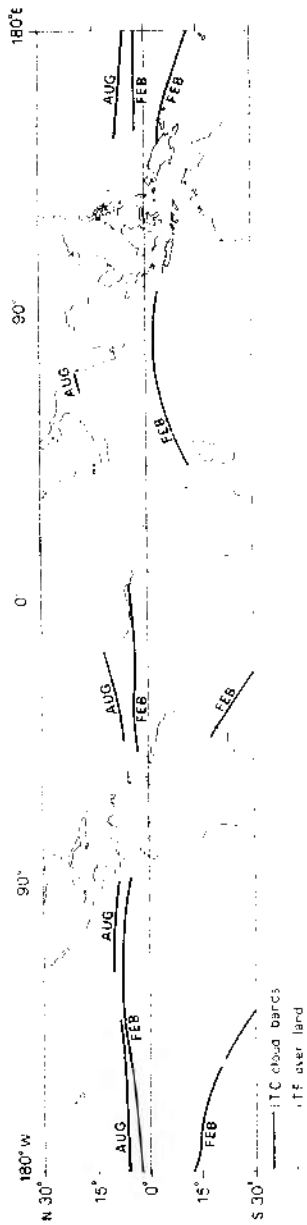


Fig. 6.1. The position of the Equatorial Trough (Inter-tropical Convergence Zone or Inter-tropical Front in some sectors) in February and August (after Saita 1973; Riehl 1954 and Yoshino 1969).

tive units of some 100 km across, and that these, in turn, form cloud clusters 100–1000 km in diameter (fig. 6.2; see also pl. 31) either along the ITCZ or in the troughs of lower tropospheric wave disturbances which have wavelengths of 2000–3000 km. In view of the discontinuity of convergence in time and space, the term *Intertropical Confluence* (ITC) is now preferred.

As climatic features the Equatorial Trough and ITC appear to move seasonally away from the equator (fig. 6.1) in association with the *Thermal Equator* (zone of seasonal maximum temperature), although detailed studies seem to contradict this connection. The location of the Thermal Equator is directly related to solar heating (figs. 1.11 and 1.13) and there is an obvious link between this and the Equatorial Trough in terms of thermal lows. However, this is oversimplified since the Equatorial Trough is also connected with the largely independent dynamics of air circulation in low latitudes. Observations (see fig. 6.22, for example) show that maximum convergence and uplift is frequently located several degrees equatorward of the Equatorial Trough. Seasonal shifts of the wind field convergence are partly a response to alternating activity in the subtropical high-pressure cells of the two hemispheres but, on a shorter time scale, the synoptic activity along the ITC obscures any simple relationships. Several satellite studies of cloudiness indicate that in the western Pacific Ocean and in the western Atlantic Ocean there may be two semi-permanent confluence zones (fig. 6.1). These do not occur, however, where there are cold ocean currents as in the eastern South Atlantic and South Pacific.

C Tropical disturbances

It was not until the 1940s that detailed accounts were given of types of tropical disturbance other than the long-recognized tropical cyclone. However, our view of tropical weather systems has been radically revised following the advent of operational meteorological satellites in the 1960s. Special programs of meteorological measurements at the surface and in the upper air together with aircraft and ship observations have been carried out in the Pacific and Indian Oceans and the Caribbean, and in the tropical Atlantic in 1974.

Although the picture is still incomplete it appears that five categories of weather system can be distinguished according to their space and time scales. The smallest, with a life span of a few hours, is the *individual cumulus*. In fair weather, cumulus clouds are generally aligned in 'cloud

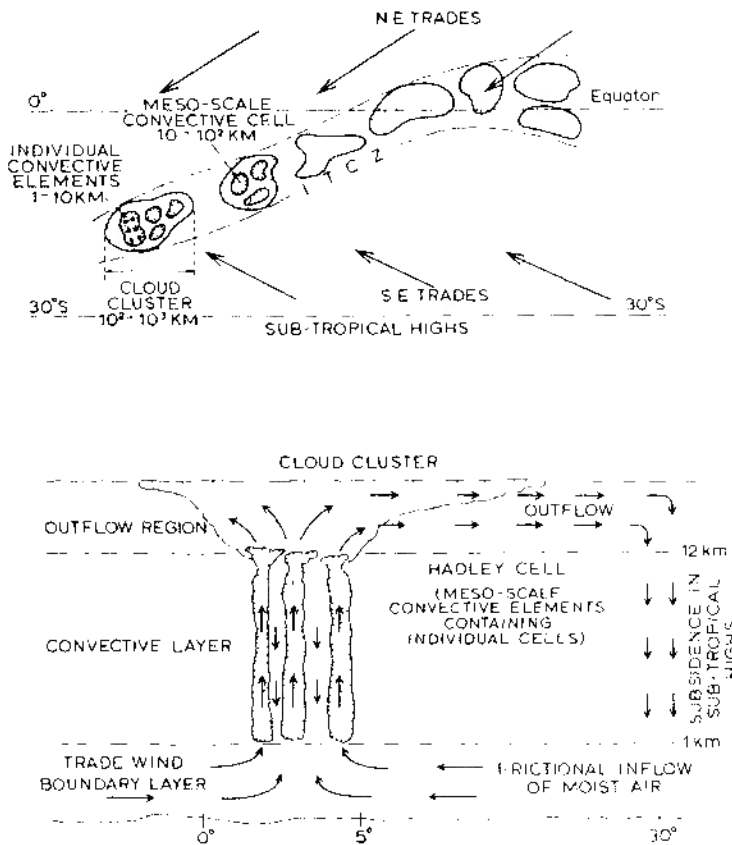


Fig. 6.2. The mesoscale and synoptic structure of the inter-tropical convergence zone (ITCZ), showing a model of the spatial distribution (above) and of the vertical structure (below) of convective elements which form the cloud clusters (from Mason 1970).

'streets', more or less parallel to the wind direction (pl. 26), rather than scattered at random. This seems to be related to the boundary layer structure and wind speed. There is little interaction between the air layers above and below the cloud base under these conditions, but in disturbed weather conditions up and downdraughts cause interaction between the two layers which intensifies the convection. In this way the smallest scale of system can aid the development of larger disturbances.

The second category is the mesoscale system (cf. pp. 216–20); such systems are particularly associated with land/sea boundaries, heated oceanic islands, and topography. A distinctive feature of the tropics, identified from satellite imagery, is the *cloud cluster* which is of subsynoptic scale and may persist for 1–3 days (see fig. 6.2). The fourth category includes the synoptic scale wave disturbances and cyclonic vortices and the final group is the planetary waves.

The planetary waves (with a wavelength from 10,000 to 40,000 km) need not concern us in detail. Two types occur in the equatorial stratosphere and another in the equatorial upper troposphere. While they may interact with lower tropospheric systems, they do not appear to be direct weather mechanisms. The synoptic scale systems which determine much of the 'disturbed weather' of the tropics are sufficiently important and varied as to be discussed under the headings of wave disturbances and cyclonic storms.

1 Wave disturbances

There are several types of wave travelling westward in the equatorial and tropical tropospheric easterlies; the differences between them probably result from regional and seasonal variations in the structure of the tropical atmosphere. Their wavelength is between about 2000–4000 km and they have a life span of 1–2 weeks, travelling some 6–7° longitude per day.

The first wave type to be described in the Tropics was the *Easterly Wave* of the Caribbean area. This system is quite unlike a mid-latitude depression. There is a weak pressure trough which usually slopes eastward with height (fig. 6.3) and typically the main development of cumulonimbus cloud and thundery showers *behind* the trough line. This pattern is associated with horizontal and vertical motion in the easterlies. Behind the trough low-level air undergoes convergence, while ahead of it there is divergence (ch. 3, B.1). This follows from the equation for the conservation of potential vorticity (compare ch. 4, F), which assumes that the air travelling at a given level does not change its potential temperature (i.e. dry-adiabatic motion; see ch. 2, D):

$$\frac{f + \zeta}{\Delta p} = k$$

f = the Coriolis parameter, ζ = relative vorticity (cyclonic positive) and Δp = the depth of the tropospheric air column. Air overtaking the trough line is moving both polewards (f increasing) and towards a zone of cyclonic curvature (ζ increasing), so that if the left-hand side of the equa-

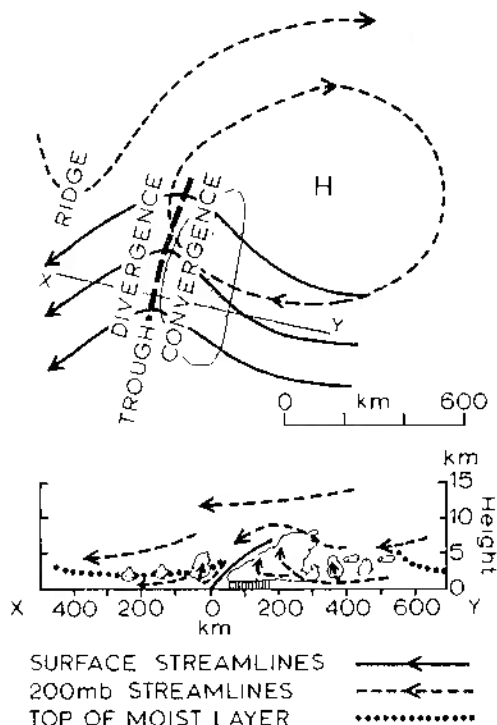


Fig. 6.3. A model of the areal (above) and vertical (below) structure of an easterly wave. Cloud is stippled and the precipitation area is shown in the vertical section. The streamline symbols refer to the areal structure, and the arrows on the vertical section indicate the horizontal and vertical motions (partly after Riehl and Malkus).

tion is to remain constant Δp must increase. This vertical expansion of the air column necessitates horizontal contraction (convergence). Conversely there is divergence in the air moving southward ahead of the trough and curving anticyclonically. The divergent zone is characterized by descending, drying air with only a shallow moist layer near the surface, while in the vicinity of the trough and behind it the moist layer may be 4500 m (15,000 ft) or more deep. When the easterly air flow is slower than the

speed of the wave, the reverse pattern of low-level convergence ahead of the trough and divergence behind it is observed as a consequence of the potential vorticity equation. Often this is the case in the middle troposphere so that the pattern of vertical motion shown in fig. 6.3 is augmented.

The passage of such a transverse wave in the trades commonly produces the following weather sequence:

In the ridge ahead of the trough	fine weather, scattered cumulus cloud, some haze.
Close to the trough line	well-developed cumulus, occasional showers, improving visibility.
Behind the trough	veer of wind direction, heavy cumulus and cumulonimbus, moderate or heavy thundery showers and a decrease of temperature.

Satellite photography indicates that the simple easterly wave is rather less common than has been supposed. Many Atlantic disturbances show an 'inverted V' wave-form in the low level wind-field and associated cloud, or a 'comma' related to cloud in a vortex. They are often apparently linked with a wave pattern on the ITC further south. Many disturbances in the easterlies have a closed cyclonic wind circulation at about the 600 mb level.

It is obviously difficult to trace the growth of wave disturbances over the oceans and in continental areas with sparse data coverage. However, some generalizations can be made. At least 8 out of 10 disturbances develop some 2–4° latitude poleward of the equatorial trough. Convection is probably set off by convergence of moisture in the airflow, accentuated by friction, and then maintained by entrainment into the thermal convective plumes (fig. 6.2). About 100 tropical disturbances develop during the June–November hurricane season in the tropical Atlantic. More than half of those disturbances originate over Africa in association with the baroclinic zone between Saharan air and cooler, moist monsoon air. Many of them can be tracked westward into the eastern North Pacific. A quarter of the disturbances intensify into tropical depressions and 10% become 'named' storms.

Developments in the Atlantic are closely related to the structure of the

trades. In the southeastern sectors of the subtropical anticyclones active subsidence maintains a pronounced inversion at 450 to 600 m (1500 to 2000 ft) (fig. 6.4). Downstream the height of the inversion base rises (fig. 6.5) because the subsidence decreases away from the eastern part of the anticyclone and cumulus towers penetrate through the inversion from

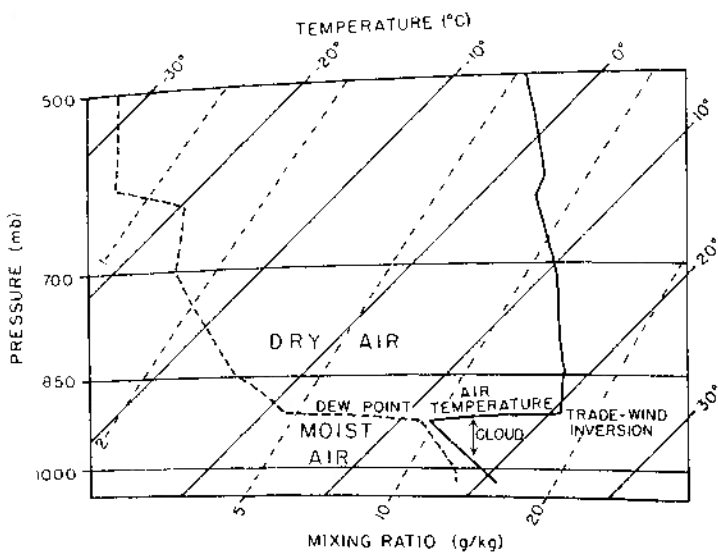


Fig. 6.4. The vertical structure of trade wind air at 30°N, 140°W at 0300 G M T on 10 July 1949. The mixing ratio is the saturation value (*based on Riehl 1954*).

time to time, spreading moisture into the dry air above. Easterly waves tend to develop in the Caribbean when the trade-wind inversion is weak or even absent during summer and autumn, whereas in winter and spring accentuated subsidence aloft inhibits their growth although disturbances may move westward above the inversion. Another factor which may initiate waves in the easterlies is the penetration of cold fronts into low latitudes. This is common in the sector between two subtropical high-pressure cells where the equatorward portion of the front tends to fracture, generating a westward-moving wave.

The influence of these features on regional climate is illustrated by the

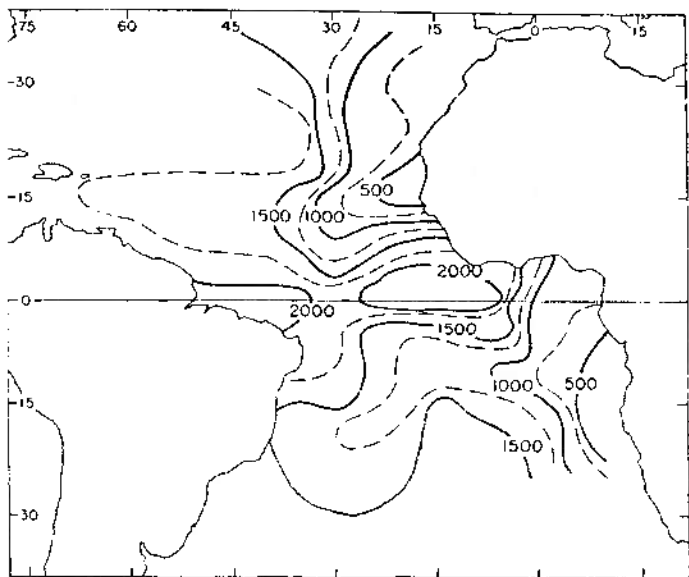


Fig. 6.5. The height (in metres) of the base of the trade-wind inversion over the tropical Atlantic (*from Riehl 1954*).

rainfall regime. For example, there is a late summer maximum at Martinique (fig. 6.6) in the Windward Islands (15°N) when subsidence is weak, although some of the autumn rainfall is associated with tropical storms. In many trade-wind areas the rainfall occurs in a few rainstorms associated with some form of disturbance. Over a ten-year period Oahu (Hawaii) had an average of 24 rainstorms per year of which 10 accounted for more than two-thirds of the annual precipitation. There is quite high variability of rainfall from year to year in such areas, since a small reduction in the frequency of disturbances can have a large effect on rainfall totals.

In the central equatorial Pacific the trade-wind systems of the two hemispheres converge in the Equatorial Trough and wave disturbances may be generated if the trough is sufficiently removed from the equator (usually to the north) to provide a small Coriolis force to begin cyclone motion. These disturbances quite often become unstable forming a cyclonic vortex as they travel westwards towards the Philippines, but the winds do not necessarily attain hurricane strength. The synoptic chart for

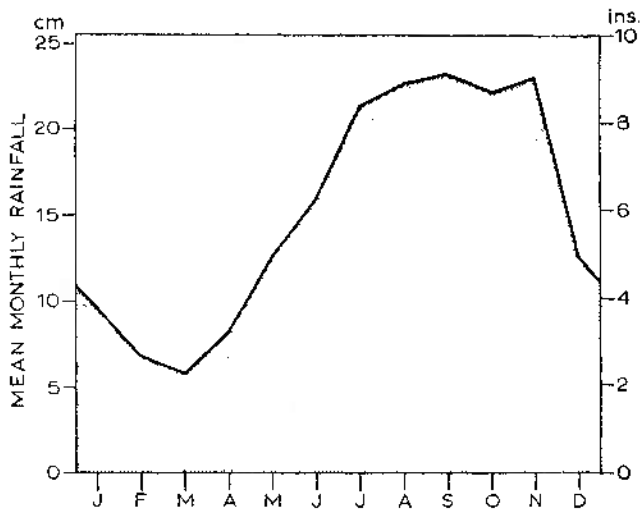


Fig. 6.6. Average monthly rainfall at Fort de France, Martinique (based on 'CLIMAT', normals of the World Meteorological Organization for 1931–60). The mean annual rainfall is 72.45 in (184 cm).

part of the north-west Pacific on 17 August 1957 (fig. 6.7), shows three developmental stages of tropical low-pressure systems. An incipient easterly wave has formed west of Hawaii which, however, filled and dissipated during the next 24 hours. A well-developed wave is evident near Wake Island, having spectacular cumulus towers extending up to over 9100 m (30,000 ft) along the convergence zone some 480 km (300 miles) east of it (pl. 28). This wave developed within 48 hours into a circular tropical storm with winds up to 20 m sec^{-1} (46 mph), but not into a full hurricane. A strong, closed, north-west moving circulation is situated east of the Philippines. Equatorial waves may form on both sides of the equator in an easterly current located between about 5°N and S. In such cases divergence ahead of a trough in the northern hemisphere is paired with convergence behind a trough line located further to the west in the southern hemisphere. The reader may confirm that this should be so by applying the equation for the conservation of potential vorticity, remembering that both f and ζ operate in the reverse sense in the southern hemisphere.

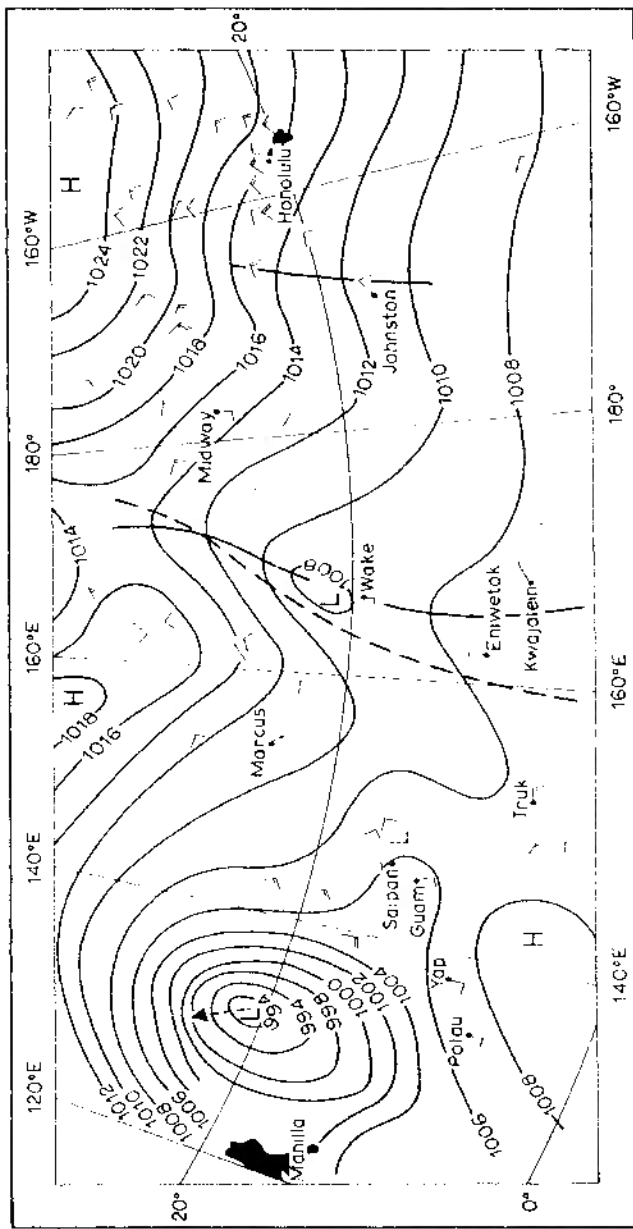


Fig. 6.7. The surface synoptic chart for part of the north-west Pacific on 17 August 1957. The movements of the central wave trough and of the closed circulation during the following 24 hours are shown by the dashed line and arrow, respectively. The dashed L just east of Saipan indicated the location in which another low pressure system subsequently developed. Plate 28 shows the cloud formation along the convergence zone just east of Wake Island (from Malitus and Riehl 1964).

2 Cyclones

a Hurricanes. The most notorious type of cyclone is the tropical hurricane (or typhoon). Because these cause widespread damage over land areas and are a serious shipping hazard, considerable attention has been given to forecasting their development and movement so that their origin and structure are beginning to be understood. Naturally the catastrophic force of a hurricane makes it a very difficult phenomenon to investigate, but some assistance is now obtained from aircraft reconnaissance flights sent out during the 'hurricane season', from radar observations of cloud and precipitation structure, and from satellite photography (see pls. 29 and 30).

The typical hurricane system has a diameter of about 650 km (400 miles), less than half that of a mid-latitude depression, although typhoons in the China Sea are often much larger. The central pressure at sea-level is commonly 950 mb and exceptionally falls below 920 mb. Hurricane winds are defined arbitrarily as 33 m sec^{-1} (74 mph) or more and in many storms they exceed 50 m sec^{-1} (120 mph). The great vertical development of cumulonimbus clouds with tops at over 12,000 m (40,000 ft) reflects the immense convective activity concentrated in such systems. Radar studies show that the convective cells are normally organized in bands which spiral inward towards the centre.

A number of conditions are necessary, even if not always sufficient, for hurricane formation. One requirement as shown by fig. 6.8 is an extensive ocean area with a surface temperature greater than 27°C (80°F). Cyclones rarely form near the equator, where the Coriolis parameter is close to zero, or in zones of strong vertical wind shear (i.e. beneath a jet stream), as both factors inhibit the development of an organized vortex. There is also a definite connection between the seasonal position of the Equatorial Trough and zones of hurricane formation, which is borne out by the fact that no hurricanes occur in the South Atlantic (where the trough never lies south of 5°S) or in the south-east Pacific (where the trough remains north of the equator). On the other hand, recent satellite photographs over the north-east Pacific show an unexpected number of cyclonic vortices in summer, many of which move westwards near the trough line about $10\text{--}15^\circ\text{N}$. About 60% of tropical cyclones seem to originate $5\text{--}10^\circ$ latitude poleward of the Equatorial Trough in the doldrum sectors, where the trough is at least 5° latitude from the equator. The development regions of hurricanes mainly lie over the western sections of the Atlantic, Pacific and Indian Oceans where the subtropical

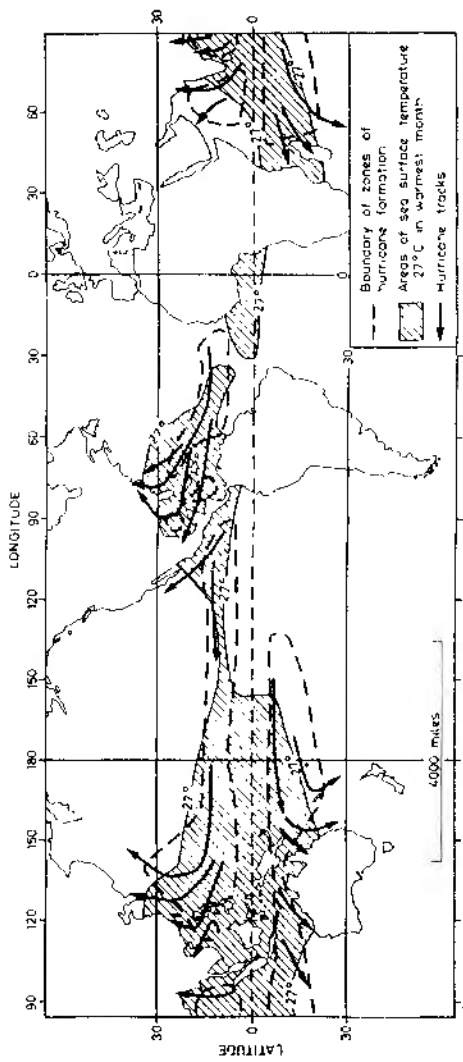


Fig. 6.8. Areas of hurricane formation, their principal tracks and mean sea-surface temperatures of the warmest month (after Palmer 1948 and Bergeron 1954).

high-pressure cells do not cause subsidence and stability and the upper flow is divergent.

The main hurricane (and typhoon) activity in the northern hemisphere is in late summer and autumn during the time of the Equatorial Trough's northward displacement. The 'hurricane season' occurs in the western Atlantic mainly between July and October with a marked peak in September, and the western Pacific between July and October. A small number of storms may affect both areas as early as May and as late as December. The late summer-autumn maximum is also found in the other areas, although there is a secondary, early summer maximum in the Bay of Bengal.

Annual frequencies of tropical cyclones are shown in table 6.1. The figures are only approximate since in some cases it may be uncertain as to whether or not the winds actually exceeded hurricane force and storms in the more remote parts of the South Pacific and Indian Oceans frequently escaped detection prior to the use of weather satellites.

Table 6.1
(After Atkinson 1971 and Baum 1974)

	<i>Tropical storms and cyclones</i> <i>Winds $\geq 17 \text{ m s}^{-1}$</i>	<i>Tropical cyclones</i> <i>Winds $\geq 33 \text{ m s}^{-1}$</i>
Western North Pacific (1959–68)	30.5	20.6
Eastern North Pacific (1966–73)	14.9	6.8
Western North Atlantic (1941–68)	9.2	5.7
Bay of Bengal (1948–69)	3.6	
Arabian Sea (1890–1967)	1.1	
South-west Indian Ocean (1931–60)	7.8	
South-east Indian Ocean (1962–67)	6.0	
Western South Pacific (1947–61)	6.6	

Early theories of hurricane development held that convection cells generated a sudden and massive release of latent heat to provide energy for the storm. Although convection cells were regarded as an integral part of the hurricane system, their scale was thought to be too small for them to account for the growth of a storm hundreds of kilometres in diameter. Recent research, however, is modifying this picture considerably. Energy is apparently transferred from the cumulus-scale to the large-scale circulation of the storm through the organization of the clouds into spiral bands (fig. 6.9 and pl. 30) although the nature of the process is still being

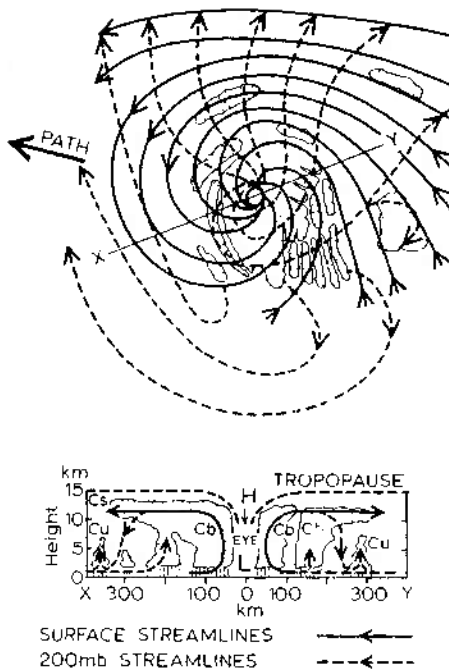


Fig. 6.9. A model of the areal (above) and vertical (below) structure of a hurricane. Cloud is stippled and areas of precipitation are shown in the vertical section. The streamline symbols refer to the upper diagram (based on La Seur and Hawkins 1963, and Fett 1964).

investigated. There is now ample evidence to show that hurricanes form from pre-existing disturbances, but while many of these disturbances develop as closed low-pressure cells few attain full hurricane intensity. The key to this problem appears to be the presence of an anticyclone in the upper troposphere. This is essential for high-level outflow (see figs. 3.6 and 3.13), which in turn allows the development of very low pressure and high wind speeds near the surface. A distinctive feature of the hurricane is the warm vortex, since other tropical depressions and incipient storms have a cold core area of shower activity. The warm core develops through the action of 100–200 cumulonimbus towers releasing latent heat of condensation. Observations show that although these 'hot towers' form

less than 1% of the storm area within a radius of about 400 km (230 miles), there effect is sufficient to change the environment. The warm core is vital to hurricane growth because it intensifies the upper anticyclone, leading to a 'feedback' effect by stimulating the low-level influx of heat and moisture which further intensifies convective activity, latent heat release and therefore the upper-level high pressure. The thermally-direct circulation converts the heat increment into potential energy and a small fraction of this – about 3% – is transformed into kinetic energy. The remainder is exported by the anticyclonic circulation at about the 12 km (200 mb) level.

In the eye, or innermost region of the storm (fig. 6.9), adiabatic warming of descending air accentuates the high temperatures, although since high temperatures are also observed in the eye-wall cloud masses, subsiding air can only be one contributory factor. The eye has a diameter of some 300–500 km (200–300 miles), within which the air is virtually calm and the cloud cover may be broken. The mechanics of the eye's inception are still largely unknown. If the rotating air conserved absolute angular momentum, wind speeds would become infinite at the centre and clearly this is not the case. The strong winds surrounding the eye are more or less in cyclostrophic balance, with the small radial distance providing a large centripetal acceleration (see p. 134). The air rises when the pressure gradient can no longer force it further inward. It is possible that the cumulonimbus anvils play a vital role in the complex link between the horizontal and vertical circulations around the eye by redistributing angular momentum in such a way as to set up a concentration of rotation near the centre.

The supply of heat and moisture combined with low frictional drag at the sea surface, the release of latent heat through condensation and the removal of the air aloft are essential conditions for the maintenance of hurricane intensity. As soon as one of these ingredients diminishes the storm decays. This can occur quite rapidly if the track (determined by the general upper tropospheric flow) takes the vortex over a cool sea surface or over land. In the latter case the increased friction hastens the process of filling while the cutting-off of the moisture supply removes one of the major sources of heat. Rapid decay also occurs when cold air is drawn in circulation or when the upper-level divergence pattern moves away from the storm.

Hurricanes usually move at some 16–24 kmph (10–15 mph), controlled primarily by the rate of movement of the upper warm core. Almost invariably they recurve poleward around the western margins of the subtropical high-pressure cells, entering the circulation of the westerlies,

where they die out or degenerate into extra-tropical depressions (pl. 18). Some of these systems retain an intense circulation and the high winds and waves can still wreak havoc. This is not uncommon along the Atlantic coast of the United States and occasionally eastern Canada. Similarly, in the western North Pacific, recurved typhoons are a major element in the climate of Japan (see ch. 6, D.4) and may occur in any month. There is an average frequency of 12 typhoons per year over southern Japan and neighbouring sea areas.

To sum up. The hurricane develops from an initial disturbance which, under favourable environmental conditions, grows first into a tropical depression and then a tropical storm (with wind speeds of 17–33 m sec⁻¹ or 39–73 mph). The tropical storm stage may persist 4–5 days, whereas the hurricane stage usually lasts for only 2–3 days. The main energy source is latent heat derived from condensed water vapour, and for this reason hurricanes are generated and continue to gather strength only within the confines of warm oceans. The cold-cored tropical storm is transformed into a warm-cored hurricane in association with the release of latent heat in cumulonimbus towers, and this establishes or intensifies an upper tropospheric anticyclonic cell. Thus high-level outflow maintains the ascent and low-level inflow in order to provide a continual generation of potential energy (from latent heat) and the transformation of this into kinetic energy. The inner eye which forms during the cold-core tropical storm stage is an essential element in the life cycle.

b *Other tropical depressions.* Not all cyclonic systems in the tropics are of the intense hurricane variety. There are two other major types of cyclonic vortex. One is the *monsoon depression* which affects southern Asia during the summer. This disturbance is somewhat unusual in that the flow is westerly at low levels and easterly in the upper troposphere (see fig. 6.22). It is more fully described in ch. 6, D.4.

The second type of system is usually relatively weak near the surface, but well-developed in the middle troposphere. In the eastern North Pacific such lows are referred to as *subtropical cyclones*. Many of them develop from the cutting-off in low latitudes of a cold upper-level wave in the westerlies (compare ch. 4, G.4). They possess a broad eye of some 150 km (100 miles) in radius with little cloud, surrounded by a belt of cloud and precipitation about 300 km (200 miles) wide. In late winter and spring a few such storms make a major contribution to the rainfall of the Hawaiian Islands. These cyclones are very persistent and tend eventually to be reabsorbed by a trough in the upper westerlies. Similar disturbances occur over the Arabian Sea in summer and make a major contribution to

summer ('monsoon') rains in northwestern India. These systems show upward motion mainly in the upper troposphere. Their development may be linked to air export at upper levels of cyclonic vorticity from the persistent heat low over northern India.

3 Subsynoptic systems

Cloud clusters have been studied primarily from satellite photographs of the tropical Atlantic and Pacific oceans. Their definition is rather arbitrary, but they may extend over an area 2° square up to 12° square. It is important to note that the peak convective activity has passed when cloud cover is most extensive through the spreading of cirrus canopies. Clusters in the Atlantic, defined as more than 50% cloud cover extending over an area of 3° square, show maximum frequencies of 10–15 clusters per month near the ITC and also at $15\text{--}20^{\circ}\text{N}$ in the western Atlantic over zones of high sea-surface temperature. They consist of a cluster of mesoscale convective cells with the system having a deep layer of convergent airflow (see fig. 6.2). Some persist for only 1–2 days but many develop within synoptic-scale waves. Many aspects of their development and role remain to be determined.

4 Mesoscale systems

Two well-known linear systems may be described in this category. They are the *disturbance lines* of West Africa and the line squalls (known as *sumatras*) of Malaya. The latter cross Malaya from the west in the early morning during the south-west monsoon and appear to be initiated by the convergent effects of land breezes in the Malacca Straits. The disturbance line occurs in West Africa in the summer half-year when low-level southwesterly monsoon air is overrun by dry, warm Saharan air. The physical process is analogous to that in the mid-latitude squall line (fig. 4.21; cf. also p. 218). They are several hundred kilometres long and travel westwards across West Africa at about 50 kmph (30 mph) giving squalls and thundery showers before dissipating over cold water areas of the North Atlantic. Spring and autumn rainfall in West Africa is derived in large part from these disturbances. Figure 6.10 for Kortright (Freetown, Sierra Leone) illustrates the daily rainfall amounts in 1960–1 associated with disturbance lines at 8°N . The summer monsoon rains make up the greater part of the total here, but their contribution diminishes northward. For example, in 1955 disturbance lines contributed about 30% of the annual rainfall over coastal Ghana and 90% in the north of the territory. Mesoscale wind systems in the Tropics are discussed on pp. 315–321.

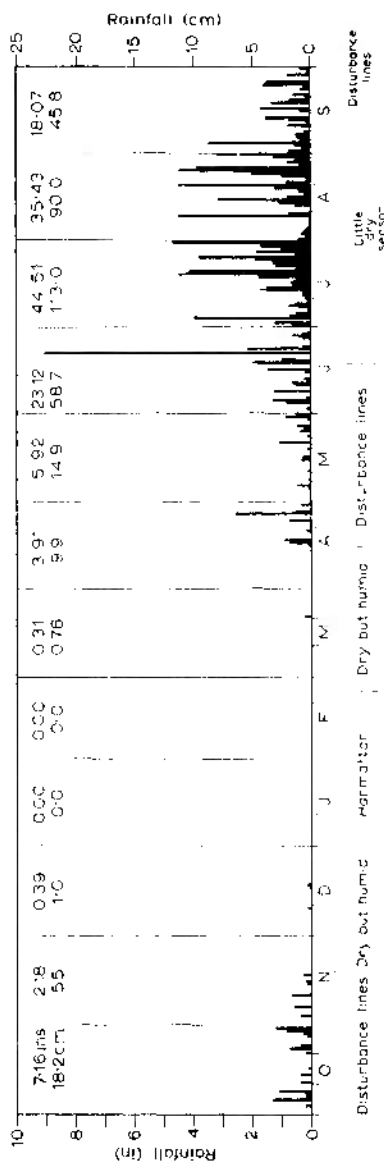


Fig. 6.10. Daily rainfall at Kortwright, Freetown, Sierra Leone. October 1960–September 1961 (after Gregory 1965).

D The Asian monsoon

The name *monsoon* is derived from the Arabic word (*mausim*) which means season, so explaining its application to large-scale seasonal reversals of the wind regime. The Asiatic seasonal wind reversal is notable for its immense extent and the penetration of its influence beyond tropical latitudes. For example, the surface circulation over China reflects this seasonal change:

	January	July
North China	60% of winds from W, NW and N	57% of winds from SE, S and SW
South-east China	88% of winds from N, NE and E	56% of winds from SE, S and SW

However, such seasonal wind shifts at the surface are quite widespread and occur in many regions which would not traditionally be considered as monsoonal (fig. 6.11). Although there is a rough accordance between these traditional regions and those experiencing over 60% frequency of the prevailing octant, it is obvious that a variety of unconnected mechanisms can produce significant seasonal wind shifts. Nor is it possible to establish a simple relationship between seasonality of rainfall (fig. 6.12) and

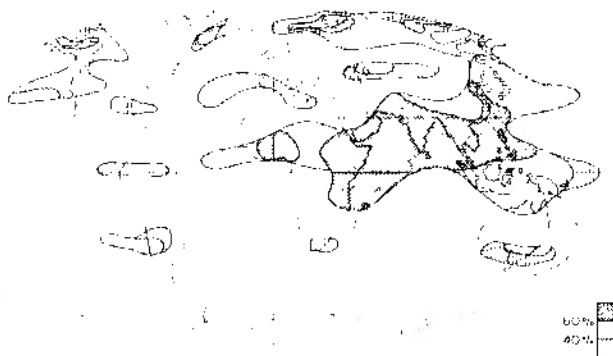


Fig. 6.11. Regions experiencing a seasonal surface wind shift of at least 120° , showing frequency of the prevailing octant (after Chromov. Adapted from Flohn 1960).



Fig. 6.12. The annual distribution of tropical rainfall. The shaded areas refer to periods during which more than 75% of the mean annual rainfall occurs. Areas with less than 250 mm/year (10 in) are classed as deserts, and the unshaded areas are those needing at least 7 months to accumulate 75% of the annual rainfall and are thus considered to exhibit no seasonal maximum (after Ramage 1971).

seasonal wind shift. Areas traditionally designated as 'monsoonal' include some of the tropical and near-tropical regions experiencing a summer rainfall maximum and most of those having a double rainfall maximum. It is clear that a combination of criteria (for example, from figs. 6.11 and 6.12) is necessary to approach an adequate definition of monsoonal areas.

In summer the Equatorial Trough and the subtropical anticyclones are everywhere displaced northwards in response to the changing pattern of solar heating of the earth, and in southern Asia this movement is magnified by the effects of the land mass. However, the attractive simplicity of the traditional explanation, which envisages a monsoonal 'sea breeze' directed towards a summer thermal low pressure over the continent, unfortunately provides an inadequate basis for understanding the workings of the system. The Asiatic monsoon regime is a consequence of the interaction of both planetary and regional factors, both at the surface and in the upper troposphere. It is convenient to look at each season in turn.

1 Winter

Near the surface this is the season of the outblowing 'winter monsoon', but aloft the westerly airflow dominates. This, as we have seen, reflects the general pressure distribution. A shallow layer of cold, high-pressure air is centred over the continental interior, but this has disappeared even at 700 mb (see fig. 3.17) where there is a trough over eastern Asia and zonal circulation over the continent. The upper westerlies split into two currents to the north and south of the high Tibetan plateau (fig. 6.13), which exceeds 4000 m (13,000 ft) over a vast area, to reunite again off the east coast of China (fig. 6.14). These two branches have been attributed to the disruptive effect of the topographic barrier on the airflow, but the northern jet may be located far from the Tibetan plateau and two currents are also found to occur farther west where there is no obstacle to the flow. The branch over northern India corresponds with a strong latitudinal thermal gradient (from November to April) and it is probable that this factor, combined with the effect of the barrier to the north, is responsible for the anchoring of the southerly jet. This southern branch is the stronger, with an average speed of more than 66 m sec^{-1} (148 mph) at 200 mb, compared with about $20-25 \text{ m sec}^{-1}$ (45-55 mph) in the northern one. Where the two unite over north China and south Japan the average velocity exceeds 66 m sec^{-1} (148 mph).

Air subsiding beneath this upper westerly current gives dry outblowing northerly winds from the subtropical anticyclone over northwestern India

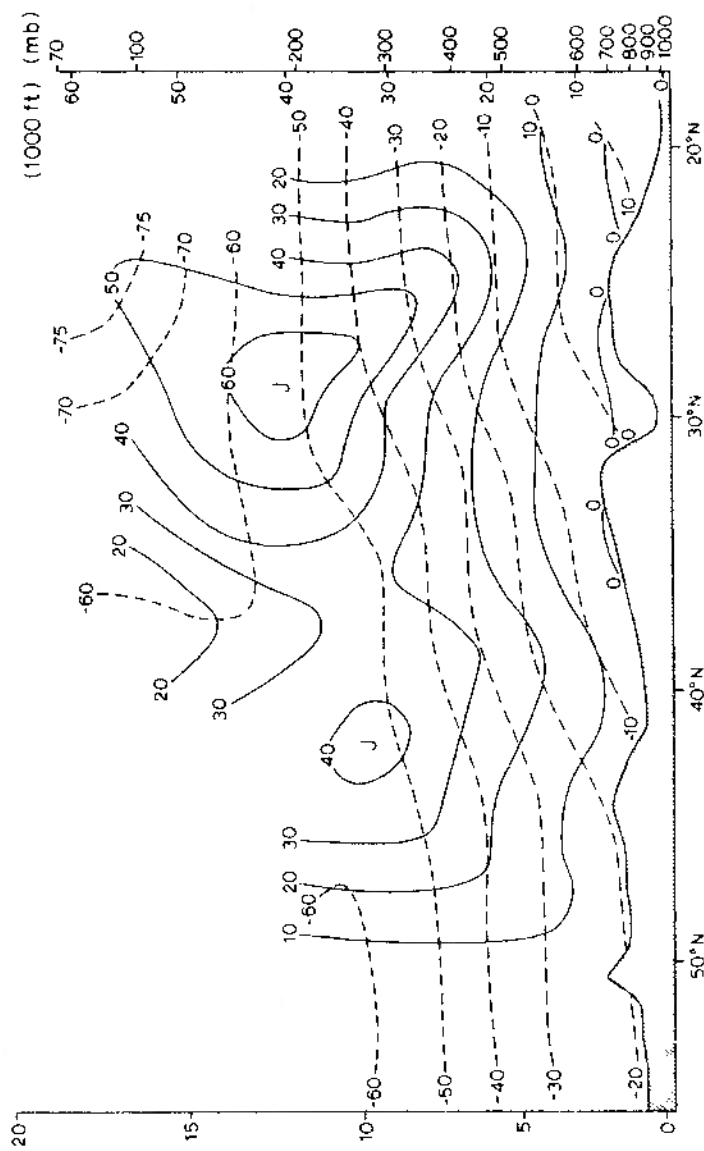


Fig. 6.13. The mean zonal geostrophic wind (in m sec^{-1} ; solid lines) and temperatures (in $^{\circ}\text{C}$; dashed lines) along longitude 105°E for January–March 1956. The numbers along the base refer to upper-air observing stations (from *Accademia Sinica 1957*).

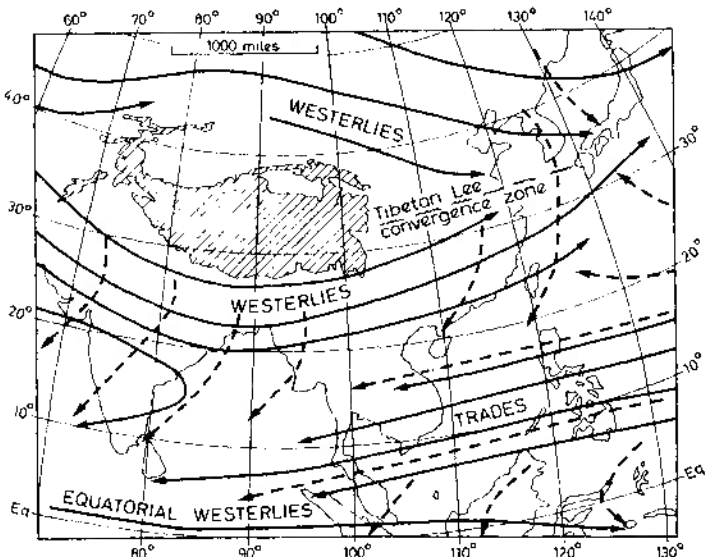


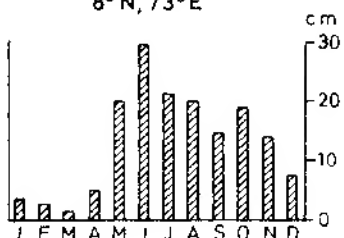
Fig. 6.14. The characteristic air circulation over southern and eastern Asia in winter (after Thompson 1951; Flohn 1960; Frost and Stephenson 1965; and others). Solid lines indicate air flow at about 3000 m (10,000 ft), and dashed lines that at about 600 m (2000 ft). The names refer to the wind systems aloft.

and Pakistan. The surface wind direction is northwesterly over most of northern India, becoming northeasterly over Burma and Bangladesh and easterly over peninsular India. Equally important is the steering of winter depressions over northern India by the upper jet. The lows, which are not usually frontal, appear to penetrate across the Middle East from the Mediterranean and are important sources of rainfall for northern India and Pakistan (e.g. Kalat, fig. 6.15), especially as it falls when evaporation is at a minimum.

Some of these westerly depressions continue eastwards, redeveloping in the zone of jet-stream confluence about 30°N , 105°E over China, beyond the area of subsidence in the immediate lee of Tibet (fig. 6.13), and it is significant that the mean axis of the winter jet stream over China shows a close correlation with the distribution of winter rainfall (fig. 6.16). Other depressions affecting central and north China travel within the westerlies north of Tibet or are initiated by outbreaks of fresh cP air.

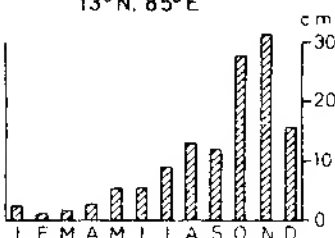
MINICOY (62'')

8°N, 73°E



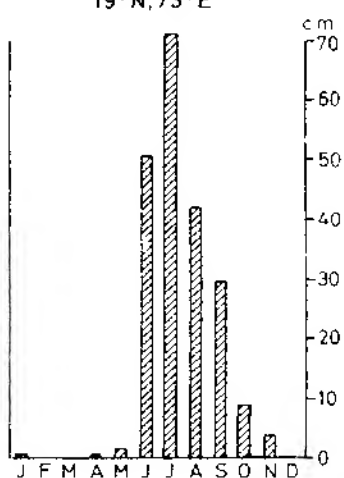
MADRAS (49'')

13°N, 85°E



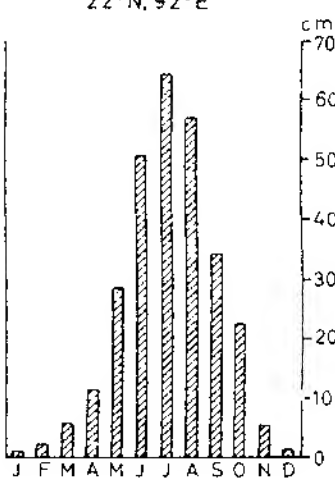
BOMBAY (82'')

19°N, 73°E



CHITTAGONG (113'')

22°N, 92°E



KALAT (9'')

29°N, 67°E



BIKANER (12'')

28°N, 73°E

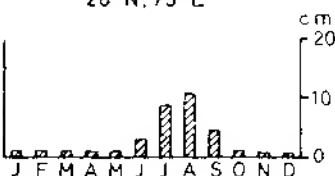


Fig. 6.15. Average monthly rainfall at six stations in the Indian region (based on 'CLIMAT', normals of the World Meteorological Organization for 1931-60). The annual total in inches is given after the station name.

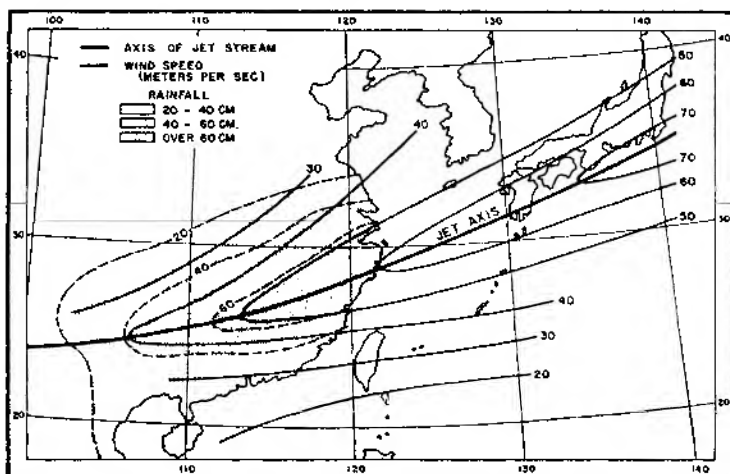


Fig. 6.16. The mean winter jet stream axis at 12 km over the Far East and the mean winter precipitation over China in cm (after Mohrl and Yeh. From Trewartha 1961).

In the rear of these depressions there are invasions of very cold air (e.g. the *buran* blizzards of Mongolia and Manchuria). The effect of such cold waves, comparable with the *northers* in the central and southern United States, is greatly to reduce mean temperatures. Winter mean temperatures in less-protected southern China are considerably below those at equivalent latitudes in India and, for example, temperatures at Calcutta and Hong Kong (both approximately 22°N) are, respectively, 19°C (67°F) and 16°C (60°F) in January and 22°C (71°F) and 15°C (59°F) in February.

2 Spring

The key to change during this transition season once again seems to be found in the pattern of the upper airflow. In March the upper westerlies begin their seasonal migration northwards, but whereas the northerly jet strengthens and begins to extend across central China and into Japan, the southerly branch remains positioned south of Tibet, although weakening in intensity.

The weather over northern India becomes hot, dry and squally in response to the greater insolation. Mean temperatures at Delhi rise from

23°C (74°F) in March to 33°C (92°F) in May. The thermal low-pressure cell (see ch. 4, G.2) reaches its maximum intensity at this time, but although onshore coastal winds develop the break of the monsoon is still a month away and other mechanisms cause only limited precipitation. Some precipitation occurs in the north with 'westerly disturbances', particularly towards the Ganges delta where the low-level inflow of warm, humid air is overrun by dry, potentially cold air, triggering convective storms known as *nor'westers*. In the north-west, where less moisture is available the convection generates violent squalls and dust-storms termed *andhis*. The mechanism of these storms is not yet fully known, though high-level divergence in the waves of the subtropical westerly jet stream appears to be essential. The early onset of summer rains in Bengal, Bangladesh, Assam and Burma (e.g. Chittagong, fig. 6.15) is favoured by an orographically produced trough in the westerlies at 300 mb, which is located at about 85°–90°E in May. Low-level convergence of maritime air from the Bay of Bengal, combined with the upper level divergence ahead of the 300 mb trough, generates thunder squalls. Tropical disturbances in the Bay of Bengal are another source of these early rains. Rain also falls during this season over Ceylon and south India (e.g. Minicoy, fig. 6.15) in response to the northward movement of the Equatorial Trough.

China has no equivalent of India's hot, pre-monsoon season. The low-level, north-easterly winter monsoon (reinforced by subsiding air from the upper westerlies) persists in north China and even in the south it only begins to be replaced by maritime tropical air in April–May. Thus, at Canton mean temperatures rise from only 17°C (63°F) in March to 27°C (80°F) in May, some 6°C (12°F) less than the mean values over northern India.

Westerly depressions are most frequent over China in spring. They form more readily over central Asia at this season as the continental anti-cyclone begins to weaken; also many develop in the jet-stream confluence zone. The average number crossing China per month during 1921–31 was as follows:

J	F	M	A	M	J	S	A	S	O	N	D	Year
7	8	9	11	10	8	5	3	3	6	7	7	86

Hence spring is wetter than winter and over most of central and southern China, the three months March–May contribute a quarter to a third of the annual rainfall.

3 Early summer

Generally during the last week in May the southern jet begins to break down, becoming first intermittent and then finally being diverted altogether to the north of the plateau. Over India the Equatorial Trough pushes northwards with each weakening of the upper westerlies south of Tibet, but the final *burst* of the monsoon, with the arrival of the humid, low-level south-westerlies, is not accomplished until the upper-air circulation has switched to its summer pattern (fig. 6.17). The low-level changes

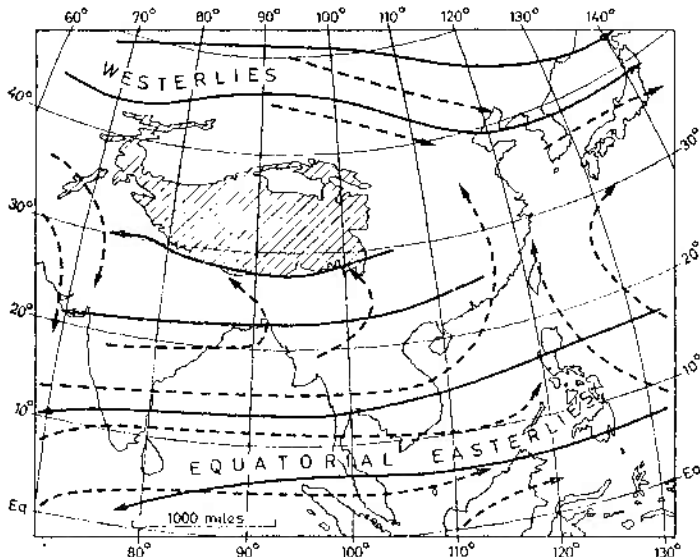


Fig. 6.17. The characteristic air circulation over southern and eastern Asia in summer (after Thompson 1951; Flohn 1960; Frost and Stephenson 1965; and others). Solid lines indicate air flow at about 6000 m (20,000 ft) and dashed lines that at about 600 m (2000 ft). Note that the low-level flow is very uniform between about 600 and 3000 m.

are related to the establishment of a high-level easterly jet stream over southern Asia about 15°N. One theory suggests that this takes place in June as the col between the subtropical anticyclone cells of the west Pacific and the Arabian Sea at the 300 mb level is displaced north-westwards from a position about 15°N, 95°E in May towards central India. The north-

westward movement of the monsoon (fig. 6.18) is apparently related to the extension over India of the upper tropospheric easterlies.

The reorganization of the upper airflow has widespread effects in southern Asia. It is directly linked with the *Mai-yu* rains of China (which reach a peak about 10–15 June), the onset of the south-west Indian monsoon and the northerly retreat of the upper westerlies over the whole of the Middle East.

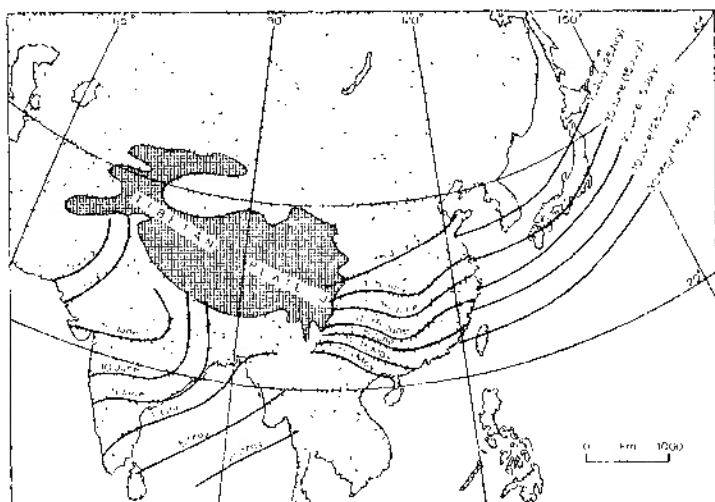


Fig. 6.18. The advance of the summer monsoon over south and east Asia, based on: For India, the beginning of the rainy season (after Chatterjee 1953); For China, the northward shift of the 5-day mean wet-bulb temperature of 24°C (after Tu and Hwang 1944); For Japan, the onset of the 'bai-u rains' (after Takahashi 1955 and, in parenthesis, after Kurashima 1968).

It must nevertheless be emphasized that it is still uncertain how far these changes are caused by events in the upper air or indeed whether the onset of the monsoon initiates a readjustment in the upper-air circulation. The presence of the Tibetan plateau is certainly of importance even if there is no significant barrier effect on the airflow. Heating of the plateau in early summer results in the formation of a thermal high-pressure cell (see fig. 3.13) over the area at the level of its surface (about 600–500 mb) and, by producing easterly flow on the south side of the anticyclone, this un-

doubtedly assists the breakdown of the southern westerly jet. At the same time, the pre-monsoonal convective activity over the south-eastern Tibetan Highlands provides a further heat source, by latent heat release, for the upper tropospheric anticyclone. Clearly, the interactions between the Indian monsoon regime and the Tibetan Highlands are decidedly complex.

Over China, the zonal westerlies retreat northwards in May–June and the westerly flow becomes concentrated north of the Tibetan plateau. The equatorial westerlies spread across south-east Asia from the Indian Ocean, giving a warm, humid air mass at least 3000 m deep. Contrary to earlier views, the Pacific is only a moisture source when tropical south-easterlies extend westwards to affect the east coast. Most of the summer precipitation over China south of 30°–35°N is derived from the north-eastward extension of the south Asian monsoon current, seemingly in relation to surges in the flow causing zones of speed convergence (see fig. 3.6A). Central China is also affected by weak disturbances moving eastward along the Yangtze valley and by occasional cold fronts from the north-west.

4 Summer

By mid-July monsoon air covers most of southern and south-eastern Asia (fig. 6.17) and in India the Equatorial Trough is located about 25°N. North of the Tibetan plateau there is a rather weak upper westerly current with a (subtropical) high-pressure cell over the plateau. The south-west monsoon in southern Asia is overlain by strong upper easterlies with a pronounced jet at 150 mb (about 15 km or 50,000 ft) which extends westwards across South Arabia and Africa (fig. 6.19). No easterly jets have so far been observed over the tropical Atlantic or Pacific. The jet is related to a steep lateral temperature gradient with the upper air getting progressively colder to the south.

An important characteristic of the tropical easterly jet is the location of the main belt of summer rainfall on the right (i.e. north) side of the axis upstream of the wind maximum and on the left side downstream, except for areas where the orographic effect is predominant (fig. 6.19). The mean jet maximum is located about 15°N, 50–80°E.

The monsoon current does not give rise to a simple pattern of weather over India, despite the fact that much of the country receives 80% or more of its annual precipitation during the monsoon season (fig. 6.20). In the north-west a thin wedge of monsoon air is overlain by subsiding continental air (fig. 6.21) and it is evident that the frontal surface is inactive in

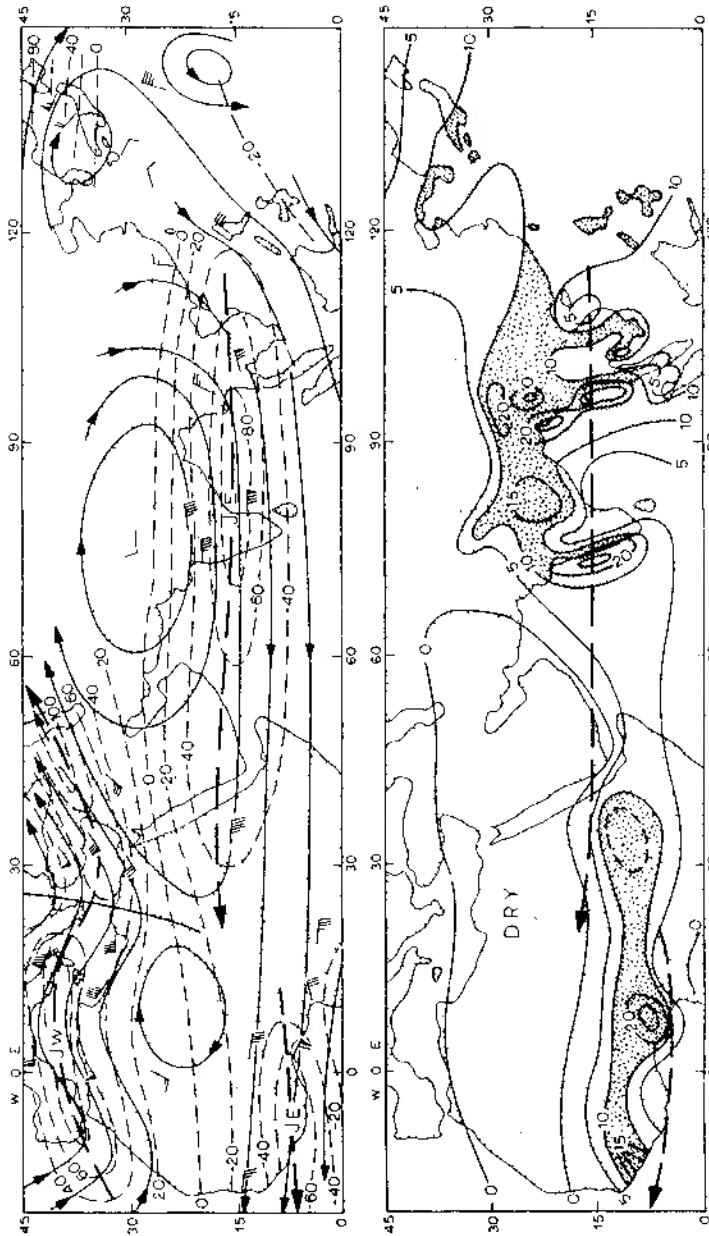


Fig. 6.19 The easterly tropical jet stream (from Kateswaram 1958). *Above*, The location of the easterly jet streams at 200 mb on 25 July 1955. Streamlines are shown in solid lines and isotachs (wind speed) dashed. Wind speeds are given in knots (westerly components positive, easterly negative). *Below*, The average July rainfall (shaded areas receive more than 10 in or 25 cm) in relation to the location of the easterly jet streams.

terms of weather. The inversion prevents convection and consequently little or no rain falls in the summer months in the arid north-west of the subcontinent (e.g. Bikaner and Kalat, fig. 6.15).

Around the head of the Bay of Bengal and along the Ganges valley the main weather mechanisms in summer are the 'monsoon depressions' (see p. 295) which usually move westwards or north-westwards across India, steered by the upper easterlies. On average, they occur about twice a month, apparently when an upper trough becomes super-imposed over a surface disturbance in the Bay of Bengal. Figure 6.22 shows that the main

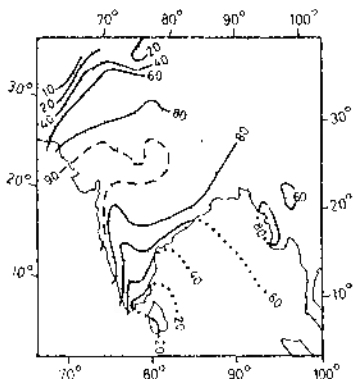


Fig. 6.20. The percentage contribution of the monsoon rainfall (June to September) to the annual total (after Rao and Ramamoorthy 1960, in Indian Meteorological Department 1960; and Ananthakrishnan and Rajagopalachari 1964 in Hutchings 1964).

rain areas lie south of the Equatorial Trough (in the south-west quadrant of the monsoon depressions, resembling an inverted mid-latitude depression), and also tend to occur on windward coasts and mountains of India, Burma and Malaya. Without such disturbances the distribution of monsoon rains would be controlled to a much larger degree by orography.

It has recently been discovered that the south-west monsoonal flow takes place partly in the form of a $15-45 \text{ m sec}^{-1}$ (30–100 mph) jet stream at a level of only 1000–1500 m (3250–5000 ft). This jet flows north-westward from Madagascar, crosses the equator from the south

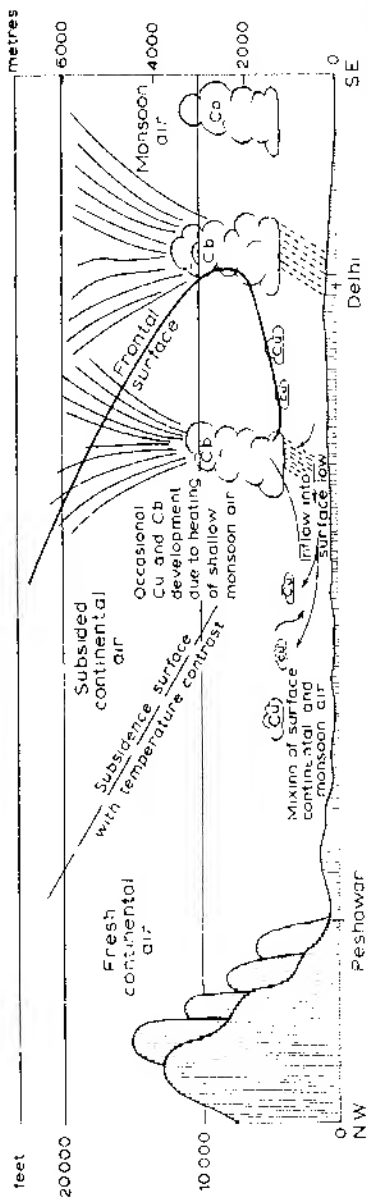
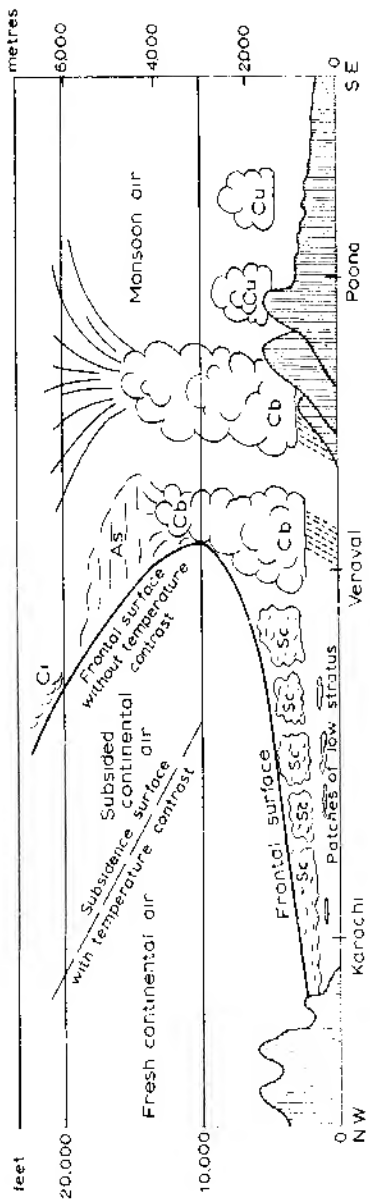


Fig. 6.21. The structure of the 'Inter-tropical Front' over the north-western part of the Indian sub-continent (from Sawyer 1947).

312 Atmosphere, weather and climate

over East Africa where its core is often marked by a streak of cloud (similar to that in pl. 10) and where it may bring excessive local rainfall, and is then deflected towards the north-east across the Arabian Sea towards the west coast of the Indian peninsula. The south-westerly current over the Indian Ocean is quite dry near the equator, apart from a shallow moist layer at the surface. Moisture is acquired over the Arabian

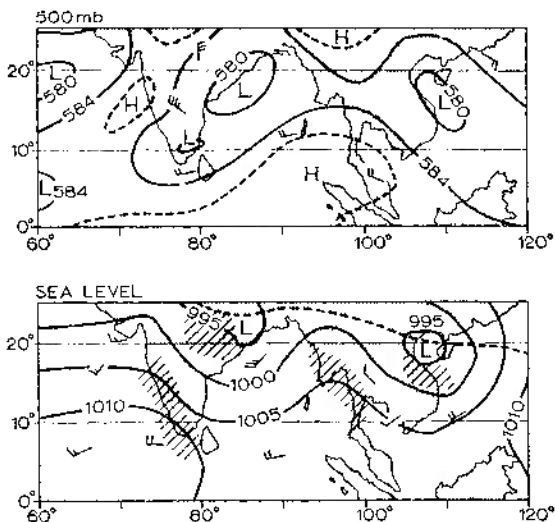


Fig. 6.22. Monsoon depressions of 1200 GMT, 4 July 1957. The upper diagram shows the height (in tens of metres) of the 500-mb surface, the lower one the sea-level isobars. The broken line in the lower diagram represents the Equatorial Trough, and precipitation areas are shown by the oblique shading (based on the IGY charts of the Deutscher Wetterdienst).

Sea, although even there an inversion indicates the presence of dry upper air originating perhaps over Arabia or East Africa. Convective instability is only released as the air slows down and converges at the coast and is forced over the Western Ghats. At Mangalore (13°N) there are on average 25 rain-days per month in June, 28 in July and 25 in August. The monthly rainfall averages are respectively 98 cm (38.6 in), 106 cm (41.7 in) and 58 cm (22.8 in), accounting for 75% of the annual total. In the lee

of the Ghats amounts are much reduced and there are semi-arid areas receiving less than 64 cm (25 in) per year.

In southern India, excluding the south-east, there is a marked tendency for less rainfall when the Equatorial Trough is farthest north. Figure 6.15 shows a maximum at Minicoy in June with a secondary peak in October as the Equatorial Trough and its associated disturbances withdraw southward. This double peak occurs in much of interior peninsular India south of about 20°N and in western Ceylon, although autumn is the wettest period.

It is important to realize that the monsoon rains are highly variable from year-to-year, emphasizing the role played by disturbances in generating rainfall within the favourable environment created by the moist south-westerlies. *Breaks* occur in the monsoon rains when, during low-index periods, mid-latitude westerlies accompanied by the jet push southwards, weakening the Tibetan anticyclone or displacing it north-eastwards. Westerly troughs travel along the southern edge of the Himalayas, giving heavy rain on the mountain slopes but little rain elsewhere. In parts this may be due to the eastward extension across central India of the subtropical high over Arabia.

To the east over China, the surface airflow is south-westerly and the upper winds are weak with only a diffuse easterly current over southern China. According to traditional views the monsoon current reaches northern China by July. The annual rainfall regime shows a distinct summer maximum with, for example, 64% of the annual total occurring at Tientsin (39°N) in July and August. Nevertheless, much of the rain falls during thunderstorms associated with shallow lows and the existence of the ITCZ in this region is doubtful (see fig. 6.1). The southerly winds, referred to above, which predominate over northern China in summer are not necessarily linked with the monsoon current farther south. Indeed this idea is the result of incorrect interpretation of streamline maps (of instantaneous airflow direction) as ones showing air trajectories (or the actual paths followed by air parcels). The depiction of the monsoon over China on fig. 6.18 is, in fact, based on a wet-bulb temperature value of 24°C. Cyclonic activity in northern China is attributable to the West Pacific Polar Front, forming between cP air and much-modified mT air.

In central and southern China the three summer months account for about 40–50% of the annual average precipitation, with another 30% or so being received in spring. In south-east China there is a rainfall singularity in the first half of July; a secondary minimum in the profile seems to result from the westward extension of the Pacific subtropical anticyclone over the coast of China.

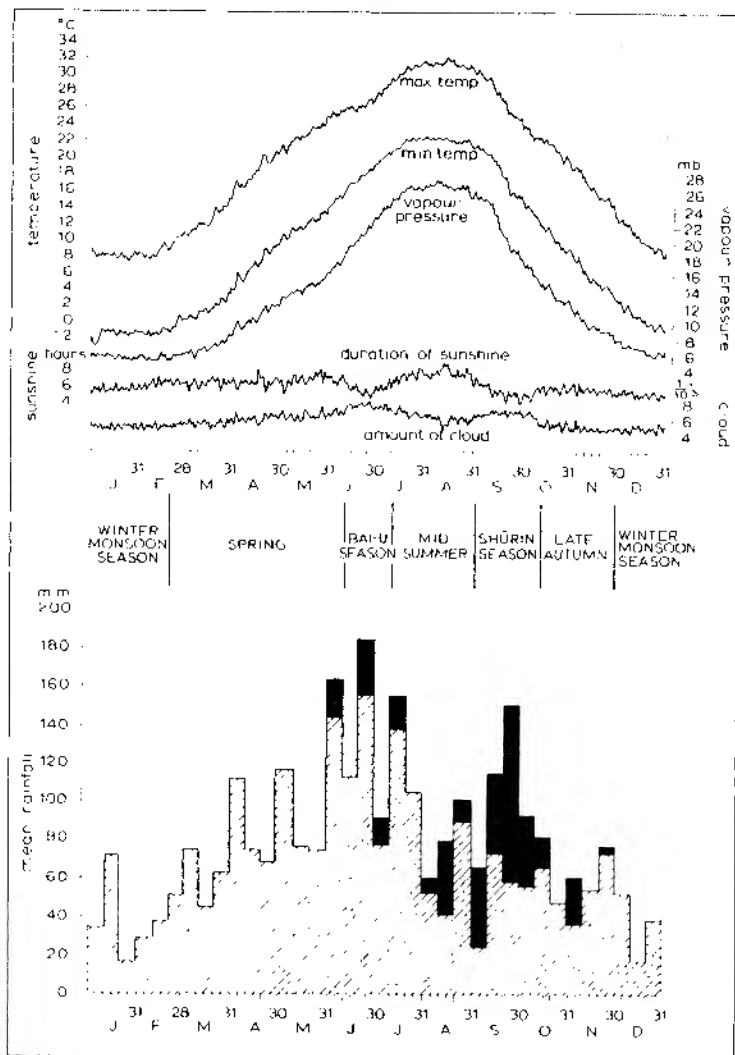


Fig. 6.23. Seasonal variation of daily normals at Nagoya, southern Japan (above), suggesting six natural seasons (from Maejima 1967). Below are average 10-day precipitation amounts for a station in southern Japan, indicating in black the proportion of rainfall produced by typhoon circulations. The latter reaches a maximum during the Shurin season (after Saito 1959. From Trewartha 1961).

A similar pattern of rainfall maxima occurs over southern and central Japan (fig. 6.23), comprising two of the six natural seasons which have been recognized there. The main rains occur during the *Bai-u* season of the south-east monsoon resulting from waves, convergence zones and closed circulations moving mainly in the tropical airstream round the Pacific subtropical anticyclone, but partly originating in a south-westerly stream which is the extension of the monsoon circulation of south Asia. The south-east circulation is displaced westwards from Japan by a zonal expansion of the subtropical anticyclone during late July and August giving a period of more settled sunny weather. The secondary precipitation maximum of the *Shurin* season during September and early October coincides with an eastward contraction of the Pacific subtropical anticyclone allowing low-pressure systems and typhoons from the Pacific to swing north towards Japan. Although much of the Shurin rainfall is believed to be of typhoon origin (fig. 6.23) some of it undoubtedly associated with the southern sides of depressions, moving along the southward-migrating Pacific Polar Front to the north, because there is a marked tendency for the autumn rains to begin first in the north of Japan and to spread southwards.

5 Autumn

Autumn sees the southward retreat of the Equatorial Trough and the break-up of the summer circulation systems (pl. 27). By October the easterly trades of the Pacific affect the Bay of Bengal at the 500-mb¹ level and generate disturbances at their confluence with the equatorial westerlies. This is the major season for Bay of Bengal cyclones and it is these disturbances rather than the onshore northeasterly monsoon, which cause the October/November maximum of rainfall in south-east India (e.g. Madras, fig. 6.15).

During October the westerly jet re-establishes itself south of the Tibetan plateau, often within a few days, and cool season conditions are restored over most of southern and eastern Asia.

E Other sources of climatic variations in the tropics

The major systems of tropical weather and climate have now been discussed, yet various other elements help to create contrasts in tropical weather both in space and time.

1 Diurnal variations

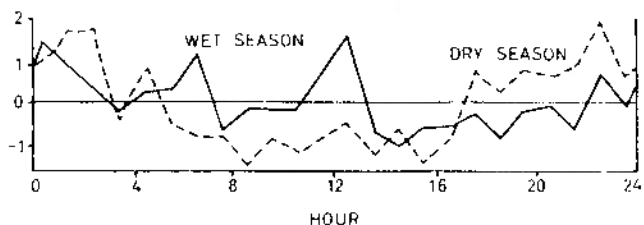
Diurnal weather variations are most evident at coastal locations in the

316 Atmosphere, weather and climate

trade-wind belt. Land and sea breeze regimes (see ch. 3, C.3) are well developed, as the heating of tropical air over land can be up to five times that over adjacent water surfaces. The sea breeze normally sets in between 0800 and 1100, reaching a maximum velocity of 6–15 m sec⁻¹ (13–33 mph) about 1300 to 1600 and subsiding around 2000. It may be up to 1000–1200 m (about 3000–4000 ft) in height with a maximum velocity at an elevation of 200–400 m (650–1300 ft) and normally penetrates some 20–30 km (about 12–20 miles) inland, although its extent may be up to 150 km (more than 90 miles) at times. Sea breezes are usually associated with a heavy build-up of cumulus cloud and afternoon downpours. On large islands under calm conditions the sea breezes converge towards the centre so that an afternoon maximum of rainfall is observed. Under steady trade winds the pattern is displaced downwind so that descending air may be located over the centre of the island. A typical case of afternoon maximum is illustrated by fig. 6.24 for Nandi (Viti Levu, Fiji) in the south-west Pacific. The station has a lee exposure in both wet and dry season. This rainfall pattern is commonly believed to be widespread in the tropics, but over the open sea and on small islands a night-time maximum (often with a peak near dawn) seems to occur and even large islands can display this nocturnal regime when there is little synoptic activity. At Rarotonga (fig. 6.24) 54% of the annual precipitation falls between 0800 and 2000. One theory is that the nocturnal radiative cooling of cloud tops makes the cloud layer less stable and encourages droplet growth by mixing of droplets at different temperatures (see ch. 2, G). This effect would be at a maximum near dawn. Another factor is that the sea-air temperature difference, and consequently the oceanic heat supply to the atmosphere, is largest about 0300–0600 hours. Yet a further hypothesis suggests that the semi-diurnal pressure oscillation encourages convergence and therefore convective activity in the early morning and evening, but divergence and suppression of convection around midday.

The Malayan peninsula displays very varied diurnal rainfall regimes in summer. The effects of land and sea breezes, anabatic and katabatic winds and topography greatly complicate the rainfall pattern by their interactions with the low-level south-westerly monsoon current. For example, there is a nocturnal maximum in the Malacca Straits region associated with the convection set off by the convergence of land breezes from Malaya and Sumatra, whereas on the east coast of Malaya the maximum occurs in the late afternoon-early evening when sea breezes extend about 30 km inland against the monsoon south-westerlies, and convective

RAROTONGA 21°S. 160°W



PERCENTAGE DEVIATION OF MEAN HOURLY RAINFALL FROM THE 24-HOUR AVERAGE

NANDI 18°S. 178°E

WET SEASON

DRY SEASON

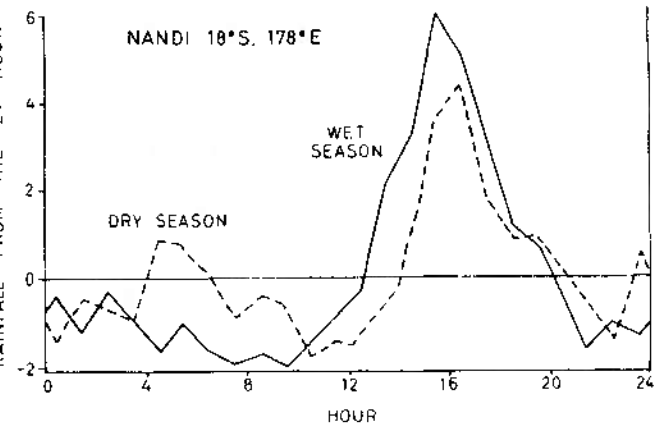


Fig. 6.24. The diurnal variation of wet and dry season rainfall in the southwest Pacific (after Finkelstein 1964, in Hutchings 1964). Amounts are shown as percentage deviations from the 24-hour average.

cloud develops in the deeper sea breeze current over the coast strip. On the interior mountains the summer rains have an afternoon maximum due to the unhindered convection process.

2 Topographic effects

Relief and surface configuration have an especially marked effect on rainfall amounts in tropical regions where hot, humid air masses are frequent. In the Hawaiian Islands the mean annual total exceeds 760 cm (300 in) on

318 Atmosphere, weather and climate

the mountains, with the world's largest mean annual total of 1199 cm (472 in) on Mt Waialeale (Kauai), but land on the lee side suffers correspondingly accentuated sheltering effects with less than 50 cm (20 in) over wide areas. On Hawaii itself the maximum falls on the eastern slopes at about 900 m, while the 4200-m summits of Mauna Loa and Mauna Kea, which rise above the trade-wind inversion, and their western slopes receive only 25–50 cm (10–20 in). On the Hawaiian island of Oahu, the maximum precipitation occurs on the western slopes, just leeward of the 850-m (2785-ft) summit with respect to the easterly trade winds. The following measurements in the Koolau Mountains, Oahu, show that the orographic factor is pronounced during summer when precipitation is associated with the easterlies, but in winter when precipitation is from cyclonic disturbances it is more evenly distributed:

Location	Elevation		Source of Rainfall		
	metres	feet	Trade Winds	Cyclonic disturbances	
			28 May— 3 Sept. 1957	2–28 Jan. 1957	5–6 Mar. 1957
Summit	850	(2785)	71.3 cm (28.09 ins)	49.9 cm (19.63 ins)	32.9 cm (12.94 ins)
760 m (2500 ft) west of summit	625	(2050)	121.0 cm (47.64 ins)	54.4 cm (21.41 ins)	37.0 cm (14.56 ins)
7600 m (25,000 ft) west of summit	350	(1150)	39.9 cm (12.97 ins)	46.7 cm (18.38 ins)	33.4 cm (13.16 ins)

(After Mink 1960)

The Khasi Hills in Assam are an exceptional instance of the combined effect of relief and surface configuration. Part of the monsoon current from the head of the Bay of Bengal (fig. 6.17) is channelled by the topography towards the high ground and the sharp ascent, which follows the convergence of the airstream in the funnel-shaped lowland to the south, results in some of the heaviest annual rainfall totals recorded anywhere. Cherrapunji, at an elevation of 1340 m, has a mean annual precipitation of 1144 cm (451 in) and the extremes recorded there include 569 cm (224 in) in July and 2299 cm (905 in) in a calendar year (see fig. 2.23).

Really high relief produces major changes in the main weather characteristics and is best treated as a special climatic type. The Kenya plateau, situated on the equator, has an average elevation of about 1500 m, above which rise the three volcanic peaks of Mt Kilimanjaro (5800 m), Mt Kenya (5200 m) and Ruwenzori (5200 m) nourishing permanent glaciers above 4270 m. Annual precipitation on the summit of Mt Kenya is about 114 cm (44 in), similar to amounts on the plateau to the south, but on the southern slopes between 2100 and 3000 m, and on the eastern slopes between about 1400 and 2400 m totals exceed 250 cm (100 in). Kabete (at an elevation of 1800 m near Nairobi) exhibits many of the features of tropical mountain climates, having a small annual temperature range (mean monthly temperatures are 19°C (67°F) for February and 16°C (60°F) for July), a high diurnal temperature range (averaging 9.5°C (17°F) in July and 13°C (24°F) in February) and a large average cloud cover (mean 7–8/10ths).

3 Cool ocean currents

Between the western coasts of the continents and the eastern rims of the subtropical high-pressure cells the ocean surface is relatively cold (see fig. 3.34). This is a result of the importation of water from higher latitudes by the dominant currents and the slow upwelling (sometimes at the rate of about 1 m in 24 hours) of water from intermediate depths due to the Ekman effect (ch. 3, F.3) and to the coastal divergence (ch. 3, B.1). This concentration of cold water gently cools the local air to dew point. As a result, dry warm air degenerates into a relatively cool, clammy, foggy atmosphere with a comparatively low temperature and little range along the west coast of South America between latitudes 4°S and 31°S, and off South-West Africa (8°S and 32°S). Thus Lima (Peru, elevation 111 m) has a mean annual temperature of only 18.3°C (65°F) and a mean annual temperature range of only 6.8°C (12°F). Callao, on the Peruvian coast, has a similarly low mean annual temperature of 19.4°C (67°F), whereas Bahia (at the same latitude on the Brazilian coast) has a corresponding figure of 25°C (77°F).

Nor is this cooling effect limited to stations near the coasts, for it is carried inland during the day at all times of the year by a pronounced sea-breeze effect (ch. 3, C.3). Along the west coasts of South America and South-West Africa the sheltering effect from the dynamically-stable easterly trades aloft provided by the nearby Andes and Namib Escarpment, respectively, allows incursions of shallow tongues of cold air to roll in from the south-west. These tongues of air are capped by strong

inversions at between 600 and 1500 m (2000 and 5000 ft) reinforcing the regionally low trade-wind inversions (see fig. 6.5) and thereby precluding the development of strong convective cells, except where there is orographically-forced ascent. Thus, although the cool maritime air perpetually bathes the lower western slopes of the Andes in mist and low stratus cloud and Swakopmund (South-West Africa) has an average of 150 foggy days a year, little rain falls on the coastal lowlands. Lima has a total mean annual precipitation of only 4.6 cm (1.8 in), although it receives frequent drizzle during the winter months of June to September, and Swakopmund has a mean annual rainfall of 1.6 cm (0.65 in). Heavier rain occurs on the rare instances when large-scale pressure changes cause a cessation of the diurnal sea breeze or when modified air from the South Atlantic or South Indian Ocean is able to cross the continents at a time when the normal dynamic stability of the trade-wind is disturbed. In South-West Africa the inversion is most likely to break down during either October or April allowing convectional storms to form, and Swakopmund recorded some 5.1 cm (2 in) of rain on a single day in 1934. Under normal conditions, however, the occurrence of precipitation is

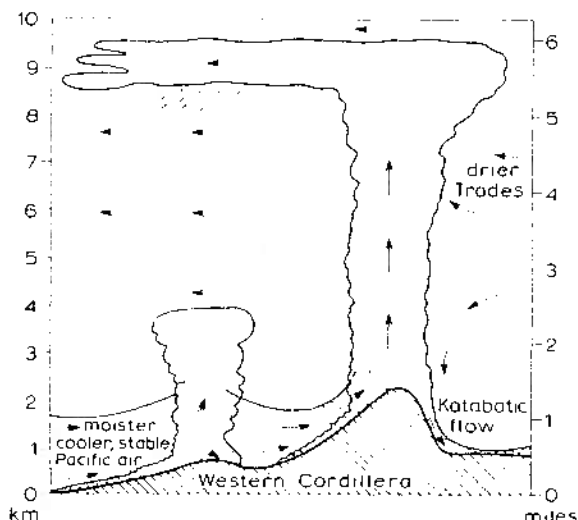


Fig. 6.25. The structure of the sea breeze in western Colombia (after Lopez. From Fairbridge 1967).

mainly limited to the higher seaward mountain slopes. From central Columbia to northern Peru the diurnal tide of cold air rolls inland for some 60 km (38 miles), rising up the seaward slopes of the Western Cordillera and overflowing into the longitudinal Andean valleys like water over a weir (fig. 6.25). Where this flow ascends or banks up against west-facing slopes it may under suitable conditions trigger off convectional instability in the overlying trades and produce thunderstorms. In South-West Africa, however, the 'tide' flows inland for some 130 km (80 miles) and rises up the 6000-ft (1800-m) Namib Escarpment without producing much rain because convectional instability is not produced and the adiabatic cooling of the air is more than offset by the radiational heating from the warm ground.

7 Urban and forest climates

The effects of climate upon all organisms and especially upon man have been recurrent themes in geography, but the growth of ideas relating to the wide field of ecology has brought about an increasing awareness of the influence exerted by the biosphere on weather and climate. The most extreme floristic environment – the forest – and the unintentional effects of man on local climate through his urban and industrial environments are considered in this chapter. However, since increasing interest is being shown in such topics as those relating to the possibility of weather modification and control, we begin with a brief résumé of some progress in applied meteorology.

On the smallest scale, man from earliest times has been concerned with modifying his most immediate environment to produce and sustain bodily comfort. Although advancing technology has made these efforts strikingly successful, their geographical significance lies both in spatial variety of man's dwellings and in the economic cost of maintaining bodily comfort (fig. 7.1) which, for modern advanced societies in extremely hot or cold conditions, can be very high. For example, Sweden's 'winter bill' is estimated at 5% of the national income, of which about one half is spent on the insulation and heating of buildings.

Meteorological modifications by man involve temporary interventions with respect to short-term weather systems or conditions, and here some progress has also been made. Cold fogs can be locally dissipated by the use of dry ice or the release of propane gas through expansion nozzles to

produce freezing. Warm fogs (i.e. having drops above freezing temperatures) present bigger problems, but attempts at dissipation have shown some limited success in evaporating droplets by artificial heating, the use of large fans to draw down dry air from above, the sweeping out of fog particles by jets of water, and the injection of electrical charges into the fog to produce coagulation. Attempts to produce precipitation have already been described in ch. 2, G.1, and all that can be claimed is that the seeding of some cumulus clouds at temperatures of -10°C to -15°C with dry ice or silver iodide probably produces a mean increase of precipitation of 10–15% from clouds which are already precipitating or

Table 7.1 Total energy of various individual phenomena and localized processes in the atmosphere (from Sellers 1965)

[Rates are relative to total solar energy intercepted by the earth (3.67×10^{21} cal/day)]

Solar energy received per day	1
Melting of average winter snow during the spring season	10^{-1}
Monsoon circulation	10^{-2}
World use of energy in 1950	10^{-2}
Strong earthquake	10^{-2}
Average depression	10^{-3}
Average hurricane	10^{-4}
Krakatoa explosion of August 1883	10^{-5}
Detonation of 'thermonuclear weapon' in April 1954	10^{-5}
Kinetic energy of the general circulation	10^{-5}
Average squall-line	10^{-6}
Average magnetic storm	10^{-7}
Average summer thunderstorm	10^{-8}
Detonation of Nagasaki bomb in August 1945	10^{-8}
Average earthquake	10^{-8}
Burning of 7000 tons of coal	10^{-8}
Daily output of Hoover Dam	10^{-8}
Moderate rain (10 mm over Washington, D.C.)	10^{-8}
Average forest fire in the United States, 1952–3	10^{-9}
Average local shower	10^{-10}
Average tornado	10^{-11}
Street lighting on average night in New York City	10^{-11}
Average lightning stroke	10^{-13}
Average dust devil	10^{-15}
Individual gust near the earth's surface	10^{-17}
Meteorite	10^{-18}

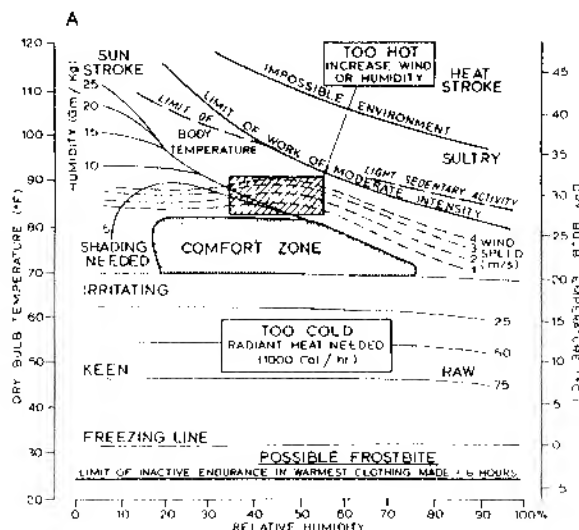


Fig. 7.1. The human relevance of climatic ranges (after Olgay 1963).

A. Atmospheric comfort, discomfort and danger for inhabitants of temperate climatic zones. Within the stippled limits of dry-bulb temperature and relative humidity the body feels comfortable at elevations of less than 300 m with customary indoor clothing, and performing sedentary or light work. Outside these limits corrective measures are necessary to restore the feeling of comfort. Below the 'comfort zone' radiant heat is needed, above it the skin temperature can be lowered by increasing the evaporation and heat convection either by raising the wind speed (for humid air) or by an increase of atmospheric moisture (for dry air).

are 'about to precipitate', with comparable increases up to 250 km downwind, whereas increases of up to 10% have resulted from seeding winter orographic storms. However, the seeding of depressions has produced no apparent precipitation increases, and it appears likely that clouds with an abundance of natural ice crystals or with above-freezing temperatures throughout are not susceptible to *rain-making*. The Russians have claimed some success in dissipating damaging hailstorms by the use of radar-directed artillery shells and rockets to inject silver iodide into high-liquid-water-content portions of clouds which freezes the available super-cooled water, so preventing it from accreting as shells on

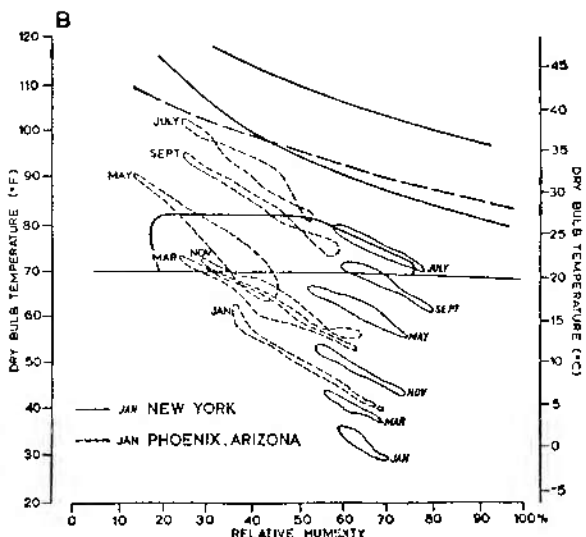


Fig. 7.1.
B. Mean daily dry-bulb temperatures and relative humidities during alternate months for New York City and Phoenix, Arizona, plotted on the 'comfort chart', indicating the need for both central heating and air conditioning.

growing ice crystals. Attempts to 'drain off' lightning charges by seeding clouds with silver iodide or with millions of metallic needles have produced even less certain results. Of all current attempts by man to control meteorological events none are more important than those relating to hurricanes. There is some indication that the seeding of the rising air in the cumulus eyewall may widen the ring of condensation and updraught, decrease the angular momentum of the storm, and thus the maximum speed of the winds. Such attempts are still in their infancy, as are plans to cut off surface evaporation ahead of hurricanes by spreading the ocean surface with oily materials.

Climatic modifications by man, the long-term continuation of large-scale meteorological controls, are for the most part of a highly speculative character. They vary from suggestions to produce widespread cirrus covers by rocket or aircraft seeding, to plans for locally changing sea temperatures and altering the surface patterns of insolation receipt by putting huge quantities of dust or metallic needles into orbit high above

326 Atmosphere, weather and climate

the earth. A particularly interesting idea is the creation of *thermal mountains* by painting desert surfaces black to decrease the albedo, stimulate convection and thereby increase cloudiness and precipitation downwind. Another suggestion is to create major inland seas in arid basins with interior drainage, such as Lake Eyre, Australia, and thereby modify the moisture balance. The proposed use of nuclear energy and, in particular, thermonuclear explosions in large-scale *geographical engineering* projects also has possible climatic implications. The excavation of huge lakes, the production of open cuts to divert water through mountains, the removal of pack-ice, the melting of ice-caps, the truncation of mountain ranges and the diversion of ocean currents (i.e. by blocking the Bering Straits) have all been seriously proposed, but both the energy (table 7.1) and expenditure involved and, particularly, the unknown attendant dangers in such permanent large-scale tampering with the earth's surface and atmosphere will postpone such schemes — perhaps permanently!

The first step must be to develop adequate mathematical models simulating the behaviour of the earth-atmosphere system so that all the possible effects of these schemes can be predicted in advance. The realization of the full potential of these models awaits the collection of more data (largely from satellites) relating to the earth-atmosphere thermal and radiative properties, albedo, roughness, soil moisture content, etc., as well as the development of better representations of small-scale processes in the models.

A Urban climates

Until man develops more direct methods of controlling the mechanisms of the atmosphere, his most profound climatic influence will remain the modification of local climates by the construction of large cities, although it should be recognized that urban climatic influences are also experienced at both the regional and global levels (see chs. 1, A.4 and 8.C). The construction of every house, road or factory destroys existing microclimates and creates new ones of great complexity depending on the design, density and function of the building. Despite the great internal variation of urban climatic influences, it is possible to make certain generalizations regarding the effects of urban structures under three main headings:

1. Modification of atmospheric composition.
2. Modification of the heat budget.
3. Other effects of modifications of surface roughness and composition.

I Modification of atmospheric composition

The city atmosphere is notoriously liable to pollution, particularly as the result of combustion, and this has effects which involve changes in the thermal properties of the atmosphere, cutting down the passage of sunlight, and providing abundant condensation nuclei. Although pollution poses a general problem both for city dwellers and planners, it is convenient to examine its sources under the following headings:

- (a) *Aerosols.* The production of suspended particulate matter (measured in mg m^{-3} or $\mu\text{g m}^{-3}$) chiefly of carbon, lead and aluminium compounds and silica.
- (b) *Gases.* The production of gases (measured in parts per million: ppm) can be viewed either from the traditional standpoint with its concentration on industrial and domestic coal burning and the production of such gases as sulphur dioxide, or from the newer standpoint of petrol and oil combustion and the production of carbon monoxide, hydrocarbons, nitrogen oxides, ozone and the like.

a. *Aerosols.* As has already been pointed out (see ch. 1, A.2 and 4), the thermal economy of the globe is significantly affected by the natural production of aerosols which are deflated from deserts, erupted from volcanoes, produced by fires, etc. Their overall thermal effect is probably one of cooling, due to the lowering of atmospheric transmissivity, and this counteracts the increases of heat associated with rises in the amount of carbon dioxide and other gases (see fig. 1.3). During the last century the average dust concentration has increased, particularly in Eurasia, due only in part to such eruptions as those of Mt Agung in Bali (1963) and Kamchatka (1966). The proportion of atmospheric dust directly or indirectly attributable to human activity has been estimated at 30% (see ch. 1, A.4). As an example of the latter, it is interesting that the North African tank battles of World War II disturbed the desert surface to such an extent that the material subsequently deflated was visible in clouds over the Caribbean.

The concentration of small nuclei ($0.01\text{--}0.1 \mu\text{m}$ diameter) averages some 9500 cm^{-3} in the British countryside, but is typically $150,000 \text{ cm}^{-3}$ and can reach $4,000,000 \text{ cm}^{-3}$ in cities, as was measured near ground level in the industrial section of Vienna in 1946. Similarly, the concentration of larger particles ($0.5\text{--}10 \mu\text{m}$ diameter) has been measured at $25\text{--}30 \text{ cm}^{-3}$ in the city of Leipzig, as against $1\text{--}2 \text{ cm}^{-3}$ in the rural environs. The

greatest concentrations of smoke generally occur with low wind speeds, low vertical turbulence, temperature inversions, high relative humidities and air moving from the pollution sources of factory districts or areas of high density housing (pl. 32). The character of domestic heating and power demands causes city smoke pollution to take on striking seasonal and diurnal cycles, with the greatest concentrations occurring about 0800 in early winter (fig. 7.2). The sudden morning increase is also partly a

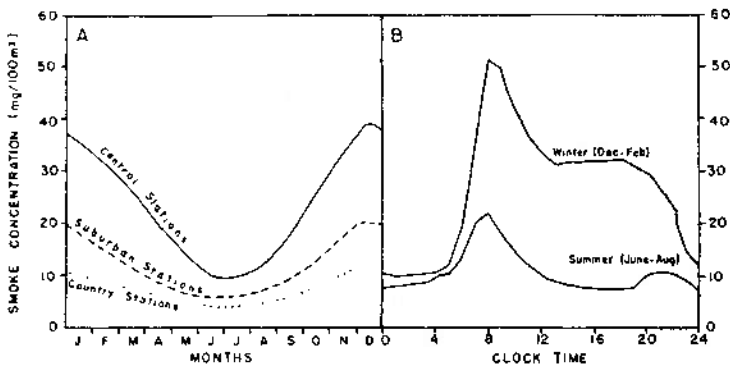


Fig. 7.2. Annual (A) and daily (B) cycles of smoke pollution at Leicester for the period 1937-9 (after Meeham 1952).

result of natural processes. Pollution trapped during the night beneath a stable layer a few hundred metres above the surface may be brought back to ground level when thermal convection sets off vertical mixing. This process is known as *fumigation*. Figure 7.3 shows the striking results of the accumulation of air pollution which occurred over the British industrial city of Sheffield in mid-December 1964 during a period of cloudless skies, weak air flow, maximum long-wave radiation, and the development of near-surface temperature inversions and radiation fog. These conditions were associated with a smoke concentration of 10% above the monthly average on 14 December, which increased to 100% above the average on 16 December.

The most direct effect of particulate pollution is to reduce incoming radiation and sunshine. Pollution, plus the associated fogs (termed *smog*), used to cause some British cities to lose 25-55% of the incoming solar radiation during the period November to March. In 1945 it was estimated that the city of Leicester lost 30% of incoming radiation in winter, as against 6% in summer. These losses are naturally greatest when the sun's

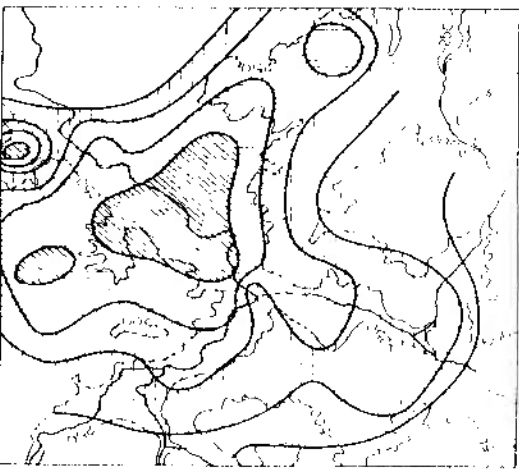
rays strike the smog layer at low angle. Compared with the radiation received in the surrounding countryside, Vienna loses 15–21% of radiation when the sun's altitude is 30°, but the loss rises to 29–36% with an altitude of 10°. The effect of smoke pollution is dramatically illustrated by figure 7.4 by comparing conditions before and after the enforcing of the Clean Air Act of 1956 in London. Before 1950 there was a striking difference of sunshine between the surrounding rural areas and the city centre (fig. 7.4A) which could mean a loss of mean daily sunshine of 16 minutes in the outer suburbs, 25 minutes in the inner suburbs and 44 minutes in the city centre. It must be remembered, however, that smog layers also impeded the re-radiation of surface heat at night and that this blanketing effect contributed to higher night-time city temperatures. The use of smokeless fuels and other pollution controls cut London's total smoke emission from 1.4×10^8 kg (141,000 tons) in 1952 to 0.9×10^8 kg (89,000 tons) in 1960, and figure 7.4B shows the increase in average monthly sunshine figures for the period 1958–67 as compared with those of 1931–60.

The abundance of condensation nuclei in city atmospheres, particularly those situated on low-lying land adjacent to large rivers, explains the former abundance of city fogs. Between August 1944 and December 1946, for example, suburban Greenwich had a monthly average of more than 20 days with good visibility at 0900 hours, whereas central London had less than 15. Occasionally very stable atmospheric conditions combined with excessive pollution production to give dense smog of a letal character. During the period 5–9 December 1952 a temperature inversion over London caused a dense fog with visibility less than 10 m for 48 consecutive hours, resulting in 12,000 more deaths (mainly from chest complaints) during the period December 1952 to February 1953 compared with the same period the previous year. The close association of the incidence of fog with increasing industrialization and urbanization was well shown by the city of Prague, where the mean annual number of days with fog rose from 79 during the period 1860–80 to 217 during 1900–20.

b Gases. Along with the pollution by smoke and other particulate matter produced by the traditional urban and industrial activities involving the combustion of coal and coke, has been associated the generation of pollutant gases. Before the Clean Air Act it was estimated that, whereas 80–90% of London's smoke was produced by domestic fires, these were responsible for only 30% of the sulphur dioxide released in the atmosphere – the remainder being contributed by electricity power stations (41%) and factories (29%). Figure 7.3 illustrates the association between

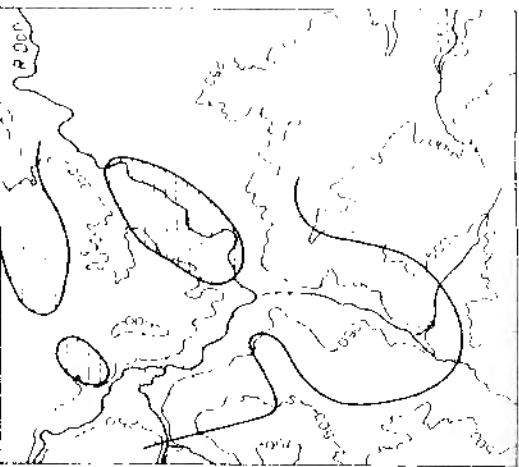
16 12 64

SMOKE



14 12 64

SMOKE



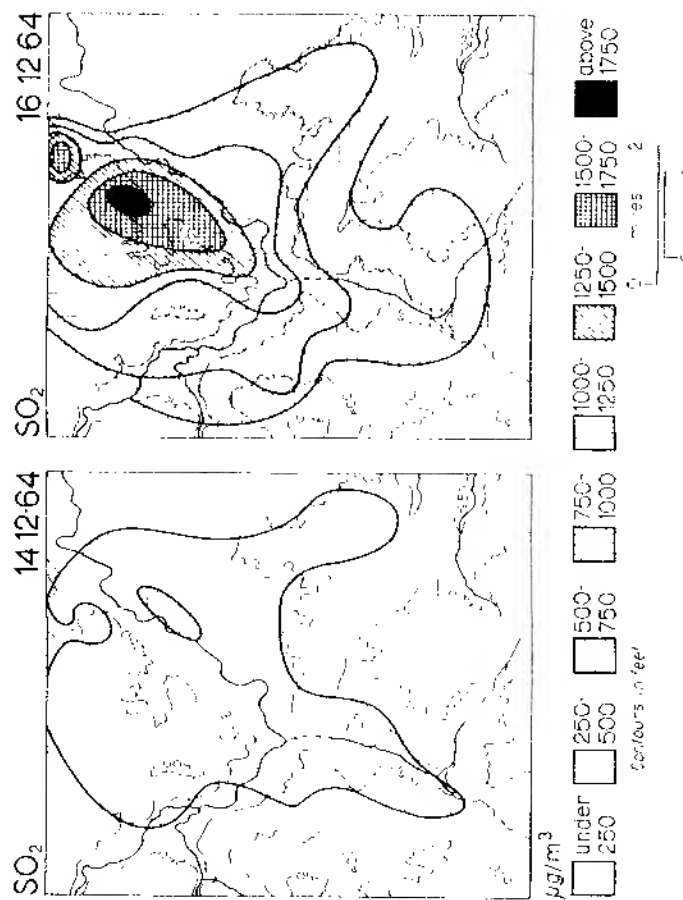


Fig. 7.3. Average values of air pollution by smoke and sulphur dioxide for Sheffield, England, on 14 and 16 December 1964 (from Garnett 1967).

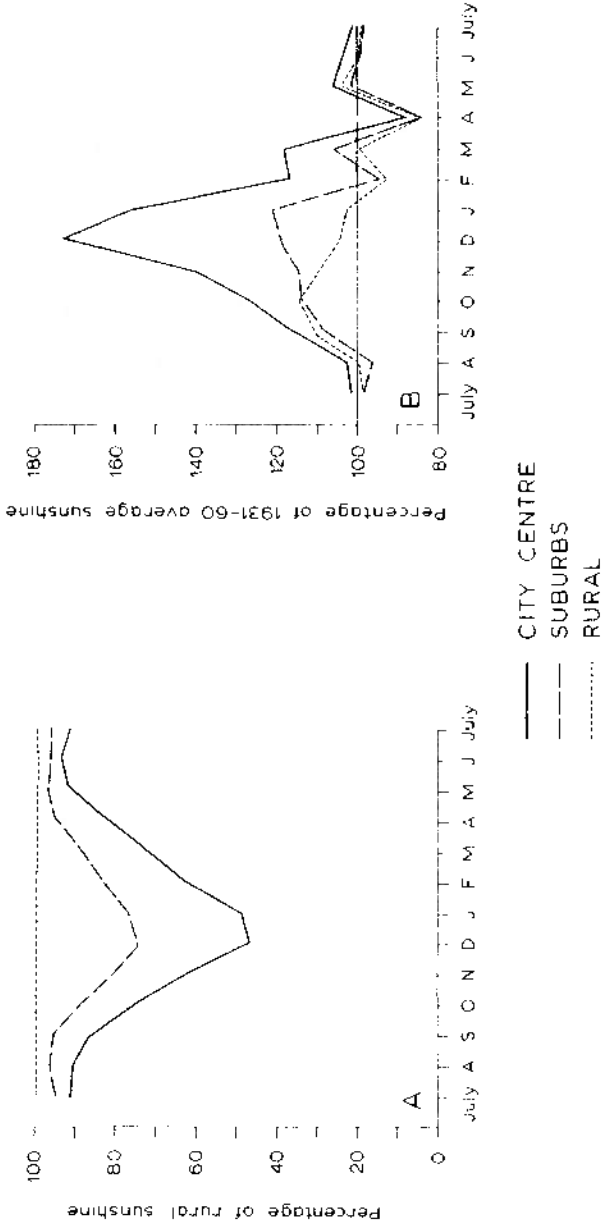


Fig. 7.4. Sunshine in and around London.

- Mean monthly bright sunshine recorded in the city and suburbs for the years 1921-50, expressed as a percentage of that in adjacent rural areas. This shows clearly the effects of winter atmospheric pollution in the city (after Chandler 1965).
- Mean monthly bright sunshine recorded in the city, suburbs and surrounding rural areas during the period 1958-67, expressed as a percentage of the averages for the period 1931-60. This shows the effect of the 1956 Clean Air Act in increasing the receipt of winter sunshine, in particular, in central London (after Jenkins 1969).

pollution by smoke and that by sulphur dioxide in Sheffield some 10 years ago; it is significant that on 16 December 1964 the concentration of sulphur dioxide in the city air had risen to three times the monthly average.

Urban complexes are being affected by a newer less-obvious, but nevertheless equally serious, form of pollution resulting from the combustion of petrol and oil by cars, lorries and aircraft, as well as from petrochemical industries. Los Angeles, lying in a topographically-constricted basin and often subject to temperature inversions, is the prime example of such pollution, although this affects all modern cities to some extent. In Los Angeles 7 million people use some 4 million private cars, consuming 30 million litres of petrol per day and producing more than 12,000 tons of pollutants. To this is added the results of the consumption of 0.5 million litres per day of diesel fuel by 13,500 lorries and buses and 2.5 million litres of aviation fuel consumed in the vicinity of the city. Even with controls, 7% of the petrol from private cars is emitted in an unburned or poorly-oxidized form, another 3.5% as petro-chemical smog and 33–40% as carbon monoxide. The production of the Los Angeles smog which, unlike traditional city smogs, occurs characteristically during the daytime in summer and autumn, is the result of very complex chains of chemical reactions. For example, cars emit nitric oxide (NO) which the action of sunlight, in the presence of hydrocarbons, turns into nitrogen dioxide (NO_2). This is a very efficient absorber of ultra-violet radiation and hence there is a positive feedback reaction which also involves the production of ozone. The effect of this smog is not only to modify the radiation budget of cities but to produce such a human health hazard that in Tokyo, for instance, citizens sometimes wear respiratory masks in the street in self-defence!

Polluted atmospheres commonly assume well-marked physical configurations around urban areas, particularly the dome and the plume (fig. 7.5). These configurations are very dependent upon environmental lapse rates, the presence of temperature inversions and, particularly, on wind speed. A wind speed as low as 2 m sec^{-1} (5 mph) is sufficient to displace the Cincinnati pollution dome downwind and a speed of 3.5 m sec^{-1} (8 mph) will disperse it into a plume. Under conditions of an intense pollution source, steady large-scale surface airflow and vertical atmospheric stability, pollution plumes may extend downwind for hundreds of kilometres. Pollution plumes originating in the Chicago-Gary conurbation have been observed from high-flying aircraft to extend almost to Washington D.C.

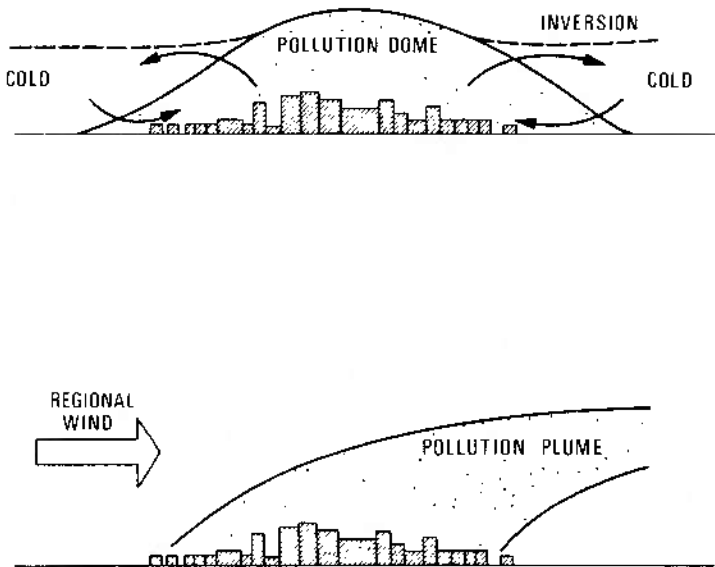


Fig. 7.5. Urban pollution dome and plume.

2 Modification of the heat budget

The thermal characteristics of urban areas are in marked contrast to those of the surrounding countryside, and the generally higher urban temperatures are the result of the interaction of the following factors:

- Changes in the radiation balance due to atmospheric composition.
- Changes in the radiation balance due to albedo, heat conductivity and thermal capacity of urban surface materials.
- The production of heat by human activities.
- The reduction of heat diffusion due to changes in airflow patterns as the result of urban surface roughness.
- The reduction in thermal energy required for evaporation and evapotranspiration due to the surface character, rapid drainage and generally lower wind speeds of urban areas.

Consideration of the last two factors will be left to ch. 7, A.3.

a Atmospheric composition. Air pollution makes the transmissivity of

urban atmospheres significantly less than that of nearby rural areas. For example, during the period 1960–69 the atmospheric transmissivity over Detroit averaged 9% less than that for nearby areas, and reached 25% less under calm conditions. Table 7.2 gives comparable urban and rural energy budget figures for the Cincinnati region during the summer of 1968 under anticyclonic conditions with $\leq 3/10$ cloud and a wind speed of $\leq 2 \text{ m sec}^{-1}$ (5 mph).

Table 7.2 Energy budget figures for the Cincinnati region during the summer of 1968 (from Bach and Patterson 1969). (10^3 ly min^{-1}).

	<i>Central business district</i>			<i>Surrounding country</i>		
	0800	1300	2000	0800	1300	2000
Short wave, incoming ($Q + q$)	413*	1094	—	439	1165	—
Short wave, reflected [$Q + q$]a†	61†	172†	—	114	228	—
Net long wave radiation (L_n)	-88	-144	-140	-88	-96	-96
Net radiation (R_n)	264	778	-140	237	841	-96
Heat produced by human activity	52	41	37†	0	0	0

* Pollution peak.

† An urban surface reflects less than agricultural land, and a rough skyscraper complex can absorb up to 6 times more incoming radiation.

| Replaces more than $\frac{1}{2}$ of the long wave radiation loss in the evening.

b Urban surfaces. Primary controls over a city's thermal climate are the character and density of urban surfaces, that is, the total surface area of buildings and roads, as well as the building geometry. Table 7.2 shows the relatively high heat absorption of the city surface. A problem of measurement is that, the stronger the urban thermal influence, the weaker is the heat absorption at street level, and, consequently, observations made only in streets may lead to erroneous results.

c Human heat production. It has been estimated that large German cities produce $15\text{--}30 \text{ ly day}^{-1}$ from combustion, which compares with the amounts received by direct insolation of 52 ly day^{-1} in December and

336 Atmosphere, weather and climate

more than 500 ly day⁻¹ in June. In Hamburg, prior to 1956, the average heat supply from coal burning during December was 40 ly day⁻¹, compared with a radiation from the sun and sky to 34 ly day⁻¹. Calculations for London in the 1950s suggested that winter domestic fuel consumption produced a temperature increase of about 0.6° C in the city, and that made up about $\frac{1}{3}$ of the total city heat excess over adjacent rural areas. Table 7.2 shows the significant proportion of Cincinnati's energy budget which is produced by human activity, even in summer. This heat production averaged 37×10^{-3} ly min⁻¹ for both day and night, of which $\frac{2}{3}$ was produced by industrial, commercial and domestic sources and $\frac{1}{3}$ by cars. In terms of the future, it has been estimated that by AD 2000 the Boston-Washington megalopolis may accommodate up to 56 million people in a continuous urban area of 30,000 km² (11,600 sq. miles), and that this concentration of human activity would produce heat equivalent to 50% of the total winter solar radiation recorded on a horizontal surface and 15% of the total summer solar radiation.

d. Heat islands. The net effect of the urban thermal processes is to make city temperatures generally higher than those in the surrounding rural areas, mainly due to the turbulent diffusion of sensible heat from warm buildings and the absorption of long wave radiation emitted by the city surface and its pollution blanket. This *heat island* effect may result in minimum urban temperatures being 5–6°C (9–11°F) greater than those of the surrounding countryside, and these differences may be as much as 6–8°C (11–14°F) in the early hours of calm, clear nights in large cities. It should be noted that, because this is a *relative* phenomena, the heat island effect also depends on the rate of rural cooling, which is influenced by the magnitude of the regional environmental lapse rate.

For the period 1931–60, the centre of London had a mean annual temperature of 11.0°C (51.8°F), comparing with 10.3°C (50.5°F) for the suburbs, and 9.6°C (49.2°F) for the surrounding countryside. Differences are even more marked during still air conditions, especially at night under a regional inversion (fig. 7.6). For this heat island effect to operate effectively there must be wind speeds of less than 5–6 m sec⁻¹ (12–14 mph), and it is especially in evidence on calm nights during summer and early autumn when it has steep cliff-like margins and the highest temperatures associated with the highest density of urban dwellings. In the absence of regional winds, a well-developed heat island may even generate its own inward local wind circulation at the surface. Thus the thermal contrasts of a city, like those of many other of its climatic features, depend on its topographic situation, and are greatest for

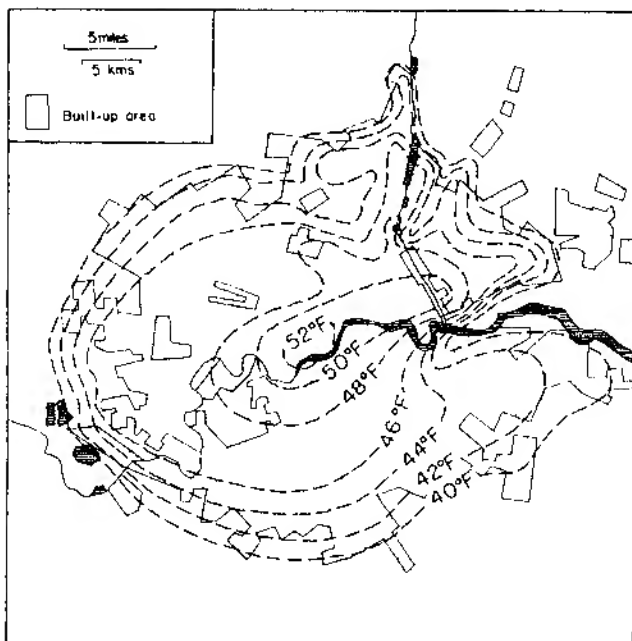


Fig. 7.6. Distribution of minimum temperatures ($^{\circ}\text{F}$) in London on 14 May 1959, showing the relationship between the 'urban heat island' and the built-up area (after Chandler 1965).

sheltered sites with light winds. The fact that for London urban/rural temperature differences are greatest in summer, when direct heat combustion and atmospheric pollution are at a minimum, indicates that heat loss from buildings by radiation is the most important single factor contributing to the heat island effect. Seasonal differences are not necessarily the same, however, in other macroclimatic zones.

The effects on minimum temperatures are especially significant. Cologne, for example, has an average of 34% less days with minima below 0°C (32°F) than its surrounding area, the corresponding figure for Basle being 25% less. In London, Kew has an average of some 72 more days with frost-free screen temperatures than rural Wisley. Precipitation characteristics are also affected and in pre-1917 Berlin 21% of the incidences of rural snowfall were associated with either sleet or rain in the city centre.

Although it is difficult to isolate changes in temperatures which are due to urban controls from those due to other influences (see ch. 8), it has been suggested that city growth is often accompanied by an increase in mean annual temperature, that of Osaka, Japan, rising by 2.6°C (4.5°F) in the last 100 years and that of Tokyo by 1.5°C (3°F). These results may be coincidental, however, since there appears to be no simple relationship between city size and intensity of the heat island. Chandler has shown that Leicester, with a population of 270,000, exhibits warming comparable in intensity with that of central London over smaller sectors. This suggests that the thermal influence of city size is not as important as that of urban density. The vertical extent of the heat island is little known, although this is now a subject of study. In the case of cities with skyscrapers the vertical and horizontal patterns of wind and temperature must be very complex.

3 Modification of surface characteristics

Urban structures have considerable effects on the movement of air both by producing turbulence as a result of their roughening the surface and by the channelling effects of the street 'gorges'. On the average, city wind speeds are lower than those recorded in the surrounding open country owing to the sheltering effect of the buildings, and central average wind speeds are usually at least 5% less than those of the suburbs. In 1935, for example, winds exceeding 10.5 m sec^{-1} (24 mph) were recorded on the relatively open Croydon Airport (London suburbs) for a total of 371 hours, whereas the corresponding figure was only 13 hours for the closely built-up South Kensington. However, the urban effect on air motion varies greatly depending on the time of day and season. During the day city wind speeds are considerably less than those of surrounding rural areas, but during the night the greater mechanical turbulence over the city means that the higher wind speeds aloft are transferred to the air at lower levels by turbulent mixing. During the day (1300 hours) the mean annual wind speed for London Airport (open country within the suburbs) was 2.9 m sec^{-1} (6.4 mph), compared with a 2.1 m sec^{-1} (4.7 mph) in central London for the period 1961–62. The comparative figures for night (0100 hours) were 2.2 m sec^{-1} (4.9 mph) and 2.5 m sec^{-1} (5.6 mph). Rural-urban wind speed differences are most marked with strong winds and the effects are therefore more evident during winter than during summer, when a higher proportion of low speeds is recorded in temperature latitudes.

The effect of urbanization on surface moisture relationships is also important. The absence of large bodies of standing water and the rapid

removal of surface run-off through drains decreases local evaporation. In addition, the lack of an extensive vegetational cover eliminates much evapotranspiration and this is an important source of augmenting urban heat. For these reasons the air of mid-latitude cities has a tendency towards lower absolute humidities than that of their surroundings, especially under conditions of light wind and cloudy skies. On other occasions of calm, clear weather the streets trap warm air, which retains its moisture because less dew is deposited on the warm surfaces of the city. Humidity contrasts between urban and rural areas are most noticeable in the case of relative humidity, which can be as much as 30% less in the city by night as a result of the higher temperatures.

Urban influences on precipitation (excluding fog) are much more difficult to determine with any precision, partly because there are few rain gauges in cities and because air turbulence makes their 'catch' unreliable. It is now fairly certain, however, that urban areas in Europe and North America are responsible for local conditions which, in summer especially, can trigger-off excesses of precipitation under marginal conditions. These triggers involve the orographic and turbulence effects of the buildings, the increased density of condensation nuclei, and thermal convection. Recordings for Munich showed 11% more days of light rain (0.1–0.5 mm or 0.004–0.12 in) than in the surrounding countryside, and Nürnberg has recorded 14% more thunderstorms than its rural environs. European and North American cities apparently record 6–7% more days with rain per year than their surrounding regions, giving 5–10% increase in urban precipitation. The effect is generally more marked in the cold season in North America, although urban areas in the midwest of the United States significantly increase summer convective activity with more frequent thunderstorms (20–30% more downwind of industrial areas of St Louis, for example) compared with rural areas. Over south-east England during 1951–60, summer thunderstorm rain (which comprised 5–15% of the total precipitation) was especially concentrated in west, central and southern London (fig. 7.7) and contrasted strikingly with the distribution of mean annual total rainfall. During this period London's thunderstorm rain was of the order of 20–25 cm (8–10 in) greater than that in rural south-east England. There has been some suggestion that an increase in urban industrialization might be reflected in increased precipitation, and between 1941 and 1969 the region 20 km (13 miles) downwind of the rapidly-expanding Bombay urban industrial complex recorded an increase in rainfall of up to 15% over that of the surrounding countryside. Similarly, the mean annual precipitation of the town of Rochdale, Lancashire, is held to have increased during its industrial growth from 108.7

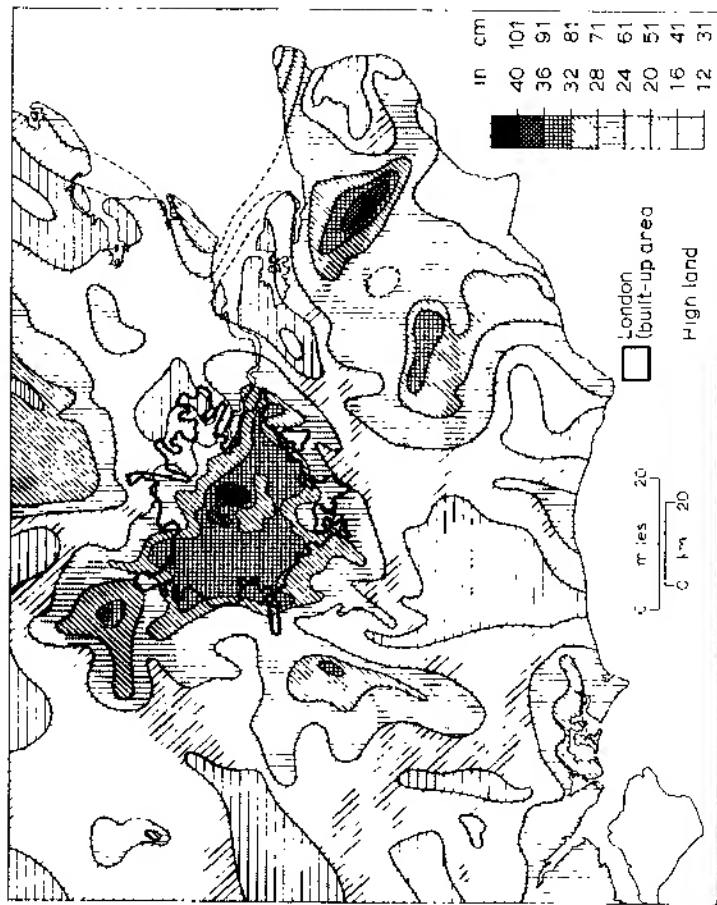


Fig. 7.7. The distribution of total thunderstorm rain in south-east England during the period 1951-60
(after Atkinson 1968).

cm (42.81 in) in 1898–1907 to 123.6 cm (48.65 in) in 1918–27. In the latter instance the greatest increases appear to have occurred on weekdays, when the factories were working. Even so, it is quite possible that such differences represent chance fluctuations or widespread climatic trends. These trends will be examined in ch. 8. Table 7.3 summarizes some of the more secure climatic differences between cities and surrounding rural areas.

Table 7.3 Average urban climatic conditions compared with those of surrounding rural areas. (Partly after W.M.O. 1970)

Atmospheric composition	Carbon dioxide	× 2
	Sulphur dioxide	× 200
	Nitrogen oxides	× 10
	Carbon monoxide	× 200 (+)
	Total hydrocarbons	× 20
	Particulate matter	× 3 to 7
Radiation	Global solar	– 15 to 20%
	Ultra-violet (winter)	– 30%
	Sunshine duration	– 5 to 15%
Temperature	Winter minimum (average)	+ 1° to 2°C
	Heating degree days	– 10%
Wind speed	Annual mean	– 20 to 30%
	Number of calms	+ 5 to 20%
Fog	Winter	+ 100%
	Summer	+ 30%
Cloud		+ 5 to 10%
Precipitation	Total	+ 5 to 10%
	Days with < 5 mm (< 0.2 in.)	+ 10%

B Forest climates

Geographers have been accustomed to considering the effects of climate on the surface vegetational cover, but it must be recognized that any variation of surface characteristics affects the local climate to some extent. Indeed, much research is currently being directed towards the microclimatic conditions associated with growing crops. When vegetation assumes its most dense and elevated forms in forests, the effects on local, and sometimes regional, climates are extremely important.

The vertical structure of a forest conditions to a great extent the control which it will exercise over local atmospheric conditions. At the same time it must be recognized that botanical differences are usually very important, and that the same type of forest stand may have differing climatic influences at different elevations, within different climatic zones, and at different times of the year. The nature of this organization of the stand in space depends in turn on the vegetational species, the ecological associations, the age of the stand, and other botanical considerations. Much of the climatic influence of a forest can be explained in simple terms of the geometry of the forest, including morphological characteristics, size, coverage and stratification. Morphological characteristics include amount of branching (bifurcation), the periodicity of growth (i.e. evergreen or deciduous), together with the size, density and texture of the leaves. Tree size is obviously important, but this may be greatly confused, particularly in tropical forests, by the great variety of sizes present locally. Crown coverage is important in terms of the physical obstruction presented by the canopy to radiation exchange and air movements. Considerations of stratification imply that one needs a particularly detailed view of the vertical forest structure in considering its climatic effects.

An obvious example of the microclimatic effects of different spatial forest organizations can be gained from a comparison of the features of tropical rain forests and temperate forests. In tropical forests the average height of the taller trees is of the order of 46–55 m (150–180 ft), individuals rising to over 60 m (200 ft). The dominant height of temperate forests is up to 30 m, so that neither temperate nor most tropical forests can compare in height with the western American redwoods (*Sequoia sempervirens*). Tropical forests commonly possess a great variety of species, there being seldom less than 40 per hectare (100 hectares = 1 km²) and sometimes over 100; comparing with less than 25 (occasionally only one) tree species with a trunk diameter greater than 10 cm or 4 in in Europe and North America. Many British woodlands, for example, have almost continuous canopy stratification from low shrubs to the tops of 36-m beeches, whereas tropical forests are strongly stratified with dense undergrowth, unbranching trunks, and commonly two upper strata of foliage. This stratification, the second or lower of which is usually the more dense, results in rather more complex microclimates in tropical forests than in temperate stands.

It is convenient to describe the climatic effects of forest stands in terms of their modification of energy transfers and of the airflow, their

modification of the humidity environment, and their modification of the thermal environment.

1 Modification of energy transfers

A major effect of a forest canopy is to blanket both incoming and outgoing radiation. The reflectivity of vegetated surfaces to incoming radiation (or albedo) has a wide range depending on the character of the vegetation and its density. For a complete covering of short, green crops the albedo is about 26%, but for temperate forests the figures range between 10 and 20% (fir 10%, young pine 14%, young oak 18%). Species of drier regions possess much higher albedos, with figures of the order of 30–38% for desert shrubs.

Besides reflecting energy, the forest canopy traps energy, and it has been calculated that for dense red beeches (*Fagus sylvatica*) 80% of the incoming radiation is intercepted by the tree-tops and less than 5% reaches the forest floor. The greatest trapping occurs in sunny conditions, for when the sky is overcast the incoming diffuse radiation has greater possibility of penetration laterally to the trunk space (fig. 7.8A). Visible light, however, does not give an altogether accurate picture of total energy penetration for more ultraviolet than infrared radiation is absorbed in the

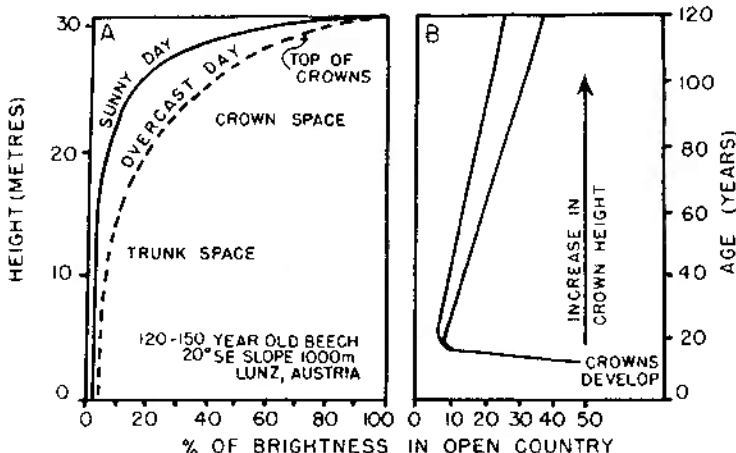


Fig. 7.8. Amount of light as a function of height (A) for a thick stand of red beeches (*Fagus sylvatica*) in Austria, and as a function of age (B) for a Thuringian spruce forest (after Geiger 1965).

crowns. For example, only 7.6% of short-wave radiation (less than 5000 Å) reached a forest floor in Nigeria, as against 45.3% greater than 6000 Å. As far as light penetration is concerned there are obviously great variations depending on type of tree, time of year, age, crown density and height. About 50–75% of the outside light intensity may penetrate to the floor of a birch-beech forest, 20–40% for pine, 10–25% for spruce and fir; but for tropical Congo forests the figure may be as low as 0.1% and one of 0.01% has been recorded for a dense elm stand in Germany. Of course, one of the most important effects of this is to reduce the length of daylight. For deciduous trees, more than 70% of the light may penetrate when they are leafless. Tree age is also important in that this controls both crown cover and height. Figure 7.8B shows this rather complicated effect for spruce in the Thuringian Forest, Germany. For a Scots pine (*Pinus sylvestris*) forest in Germany 50% of the outside light intensity was recorded at 1.3 years, only 7% at 20 years and 35% at 130 years. Figure

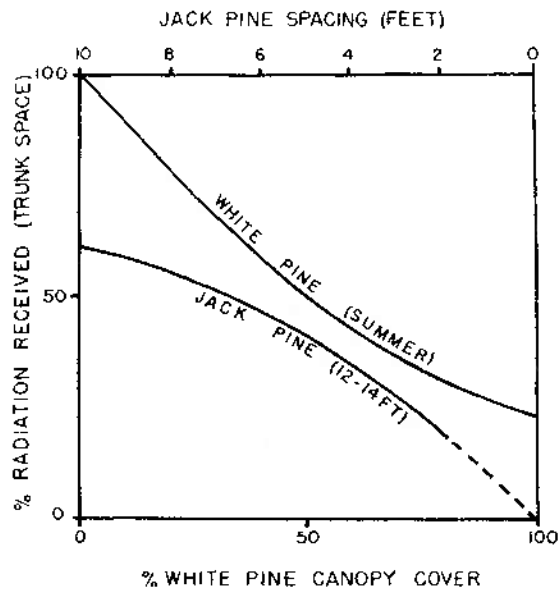


Fig. 7.9. Percentage of outside radiation received in pine forest trunk spaces, as a function of white pine (*Pinus strobus*) canopy cover in Massachusetts, and of jack pine (*Pinus banksiana*) spacing in Vermont (data from Kittredge 1948).

7.9 shows the effects of canopy cover and tree-spacing on the amount of trunk-space radiation received. In a 25-year-old stand of red pine (*Pinus resinosa*) in Minnesota the interior light intensity fell from 60% with a tree density of 1300 trees per hectare to 15% with 6500 trees per hectare. Yet most tree-spacing is irregular and it has been estimated that only 0.5–2.5% of a forest floor in Guyana receives direct illumination.

2 Modification of the airflow

Forests impede both the lateral and vertical movement of air, but as it is more convenient to treat the latter in connection with thermal modifications we shall be concerned here with forests as obstructions to lateral air displacements. In general air movement within forests is slight compared with that in the open, and quite large variations of outside wind velocity have little effect inside woods (fig. 7.10A). Measurements for

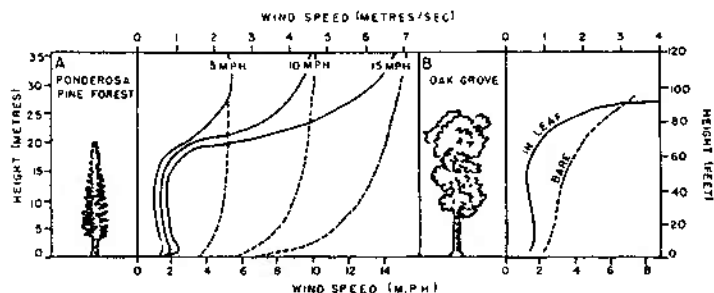


Fig. 7.10. Influence on wind velocity profiles exercised by (A) a dense 45-year-old ponderosa pine (*Pinus ponderosa*) stand in the Shasta Experimental Forest, California (after Fons, and Kittridge 1948), the dashed lines indicating the wind profile over open country; and (B) an oak grove (after R. Geiger and H. Amann, and Geiger 1965).

European forests show that 30 m (100 ft) of penetration reduces wind velocities to 60–80%, 60 m (200 ft) to 50%, and 120 m (400 ft) to only 7%. A speed of 2.2 m sec^{-1} (4.9 mph) outside a Brazilian evergreen forest was found to be reduced to 0.5 m sec^{-1} (1.1 mph) at about 100 m (300 ft) within, and to be negligible at 1000 m. In the same location external storm winds of 28 m sec^{-1} (62.7 mph) were reduced to 2 m sec^{-1} (4.2 mph) some 11 km (7 miles) deep in the forest. Where there is a complex vertical structuring of the forest wind velocities become more complex. Thus whereas in the crowns (23 m; 75 ft) of a Panama rain forest the wind

velocity was 75% of that outside, it was only 20% in the undergrowth (2 m; 6·5 ft). Other influences include the density of the stand and the season. For dense pine stands in Idaho simultaneous recordings showed the wind velocity to be $0\cdot6 \text{ m sec}^{-1}$ (1·3 mph) in a cut area, $0\cdot4 \text{ m sec}^{-1}$ (0·9 mph) half cut, and $0\cdot1 \text{ m sec}^{-1}$ (0·2 mph) in the uncut stand. The effect of season on wind velocities in deciduous forests is shown by fig. 7.10B. Observations in a Tennessee mixed-oak forest showed January forest wind velocities to be 12% of those in the open whereas those in August had dropped to 2%.

Knowledge of the effect of forest barriers on winds has been utilized in the construction of wind breaks to protect crops and soil, and, for example, the cypress breaks of the southern Rhone valley and the Lombardy poplars (*Populus nigra*) of the Netherlands form distinctive features of the landscape. It has been found that the denser the obstruction the greater the shelter immediately behind it, although the downwind extent of its effect is reduced by lee turbulence set up by the barrier. The maximum protection is given by the filtering mechanism produced by a break of about 40% penetrability (fig. 7.11A). An obstruction begins to have an effect about 18 times its own height upwind (fig. 7.11B), and the downwind effect can be increased by the *back coupling* of more than one belt (fig. 7.11A).

There are also some less obvious microclimatic effects of forest barriers. One of the most important is that the reduction of horizontal air movement in forest clearings increases the frost hazard on winter nights. A less important aspect is the removal of dust from the air by the filtering action of forests; measurements $1\frac{1}{2}$ km upwind, on the lee side and $1\frac{1}{2}$ km downwind of a kilometre-wide German forest gave dust counts (particles per litre) of 9000, less than 2000 and more than 4000, respectively.

The catch of moisture in the form of horizontally moving fog particles is another aspect of the obstructive features of forest microclimatology. Measurements in association with a 2-m high and 13-m thick shelter belt on the south-east Hokkaido coast, Japan, in July 1952 showed this filtering effect on advection fog rolling in from the sea, in that 20 m downwind of the obstruction the humidity was only $0\cdot1 \text{ g m}^{-3}$ (mean wind velocity $2\cdot55 \text{ m sec}^{-1}$), compared with $0\cdot3 \text{ g m}^{-3}$ (mean wind velocity $3\cdot4 \text{ m sec}^{-1}$) a similar distance upwind. In extreme cases so much fog can be filtered from laterally moving air that *negative interception* can occur, where there is a higher precipitation catch within a forest than outside. The winter rainfall catch outside a eucalyptus forest near Melbourne, Australia was 50 cm (19·7 in), whereas inside the forest it was 60 cm (23·6 in).

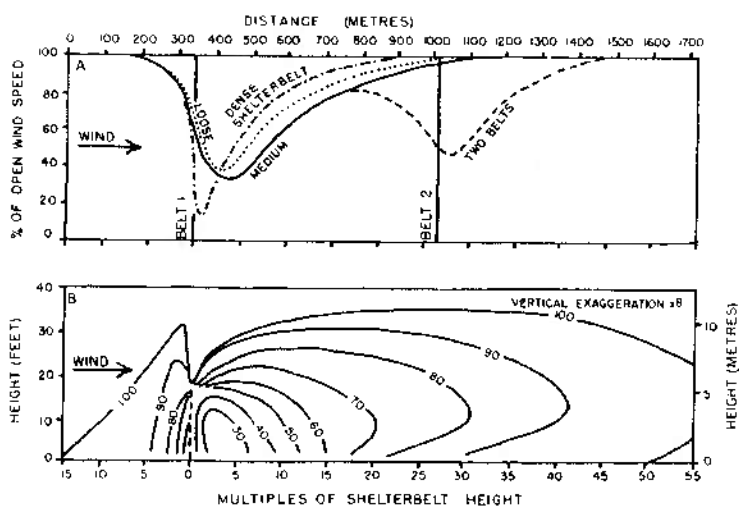


Fig. 7.11. The influence of shelterbelts on wind-velocity distributions (expressed as percentages of the velocity in the open).

A. The effects of one shelterbelt of three different densities, and of two back-coupled medium-dense shelterbelts (after W. Nägeli, and Geiger 1965).

B. The detailed effects of one half-solid shelterbelt (after Bates and Stoeckeler, and Kittredge 1948).

3 Modification of the humidity environment

The humidity conditions within forest stands contrast strikingly with those in the open. Evaporation from the forest floor is usually much less because of the decreased direct sunlight, lower wind velocities, lower maximum temperatures, and generally higher forest air humidity. Evaporation from the bare floors of pine forests is 70% of that in the open for Arizona in summer and only 42% for the Mediterranean region, although such measurements have little real significance in that water losses from vegetated surfaces are controlled by the plant evapotranspiration.

During daylight leaves transpire water through open pores, or *stomata*, so that this loss is controlled by the length of day, the leaf temperature (modified by evaporational cooling), the leaf surface area, the tree species and its age, as well as by the meteorological factors of available radiant energy, atmospheric vapour pressure and wind speed (see ch. 2, A). Total evaporation figures are therefore extremely varied; also the evaporation of water intercepted by the vegetation surfaces enters into the totals, in

addition to direct transpiration. Calculations made for a catchment covered with Norway spruce (*Picea abies*) in the Harz Mountains of Germany showed an estimated annual evapotranspiration of 34 cm and additional interception losses of 24 cm.

The humidity of forest stands is very much linked to the amount of evapotranspiration and increases with the density of vegetation present (fig. 7.12A). The increase of forest humidity over that outside averages

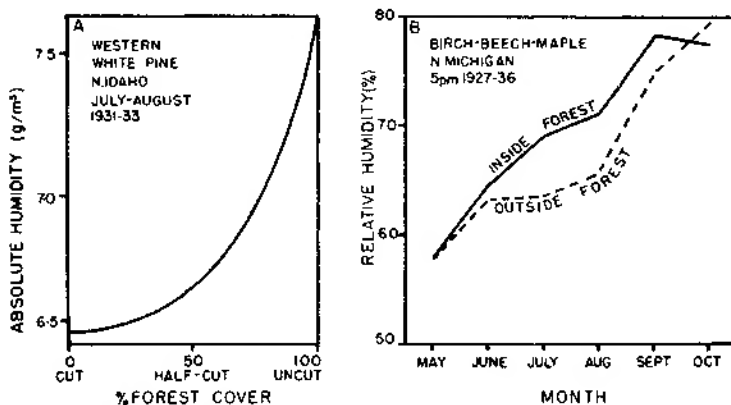


Fig. 7.12. The effects of (A) percentage of white pine (*Pinus monticola*) cover on summer absolute humidity in Idaho (after Kittredge 1948); and (B) season on relative humidity in a Michigan birch-beech-maple forest (after U.S. Dept. Agriculture Yearbook 1941).

some 3–10% of relative humidity and is especially marked in summer (fig. 7.12B). Mean annual relative humidity forest excesses for Germany and Switzerland are for beech 9·4%, Norway spruce (*Picea abies*) 8·6%, larch 7·9%, and Scots pine (*Pinus sylvestris*) 3·9%. However, humidity comparisons in these terms are rather unsatisfactory in that forest temperatures differ strikingly from those in the open. Forest vapour pressures were found to be higher within an oak stand in Tennessee than outside for every month except December. Tropical forests exhibit almost complete night saturation irrespective of elevation in the trunk space, whereas during the day humidity is inversely related to elevation.

The influence of forest structures on precipitation is still very much an unresolved problem. This is partly due to the difficulties of comparing rain-gauge catches in the open with those near forests, within clearings or beneath trees. For example, on the windward side of a forest the

dominance of low-level upcurrents decreases the amount of precipitation actually caught in the rain gauge, whereas the reverse occurs where there are lee side downdraughts. In small clearings the low wind velocities cause little turbulence around the opening of the gauge and catches are generally greater than outside the forest, although the actual precipitation amounts may be identical. On the other hand, it is sometimes found that the larger the clearing the more prevalent are downdraughts and consequently the precipitation catch increases. In a 25-m-high pine and beech forest in Germany, catches in clearings of 12 m diameter were only 87% of that upwind of the forest, but this catch rose to 105% in clearings of 38 m diameter. An analysis of precipitation records for Letzlinger Heath (Germany) before and after afforestation suggested a mean annual increase of 6%, with the greatest excesses occurring during drier years. It is generally agreed, however, that forests have little effect on cyclonic rain, but that they may have a marginal orographic effect in increasing lifting and turbulence, which is of the order of 1–3% in temperate regions.

A far more important obstructional influence of forests on precipitation is in terms of the direct interception of rainfall by the canopy. This obviously varies with crown coverage, with season, and with the rainfall intensity. Measurements in German beech forests indicate that, on average, they intercept 43% of precipitation in summer and 23% in winter. Pine forests may intercept up to 94% of low-intensity precipitation but as little as 15% of high intensities, the average for temperate pines being about 30%. The intercepted precipitation either evaporates on the canopy, runs down the trunk, or drips to the ground. Assessment of the total precipitation reaching the ground (the *throughfall*) requires very detailed measurements of the stem flow and the contribution of drips from the canopy. Canopy evaporation is not necessarily a total loss of moisture from the woodland, since the solar energy used in the evaporating process is not available to remove soil moisture or transpiration water, but the vegetation does not derive the benefit of the cycling of the water through it via the soil. Evaporation from the canopy is very much a function of net radiation receipts (20% of the total precipitation evaporates from the canopy of Brazilian evergreen forests), and of the type of species. Some Mediterranean oak forests yield virtually no stem-flow and their 35% interception almost all evaporates from the canopy. Recent investigations of the water balance of forests provide some evidence that evergreen forests may be subject to greater evapotranspiration than grass in the same climatic conditions. Grass normally reflects 10–15% more solar radiation than coniferous tree species and hence less energy is available for evaporation. In addition evergreens allow

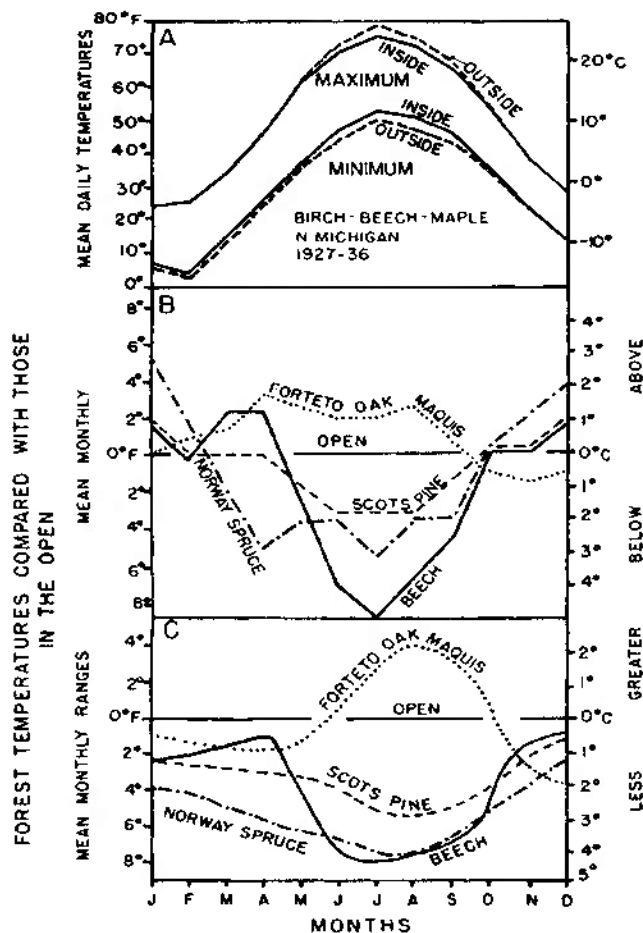


Fig. 7.13. Seasonal regimes of forest temperatures.

- A. Mean daily maximum and minimum temperatures inside and outside a birch-beech-maple forest in Michigan (after U.S. Dept. Agriculture Yearbook 1941).
- B. Mean monthly temperatures and C mean monthly temperature ranges, compared with those in the open, for four types of Italian forest (FAO 1962). Note the anomalous conditions associated with the *forteto oak maquis*, which transpires little.

transpiration to occur throughout the year. Nevertheless many more detailed and careful studies are required to check these results and to test the various hypotheses.

4 Modification of the thermal environment

From what has been said it is apparent that forest vegetation has an important effect on microscale temperature conditions. Shelter from the sun, blanketing at night, heat loss by evapotranspiration, reduction of wind speed, and the impeding of vertical air movement all influence the temperature environment. The most obvious effect of canopy blanketing is that inside the forest daily maximum temperatures are lower and minima are higher (fig. 7.13A). This is particularly apparent during periods of high summer evapotranspiration which depress daily maximum temperatures and cause mean monthly temperatures in tropical and temperate forests to fall well below those outside. In temperate forests at sea-level the mean annual temperature may be about 0.6°C (1°F) less

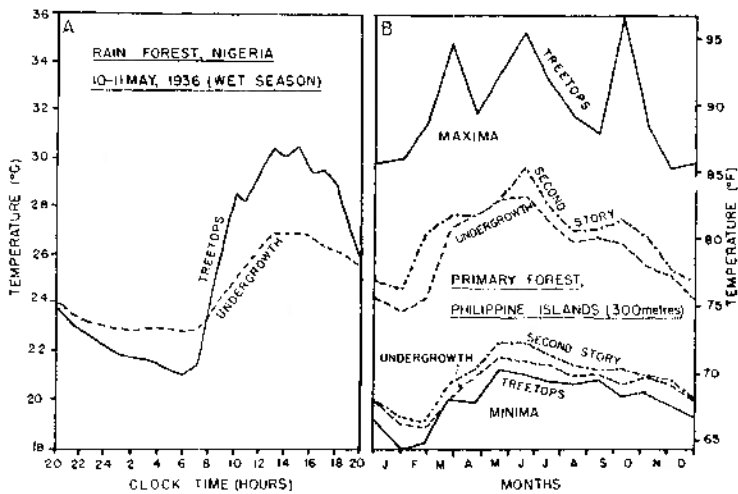


Fig. 7.14. The effect of tropical rain forest stratification on temperature (after Richards 1952).

A. Daily march of temperature 10–11 May 1936 in the treetops (24 m) and in the undergrowth (0.7 m) during the wet season in primary rain forest at Shasha Reserve, Nigeria (after Evans).

B. Average weekly maximum and minimum temperatures in three layers of primary (Dipterocarp) forest, Mt Maquiling, Philippine Islands (after Brown).

352 Atmosphere, weather and climate

than that in surrounding open country, the mean monthly differences may reach 2.2°C (4°F) in summer but not exceed 0.1°C in winter, and on hot summer days the difference can be more than 2.8°C (5°F). Mean monthly temperatures and temperature ranges for temperate beech, spruce and pine forests are given in fig. 7.13B and C, which also show that when trees do not transpire greatly in the summer (e.g. the *Forteto* oak maquis of the Mediterranean) the high day temperatures reached in the sheltered woods may cause mean monthly figures to reverse the trend exhibited by temperate forests. Even within individual climatic regions it is difficult to generalize, however, for at elevations of 1000 m the lowering of temperate forest mean temperatures below those in open country may be double that at sea-level.

The complex vertical structure of forest stands is a further factor in complicating forest temperatures. Even in relatively simple stands vertical differences are very apparent. For example, in a ponderosa pine forest (*Pinus ponderosa*) in Arizona the recorded mean June-July maximum was increased by 0.8°C (1.5°F) simply by raising the thermometer from 1.5 to 2.4 m (5 to 8 ft) above the forest floor. In stratified tropical forests the thermal picture is much more complicated. The dense canopy heats up very much during the day and quickly loses its heat at night, showing a much greater diurnal temperature range than the undergrowth (fig. 7.14A). Whereas daily maximum temperatures of the second story are intermediate between those of the tree-tops and the undergrowth, the nocturnal minima are higher than either tree-tops or undergrowth because the second story is insulated by trapped air both above and below (fig. 7.14B).

8 Climatic variability, trends and fluctuations

Probably the aspect of climate which most interests the layman is speculation regarding its possible trends. Unfortunately, as well as being the most interesting, it is also the most uncertain aspect of meteorological research. Realization that climate has changed radically with time came only during the 1840s when indisputable evidence of former ice ages was obtained, yet in many parts of the world the climate has altered sufficiently, even within the last few thousand years, to affect the possibilities for agriculture and settlement. Reliable weather records have only been kept during the last hundred years or so and therefore it is only the recent climatic fluctuations which can be investigated adequately. The discussion in this chapter is mainly limited to these events, but first it is worthwhile considering the methods of handling the meteorological records which are available.

A Climatic data

1 Averages

The climate of a place is often regarded simply as its 'average weather', but vital climatic information is overlooked if the range and frequency of extremes are neglected. Averages can be markedly affected by extreme values and this is particularly true of the arithmetic mean (which is obtained by totalling the individual values and dividing by the number of occurrences). For this reason a 30- or 35-year period is normally required

for the determination of climatic averages. Even so, certain types of data are very inadequately summarized by the arithmetic mean, especially when small values are frequent but very large ones occur occasionally. This situation is illustrated by fig. 8.1, where the *histograms* or frequency-distribution graphs of annual rainfall at Helwan (Egypt) and Aden are clearly dissimilar to those at Greenwich (England) and Padua (Italy). The profile for Padua approximates a symmetrical 'normal' distribution,

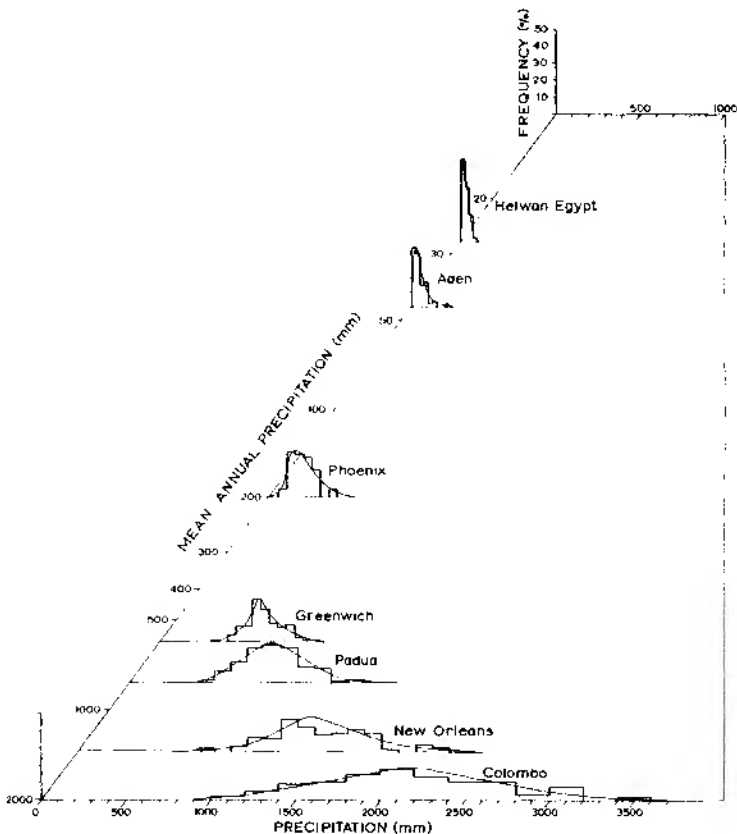


Fig. 8.1. Frequency distribution curves of annual rainfall for: Helwan (Cairo), Egypt (averaged over 37 years); Aden (55 years); Phoenix, Arizona (45 years); Greenwich (London), England (100 years); Padua, Italy (200 years); New Orleans (88 years); and Colombo, Ceylon (70 years).

where half the values lie above and half below the mean, and where the most frequent (or *modal*) category is equal to the mean.¹ For 1725–1924, the annual rainfall at Padua has a mean of 859 mm, and a mode of about 884 mm. The *median* for the same period at Padua is 847 mm. This is another useful measure of central tendency, which has exactly half the number of items in the data series above it and half below it. Consequently it is not biased by the occurrence of a few extreme figures. Modal or median values would be much more meaningful indicators of annual precipitation at Aden and Helwan where the graphs exhibit strong 'positive' skewness i.e. 'tail' of the distribution is towards values greater than the mean. Positive skewness is especially marked when the mean of the distribution approaches zero, when a large number of records includes some infrequent events of high magnitude, and when the length of time to which the event is related is short (for example, rainfall figures referring to any one month are usually more skewed than those relating to the whole year). Another problem of frequency distributions is that they may be bimodal, as shown in fig. 8.1 for New Orleans.

2 Variability

Variability about the average can be expressed in several ways. When the median is used it is common also to determine the upper and lower quartiles (Q_1 and Q_3), which are the central values between the median and the upper and lower extremes, respectively. The average deviation from the median is given by $(Q_3 - Q_1)/2$. A more widely used measure of variability is the standard deviation (σ , pronounced *sigma*) which is calculated by summing the square of the deviation of each value from the mean, dividing by the number of cases and then taking the square root.

$$\sigma = \sqrt{\frac{\sum(x_i - \bar{x})^2}{n}}$$

where:

x = an individual value

$$\bar{x} = \frac{\sum x_i}{n} \text{ (the mean)}$$

n = number of cases

Σ = sum of all values for $i = 1$ to n .

¹ Fuller details of elementary statistical procedures may be found in S. Gregory, *Statistical Methods and the Geographer* (Longmans, 1973), or M. J. Moroney, *Facts from Figures* (Pelican, 1951) and later editions.

356 Atmosphere, weather and climate

It is therefore a measure of average deviation, where the difficulty created by positive and negative departures (i.e. values greater and less than the mean) is removed by squaring each deviation and rectifying this by finally calculating the square root. Variability of rainfall may be compared between stations if the standard deviation is expressed as a percentage of the mean (the *coefficient of variation, CV*).

$$CV = \frac{\sigma}{\bar{x}} \times 100(\%)$$

Where the standard deviation is not available, use has often been made in the past of the mean deviation, *MD*.

$$MD = \frac{\sum |x_i - \bar{x}|}{n}$$

where $| - |$ denotes the absolute difference, disregarding sign.

This measure of variability, standardized against the mean, ranges for annual precipitation from about 10–20% in western Europe and parts of monsoon India to over 50% in arid areas of the world (fig. 8.2). It is in such areas that a small change in the frequency of rainstorms can markedly affect the ‘average’ rainfall over a given period of years. It should be noted, however, that detailed examination of the precipitation in many diverse climatic regions shows that the apparent inverse relationship between annual total and variability is only very approximate. Moreover, a coefficient of variation $\geq 50\%$ in fact violates the statistical assumption of a normal frequency distribution on which this statistic is based.

3 Trends

It is obvious that the great year-to-year variability of climatic conditions may conceal gradual trends from one type of regime towards another. The effect of short-term irregularities can be removed by various statistical techniques, of which the simplest is the *running mean* (or *moving average*). The method is to calculate mean values for successive, overlapping periods of perhaps 5, 10 or 30 years, e.g.

$$\frac{\text{Year 1} + \text{Year 2} + \text{Year 3} + \text{Year 4} + \text{Year 5}}{5} = \text{Mean for Year 3}$$

$$\frac{\text{Year 2} + \text{Year 3} + \text{Year 4} + \text{Year 5} + \text{Year 6}}{5} = \text{Mean for Year 4, etc.}$$

This device smooths out the short-term fluctuations if periods of 20 or 30 years are used, thereby emphasizing the long-term trends. Caleendar has

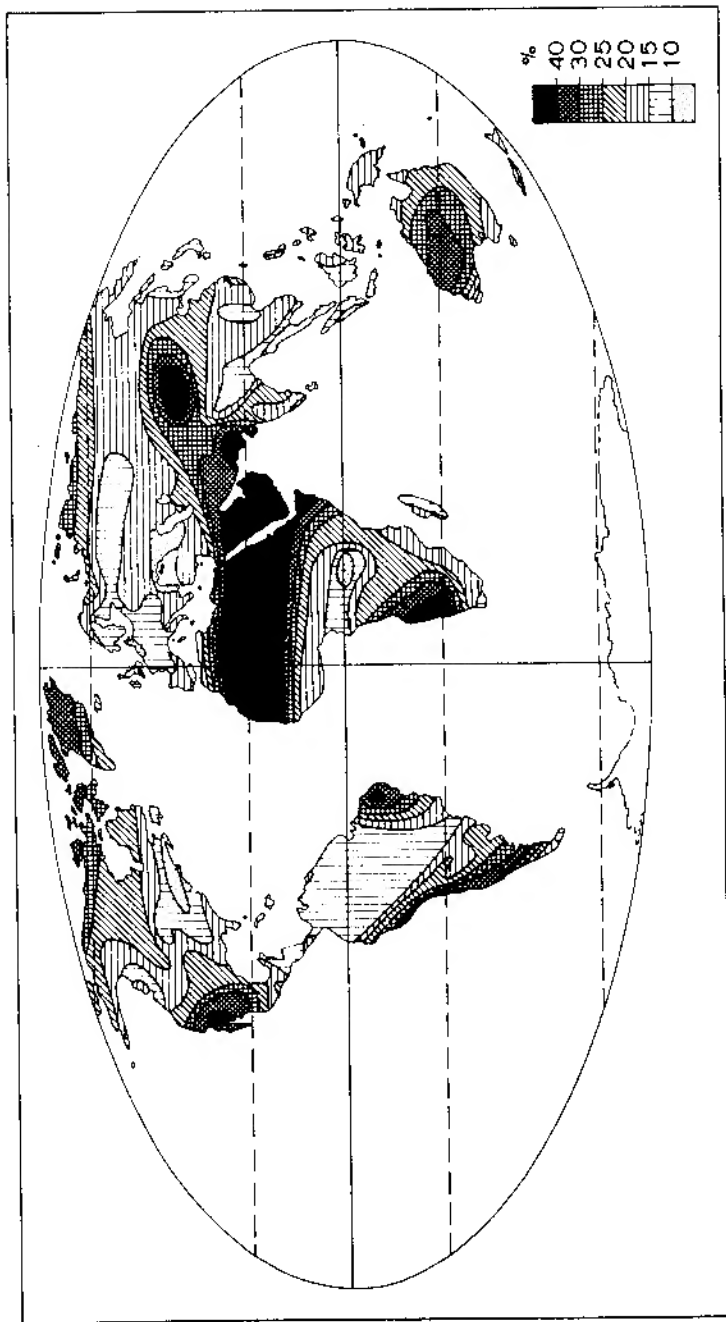


Fig. 8.2. Distribution of rainfall variability over the continents (after Erwin Blei).

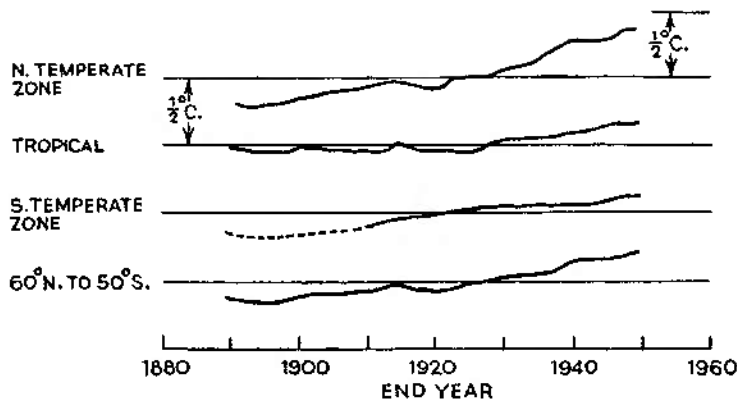


Fig. 8.3. Temperature trends for generalized latitude zones. The graphs show the departure of 20-year moving averages from the mean temperature for 1901–30 (from Callendar 1961).

used this method to show that there has been an increase in warmth since the end of the last century, particularly in the north temperate zone (fig. 8.3). The change appears to have been least in the tropics and the largest in the Sub-Arctic; the changes of annual mean temperature between the 30-year periods 1890–1919 and 1920–49 were approximately +0.2°C (0.3°F) for the tropics and +0.4°C (0.6°F) for the north temperate zone,

Table 8.1 The frequency of January and July temperatures at Copenhagen (After Lysgaard 1963)

	1811–40	1841–70	1871–1900	1901–30	1931–60
<i>January</i>					
<i>Mean (°C)</i>					
≤ −1.5	14	13	6	6	4
−1.4 to 1.4	11	12	15	17	18
≥ 1.5	5	5	7	7	8
<i>July</i>					
<i>Mean (°C)</i>					
≤ 15.5	7	9	4	3	1
15.6 to 18.4	18	19	24	22	21
≥ 18.5	5	2	2	5	8

while the rise in the Svalbard-Greenland Sea area amounted to +2.8°C (5.0°F) between 1900-19 and 1920-39.

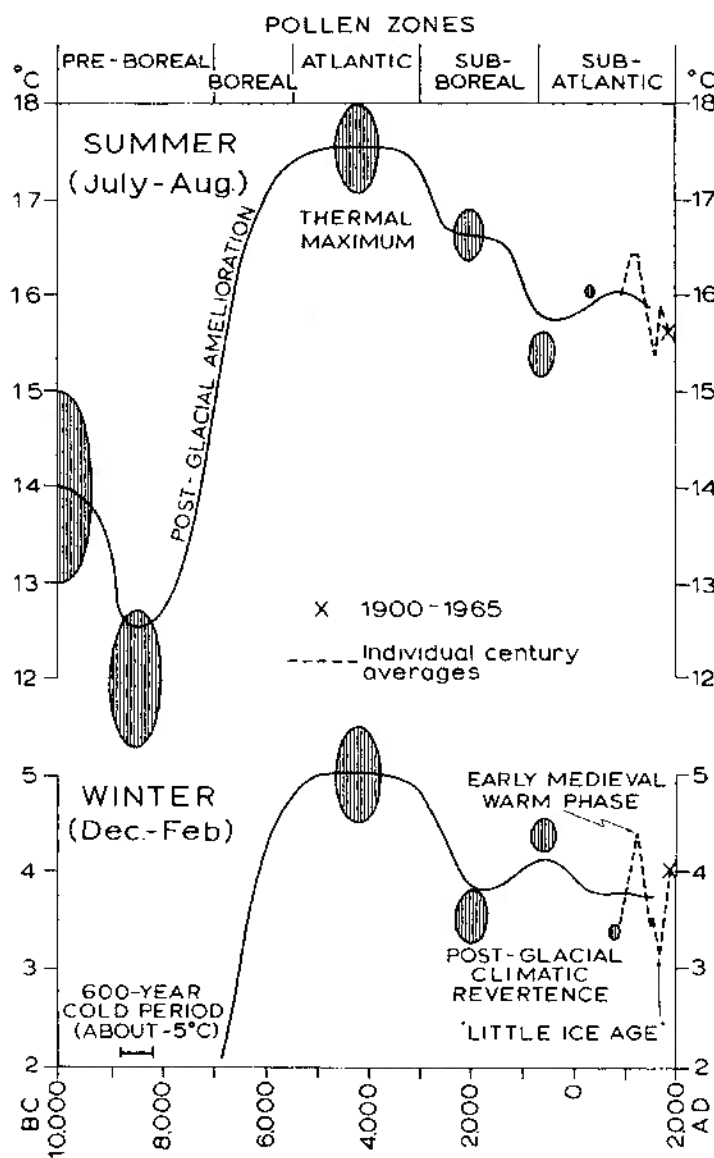
These changes represent an increased frequency of warm months rather than a slight overall temperature increase. For instance, the records at Copenhagen (table 8.1) show that warm winter and summer months have become more frequent, and cold ones less frequent, during the present century.

B The climatic record

To understand the significance of climatic trends over the last hundred years they need to be viewed against the background of our general knowledge about the post-glacial climatic record. The available information is based on archaeological evidence, analysis of the vegetation history by means of pollen remains preserved in peat bogs, dendroclimatology and, for more recent periods, documentary sources. Although these rarely provide precise quantitative data the general pattern is nevertheless clear.

1 The major post-glacial epochs

Following the final retreat of the continental ice sheets from Europe and North America between 10,000 and 7000 years ago the climate rapidly ameliorated in middle and higher latitudes. A thermal maximum was reached about 5000 to 3000 BC when summer temperatures are known to have been several degrees higher than today. Thereafter a decline set in with cold, wet conditions in Europe around 900-500 BC. Although temperatures have not since equalled those of the thermal maximum there was certainly a warmer period in many parts of the world between about AD 1000 and 1250, and this phase was marked by the Viking colonization of Greenland and the occupation of Ellesmere Island in the Canadian Arctic by Eskimos. A further deterioration followed and severe winters between AD 1550 and 1700 gave a 'Little Ice Age' with extensive Arctic pack-ice and glacier advances in some areas to maximum positions since the end of the Ice Age. These advances occurred at dates ranging from the mid-seventeenth to the late nineteenth century in different areas, as a result of the lag in glacier response and minor climatic fluctuations. Figure 8.4 attempts to summarize these trends, but it must be stressed that at present only the gross features are represented, as we know little or nothing about short-term fluctuations before the Medieval period, for example, and even the relative magnitudes of the changes prior to about AD 1700 can only be indicated in a very general way.



2 The recent warming trend

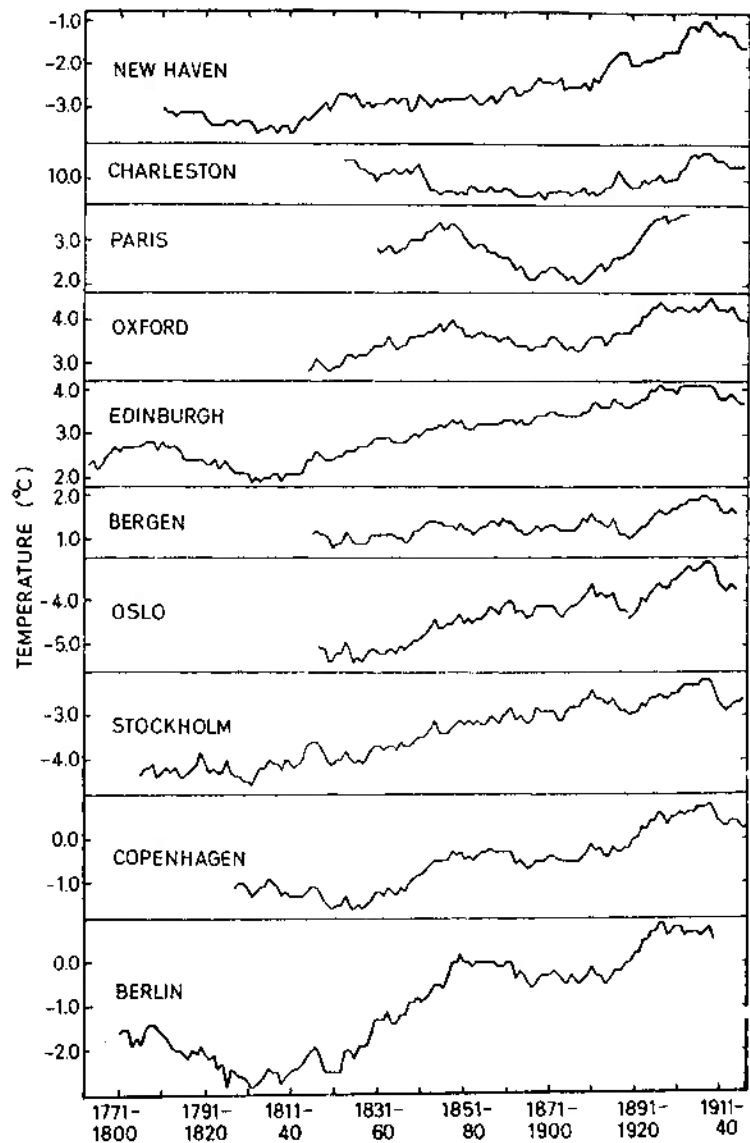
Long instrumental records for a few stations in Europe indicate that the warming trend which ended the 'Little Ice Age' began early in the nineteenth century, although it was interrupted in some areas about 1880–90 (fig. 8.5). Winter temperatures have been most affected and on Svalbard the 20-year change in January mean temperature from 1900–19 to 1920–39 amounted to +7.8°C (14.0°F).

The effects of the temperature rise are apparent in many ways. There has been, for example, a rapid retreat of most of the world's glaciers (e.g. measurement of the Muir Glacier in Alaska shows it has retreated 3 km in 10 years). Glaciers in the North Atlantic area seem to be universally shrinking at present, due largely to temperature increases which have the effect of lengthening the ablation season, rather than to decreases in snowfall. The world rise in temperature has caused a corresponding raising of the snowline. Since 1900 it has risen 800 m in Peru, and in Sweden the timberline on some mountain slopes has risen as much as 20 m since 1930. Associated with the melting of glaciers has been a general rise in sea level which has been estimated at about 15 cm between 1930 and 1948, a rise of four times the average rate experienced during the last 9000 years. The rate became six times the average in the mid-1920s, the time when glacier melting showed a particularly marked increase. Another tendency illustrating world warming has been the retreat of the tundra margin. In Alaska and Siberia trees are beginning to annex former tundra areas to the north. In Siberia the southern limit of permanently frozen ground is retreating northwards at the rate of several dozen metres a year. At the same time ports in the Arctic are remaining free of ice for longer periods each year and cod have extended their feeding northwards off west Greenland by 9° of latitude between 1919 and 1948.

Unfortunately the latest evidence (see fig. 1.3) suggests that the warm period of 1920–40 has come to an end. Cooling has taken place especially over northern Siberia, the eastern Canadian Arctic and Alaska, with changes of the order of -2° to -3°C (-4° to -6°F) in winter mean

Fig. 8.4. Air temperatures in the lowlands of central England. Trends of the supposed 1000-year and 100-year averages since 10,000 bc (the latter calculated for the last millennium) (after Lamb 1966). Shaded ovals indicate the approximate ranges within which the temperature estimates lie and error margins of the radiocarbon dates. Note that the pre-boreal phase begins about 8,000 bc following the end of the glacial period.

362 Atmosphere, weather and climate



temperature from 1940–9 to 1950–9. Perhaps in compensation slight winter warming has at the same time affected the United States, eastern Europe and Japan. Whether or not this *downturn* of temperature represents a minor fluctuation or a longer-term trend remains to be seen, but it is clear that the latter would have important economic implications in many parts of the northern hemisphere.

3 Recent changes in tropical rainfall

While temperatures in the tropics seem to have undergone little change since the 1880s, the same is not true of rainfall totals. Over extensive areas there is evidence of a marked decrease of annual rainfall at the end of the nineteenth century. Kraus illustrates the magnitude of this change at Freetown (Sierra Leone):

Seasonal rainfall averages at Freetown

	<i>May–October</i>	<i>November–April</i>
1875–1896	452.3 cm (178.05 in)	41.7 cm (16.41 in)
1907–1931	312.1 cm (122.85 in)	23.1 cm (9.10 in)

The early rains (May–June) and the late rains (September–October) show a greater *relative* decrease than the very wet months of July and August, which points to a lengthening of the dry season as the main factor.

The greater aridity in the tropics was apparently not accompanied by any compensating increase in temperate latitudes, indeed rainfall also decreased in south-east Australia and eastern North America. This suggests that a general weakening of the moisture cycle, particularly a reduction of evaporation, was probably responsible, but the underlying reason for such a change is not yet clear.

Recently, a marked decrease in the summer monsoon rains of India and Africa has been identified by D. Winstanley, amounting to more than 50% between 1957 and 1970. This seems to be a response to a slight southward shift of the subtropical anticyclone belt with a restricted

Fig. 8.5. January temperature trends since 1800. 30-year moving averages (*from Lysgaard 1949*).

northward penetration and intensity of the tropical circulation. The tragic consequences of this minor climatic fluctuation have been dramatically evident in the Sahel zone of Africa with recurrent widespread crop failures and starvation. By contrast, the winter and spring rains which decreased generally across subtropical Africa, the Middle East and India from 1950 into the early 1960s, increased sharply in the late 1960s in association with more frequent northerly meridional airflows over each of these three sectors.

C Possible causes of climatic change

The immediate cause of the recent climatic fluctuations appears to be the strength of the global wind circulation. The first 30 years of this century saw a pronounced increase in the vigour of the westerlies over the North Atlantic, the north-east trades, the summer monsoon of southern Asia and the southern hemisphere westerlies (in summer). In the north-east North Atlantic this trend was already under way early in the nineteenth century. It has been accompanied by more northerly depression tracks across the Atlantic and by independent changes in the meridional (north-south) components of airflow. A comparison of pressure readings for the period 1900–19 with the period 1920–39 shows that the Siberian high-pressure cell spread westward (5–10° of longitude) towards Scandinavia. At the same time the Icelandic and winter Mediterranean low-pressure cells deepened (decreasing by 2 and 1 mb, respectively) and the North American high-pressure cell may have spread eastward. The Aleutian and Icelandic low-pressure cells also tended to move 5–10° of longitude eastward.

The picture over the North Atlantic thus consisted of an increased pressure gradient between the Azores high and the Icelandic low, on the one hand, and between the Siberian high and the Icelandic low on the other. This resulted in a significant increase in the frequency of mild southwesterly airflow over the British Isles between about 1900 and 1930, as reflected by the average annual frequency of Lamb's Westerly airflow type (see ch. 5, A.3). For 1873–97, 1898–1937 and 1938–61, the figures are 27, 38 and 30%, respectively. The recent decrease of westerly airflow, especially in winter, is linked with an increase of northerly airflow, giving more frequent snowfalls, while the southward shift of the main depression tracks has produced a number of cool, wet summers in Britain (notably 1954, 1956, 1958 and 1960). These regional indicators (together with those discussed above), reflect a general decline in the overall strength of

the midlatitude circumpolar westerlies, accompanying an apparent expansion of the polar vortex, and a parallel decrease in the intensity of the tropical Hadley circulation.

The key to these atmospheric variations must be linked to the heat balance of the earth-atmosphere system and this forces us to return to the fundamental energy considerations with which we began this book. It is possible that there have been changes in the amount of energy sent out by the sun, but the present evidence for fluctuations in the 'solar constant' is inconclusive. However, variations apparently do occur in the emission of high-energy particles and ultraviolet radiation during brief solar flares. All solar activity follows the well-known cycle of approximately 11 years, which is usually measured with reference to the period between sunspot maximum and minimum and, although numerous attempts have been made to correlate sunspot numbers with meteorological events, the results so far obtained are conflicting. For instance, tropical temperatures show positive correspondence with sunspot numbers between 1930 to 1950, but from 1875 to 1920 the relationship was an inverse one. Such phase changes may be capable of interpretation when more is known about the effect of solar activity on the upper atmosphere, although only very tentative hypotheses have yet been advanced. A recent one suggests that stratospheric ozone is more abundant about 2 years before a sunspot minimum. The latter is accompanied by lower solar latitudes of sunspot activity causing solar radiation to be pointed more directly at the earth. The resulting increase of ultraviolet radiation yields more ozone with consequently greater absorption of solar insolation. It is postulated that warming of the stratosphere weakens the subtropical high-pressure belt and in turn the westerlies, giving lower than average rainfall in temperate oceanic climates. In continental areas the weaker westerlies may favour greater convectional rainfall, so that complex phase relationships can be envisaged between weather and the sunspot cycle.

Another possible factor, which is not necessarily an alternative, is a change in the tropospheric heat budget. It has previously been noted that the amount of carbon dioxide in the atmosphere seems to bear a direct relationship with temperature. In the last 70 years world measurements of carbon dioxide have shown an increase of 10% (see fig. 1.3). This would naturally lead to an increase of heat absorption by the atmosphere from the earth's outgoing long-wave re-radiation and an estimated warming of the entire lower atmosphere by 0.3°C. However, as pointed out earlier, the warming trend of the early part of this century now appears to have ended!

Other factors may also have modified the atmospheric heat budget. The presence of increased amounts of volcanic dust in the atmosphere is one suggested cause of the 'Little Ice Age' and, while this may be the case, it seems doubtful that reduced dust content was responsible for the early twentieth-century warming, since the trend was least in the tropics and greatest in cloudy, maritime regions of high latitudes. In fact this pattern is strong evidence of a heat-transporting mechanism. Increased storminess might cause more frequent movement of warm air masses towards high latitudes, yet increases in winter temperatures also occur in areas which are predominantly affected by northerly winds and therefore cannot receive heat directly from the source regions of warm air. It has been suggested that increasing atmospheric pollution in the twentieth century may have caused the recent temperature downturn. Evidence from the Soviet Union shows a sharp rise in dust-fall on mountain snowfields since 1930 and atmospheric turbidity has increased by 57% over Washington D.C., between 1905–64, and by 85% over Davos, Switzerland (1920–58). The presence of dust in the atmosphere increases the backscatter of short-wave radiation, thereby increasing the planetary albedo and causing cooling, but the effect on infrared radiation is one of surface warming. The net result is complicated by the surface albedo. Man-made aerosols cause net warming over land areas, cooling over the oceans. Natural aerosols probably cause general cooling. The overall effect on surface temperature remains uncertain.

The interactions between ocean and atmosphere also introduce a variety of complications. The sea can store vast quantities of heat and may therefore greatly modify the heat and moisture exchanges with the air above. However, recent detailed investigations by J. Bjerknes show that variations in Atlantic sea-surface temperatures are due to initial changes in the wind regime. Hence, although feedback effects may operate, the atmospheric changes appear to be the primary mechanism. In the short-term these may be the result of inherent instability in the atmospheric circulation, but the occurrence of Ice Ages probably demands the existence of distinct causative factors. Whether these are terrestrial or extra-terrestrial remains a problem for future research to solve.

Bibliography

General

- BARRETT, E. C. (1974) *Climatology from Satellites*. Methuen, London. 418 pp.
- BARRY, R. G. and PERRY, A. H. (1973) *Synoptic Climatology: Methods and Applications*. Methuen, London. 555 pp.
- BATES, D. R. (1957) *The Planet Earth*. Pergamon Press, London. 312 pp.
- *BATTAN, L. J. (1959) *Radar Meteorology*, Univ. of Chicago Press, Chicago, Ill. 161 pp.
- *BERRY, F. A., BOLLAY, E. and BEERS, N. R. (eds.) (1945) *Handbook of Meteorology*. McGraw-Hill, New York, 1068 pp.
- BLAIR, T. A. and FITE, R. C. (1965) *Weather Elements: A text in elementary meteorology*, 5th edn. Prentice-Hall, New York. 364 pp.
- BLÜTHGEN, J. (1966) *Allgemeine Klimageographie*, 2nd edn. W. de Gruyter, Berlin, 720 pp.
- BRUCE, J. P. and CLARK, R. H. (1966) *Introduction to Hydrometeorology*. Pergamon Press, Oxford and London. 319 pp.
- *BYERS, H. R. (1974) *General Meteorology*, 4th edn. McGraw-Hill, New York. 480 pp.
- CHANG, J. H. (1972) *Atmospheric Circulation Systems and Climates*. Oriental Publishing Co., Honolulu. 326 pp.
- CRAIG, R. A. (1968) *The Edge of Space*. Doubleday, New York. 150 pp.
- CROWE, P. R. (1971) *Concepts in Climatology*. Longmans, London. 589 pp.
- *DOBSON, G. M. B. (1968) *Exploring the Atmosphere*, 2nd edn. O.U.P., London. 209 pp.
- DONN, W. T. (1965) *Meteorology*, 3rd edn. McGraw-Hill, New York. 484 pp.
- FAIRBRIDGE, R. W. (ed.) (1967) *The Encyclopaedia of Atmospheric Sciences and Astrogeology*. Rheinold, New York. 1200 pp.

* Indicates more advanced texts with reference particularly to the physical bases of meteorology, often including mathematical material.

368 Atmosphere, weather and climate

- FLOHN, H. (1969) *Climate and Weather*. Weidenfeld and Nicolson, London. 253 pp.
- FRITZ, S. (1964) Pictures from meteorological satellites and their interpretation. *Space Science Reviews* 3. 541-80.
- GEIGER, R. (1965) *The Climate near the Ground*, 2nd edn. Harvard Univ. Press, Cambridge, Mass. 611 pp.
- *HALTINER, G. J. and MARTIN, F. L. (1957) *Dynamical and Physical Meteorology*. McGraw-Hill, New York. 470 pp.
- HARE, F. K. (1953) *The Restless Atmosphere*. Hutchinson, London, 192 pp.
- HARE, F. K. (1955) Dynamic and synoptic climatology. *Ann. Assn. Amer. Geog.* 45, 152-62.
- HARE, F. K. (1957) The dynamic aspects of climatology. *Geografiska Annaler* 39, 87-104.
- HAURWITZ, B. and AUSTIN, J. M. (1944) *Climatology*. McGraw-Hill, New York. 410 pp.
- *HESS, S. L. (1959) *Introduction to Theoretical Meteorology*. Henry Holt, New York. 362 pp.
- HEWSON, E. W. and LONGLEY, R. W. (1944) *Meteorology, Theoretical and Applied*. Wiley, New York. 468 pp.
- *HUMPHREYS, W. J. (1929) *Physics of the Air*. McGraw-Hill, New York. 654 pp.
- HUSCHKE, R. E. (ed.) (1959) *Glossary of Meteorology*. American Meteorological Society, Boston. 638 pp.
- HUTCHINSON, G. E. (1957) *A Treatise on Limnology* I. Wiley, New York. 1015 pp.
- KENDREW, W. G. (1949) *Climatology*. O.U.P., London. 383 pp. (2nd edn, 1957, 400 pp.).
- KENDREW, W. G. (1961) *The Climates of the Continents*, 5th edn. O.U.P., London. 608 pp.
- LAMB, H. H. (1964) *The English Climate*. English Universities Press, London. 212 pp.
- LAMB, H. H. (1972) *Climate: Present, Past and Future*, Vol. I. *Fundamentals and Climate Now*. Methuen, London. 613 pp.
- LIST, R. J. (1951) *Smithsonian Meteorological Tables*, 6th edn. Smithsonian Institution, Washington. 527 pp.
- LOCKWOOD, J. G. (1974) *World Climatology: An environmental approach*. Arnold, London. 330 pp.
- MICHAELSON, G. (ed.) (1973) *Climate in Review*. Houghton-Mifflin, Boston. 314 pp.
- MCINTOSH, D. H. (1963) *Meteorological Glossary*, 2nd edn. H.M.S.O., London. 288 pp.
- MCINTOSH, D. H. and THOM, A. S. (1972) *Essentials of Meteorology*. Wykeham Publications, London. 239 pp.
- *MALONE, T. F. (ed.) (1951) *Compendium of Meteorology*. American Meteorological Society, Boston. 1334 pp.

- MANLEY, G. (1952) *Climate and the British Scene*. Collins, London. 314 pp.
- METEOROLOGICAL OFFICE (1958) *Tables of Temperature, Relative Humidity, and Precipitation for the World*, 6 vols. H.M.S.O., London.
- MILLER, A. (1966) *Meteorology*. Merrill, Columbus, Ohio. 128 pp.
- MILLER, A. A. (1957) *Climatology*, 8th edn. Methuen, London. 318 pp.
- MONTEITH, J. L. (1973) *Principles of Environmental Physics*. Arnold, London. 241 pp.
- MUNN, R. E. (1966) *Descriptive Micrometeorology*. Academic Press, New York. 245 pp.
- NATIONAL AERONAUTICS AND SPACE ADMINISTRATION (1966) *NIMBUS II Users' Guide*. Goddard Space Flight Center, Greenbelt, Maryland. 229 pp.
- NEIBURGER, M., EDINGER, J. G. and BONNER, W. D. (1973) *Understanding Our Atmospheric Environment*. W. H. Freeman, San Francisco. 293 pp.
- OLIVER, J. E. (1973) *Climate and Man's Environment*. Wiley, New York. 517 pp.
- *PALMÉN, E. and NEWTON, C. W. (1969) *Atmosphere Circulation Systems: Their structure and physical interpretation*. Academic Press, New York. 603 pp.
- PEDGLEY, D. E. (1962) *A Course of Elementary Meteorology*. H.M.S.O., London. 189 pp.
- *PETTERSSON, S. (1956) *Weather Analysis and Forecasting*, 2 vols. McGraw-Hill, New York. 428 pp and 266 pp.
- PETTERSSON, S. (1969) *Introduction to Meteorology*, 3rd edn. McGraw-Hill, New York. 333 pp.
- *REITER, E. R. (1963) *Jet Stream Meteorology*. Univ. of Chicago Press, Chicago, Ill. 515 pp.
- RIEHL, H. (1965) *Introduction to the Atmosphere*. McGraw-Hill, New York. 365 pp.
- *SELLERS, W. D. (1965) *Physical Climatology*. Univ. of Chicago Press, Chicago, Ill. 272 pp.
- STRAHLER, A. N. (1965) *Introduction to Physical Geography*. Wiley, New York. 455 pp.
- STRINGER, E. T. (1972a) *Foundations of Climatology*. W. H. Freeman, San Francisco. 586 pp.
- STRINGER, E. T. (1972b) *Techniques of Climatology*. W. H. Freeman, San Francisco. 539 pp.
- SUTCLIFFE, R. C. (1941) *Meteorology for Aviators*. H.M.S.O., London. 274 pp (and later editions).
- SUTTON, O. G. (1960) *Understanding Weather*. Pelican, London. 215 pp.
- SUTTON, O. G. (1962) *The Challenge of the Atmosphere*. Hutchinson, London. 227 pp.

370 Atmosphere, weather and climate

- SVERDRUP, H. V. (1945) *Oceanography for Meteorologists*. Allen and Unwin, London, 235 pp.
- SVERDRUP, H. V., JOHNSON, M. W. and FLEMING, R. H. (1942) *The Oceans; Their physics, chemistry and general biology*. Prentice-Hall, New York, 1087 pp.
- TAYLOR, J. A. and YATES, R. A. (1967) *British Weather in Maps*, 2nd edn. Macmillan, London. 315 pp.
- TREWARTH, G. T. (1968) *An Introduction to Climate*, 4th edn. McGraw-Hill, New York. 408 pp.
- TREWARTH, G. T. (1961) *The Earth's Problem Climates*. McGraw-Hill, New York. 334 pp.
- VAN ROOY, M. P. (1957) *Meteorology of the Antarctic*. Weather Bureau, Pretoria. 240 pp.
- WILLETT, H. C. and SANDERS, F. (1959) *Descriptive Meteorology*, 2nd edn. Academic Press, New York. 355 pp.
- WORLD METEOROLOGICAL ORGANIZATION (1962) *Climatological Normals (CLINO) for CLIMAT and CLIMAT SHIP stations for the period 1931-60*. World Meteorological Organization, Geneva.
- WORLD METEOROLOGICAL ORGANIZATION (1973) The use of satellite pictures in weather analysis and forecasting. *W.M.O. Technical Note* 124, Geneva. 275 pp.

Chapter 1 Atmospheric composition and energy

- BARRY, R. G. and CHAMBERS, R. F. (1966) A preliminary map of summer albedo over England and Wales. *Quart. J. Roy. Met. Soc.* 92, 543-8.
- BECKINSALE, R. P. (1945) The altitude of the zenithal sun: A geographical approach. *Geog. Rev.* 35, 596-600.
- RUDYKO, M. I. et al (1962) The heat balance of the surface of the earth. *Soviet Geography* 3(5), 3-16.
- CRAIG, R. A. (1965) *The Upper Atmosphere; Meteorology and Physics*. Academic Press, New York. 509 pp.
- DEFANT, F. R. and TABA, H. (1957) The threefold structure of the atmosphere and the characteristics of the tropopause. *Tellus* 9, 259-74.
- GARNETT, A. (1937) Insolation and relief. *Trans. Inst. Brit. Geog.* 5, 71 pp.
- GODSON, W. L. (1960) Total ozone and the middle stratosphere over arctic and sub-arctic areas in winter and spring. *Quart. J. Roy. Met. Soc.* 86, 301-17.
- HARE, F. K. (1962) The stratosphere. *Geog. Rev.* 52, 525-47.
- HASTENRATH, S. L. (1968) Der regionale und jahrzeitliche Wandel des vertikalen Temperaturgradienten und seine Behandlung als Wärmhaushaltsproblem. *Meteorologische Rundschau*. 21, 46-51.
- KEELING, C. D. (1973) The carbon dioxide cycle: reservoir models to depict the exchange of atmospheric carbon dioxide with the oceans and land plants; In

- RASOOL, S. I. (ed.) *Chemistry of the Lower Atmosphere*, Plenum Press, New York. pp. 251-329.
- KUNG, F. C., BRYSON, R. A. and LENSCHOW, D. H. (1964) Study of a continental surface albedo on the basis of flight measurements and structure of the earth's surface cover over North America. *Monthly Weather Review*, 92, 543-64.
- LAUTENSACH, H. and BOGEL, R. (1956) Der Jahrgang des mittleren geographischen Höhengradienten der Lufttemperatur in den verschiedenen Klimagebieten der Erde. *Erdkunde*, 10, 270-82.
- LONDON, J. and SASAMORI, T. (1971) Radiative energy budget of the atmosphere. *Space Research* 11, 639-49.
- LUMB, F. E. (1961) *Seasonal variation of the sea surface temperature in coastal waters of the British Isles*, Sci. Paper No. 6. Meteorological Office, H.M.S.O., London. 21 pp.
- MCFADDEN, J. D. and RACOTZKIE, R. A. (1967) Climatological significance of albedo in central Canada. *Jour. Geophys. Res.* 72, 1135-43.
- MACHTA, L. (1972) The role of the oceans and biosphere in the carbon dioxide cycle; In Dyrssen, D. and Jagner, D. (eds.), *The Changing Chemistry of the Oceans*, Nobel Symposium 20. Wiley, New York. p. 121-45.
- MILLER, D. H. (1968) A Survey Course: The Energy and Mass Budget at the Surface of the Earth Pub. No. 7, Assn. Amer. Geog. Washington, D.C. 142 pp.
- NEWELL, R. E. (1963) Transfer through the tropopause and within the stratosphere. *Quart. J. Roy. Met. Soc.* 89, 167-204.
- NEWELL, R. E. (1964) The circulation of the upper atmosphere. *Sci. American* 210, 62-74.
- NEWTON, H. W. (1958) *The Face of the Sun*. Pelican, London. 208 pp.
- PAFFEN, K. (1967) Das Verhältniss der Tages-zur Jahreszeitlichen Temperaturschwankung. *Erdkunde* 21, 94-111.
- PLASS, G. M. (1959) Carbon dioxide and climate. *Sci. American* 201, 41-7.
- RADOS, R. M. (1967) The evolution of the TIROS meteorological satellite operational system. *Bull. Amer. Met. Soc.* 48, 326-37.
- RANSOM, W. H. (1963) Solar radiation and temperature. *Weather* 8, 18-23.
- RATCLIFFE, J. A. (ed.) (1960) *Physics of the Upper Atmosphere*. Academic Press, New York and London. 586 pp.
- SHEPPARD, P. A. (1968) Global atmospheric research. *Weather* 23, 262-83.
- STONE, R. (1955) Solar heating of land and sea. *Geography* 40, 288.
- SUTTON, G. (1963) Scales of temperature. *Weather* 18, 130-4.
- VALLEY, S. L. (ed.) (1965) *Handbook of Geophysics and Space Environments*. McGraw-Hill, New York.
- VONDERHAAR, T. H. and SUOMI, V. E. (1971) Measurements of the earth's radiation budget from satellites during a five-year period. Part I. Extended time and space means. *J. Atmos. Sci.*, 28, 305-14.
- WORLD METEOROLOGICAL ORGANIZATION (1964) Regional basic networks. *W.M.O. Bulletin* 13, 146-7.

Chapter 2 Atmospheric moisture

- ARMSTRONG, C. F. and STIDD, C. K. (1967) A moisture-balance profile in the Sierra Nevada. *J. of Hydrology* 5, 258-68.
- BANNON, J. K. and STEELE, L. P. (1960) Average water-vapour content of the air. *Geophysical Memoirs Meteorological Office* 102, 38 pp.
- BERGERON, T. (1960) Problems and methods of rainfall investigation. In *The Physics of Precipitation*, Geophysical Monograph. 5 Amer. Geophys. Union, Washington. 5-30.
- BORCHERT, J. R. (1971) The dust bowl in the 1970's. *Ann. Assn. Amer. Geogr.* 61, 1-22.
- BRAHAM, R. R. (1959) How does a raindrop grow? *Science* 129, 123-9.
- BYERS, H. R. and BRAHAM, R. R. (1949) *The Thunderstorm*. U.S. Weather Bureau.
- DALBY, D. and HARRISON CHURCH, R. J. (eds.). (1973) *Drought in Africa*. Centre for African Studies, School of Oriental and African Studies, Univ. of London. 124 pp.
- DEACON, E. I. (1969) Physical processes near the surface of the earth. In Flohn, H. (ed.), *General Climatology*, World Survey of Climatology 2. Elsevier, Amsterdam. pp. 39-104.
- DURBIN, W. G. (1961) An introduction to cloud physics. *Weather* 16, 71-82 and 113-25.
- FAST, T. W. R. and MARSHALL, J. S. (1954) Turbulence in clouds as a factor in precipitation. *Quart. J. Roy. Met. Soc.* 80, 26-47.
- GARCIA-PRIETO, P. R., LUDLAM, P. H. and SAUNDERS, P. M. (1960) The possibility of artificially increasing rainfall on Tenerife in the Canary Islands. *Weather* 15, 39-51.
- GILMAN, C. S. (1964) Rainfall. In Chow, V. T. (ed.), *Handbook of Applied Hydrology*. McGraw-Hill, New York. Section 9.
- HARROLD, T. W. (1966) The measurement of rainfall using radar. *Weather* 21, 247-9 and 256-8.
- HASTENRATH, S. L. (1967) Rainfall distribution and regime in Central America. *Archiv. Met. Geophys. Biokl. B*, 15 (3), 201-41.
- HERSFIELD, D. M. (1961) Rainfall frequency atlas of the United States for durations from 30 minutes to 24 hours and return periods of 1 to 100 years. U.S. Weather Bureau, Tech. Rept. 40.
- HOPKINS, M. M. JR. (1967) An approach to the classification of meteorological satellite data. *J. Appl. Met.* 6, 164-78.
- HOWE, G. M. (1956) The moisture balance in England and Wales. *Weather* 11, 74-82.
- JIUSTO, J. E. and WEICKMANN, H. K. (1973) Types of snowfall. *Bull. Amer. Met. Soc.* 54, 148-62.
- LANDSBERG, H. E. (1974) Drought, a recurring element of climate. *Graduate Program in Meteorology, University of Maryland*, Contribution No. 100. 47 pp.

- LATHAM, J. (1966) Some electrical processes in the atmosphere. *Weather* 21, 120-7.
- LIGDA, M. G. H. (1951) Radar storm observation. In Malone, T. F. (ed.), *Compendium of Meteorology*. American Meteorological Society, Boston, Mass. pp. 1265-82.
- LINSLEY, R. K. and FRANZINI, J. B. (1964) *Water-Resources Engineering*. McGraw-Hill, New York. 654 pp.
- LUDLAM, F. H. (1956) The structure of rainclouds. *Weather* 11, 187-96.
- MCDONALD, J. E. (1962) The evaporation-precipitation fallacy. *Weather* 17, 168-77.
- MASON, B. J. (1959) Recent developments in the physics of rain and rainmaking. *Weather* 14, 81-97.
- MASON, B. J. (1962a) *Clouds, Rain and Rainmaking*. C.U.P., Cambridge. 145 pp.
- MASON, B. J. (1962b) Charge generation in thunderstorms. *Endeavour* 21, 156-63.
- MÖLLER, F. (1951) Vierteljahrkarten des Niederschlags für die ganze Erde. *Petermanns Geographische Mitteilungen*, 95 Jahrgang, 1-7.
- MORE, R. J. (1967) Hydrological models and geography. In Chorley, R. J. and Haggett, P. (eds.), *Models in Geography*. Methuen, London. p. 145-85.
- NORDBERG, W. and PRESS, H. (1964) The 'Nimbus I' meteorological satellite. *Bull. Amer. Met. Soc.* 45, 684-7.
- PAULHUS, J. L. H. (1965) Indian Ocean and Taiwan rainfall set new records. *Monthly Weather Review* 93, 331-5.
- PEARL, R. T. et al. (1954) *The calculation of irrigation need*. Tech. Bull. No. 4, Min. Agric., Fish and Food. H.M.S.O., London. 35 pp.
- PENMAN, H. L. (1963) *Vegetation and Hydrology*. Tech. Comm. No. 53. Commonwealth Bureau of Soils, Harpenden. 124 pp.
- REITAN, C. H. (1960) Mean monthly values of precipitable water over the United States, 1946-56. *Monthly Weather Review* 88, 25-35.
- SAWYER, J. S. (1956) The physical and dynamical problems of orographic rain. *Weather* 11, 375-81.
- SCHERMERHORN, V. P. (1967) Relations between topography and annual precipitation in western Oregon and Washington. *Water Resources Research* 3, 707-11.
- SIMPSON, C. G. (1941) On the formation of clouds and rain. *Quart. J. Roy. Met. Soc.* 67, 99-133.
- SUTCLIFFE, R. C. (1956) Water balance and the general circulation of the atmosphere. *Quart. J. Roy. Met. Soc.* 82, 385-95.
- WARD, R. C. (1963) Measuring potential evapotranspiration. *Geography* 47, 49-55.
- WEISCHET, W. (1965) Der tropische-konvektive und der ausser tropische-advektive Typ der vertikalen Niederschlagsverteilung. *Erdkunde* 19, 6-14.
- WIDGER, W. K. (1961) Satellite meteorology - fancy and fact. *Weather* 16, 47-55.

- WINSTANLEY, D. (1973) Rainfall patterns and the general atmospheric circulation. *Nature* 245, 190-4.
- WINSTON, J. S. (1962) The operational use of meteorological satellite data. *Ann. New York Acad. Sci.* 93, 775-812.
- WORLD METEOROLOGICAL ORGANIZATION (1956) *International Cloud Atlas*. Geneva.
- WORLD METEOROLOGICAL ORGANIZATION (1972) *Distribution of precipitation in mountainous areas*, 2 vols. W.M.O. No. 326. Geneva. 228 and 587 pp.
- YARNELL, D. L. (1935) Rainfall intensity-frequency data. *U.S. Dept. Agr., Misc. Pub.* 204.

Chapter 3 Atmospheric motion

- BARRY, R. G. (1967) Models in meteorology and climatology. In Chorley, R. J. and Haggett, P. (eds.), *Models in Geography*. Methuen, London, pp. 97-144.
- BERAN, W. D. (1967) Large amplitude lee waves and chinook winds. *J. Appl. Met.* 6, 865-77.
- BORCHERT, J. R. (1953) Regional differences in world atmospheric circulation. *Ann. Assn. Amer. Geog.* 43, 14-26.
- BRINKMANN, W. A. R. (1971) What is a foehn? *Weather* 26, 230-9.
- BRINKMANN, W. A. R. (1974) Strong downslope winds at Boulder, Colorado. *Mon. Wea. Rev.* 102, 592-602.
- BUETTNER, K. J. and THYER, N. (1965) Valley winds in the Mount Rainier area. *Archiv. Met. Geophys. Biokl. B*, 14, 125-47.
- CORBY, G. A. (ed.) (1970) *The global circulation of the atmosphere*. Roy. Met. Soc., London. 257 pp.
- CROWE, P. R. (1950) The seasonal variation in the strength of the trades. *Trans. Inst. Brit. Geog.* 16, 23-47.
- DEFANT, F. and TABA, H. (1957) The threefold structure of the atmosphere and the characteristics of the tropopause. *Tellus* 9, 259-74.
- DIETRICH, G. (1963) *General Oceanography: An Introduction*. Wiley, New York. 588 pp.
- EDDY, A. (1966) The Texas coast sea-breeze: A pilot study. *Weather* 1, 162-50
- FLOHN, H. (1969) Local wind systems. In Flohn, H. (ed.) *General Climatology, World Survey of Climatology*, 2. Elsevier, Amsterdam. pp. 139-71.
- GARRELL, M. A. (1947) *Tropical and Equatorial Meteorology*. Pitman, London. 237 pp.
- GEIGER, R. (1969) Topoclimates. In Flohn, H. (ed.), *General Climatology, World Survey of Climatology*, 2. Elsevier, Amsterdam. pp. 105-38.
- GLENN, C. L. (1961) The chinook. *Weatherwise* 14, 175-82.
- HARE, F. K. (1965) Energy exchanges and the general circulation. *Geography* 50, 229-41.
- JOHNSON, A. and O'BRIEN, J. J. (1973) A study of an Oregon sea breeze event. *J. Appl. Met.* 12, 1267-83.

- KUENEN, PH. H. (1955) *Realms of Water*. Cleaver-Hulme Press, London, 327 pp.
- LAMB, H. H. (1960) Representation of the general atmospheric circulation. *Met. Mag.* 89, 319-30.
- LOCKWOOD, J. G. (1962) Occurrence of föhn winds in the British Isles. *Met. Mag.* 91, 57-65.
- LORENZ, E. N. (1967) *The nature and theory of the general circulation of the atmosphere*. World Meteorological Organization, Geneva. 161 pp.
- MCDONALD, J. E. (1952) The Coriolis effect. *Sci. American* 186, 72-8.
- NAMIAS, J. (1972) Large-scale and long-term fluctuations in some atmospheric and ocean variables. In Dyrssen, D. and Jagner, D. (eds.), *The Changing Chemistry of the Oceans*, Nobel Symposium 20. Wiley, New York, pp. 27-48.
- O'CONNOR, J. F. (1961) Mean circulation patterns based on 12 years of recent northern hemispheric data. *Monthly Weather Review* 89, 211-28.
- PALMÉN, E. (1951) The role of atmospheric disturbances in the general circulation. *Quart. J. Roy. Met. Soc.* 77, 337-54.
- PFEIFFER, R. L. (1964) The global atmospheric circulation. *Trans. New York Acad. Sci.*, ser. 11, 26, 984-97.
- RIEHL, H. (1962a) General atmospheric circulation of the tropics. *Science* 135, 13-22.
- RIEHL, H. (1962b) *Jet streams of the atmosphere*. Tech. Paper No. 32. Colorado State Univ. 117 pp.
- RIEHL, H. (1969) On the role of the tropics in the general circulation of the atmosphere. *Weather* 24, 288-308.
- RIEHL, H. et al. (1954) The jet stream *Met. Monogr.* 2 (7). American Meteorological Society, Boston, Mass. 100 pp.
- ROSSBY, C.-G. (1941) The scientific basis of modern meteorology. U.S., Dept. of Agriculture Yearbook *Climate and Man*. pp. 599-655.
- ROSSBY, C.-G. (1949) On the nature of the general circulation of the lower atmosphere. In Kuiper, G. P. (ed.), *The Atmosphere of the Earth and Planets*. Univ. of Chicago Press, Chicago, Ill. pp. 16-48.
- ROWNTREE, P. R. (1972) The influence of the tropical east Pacific Ocean temperatures on the atmosphere. *Quart. J. Roy. Met. Soc.* 98, 290-321.
- SAWYER, J. S. (1957) Jet stream features of the earth's atmosphere. *Weather* 12, 333-4.
- SCORER, R. S. (1958) *Natural Aerodynamics*. Pergamon Press, Oxford. 312 pp.
- SCORER, R. S. (1961) Lee waves in the atmosphere. *Sci. American* 204, 124-34.
- STARR, V. P. (1956) The general circulation of the atmosphere. *Sci. American* 195, 40-5.
- TALJAARD, J. J., VAN LOON, H., CRUTCHFIELD, H. L. and JENNE, R. L. (1969) *Climate of the upper Air, Part 1. Southern Hemisphere*, Vol. 1. Naval Weather Service Command, Washington, D.C. NAVAIR 50-1C-55.
- TUCKER, G. B. (1961) Some developments in climatology during the last decade. *Geography* 46, 198-207.

376 Atmosphere, weather and climate

- TUCKER, G. B. (1962) The general circulation of the atmosphere. *Weather* 17, 320-40.
- VAN ARK, W. S. (1962) *Introduction to Physical Oceanography*. Addison-Wesley, Reading, Mass. 422 pp.
- VAN LOON, H. (1964) Mid-season average zonal winds at sea level and at 500 mb south of 25°S and a brief comparison with the northern hemisphere. *J. Appl. Met.* 3, 554-63.
- WACO, D. E. (1968) Frost pockets in the Santa Monica Mountains of southern California. *Weather* 23, 456-61.
- WALKER, J. M. (1972) Monsoons and the global circulation. *Met. Mag.* 101, 349-55.
- WALLINGTON, C. E. (1960) An introduction to lee waves in the atmosphere. *Weather* 15, 269-76.
- WALLINGTON, C. F. (1969) Depressions as moving vortices. *Weather* 24, 42-51.
- WICKHAM, P. G. (1966) Weather for gliding over Britain. *Weather* 21, 154-61.

Chapter 4 Air masses, fronts and depressions

- BARRETT, E. C. (1964) Satellite meteorology and the geographer. *Geography* 49, 377-86.
- BATES, F. C. (1962) Tornadoes in the central United States. *Trans. Kansas Acad. Sci.* 65, 215-46.
- BELASCO, J. E. (1952) Characteristics of air masses over the British Isles. *Geophysical Memoirs*, Meteorological Office, 11 (87) 34 pp.
- BOUCHER, R. J. and NEWCOMB, R. J. (1962) Synoptic interpretation of some TIROS vortex patterns: A preliminary cyclone model. *J. Appl. Met.* 1, 122-36.
- BOYDEN, C. J. (1960) The use of upper air charts in forecasting. *The Marine Observer* 30, 27-31.
- BOYDEN, C. J. (1963) Development of the jet stream and cut-off circulations. *Met. Mag.* 92, 287-99.
- BROWNING, K. A. (1968) The organization of severe local storms. *Weather* 23, 429-34.
- BRUNK, I. W. (1953) Squall Lines. *Bull. Amer. Met. Soc.* 34, 1-9.
- CRESSMAN, G. P. (1965) Numerical weather prediction in daily use. *Science* 148, 319-27.
- CROWE, P. R. (1949) The trade wind circulation of the world. *Trans. Inst. Brit. Geog.* 15, 38-56.
- CROWE, P. R. (1965) The geographer and the atmosphere. *Trans. Inst. Brit. Geog.* 36, 1-19.
- FAWBUSH, E. J. and MILLER, R. C. (1954) The types of airmasses in which North American tornadoes form. *Bull. Amer. Met. Soc.* 35, 154-65.
- FREEMAN, M. H. (1961) Fronts investigated by the Meteorological Research Flight. *Met. Mag.* 90, 189-203.

- FULKS, J. R. (1951) The instability line. In Malone, T. F. (ed.), *Compendium of Meteorology*. American Meteorological Society, Boston, Mass. pp. 647–52.
- GALLOWAY, J. L. (1958a) The three-front model; its philosophy, nature, construction and use. *Weather* 13, 3–10.
- GALLOWAY, J. L. (1958b) The three-front model, the tropopause and the jet stream. *Weather* 13, 395–403.
- GALLOWAY, J. L. (1960) The three-front model, the developing depression and the occluding process. *Weather* 15, 293–309.
- GENTILLI, J. (1949) Air masses of the southern hemisphere. *Weather* 4, 258–61 and 292–7.
- GODSON, W. L. (1950) The structure of North American weather systems. *Cent. Proc. Roy. Met. Soc.* London. pp. 89–106.
- HARE, F. K. (1960) The westerlies. *Geog. Rev.* 50, 345–67.
- HARMAN, J. R. (1971) Tropical waves, jet streams, and the United States weather patterns. *Association of American Geographers, Commission on College Geography, Resource Paper No. 11.* 37 pp.
- HARROLD, T. W. (1973) Mechanisms influencing the distribution of precipitation within baroclinic disturbances. *Quart. J. Roy. Met. Soc.* 99, 232–51.
- HOUGHTON, D. M. (1965) Current forecasting practice. *Quart. J. Roy. Met. Soc.* 91, 524–6.
- KLEIN, W. H. (1948) Winter precipitation as related to the 700-mb circulation. *Bull. Amer. Met. Soc.* 29, 439–53.
- KLEIN, W. H. (1957) Principal tracks and mean frequencies of cyclones and anti-cyclones in the Northern Hemisphere. *Research Paper No. 40, Weather Bureau.* Washington. 60 pp.
- KNIGHTING, F. (1958) Numerical weather forecasting. *Weather* 13, 39–50.
- LAMB, H. H. (1951) Essay on frontogenesis and frontolysis. *Met. Mag.* 80, 55–6, 65–71 and 97–106.
- LUDLAM, F. H. (1961) The hailstorm. *Weather* 16, 152–62.
- LYALL, I. T. (1972) The polar low over Britain. *Weather* 27, 378–90.
- MASON, B. J. (1968) Forecasting the weather by computer. *The Advancement of Science* 24, 263–72.
- MASON, B. J. (1974) The contribution of satellites to the exploration of the global atmosphere and to the improvement of weather forecasting. *Met. Mag.* 103, 181–201.
- MILES, M. K. (1961) The basis of present-day weather forecasting. *Weather* 16, 349–63.
- MILES, M. K. (1962) Wind, temperature and humidity distribution at some cold fronts over S.E. England. *Quart. J. Roy. Met. Soc.* 88, 286–300.
- MILLER, R. C. (1959) Tornado-producing synoptic patterns. *Bull. Amer. Met. Soc.* 40, 465–72.
- MILLER, R. C. and STARRETT, I. G. (1962) Thunderstorms in Great Britain. *Met. Mag.* 91, 247–55.
- NEWTON, C. W. (1966) Severe convective storms. *Adv. Geophys.* 12, 257–308.

378 Atmosphere, weather and climate

- NEWTON, C. W. (ed.) (1972) *Meteorology of the Southern Hemisphere*. Met. Monogr. 13, (35). American Meteorological Society, Boston, Mass. 263 pp.
- PEDGLEY, D. E. (1962) A meso-synoptic analysis of the thunderstorms on 28 August 1958. *Geophysical Memoirs Meteorological Office* 14 (1) 30 pp.
- PENNER, C. M. (1955) A three-front model for synoptic analyses. *Quart. J. Roy. Met. Soc.* 81, 89-91.
- PETTERSEN, S. (1950) Some aspects of the general circulation of the atmosphere. *Cent. Proc. Roy. Met. Soc. London*, pp. 120-55.
- POTHECARY, I. J. W. (1956) Recent research on fronts. *Weather* 12, 147-50.
- REED, R. J. (1960) Principal frontal zones of the northern hemisphere in winter and summer. *Bull. Am. Met. Soc.* 41, 591-8.
- RICHTER, D. A. and DAHL, R. A. (1958) Relationship of heavy precipitation to the jet maximum in the eastern United States. *Monthly Weather Review* 86, 368-76.
- SAWYER, J. S. (1967) Weather forecasting and its future. *Weather* 22, 350-9.
- SHOWALTER, A. K. (1939) Further studies of American air mass properties. *Monthly Weather Review* 67, 204-18.
- SUTCLIFFE, R. C. (1964) Weather forecasting by electronic computer. *Endeavour* 23, 27-32.
- SUTCLIFFE, R. C. and FORSDYKE, A. G. (1950) The theory and use of upper air thickness patterns in forecasting. *Quart. J. Roy. Met. Soc.* 76, 189-217.
- VEDERMAN, J. (1954) The life cycles of jet streams and extratropical cyclones. *Bull. Amer. Met. Soc.* 35, 239-44.
- WALLINGTON, C. E. (1963) Mesoscale patterns of frontal rainfall and cloud. *Weather* 18, 171-81.
- WASHINGTON, W. (1968) Computer simulation of the earth's atmosphere. *Science Jour.* 4, 37-41.
- WICK, G. (1973) Where Poseidon courts Aeolus. *New Scientist*, 18 January, pp. 123-26.
- YOSHINO, M. M. (1967) Maps of the occurrence frequencies of fronts in the rainy season in early summer over east Asia. *Science Reports of the Tokyo University of Education*, (89), 211-45.

Chapter 5 Weather and climate in temperate latitudes

- BAILEY, H. P. (1964) Toward a unified concept of the temperate climate. *Geog. Rev.* 54 (4), 516-45.
- BARRY, R. G. (1963) Aspects of the synoptic climatology of central south England. *Met. Mag.* 92, 300-8.
- BARRY, R. G. (1967a) Seasonal location of the arctic front over North America. *Geog. Bull.* 9, 79-95.
- BARRY, R. G. (1967b) The prospect for synoptic climatology: A case study. In Steel, R. W. and Lawton, R. (eds.), *Liverpool Essays in Geography*. Longmans, London. pp. 85-106.

- BARRY, R. G. (1973) A climatological transect on the east slope of the Front Range, Colorado. *Arct. Alp. Res.* 5, 89-110.
- BARRY, R. G. and HARE, F. K. (1974) Arctic climate. In Ives, J. D. and Barry, R. G. (eds.), *Arctic and Alpine Environments*. Methuen, London. pp. 17-54.
- BELASCO, J. E. (1948) The incidence of anticyclonic days and spells over the British Isles. *Weather* 3, 233-42.
- BILHAM, E. G. (1938) *The Climate of the British Isles*. Macmillan, London. 347 pp.
- BLEEKER, W. and ANDRE, M. J. (1951) On the diurnal variation of precipitation, particularly over central U.S.A., and its relation to large-scale orographic circulation systems. *Quart. J. Roy. Met. Soc.* 77, 260-77.
- BOAST, R. and MCQUINNIGLE, J. B. (1972) Extreme weather conditions over Cyprus during April 1971. *Met. Mag.* 101, 137-53.
- BORCHERT, J. (1950) The climate of the central North American grassland. *Ann. Assn. Amer. Geog.* 40, 1-39.
- BRYSON, R. A. (1966) Air masses, streamlines and the boreal forest. *Geog. Bull.* 8, 228-69.
- BRYSON, R. A. and HARE, F. K. (eds.) (1974) *Climates of North America*. World Survey of Climatology, Vol. 11. Elsevier, Amsterdam. 420 pp.
- BRYSON, R. A. and LAHEY, J. F. (1958) *The March of the Seasons*. Meteorological Department, University of Wisconsin. 41 pp.
- BRYSON, R. A. and LOWRY, W. P. (1955) Synoptic climatology of the Arizona summer precipitation singularity. *Bull. Amer. Met. Soc.* 36, 329-39.
- BURBIDGE, F. E. (1951) The modification of continental polar air over Hudson Bay. *Quart. J. Met. Soc.* 77, 365-74.
- BUTZER, K. W. (1960) Dynamic climatology of large-scale circulation patterns in the Mediterranean area. *Meteorologische Rundschau* 13, 97-105.
- ENVIRONMENTAL SCIENCE SERVICES ADMINISTRATION (1965) *APT Users' Guide*. U.S. Department of Commerce, Washington D.C. 80 pp.
- ENVIRONMENTAL SCIENCE SERVICES ADMINISTRATION (1968) *Climatic Atlas of the United States*. U.S. Department of Commerce, Washington D.C. 80 pp.
- FLOHN, H. (1954) *Witterung und Klima in Mitteleuropa*. Zurich. 218 pp.
- GENTILLI, J. (ed.) (1971) *Climates of Australia and New Zealand*. World Survey of Climatology, 13. Elsevier, Amsterdam. 405 pp.
- GORCZYNSKI, W. (1920) Sur le calcul du degré du continentalisme et son application dans la climatologie. *Geografiska Annaler* 2, 324-31.
- GREEN, C. R. and SELLERS, W. D. (1964) *Arizona Climate*. University of Arizona Press, Tucson. 503 pp.
- HALES, J. E., JR. (1974) Southwestern United States summer monsoon source - Gulf of Mexico or Pacific Ocean. *J. Appl. Met.* 13, 331-42.
- HARE, F. K. (1968) The Arctic. *Quart. J. Roy. Met. Soc.* 74, 439-59.
- HAWKE, E. L. (1933) Extreme diurnal range of air temperature in the British Isles. *Quart. J. Roy. Met. Soc.* 59, 261-5.

380 Atmosphere, weather and climate

- HORN, L. H. and BRYSON, R. A. (1960) Harmonic analysis of the annual march of precipitation over the United States. *Ann. Assn. Am. Geog.* 50, 157-71.
- HUTTARY, J. (1950) Die Verteilung der Niederschläge auf die Jahreszeiten im Mittelmeergebiet. *Meteorologische Rundschau* 3, 111-19.
- KENDREW, W. G. and CURRIE, B. W. (1955) *The Climate of Central Canada*. Queen's Printer, Ottawa. 194 pp.
- KLEIN, W. H. (1963) Specification of precipitation from the 700-mb circulation. *Monthly Weather Review* 91, 527-36.
- LAMB, H. H. (1950) Types and spells of weather around the year in the British Isles: Annual trends, seasonal structure of the year, singularities. *Quart. J. Roy. Met. Soc.* 76, 393-438.
- LONGLEY, R. W. (1967) The frequency of Chinooks in Alberta. *The Albertan Geographer* 3, 20-2.
- LUMB, F. E. (1961) Seasonal variations of the sea surface temperature in coastal waters of the British Isles. *Met. Office Sci. Paper No. 6*, M.O. 685. 21 pp.
- MANLEY, G. (1944) Topographical features and the climate of Britain. *Geog. Jour.* 103, 241-58.
- MANLEY, G. (1945) The effective rate of altitude change in temperate Atlantic climates. *Geog. Rev.* 35, 408-17.
- METEOROLOGICAL OFFICE (1952) *Climatological Atlas of the British Isles*, M.O. 488. H.M.S.O., London. 139 pp.
- METEOROLOGICAL OFFICE (1962) *Weather in the Mediterranean*. H.M.S.O., London. I, General Meteorology, 2nd edn., 362 pp.
- METEOROLOGICAL OFFICE (1964a) *Weather in the Mediterranean*. M.O. 391b. H.M.S.O., London. 2, 372 pp.
- METEOROLOGICAL OFFICE (1964b) *Weather in Home Fleet Waters*, M.O. 732a. H.M.S.O., London. Vol. 1, The Northern Seas, Part 1, 265 pp.
- NAMIAS, J. (1964) Seasonal persistence and recurrence of European blocking during 1958-1960. *Tellus* 16, 394-407.
- RAYNER, J. N. (1961) *Atlas of Surface Temperature Frequencies for North America and Greenland*. Arctic Meteorological Research Group, McGill University, Montreal.
- REX, D. F. (1950-51) The effect of Atlantic blocking action upon European climate. *Tellus* 2, p. 196-211 and 275-301, 3, 100-11.
- SCHICK, A. P. (1971) A desert flood. *Jerusalem Studies in Geography* 2, 91-155.
- SHAW, E. M. (1962) An analysis of the origins of precipitation in Northern England, 1956-60. *Quart. J. Roy. Met. Soc.* 88, 539-47.
- SIVALL, T. (1957) Sirocco in the Levant. *Geografiska Annaler* 39, 114-42.
- SUMNER, E. J. (1959) Blocking anticyclones in the Atlantic-European sector of the northern hemisphere. *Met. Mag.* 88, 300-11.
- THOMAS, M. K. (1964) A survey of Great Lakes snowfall. *Great Lakes Research Division, Univ. Of Michigan, Publication No. 11* pp. 294-310.
- THORNTONTHWAITE, C. W. and MATHER, J. R. (1955) *The Moisture Balance*, Publications in Climatology, 8 (1). Laboratory of Climatology, Centerton, N.J. 104 pp.

- UNITED STATES WEATHER BUREAU (1947) *Thunderstorm Rainfall*. Vicksburg, Mississippi. 331 pp.
- VILLMOW, J. R. (1956) The nature and origin of the Canadian dry belt. *Ann. Assn. Amer. Geog.* 46, 221-32.
- VISHER, S. S. (1954) *Climatic Atlas of the United States*. Harrd. 403 pp.
- WALLÉN, C. C. (1960) Climate. In Somme, A. (ed.), *The Geography of Norden*. Cappelens Forlag, Oslo. pp. 41-53.
- WALLÉN, C. C. (ed.) (1970) *Climates of Northern and Western Europe*, World Survey of Climatology, 5. Elsevier, Amsterdam. 253 pp.

Chapter 6 Tropical weather and climate

- ACADEMICA SINICA (1957-58) On the general circulation over eastern Asia. *Tellus*, 9, 432-46, 10, 58-75 and 299-312.
- ARAKAWA, H. (ed.) (1969) *Climates of Northern and Eastern Asia*, World Survey of Climatology, 8. Elsevier, Amsterdam. 248 pp.
- ATKINSON, G. D. (1971) *Forecasters Guide to Tropical Meteorology*. Headquarters Air Weather Service, U.S. Air Force, Tech. Rep. 240. 360 pp.
- BAUM, R. A. (1974) Eastern North Pacific hurricane season of 1973. *Monthly Weather Review* 102, 296-306.
- BECKJNSALE, R. P. (1957) The nature of tropical rainfall. *Tropical Agriculture*, 34, 76-98.
- BERGERON, T. (1954) The problem of tropical hurricanes. *Quart. J. Roy. Met. Soc.* 80, 131-64.
- BLUMENSTOCK, D. I. (1958) Distribution and characteristics of tropical climates. *Proc. 9th Pacific Sci. Congr.* 20, 3-23.
- CHANG, J.-H. (1957) Air mass maps of China proper and Manchuria. *Geography* 42, 142-8.
- CHANG, J.-H. (1962) Comparative climatology of the tropical western margins of the northern oceans. *Ann. Assn. Amer. Geog.* 52, 221-7.
- CHANG, J.-H. (1967) The Indian summer monsoon. *Geog. Rev.* 57, 373-96.
- CHOPRA, K. P. (1973) Atmospheric and oceanic flow problems introduced by islands. *Advances in Geophysics*, 16, 297-421.
- CROWE, P. R. (1949) The Trade Wind circulation of the world. *Trans. Inst. Brit. Geog.* 15, 37-56.
- CROWE, P. R. (1951) Wind and weather in the equatorial zone. *Trans. Inst. Brit. Geog.* 17, 23-76.
- CRY, G. W. (1965) Tropical cyclones of the North Atlantic Ocean. *Tech. Paper No. 55, Weather Bureau*. Washington. 148 pp.
- CURRY, L. and ARMSTRONG, R. W. (1959) Atmospheric circulation of the tropical Pacific ocean. *Geografiska Annaler* 41, 245-55.
- DUNN, G. F. and MILLER, B. I. (1960) *Atlantic Hurricanes*. Louisiana State University Press. 326 pp.
- ELDRIDGE, R. H. (1957) A synoptic study of West African disturbance lines. *Quart. J. Roy. Met. Soc.*, 83, 303-14.

382 Atmosphere, weather and climate

- FINDLATER, J. (1974) An extreme wind speed in the low-level jet-stream system of the western Indian Ocean. *Met. Mag.* 103, 201-5.
- FLOHN, H. (1968) *Contributions to a meteorology of the Tibetan Highlands*. Atmos. Sci. Paper No. 130. Colorado State Univ., Fort Collins. 120 pp.
- FLOHN, J. (1971) Tropical circulation patterns. *Bonn. Geogr. Abhandl.* 15, 55 pp.
- FOSBERG, F. R., GARNIER, B. J. and KÜCHLER, A. W. (1961) Delimitation of the humid tropics. *Geog. Rev.*, 51, 333-47.
- FRANK, N. L. and HUBERT, P. J. (1974) Atlantic tropical systems of 1973. *Monthly Weather Review* 102, 290-5.
- FROST, R. and STEPHENSON, P. H. (1965) Mean streamlines and isotachs at standard pressure levels over the Indian and west Pacific Oceans and adjacent land areas. *Geophys. Mem.* 14, (109) H.M.S.O., London. 24 pp.
- GARRELL, M. A. (1947) *Tropical and Equatorial Meteorology*. Pitman, London. 237 pp.
- GARNIER, B. J. (1967) Weather conditions in Nigeria. *Climatological Research Series No.* 2. McGill Univ. Press, Montreal. 163 pp.
- GRAY, W. M. (1968) Global view of the origin of tropical disturbances and hurricanes. *Monthly Weather Review* 96, 669-700.
- GREGORY, S. (1965) *Rainfall over Sierra Leone*; Geography Department, University of Liverpool, Research Paper No. 2. 58 pp.
- GRIFFITHS, J. R. (ed.) (1971) *Climates of Africa*, World Survey of Climatology, 10. Elsevier, Amsterdam. 604 pp.
- HUTCHINGS, J. W. (ed.) (1964) *Proceedings of the Symposium on Tropical Meteorology*. New Zealand Meteorological Service, Wellington. 737 pp.
- INDIAN METEOROLOGICAL DEPARTMENT (1960) *Monsoons of the World*. Delhi. 270 pp.
- JORDAN, C. L. (1955) Some features of the rainfall at Guam. *Bull. Amer. Met. Soc.* 36, 446-55.
- KOTESWARAM, P. (1958) The easterly jet stream in the tropics. *Tellus* 10, 43-57.
- KURASHIMA, A. (1968) Studies on the winter and summer monsoons in east Asia based on dynamic concept. *Geophys. Mag.* Tokyo 34, 145-236.
- LOCKWOOD, J. G. (1965) The Indian monsoon - a review. *Weather* 20, 2-8.
- LOGAN, R. F. (1960) The Central Namib Desert, South West Africa. *National Academy of Sciences, National Research Council, Publication* 758. Washington D.C. 162 pp.
- LOWELL, W. E. (1954) Local weather of the Chicama Valley, Peru. *Archiv Met. Geophys. Biokl. B*, 5, 41-51.
- LYDOLPH, P. E. (1957) A comparative analysis of the dry western littorals. *Ann. Assn. Amer. Geog.* 47, 213-30.
- MAEJIMA, I. (1967) Natural seasons and weather singularities in Japan. *Geog. Rept. No.* 2. Tokyo Metropolitan University. p. 77-103.
- MALKUS, J. S. (1955-56) The effects of a large island upon the trade-wind air stream. *Quart. J. Roy. Met. Soc.* 81, 538-50, and 82, 235-38.

- MALKUS, J. S. (1958) Tropical weather disturbances: why do so few become hurricanes? *Weather* 13, 75-89.
- MALKUS, J. S. and RIEHL, H. (1964) *Cloud Structure and Distributions over the Tropical Pacific Ocean*. Univ. of California Press, Berkeley and Los Angeles. 229 pp.
- MASON, B. J. (1970) Future developments in meteorology: An outlook to the year 2000. *Quart. J. Roy. Met. Soc.* 96, 349-68.
- MILLER, B. J. (1967) Characteristics of hurricanes. *Science* 157, 1389-99.
- MINK, J. F. (1960) Distribution pattern of rainfall in the leeward Koolau Mountains, Oahu, Hawaii. *J. Geophys. Res.* 65, 2869-76.
- PALMÉN, E. (1948) On the formation and structure of tropical hurricanes. *Geophysica*, 3, 26-38.
- PALMER, C. F. (1951) Tropical meteorology. In Malone, T. F. (ed.), *Compendium of Meteorology*. American Meteorological Society, Boston, Mass. pp 859-80.
- PÉDALABORDE, P. (1958) *Les Moussons*. Armand Colin, Paris, 208 pp. (English edn, Methuen, London, 1963, 196 pp.).
- RAGHARAN, K. (1967) Influence of tropical storms on monsoon rainfall in India. *Weather* 22, 250-5.
- RAMAGE, C. S. (1952) Relationships of general circulation to normal weather over southern Asia and the western Pacific during the cool season. *J. Met.* 9, 403-8.
- RAMAGE, C. S. (1964) Diurnal variation of summer rainfall in Malaya. *J. Trop. Geog.* 19, 62-8.
- RAMAGE, C. S. (1968) Problems of a monsoon ocean. *Weather* 23, 28-36.
- RAMAGE, C. S. (1971) *Monsoon Meteorology*. Academic Press, New York and London. 296 pp.
- RAMASWAMY, C. (1956) On the sub-tropical jet stream and its role in the development of large-scale convection. *Tellus* 8, 26-60.
- RAMASWAMY, C. (1962) Breaks in the Indian summer monsoon as a phenomenon of interaction between the easterly and the sub-tropical westerly jet streams. *Tellus* 14, 337-49.
- REITER, E. R. and HEUBERGER, H. (1960) A synoptic example of the retreat of the Indian summer monsoon. *Geografiska Annaler* 42, 17-35.
- RIEHL, H. (1954) *Tropical Meteorology*. McGraw-Hill, New York. 392 pp.
- RIEHL, H. (1963) On the origin and possible modification of hurricanes. *Science* 141, 1001-10.
- SAHA, R. R. (1973) Global distribution of double cloud bands over the tropical oceans. *Quart. J. Roy. Met. Soc.* 99, 551-5.
- SAITO, R. (1959) The climate of Japan and her meteorological disasters. *Proceedings of the International Geophysical Union, Regional Conference in Japan*, Tokyo 173-83.
- SAWYER, J. S. (1947) The structure of the Intertropical Front over N.W. India during the S.W. Monsoon. *Quart. J. Roy. Met. Soc.* 73, 246-69.

- SAWYER, J. S. (1970) Large-scale disturbance of the equatorial atmosphere. *Met. Mag.* 99, 1-9.
- SCORER, R. S. (1966) Origin of cyclones. *Science Jour.* 2 (3), 46-52.
- THOMPSON, B. W. (1951) An essay on the general circulation over South-East Asia and the West Pacific. *Quart. J. Roy. Met. Soc.* 569-97.
- THOMPSON, B. W. (1965) *The Climate of Africa* (Atlas). O.U.P., Nairobi.
- TREWARTH, G. T. (1958) Climate as related to the jet stream in the Orient. *Erdkunde* 12, 205-14.
- WATTS, I. E. M. (1955) *Equatorial Weather, with particular reference to South-east Asia*. O.U.P., London. 186 pp.
- WORLD METEOROLOGICAL ORGANIZATION (1972) Synoptic analysis and forecasting in the tropics of Asia and the southwest Pacific. *W.M.O. No. 321*, Geneva. 524 pp.
- YIN, M. T. (1949) A synoptic-aerologic study of the onset of the summer monsoon over India and Burma. *J. Met.* 6, 393-400.
- YOSHINO, M. M. (1969) Climatological studies on the polar frontal zones and the intertropical convergence zones over South, Southeast and East Asia. *Climatol. Notes*, Hosei University, 1, 71 pp.
- YOSHINO, M. M. (ed.) (1971) *Water Balance of Monsoon Asia*. University of Tokyo Press. 308 pp.
- YOUNG, J. A. (coordinator) (1972) *Dynamics of the Tropical Atmosphere*, (Notes from a Colloquium). National Center for Atmospheric Research, Boulder, Colorado. 587 pp.

Chapter 7 Urban and forest climates

- ATKINSON, B. W. (1968) A preliminary examination of the possible effect of London's urban area on the distribution of thunder rainfall 1951-60. *Trans. Inst. Brit. Geog.* 44, 97-118.
- BACH, W. (1971) Atmospheric turbidity and air pollution in Greater Cincinnati. *Geog. Rev.* 61, 573-94.
- BACH, W. and PATTERSON, W. (1969) Heat budget studies in Greater Cincinnati. *Proc. Assn. Amer. Geog.* 1, 7-16.
- BRYSON, R. A. and KUTZBACH, J. E. (1968) Air pollution. *Association of American Geographers, Commission on College Geography, Resource Paper* 2. 42 pp.
- CABORN, J. M. (1955) The influence of shelter-belts on microclimate. *Quart. J. Roy. Met. Soc.* 81, 112-5.
- CHAGNON, S. A., Jr. (1969) Recent studies of urban effects on precipitation in the United States. *Bull. Amer. Met. Soc.* 50, 411-21.
- CHANDLER, T. J. (1965) *The Climate of London*. Hutchinson, London. 292 pp.
- CHANDLER, T. J. (1967) Absolute and relative humidities in towns. *Bull. Amer. Met. Soc.* 394-9.
- COMMITTEE ON AIR POLLUTION (1955) *Report*, Crnd 9322. H.M.S.O., London.

- COUTTS, J. R. H. (1955) Soil temperatures in an afforested area in Aberdeenshire. *Quart. J. Roy. Met. Soc.* 81, 72-9.
- DUCKWORTH, F. S. and SANDBERG, J. S. (1954) The effect of cities upon horizontal and vertical temperature gradients. *Bull. Amer. Met. Soc.* 35, 198-207.
- FOOD AND AGRICULTURE ORGANISATION OF THE UNITED NATIONS (1962) *Forest Influences*, Forestry and Forest Products Studies No. 15, Rome. 307 pp.
- GARNETT, A. (1967) Some climatological problems in urban geography with special reference to air pollution. *Trans. Inst. Brit. Geog.* 42, 21-43.
- GOLDSMITH, J. R. (1969) Los Angeles smog. *Science Jour.* 5, 44-49.
- HEWSON, E. W. (1951) Atmospheric pollution. In Malone, T. F. (ed.), *Compendium of Meteorology*. American Meteorological Society, Boston, Mass. pp. 1139-57.
- JENKINS, I. (1969) Increases in averages of sunshine in Greater London. *Weather* 24, 52-4.
- KITTREDGE, J. (1948) *Forest Influences*. McGraw-Hill, New York. 394 pp.
- LANDSBERG, H. E. (1956) The climate of towns. In Thomas, W. L. (ed.), *Man's Role in Changing the Face of the Earth*. Chicago. pp. 584-603.
- LANDSBERG, H. E. (1970) Man-made climatic changes. *Science* 170, 1265-74.
- LOWRY, W. P. (1969) *Weather and Life*. Academic Press, New York. 305 pp.
- MACDONALD, G. J. F. (Chairman) (1966) Weather and climate modification: Problems and prospects. *Bull. Amer. Met. Soc.* 47, 4-19.
- MARSHALL, W. A. L. (1952) *A Century of London Weather*, Met. Office, Air Ministry, Rept MO 508. H.M.S.O., London. 103 pp.
- MEETHAM, A. R. (1952) *Atmospheric Pollution*. Pergamon Press, Oxford and London. 268 pp.
- MEETHAM, A. R. (1955) Know your fog. *Weather* 10, 103-5.
- NATIONAL ACADEMY OF SCIENCES (1966) *Spacecraft in Geographic Research*, National Research Council, Publication 1353. Washington. pp. 23-38.
- OLGYAY, V. (1963) *Design with Climate: Bioclimatic approach to architectural regionalism*. Princeton Univ. Press, Princeton, N.J. 190 pp.
- PARRY, M. (1966) The urban 'heat island'. In Tromps, W. and Weite, W. H. (eds.), *Biometeorology 2*. Pergamon Press, Oxford and London. pp. 616-24.
- RAMDAS, L. A. (1957) Natural and artificial modification of microclimate. *Weather* 12, 237-40.
- REYNOLDS, F. R. C. and LEYTON, L. (1963) Measurement and significance of through-fall in forest stands. In Whitehead, F. M. and Rutter, A. J. (eds.), *The Water Relations of Plants*. Blackwell Scientific Publications, Oxford. pp. 127-41.
- RICHARDS, P. W. (1952) *The Tropical Rain Forest*. Cambridge. 450 pp.
- RUTTER, A. J. (1967) Evaporation in forests. *Endeavour* 97, 39-43.
- SARGENT, F. (1967) A dangerous game: Taming the weather. *Bull. Am. Met. Soc.* 48, 452-8.

- SCORER, R. (1968) *Air Pollution*. Pergamon Press, Oxford and London. 151 pp.
- SEWELL, W. R. D. (ed.) (1966) Human dimensions of weather modification. *Univ. Chicago, Dept. of Geography, Research Paper* 105. 423 pp.
- SIMPSON, R. H. and SIMPSON, J. (1966) 'Why experiment on tropical hurricanes?' *Trans. New York Acad. Sci.*, II, 28 (8). 1045-62.
- SOPPER, W. E. and LULL, H. W. (eds.) (1967) *International Symposium on Forest Hydrology*. Pergamon Press, Oxford and London. 813 pp.
- STEARNS, A. C. (ed.) (1968) *Atmospheric Pollution*, 3 vols. Academic Press, New York.
- SUKACHEV, V. and DYLIS, N. (1968) *Fundamentals of Forest Biogeocoenology*. Oliver and Boyd, Edinburgh. 672 pp.
- TERJUNG, W. H. (1970) Urban energy balance climatology. *Geog. Rev.* 60, 31-53.
- TERJUNG, W. H. and LOUIS, S. S.-F. (1973) Solar radiation and urban heat islands. *Ann. Assn. Amer. Geog.* 63, 181-207.
- TURNER, W. C. (1955) Atmospheric pollution. *Weather* 10, 110-19.
- TYSON, P. D., GARSTANG, M. and EMMITT, G. D. (1973) The structure of heat islands. *Occasional Paper No. 12*. Dept. of Geography and Environmental Studies, University of the Witwatersrand, Johannesburg. 71 pp.
- WORLD METEOROLOGICAL ORGANIZATION (1970) Urban climates. *W.M.O. Technical Note No. 108*. 390 pp.
- ZON, R. (1941) Climate and the nation's forests. U.S. Dept. of Agriculture Yearbook *Climate and Man*. pp. 477-98.

Chapter 8 Climatic variability, trends and fluctuations

- AHLMANN, H. W. (1948) The present climatic fluctuation. *Geog. Jour.* 113, 165-93.
- BECKINSALE, R. P. (1965) Climatic change: A critique of modern theories. In Whittow, J. B. and Wood, P. D. (eds.), *Essays in Geography for Austin Miller*. Univ. of Reading Press. pp. 1-38.
- BRYSON, R. A. (1968) All other factors being constant . . .; *Weatherwise*. 21, 51-61.
- BRYSON, R. A. (1974) A perspective on climatic change. *Science* 184, 753-60.
- CALLendar, G. S. (1961) Temperature fluctuations and trends over the earth. *Quart. J. Roy. Met. Soc.* 87, 1-12.
- CONRAD, V. and POLLAK, L. W. (1950) *Methods in Climatology*. Harvard Univ. Press. Cambridge, Mass. See ch. 2, Statistical analysis of climatic elements, pp. 17-60.
- DAVITAYA, F. F. (1969) Atmospheric dust content as a factor affecting glaciation and climatic change. *Ann. Assoc. Amer. Geog.* 59, 552-60.
- DORF, F. (1960) Climatic changes of the past and present. *Amer. Scientist* 48, 341-64.
- GREGORY, S. (1962) *Statistical Methods and the Geographer*. Longmans, London. 240 pp. (and subsequent editions).

- GREGORY, S. (1969) Rainfall reliability. In Thomas, M. F. and Whittington, G. W. (eds.), *Environment and Land Use in Africa*. Methuen, London. pp. 57-82.
- KRAUS, E. B. (1955) Secular changes of tropical rainfall regimes. *Quart. J. Roy. Met. Soc.* 81, 198-210.
- LAMB, H. H. (1965) Frequency of weather types. *Weather* 20, 9-12.
- LAMB, H. H. (1966) *The Changing Climate: Selected Papers*. Methuen, London. 236 pp.
- LAMB, H. H. (1970) Volcanic dust in the atmosphere; with a chronology and an assessment of its meteorological significance. *Phil. Trans. Roy. Soc., A*, 266, 425-533.
- LAWRENCE, E. N. (1965) Terrestrial climate and the solar cycle. *Weather* 20, 334-43.
- LEOPOLD, L. B. (1951) Rainfall frequency: An aspect of climatic variation. *Trans. Amer. Geophys. Union*, 32 (3), 347-57.
- LEWIS, P. (1960) The use of moving averages in the analysis of time-series. *Weather* 15, 121-6.
- LYSGAARD, L. (1949) Recent climatic fluctuations. *Folia Geographica Danica*. Kongelige Danske Geog., Selskab 5, 215.
- MANLEY, G. (1958) Temperature trends in England, 1698-1957. *Archiv Met. Geophys. Biokl.*, B (Vienna), 9, 413-33.
- MATHER, J. R. (1954) The present climatic fluctuation and its bearing on a reconstruction of Pleistocene climatic conditions. *Tellus* 3, 287.
- MITCHELL, J. M., JR. (ed.) (1968) Causes of climatic change. *Amer. Met. Soc. Monogr.* 8 (30) 159 pp.
- MITCHELL, J. M., JR. (1972) The natural breakdown of the present interglacial and its possible intervention by human activities. *Quat. Res.* 2, 436-45.
- PLASS, G. N. (1959) Carbon dioxide and climate. *Sci. American* 201, 41-7.
- SCHNEIDER, S. H. and KELLOGG, W. W. (1973) The chemical basis for climate change. In Rasool, S. I. (ed.), *Chemistry of the Lower Atmosphere*. Plenum Press, New York. pp. 203-49.
- SHAPLEY, H. (ed.) (1953) *Climatic Change*. Harvard Univ. Press, Cambridge, Mass. 318 pp.
- Study of Man's Impact on Climate (SMIC) (1971) *Inadvertent Climate Modification*. Massachusetts Institute of Technology Press, Cambridge, Mass. 308 pp.
- TUCKER, G. B. (1964) Solar influences on the weather. *Weather* 19, 302-11.
- UNESCO (1963) Changes of Climate. *Arid Zone Research*, 20. UNESCO, Paris. 488 pp.
- WINSTANLEY, D. (1973) Recent rainfall trends in Africa, the Middle East and India. *Nature* 243 (5408), 464-65.

Appendix 1 Climatic classification

The purpose of any classification system is to obtain an efficient arrangement of information in a simplified and generalized form. Thus, climatic statistics can be organized in order to describe and delimit the major types of climate in quantitative terms. Obviously no single classification can serve more than a limited number of purposes satisfactorily and many different schemes have therefore been developed. Some schemes merely provide a convenient nomenclature system, whereas others are an essential preliminary to further study. Many climatic classifications, for instance, are concerned with the relationships between climate and vegetation or soils, but surprisingly few attempts have been made to base a classification on the direct effects of climate on man.

Only the basic principles of the three groups of the most widely known classification systems are summarized here. Further information may be found in the listed references.

A General classifications related to plant growth or vegetation

The numerous schemes which have been suggested for relating climatic limits to plant growth or vegetation groups rely on two basic criteria — the degree of aridity and of warmth.

Aridity is not simply a matter of low precipitation, but of the 'effective precipitation' (i.e. precipitation minus evaporation). The ratio of rainfall/temperature has been used as such an index of precipitation effectiveness, on the grounds that higher temperatures increase evaporation.

The ratio r/t was proposed by R. Lang in 1915 (where r = mean annual rainfall in mm, and t = mean annual temperature in °C), such that $r/t < 40$ is considered arid and $r/t > 160$ perhumid.

The work of W. Köppen is the prime example of this type of classification. Between 1900 and 1936 he published several classification schemes involving considerable complexity in their full detail. Nevertheless, the system has been used extensively in geographical teaching. The key features of Köppen's final classification are:

Temperature criteria: Five of the six major climatic types are recognized on the basis of monthly mean temperature.

- A. Tropical rainy climate. Coldest month $> 18^{\circ}\text{C}$ (64.4°F).
- B. Dry climates.
- C. Warm temperate rainy climates. Coldest month between -3° and 18°C , warmest month $> 10^{\circ}\text{C}$ (50°F).
- D. Cold boreal forest climates. Coldest month $< -3^{\circ}\text{C}$ (26.6°F),* warmest month $> 10^{\circ}\text{C}$.
- E. Tundra climate. Warmest month 0° – 10°C .
- F. Perpetual frost climate. Warmest month $< 0^{\circ}\text{C}$.

The arbitrary temperature limits stem from a variety of criteria, the supposed significance of the selected values being as follows: the 10°C summer isotherm correlates with the poleward limit of tree growth; the 18°C winter isotherm is critical for certain tropical plants; and the -3°C isotherm indicates a few weeks of snow cover. However, these correlations are far from precise! The criteria were determined from the study of vegetation groups defined on a physiological basis (i.e. according to the internal functions of plant organs) by De Candolle in 1874.

Aridity criteria:

	<i>Steppe (BS)/Desert (BW) boundary</i>	<i>Forest/Steppe boundary</i>
Winter precipitation maximum	$r/t = 1$	$r/t = 2$
Precipitation evenly distributed	$r/(t+7) = 1$	$r/(t+7) = 2$
Summer precipitation maximum	$r/(t+14) = 1$	$r/(t+14) = 2$

* Note that many American workers use a modified version with 0°C as the C/D boundary.

390 Atmosphere, weather and climate

Where: r = annual precipitation (in cm)

t = mean annual temperature (in °C).

The criteria imply that, with winter precipitation, arid (desert) conditions occur where $r/t < 1$, semi-arid conditions where $1 < r/t < 2$. If the rain falls in summer a larger amount is required to offset evaporation and maintain an equivalent total of effective precipitation.

Subdivisions of each major category are made with reference, firstly, to the seasonal distribution of precipitation (the most common of which are: f = no dry season; m = monsoonal, with a short dry season and heavy rains during the rest of the year; s = summer dry season; w = winter dry season) and, secondly, to additional temperature characteristics. (For the B climates: h = mean annual temperature $> 18^{\circ}\text{C}$; k = mean annual temperature $< 18^{\circ}\text{C}$ (warmest month $> 18^{\circ}\text{C}$); k' = mean annual temperature (and warmest month) $< 18^{\circ}\text{C}$). Figure app. 1.1A illustrates the distribution of the major Köppen climatic types on a hypothetical continent of low and uniform elevation.

A somewhat similar scheme has been proposed more recently by A. A. Miller (1951), using the following criteria:

Boundary of arid conditions: $r/t = 1/5$.

Boundary of semi-arid conditions: $r/t = 1/3$.

Where: r = mean annual rainfall (in in.)

t = mean annual temperature (in °F).

The thermal units relate to the *accumulated temperature*, which Miller estimated approximately by using 'month-degrees' – the excess of mean monthly temperatures above 43°F (6°C) – rather than the usual day-degrees based on daily mean temperatures above this limit.

C. W. Thornthwaite introduced a complex, empirical classification in 1931. An expression for *precipitation efficiency* was obtained by relating measurements of pan evaporation to temperature and precipitation. For each month the ratio

$$11.5(r/t - 10)^{10/9}$$

where: r = mean monthly rainfall (in in)

t = mean monthly temperature (in °F)

is calculated. The sum of the 12 monthly ratios gives the *precipitation efficiency (P-E)* index. By determining boundary values for the major